5TH INTERNATIONAL WORKSHOP

STABILITY AND OPERATIONAL SAFETY OF SHIPS

University of Trieste
12-13 September 2001

PROCEEDINGS
OF THE
5TH INTERNATIONAL WORKSHOP "STABILITY AND OPERATIONAL SAFETY OF SHIPS"

University of Trieste, Italy, 12-13 September 2001

Edited by Alberto FRANCESCUTTO

Welcome in Trieste!

Dear participant to the 5th International Workshop on Ship Stability and Operational Safety, on behalf of the Organising Committee I welcome you in Trieste.
Tourist guides qualify Trieste as a crossroad between the Central-European and the Mediterranean cultures and as such a pole of attraction. On the other hand, its particular position was at the origin of the opening of a Nautical School since 1753, followed by the foundation of the Royal Academy of Business and Navigation in 1816. The presence of Fincantieri Shipyards and the opening of the curriculum for Naval Architecture and Marine Engineeing at University in 1942 witness the importance of Maritime affairs for this region. I hope you will enjoy both the Workshop and the nice geographic position of the town.

Prof. Alberto Francescutto

The Workshop on Ship Stability and Operational Safety

This is the 5th Workshop of the series, after Strathclyde (UK), Osaka (JAPAN), Hersonissos (GREECE), St.Johns (CANADA). Since its formation in 1995, the Ship Stability Workshop has presented a unique opportunity for experts in the field to gather together and present their latest research results. The Workshop provides an overview of the state of the art and the discussion developed from the presentations is an important part of the meeting.
The following is a list of typical Sessions held during the first four Workshops:

Surf-riding, Broaching and Capsizing in Following/Quartering Seas
Capsizing in Beam Seas
Capsize Model Experiments with a Damaged Ship
Dynamics of Ship Capsize with Flooded Internal Space Including Cargo Shift
Probabilistic Approach to Damage Stability and Survivability Assessment
Ship Capsize Simulation in Stability Research
Model Capsize Experiments in Heavy Seas
Non-Linear Dynamics and Ship Capsize
Dynamic Stability Software Validation Techniques
Standardisation of Model Experiments for Extreme Tests
Simulation of Damaged Ship Motions with Progressive Flooding
Interface and Overlaps on the Seakeeping, Manoeuvring and Stability of Ships
The Impact of Recent Stability Regulations on Existing and New Ships
Numerical and Physical Modelling of Intact Stability
Numerical and Physical Modelling of Damage Stability
Applications to Ship Design and Operation

Sessions Development

The Workshop will be held in an amphiteater room. Following the tradition of previous Stability Workshops, the Session Organisers of each Session (acting as chair/vice chair during the Session) will select discussers to seat in the first row (the "hot" seats) to act as "prime discussers" to boost and direct discussion which is the most important feature of the workshop.

Venue

- The Workshop will be held at the University of Trieste, Lecture Hall of Building H3, Via A. Valerio 10, 34127 Trieste, Italy;
- The preliminary sessions on September 10th-11th and the meetings on 14th-15th will be held at the University of Trieste, Department of Naval Architecture, Ocean and Environmental Engineering (DINMA), 2nd floor of Building C5, Via A. Valerio 10, 34127 Trieste, Italy;
- The International Maritime Academy is close to University (transportation provided).

The University is easily reachable by a 10 minutes bus ride from major hotels centrally located by using bus lines 3, 4, 17, 17(/), 39; no tickets selling on board → tobacconists, newsstands. For more information about Trieste University, visit the web site:
http://www.univ.trieste.it/english.html
For more information about Trieste, visit the web sites:
http://www.ts.camcom.it/english/home.htm
http://www-dft.ts.infn.it/TS/TS.html
These sites contain information about hotels, flights, weather forecast, etc.

Contact person:

Prof. Alberto Francescutto
DINMA, University of Trieste
Via A. Valerio 10
34127 Trieste, Italy
fax: +39-040-6763443
Phone: +39-040-6763425
e-mail: francesc@univ.trieste.it

Congress Secretariat:

Università degli Studi di Trieste
RIPARTIZIONE PROMOZIONE
P.le Europa 1
34100 Trieste - Italy
Phone: +39 - 040 - 6763464 /6763551
Fax : +39 - 040 - 574925
e-mail: promozione@amm.univ.trieste.it

SPONSORED BY:

FINCANTIERI SpA
International Maritime Academy, Trieste

Workshop held under the patronage of Regione Autonoma Friuli-Venezia Giulia

Proceedings printed with the financial support of "Fondazione Cassa di Risparmio di Trieste"

International Standing Committee Members

Prof. A. Francescutto
Prof. X.L. Huang
Mr. H. Hormann
Prof. Y. Ikeda
Dr. J.O. de Kat
Mr. D. Molyneaux
Prof. Marcello Neves
Prof. A. Papanikolaou
Prof. L. Perez-Rojas
Prof. N. Rakhmanin
Dr. M. Renilson
Prof. O. Rutgersson
Prof. K. Spyrou
Mr. Robert Tagg
Prof. N. Umeda
Prof. D. Vassalos (Chairman)
Prof. B.H. Nehrling

Organising Committee

Prof. Antonio Cardo, University of Trieste (Chairman)
Prof. Giacomo Borruso, International Maritime Academy, Trieste
Prof. Alberto Francescutto, University of Trieste (Secretary & Contact Person)
Ing. Livio Marchesini, Fincantieri SpA Trieste

A special thank to the Session Organisers of 5th International Workshop:

Jan deKat and Rubin Sheinberg: *"Operational issues and on-board stability guidance"*
Dracos Vassalos & Yoshiho Ikeda: *"Damage Stability I"*
Apostolos D. Papanikolaou & Robert Tagg: *"Damage Stability II"*
Kostas Spyrou & Alberto Francescutto: *"Large amplitude rolling motion and nonlinear ship dynamics"*
Shigeru Naito & Giorgio Contento: "*CFD Approaches to Ship Stability"*
Naoya Umeda & Martin Renilson: *"Intact Ship Stability: Simulation Tools for Capsizing - Validation and ITTC Benchmarking"*
Osman Turan & Andrzej Jasionowsky: *"Damage Ship Stability: Simulation Tools for Capsizing - Validation and ITTC Benchmarking"*
Bruce Johnson & Pasquale Cassella: "*SNAME Working Group on Fishing Vessel Stability Criteria"*

INDEX

ROUND TABLE DISCUSSION: "THE VIRTUOUS CIRCLE OF MARTIME SAFETY"

The International Maritime Organisation (Tom Allan)
The European Commission (Claudia Vivalda, Research Directorate General)
A Classification Society (Mario Dogliani, RINA)
A Shipping Company (Rolf Kjaer, Color Line)
A Towing Tank (Jan deKat, MARIN)
A Shipyard Design Office (Gianfranco Bertaglia, Fincantieri, Trieste)
A University (Apostolos Papanikolaou, NTUA)
The ITTC Stability Committee (Dracos Vassalos, NAME –SSRC, Chairman)

SUMMARY

This round table discussion attempts to address and discuss what is in essence a simple question: conceptualising the safety regime as a "wheel" with the number of stakeholders involved as the "teeth" of this wheel, what would be needed to render it virtuous, aiming at maximising maritime safety cost-effectively? Following a description of the said regime, the views of the key players in our industry are presented with the view to providing the stimuli for a constructive discussion in this fifth International Workshop on the "Stability and Operational Safety of Ships".

SAFETY REGIME [D. Vassalos]

The operation of merchant shipping is international, specialised and complex, currently governed by comprehensive rules and regulations developed by national and international authorities to provide a basis for common action. Legislation governing ship and environmental protection has progressed over time through a number of stages but in the main assurance of safety has always been sought through regulating widely existing best practices in ship design, construction and operation. In this evolutionary process, three co-existing and interacting ship safety regimes can be identified and are explained briefly next.

Punishment Regime: This relies on identifying and apportioning blame, frequently to the last person in the chain of events. The underlying principle is that the threat of punishment influences company and individual behaviour to the extent that safety gains a higher priority.
Compliance Regime: This constitutes the core of ship safety assurance today and involves mainly the regulation of ship safety by prescription with external rules.
Self-Regulation Regime: This concentrates on external management and organisation for safety and encourages individual companies to establish targets for safety performance. It is very much the result of a general acceptance by the shipping industry of the inadequacy of the previous two, to rely solely on regulations as a means of improving ship safety standards, and is in the heart of current and future developments. The adoption of the ISM Code, which became mandatory on 1 July 1998 by all IMO member states, constitutes an important step towards the establishment of a self-regulation regime.

The prevailing philosophy therefore is that of compliance, characterised by the following main steps and associated players:

Development of international instruments through the International Maritime Organisation (IMO)

IMO is an agency of the United Nations and has its headquarters in London. It was established in 1948 in response to the need for uniformity in shipping legislation with the task of developing a comprehensive body of international law dealing with maritime safety that would be applied by all shipping nations to ships under their flag. The IMO membership since then has grown to 155 countries, with more than 40 conventions, agreements and protocols developed in the process under the IMO aegis. The Maritime Safety Committee (MSC), which is responsible for all safety matters except marine pollution, has 12 sub-committees covering a wide spectrum of safety-related areas.

IMO have in the past been subject to criticism: too slow and by implication inefficient; a toothless tiger; responding to every crisis with a new piece of legislation; minimum standards fostered by a consensus approach; political rather than technical arguments often dominate. IMO, however, is undergoing major transformations involving changes in attitude, philosophy and approach to ship safety and environmental protection and this process is likely to continue at an accelerated pace. The legislation at IMO on ferries and the work of the Panel of Experts certainly demonstrated that IMO can move fast and the ISM Code and STCW Convention are clear indications of positive actions to improve safety.

Implementation of regulatory instruments by Ship Owners/Operators

With the exception of the master who has the ultimate responsibility for the safety of the ship, ship owners are top in the order of priority for the responsibility of implementing and maintaining safety standards. They

cannot, however, be relied upon universally and the existence of sub-standard ships is evidence to that. It is said that behind a sub-standard ship there is a sub-standard owner and it is common belief that enforcement and verification by the flag and port states and the classification societies are no substitute for the all-embracing responsibility of the owner. As with the safety regimes described above, it would be appropriate to classify the prevailing cultures of ship owners into the following three, Figure 1.

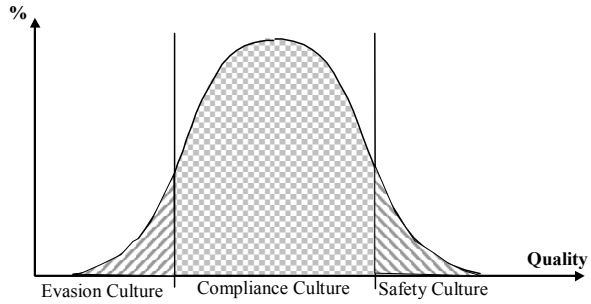

Figure 1: Ship Owners Prevailing Cultures Distribution

Evasion Culture: Evading rules and regulations, cutting corners. Taking the risk in the belief they can get away with it or yielding to economic pressures or as a result of failure in the enforcement and verification processes.
Compliance Culture: Simplistic compliance with prescriptive legislation is currently the industry norm aimed at satisfying minimum safety requirements and nothing more. The existence of this norm is demonstration of the passivity inculcated through prescription.
Safety Culture: Continuous safety improvements with safety becoming an almost subconscious priority and safe operation a matter of course.

Enforcement of regulatory instruments by Flag States and Classification Societies

Flag States
The next level of responsibility is that of the Flag State. Considering the tendency at IMO of adopting minimum standards, some countries enhance such standards through national rules and regulations. After all, the state has the ultimate responsibility, that of protection of human life. The duty and commitment of the state must not be confined to the satisfaction of IMO rules. Promotion of scientific research, improved vocational training, improved efficiency in port organisation, increased surveillance and assistance at sea are the duties of the state. The attitude of flag states to these duties and responsibility range quite widely. This is reflected in the casualty rates of individual flags, clear indication that regulations are implemented differently form country to country. The prevailing cultures of flag states could quite easily be classified in a way similar to the ship owners. In some cases, however, it is the lack of resources to enforce regulations that leads to evasion. "Flags of Convenience" are born out of the inability of a state to supervise the safety of its ships effectively. What is worrying in this respect is the fact that there is a significant number of flags of convenience with figures produced by the Institute of London Underwriters showing that, in general, registers with a higher percentage of total losses are expanding at the expense of those with a better safety record.

Classification Societies
Classification societies are independent, non-profit making organisations concerned primarily with the standards of construction and maintenance of ships. As such they contribute greatly to the advancement of the art and are a potential source of considerable technical experience gained worldwide. By means of the development of their rules for construction and periodical surveys they are in a position to influence the standards of ship construction and operation and their contribution to these matters and to ship safety generally has been considerable. Originally established to designate minimum standard, on which underwriters could rely before insuring a vessel as a form of risk management, they have in fact emerged as the unique arbiters of a standard, which is relied upon not only by underwriters but also by every section of the shipping community. In fact, from July 1998 an amendment to the SOLAS Convention comes into force making compliance with the classification society rules for ship structures and essential engineering systems a mandatory requirement. Notwithstanding this, today it is not possible for a ship to trade unless it is 'class maintained'. From this it follows that all vessels at sea (good or bad) are registered with one of the classification societies. Included among these are vessels, invariably brought to light by a casualty, the condition of which is such that they should not have been registered. In many cases it will transpire that the vessel is in possession of a special survey certificate of recent issue, notwithstanding the fact that numerous serious defects are long-standing. This is a serious problem facing all classification societies and it reflects the difficulty of maintaining consistent standards. The eleven major classification societies have a co-operative organisation, the international Association of Classification Societies (IACS), which enjoys consultative status with IMO, co-ordinates the policy of societies and issues unified recommendations for the standard to be applied in essential technical matters. In response, to the aforementioned criticism, IACS has developed a quality assurance concept, which all the members must comply with.

Verification of the proper implementation and enforcement of all applicable international requirements by Port States

Port state control is the first line of defence in the enforcement and verification of safety standards but can never be as effective as good flag state control, because

port states have to accept international certificates at face value unless there are clear grounds for disputing their validity. If not so, the ship owners are entitled according to SOLAS to be compensated if their ship is unreasonably delayed. Port state control alone has inherent limitations. Primarily it is a spot check but even when targeting those ships most likely to have shortcomings, it will be impossible to identify all substandard ships. Often it is impossible to inspect the holds if the ship is fully laden, and it may not be possible to assess fully the competence of those onboard.

General Remarks

This introspective look demonstrates that the prevailing safety regime is hard pushed to retain its integrity at the larger scale and allows for a worrying imbalance in the assurance for safety between property (ships and cargoes) and lives (seafarers and passengers). Those concerned with property have sophisticated insurance markets at their disposal, which compete for the insurance of ship and cargoes. The classification societies play a central role in this process in that they provide independent quality assurance to shipbuilders and expert advice to ship owners and insurers. The latter normally comprise a large percentage in the constitution of classification societies and are therefore in a position to either insist upon higher classification standards or quote higher premia for ships with greater risks. Thus, if ships and cargoes are lost, the sensible owners will be compensated by their insurers and, for their part, the insurers can make profit at any predictable level of risk. Therefore, ship loses are recorded, analysed and published, allowing the organisations concerned with classifying and insuring property to assess risk. By contrast, however, there is not a mechanism formal or informal in place to record systematically and assess the effectiveness of legislation aimed at improving the safety of life at sea. Fatalities have been reported since 1978 but not with the rigour necessary to draw conclusions from statistics. There are no incentives to do so.

This is a state of affairs that the marine industry simply could not afford as was amply demonstrated by the recent well-publicised ferry disasters. Furthermore, with passenger ships being built carrying 5,000 passengers such as the Eagle Class of the Royal Caribbean Cruise Lines, safety must become an integral part of ship design, construction and operation with the focus particularly on passenger safety. Added to this are the new challenges and new risks associated with the escalation of speed at sea. Historically, significant changes in the design, operation and management of ships have brought about new hazards and more casualties. Reliance on experience with conventional ships provided in most cases a cushion against impending disasters. But what is to be expected when this cushion is removed?

Could the answer to this question lie on what is (surprisingly) coming out from the IMO "furnace": ALTERANTIVE DESIGN AND SAFETY EQUIVALENCE? Could this approach provide the "fuel" that would make the wheel (Figure 2) of maritime safety turn?

Figure 2: The Virtuous Circle of Maritime Safety

SAFETY DRIVERS – PASSENGER SHIP SAFETY STAKEHOLDERS [A. Papanikolaou]

This input is wholly based on the MSC 70/INF paper on the Formal Safety Assessment (FSA) of Bulk Carriers, submitted by the United Kingdom to the Bulk Carriers Working Group. This has been properly amended to account for the fundamental differences between the Bulk Carrier's and the Passenger Ship's design and operation.

1 A key feature of the FSA methodology is that it should be able to recognize and account for the various interests and positions of those who will be affected by any changes to regulations resulting from the study.
2 *Interested entities or stakeholders, herein also understood as safety drivers,* are defined as any person, organization, company or state who is directly or indirectly affected by an accident or by the cost effectiveness of any proposed new regulatory requirements.
3 Stakeholders may be voluntary (e.g. ship owners) involuntary (e.g. cost state) or a combination of both (e.g. passengers, cargo owners). Similarly, the interests of stakeholders may be either beneficial or prejudicial in nature, or a combination of both. Stakeholders may be represented directly, indirectly or by representative groups where their interests are similar.
4 Each stakeholder creates and/or suffers a risk as a result of his involvement with the maritime venture and receives benefit and/or suffers cost of liability. The returns obtained by individual stakeholders will

not necessarily reflect their investment in the venture. Some stakeholders will obtain disproportionate returns in relation to the risk they create whilst others will obtain no return whatsoever. From this, the concept of Risk Balance is introduced, as shown in Figure 3.

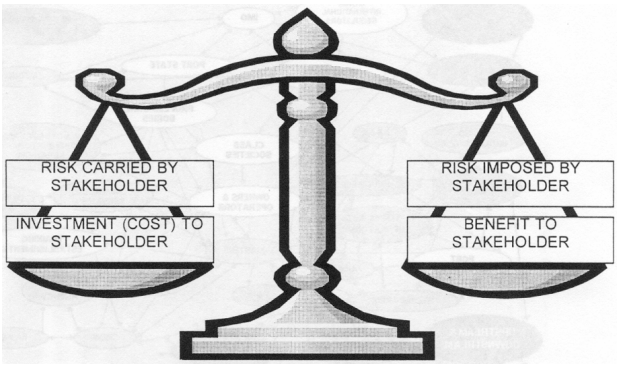

Figure 3: Concept of Risk Balance

5 Stakeholders with any degree of voluntary participation in the exercise will clearly expect that the benefit side of the balance will outweigh the cost side, however the proportion by which the benefit outweighs cost will generally be different for each stakeholder.

6 Ideally, the risks, costs and benefits derived from the maritime venture would be assessed for each stakeholder to determine whether the balance is equitable in relation to the other stakeholders. In practice, such an absolute solution would be very difficult to achieve due to historical factors. The final recommendations for the decision-making should, where practicable, seek to redress any imbalance between those stakeholders who impose risk and those who carry disproportionate risk in relation to the return they receive – i.e. the Risk-Imposer pays.

Stakeholder Map

7 The role of each stakeholder should be considered in the context of accident prevention and mitigation. The influences of, and interactions among, stakeholders should be assessed. In particular, a FSA study should recognize that the relative positions and prominence of stakeholders will vary at different stages of an accident (e.g. prior to, during and after).

8 The principal stakeholders of Passenger Ship operations have been identified and their interrelationships considered as shown in Figure 4 and listed with the effect of a casualty of their interests in Table 1 and 2.

9 It should be noted that only the principal influences are shown. Many secondary influences will be present in any given scenario.

10 Whilst legal services and consultants are considered stakeholders, it is considered that their influences may be represented on the influence map by those of their clients.

11 Only the principal insurance interests are shown. All stakeholders would probably have insurance cover (and many insurers would probably have re-insurance). As with legal and consulting services, insurance interests are considered to be represented on the influence map by their insurers.

12 Upstream and Downstream stakeholders are those stakeholders who are generally physically remote from the vessel but are affected by the consequences of an incident to it.

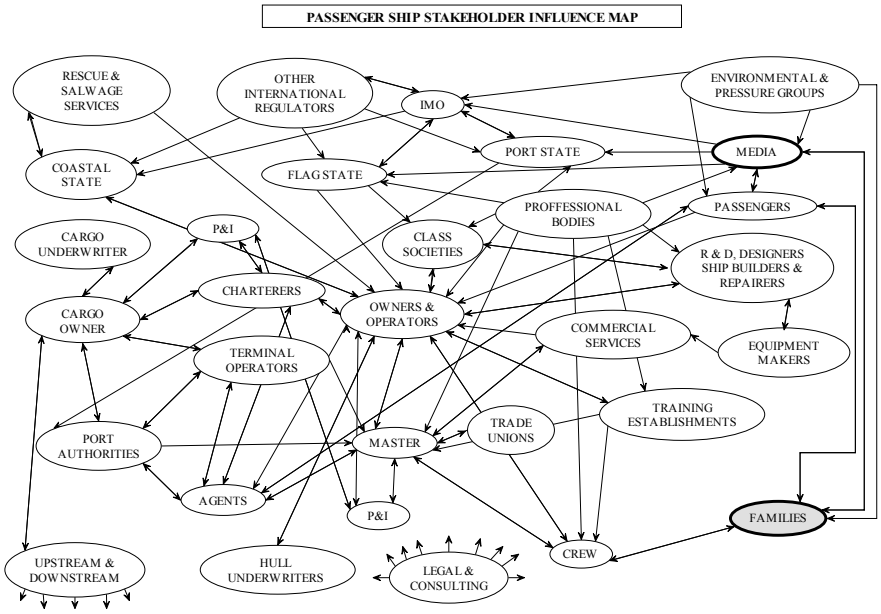

Figure 4: Stakeholder Influence Map - Passenger Ships

STAKEHOLDERS	EFFECT OF A CASUALTY
Owner, Operator or Manager	Loss of ship, direct and indirect loss of income (incl. possible losses in the stock market), loss of reputation, contract liabilities, employee liabilities and 3rd Party liabilities, possible indictment by jurisdiction.
Master	Loss of life, loss of reputation, loss of income, possible indictment by jurisdiction.
Crew	Loss of life and loss of income, possible indictment by jurisdiction.
Passengers	Loss of life and property.
Trade Unions	Representation expenses.
Families	Personal loss and loss of income.
Designers, Ship-builders & Repairers	Loss of reputation, liability and loss of income. Increase in income.
Equipment makers	Loss of reputation, liability loss of income. Increase in income.
I M O	Loss of reputation.
International Regulators	Loss of reputation.
Port State Control	Loss of reputation, possible indictment by jurisdiction.
Flag State	Loss of reputation, loss of income, possible indictment by jurisdiction.
Port Authority	Pollution, cost of removal of wreck and loss of income (trade).
Classification Societies	Loss of income and loss of reputation, possible indictment by jurisdiction.
Professional Bodies	Loss of reputation.
Training Establishments	Loss of reputation and loss of income.
Environmental and Pressure Groups	Increase of income, greater awareness.
Cargo Owner	Loss of goods, loss of income, loss of reputation, contract liability and downstream supply failure.
Charterer	Loss of income, contract liabilities and loss of reputation.
Terminal Operator	Damage to facility, disruption of facility and loss of income.
Hull Underwriters	Liability.
Cargo Underwriters	Liability.
P & I Club(s)	Liability.
Rescue Services	Possible loss of life and property damages (non-professional rescuers), 3rd party liability. Increase in income (professional rescuers)
Salvors	Increase in income.
Coastal State	Pollution and cost of removal the wreck.
Media	Increase in income and increase in ratings.
Legal Services	Increase in income.
Marine Consultants	Increase in income.

Table 1: Stakeholders

STAKEHOLDERS	EFFECT OF A CASUALTY
Regional & State Groups	Loss of trade. Additional trade.
Other Trading Nations	Additional trade.
Suppliers upstream	Loss of trade.
Alternative Suppliers	Additional trade.
Consumers downstream	Additional costs.

Table 2: Upstream & Downstream Stakeholders

Stakeholder Groupings

13 The stakeholders may be grouped into 'primary' groups to assist in identifying common interests and influences. This will serve to reduce duplication of effort in considering the effects of Risk Control Options (RCOs) on the various stakeholders. With each RCO, it will be necessary to verify that the grouping is valid. The FSA study should take account of the fact that Stakeholders within a group may not have exactly parallel interests and that the other Stakeholders and influences may emerge. The Stakeholder groups presently identified are:

.1 Owners & Operators;
.2 Staff and Support (Master, Crew, Crew Agency, Trade Unions, Families);
.3 Passengers (incl. families);
.4 Hardware (Ship designers, Ship builders, Ship Repairers, Equipment Makers, Port Commercial (supply) Services;
.5 Regulatory (IMO, International Regulators, Port State, Flag State, Port Authority);
.6 Non-Governmental Bodies and Pressure Groups (Classification Societies, Professional Bodies, Trade Associations, Training Establishments, Environmental Groups);
.7 Cargo Group (Cargo Owner, Charterer(s), Terminal Operators);
.8 Insurance Group (Hull & Machinery Underwriters, Cargo Underwriters, P&I);
.9 Response Services (Rescue & Emergency Services, Salvors, Coastal State)
.10 Media
.11 Service Group (Legal Services, Marine Consultancy and Surveying Services, General Insurance)

Upstream and Downstream Groups (Commercially or Geographically Dependant Region or States, Other Trading Nations, Suppliers, Consumers).

LEGISLATION/PROCEDURALISATION [T. Allan]

Dracos has set a few tasks for each of the members of the round table discussion to address "The Virtuous Circle of Maritime Safety". I have been allocated the task of considering "legislation / proceduralisation".

"Proceduralisation" not sure if there is such a word but it does seem to encapsulate the issue. Are Rules the answer? In an ideal world the answer has got to be NO! In such a world we could leave it to the ship owner to apply a full risk analysis to his particular vessel for specific operational requirements and then design according to his perceived risks. However in an international world-wide industry is this a practical proposition?

At present we have 158 member states of IMO. Is it practical in a business, where shipping can trade world wide, to have or operate ships which have been subject to 158 differing interpretations on something as fundamental as ship survivability? While it may be possible for a few like minded countries to accept the same version of perceived risk, there is no doubt that this approach could not achieve agreement on an international basis. Could a ship owner take the risk and build his ship to one set of requirements which a) may not be acceptable to all States to which he wishes to trade; or b) could limit his opportunities for the future sale of the vessel. I doubt it.

Obviously this is a very diverse and complex issue which could only be taken by the owner / State on a case by case basis. There may very well be a situation whereby a ship could be built to suit a specific operation and where the problems of the views or acceptance by others were not material. But I would suggest that this would be a minority of cases. The use of equivalence has been an accepted IMO procedure for a long time now but this is within very strict limits. That is equipment equivalents although lately we did address the model test procedure as an equivalence to a set standard. However here again it was within limits in that the prime standard (SOLAS '90) had to be achieved first and the equivalence addressed the additional element of survivability "water on the car deck". Equivalence will always be with us but I do not think it will be accepted as an overall concept, which could a request to the owner to prove that his vessel was "safe". Safety Codes are another possibility; here IMO has used Codes of Safety for specific types of ships. These Codes acknowledge the differing concepts of design and operation for example between conventional ships and high-speed craft. This is a concept worthy of further consideration where further elements of risk acceptance criteria could be applied.

A virtuous circle however requires all within the circle to accept an agreed set of aims and objectives. To develop a set of objectives were each owner / State could demonstrate that their ship can meet those aims e.g. "for the vessel to be safe and operable with two compartments damaged and flooded" requires some form of International collaboration. This is where the International Maritime Organisation achieves its goal.

Member States at IMO, supported by their industry, are very much against unilateral action either by a single State or on a regional basis. One of the goals of IMO is to achieve a safety culture throughout all member Flag States, operators, charterers, brokers and financiers i.e. the full circle of stakeholders. Or to use the phrase given to us "the virtuous circle of maritime safety. One positive example, as I understand the situation, is the probabilistic approach. This accomplishes the aim in that once we agree a level of achievable safety then all that the owner / State has to do is demonstrate that level of achievement. How he achieves it is up to the owner and his designers. The main point is that the level can be demonstrated and accepted by all States to which the vessel trades.

Therefore as much as I would wish otherwise some form of Internationally agreed regulation is, I believe, essential to maintain a level playing field. With the help of the "virtuous" or "safety culture" that should assist in raising the playing field to an acceptable safety standard. Or am I wrong?

IMPLEMENTATION - GOALS OF SAFETY CONCERNED PASSENGER SHIP COMPANY [R. Kjaer]

- Leading operator within transport and short cruise segment
- High quality of:
  - *Safety*
  - *Service*
  - *Environmental policy*
  - *Competitiveness*
- Economy for growth
- Qualified operation of relevant tonnage
- Meet future requirements for high competence

INFLUENCE OF EXTERNAL FACTORS PEFORMANCE OF COMPANY

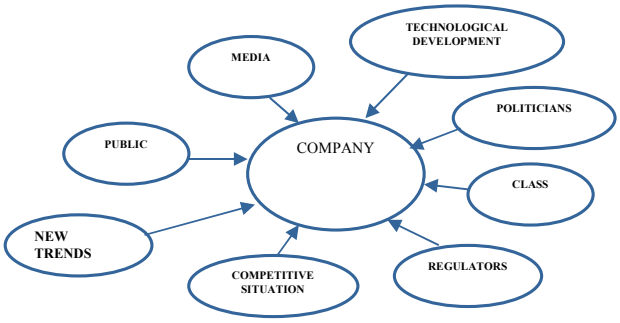

SAFETY AND ENVIRONMENTAL FACTORS

- Safe, economic operation
- Control/secure authorities requirements for operation
- Meet challenges according to new rules
- Future environmental requirements
- Provide cluster of experts for technical/maritime operation
- Competitiveness with high safety and environmental profile

MEDIA FOCUS

- Examples from large accidents
  - *"Scandinavian Star"*
  - *"Estonia"*
  - *"Prinsesse Ragnhild"*
- Proactive
- Open society, media
  easy access standard of operation
- Media create actions by politicians

CO-OPERATION RE SAFETY

- Important that operator is responsible for own operation
- Authorities/Class auditors re safety
- Importance co-operation all parties associated with safety:
  - *Regulators*
  - *Research*
  - *Operators*
  - *Class*
- Co-operation from day one
- Open co-operation also between operators ex NORDKOMPASS

OPERATORS VIEW

- View regulations should be channeled through IMO
- New regulations must be understood to be important
- Importance re co-operation regulators/-owners when discussing new rules
- New regulations should be based on safety assessment, not on accidents
- Important that regulators ensure influence operation friendly solutions
- Cost benefit factor, industry must survive

OPERATORS VIEW RE RESEARCH

- Closer contact operators/universities
- Importance useful research
- Operators must understand academic society - eliminate borders - vice versa
- Importance research projects participation different players
- Importance seminars establishing closer contact with parties

FUTURE WORK

- Rules through IMO
- If no success IMO, regional solutions
- Proactive safety rôle, large passenger ships
- Establish fora for co-operation
- Importance EU research projects
- **Safety assessment**

ENFORCEMENT [M. Dogliani]

Safety = money

- Effective monitoring incentives
  decentives
- Standards (IMO's, Class, ..) = minimum acceptable safety level
- Minumum standard operator: cost driven = decentives
- Higher standard operator: revenue driven = incentives

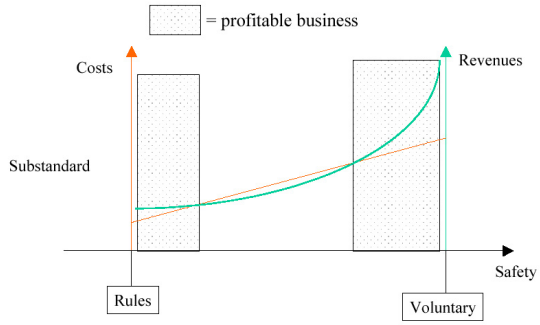

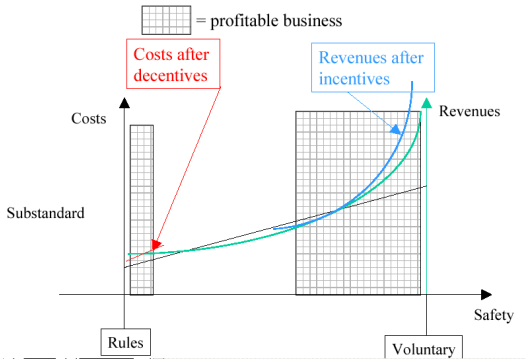

How to achieve this? Partnership

LIFE-CYCLE DESIGN FOR SAFE OPERATION
Safety on the cruise ships – The FINCANTIERI Experience [G. Bertaglia]

Fincantieri developed the design of the Cruise Ship "Crown Princess" (70000 GT) in 1985 and in relationship to safety evaluation the following decisions was adopted:

- Embarkation deck and Lifeboats, was fitted at a height of less than 15 m from the sea level; this solution became recommendation in 1991 and rule in 1998.
- Having present the diesel-alternator room layout (the Diesel motors in one watertight compartment and the alternator in another), it has been verified the damage stability for three compartment flooded.
- Having the need to deploy a restaurant longer than 48 meters, the room has been divided with a water curtain (screen) of high flow rate, it has been oversized the sprinkler system and, in relationship with the stability problems of free surfaces effect of water on the floor of the restaurants, scuppers oversized in diameter has been provided to discharge overboard the water of the sprinkler system and non return valves was fitted for avoid problems to the air conditioning plant.

In 1992, during the design of the Cruise Ship "Destiny", at the time the biggest Ship in the world (101000 GT), Fincantieri proposed to the Owner, the passengers direct embarkation on the Lifeboats on the stowed position, defining a space not furnished completely protected for the muster stations. The Owner approved the proposal, considering it an investment for giving more safety to the passengers both real than psychological and for abbreviate the embarkation time.
Today, this Ship series, are the only with this layout.
In 1994 during the design of the Cruise Ship "Grand Princess" (109000 GT), Fincantieri developed:

- Safety availability studies with a flooding approach
- Smoke strategy

The above mentioned, to underline the importance of the safety for the Cruise Ships, that are grooving in number and in dimension. Today, many of these, have a maximum number of person on board of 4000-5000, others in designing reach 6000.

Flooding analysis

Flooding risk analysis has been carried out on Grand Princess design, as part of the overall safety and availability assessment. Hazard identification exercises were performed, examining historical casualty data (distribution, location and extent of damage along the hull) including hull, machinery systems and operational factors. The consequences of flooding were estimated on a compartment-by-compartment basis, and then to simultaneous flooding of two or more compartments. The predicted frequencies of the risks were estimated together with a detailed consequence and escalation assessment.

The results allowed some improvements in the design: It was found, for instance, that the probability of flooding two adjacent compartments was greater than flooding just one. As a consequence, the location of equipment was modified, either in compartments within B/5 boundaries or in non-adjacent compartments.

Therefore, in case or damage, the availability of the ship and her systems was improved As a general comment, the identification of modifications during basic design can prevent major changes being made during detailed design.

Smoke strategy (smoke control and ventilation)

Several F/C ships (all P&O cruise ships) have been designed having in mind a smoke strategy, based on a pre-planned strategy of the air conditioning and ventilation systems to contain the fire and the smoke in the place of origin. The statutory SOLAS requirements

simply consider the emergency shut-down of the complete Main Vertical Zone in case of fire. The smoke strategy allows the master and the senior officers of the ship to monitor and control the development of the fire with a direct control of the following aspects:

- air inlet (cutting off ventilation and fresh air)
- air exhaust (to keep extracting the smoke from the place of origin)
- controlled atmosphere and pressure along escape ways (corridors and stairs)

The correct implementation of the smoke strategy is a basic design requirement, since it involves the basic design of the air conditioning and ventilation systems from the beginning.

At the time being, the smoke control on passenger ships is voluntary and not mandatory, although discussions have been made at IMO Fire Protection (FP) sub-committee to draft Guidelines with a view toward keeping assembly stations and atriums smoke-free during a fire. The delegation of Italy at the IMO offered to prepare draft Guidelines on smoke control and ventilation based upon document FP 45/5 for consideration bv FP 46.

Post Panamax cruise ships safety

SOLAS rules, developed on the basis of past experience and incidents, have been defined with reference to all cruise ships, regardless of their size. The application of such rules to ships "up to panamax size" (as in past years) has proved fairly successful, as demonstrated by the very low rate of incident, which has qualified the cruise industry in these years of growth. Recently, however, the increasing trend of the cruise industry towards ships of much bigger size (Post Panamax) has evidenced some problem and concern about the "literal" application of SOLAS rules. Particularly there are two basic questions which need to be answered:

(1) Are these rules, as presently formulated, really effective for ensuring the safety standards of very big cruise ships (Post panamax)?
(2) Does the present obligation to strictly comply with to the individual rules and regulations as formulated cause problems in the development of the design of these big ships?

For answering to the first question in a factual way, it is necessary to actually measure and compare the "safety standards" of corresponding areas and arrangements on board of "consolidated" Panamax and Post Panamax ships. Such comparison has to be based on a detailed risk analysis, focused on the main "safety" factors (such as volume of each area, time needed for actually ensure the evacuation of an area, distance for the lifeboat embarkation deck a.s.o.), and developed with the same criteria and parameters on both Panamax and Post Panamax ships. Also the comparison with the results achieved in corresponding land based applications could offer useful terms of comparison.

Preliminary results of these risk analysis - focused on the measurement of the "evacuation time" - evidence that the ships up to Panamax size are safer than the corresponding land based applications, while the "Over-panamax size ships are, from the safety point of view, equivalent or even more effective than Panamax ones.

For what instead concerns the limits in the Post Panamax ship's design linked to the "literal" application of SOLAS rules, (such as, for example, the combined requirements of maximum length and maximum surface of a fire zone, which appear to be very demanding when applied to an "extra – wide" cruise ship), industry opinion seem to converge towards a "concept idea" of "equivalence", focusing on the "core" parameters and targets peculiar to the individual rules rather than on the application of individual prescriptions. A possible example of this approach, which aims to grant levels of safety equivalent or (due to the peculiar characteristics of Post Panamax cruise ships) even higher respective to the literal application of prescriptions, could possibly be found in the above mentioned limits to fire zone length and surface.
In this case the "core" targets of the SOLAS rules could possibly be anyhow reached by operating in terms of:

- equivalence of volume of the zone, in comparison with the maximum allowed by the standard criteria;
- reduced distance from muster stations deck
- specific provisions for reducing escape times
- introduction of specific further "risk reduction devices", in order to further ensure the correspondence between the safety standards achieved with the new arrangements and the ones ensured by the standard rules application:
  - further reduction of combustible materials;
  - area partition with "spray water" curtains
  - increase of active protection devices
  - positioning of the area respective to lifeboats embarkation decks
  - increase in the quantity and dimensions of escape doors
  - direct connection between the area and the open decks with one-only flight of steps
  - special emergency ventilation systems

Safety could be considered by more aspects:

- Fire
- Lifeboats position / evacuation
- Grounding
- Collision
- Damage

Many are the approach of the Industry and the Owners for improve safety: for example technical solutions, behaviour's standards, crew and passengers training, etc. The above mentioned increase the safety, but isn't clear how much, and so it is not easy to correlate the investment made with the result.

One possible solution is to determine the entity of the improvement: for example applying an opportune theory to a certain standard responding to the rules, quantifying some meaningful parameters. Then applying a modification and assess the results applying the same analysis. Comparing the results, it would be possible to quantify the variation of the safety aspect assessed, correlating, not the least, with the cost.

LIFE-CYCLE DESIGN FOR SAFE OPERATION [J. de Kat]

+*Design and operation should be coupled in an interactive fashion*- establish feedback from owners and seafarers to designers and yards
- reporting and analysis of extreme events and "near-misses"
- education and training with state-of-art tools: officers, seafarers
- operational guidance (dynamic stability, loads, etc.)
- on-board measurement systems (motions, stresses, sea state)
    - quantify operational profiles in design stage, incl. climate
        - stability/strength/… characteristics as function of time
            - account for human factors (MIS, MII, MIF), ergonomics
            - consider design and off-design conditions
            - incorporate surveys into design

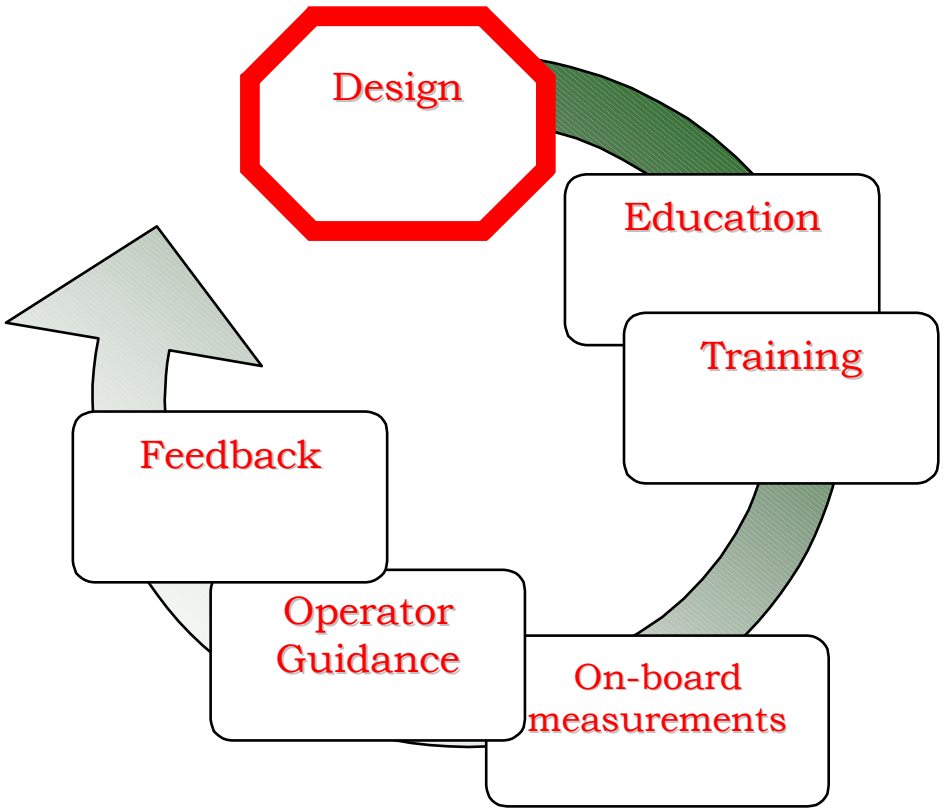

Stability and safe operation

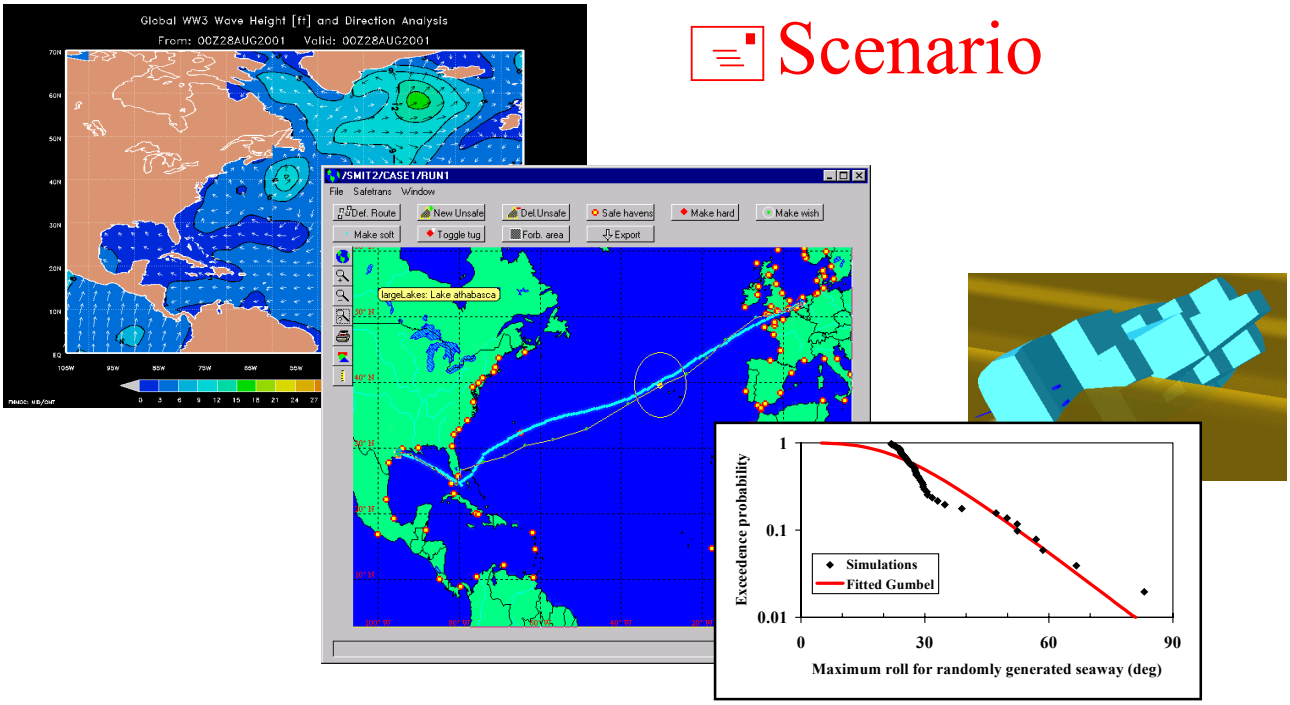

Maritime safety

- Safety: not a closed loop, but open and multi-faceted system
- Many associated parties/stakeholders: fragmented, few links; some have conflicting demands w.r.t. safety
- Fuzzy relationship between safety and economic performance of shipping operations (which tend to be marginal)
- Accidents will remain part of shipping operations -- ALARP?
- Why invest in R&D?

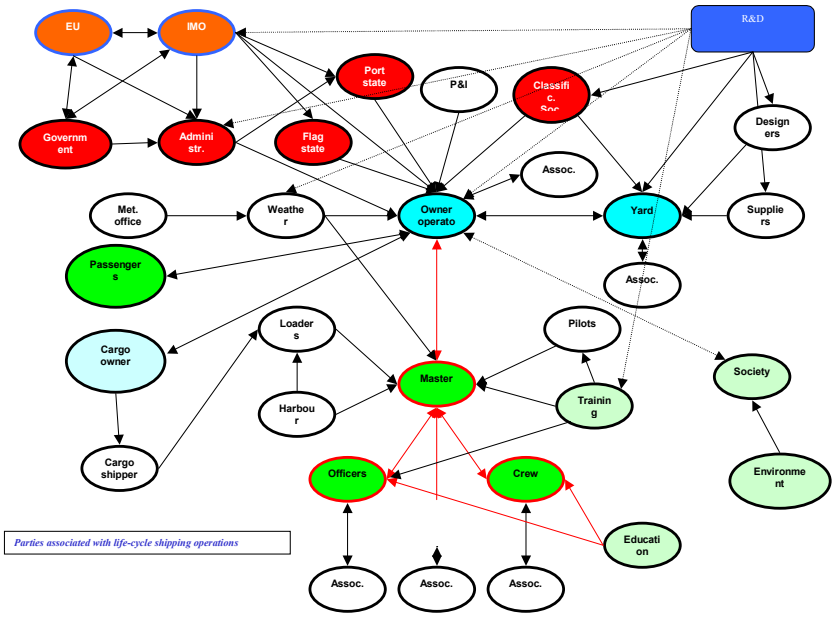

Role R&D

+ Cluster R&D with different disciplines and create process of interaction with stakeholders on different themes, including (but not solely) safety

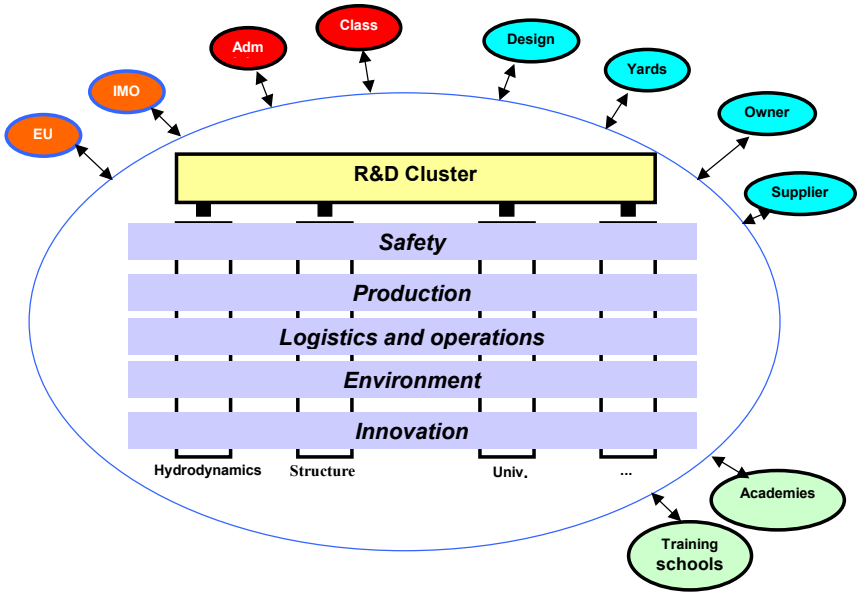

Life-cycle design for safe operation

Design and operation should be coupled in an interactive fashion

- establish feedback from owners and seafarers to designers and yards
- reporting and analysis of extreme events and "near-misses"
- education and training with state-of-art tools: officers, seafarers
- operational guidance (dynamic stability, loads, etc.)
- on-board measurement systems (motions, stresses, sea state)
  - quantify operational profiles in design stage, incl. climate
    - stability/strength/… characteristics as function of time
      - account for human factors (MIS, MII, MIF), ergonomics
      - consider design and off-design conditions
      - incorporate surveys into design

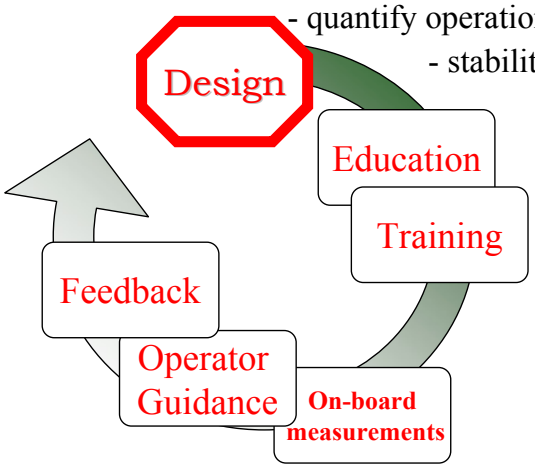

De Kat, Aug. 2001

Stability and safe operation

Scenario analysis, risk management

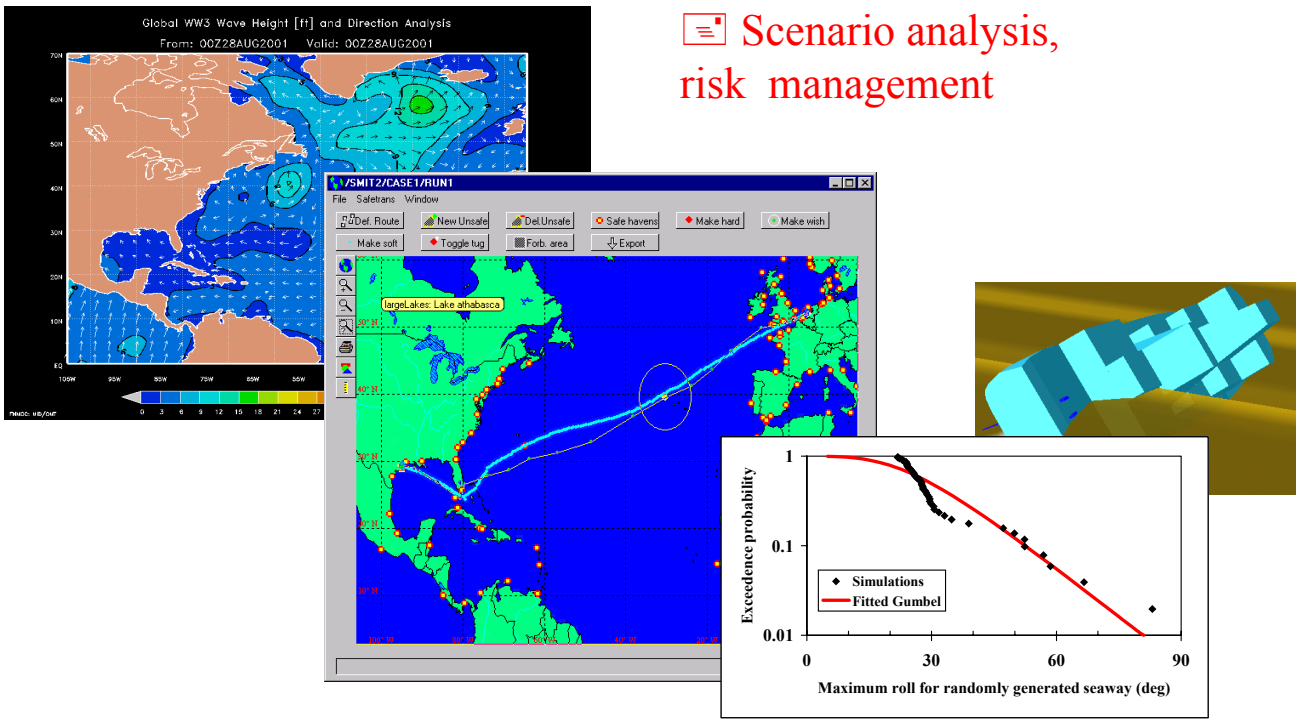

De Kat, Aug. 2001

Maritime safety

- Safety: not a closed loop, but open and multi-faceted system
- Many associated parties/stakeholders: fragmented, few links; some have *conflicting* demands w.r.t. safety
- Fuzzy relationship between safety and economic performance of shipping operations (which tend to be marginal)
- Accidents will remain part of shipping operations -- ALARP?
- Why invest in R&D?

Multi-disciplinary problem ↓ integrated approach is a necessity

Combine performance and safety ↓ optimization depends on stakeholder groups

R&D can and should play a definitive role

De Kat, Aug. 2001

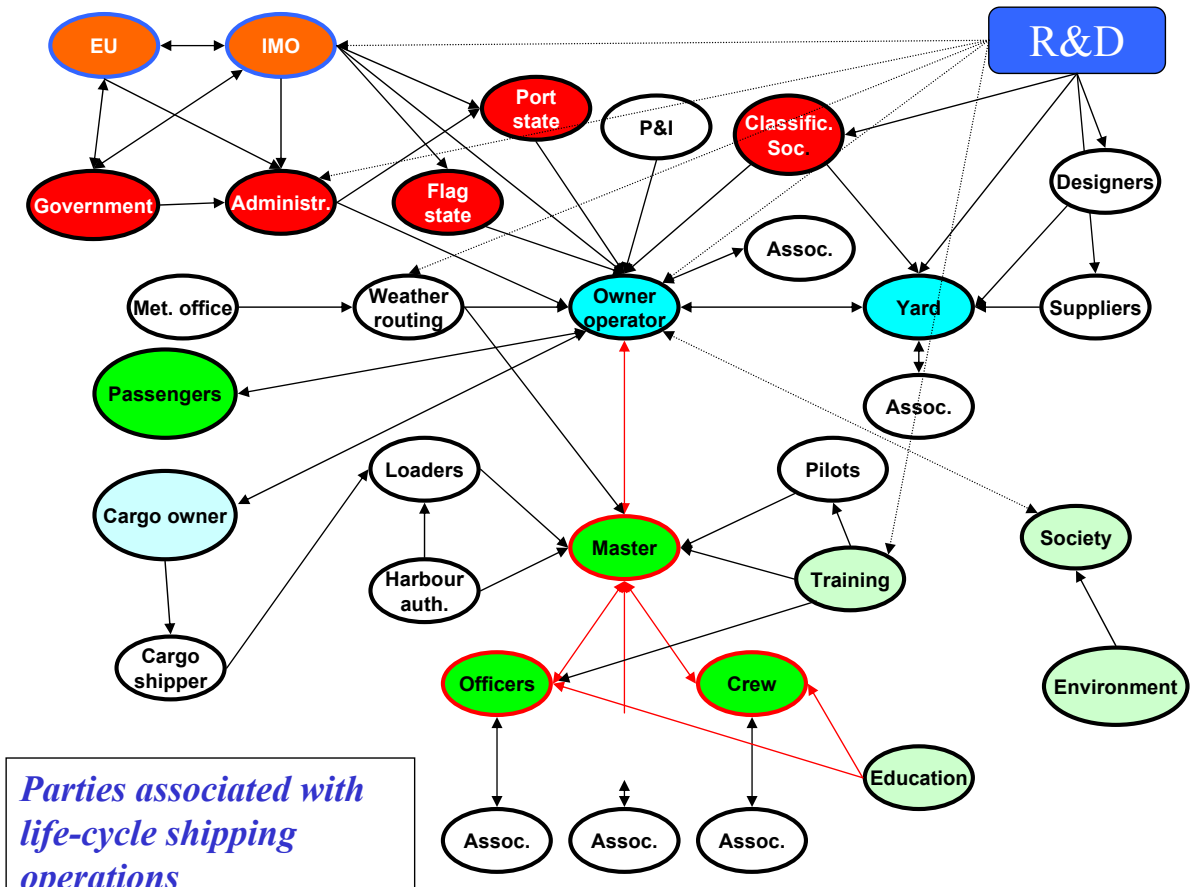

Parties associated with life-cycle shipping operations

De Kat, Aug. 2001

Role R&D

- Cluster R&D with different disciplines and create process of interaction with stakeholders on different themes, including (but not solely) safety

De Kat, Aug. 2001

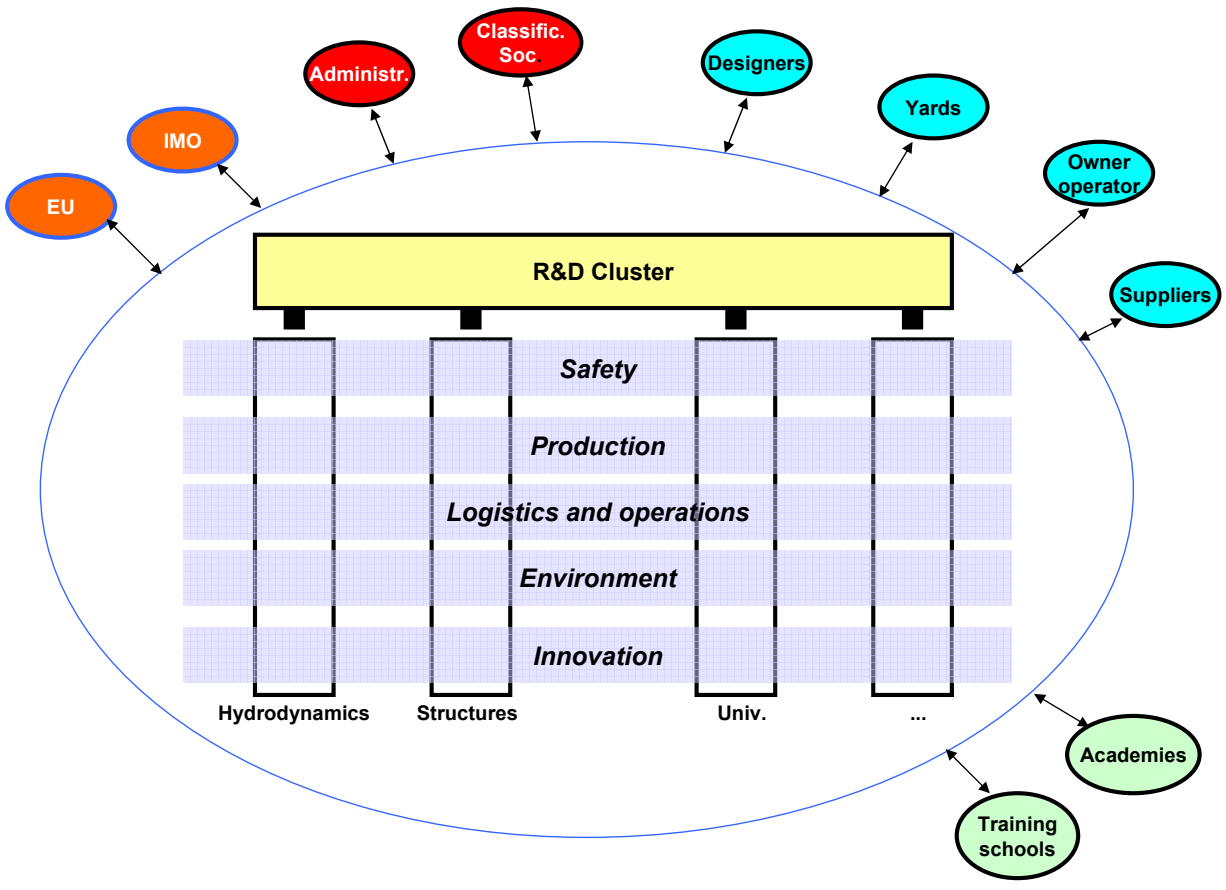

De Kat, Aug. 2001

- Safety = money

- Effective monitoring incentives

decentives

- Standards (IMO's, Class, ..) = minimum acceptable safety level
- Minumum standard operator: cost driven = decentives
- Higher standard operator: revenue driven = incentives

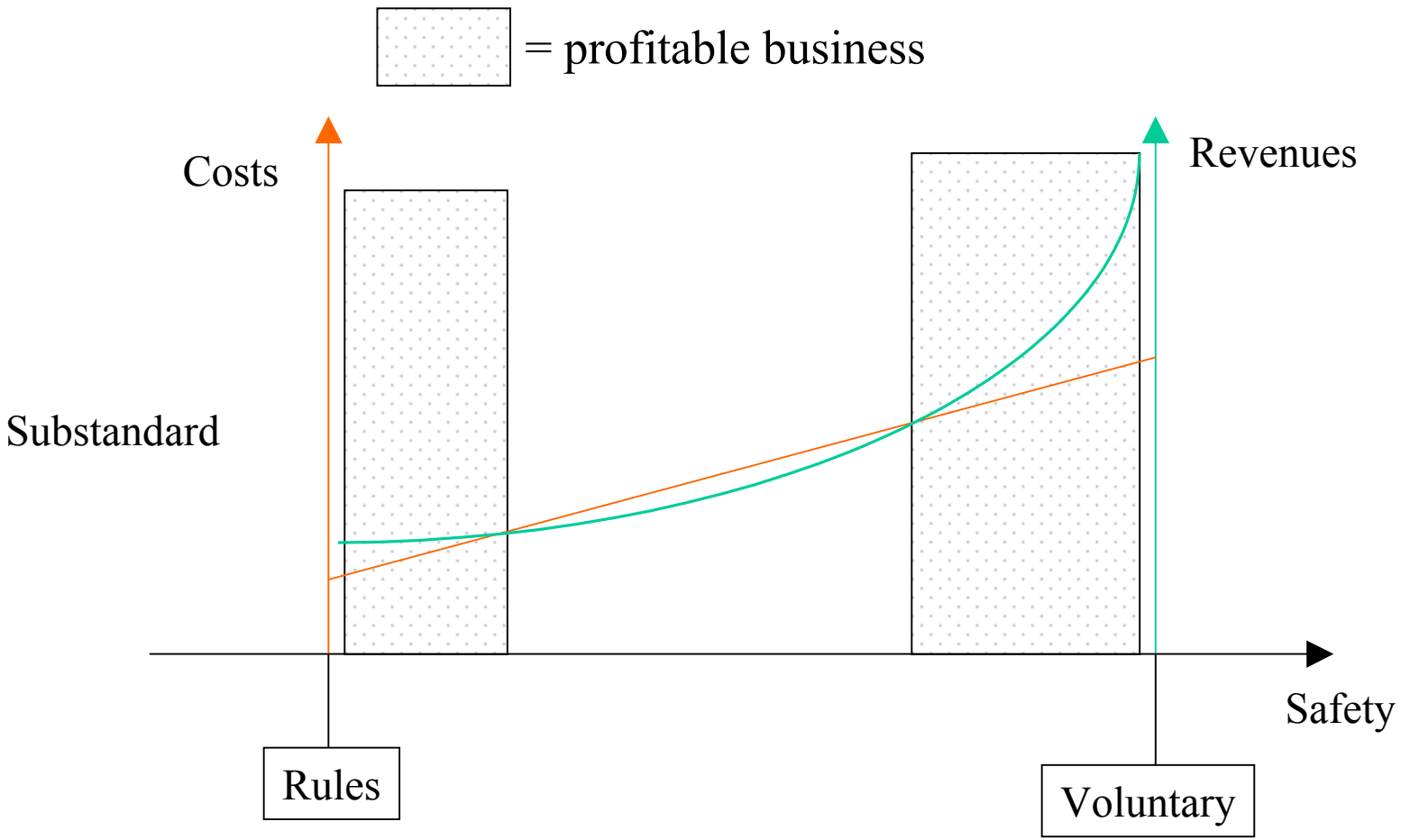
= profitable business
Costs
Revenues
Substandard
Safety
Rules
Voluntary

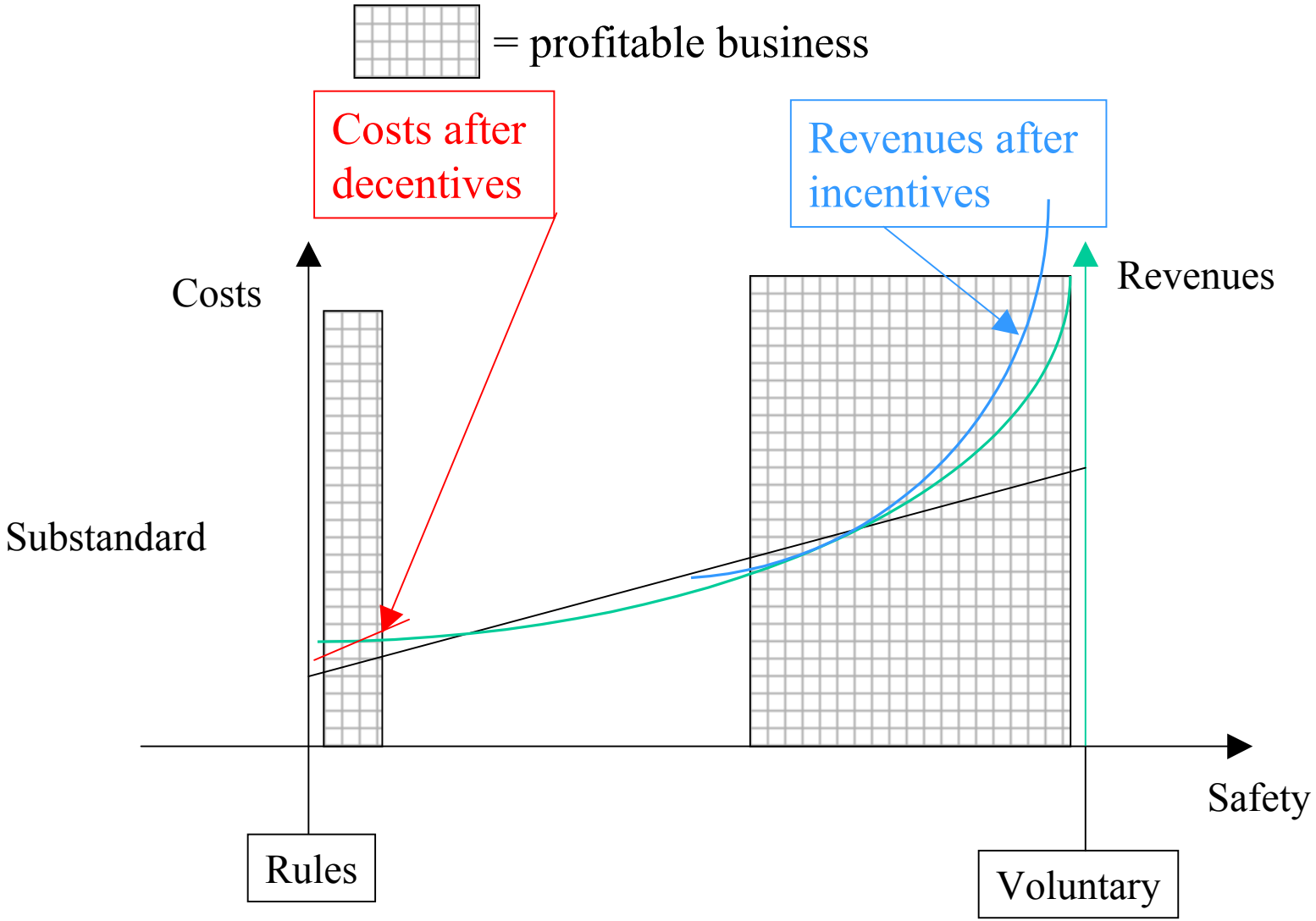
= profitable business
Costs after decentives
Revenues after incentives
Costs
Revenues
Substandard
Safety
Rules
Voluntary

How to meet this?

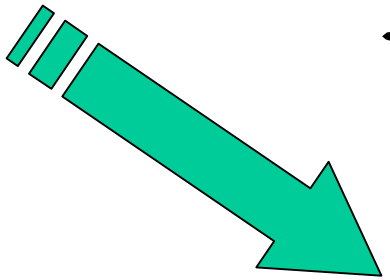

Parternship

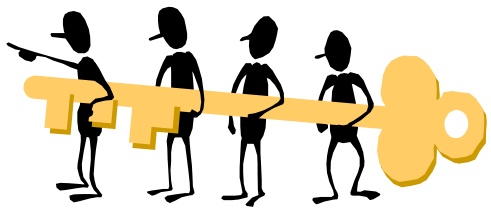

AGENDA

- Goals of safety concerned passenger ship company
- Influence externally on performance of company
- Safety and environmental factor
- Media focus
- Co-operation re safety
- Operators view regarding regulators/class
- Operators view regarding universities, consulting companies etc
- Future work

GOALS OF SAFETY CONCERNED PASSENGER SHIP COMPANY

- Leading operator within transport and short cruise segment
- High quality of:
  - Safety
  - Service
  - Environmental policy
  - Competitiveness
- Economy for growth
- Qualified operation of relevant tonnage
- Meet future requirements for high competence

INFLUENCE EXTERNAL FACTORS PEFORMANCE OF COMPANY

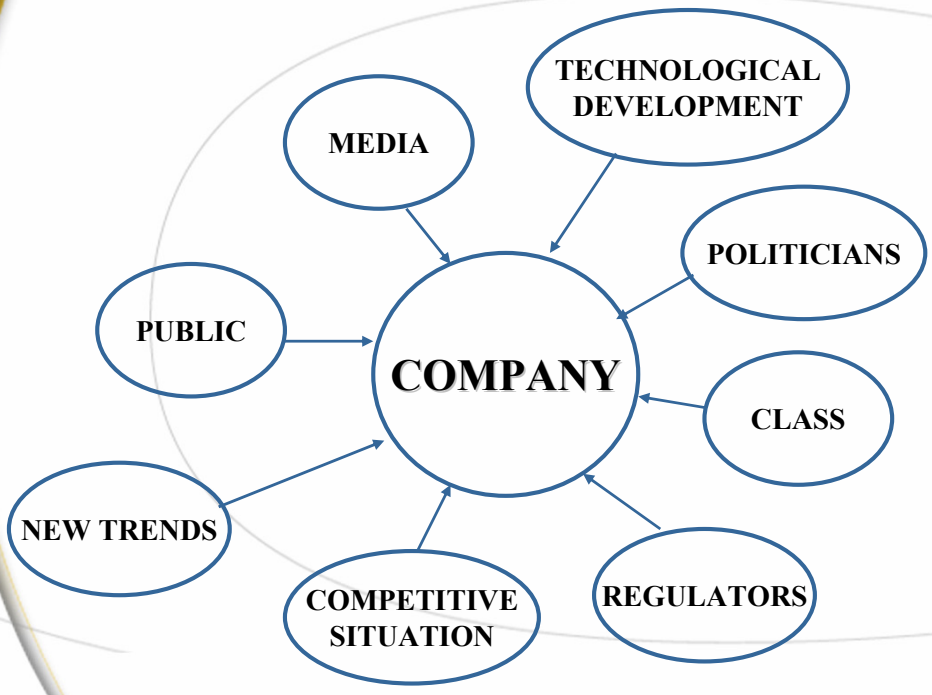

Color Line

SAFETY AND ENVIRONMENTAL FACTORS

- Safe, economic operation
- Control/secure authorities requirements for operation
- Meet challenges according to new rules
- Future environmental requirements
- Provide cluster of experts for technical/maritime operation
- Competitiveness with high safety and environmental profile

Color Line

MEDIA FOCUS

- Examples from large accidents
  - "Scandinavian Star"
  - "Estonia"
  - "Prinsesse Ragnhild"
- Proactive
- Open society, media
  easy access standard of operation
- Media create actions by politicians

CO-OPERATION RE SAFETY

- Important that operator is responsible for own operation
- Authorities/Class auditors re safety
- Importance co-operation all parties associated with safety:
  - Regulators
  - Research
  - Operators
  - Class
- Co-operation from day one
- Open co-operation also between operators ex NORDKOMPASS

OPERATORS VIEW

- View regulations should be channeled through IMO
- New regulations must be understood to be important
- Importance re co-operation regulators/-owners when discussing new rules
- New regulations should be based on safety assessment, not on accidents
- Important that regulators ensure influence operation friendly solutions
- Cost benefit factor, industry must survive

OPERATORS VIEW RE RESEARCH

- Closer contact operators/universities
- Importance useful research
- Operators must understand academic society - eliminate borders - vice versa
- Importance research projects participation different players
- Importance seminars establishing closer contact with parties

FUTURE WORK

- Rules through IMO
- If no success IMO, regional solutions
- Proactive safety rôle, large passenger ships
- Establish fora for co-operation
- Importance EU research projects
- Safety assessment

Color Line

Heavy Weather Guidance and Capsize Risk

Philip R. Alman, Naval Sea Systems Command, **Kevin A. McTaggart**, Defence Research Establishment Atlantic, **Peter V. Minnick**, USCG Engineering Logistics Center, **William L. Thomas III**, Carderock Division, Naval Surface Warfare Center

ABSTRACT

Recent advances in simulation of capsize in severe seas have opened the door to the application of risk assessment techniques to capsize survivability assessment, and seaway specific heavy weather guidance for the ship operator. Communication of risk of operation based on seaway severity, ship heading, speed, and loading is essential in providing useful heavy weather guidance to the operator. Members of the Cooperative Research Group, Navies, (CRNAV), and the Naval Stability Standards Working Group (NSSWG) have been developing risk methodologies and techniques to determine both the risk of capsize on an annual basis, as well as for seaway specific conditions. The authors will summarize the methodologies for risk assessment, involving both fitted statistical data and distribution free approaches, and their application to annual capsize risk statistics, and seaway specific operational risks. The development of capsize risk criteria is an essential link in providing heavy weather guidance and tactical shiphandling information for severe seaway operation

NOMENCLATURE

a_X	=	Gumbel distribution scale parameter
b_X	=	Gumbel distribution location parameter
C	=	ship capsize
$F(X)$	=	cumulative distribution function for X
Hs	=	significant wave height
KG	=	height of the center of gravity above the keel
N_C	=	number of ship capsizes
N_S	=	number of simulations
$P(C_D)$	=	probability of capsize in duration D
$p(X)$	=	disretized probability of X
$Q(X)$	=	exceedance probability for X
Tp	=	peak wave period
V	=	ship speed
X_i	=	random variable sample of rank i
β	=	relative wave heading
λ	=	wavelength
$\varphi_{max,D}$	=	max absolute roll angle in duration D

Head Seas are 000^o relative wave heading and seas on starboard beam are from 090^o.

INTRODUCTION

Design criteria and operator guidance for stability in heavy weather are typically treated as distinct and separate issues. In the past, stability criteria based on righting energy relationships have provided a measure for intact stability. This measure ensured a level of safety, but did not provide specific guidance for capsize avoidance in severe seaway conditions. After nearly 60 years we still don't have that "red light" that comes on indicating that the current combination of speed and heading is no longer safe and that evasive action must be taken to save the ship.

Several references can be found on shiphandling in heavy weather. These typically give general rules of thumb for avoidance of tropical storms, and provide generic guidance to the mariner in the event his ship gets caught in the storm. "Heavy Weather Guide" (Harding, 1965), "Summary of a Course in Shiphandling in Rough Weather" (USCG, 1981), "Knight's Modern Seamanship" (Noel, 1972), "IMO Assembly Resolution 1994, Guidance to the Master for Avoiding Dangerous Situations in Following and Quartering Seas", (IMO, 1994) are a few of the publications available for reference and training of deck officers. Interestingly, there is a

progressive trend towards more specific guidance on dangerous zones both in terms of storm avoidance and dangerous headings and speeds.

In recent years the maritime community has started to recognize that capsize sensitivity is related to ship dynamics and subject to several parameters including hull geometry, loading condition, size, heading, speed, and seaway (De Kat, Paulling, 1989). Capsize risk in extreme seas can be expected to vary considerably from ship to ship (IMO 1994). Thus, a ship handler must rely on his wits, experience, and judgement, in maintaining safe speed and heading under the most adverse conditions. Very little information exists today which can provide ship-specific operator guidance to avoid potentially hazardous zones of speed and heading in a severe seaway.

Practical experience in heavy weather shiphandling may be limited to some mariners, especially in the case of naval officers who might not be aboard a particular ship for more than a few years. The advent of weather routing has deliberately (and for good reason) reduced encounters with extreme weather. Thus, practical experience in heavy weather shiphandling may be limited.

The use of innovative features in ship hull designs can provide additional challenges for the ship operator because the dynamic characteristics can substantially differ from conventional ships in severe seaways (De Kat, et. al, 1994). Consequently, the need for ship specific operator guidance becomes even more crucial to ship safety.

Recent work in capsize simulation and probabilistic analysis has opened the door for the development of risk based operator guidance in heavy weather. The use of risk data if properly presented, can provide a powerful tool in communicating potential shiphandling hazards to the operator. Simulations and probabilistic analyses conducted in recent years have shown that some of the traditional storm avoidance guidance should be reevaluated since it can actually put a ship at hazard due to dynamic capsize (Alman et al., 1999).

A good example of this is the situation of hurricane avoidance. Traditionally, the guidance offered to a ship's master is based on determining whether the vessel is in the dangerous semicircle or navigable semicircle and placing the ship's head relative to the wind direction accordingly to depart the area. Shown in Figure 1 is the guidance for departing the dangerous semicircle of a tropical cyclone in the Northern Hemisphere. In this situation the advice would be to bring the wind on the starboard bow (45° relative) and make as much headway as possible in order to evade the storm. Unfortunately, this guidance places the waves on the starboard quarter (i.e.; the waves are coming from 160° relative assuming that the wind is placed at 045° relative). A ship underway at high speed may actually be placed in hazardous following or quartering seas and run the risk of capsizing. Based on present understanding of the physics of ship capsize behavior, placing a ship in following or quartering seas and making as much speed as possible in mountainous seas will likely place the ship in regions where capsizing becomes a distinct possibility.

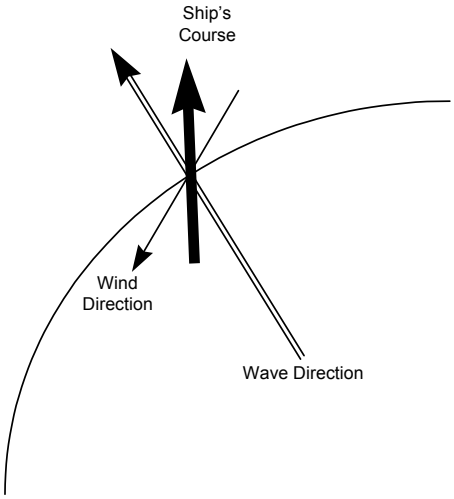

Figure 1. Traditionally recommended ship's course to depart the dangerous semicircle of a tropical cyclone (Northern Hemisphere).

Ships do get caught in storms despite best efforts to avoid them. Guidance given to the operator to avoid capsize must provide two things. The first is a display of the change in risk in a seaway as a function of heading and speed. Such guidance can be provided in capsize risk polar plots, as displayed in Figure 2. The polar plot depicts ship heading relative to the waves with head seas at the top of the plot and following seas at the bottom. Ship speed is depicted by concentric circles starting at the speed of zero knots in the center of the plot, increasing in 5-knot increments.

The second requirement, is for heavy weather maneuvering guidance that describes when it is safe (or unsafe) to execute a maneuver that could entail a risk of capsize. Frequently maneuvers must be undertaken in severe seas to change course and heading for reasons other than stability. Structural damage in head seas may force a ship to come about and run with the waves. Operational planning should also entail operator guidance for when to utilize weather routing for storm avoidance.

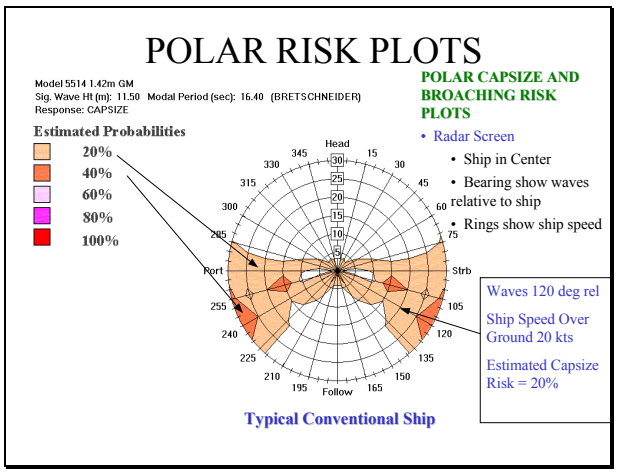

Figure 2. Capsize risk polar plot for a notional destroyer in Sea State 8

The Canadian Navy and the U.S. Navy have jointly pursued development of probabilistic capsize risk assessments for both design and operator guidance. The development of operator guidance for shiphandling in heavy weather can be linked to design criteria, providing continuity in a system safety approach to capsize risk mitigation. Capsize risk based operator guidance and weather routing criteria can provide vital information to the ship handler and operations planner, helping to break the "chain of events" leading to capsize and loss of a ship in heavy weather (Alman et al., 1999). The key to providing vital design and operator capsize risk guidance is in the evaluation of capsize probability using time domain simulations.

ASSESSING CAPSIZE PROBABILITY WITH TIME DOMAIN SIMULATIONS

In recent years, progress in numerical models and computing power has made it possible to evaluate capsize probability in random seaways using time domain simulation. The numerical model FREDYN (De Kat et al., 1994) has been developed by the Cooperative Research Navies Dynamic Stability Project for simulating ship capsize in both regular and random wave conditions.

Extensive validation with experiments (De Kat and Thomas, 1998) has shown that FREDYN gives good predictions of capsize for naval frigates. To enable useful application for ship design and operation, a method has been developed for predicting capsize probability of intact ships in long-crested, random seaways (McTaggart and De Kat, 2000).

Overview of probabilistic approach

The probability of ship capsize during duration D (e.g., one hour) is given by:

$$P(C_D) = \sum\sum\sum\sum\sum p(V)p(\beta)p(Hs,Tp)P(C_D \mid V,\beta,Hs,Tp) \quad (1)$$

where $p(X)$ is discretized probability of random variable X, V is ship speed, β is ship heading, Hs is significant wave height, Tp is peak wave period, and $P(C_D|V,\beta,Hs,Tp)$ is capsize probability given V, β, Hs, and Tp. Similarly, the exceedance probability for maximum roll angle can be evaluated as:

$$Q(\phi_{\max D}) = \sum\sum\sum\sum\sum p(V)p(\beta)p(Hs,Tp)Q(\phi_{\max D} \mid V,\beta,Hs,Tp) \quad (2)$$

where $Q(\varphi_{max,D}|V,\beta,Hs,Tp)$ is exceedance probability of maximum roll angle given V, β, Hs, and Tp.

Distribution statistics for maximum roll angle in given conditions

The occurrence of capsize for given conditions (i.e., ship speed, heading, significant wave height, and peak wave period), will depend on the realization of the randomly generated seaway. Ideally, the probability of capsize for given conditions could be determined by running a very large number of simulations and using the following equation:

$$P(C_D \mid V,\beta,Hs,Tp) = \frac{N_C}{N_S} \quad (3)$$

where N_C is the number of observed capsize in N_S simulations. The cumulative distribution function (CDF) of maximum roll angle for given conditions can be estimated in a similar manner. For brevity, the random variable X is introduced here, which could represent maximum roll angle for given conditions. Madsen et al. (1986) indicate that the estimated CDF values from N_S samples will be:

$$F(X_i) = \frac{i}{N_S + 1} \quad (4)$$

where i is the rank of sample X_i. When predicting roll exceedance probabilities, the main disadvantage of Equation 4 is that it cannot extrapolate beyond observed values. However, Equation 4 is useful because it provides an unbiased estimate and it requires no assumptions regarding the distribution of the variable X, and is thus referred to as a "distribution free" estimate.

Ongoing work (McTaggart, 2000) has indicated that capsize risk in given conditions can be efficiently estimated by modeling maximum roll angle using a Gumbel distribution as follows:

$$F(X) = \exp\left[-\exp\left(\frac{b_X - X}{a_X} \right) \right] \quad (5)$$

where a_X and b_X are scale and location parameters, with b_X being the 36.8'th percentile of X. The Gumbel parameters a_X and b_X can be determined using maximum roll angles obtained from a number of simulations (typically at least ten) in seaways of duration D. Experience predicting ship capsize risk indicates that it is preferable to determine a_X and b_X by minimizing the error in ln[-ln($F(X)$)] from simulated samples. Figure 3 shows an example of a Gumbel distribution fitted to maximum hourly roll angles simulated by FREDYN for a ship in stern quartering seas. The fitted Gumbel distribution provides good agreement with the observed values, particularly in the upper range of roll angles of greatest interest for ship capsize.

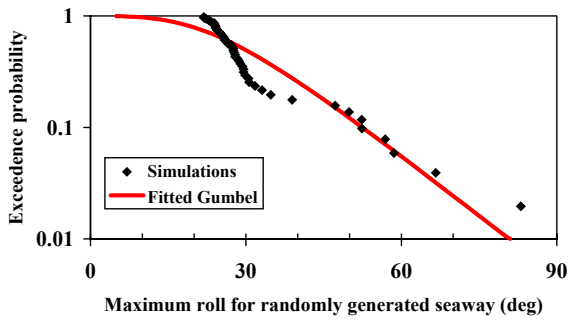

Figure 3. Maximum hourly roll angle, 10 knots, stern quartering seas (150°), *Tp* 12.4 s, *Hs* 9.5 m

In additional to the Gumbel distribution, the type II maximum and generalized extreme value distributions have been tried for modeling maximum roll exceedance probabilities in given conditions. The Gumbel distribution consistently gives more reliable predictions of capsize probability than the other distributions. When deciding between using fitted Gumbel distributions or distribution free estimates for predicting capsize probability, fitted Gumbel distributions have the advantage of permitting extrapolation beyond observed roll angles. Experience computing capsize probability based on fitted Gumbel distributions and distribution free estimates indicates that the two approaches provide very similar results (McTaggart, 1999).

The distribution free approach is especially suited to developing statistics for phenomena such as broaching, which cannot be easily described by a single parameter suited to modelling by a statistical distribution. It is likely that certain ships have roll responses that are not well suited to the Gumbel fit procedure described above; thus, the distribution free approach would be more appropriate for prediction of their capsize risk.

APPLICATION OF PROBABILISTIC METHODS

Probabilistic methods have a variety of applications for design and operation of safe ships. In the design phase, probabilistic methods can determine whether a ship has sufficient intact stability to minimize risk of capsize both in comparison to other ships, and in specific seaway conditions. Probabilistic methods can also be used to determine design feasibility by utilizing capsize probabilities as a measure of suitability. In addition, probabilistic methods can be used to develop relatively simple design guidelines that will ensure adequate intact stability. For example, a suitable range of positive stability (e.g., 90 degrees) for a certain vessel type could be determined by probabilistic methods

For the ship operator, probabilistic methods can indicate which combinations of speed and heading are dangerous for given environmental conditions. Such knowledge can be invaluable when making critical decisions in situations such as search and rescue operations. Capsize and broaching risk polar diagrams show promise as a tool for operational guidance. The resultant probabilities are plotted as isoclines on capsize-broaching polar diagrams, as shown in Figure 2.

Assumptions Regarding Ship Operations

Capsize risk assessments typically make idealized assumptions regarding the operation of a ship. For example, ship speed and heading are often assumed to be independent of seaway. When performing comparative studies between two ships, they are often assumed to have identical speed and heading profiles. These assumptions do not account for shiphandling tactics, machinery limitations, or operational restrictions that may be unique to a class of ships. All of these factors may drastically affect the final statistics. Currently, sufficient data do not exist to permit a more extensive consideration of machinery characteristics and shiphandling tactics in extreme seas. The Naval Stability Standards Working Group NSSWG, is currently considering how data on shiphandling tactics in extreme seas may be gathered and assessed.

Required number and duration of simulations

Of great practical importance is the required duration of simulations for predicting capsize risk for given conditions (i.e., ship speed, heading, significant wave height, and peak wave period). Several different seaway realizations must be simulated for given conditions. Experience has shown that somewhere between 10 and

50 simulations of 30 minute duration should be run to determine hourly capsize statistics. For the distribution free approach, a minimum of 25 realizations is typically used. Using the fitted Gumbel approach, 10 initial simulations can be run to estimate if capsize risk is non-negligible. The number of simulations can be increased (e.g., to 50) if capsize risk appears to be significant.

Computational experience

The use of time domain simulations in the probabilistic assessment of capsize risk is largely constrained by limits on computational speed. For example, the capsize risk polar plot displayed in Figure 2, required 4.5 days of run time to perform 4200 FREDYN simulations on a 933 MHz Pentium III desktop computer. Comprehensive risk assessments using multiple wave height and modal period combinations (see Equation 1) can be performed in approximately one month using between five and seven Pentium III computers. Efforts to continue the development of non-linear CFD codes to improve the precision of predictions are supported by the authors, however, the slowness of the CFD codes (slower than FREDYN by factors in excess of 700) have not yet made them practical in capsize risk assessments.

Climatology

Application of equations (1) and (2) requires the joint probability distribution of significant wave height and peak wave period in the form of a wave climate scattergram. Experience has shown that predicted capsize probability can be highly dependent upon wave climate. Initial capsize predictions based upon the electronic version of BMT Global Statistics for Area 15 gave unrealistically high capsize probabilities for naval frigates. Further investigation revealed that the wave climate scattergram had unrealistically large nominal wave steepnesses, defined by:

$$H \tilde{/} \lambda = \frac{Hs}{g /(2\pi)Tp^2} \qquad (7)$$

For comparison of different data sources, the following relationship for a Bretschneider spectrum relates peak wave period to zero-crossing wave period:

$$Tp = 1.408\, Tz \qquad (8)$$

Shown in Figure 4 is the maximum significant wave height versus peak wave period from three different sources. The Buckley (1994) data are based on wave buoy observations. For several wave periods, the data from BMT Global Wave Statistics (1986) Area 15 has significant wave heights much higher than those from Buckley do. The hindcast data of Bales (1984) give a limiting wave height envelope that is more consistent with Buckley. Computed capsize probabilities based on the hindcast wave data of Bales appear to give credible capsize probabilities for naval ships.

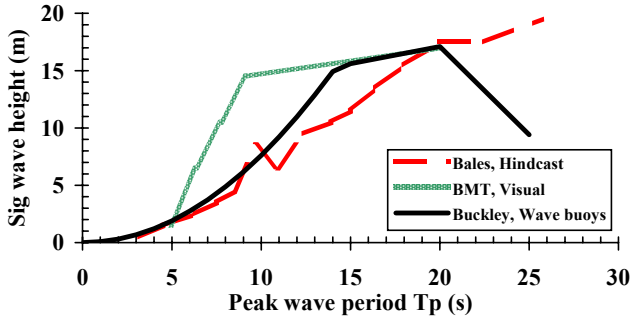

Figure 4. Maximum significant wave height versus peak wave period

McTaggart and De Kat (2000) and the discussion for their paper consider why BMT Global Wave Statistics gives unrealistic nominal wave steepnesses. The problem stems from extrapolation of wave height exceedance probabilities for given wave periods. In the printed version of Global Wave Statistics, the resolution of 0.001 in the wave scattergram data gives reasonable nominal wave steepnesses; however, the electronic version of Global Wave Statistics gives wave scattergrams to a resolution of one millionth, leading to extrapolation problems.

GUIDANCE TO OPERATORS DURING SEVERE CONDITIONS

Efforts to date have focused on understanding the process of capsize behavior and the effects of dynamic stability. Most recently (as presented earlier in the paper) the effort has been to explore the probability of capsize both in a over-the-ship-lifetime global approach and as an assessment of the probability of capsize within given conditions. These approaches will be very useful in the design of a new vessel or class of vessels as a means to compare the relative merits of competing designs in terms of their true heavy weather operability. However, global capsize probability by itself does little to assist the operators of an as-built vessel.

To provide useful guidance to a ship's officer operating in a severe seaway, the polar capsize risk plot (Figure 2) has emerged as a useful tool. A shaded portion of a polar plot is referred to as a capsize region, and indicates combinations of speed and heading where capsize risk is non-negligible. An assessment of capsize

behavior within the mapped capsize region offers additional useful information to the ship's officer, and can provide the basis for operator guidance on shiphandling in heavy weather. A first step was described by Alman et al. (1999) for safe operation in the vicinity of tropical cyclones. It was recognized that the traditional guidelines for course and speed to avoid an oncoming hurricane represent the fastest means to get out of the way of the storm. Hurricane avoidance action should be followed as soon as the danger is recognized and before sea conditions worsen. Unfortunately, it is not always possible to successfully avoid a hurricane, and the strategy must be changed from one of avoidance to survival. In such severe conditions, following and quartering seas can become a hazard to the vessel. To mitigate the risk of capsize, either the speed of the vessel should be reduced, the course of the vessel altered, or some combination of speed reduction and course change executed in order to keep the vessel out of its potential capsize regions. This ship-specific information could be computed for the vessel and made available to the master and ship officers in the form of polar plots presented in a heavy-weather stability guidance booklet or by other suitable means such as computer display.

Continuing with the hurricane avoidance scenario, the first choice of a modified course and speed should, if possible, continue to remove the ship from the storm area. However, if sea conditions continue to worsen, again potentially placing the vessel in an expanding capsize region, preparations should be made to weather the storm. Here the maneuvering and powering performance of the ship must be taken into account in developing effective guidance. Care must be taken on board the vessel such that the decision to alter course from hazardous quartering seas and come about in order to weather the seas on the bow is not made after the point at which the vessel becomes unable to complete its turn due to the state of the seas. Dynamic stability analysis using time-domain dynamic stability simulations can determine the limits of a vessel's turning and maneuvering capability.

Effective guidance therefor falls into three categories. These represent a triad for the ship/seaway system. Each is fundamentally important to minimize capsize risk.

1. Ship capsize behavior
2. Ship system capability and configuration
3. Real-time knowledge of seaway conditions

Guidance based on an understanding of ship capsize behavior

Efforts have been undertaken for a few ships and designs to quantify the probability of capsize within the capsize region. These efforts have served to identify the real risk involved for a design over-and-beyond a set of polar plots with just the capsize region indicated. Given a sea condition, one vessel may have a larger capsize region but with very little probability of capsize within the region. Another ship by contrast may have a distinctly small capsize region but is inherently unsafe for operation within the region. Capsize region mapping in this manner results in "isobars" of equivalent capsize probability within the capsize region.

A related approach would involve mapping the interior of the capsize region for the dynamic stability process (or processes from different seed numbers) that results in capsize. In order to develop effective operator guidance, the failure mechanism needs to be known. The mitigation strategy can then be developed to remove the ship from the capsize region, or from near proximity to the capsize region, without initiating a catastrophic dynamic stability response. It is hypothesized that severe ship dynamic response related to stability behavior within a sub-region of the overall capsize region will also be present to a reduced magnitude at headings and speeds just outside the capsize region. Mitigation strategies developed to combat a potential dynamic stability hazard would then be used on the ship in a manner similar to monitoring a ship's GM at sea by observation of its natural roll period. In this case, if the ship's roll constant is known and the ship's natural roll period is observed by using the rudder to induce roll in calm water, then an estimate of GM can be computed. A large increase in natural roll period at sea is thus an indication that GM may have been reduced and corrective action can be initiated.

The same approach can be adapted to dynamic stability guidance while at sea. Suppose through simulation in a given sea condition it is found that a vessel has a propensity to surfride severely, resulting in broaching and capsize at known headings and speeds within the capsize region. Then the mitigation strategy would probably involve a speed reduction rather than a course change because the course change could very possibly lead to further loss of control and broaching. However, if the vessel tends to capsize by loss of transverse stability after wave capture, but possesses good directional control, then a course change might be the safer mitigation strategy.

Naturally, while underway in heavy seas, efforts should be made to stay removed from the ship's known capsize region. But as the true wave steepness is not known with certainty, or the wave direction could change or the ship could be forced off course placing the ship into the capsize region, reliance on specific headings and speeds just outside the capsize region pose an increased level of risk. At these headings and speeds, specific ship

motions or response behaviors could serve as indicators of the potential hazard, and the appropriate mitigation strategy would dictate the shiphandling maneuver to employ.

Guidance based on an understanding of ship system capability and configuration

Ship specific guidance also has to take into account the performance capability of the ship. A generally safe heading in severe seas may become threatening if sea conditions worsen, thus necessitating a heavy seas shiphandling maneuver. Using an example of hurricane avoidance guidance, the "safe" heading in quartering seas may become unsafe, forcing the master to attempt to come about into the seas. However, there may not be sufficient power to execute the maneuver, and the longitudinal distribution of a large sail area may make the maneuver physically impossible.

The key issues to address in guidance for heavy seas shiphandling maneuvers are whether the vessel can complete the maneuver; whether the maneuver increases the risk to the vessel; and possibly, whether the new combination of heading and speed is actually less dangerous for the vessel.

Selection of the best heading and speed in terms of avoiding extreme capsize risk can be greatly impacted by secondary affects caused by wind drag on the exposed topside. Wind can play a critical role in determining whether a ship survives a maneuver, especially where a loss of power occurs. Figure 5 shows results from simulations conducted on a frigate type ship executing typhoon avoidance. When power to the ship is lost, capsize probability is very dependent on the wind direction relative to waves. This phenomenon is largely due to the heading that the ship assumes once it is dead in the water. The combination of wind direction relative to sea direction and the longitudinal position of the center of wind pressure can result in either a dead ship riding with the waves or broaching in the trough.

In order to develop appropriate, ship-specific guidance, an understanding of the ship's maneuvering and powering characteristics is needed. Sail area location may be an important factor for some ship configurations. In the case of windage, variance in loading condition may be more important to consider for naval auxiliaries than for naval combatants due to the relatively small changes in draft of the latter. Turning circle maneuvers can be executed using time-domain simulations with different power levels and rudder angles in different sea conditions to determine how the ship responds. Other scenarios can be developed that address hazardous circumstances arising from common ship system failures.

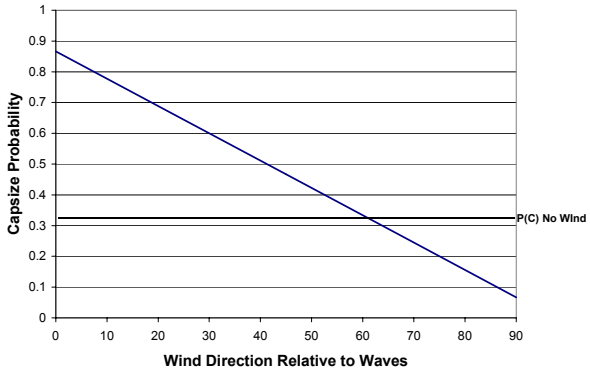

Figure 5. Power loss scenario: P(C) variation with wind direction in hurricane Camille

In order to determine the maneuvering characteristics of a ship in calm water, a set of standard scenarios including zigzags and turning circles has been employed. Maneuvering characteristics in heavy weather are also very ship specific; thus, a set of simulation scenarios for heavy weather can provide critical information concerning capsize risk avoidance which the master should be aware of when planning tactical maneuvers.

Guidance based on real-time measurement of sea conditions

"What is it doing out there?" seems a simple question, but even so requires a quick accurate answer. To date, little work has been done to develop onboard wave measurement systems beyond "Mark I eye ball". The loading condition of a ship can have a significant impact on capsize probability with changes in draft, trim and KG. Likewise, the seaway characteristics can directly impact capsize probability.

It is important that the operator have accurate measurements of significant wave height, modal period and wind speed for the seaway his ship is in. "Eye ball" estimates of wave height and period may not be accurate enough where the ship is sensitive to seaway tuning due to modal wave period and roll natural frequency. McTaggart and De Kat (2000) show that capsize probabilities can change greatly for seaways of the same significant wave height but varying modal periods.

Consequently, usable and accurate operator guidance will depend on availability of reliable environmental data in the immediate vicinity of the ship. Real-time onboard wave sensors are the best way to provide seaway data to the ship.

CONCLUSIONS

Simulation techniques coupled with risk assessment methodologies can provide significant information on capsize risk in severe seaways. Both the Gumbel distribution and distribution free techniques can be employed effectively in developing an awareness of the hazardous areas of ship operation in heavy seas. The fitted Gumbel distribution can be used for estimating roll exceedance probabilities for given conditions. The distribution free approach must be used for assessing phenomena such as broaching that are not easily modelled by statistical distributions. However, for at-sea shiphandling guidance, capsize risk polar diagrams are not enough to provide a complete picture when considering all factors in tactical decision making. A knowledge of the physical capsize mechanisms at play in a particular section of the capsize region will help to develop effective mitigation strategies. A series of scenarios involving ship system failures, wind, and standard maneuvers can be employed to judge the risk of carrying out shiphandling tactical maneuvers to ensure that the maneuver selected will actually lessen the risk to the ship and crew.

REFERENCES

Alman, P.R., Minnick, P.V., Sheinberg, R., Thomas, W. L. III, "Dynamic Capsize Vulnerability: Reducing the Hidden Operational Risk", SNAME Transactions, Society of Naval Architects and Marine Engineers, Vol. 107, New York, 1999.

Bales, S.L., "Development and Application of a Deep Water Hindcast Wave and Wind Climatology," *Royal Institute of Naval Architects Wave and Wind Climate World Wide Symposium,* 1984.

Buckley, W.H., "Stability Criteria: Development of a First Principles Methodology," *STAB '94, Fifth International Conference on Stability of Ships and Ocean Vehicles,* Vol. 3, Melbourne, Florida, 1994.

De Kat, J. O., R. Brouwer, K. A. McTaggart and W. L. Thomas, "Intact Ship Survivability in Extreme Waves: New Criteria from a Research and Navy Perspective", *Fifth International Conference on Stability of Ships and Ocean Vehicles, STAB '94* Conference, Melbourne, Florida, Nov. 1994.

De Kat, Jan O., and J. Randolph Paulling, "The Simulation of Ship Motions and Capsizing in Severe Seas", SNAME Transactions, Society of Naval Architects and Marine Engineers, New York, Vol. 97, 1989.

De Kat, Jan O., and W. L. Thomas III, "Extreme Rolling, Broaching, and Capsizing-Model Tests and Simulations of a Steered Ship in Waves", *Twenty-Second Symposium on Naval Hydrodynamics*, Washington, D.C., August 1998.

Global Wave Statistics, British Maritime Technology Limited, Unwin Brothers, London, 1986.

Harding, Edwin T., Captain, USN, and William J. Kotsch, Captain, USN, Heavy Weather Guide, United States Naval Institute, Annapolis, Maryland, 1965.

IMO, "Guidance to the Master for Avoiding Dangerous Situations in Following and Quartering Seas", 1994, Draft Assembly Resolution.

McTaggart, K. A., "Ship Capsize Risk in a Seaway Using Time Domain Simulations and Fitted Gumbel Distributions", *18th International Conference on Offshore Mechanics and Arctic Engineering-ONMAE99*, St. John's Newfoundland, July 1999.

McTaggart, K.A., "Ship Capsize Risk in a Seaway Using Fitted Distributions To Roll Maxima," Transactions of the ASME, Journal of Offshore Mechanics and Arctic Engineering, May 2000.

McTaggart, K., De Kat, J.O., "Capsize Risk of Intact Frigates in Irregular Seas", SNAME Transactions, Society of Naval Architects and Marine Engineers, 2000.

Madsen, H.O., S. Krenk, and N.C. Lind, Methods of Structural Safety, Prentice-Hall, Englewood Cliffs, New Jersey, 1986.

Noel, John V., Jr., Captain, USN, Knight's Modern Seamanship, 15th ed., revised by Noel, Van Nostrand Reihold Co., New York, 1972.

U.S. Coast Guard, "Summary of a Course in Shiphandling in Rough Weather", 1981.

MONITORING WAVE ENVIRONMENT AND SHIP RESPONSE

Koning, Jos, Trials & Monitoring Dept. Marin, Netherlands Wageningen. J.Koning@Marin.NL

SUMMARY

This papers covers the summer 2001 state of the art on the possibilities of environment monitoring and coupling of the measured data with ship response models. The operational relevance and use of monitoring systems is discussed. For this purpose the paper reviews the methods to model waves, focuses on wave sensors and describes methods to calculate ship response to waves.

NOMENCLATURE

ω	Circular frequency
ρ	Density of water
β	Wave direction relative to ships heading
ζ	Wave surface elevation

1. INTRODUCTION

All vessels and structures operating in the marine environment are subject to actions of waves, wind and current. Merchant shipping, yachting, dredging, fishery, and offshore, heavy transport and cable laying industries have a quit different approach to handle and deal with wave loads. Depending on the affected operational parameters, the attention is focused on various issues. Some of these are:

- Extreme motion and acceleration levels, crew discomfort, cargo damage, workability, operability.
- Relative wave motions, slamming, whipping and springing, side shell fatigue, wave bending moments.
- Green water structural- and cargo- damage.
- Ultimate stability issues, capsizing, parametric roll.
- Manoeuvrability.
- Mooring and structural dynamics.

Standing in the wheelhouse of a particular ship there is nothing much that can be done to the wave environment itself. It is however useful to be able to recognise particular effects in the sea state, before they are experienced in the response of the structure as mentioned above. Crews might be able to change the operational parameters of the vessel e.g. heading and speed in order to avoid damage before it occurs.

In this paper the outline of advisory systems will be discussed. For this the mathematical representation of a sea state will be described briefly. Also the behaviour of ships in waves will be discussed. Several types of sensors available for measuring the sea state parameters will be discussed and finally the state of the art in nowadays wave measurements and advisory systems will be summarized.

2. GENERAL OPERATIONAL SEEKEEPING GUIDANCE AND ASSISTANCE SYSTEM

The effects as mentioned in the introduction can be thought of as caused directly by waves or motions or by a combination of these. The first target of operational seakeeping advisory tools should be to provide information on the actual sea state in the direct vicinity of the vessel combined with the motion response and relative wave heights around the vessel. The latter with the ship sailing with arbitrary speed and relative wave headings.
With this information the likelihood of exceedance of specific operational limiting parameters can be derived using dedicated (software) models as shown in Figure 1.

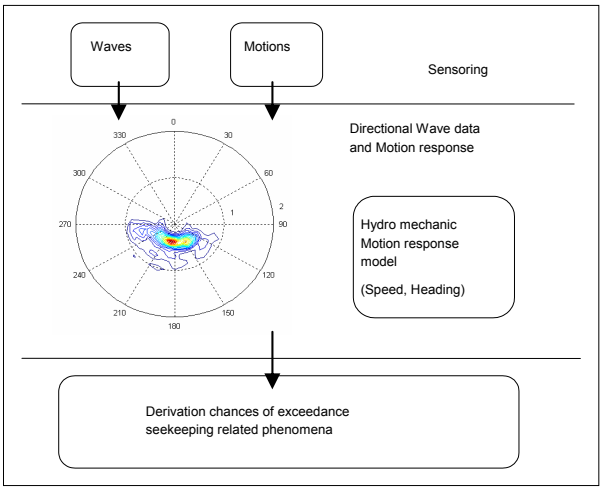

Figure 1. System outline

The scope of this paper is limited to the measurement of the wave data and the derivation of ship motions. The models required for the evaluation of the chances for exceeding specific operational envelopes are not discussed in detail.

3 THE WAVE ENVIRONMENT

How is a wave environment described? Looking at a sea surface one may be wondering at the apparent incomprehensible ever-changing behaviour of the waves.

In general most waves are wind driven. Depending on the wind condition and history the waves may be building, fully developed or decaying. Older waves systems coming in from other locations may have different characteristics from the locally building sea. Developing seas are usually short crested. Older swell components may have long regular crests. Obviously it is difficult to describe a sea state in detail. Following is a brief resume of the used models.

3.1 2D SEA SURFACE IN TIME

The sea comprises of travelling gravity waves coming from various directions. Wavelength and height, travelling speed and direction describe the characteristics for separate wave components. The water surface in a particular area and time window is defined by a number of wave components that passes by in that period. The combined effect of these passing waves will produce the actual sea surface.
In linear wave theory the behaviour of separate waves can be described in reasonable detail. The behaviour of a sea comprised of many waves can be described using a summation of many separate waves coming from various directions. For deep water and non-breaking waves the following describes a multi-directional sea state typically producing short crested waves.

$$\zeta(x,y,t) = \sum_{k=1}^{M}\sum_{j=1}^{N} A_{jk}\sin\left(\omega_j.t - k_j\left(x.\cos\left(\beta_{jk}\right) + y.\sin\left(\beta_{jk}\right)\right) + \varepsilon_{jk}\right)$$

where j indicates the number of wave components $(1-N)$

k_j *is the wavelength of the* j^{th} *wave component,*

and the index k indicates the var*ious wave directions* $(1-M)$

Each separate wave component has a circular frequency ω_j, wavelength k_j, direction β_{jk} and height A_{jk}.

3.2 WAVE SPECTRA

The coefficients A_{jk} may be written in the form of a so-called frequency spectrum as follows:

$$\tfrac{1}{2}A_{jk}^{\ 2} = S\left(\omega_j,\beta_k\right)\Delta\omega\Delta\beta$$

Where $S(\omega)$ is the wave spectrum or wave variance spectrum. It can be derived that the variance of the sea surface at a particular location behaves as:

$$\sigma^2 = \sum_{j=1}^{N}\sum_{k=1}^{M} A_{jk}^2/2 = \int_{\omega=0}^{\infty}\int_{\beta=0}^{2\pi} S(\omega,\beta)\,d\omega\,d\beta$$

If for a particular sea state the directional wave spectrum is known then a statistically representative sea surface can be calculated. If the phase angles of the separate wave components are known as well then also the actual sea surface can be calculated.

The so-called full directional wave spectrum is therefore a very powerful tool to represent a particular sea state. It is however not easily measured. What can be easily measured is the non-directional or Point Spectrum. This is the Variance spectrum of the wave elevation at one single X, Y position.

This spectrum is usually represented as S (ω) and follows

$$\zeta(t) = \sum_{j=1}^{N} A_j\sin\left(\omega_j.t + \varepsilon_j\right)$$

$$\tfrac{1}{2}A_j^{\ 2} = S\left(\omega_j\right)\Delta\omega$$

This spectrum can be easily estimated from measurements by interpretation of a measured time series of vertical wave displacements.

Short crested waves cannot be described using the one-dimensional spectrum. In order to account for this the wave spreading principle was introduced. It is assumed that the combined wave energy from a point spectrum is distributed around a principal direction. Spreading has a bandwidth that is described by the spreading function. An example is as indicated in:

$$S\left(\omega_j,\beta_k\right) = S\left(\omega_j\right)f(\theta)$$

where:

$$f(\theta) = \tfrac{2}{\pi}\cos^2(\theta),\quad -\pi/2 < \theta < \pi/2,\quad \theta = \beta_k - \beta_{mean}$$

$$f(\theta) = 0,\quad elsewhere$$

A synthesised full directional spectrum can be derived from a single point spectrum using a mean direction and (standard) spreading function. This easily derived directional spectrum has been widely adopted in wave measurements recently.

3.3 STATISTICS AND SPECTRAL MOMENTS

Apart from the spatial and the spectral representation, the behaviour of the wave surface can also be described in a statistical manner. The sea surface has a mean level with a particular variance, dominant wave direction and period as mentioned earlier. Ship crews observing wave environments describe the sea state in terms of significant wave height, wave period and direction. If older wave systems are also present a subdivision in a wind sea and a swell component is made. For each of these a significant wave height, a period and a wave direction is usually logged. It is found that particular relations exist between the visually observed data, statistical information and wave spectra. First the concept of spectral moments is introduced.

$$m_k = \int_0^{\infty}\omega^k\ S(\omega)\,d\omega$$

For k=0 this indicates the variance m_o. Then m_1 and m_2 are referred to as the first and the second spectral moment.

It is found that the estimates of the significant wave height correspond to the average of the highest 1/3 of the

measured waves. Usually the significant wave height is written as $H_{1/3}$. The period corresponds to the mean zero upward crossing period T_{mzup}. Following expressions link these observed values to spectral parameters.

$$H13 = 4\,\sigma = 4\sqrt{m_0}$$
$$T_{mzup} = 2\pi\sqrt{m_0 / m_2}$$

Using these expressions the estimates for the spectral parameters m_o, m_1, and m_2 can thus be retrieved from visual observations. A frequency point spectrum can be now be derived using the spectral moments and application of a standard sea state spectrum description, for instance PM, Jonswap or ITTC formulations.

3.4 EFFECT OF FORWARD SPEED

A ship sailing in a wave field at particular speed V encounters the waves at different frequencies depending on speed and relative direction to the waves. The shape of the wave and its geometric effect on the vessel do not change at varying speeds. It is only the frequency that changes. In the frequency domain using wave spectra this transformation can be done relatively straightforward.

The transformation of the wave frequencies to encounter frequencies is governed by the wavelength, propagation speed, the relative wave direction and the ship speed. Water depth affects greatly the wave propagation speed. For this discussion we limit the scope to deep water (in general greater than 300 meter). For deep water the relation between encounter and global wave frequency is:

$$\omega_e = \omega\left(1 - \frac{\omega V \cos(\alpha)}{g}\right)$$

With this transformation the spectral densities S (ω) can be mapped to corresponding S (ω_e). As the variance for the encounter sea state and the global sea state should be the same it follows that besides the scaling of the frequency axis also the spectral density itself must change. This is illustrated as follows:

$$S(\omega_e)\,d\omega_e = S(\omega)\,d\omega$$
$$S(\omega_e) = S(\omega)\frac{d\omega}{d\omega_e}$$
$$\frac{d\omega}{d\omega_e} = 1 \Big/ \frac{d\omega_e}{d\omega}$$
$$\frac{d\omega_e}{d\omega} = 1 - \frac{2\omega V \cos(\alpha)}{g}$$

The derivative dw/dw_e is not analytically continuous because of the zero point in dw_e/dw. When using discretized wave spectra the contributions for discrete frequency bands can however consequently be mapped from frequency band to frequency band without problems.

The transformation also applies for each frequency band in the directional wave spectrum. The full 2D spectrum may be transformed to an encounter spectrum. The wave encounter spectrum may be used to generate a wave surface as it is "felt" by the vessel.
Higher wave frequencies (short wavelengths) will result in negative encounter frequencies indicating that the ship is overtaking the waves. Their apparent frequency is $|\omega_e|$.
When the direction and length of the wave components is unknown the transformation from encounter to earth fixed frequency is not unique as indicated in Figure 2 for following or stern quartering waves. The figure illustrates that three different wave components have the same encounter frequency of 0.1 rad/s.

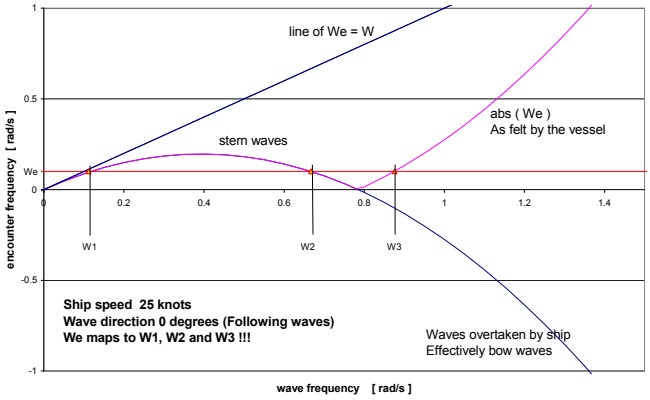

Figure 2 . Wave freq - Encounter wave freq

This ambiguity in the wave encounter frequency makes it difficult to do numerical wave calculations in the ω_e domain. In fact it is not possible to scale a point spectrum in ω_e back to the ω domain without information on the direction of the corresponding wave component. An assumption for the wave direction and wave length is required to make this transformation possible.

3.5 SUMMARIZING WAVE PARAMETERS.

The description of the wave surface has been briefly discussed from detailed back to few parameters. Summarizing, a sea state may be described as:

- A sum of an old wave system called swell and a wind driven newer system called wind sea.
- Each of these components has a significant wave height, mean zero upward crossing period and direction and spreading.
- A wave point variance spectrum can be derived from the $H_{1/3}$ and T_z or be calculated from a measured time series of wave elevations.
- Using the mean direction and spreading the point spectrum can be converted into a full 2D directional

wave spectrum. This spectrum may also be derived from measurements if the direction of separate wave components can be determined.

- A vessel with forward speed perceives the actual sea state through changing encounter frequencies. The variance in the sea state does not.
- The transformation from the global or earth fixed sea state description to the ship encounter frequency is possible. The transformation from ship encounter back to the global system of coordinates is difficult.
- The full 2D wave spectrum can be transformed into a representative 2 dimensional wave surface. If the phase angles of the wave components are also known then the actual sea state surface may be reproduced as indicated by:

$$\zeta(x,y,t) = \sum_{k=1}^{M}\sum_{j=1}^{N}\sqrt{2\,S(\omega_j,\beta_k)\Delta\omega\Delta\beta} \quad * \quad \cdots$$
$$\cdots \quad \sin\left(\omega_j t - k_j\left(x.\cos(\beta_k) + y.\sin(\beta_k)\right) + \varepsilon_{jk}\right)$$

This completely describes the wave surface both in time and space. In theory the actual surface could be predicted even into the future. The problems and inaccuracies that make that difficult are the deep water condition and the linear theory. In shallow water the bottom geometry usually makes the water depth a significant function of the x,y position. The different propagation speed and wave profiles disturb the linear summation criteria. The linearity assumptions fail in higher wave conditions. The energy dissipation due to breaking waves is not covered. Extreme waves can thus not accurately be represented.

4 WAVE SENSORS

A wave sensor for operational purposes implies that the results are directly available for interpretation on board. In the above the various means to describe a sea state have been covered. What equipment does exist to measure either earth or encounter frequent information for the parameters describing the sea surface? That is:

- 2D wave surface outline ζ (t, x,y)
- 1D wave elevation history ζ (t)
- Variance spectra (S (ω,β) and S (ω))
- Peak and valley distributions (H13 & Tz)

Shipborne possibilities for obtaining wave information can be categorized as follows:

- visual estimates
- of the bow down looking level gauges
- submerged pressure gauges in bow & side plating
- reverse engineering using ship motions
- radar back scatter directional systems
- coherent radar directional radar systems
- now- and forecasts based on :
  - fixed platform level gauge(s)
  - (directional) wave rider buoys
  - seabed ADCP
  - sea roughness (SAR)
  - Doppler shift systems.

4.1 VISUAL

Visual observations from crews provide information on swell and wind sea contributions. For these the significant wave height, zero upward crossing period and dominant direction are given. It is found that the results from various crews depend on the experience and ship size. Crews on larger ships appear to provide lower wave estimates than on smaller vessels. Ship motions may play a major part in this. During night-time no visual observations are possible. This illustrates the value of instrumented wave measurements for night-time operation.

4.2 RELATIVE WAVE HEIGHT

A number of sensors work based on the measurement of relative wave height around the ship. Examples of these sensors are: vertical radar level gauge, acoustic level gauge and pressure gauges measuring pressure or local water column height.

In the value of a relative wave height the following parameters are included:

- Undisturbed wave profile
- Sensor displacement (1st order ship motions)
- Diffraction wave profile by ship motions
- Refracted wave effects (“upwind effect”)
- Wave shielding effects (“downwind”)

It is clear that a relative wave height sensor requires corrections. The effect of vertical sensor displacement is easily corrected by measuring local displacement. The wave disturbance due to the vessel is however highly sensitive for direction. The sensor does not measure information on the wave direction. The effect can thus not be accounted for automatically. Commercial relative wave height sensors usually assume undisturbed waves.

The sensors are usually placed at the bow in the centreline. Pressure gauges are highly influenced by local dynamic pressure effects. Diffraction pressures, wave refraction, intermittent submerging of the sensor and slams make it difficult to get sensible data from pressure gauges.
The often applied over the bow down-looking surface radar is highly influenced by the local wave pattern induced by the vessel. Following waves are shielded, Bow waves are refracted, ship motions cause diffraction waves etc. Acoustic systems are in addition to this much influenced by presence of spray in the measurement area.
In general measurements taken from the sea surface in the close vicinity of the ship are too affected by the

presence of the ship to allow reliable wave observations under all conditions (e.g. relative headings). For slender ships the accuracy is best particularly in bow waves. More blunt bow shapes introduce large errors in the results due to wave refraction and dynamic swell up.

4.3 RADAR BACK SCATTER SYSTEMS

Radar backscatter systems are based on the radar reflections coming from wind ripples on wave crests. Depending on wave height and wind strength, wave crests show up in received X-band radar data. In the radar plots the wave crests show up allowing the distinction of wavelengths and "crest intensity". Using 2D and 3D Fourier algorithms the wave surface can be derived when assuming a relation between the intensity of the reflection and the wave height. The result is a full 2D directional sea state description in terms of wave -lengths, -speeds and -heights per direction. By using the dispersion relation the wavelengths can be transformed to the frequency domain and be put into wave variance spectra as earlier described. This approach promises complete wave data providing all information required to model the sea state. In fact it should be possible to obtain all required data to predict the behaviour of the sea in the direction of the wave propagation in the close future.

The problem with the backscatter technology lies in the reliability of the scaling function from reflection intensity to wave height. In lack of wind speed there are no reflections so no wave crests are shown. In high seas the effects of shadowing of waves and the fact that the sea is already at maximum roughness may be problematic. Validations are still in progress. The produced results are increasingly accurate from various providers. Two comparisons between off the bow radar and a X-band radar based system are shown in Figure 3.

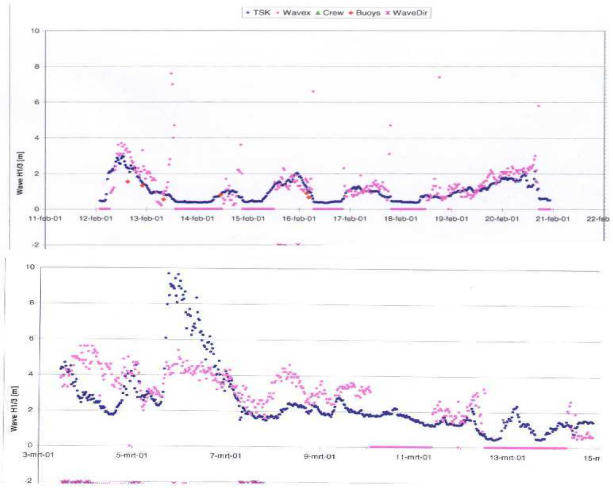

Figure 3. Long term comparisons of vertical relative wave height. Radar and directional wave radar results. Above good registration, below poor correlation.

The lighter dots referring to measurements by a Marine Radar based system, the darker taken from of the bow vertical wave radar. The systems were installed on a 24 knots container vessel.

4.4 COHERENT DIRECTIONAL WAVE RADAR

Coherent directional wave radars (CORA) are based on the fact that is it possible to derive the speed of the wave surface from the received radar reflection. The wave surface speed is related directly to the orbital motions. The orbital motions are related to the wave height and length. As such it is possible to derive the actual wave height distribution from coherent radar measurements. Operational systems have not been widely adopted yet on sailing ships as to the author's awareness.

4.5 REVERSED ENGINEERING

Reversed engineering comprises the derivation of undisturbed wave information from a combination of the measured ship motions with calculated motion and relative wave height RAOs.

The simplest approach is to directly derive the undisturbed encounter spectrum from the measured ship motions using numerically calculated RAOs. This is relatively straightforward but depends on the ship size and its sensitivity to the actual waves. I.e. it is not possible to derive wave estimates from the motions of a non-moving vessel. For smaller vessels this approach has proved to be working. In general the wavelengths should be in excess of 2/3 the ship length to induce significant motions.

A related approach is to derive the wave environment by interpreting the wave distributions around the vessel on all sides. (MARIN DPJIP 2001). By using the measured ship motions and the effect of the diffraction waves the measured wave data can be compared with calculations. By performing a best fitting selection of the calculated wave with measurements, the wave energy and direction can be estimated.

The latest and perhaps most feasible approach is to use wave directional information from e.g. directional wave radar systems and calculate normalized motions responses using RAOs. By comparison of the calculated motions with the measured motions the wave energy can be estimated. The combination of wave energy and wave directional spectrum provides a full complete wave description.

4.6 REMOTE WAVE MEASUREMENTS

There are various sources of information that can be used to obtain remote wave data on board. These vary from networks of moored wave rider buoys to now-, fore- and hind-cast data and satellite observations. Fixed buoys information is usually accurate. The buoy grid is however restricted to just few areas in the coastal

regions. The same goes for under water ADCP set-ups and fixed platform wave radar.
Satellite observations based on Doppler shift and SAR technology have a much wider coverage across the world. They are increasing their accuracy for wave height and direction estimations. The update rate at any particular position is however rather low. Satellites pass each grid position of 1.5x1.5 degrees about once every day.
Regular ships weather forecast and now cast information is usually based on models that are fed with observations from vessels sailing offshore. Due to the accuracy in the input data the provided results are usually indicative at best. No short term or local effects are included.

5 SHIP MOTION RESPONSE IN WAVES

Ship responses to the wave environment vary from:

- Added resistance, speed reduction, fuel consumption
- Structural loads caused by waves. E.g. slamming, green water, general wave bending and torsion, side shell fatigue.
- High motion and acceleration levels due to direct (linear) wave response.
- Induced motions caused by non linear wave response

If the wave environment is known or described then what other basic information is needed to allow an operational approach to the mentioned topics?

The induced ship motions in the encountered wave field play a major role in all mentioned issues. Added resistance is partly caused by the energy that is lost into the generated waves. The chances of occurrence for high peak loads can be numerically estimated when a reliable model is available calculating ship motions and local relative wave heights and relative wave speeds. Induced linear and non linear motions can be directly used to calculate the motion and acceleration levels at any point on the (rigid body) ship.

For a sound operational application of measured wave data it is therefor required to have an online model to predict and evaluate effected ship motion response. The comparison of the actual ship motion state with the limiting criteria will be done using the measured wave data, the measured ship motions and the predicted ship motions and relative wave heights.
Specialized software modules can use the wave data and the ship motions to derive information and chances of exceedance for particular events related to cargo loss, slamming etc.
Effects of other headings and speed settings on the criteria can be calculated using linear and non linear RAOs. The results may be used to show the crew operational safe envelopes in terms of speed and heading in the actual wave conditions.

5.1 WAVE INDUCED LINEAR SHIP MOTIONS

In linear theory it is assumed that a wave with a circular frequency w and coming from a particular direction, will cause a motion effect that acts in that same direction. Bow waves will cause pitch, beam seas roll etc. A twice as big a wave will cause a two times bigger motion response.

The relations between the incoming waves and effected ship motions but also between local relative wave height and motions can be expressed in so-called RAOs or Response Amplitude Operators. H(ω,β).

$$S_{xx}(\omega_{ej}) = \sum_{k=1}^{M} H^2(\omega_{ej}, \beta_k) S_{\zeta\zeta}(\omega_{ej}, \beta_k)$$

where H is a complex function in order to obtain the phase relations in the summation

The RAOs can be derived using diffraction or strip theory software. The results of these calculations can be transformed to the encounter frequency domain for direct operational application on board in the encountered waves for each ω_j. By summation of the contributions of waves with various frequencys coming from various directions the total motions response may be calculated.

5.2 NON LINEAR EFFECTS

Non linear motions and effects refer to the phenomena that are more difficult to describe than was mentioned earlier. In general for instance when a twice as big an excitation results in a three times higher response or even when without obvious loads high outputs are found. Examples are:

- Sagging/Hogging effect
- Bow flare immersion
- Bow emergence (slamming / whipping)
- Green water
- Parametric rolling

The earlier described linear theory can not predict the effects directly. For implicit calculations nonlinear approach and often time domain calculations will be required. For operational guidance and assistance systems this is still out of scope. What can be done however is to recognize the conditions under which particular non linear phenomena come into significant effect. This either by interpreting the measured wave environment, the calculated- or measured- motions or by a combination of these.

As an example the nonlinear Parametric roll response is mentioned here. Parametric roll is a phenomenon that occurs in conditions where under head or stern waves a vessel starts to roll without sideways excitation. Roll angles over 20 degrees plus minus have been reported. The roll motion may build up under particular conditions

quite rapidly and may seriously hazard stability, structural integrity of ship and cargo and crew safety.

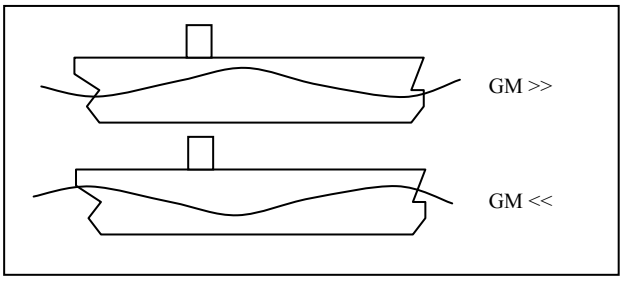

Figure 4. Effect of waves on moment of stability

Parametric roll is rooted in the fact that little excitation is required to excite a ship in its natural period roll motion. The excitation in the parametric roll case comes not from direct wave excitation but from amplification of initial roll motions by changes of the restoring moment of stability in the Roll natural period. A wave with wavelength close to equal the ships length coming from astern or forward will pass the ship with encounter frequency ω_e depending on the ship speed. Because of the outline of the waterplane area, when the midship section is on a wave crest, the moment of stability is higher then when the midship section is on a wave through. Figure 4. If the motion phase and the wave encounter phase angles vary 90 degrees than the variations in righting moment may be interpreted as a negative damping term. Figure 5. This will cause resonance when the transferred energy is higher than the dissipation by the regular roll damping. Roll motions will increase until the roll damping equals the negative excitation damping.

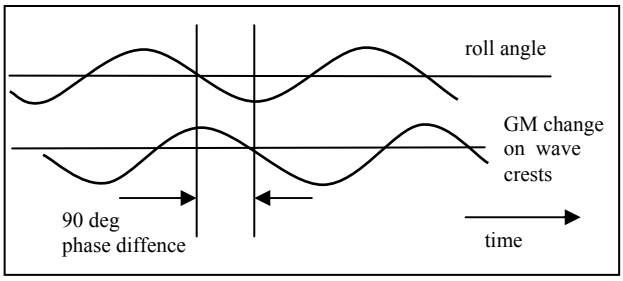

Figure 5. negative damping by varying GM

The criteria for occurrence of this effect lie therefor in the combination of:

- a wave length around the ships length with
- encounter frequency close or equal to the roll resonance period.
- significant induced variations of the GM due to the changes of the waterplane area when passing the wave profile.

The likelihood of occurrence for this condition can be evaluated by a dedicated software module from a full directional wave spectrum plus the ship speed and heading and a calculated GM response to waves.

6 STATE OF THE ART.

Having discussed the various wave representation techniques, sensor types and approaches to model ship response in the waves, we come to the current state of the are and the direction that developments will take in the coming time.

The most accepted technology for on board wave measurements is at this time still in off the bow relative wave height measurements. These provide the most cost – effective off the shelf instrumentation. The instrumentation can be done very rapidly and straightforward. No extensive calibrations are required. Problems are encountered in following waves and when blunt bow shapes are used. No directional information can yet be achieved from the systems.
The state of the art and in the very near future the equipment of choice will be based on radar back scatter systems. Combination of wavelengths and directions from the radar image with wave energy estimates from vertical wave height and ship response will provide accurate and complete wave information allowing statistical description of the wave climate in the close vicinity.

The acquisition and evaluation of the wave information from the radar images takes typically 2 minutes. The process is aimed at the statistic representation of the sea state so no separate wave component phase information is retained. The availability of fast computing systems, dsp's and algorithms will eventually allow the online calculation of the wave data. This will allow the real time decomposition of the sea surface in its separate wave components and allow prediction of the wave surface in the future in the path of the sailing ship.

It is likely that in few years it will be possible to predict the incoming wave train that a vessel will encounter in the coming minute(s). This will make it possible to allow guidance and assistance in avoiding extreme waves, assistance in extreme motion related manoeuvres, helicopter operations, station keeping, optimal dynamic positioning / tracking etc. These real time wave surface systems require faster acquisition and computation models than currently available. The use for ship crews is yet unclear because little time will remain between the recognition of a threatening condition and its moment of occurrence.
Perhaps in that area lies yet the biggest challenge: With the technology is about to be there, how to present the available information to the crew in an comprehensible way such that it is used and adopted.

ACKNOWLEDGEMENTS

Experiences mentioned and used in this paper were part of the work conducted in following MARIN projects: CRS FSM (3.12.872), CRS Probs (3.12777), Most (13.286), CRS Smacs (13.934), FPSO integrity JIP (13.777), Owase JIP (14.513) and DP JIP (17032). All of these projects comprised full-scale measurements of on line wave information from ship borne wave measurement equipment. The projects were either focusing on the acquisition of wave data directly or on the operational use of the wave data for purpose of sustained speed and added resistance, long term wave environment for fatigue and hull bending moments etc.

REFERENCES

C. Guedes Soares & PC. Viana, Sensitivity of marine structures to wave climatology. Computer modelling in Ocean Engineering. Schrefler & Zienkiewics, 1988, Balkema, Rotterdam. ISBN 90 6191 8367.

C Guedes Soares and M.F.S. Trovao. Influence of wave climate modelling on the long term prediction of wave induced responses of ship structures., Dynamics of Marine vehicles and structures in waves, Elsevier Science publishers 1991.

O.M. Faltinsen. Sea loads on ships and offshore structures. Cambridge Ocean Technology series, Cambridge university press 1990.

PRACTICAL EXPERIENCE AND OPERATIONAL REQUIREMENTS FOR ON-BOARD RISK MANAGEMENT UNDER MARGINAL STABILITY CONDITIONS

Eric. J. Shaw, Ph.D.
Commander, U.S. Coast Guard
Cutter Command and Operations School
Leadership Development Center
U.S. Coast Guard Academy New London, CT 06320

(860) 701-6675
eshaw@cga.uscg.mil

SUMMARY

This paper focuses on the second part of the workshop title, the operational safety of ships. Using experience gained from three tours aboard a U.S. Coast Guard 270-foot medium endurance cutter, including a tour as commanding officer, the author investigates their employment. This ship class shares many of their operational handling characteristics of other corvette-sized ships. While one of the most stable platforms from a damage control perspective, the 270-foot cutters are described by Jane's Fighting Ships as "Very lively in heavy seas because the length to beam ratio is unusually small for ships required to operate in Atlantic conditions." A fairly shallow draft also contributes to this "liveliness." This behavior extends into lower sea states where ships of this tonnage should be expected to operate effectively, creating shiphandling challenges for operators.

These challenges can be mitigated by inherent and ancillary design considerations. When the design process requires ships with high beam width and low length along the waterline, efforts must be made to increase not only static stability but also those stability factors that contribute to evolutions conducted in dynamic realms. Configuration of boat decks and flight decks can be designed for reduced crew and equipment motion, exposure to the elements and the dangers they present. Operators must understand remaining limitations and the operational envelope these limitations dictate.

NOMENCLATURE

C4ISR	Command, Control, Communications, Computers, Intelligence, Surveillance, Reconnaissance
CI/BI	Capsize and Broach Indices
CPB	Coastal Patrol Boat
DC	Damage Control
DDS	Design Data Sheet
HEC	High Endurance Cutter
HIFR	Helicopter In Flight Refueling
MEC	Medium Endurance Cutter
MIF	Motion Induced Fatigue
PQS	Personnel Qualifications Procedures
RHIB	Rigid Hull Inflatable Boat
VERT-REP	Vertical Replenishment

1. INTRODUCTION

Ship operators applaud recent calls for greater communication and cooperation between ship designers and operators. Recognition of the need for close alignment between the two communities during all phases of ship design and service life promises greater ship utility and safer operation. Designers can provide ship commanders and operators better information on how best to employ ships, how best to identify and avoid risk, and how best to mitigate risks that have been identified and determined to be required to be taken. Operators best understand effects of marginal stability situations on operations. Sharing this understanding provides designers with important knowledge.

Ship commanding officers steadfastly seek to minimize exposure to conditions that imperil their vessels. Emergencies or operational requirements may force them towards a point where there is potential for diminished stability and beyond that point, disaster. They are therefore most interested in gaining as much reserve static and dynamic stability as can be afforded. These situations, fortunately, are rare. More common are conditions and situations when a commander desires a more stable platform from which to conduct operations, albeit sometimes under fairly challenging conditions. This short discussion focuses on employment of undamaged ships, steps needed to reduce the potential for loss of their stability, and possible courses in the design of new ships that afford a crew a more stable platform from which to conduct their business.

As an historical aside, ship designers and engineers have been motivated by this last goal of providing more stable platforms—derived mainly by the need for stable gun decks. In one instance, this goal was pursued through

what now appears to be a somewhat unorthodox approach. The German engineer Otto Schlick and the American inventor Elmer Sperry used gyroscopes to stabilize ships, although not through the types of systems one might think of today. In 1912, the U.S. Navy installed a Sperry gyro aboard the 433-ton USS *Worden*. The gyro wheel itself weighed two tons and was 50 inches in diameter. The spinning of this massive gyroscope effectively neutralized rolls, decreasing them from 30 degrees to six. The forces it created, however, exerted excessive strain on the ship's structure. Later, in World War I the U.S. Navy installed another gyro weighing 25 tons in a 10,000-ton ship to achieve the same effect. It was only following the conclusion of WWI that engineers turned to installing smaller gyros linked to stabilizing fins (Hughes 106-110).

1.1 U.S. COAST GUARD SHIPS

The U.S. Coast Guard operates several classes of ocean-going vessels. The largest range from three polar ice breakers to twelve 378-foot 3,200 LT *Hamilton* class ships, equivalent to frigates in size and mission, and designated by the U.S. Coast Guard as High Endurance cutters (HECs). There are two classes of Medium Endurance Cutters" (MECs): thirteen 270-foot, 1800 LT *Bear* class and eighteen 210-foot 1,000 LT *Reliance* class cutters. (N.B. "Cutter" is the official and traditional nomenclature for U.S. Coast Guard ships. It hearkens back to the first cutter-rigged ships in the Service.) This paper concentrates on the *Bear* class that shares many operational handling characteristics of other corvette-sized ships. While one of the most stable platforms from a damage control perspective, the 270-foot cutters are described by Jane's Fighting Ships as "Very lively in heavy seas because the length to beam ratio is unusually small for ships required to operate in Atlantic conditions." A fairly shallow draft (14.5 ft) also contributes to this "liveliness." This behavior extends into lower sea states where ships of this tonnage should be expected to operate effectively, creating shiphandling challenges for operators.

Many of the negative aspects of the 270-foot MEC seakeeping characteristics are attributable to cost-driven compromises made during its design cycle. Attention to the results of these compromises along with reinforcement of the need to strengthen the dialogue between designers and users should be emphasized within the U.S. Coast Guard ship community. This is especially so now since the Service is in the early stages of selecting an integrated system of ships, aircraft, and support capabilities, the Deepwater Capability Replacement Program. The envisioned $15 billion 20-year program seeks to renovate, modernize, and/or replace the Coast Guard's entire inventory of ships and planes with an integrated system of surface, air, C4ISR, and logistics capabilities. The expense and expanse of the program emphasizes the need to ensure the best possible designs are selected, developed, and introduced. This, in turn, punctuates the call for greater cooperation between engineers and operators.

2. OPERATIONAL AREAS OF CONCERN FOR STABILITY

With the exception of polar icebreakers, Coast Guard ships of the ocean-going classes are armed and have military, law enforcement, and search and rescue responsibilities, as well as others. They are most often involved in one of three types of operations. These are transit, helicopter operations, and boat operations. Transit includes traveling from homeport to operational areas and between assigned areas of operation. Helicopter operations include launch and recovery, Vertical Replenishment (VERTREP) and Helicopter In-Flight Refueling (HIFR). While the first two are limited to helicopters the ship is certified to carry, the latter two can be conducted with nearly any size of properly equipped helicopter. These last two operations can also be conducted when flight deck motion parameters for embarkable helicopters have been exceeded. Boat operations include launch, recovery, and alongside evolutions.

Although conditions that affect stability, and therefore impinge on operations, are not limited to weather, it is the effect of winds, seas, and icing that most often and most severely hamper operations. A second consideration is loading. Most often this is thought of in terms of new equipment, stores, fuel and ballast. More prescient planners and managers also consider lifetime weight growth. These all require careful consideration by operators and particularly in the last instance, by decision and policy makers.

There is, however, an operational concern as well. The U.S. Coast Guard finds itself regularly called upon to transfer to its ships large numbers of passengers. Examples of large groups that might be taken aboard are survivors of disasters at sea, humanitarian evacuees, and migrants. Numbers of people taken on can easily exceed three hundred. Like other warships, Coast Guard cutters have very limited passenger spaces. For the most part, extra personnel are lodged on the level immediately above the main deck. On 378-foot HECs and 270-foot MECs, as many of these people as possible are afforded the helicopter hangar with spillover onto the flight deck (that is, if the ship is close enough to shore or another ship to transfer the helicopter. On a slightly smaller class of ship, the 210-foot medium endurance cutter, tarps and awnings are rigged over the forecastle and flight deck to afford some protection from the elements. The numbers of people, the accoutrements required to provide sanitation and protection, and their location above the main deck create a significant negative impact on

stability. The current stability criteria used by the U.S. Coast Guard and U.S. Navy, Design Data Sheet (DDS) 079-01, accounts for this to some degree in its criteria regarding the crowding of passengers to one side of the ship. Doctrine and operational guidance covering crowd control seek to mitigate the effect by limiting movement and in particular surges of large groups of people across the deck, but the concern remains.

2.1 HEAVY WEATHER AVOIDANCE AND SURVIVAL

One of the most critical transit operations for small combatants is storm avoidance. Generally speaking, traditionally hulled small combatants of the corvette and frigate size are speed limited. When it comes to heavy weather operations, ship commanders face an overwhelming dearth of advice. A standard text for U.S. Coast Guard and Navy shiphandling, Crenshaw's *Naval Shiphandling*, states that for ships in rough seas, but not experiencing hurricane strength winds, it is the seas that most effect a ship and it is rolling that should first be addressed. The advice offered is to generally run with the seas at a speed a few knots higher or lower than the speed of the waves (Crenshaw 1975, 147). In mountainous seas associated with hurricanes and typhoons the guidance is to maintain power, buoyancy, and stability—worthwhile goals in all cases. In regard to shiphandling, the author offers arguments for and against running with the seas, heading into them, and doing nothing—that is, stopping the engines and lying to. For destroyer types, this last advice is discounted while its application for merchant hulls is given due consideration. The previous advice to run down seas is applied to combatants caught in all but the most severe hurricane weather where direction is shifted to keeping the bow heading into the seas.

So, for those heavy weather conditions with the exception of the most severe hurricane conditions, Crenshaw offers the general guidance of running with the seas. What the text fails to cover is how to avoid the worst conditions. For that, another standard text, *Knight's Modern Seamanship*, offers specific guidance for ships caught within the circulation of a cyclone. A ship directly ahead of the storm's center should bring the wind on the starboard quarter and make best speed. A ship in the "navigable semicircle" (in the Northern hemisphere, the semicircle to the left of the storm path) is advised to put the wind broad on the starboard quarter and make best speed. A vessel caught in the "dangerous semicircle" is encouraged to bring the wind onto the starboard bow and make as much headway as possible (Noel 1989, 499). Since cyclonic winds curve in towards a storm's center, this guidance places waves on the port quarter for the first two situations and on the starboard quarter for the third.

A summary of the heavy weather advice offered the mariner can be stated as "except for the worst case (caught in the heart of a hurricane), a ship should place the seas on a quarter." Unfortunately, it is with the seas on the stern or quartering that yields the greatest risk for broaching and capsizing.

2.2 HEAVY WEATHER OPERATIONS

Not all storms may be avoided. This can be due to lack of anticipatory information, lack of adequate speed or seaway to avoid a storm track, or mission requirements. While purposeful exposure of one's ship to potentially fatal weather should be avoided at nearly all costs, mission requirements may force a commander into a decision balancing potential severe repercussions at the hand of weather with a compelling need to attempt a mission. Inaccurate forecasting, impartial information regarding location and on scene weather, or other similar less-than-perfectly known factors, as well as mission exigencies and humanitarian concerns may force a ship commander into areas where winds and seas imperil a ship. Search and rescue is a major mission area for the U.S. Coast Guard and one that often forces this kind of calculus.

Since heavy and extreme weather conditions present one of the greatest threats to a ship's stability and since avoidance and mitigation requires the ship to present an aspect that is less than optimal, one would think that there would be a fairly well-developed body of information available to the mariner on how to best handle a ship in these conditions. Unfortunately, with the exception of the avoidance advice described above, there is very little. One group of authors advocates the development of aids such as polar diagrams, capsize and broach indices to provide ship operators with risk management information (Alman, *et al* n.d., 21). Ship commanders endorse this whole-heartedly.

2.3 OPERATIONS AT ENVIRONMENTAL LIMITS

Bear class cutters are stationed along the east coast of the United States. They routinely operate from the Northwest Atlantic to the Caribbean. Members of the class have also operated on the Pacific coast from Alaska to the Equator. Class members have circumnavigated South America and for the last five years a 270-foot cutter has also deployed to the Baltic, Mediterranean, and in one case, the Black Seas.

With 270-foot MECs ranging across large expanses of the oceans, encountering severe weather is inevitable. The prudent mariner will always attempt to avoid the path of large storms and hurricanes. If in a port in the path of a hurricane, ships will routinely sortie for

evasion. When underway, and given the ability of today's meteorologists to forecast potential events well in advance, ships will divert away from the forecasted path of an approaching hurricane. However, for the reasons stated above, this is not always possible. Multiple reasons can appear to conspire, leaving the commander with fewer options than one might expect. For example, 270-foot MECs have a maximum speed of 19.5 knots under optimal conditions. In the seas that one may expect near an approaching hurricane, the speed available to the ship commander is much less, limiting the angle of escape courses from the path of the oncoming storm. Proximity to shore may further reduce options. In some circumstances, the best alternative to running from the storm is seeking safe haven. This author served aboard a *Bear* class cutter operating in the Caribbean basin before the path of Hurricane Gilbert in September 1988. This Category 5 hurricane had winds associated with it that were measured as high as 160 knots. The speed of the storm's westward advancement compared with the ship's maximum available speed coupled with its location in the central Caribbean closed off avoidance options. The ship sought shelter at U.S. Naval Base Guantanamo Bay, Cuba. Upon arrival at the mouth of the harbor the crew found it disconcerting to pass the larger (and faster) U.S. Navy ships heading outbound for hurricane evasion. Injury was added to insult when, having berthed and secured for the anticipated meteorological assault, the ship was recalled into the hurricane to assist a U.S. ocean-going tugboat on fire and drifting into Cuban waters. During the height of the Cold War, to prevent the potential political fallout of having a U.S. registered ship *in extremis* in Cuban waters, hazarding the cutter was apparently deemed a necessary risk. That the ship was able to rendezvous with, take into tow, and safely rescue the tug is a testament to the capabilities of the *Bear* class designers, builders, and crew.

Mission requirements that force operations in adverse weather conditions exacerbate other factors that compound difficulties regarding stability. A ship that is in no danger of capsize can still be—in terms of mission effectiveness and crew comfort—very unstable. Helicopter and boat operations are both severely hampered by deck motion. Likewise, underway replenishment can be very challenging for a ship displaying a lively ride while alongside a large supply ship. While inclusion of active fin stabilization and other design features of 270-foot MECs mitigate some of these operational challenges, particularly in the roll dimension, pitch limitations often make helicopter and boat launching difficult, if not impossible. Slow speed alongside maneuvers such as towing and personal and small boat recovery present even greater challenges since they often must occur at velocities below that at which fins are effective. An important difference lies between the helicopter and boat operations, however, that again points to the need for better quantified information. U.S. Coast Guard shipboard helicopter operations are governed by well-defined motion limits spelled out in the *Helicopter Operational Procedures Manual* (COMDTINST M3710.2A). This publication sets pitch and roll limits for the conduct of launch and recovery operations. These limits are fairly severe and all the more so for nighttime evolutions. To illustrate, nighttime pitch limits for the HH-60J Jayhawk helicopter embarked on a 270-foot MEC are +/- 1°. Given the very short bow of a 270-foot MEC and the relatively short length overall, this is a very difficult parameter within which to remain. It effectively denies a commander use of this class of helicopter at night in all but sheltered waters.

While some ship commanders may view helicopter operational limits as overly restrictive, shipboard boat operations suffer from an opposite situation. There is little empirically based information available advising commanding officers on how to conduct boat operations in marginal conditions. Likewise, there are few published guidelines suggesting what conditions operations should be suspended. Anecdotal information passed along either directly from commander to commander, or in after-action reports, or in findings of mishap investigations serve these purposes.

Design also affects boat operations. Most oceangoing U.S. Coast Guard cutters have boat decks on the level above the main deck, approximately amidships. On the 270-foot MEC the boat deck for the 26-foot motor surf boat is located there while a 7-meter RHIB is launched from a single-arm davit located on the main deck on the fan tail. Both positions afford advantages and disadvantages. The amidships placement allows for an easier establishment of a weather lee for the boat and boat deck during hoisting. However, the height of these locations exposes the boat and crew to the uncomfortable condition of swinging on the falls for a greater time and at a greater height. 378-foot HECs and 210-foot MECs can somewhat ameliorate this situation through the use of frapping lines controlled from the main deck air castle directly below. The 270-foot MEC is slab sided and therefore cannot avail itself of this technique.

On the 270-foot MEC, the RHIB's location on the fantail necessitates the use of a quartering or following sea for launch and recovery. This, again, subjects the ship to a less than optimal ride. Most 270-foot commanding officers prefer to adjust the ship's speed to slightly faster than the prevailing wave speed so as to present the RHIB with a bow-on sea and to ensure the active fin stabilizers are effective. The speed required can often be considerable.

One further class of U.S. Coast Guard ship and its boat deck need be considered. The relatively new 87-foot Coastal Patrol Boat (CPB) is equipped with a stern launching system for its RHIB. This is the first

experience of this type of system for the U.S. Coast Guard. Other navies have employed the system successfully. But there have been several mishaps on U.S. Coast Guard cutters associated with the launching system. One can be fairly certain that a contributing factor to these accidents was a lack of experience in launching from astern coupled with a lack of information on how these ships should be operated to afford the most stable platform from which to conduct small boat operations. This again leads to a call for more knowledge to the operators.

2.4 PERCEPTION

A large area of disparity exists between observers regarding conditions and their effects. Members of ship's company including those with meteorological training offer often largely divergent estimates of sea state. Wave height estimates are subject to debate. Identification of the direction of movement of the primary sea waves and swells and the detection of secondary but significant wave systems compound the range of opinions. The lack of consensus extends to the primary stations involved in flight deck and boat deck evolutions. The perceptions of bridge team, flight/boat deck members, and helicopter/boat crews vary widely with the degree of variability proportionate to the severity of the weather. What can be perceived as acceptable conditions for one station may be seen as intolerable to others. Instrumented studies verify not uncommon occurrences of vertical accelerations in excess of 0.3g and in at least one instance, 0.4g measured at the pilothouse of a 270-foot MEC (Minnick, Cleary and Sheinberg 1999, 12). The pilothouses on the class of ship are fairly high (height of eye of approximately 45 feet) and fairly far forward (approximately 50 feet from the bow). Motion at the flight or boat decks can be perceived as less than that felt by the bridge crew. On the other hand, with the RHIB boat deck on the fan tail and in following seas, the perception of wave height can be much greater than that perceived by the bridge. This points to the need to develop instrumentation beyond the inclinometer to better inform ship commanders of actual ship motion at important stations and equipment or aids to allow more quantifiable measurement of sea states. The study cited above demonstrated the ability to capture quantifiably the acceleration limits that define the "go/no-go" criterion for boat operations on this class of vessel. This was a 0.2g vertical acceleration, experienced either in the pilothouse or at a boat station. The data gathered must be able to be easily injected in to operational risk management assessment tools that factor the various elements beyond environmental conditions to yield a more comprehensive assessment before any go/no-go decision is made.

Another aspect of ship motion that must be addressed in more quantifiable terms is the effect of ship motion on the crew. Modern seasickness medication is a boon to today's cuttermen, but it is not a panacea. The medication attenuates but does not alleviate the effects of seasickness. Also, it does not prevent—and can aggravate—Motion Induced Fatigue (MIF). The study cited above also compared MIF between the crews of a 378-HEC and 270-MEC operating side-by-side in the Bering Sea. The study found significant differences in the severity of ship movement (for example, a 30-40 percent greater vertical acceleration on the 270-foot MEC) but no differences in reported sea sickness (although there was a significantly higher incidence of the use of anti-seasickness medication on the 270-foot MEC). One indicator of fatigue, the time to complete tasks, showed a significant difference between the two crews with 29 percent fewer of the crew of the 270-foot MEC reporting an ability to complete tasks in "normal time" (Minnick, Cleary, and Sheinberg 1999, 13). In interpreting this self-report data, one should not discount the possibility of natural competition between the crews as a potential source for skewing the data. *Bravado* and *esprit de corps* combined with the potential for the crews to perceive the comparison of two ships of different classes as a competition might create a reluctance to accurately report MIF. That the smaller ship was brought into the operational area of the larger one to see how it might perform in that environment might motivate its crew to under-report its MIF to a greater degree than for the 378-HEC's. Experience strongly indicate that MIF can be the source of serious degradation in crew and cutter performance.

The current drive to reduce ship personnel allowances further emphasizes personnel and equipment safety issues. This was a major consideration for the selection of the 87-foot CPB's stern launch system that was designed to require only one person to conduct launch and recovery of the small boat and its crew. Reduced crew sizes are but one dimension of the difficulty operating a ship in moderate to heavy seas and creating crew safety and fatigue concerns. Shrinking fleets and increased responsibilities within navies and coast guards around the globe place greater burdens on ships and crews, increasing their exposure to less-than-optimal operating conditions. "Human stability curves" addressing ship motion over time and its effects on personnel need to be developed and employed.

3. TRAINING AND EDUCATION

Once a ship's design cycle is complete and it is introduced, responsibility for its employment shifts towards (but not solely upon) the operators. Engineers must continue to be part of the employment team with responsibility for ensuring proper configuration management and guarding against inevitable weight growth and their effects on operational stability. For operators and their leadership, responsibilities include ensuring commanders and crew are familiar with ship characteristics and limitations. To date in the U.S. Coast

Guard, this has been done through a semi-formal personnel qualification standards (PQS) and damage control (DC) training program. The primary sources of instruction for these programs at the unit level are fellow crewmembers, supported by pipeline training, a smattering of recurrent classroom courses, and ship training availabilities. These provide a generally broad but shallow knowledge of stability issues for all but the Engineer Officer and the Damage Control Assistant.

Deck officers receive very little formal classroom and practical hands-on experience related to operational stability. In the past, sources of first-hand experiences were limited to sea stories told by those who survived, literally or figuratively, operations conducted at stability extremes. With the availability of simulators ranging from desktop personal computer applications to full-motion bridge simulators, deck officers can experience the effects of extreme stability situations with realistic fidelity. Such training should be mandated for senior enlisted and officer crew members.

4. CONCLUSION

The Coast Guard has been employing 270-foot MECs since the mid-1980s. With over fifteen years of experience with this class, these ships have ably demonstrated their capability. They have also presented areas where ships of this size may be improved. Lessons learned from these areas afford U.S. Coast Guard Deepwater designers and the designers of other naval surface ships opportunities to design and build ships that are safer and more capable across a greater range of environmental and operational spectra. The first lesson is to concentrate energy on designing ships that are inherently more tolerant of heavy weather and the motion imparted on the ship by it. This includes positioning important operational stations at places that minimize vertical and transfer acceleration, and exposure of equipment and crew. The second lesson is the requirement to develop onboard instrumentation to capture a greater knowledge of ship's motion. This information should then be provided to the commander during operation of the vessel in a usable manner like polar plots and capsize/broaching index (CI/BI) information. A third lesson is the need to establish continuous attention to stability and stable platform considerations during modeling and simulation, testing and evaluation, introduction, and operational lifetime stages to include operator education, training, and operational guidelines.

5. REFERENCES

Alman, Phillip R., Peter V. Minnick, Rubin Sheinberg, and William L. Thomas III. "Dynamic Capsize Vulnerability: Reducing the Hidden Operational Risk," n.d.

Crenshaw, R. N., Captain, U.S. Navy (Retired). *Naval Shiphandling*. 4th ed. Annapolis: Naval Institute Press, 1975.

Hughes, Thomas P. *American Genesis: A History of the American Genius for Invention*. New York: Penguin Books, 1989.

Noel, John V., Jr., Captain, U.S. Navy (Retired), ed.. *Knight's Modern Seamanship*. 18th ed. New York: Van Nostrand Reinhold, 1989.

Minnick, Christopher Cleary and Rubin Sheinberg. "Operational Comparison of the 270-foot WMEC and 378-foot WHEC Based on Full Scale Seakeeping Trials." Paper delivered to Chesapeake Section, the Society of Naval Architects And Marine Engineers, 1999.

U.S. Department of Transportation, U.S. Coast Guard. *Helicopter Operational Procedures Manual (COMDTINST M 3710.2C)*. Washington, D.S.: U.S. Government Printing Office, 1998.

The opinions expressed are those of the author and not those of the U.S. Coast Guard.

On Developing a Rational and User-friendly Approach to Fishing Vessel Stability and Operational Guidance

Bruce Johnson, NAOE Department, U. S. Naval Academy, Annapolis, MD 21402
e mail: aronj@bellatlantic.net
John Womack, Mid-Atlantic Shipwrights LLC, Cambridge, MD 21613

e-mail: Shipsjw@aol.com

Summary There is common recognition that a major shift in the commercial fishing culture is necessary. It is understood that this can only be accomplished by increased awareness of the risk and the problems faced, whether in design or operations. The key element for the SNAME Ad Hoc Panel #12 on Fishing Vessel Operations and Safety will be development and pursuit of awareness efforts while working with other like-minded organizations to affect a major shift to a safety culture. The scope of this effort is to address fishing vessel safety from a broad perspective including: basic issues affecting fishing vessel safety, vessel design, vessel construction, vessel operation, vessel maintenance, survey, safety training and awareness, voyage planning, costing, marine weather prediction, fishing regulation, risk analysis and assessment and to investigate and recommend ways to improve awareness on the part of commercial fishing vessel community to aid in getting that community embrace a safety culture.

1. INTRODUCTION

The Society of Naval Architects and Marine Engineers (SNAME) has recently organized a new Ad-Hoc Panel on Fishing Vessel Operations and Safety. As stated in our charter,
http://www.sname.org/committees/tech_ops/fishing/home.html
the initial objectives of the FV Panel, each supported by a working group, are to:

A.Investigate the feasibility of establishing risk-based fishing vessel stability criteria appropriate to the type of vessel and its operating area.
B.Evaluate the effectiveness of existing stability letters and develop better ways to communicate to the fishing community the importance of following reasonable stability and survivability guidelines.
C.Develop proposed design, production, operation and maintenance guidelines for various classes of fishing vessels that address basic safety, vessel design, vessel construction, vessel operation, vessel surveys and vessel maintenance.
D.Coordinate with SNAME Panel SC-3 in developing a long-range plan to deal with marine engineering and environmental issues of all types within the commercial fishing industry.

Working Group A (which has its organizational meeting during the Trieste workshop) is tasked to:
1. Identify hazards associated with small vessel capsizes and sinkings and develop guidelines to reduce wave impact damage and personal injuries.
2. Work with NOAA and the international meteorological community to improve predictions of dangerous local wave conditions.
3. Suggest ways to improve survivability for smaller vessels and their crews when they encounter extreme waves.
4. Review the Torremolinos Protocol, which has been criticized by the international naval architecture community a) for lacking "rational criteria" and b) for promoting capsize resistance for the vessel at the expense of operational safety conditions on board. Satisfying the IMO Torremolinos criteria for fishing vessels does not insure surviving a direct hit by rogue waves, or by other extreme (breaking) wave conditions and does not adequately address or insure crew survivability, which frequently involves escaping from a vessel that is stable while inverted.
5. Formulate a proposed fishing vessel research program to develop a new set of scalable, non-dimensional parameters for designing and building safer vessels. It is expected that the effects of variations in length, beam, draft, freeboard, sheer line, bulwark and deckhouse arrangements and loading conditions can be correlated with a new set of design parameters for increasing small vessel safety and survivability in a variety of situations.

Working Group B is charged with the following tasks related to the stability letter and operator guidance:
1. Since most fishing boat captains regard the determination of a vessel's stability letter as a lot of black magic by the naval architect/ surveyor, develop a user-friendly format that most fishermen and owners can more easily comprehend.
2. Work with fishermen, owners, surveyors, marine insurers, fishing boat designers and builders to insure that all parties understand the purpose and implication of stability letters.
3. Involve fishermen, vessel owners, insurance representatives, fishing safety trainers, Coast Guard representatives and naval architects in developing understandable, but not oversimplified, fishing vessel safety materials and training devices.

2. The Torremolinos Protocol

The IMO voluntary fishing boat safety regulations for vessels > 79 feet (24 m) in length are based on one-size-fits-all criteria derived from computer generated static stability righting-arm curves. The current version is known as the 1993 Torremolinos Protocol and can be found on the IMO web site. (For technical and historical details on its development see Bird 1986, Cleary 1993, Dyer 2000 and Kobylinski 1994 and 2000.) The Torremolinos Protocol

has been criticized 1) for lacking "rational criteria" (Kobylinski 1994 and 2000, Umeda 1994, Dahle 1995) and 2) for promoting capsize resistance at the expense of operational safety conditions on board (Boccadamo 1994 and 2000, Umeda 1999 and 2000).

The frequently used interpretation in applying the Torremolinos Protocol stability criteria is that the area under the righting arm curve represents righting energy. This is incorrect, and in the US, The Code of Federal Regulations (CFR) and NVIC 5-86 criteria are frankly wrong in making such statements!!!! (Work and energy are in lb-ft or N-m. Reference PNA 1988, Volume 1, pp 87-93 on Dynamic Stability.)

Briefly, scalability in vessel stability characteristics depends on the square-cubed rule, i.e. the heeling forces, which depend on water and wind impact areas, go up with the square of the dimensions but the righting moment depends on the displacement which goes up with the cube of the dimensions. Thus, bigger is almost always better Correctly using the Torremolinos criteria should mean that vessels double in dimensions should survive without capsizing in twice the wave height conditions but that is not the interpretation given by the existing guidelines. The wind heel criteria do scale with size, as PNA points out, since the both the heeling arm and the righting arm are divided by the vessel displacement.

In addition, existing voluntary guidelines for fishing vessel stability are intended to provide significant capsize resistance for the vessel during storms that contain few rogue waves. Satisfying the voluntary IMO Torremolinos criteria for fishing vessels longer than 24 meters, for example, does not provide the capability to survive a direct hit by rogue waves or by other extreme (breaking) waves. Capsize resistance criteria for fishing vessels generally do not address or insure crew survivability, which frequently involves escaping from a vessel that is stable while inverted. In addition crew members who abandon a vessel in a major storm can be in danger of life threatening capsizes in many types of life rafts. Of the six men who died in the 1998 Sydney-Hobart sailboat race, three were attempting to survive in a life raft that capsized repeatedly in extreme waves (Mundle 1999).

3. Capsize and Extreme Wave Research on Smaller Vessels

Most capsize research concerning vessels of all sizes has concentrated on loss of waterplane area (hull form) stability on a wave crest in steep waves and/or spilling breakers. (Grochowalski 1989, 1993 and 1997, Blume 1993, Dahle 1995, Umeda 1999 and 2000. See also an excellent review of the 2000 Stability Conference in Belenky 2001.)
On the other hand, much yacht capsizing research has concentrated on wave impact capsizes caused by extreme breaking waves, thought to be a primary cause during the 1979 Fastnet Race disaster. (Kirkman, 1983, Salsich 1983, Claughton 1984, Zseleckzy 1988) These studies showed that in beam seas, the location of the vessel relative to the breaking position of the wave is critical. If the vessel is caught in the curl of a plunging breaker, or in the secondary wave created by the jet impact of the plunger, capsize is possible in waves as small as 1.2 times the beam of the vessel, even for a yacht with a low center of gravity. The roll moment of inertia is also an important parameter because a vessel with a large value of this parameter will roll to a smaller angle on impact but expose the deckhouse and work area to the full impact of the plunging wave jet. More recently, experiments on multihull capsizing (Deakin 2001) and the re-righting of sailing yachts in waves (Renilson 2001) have been investigated.

Part of the capsize research effort suggests that the experimenter attempt to characterize the asymmetry of the breaking wave by analyzing the wave parameters suggested by Kjeldsen (Myrhaug 1983, Bonmarin 1984 and 2000, Duncan 1987, Zseleczky 1989).

As discussed at the Rogue Wave 2000 Conference (Olagnon 2000), open ocean rogue waves appear to be short-lived and the probability of measuring one from a single platform record is small. During the 1998 Sydney-Hobart race as reported in deKat 1999, from which his Figure 10 (below) is taken, the Esso Kingfish-B platform located in the Bass Strait measured no waves more than twice the significant wave height, even though the participants reported many very large breaking waves during the race (Mundle 1999). (Note that the date is incorrect and should be 27-12-98.)

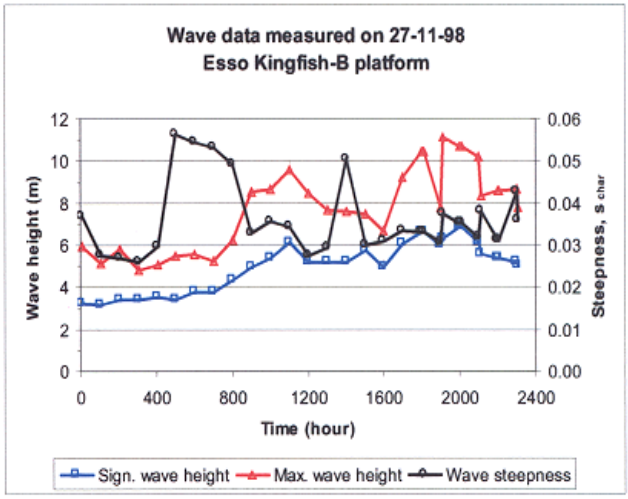

Figure 10. Wave height (significant and maximum) and direction in eastern Bass Strait.

Figure 1 from deKat 1999

The workshop presentation will also discuss and illustrate with video clips two capsize modes:
1) Loss of waterplane area (hull form) stability on a wave crest in steep waves and/or spilling breakers, *a high risk for improperly designed and or loaded vessels in storms.* and
2) Wave impact capsize caused by a plunging extreme wave, *a lower risk for stable vessels in storms, i.e. being in the wrong place at the wrong time during a low probability event.*

4. Operator Guidance

The primary means for providing stability operating guidance to small fishing boat crews is the "Stability Letter". These stability letters are generally a simplified version of the traditional "Stability Book" that is generated for large commercial boats. These simplified stability letters have been the preferred means of conveying the critical stability information and boat operating guidance to crews given the simpler configuration of small fishing boats and the lower or non-existent training levels of the crews.

For a stability letter to be effective, it must first be understandable to the crews, and second, the crews must believe that the guidance information provided is correct. While the first requirement is fairly obvious, the second requirement is equally important. The best stability letter on the most seaworthy boat in the world is of no value if the crew believes the loading requirements are wrong and ignores the stability guidance.

There are two basic stability letter types in use today, the text only version and the pictorial version. In both versions, the intent is to provide the crews with all of information to allow safe navigation of their boat under typical weather conditions and fishing operations. Unfortunately, most forms of the stability letters currently in use are neither readily comprehensible and/or are trusted by the crews. The current versions of these stability letters may suffer from one or more of the following basic flaws:

First, they may be written using terms more familiar to Naval Architects then to crews. The concept of terms such as Transverse Metacenter (KM), Metacentric Height (GM), Center of Buoyancy (KB), and Righting Arm (GZ) are unknown to most small fishing boat crews. These terms, while useful in determining if a boat has adequate stability, are simply foreign concepts to most crews and only serve to confuse them. Imagine trying to explain what Transverse Metacenter and Metacentric Height are to crews who have little or no knowledge of boat design let alone can barely read and write.

Secondly, these stability letters may use loading restrictions that are either very difficult to measure when underway or are impractical to use during typical fishing operations. One example is the specifying of minimum freeboards. While a good method in theory to specify maximum loadings, it is impracticable, and dangerous for a crew to measure freeboards while underway by hanging over the boat's side in any type of sea. The same criticism holds true for specifying maximum drafts. Draft marks on a boat's side are basically impossible to see from the deck due to flare, rubrails, or other obstructions. And the typical draft marks used are generally not sufficiently accurate to determine a good draft reading for stability purposes.

The other type of loading restrictions that may be impractical to use underway are those limiting the weight of a net catch, the loose catch on deck awaiting processing, or other similar temporary conditions during fishing. An example is the restrictions on deck loading when hauling in the net on the F/V Artic Rose (which sank on April 02, 2001). From an article in the Seattle Times on June 17, 2001, the naval architects that created the boat's stability letter stated that the maximum deck loading was 5,000 pounds in most cases, up to a maximum of 21,000 pounds under the most optimum conditions. The boat was capable of catch capacities of 40,000 pounds for each net haul back. This type of restriction requires the crew to accurately estimate the weight of the fish in the net while it is still under tow as well as accurately estimate the weight of the fish on deck. In addition, because this loading restriction is such a small percentage of what the boat can typically catch, the crew is faced with a difficult decision if they have a very successful tow that exceeds the loading restriction. In theory the crew must dump a portion of the net before bringing the net onboard to ensure the boat has adequate stability. In practice though, the extra fish are brought on board which makes this type of restriction basically useless.

Another problem is with stability letters that use a series of simple pictures of the boat under different loading conditions with a safe or unsafe notation. To adequately show the crew all possible loading conditions, both safe and unsafe, a large number of loading pictures must often be created. This creates several problems. First, to determine if the boat is safe, the crew must search through a large selection of loading pictures. And second, given the many possible loading variations of tanks, catch, and other variable loads, the crew more than likely will have to "select", (more actually guess), which loading picture best approximates the actual boat's condition. With the crews not likely to have any technical training, the potential exists that crew could guess wrong and create a dangerous stability situation.

Pictorial types of stability letters can also suffer from a lack of clarity when attempting to depict fishing boats with multiple tanks, fish holds, and other variable loading areas. For example, use a fishing boat with (3) centerline fish holds, (2) port and (2) starboard belly tanks under the holds, and (2) port and (2) starboard wing tanks alongside the holds, a typical arrangement. To adequately depict one loading condition, at least (2) inboard profiles, see Figure 2, must be used if it is assumed that port and starboard tank pairs are at equal levels. This is not always a valid

assumption for many boats that use the port and starboard tanks to compensate for built-in or temporary lists. In this case at least (4) inboard profiles, see Figure 3, must be used to show all tanks and holds. This though, can be very confusing as to which are the port tanks and which are the starboard tanks, especially to untrained crews. In addition, in two of the profiles, the fish holds must be duplicated, which can add to the confusion. Deck plan views can be added as shown, but the problem then exists in clearly indicating the level of the tank or fish hold.

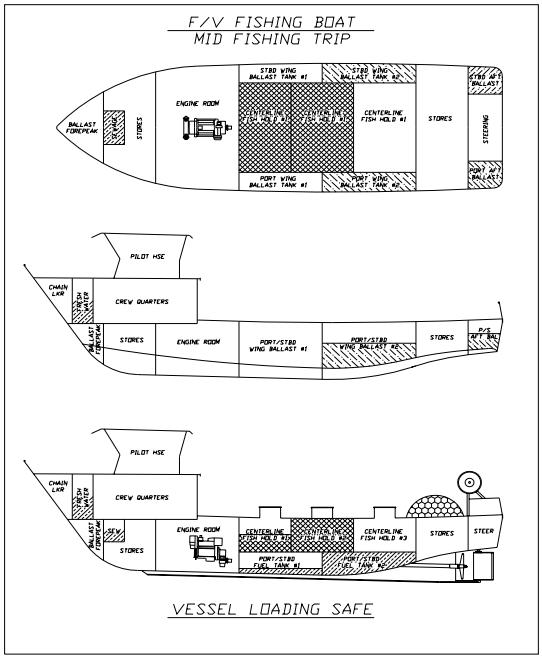

Figure 2 - Sample Pictorial Loading Page

The last problem with pictorial types of stability letters is they assume the fishing boat crews can "read" drawings to be able to transfer the real boat to the picture and vice versa. To naval architects with formal training, this ability is often blindly assumed. In practice though, this is often a poor assumption. Being able to visualize a 3-D boat with hidden tanks and then transfer that information to 2-D pictures takes formal training. From practical experience, the crews may know where all of the tanks are on the boat, but often have problems in looking at a drawing and being able to locate them.

Assuming the stability letter adequately provides the necessary stability operating guidance, the crews must also believe that the guidance provided is correct so they will follow it. Unfortunately, from many casualties reports in the US, the crews often ignore stability letters because they believe they know how to load the boat correctly. (USCG 1999)

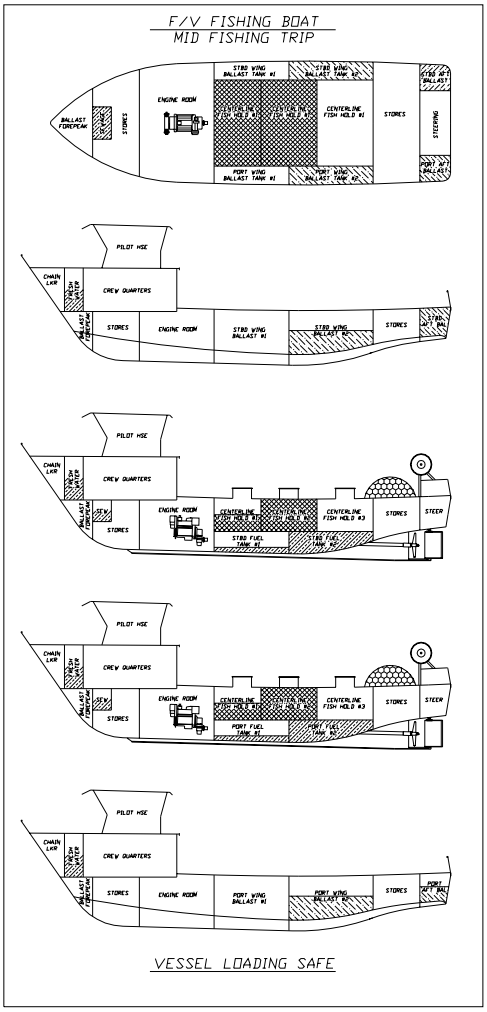

Figure 3 - Sample Pictorial Loading Page

This situation exists for several reasons. First, many of the crews have little or no formal training in seamanship and stability. Their experience comes from many years of hands-on learning under captains who themselves had little or no formal training. As an example is this excerpt from the forthcoming book "Wages of the Sea" by Douglas Campbell and published by Carroll & Graff.

> There were few in the clam industry who would have ridiculed Novack or his mate for their disregard of the stability letter carried in their boat. Many clam boat captains were either ignorant of the contents of these documents or held them in disdain. They had been on the ocean for years, and the ocean had taught them lessons. There was little that a so-called expert could tell these men that they had not already learned through their daily lives on the water. One such man was William Parlett, captain of the clam boat Richard M. Parlett, a twenty-five-year veteran of commercial fishing,

twenty of them as a skipper. At one time, he had filled in as captain of the Beth Dee Bob. He knew that boat had a stability letter. Several years later he could recall precisely where it was kept on the boat. When asked if he had ever read it, he replied stiffly: ``No, sir. " Asked why, he explained, as if it were obvious: ``Didn't need to. " But why? ``If I felt she was unsafe, I'd get off it. "

An example of Parlett's attitude toward the stability of a boat is found in his approach to the presence of water in the clam holds. How much water in the hold was okay? That amount, Parlett said, that would ``keep (the boat) on a level keel. "

``You could flood the holds completely if you wanted to," the captain said. ``All it did was make it more stable. "

Another reason for why crews may chose to ignore the stability letter occurs because of the way a typical fishing boat's stability works. A fishing boat's stability can be divided into two ranges, initial stability and overall stability. Initial stability is typically from zero degrees (no heel) to about 10 degrees of heel. Overall stability encompasses the boat's stability from zero degrees to the point of vanishing stability. For fishing boat crews, the boat's initial stability is what they encounter, "feel", during typical fishing trips. The boat's overall stability characteristics are more rarely encountered during severe storms.

The problem occurs because a boat's initial stability is not a reliable indicator of a boat's overall stability. A "tender" boat with a high freeboard or one that is too stiff may feel uncomfortable during typical operations, but may have excellent overall stability. Conversely, a boat that feels very safe during typical operations, may have poor overall stability. Because of this, crews that load their boat so that it "feels" safe during everyday operations may have little or no warning that they have significantly reduced their boat's overall stability to dangerous levels.

Figure 4, which shows the effect on a boat's stability of adding ballast low, will illustrate this point. Crews will fill ballast tanks under the fish hold to stiffen a boat's motion to make it more comfortable during everyday operations. Many crews believe they have improved the boat's stability when in fact it has been significantly reduced. The solid line indicates the righting arm curve without ballast and dashed line is righting arm curve with ballast. Note that initially the righting arms, and thus initial stability is increased by adding the ballast, which the crew feels during everyday operations. Note also that the overall stability has been significantly reduced in several critical areas; the range of positive righting arms is reduced, the area under the righting arm is reduced, and the heel angle of the maximum righting is reduced.

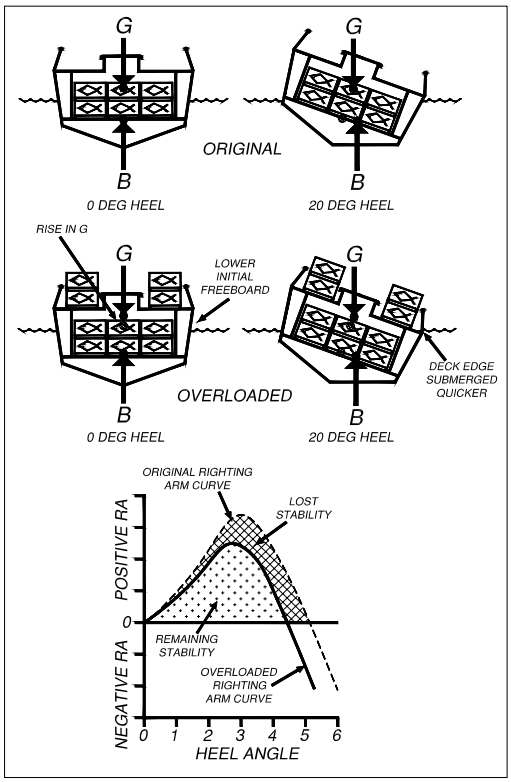

Figure 4 - Effect of Overloading on Stability

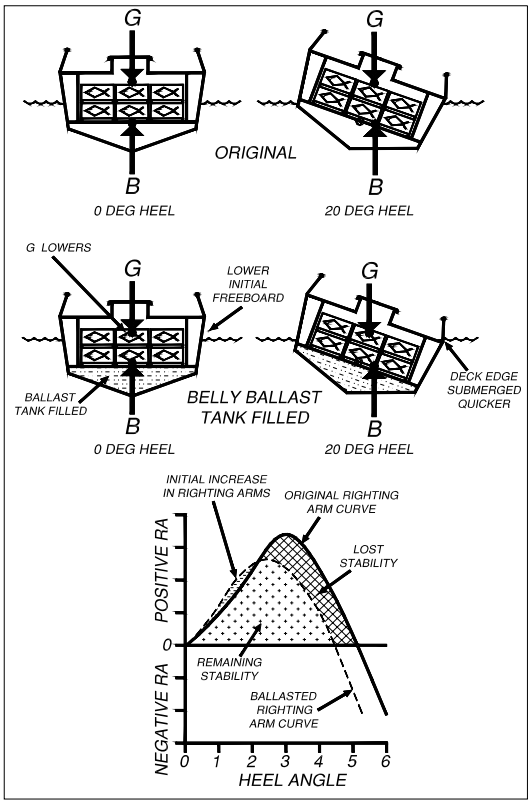

Figure 5 - Effect of Ballasting on Stability

This initial/overall stability conflict also explains why crews often disregard maximum catch limits in their stability letters. Figure 5, which shows the effect on a boat's stability from overloading, will illustrate this point. In this figure, the solid line indicates the righting arm curve before overloading and dashed line is righting arm curve after overloading. In this case, note that righting arms up to 10 to 15 degrees of heel have not been significantly reduced. The overall stability though, has been significantly reduced. Because the crews usually evaluate the "feel" of the rolling motions under initial stability conditions, the boat dose not "feel" unsafe when they bring in extra fish from a good trip. This happens several times and they understandably start to disregard their stability letter. As long as the weather remains good, they can get away with the overloading. In bad weather though, they do not realized how much their boat's stability has been degraded and the significant danger they are in. (The Workshop Presentation will include statistics from USCG on overloading losses.)

The impractical loading conditions mentioned previously can also cause crews to ignore their stability letter. Restricting a crew to catch amount of 5,000 pounds when they can catch 40,000 pounds is just asking for the crew to ignore the stability letter. Faced with having a net full of fish and bills due, human nature says most will keep the fish. And as mentioned above, because they can successfully do this in good weather with no apparent effect on their boat's stability level, they will likely continue to ignore the stability letter limits.

Finding solutions to these problems is the task of SNAME's Working Group B on Stability Letters, Stability Education, and Training. The solutions are simple: improving stability letters and the training of basic stability concepts to fishing boat crews so they understand and trust their letters. Since the principal blame for problems with stability letters lies with the naval architects and marine surveyors who create them, the solutions must then come from naval architects who understand what the fishermen need and want to fix the system.

To improve stability letters, the members of Working Group B will be working with naval architects, regulators, and fishing boat crews to develop an improved format. The basic criteria for developing the improved stability letter format will be;

1. Written to provide stability guidance, not dictate the boat's operation.
2. Present the safe loading conditions clearly, both visually and written..
3. Provide some means for conveying the stability levels, i.e. risk of capsizing, associated with each of the loading conditions.
3. Be comprehensible by crews with little or no formal training.
4. Use practical operating restrictions on variable catch limits, etc.
5. Use practical means to allow the crew to check if the boat is loaded correctly.
6. Develop a series of operating guidelines on proper seamanship and boat maintenance suitable for preserving a boat's stability.

In summary, the goal is to provide the captain with practical stability guidance and a way to gauge the risks of capsizing based on loading, weather, and other factors, and let them run their boats.

Using a safe/unsafe loading matrix is one of the formats being investigated for a new type of stability letter. These matrixes (see Figure 6 for an example) have been proposed in the past and have several advantages. First, a large number of loading conditions can be shown on a single page. And second, the matrix is relatively easy to use. With catch levels on the left column and various tank loadings across the top, it is easy for the crew to check if the boat's stability is acceptable.

F/V FISHING BOAT - STABILITY LOADING MATRIX								
		MAXIMUM CAGES IN HOLD - DREDGE FULL & ON RAMP						
PORT & STBD FUEL TANKS	POTABLE WATER	0 CAGES	10 CAGES	20 CAGES	30 CAGES	40 CAGES	50 CAGES	60 CAGES
100%	100%	SAFE	SAFE	UNSAFE	UNSAFE	UNSAFE	UNSAFE	UNSAFE
75%	100%	SAFE	SAFE	UNSAFE	UNSAFE	UNSAFE	UNSAFE	UNSAFE
75%	75%	SAFE	SAFE	SAFE	UNSAFE	UNSAFE	UNSAFE	UNSAFE
50%	75%	SAFE	SAFE	SAFE	UNSAFE	UNSAFE	UNSAFE	UNSAFE
50%	50%	SAFE	SAFE	SAFE	SAFE	UNSAFE	UNSAFE	UNSAFE
50%	25%	UNSAFE	SAFE	SAFE	SAFE	UNSAFE	UNSAFE	UNSAFE
25%	50%	UNSAFE	SAFE	SAFE	SAFE	SAFE	UNSAFE	UNSAFE
25%	25%	UNSAFE	UNSAFE	SAFE	SAFE	SAFE	SAFE	UNSAFE
10%	10%	UNSAFE	UNSAFE	UNSAFE	SAFE	SAFE	SAFE	UNSAFE

Figure 6 - Sample Safe/Unsafe Loading Matrix

Working Group B is also investigating expanding the safe/unsafe loading matrix into a risk based loading matrix (see Figure 7). In this matrix scheme, instead of a safe/unsafe (go-no go) indication for each possible loading condition, a risk level would be assigned. How to clearly indicate the risk level still needs to be investigated. Suggestions include using red, yellow, and green shading for a visual representation or using a "risk of capsizing" number.

F/V FISHING BOAT - STABILITY LOADING MATRIX								
		MAXIMUM CAGES IN HOLD - DREDGE FULL & ON RAMP						
PORT & STBD FUEL TANKS	POTABLE WATER	0 CAGES	10 CAGES	20 CAGES	30 CAGES	40 CAGES	50 CAGES	60 CAGES
100%	100%	STORMS	HEAVY SEAS	FAIR SEAS	CALM SEAS	UNSAFE	UNSAFE	UNSAFE
75%	100%	STORMS	STORMS	HEAVY SEAS	FAIR SEAS	CALM SEAS	UNSAFE	UNSAFE
75%	75%	STORMS	STORMS	STORMS	HEAVY SEAS	CALM SEAS	UNSAFE	UNSAFE
50%	75%	STORMS	STORMS	STORMS	HEAVY SEAS	FAIR SEAS	UNSAFE	UNSAFE
50%	50%	STORMS	STORMS	STORMS	STORMS	FAIR SEAS	CALM SEAS	UNSAFE
50%	25%	HEAVY SEAS	STORMS	STORMS	STORMS	HEAVY SEAS	FAIR SEAS	UNSAFE
25%	50%	HEAVY SEAS	STORMS	STORMS	STORMS	STORMS	HEAVY SEAS	CALM SEAS
25%	25%	FAIR SEAS	HEAVY SEAS	STORMS	STORMS	STORMS	STORMS	FAIR SEAS
10%	10%	CALM SEAS	FAIR SEAS	HEAVY SEAS	STORMS	STORMS	STORMS	HEAVY SEAS

Figure 7 - Sample Risk Based Loading Matrix

This risk based loading matrix scheme ties into Working Group A's review of the stability criteria currently in use. The current one size, one weather stability criteria such as the Torremolinos Convention have many flaws. This approach leads to overly conservative stability levels for good weather trips. As discussed above, crews soon learn they can overload the boat "safely" in good weather. But when bad weather occurs, the crews have no means to gauge the risk caused by the overloading. The crews have intuitively figured out that weather is an important criteria in determining a boat's potential loading levels. What can not be figured out intuitively by the crews is the overall stability levels and potential capsizing risks. This can only be done by a trained naval architect.

This type of loading matrix also has the advantage of putting the operational decisions for the boat back to the captain instead of with the naval architect as current stability letters do. This approach does require that the captain, vessel owner, and other decision makers must clearly understand the basic concepts of stability in order to select the appropriate risk level, given predicted weather conditions and other trip factors.

For teaching basic stability concepts to fishing boat crews, the working group has started the development of a new type of training course. From discussions with fishing boat crews, they are interested in understanding their stability letters. The problem is the creation of the stability letter appears to be a lot of black magic by the naval architect. From moving some weights back and forth on their boat, the architect comes back with a piece of paper on how to load their boat. And often, the stability instructions run counter to how they believe their boat should be loaded or restrict the maximum allowable catch to levels below what they are carrying now.

To teach stability to fishing boat crews will require explaining fishing boat stability and its complex interactions to crews who generally lack an education. As noted previously, the common naval architecture terms used in stability are simply unknown, and often incomprehensible, to the crews. For example, even the basic concept of center of buoyancy is unknown to many crews. The challenge will be in convincing the crew that the center of buoyancy is a real location that all of the buoyant forces are acting through, not an imaginary point on their boat that the crews may have a hard time conceiving.

The course is only intended to teach the basic concepts of stability and the effect of typical fishing operations on a boat's stability. The course is not intended to teach how stability is calculated. That is the responsibility of the naval architect. The primary goals for the proposed stability training course are:

1. Explain what center of gravity (G) and center of buoyancy (B) are.
2. Show the relationship between G and B as the boat heels and how that works to keep the boat upright.
3. Explain the basic methods of determining if a boat has adequate stability.

A. Show what a righting arm curve is.
B. Show how the righting arm curve is calculated.
C. Show the basic parts of the righting arm curve used to determine the boat's stability level.

4. Show the effect on a boat's stability level from typical boat operations.

A. Explain the difference between initial and overall stability.

i. Initial stability is what the crews typically feel and see.

ii. Overall stability is what keeps the boat upright in a storm.

iii. Initial stability is not an accurate indicator of overall stability.

B. Show the effect of free surface, overloading, lifting over the side, and other similar loading conditions.

The initial layout of the stability training course consists of two parts; a written manual and a verbal presentation. The two individual components of the training course will be developed to be mutually supporting. Figures in the written manual would be similar to the models used in the presentation, and concepts demonstrated in the presentation would be in the manual. This will allow crews that have taken the training course to use the written manual as a refresher.

The written manual will be developed to be self-explanatory to persons who have some formal education or seamanship training. The figures intended to show the basic stability concepts will be kept simple and structured to appear similar to existing fishing boats designs. It is important to make the figures believable to the crews. If they look similar to their boat, the chances are better the crew will believe the message even when it runs counter to past beliefs. Figure 8 is an example of the proposed figures (more will be shown during the Workshop) which will show the relationship between center of gravity and center of buoyancy and how the righting arm curve is developed. The preferred use of the written manual will be as follow-up take-home notes to the verbal presentation.

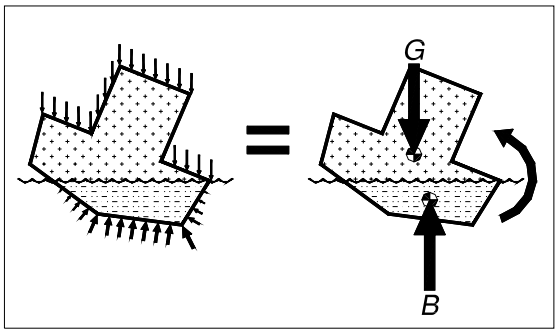

Figure 8 - Positive righting Arm

The second component of the training course, the verbal presentation, will be developed for both small and large groups. The small group is intended to be an individual fishing boat's crew and owner, with the larger groups being at meetings such as trade shows or NMFS regional council meetings. The presentation for individual boats will be made easily transportable to allow the presentation to be made onboard, at dockside, or even in the local watering hole. This will allow a naval architect to give the presentation when delivering a stability letter to a boat.

For both presentations, a series of static and dynamic demonstration models with companion posters is proposed. Figure 9 is an example of a proposed static demonstration model. By having removable sections as shown in figure 10, several different stability issues can be demonstrated. The models are an important part of the presentation as they allow the crews to see "hands-on" what is happening during typical fishing operations. As an example, the crews can see directly the loss of stability when they boat is overloaded or the negative effects of slack tanks. Actually "capsizing" the model, especially when they believe they have loaded the model to make it safer, is a very convincing training method.

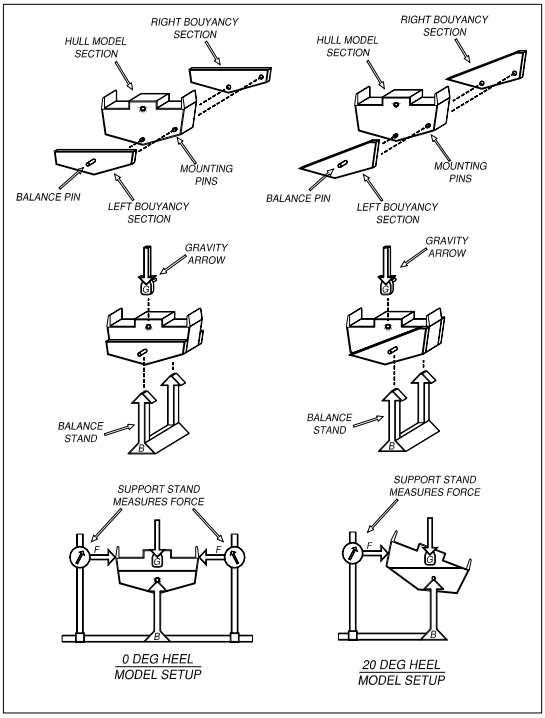

Figure 9 - Static Stability Demonstration Model

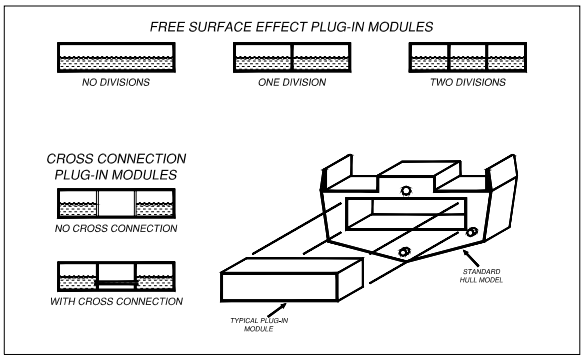

Figure 10 - Static Stability Demonstration Model

In summary, problems exist with current types of stability letters used to provide stability to small fishing boat crews. These problems are the principal reason crews are disregarding these letters, either intentionally or because the letters are incomprehensible, and putting themselves in danger. Fishing boat crews don't have a death wish, they just truly don't understand the potential adverse impacts on their boat's overall stability when they load the boat to make it "feel" better under normal fishing operations. The initial stability the crew feels is no indication of the boats overall stability levels. This "hidden flaw" is not seen by the crews because they have never been taught the basic concepts of their boat's stability.

On the positive side, experience has shown that the crews are willing to learn and do a better job following their stability letters if we, as naval architects, can give them practical, intelligent, flexible stability guidance and the tools to understand that guidance. Responsibility for the proper operation of the boat should be put back to the captain instead of being dictated by the naval architect as current stability letters are.

5. Future Work

Working Group B is considering formats for risk-based Sea State vs Loading Consequence Diagrams appropriate to the type of vessel and its operating area. It is expected that the initial versions will be based on avoiding loss of waterplane area and shipping water capsizes, for which significant prediction tools already exist (Grochowalski 1997). The breaking wave capsize probabilities are unknown at present because the statistics of the occurrence of steep waves, especially plunging breakers, in a particular geographic region are not presently included in marine forecasting models. This must eventually be addressed, even though being in the wrong place at the wrong time is a low probability event.

A longer range goal of Working Group A of the ad-hoc F/V Panel is to create a fishing vessel research program to develop a new set of scalable non-dimensional parameters for designing and building safer fishing vessels (Blume 1993, Boccadamo 1994, Buckley 1994). In order to experimentally determine fishing vessel design parameters,

which improve survivability in a severe seaway, a new "free-to-broach" towing rig will be developed. This rig will allow models of a series of existing and proposed new fishing boat designs to be investigated for capsizing resistance while being towed under computer control to a region of the tank where computer-generated irregular waves are combined with deterministic steep waves produced by wave energy concentration (Salsich 1983a, Duncan 1987, Takaishi 1994, Buckley 1994, Kriebel 2000 and several methods presented at the Rogue Wave 2000 conference). This technique avoids using radio-controlled models which are difficult to position precisely in capsizing wave conditions. It should also be useful for validating attempts to mathematically model the surf-riding phenomenon (Vassalos 1994). Towing models in quartering seas should shed light on the dynamic stability characteristics of several classes of fishing vessels, improving on the zero-speed beam-sea capsize testing previously done at the Naval Academy on sailing yachts (Salsich 1983b, Zseleczky 1988) and the USCG 44 ft and 47 ft Motor Life Boats (Zseleczky 1989).

It is expected that the effects of variations in length, beam, draft, freeboard, sheer line, bulwark and deckhouse arrangements and loading conditions can be correlated with a new set of design parameters for increasing fishing boat safety in a variety of situations (Boccadamo 1994).

References:

Belenky, Vadim L. 2001. Seventh International conference on the Stability of Ships and Ocean Vehicles (STAB' 2000) – A Review, *Marine Technology*, Vol. 38, No. 1 January 2001, pp. 1-8.

Bird, H. and Morrall, A. 1986. Research Towards Realistic Stability Criteria, *Proceedings of the International Conference on the Safeship Project: Ship Stability and Safety*, RINA, London 9-10 June 1986.

Blume, P. 1993. On Capsize Model Testing, *Proceedings of the U. S. Coast Guard Vessel Stability Symposium, New London*, CT, March 15-17, 1993.

Boccadamo, G., Cassella, P, Russo Krauss, G, and Scamardella, A. 1994. Analysis of I.M.O. Stability Criteria by Systematic Hull Series and by Ship Disasters, *Proceedings of the 5th International Conference on Stability of Ships and Ocean Vehicles (STAB 94*), Melbourne, Fl. USA.

Boccadamo, G., Cassella, P., and Scamardella, A. 2000. Stability, Operability and Working Conditions on Board Fishing Vessels*, Proceedings of the 7th International Conference on Stability of Ships and Ocean Vehicles (STAB 2000),* Launceston, Tasmania, Australia, 7-11 February 2000.

Bonmarin, P. and Ramamonjiarisoa, A. 1984, Deformation to Breaking of Deep Water Gravity Waves, *Experiments in Fluids*, vol 2, pp. 1-6.

Bonmarin, P., 2000, Some Geometric and Kinematic Properties of Breaking Waves, *Proceedings of the Rogue Wave 2000 Conference*, Brest, France, November 29-30, 2000.

Buckley, W. H., 1994. Stability Criteria: Development of a First Principles Methodology, *Proceedings of the 5th International Conference on Stability of Ships and Ocean Vehicles (STAB 94)*, Melbourne, Fl. USA.

Claughton, A. and Handley, P 1984, An Investigation into the Stability of Sailing Yachts in Large Breaking Waves, *University of Southampton Ship Science Report No. 15*, January 1984.

Cleary, W. 1993. The Regulation of Ships Stability Reserve, *Proceedings of the U. S. coast Guard Vessel Stability Symposium*, New London, CT, March 15-17, 1993.

Dahle, E. A., and Myrhaug, D., 1995. Risk Analysis Applied to Capsize of Fishing Vessels. *Marine Technology*, Vol. 32, No. 4, October 1995, pp. 245-257.

Deakin, B., 2001, Model Tests to Study Capsize and Stability of Sailing Multihulls, *Proceedings of the 15th Chesapeake Sailing Yacht Symposium*, Annapolis, MD January 26-27, 2001.

deKat, Jan O, 1999, Dynamics of Vessel Capsizing in Critical Wave Conditions, *Proceedings of the Workshop on Safety of Ocean Racing Yachts*, Sydney, 28 March 1999, pp 83-90.

Duncan, J. H., Wallendorf, L. A. and Johnson, B., 1987, An Experimental Investigation of the Kinematics of Breaking Waves, *Proceedings of the IAWR Seminar on Wave Analysis in Laboratory Basins*, 1-4 Sept. 1987, pp. 411-422.

Dyer, M. G., 2000. 'Hazard and Risk in the New England Fishing Fleet', *Marine Technology*, Vol. 37, No. 1, Winter 2000, pp. 30-49

Grochowalski, S., 1989, Investigation into the Physics of Ship Capsizing by Combined Captive and Free-Running Model Tests. *SNAME Transactions,* 1989 pp 169-212

Grochowalski, S., 1993. Effect of Bulwark and Deck Edge Submergence in Dynamics of Ship Capsizing. *Proceedings, US Coast Guard Vessel Stability Symposium*, New London, Connecticut, USA. March 1993.

Grochowalski, S., Hsiung, C. C., and Huang, Z. J. Development of a Time-Domain Simulation Program for Examination of Stability Safety of Ships in Extreme Waves. *Proceedings, International Conference on Ship and Marine Research*, NAV '97 Naples, Italy, March 1997.

Johnson, B., Wallace, D., Womack, J. and Savage, R. 2000, Developing the Foundation for an Interdisciplinary Approach to Improving Fishing Vessel Safety, *Proceedings of the IFISH Conference*, Woods Hole, MA, October 25-27, 2000

Johnson, B. 2000, Capsize Resistance and Survivability When Smaller Vessels Encounter Extreme Waves, *Proceedings of the Rogue Wave 2000 Conference*, Brest France, 29-30 November 2000

Kirkman, K., 1983 On the Avoidance of Inverted Stable Equilibrium, *Proceedings of the AIAA/SNAME Ancient Interface XIII*, 1983.

Kobylinski, L. 1994. Methodology of the Development of Stability Criteria on the Basis of Risk Evaluation, *Proceedings of the 5th International Conference on Stability of Ships and Ocean Vehicles (STAB 94)*, Melbourne, Fl. USA.

Kobylinski, L. 2000. Stability Standards - Future Outlook, *Proceedings of the 7th International Conference on Stability of Ships and Ocean Vehicles (STAB 2000)*, Launceston, Tasmania, Australia, 7-11 February 2000.

Kriebel, D. L. and Alsina, M. V. 2000 Simulation of Extreme Waves in a Background Random Sea, *Proceedings of the Tenth International Offshore and Polar Engineering Conference*, Seattle, USA, May 28-June2, 2000.

Mundle, R. 1999, *Fatal Storm: the Inside Story of the Tragic Sydney-Hobart Race*, International Marine /McGraw-HIll, 1999.

Myrhaug, D. and Kjeldsen, P. 1983, Parametric Modeling of Joint Probability Density Distributions for Steepness and Asymmetry in Deep Water Waves, *Journal of Coastal Engineering*, Amsterdam, 1983.

Olagnon, M and van Iseghem, S., 2000, Some cases of observed rogue waves and attempts to characterize their occurrence conditions, *Proceedings of the Rogue Wave 2000 Conference*, Brest France, 29-30 November 2000.

Principles of Naval Architecture (PNA 1988) Volume 1, SNAME, 1988, pp 87-93.

Renilson, M., Binns, J. R., and Tuite, A. 2001, The Re-Righting of Sailing Yachts in Waves – A Comparison of Different Hull Forms, *Proceedings of the 15th Chesapeake Sailing Yacht Symposium*, Annapolis, MD January 26-27, 2001.

Salsich, J. O., Johnson, B., and Holton, C. 1983a, A Transient Wave Generation Technique and Some Engineering Applications, *Proceedings of the 20th American Towing Tank conference*, 1983

Salsich, J. and Zseleczky, J. J. , 1983b, Experimental Studies of Capsizing in Breaking Waves, *Proceedings of the AIAA/SNAME Ancient Interface XIII*, 1983.

Takaishi, Y., Dangerous Encounter Wave Conditions for Ships Navigating in Following and Quartering Seas, *Proceedings* of the 5th International Conference on Stability of Ships and Ocean Vehicles (STAB 94), Melbourne, Fl. USA

Umeda, N., and Ikeda, Y., 1994. Rational Examination of Stability Criteria in the Light of Capsizing Probability, *Proceedings of the 5th International Conference on Stability of Ships and Ocean Vehicles (STAB 94*), Melbourne, Fl. USA.

Umeda, N., Matsuda, A., Hamamoto, M, and Suzuki, S. 1999. Stability Assessment for Intact Ships in the Light of Model Experiments. *J. of Marine Science and Technology*, SNAJ, Japan, Vol. 4, pp 45-57, 1999.

Umeda, N. and Matsuda, A. 2000. Broaching in Following and Quartering Seas - Theoretical Attempts and New Prevention Device, *Proceedings of the 7th International Conference on Stability of Ships and Ocean Vehicles (STAB 2000*), Launceston, Tasmania, Australia, 7-11 February 2000.

USCG 1986. Proposed Voluntary Stability Standards for Uninspected Commercial *Fishing Vessels, Navigation and Vessel Inspection Circular NVIC 5-86*, 1986.

USCG 1999. Dying to Fish: *Fishing Vessel Casualty Task Force Report*, USCG, March 1999.

Vassalos, D. and Maimun, A. 1994. Broaching-To: Thirty Years On, *Proceedings of the 5th International Conference on Stability of Ships and Ocean Vehicles (STAB 94),* Melbourne, Fl. USA.

Zseleczky, J. J., 1988. Evolving Methods for Estimating Capsize Resistance in Breaking Waves. *Proceedings of the SNAME New England Sailing Yacht Symposium,* New England, March 1988.

Zseleczky, J. J. and Cohen, S. H. 1989, Model Tests to Evaluate the Capsize Resistance of a Motor Lifeboat in Breaking Waves, *Proceedings of the 22nd American Towing Tank Conference*, St. Johns, Newfoundland, 1989.

5TH INTERNATIONAL WORKSHOP

STABILITY AND OPERATIONAL SAFETY OF SHIPS

Trieste, Italy, 12-13 September 2001

Paper: **Fishing Vessel Design in a Regulation Driven Environment**

Authors: Richard Birmingham and Rod Sampson

Contact: Dr. Richard Birmingham
Department of Marine Technology
The University of Newcastle
Newcastle upon Tyne
England NE1 7RU

Tel: 0191 222 6722
Fax: 0191 222 5491
E-mail: R.W.Birmingham@ncl.ac.uk

Fishing Vessel Design in a Regulation Driven Environment

Richard Birmingham and Rod Sampson
The Department of Marine Technology, the University of Newcastle upon Tyne, UK.

Dr. Richard Birmingham is a Senior Lecturer in Small Craft design in the Department of Marine Technology at Newcastle University. His research interests include stability of working craft, and the application of Formal Safety Assessment methods in the design of lifeboats and high speed craft.

Mr Rod Sampson is a student in the Department of Marine Technology at Newcastle University, and will be graduating in July 2001. Rod Sampson also has ten years experience as service technician aboard cruise liners.

ABSTRACT

Many newly constructed and currently operating fishing vessels appear to have been designed with disregard for much of the naval architect's conventional wisdom as to what constitutes a sound, sensible and safe design. In this paper recent designs will be examined in the context of the rapidly changing regulatory and legislative framework that controls the fishing industry, and the difficulties in obtaining satisfactory stability characteristics will be considered. In analysing recent safety records no evidence is found to suggest that the new vessels are less safe than more traditional forms, but it is observed that turbulence in the regulatory framework in which they operate may be contributing to the lack of progress in improving safety.

Abbreviations

DETR:	Department of Transport Environment and the Regions
FISG:	Fishing Industry Safety Group
FQA:	fixed quota allocation
FAS:	formal safety assessment
ITQ:	individual transferable quota
MAFF:	Ministry of Agriculture Fisheries and Food
MAIB:	Marine Accident Investigation Branch
MCA:	Maritime and Coastguard Agency
SFIA:	Sea Fish Industry Authority (Seafish)
TAC:	total allowable catch
VCU:	vessel capacity unit

Introduction

Regulations that are intended to ensure the sustainability of the fish stock in European waters have resulted in new vessels that have some extreme characteristics. These 'rule beaters' appear to go against the natural instincts of the naval architect. The impact of rules on the design of vessels has often been unexpected. Rules and

regulations designed with one aspect of performance in mind, can unwittingly lead to undesirable characteristics being favoured in other unrelated aspects. In his analysis of the Fastnet disaster of 1979 Marchaj [1] details how the rating rule applied to the yachts of the time unintentionally penalised stability, as a rule that was intended to ensure fair competition between racing yachts in practice compromised safety. This paper will consider how a similar phenomenon has developed in the fishing vessel fleet, and how it has influenced the stability characteristics of modern fishing vessels.

The Design of Fishing Craft and the Role of Regulations

In recent years the major factor impacting on the evolution of the design of fishing vessels in the UK has been the introduction of increasingly complex and demanding regulations for the control the fishing industry. Fishermen may work in dangerous waters, but it is turbulence in the regulatory framework that taxes the skill of the designers of these craft.

The latest additions to the UK fishing fleet are characterised by extreme length to beam ratios (often around 2.5 and on occasion as little as 2.1 in determined 'rule beater' designs) and exaggerated length to draught and depth ratios. The underwater form is exceptionally full, with the above water profile a towering rectangular slab above which perches the wheelhouse. These are the vessels that fishermen are having built today, so they must be successfully meeting their requirements. However they are a stark contrast to the traditional style of craft, and to new vessels being built in other parts of the world. In these vessels it is clear that the usual physical requirements driving the design process have been overwhelmed by the influences of the fishing regulations. When unconstrained by regulations the designer produces a hull that is moderate in all aspects: length to breadth ratios of between 3 and 4 and fine form coefficients minimise resistance when free running and enhance seakeeping performance, and a moderate superstructure height reduces windage and improves stability. Although the safety record of these vessels cannot be questioned without further work to produce relevant detailed data, it is clear that the crew of a vessel with poor seakeeping characteristics, and therefore high accelerations, will work less effectively than the crew of a more seakindly boat. In addition the working areas of these modern boats include the extreme ends of the vessels where the motions are greatest, areas that would normally be left void or used for storage in a more conventional craft. The control position is also at a far greater distance from the centres of rotation than on traditional craft, which must also impact on the crew's effectiveness. The skipper and crew would operate more happily, effectively and safely on a vessel that responded in a more orderly manner to the sea, and that was arranged with a higher priority on crew comfort.

These new style vessels are the result of an on-going tussle between the regulators, who impose the rules, and the fishermen who respond, often in unanticipated but strategically sound ways. It is the work of the naval architect to interpret these moves and counter moves as design constraints, with each new vessel being a record of the current state of play and an indicator as to the extent to which the design of fishing vessels is being driven by politically and environmentally inspired regulations rather than by physical requirements.

The Regulatory Control of the Fishing Industry

Fisheries are a totally free naturally occurring resource. Experience has demonstrated that the un-restricted use of such a common resource will lead to its over use and gradual decline, defined by Hardin as 'the tragedy of the commons' [2]. He states that each fisherman will consider their own interests and forsake the broader social costs, with the inevitable result being over capitalisation in the industry, excessive harvest and eventually stock depletion. A similar sentiment was outlined by Gordon [3]: "There appears to be some truth in the conservative dictum that everybody's property is nobody's property. Wealth that is free for all is valued by no one because he who is foolhardy enough to wait for it's proper time of use will only find that it has been taken by another… The fish in the sea are valueless to fishermen, because there is no assurance that they will be there for him tomorrow if they are left behind today". The truth of these observations made in the middle of the last century are self evident today, and the fulfilment of the prophecies is quite simply that we have too many fishing boats chasing too few fish.

If the seas are to be fished in a sustainable way then the organisation of the industry, the number and types of vessels, the way they are operated, and the way the catches are processed and monitored will all have to change. The regulations are therefore concerned with an orderly process of change management. Such a process will always be criticised as it is impossible to satisfy all parties in a time of transition, and it may even be impossible to completely satisfy any party. Given the fragmented nature of the problem it is not surprising that attempts to regulate this industry have been complex, and often unpopular with sections of it. A broad overview of the current regulatory framework can be found in the references [4], with the briefest of summaries provided here.

As with other vessels of all types fishing vessels have a long established procedure for validating that they are built and operated to recognised standards of safety. In the UK two bodies, the SFIA and the MCA, oversee the three safety elements of vessel structure, equipment and crew competence. In recent decades these safety-orientated regulations have been augmented by the measures intended to ensure the sustainability of the fisheries, and to manage the changes necessary to achieve that end. Two types of control have therefore been introduced, those to limit the total catch and so ensure conservation of stocks, and those to manage the reduction in fishing effort and so minimise the social and economic disruption due to the structural changes necessary in the industry. Both of these types of control are the responsibility of the MAFF. Here the way in which these three organisations regulate the industry will be examined in broad terms as the complexity and dynamic nature of the controls makes a detailed description inappropriate here. It is also unnecessary as the intention is not to describe the controls themselves, but to examine their nature and so obtain some insight into their interaction with the safe design of fishing vessels, and in particular the impact in their stability characteristics.

In the context of safety the SFIA acts as a Classification Society for the construction of fishing vessels, publishing scantling rules and employing surveyors to oversee the construction of fishing vessels. These guidelines cover both the hull construction and essential equipment. It also promotes crew training through the development of

courses and the provision of bursaries [5]. The Maritime and Coastguard Agency (MCA) is concerned with all aspects of marine safety. It has a long standing Code of Practice for Fishing Vessels over 12 metres and recently created a Code of Practice for vessels under 12 metres. These Codes consists of a checklist of safety equipment plus a written risk assessment that covers the operation of the vessel, watertight and weather tight integrity, stability, machinery, fire protection and fire prevention. The under 12 metre Code allows for self-certification by the owner but also requires a regular verification inspection by the MCA. The Ministry of Agriculture Fisheries and Food, MAFF, controls both the total amount of fish caught, and the catching capability of the fleet, through a license scheme. The right to fish is dependent upon possession of a licence appropriate to the type of vessel and the species targeted. The licensing scheme has developed considerably in breadth and complexity and the current licence structure limits not only the total number of vessels but also their size and power and the extent to which effort can be shifted between target stocks and between fishing methods. The licences have three elements: the authorisation to fish; the catch entitlement, or quota; and the allowable fishing capability expressed in vessel capacity units, VCUs. Since licence entitlements are transferable between ownerships and are restricted in number an active market in all three elements of the licences has developed [6].

Before exploring how the various regulations have impacted on the design of fishing vessels both the quota concept, and the measure of fishing capability (the VCU) can be considered further. The quota associated with a license is one small part of the total allowable catch (TAC) agreed by the EU for the waters of the member states of the EU. The Community shares fishing opportunities in the form of quotas among Member States [7]. Member states allocate their national quota in different ways, the UK having moved from an allocation based on a vessel's track record to a fixed quota allocation (FQA) that can be traded to a limited extent. (An alternative procedure referred to as the individual transferable quota (ITQ) has been introduced successfully in both New Zealand [8] and Iceland [9]. ITQs effectively make the fishermen owners of a share of the resource and so they encourage the fishermen to regulate fishing effort and protect stocks as they have an annual claim on the harvest. Catching rights expressed by ITQs are analogous to territorial interests held by farmers and their tenants in that they form part of their property [10]. The advantages and disadvantages of the various methods of quota allocation are discussed in detail by Symes [11].)

The measures of fishing capability, or capacity, vary between the member states, some adopting the units used at the EU level, these being a combination of engine power and tonnage. In the UK a system based on length was replaced by the vessel capacity unit, the VCU, in 1990. This followed research by the SFIA aimed at identifying the most appropriate measure of fleet capacity, and concluding that the unit should comprise the sum of the deck area and a percentage of the engine's maximum continuous rating [12], calculated thus:

$$VCU = \{\text{length (m)} \times \text{breadth (m)} + 0.45 \times \text{engine power (KW)}\}$$

Fishing craft designed to maximise their fishing capability while minimising the measured VCU are referred to as 'rule beaters'. Both halves of the above equation impact on the design of such craft. The dimensional constraints have a significant impact on the appearance of these craft, and on their stability characteristics.

Design Impact of the Licensing System

'Rule beaters' are vessels designed to flout the spirit of a set of rules, but succeed in being both legitimate and profitable by strictly following the letter of the regulations. The classification societies, and others concerned with safety-focussed rules, have long been aware that any specified requirement is not treated as a minimum, but as a design target. Similarly where different sets of rules apply to different classes of vessel it is common practice to try to gain advantage by squeezing a vessel into the most economical class, even if it is inappropriate for the vessel's true function. In the regulation of fishing vessels both of these phenomenon have long been apparent. Fortunately the robust scantlings required of these workboats have negated the impact of any tendency to 'design down'. The application of different sets of rules to different sizes of vessels has however caused a noticeable bunching of the fleet at the relevant break points, whether they be specified in terms of length or displacement, with many more vessels being built just below the defined break points (such as 12 meters and 24 meters for the scantling rules) and almost none being built in a range above these points. Some of the vessels built just below such break points could be defined as rule beaters, but in these cases the financial savings made by staying in a lower class are limited, and other efficiency losses soon outweigh them. The imposition of these rules therefore distorts the fleet profile, but does not have a significant impact on the design of individual vessels.

This contrasts markedly with the impact of regulations intended to control the catching capability of individual vessels, and of the fleet, and with the impact of the alternative methods of enforcing individual, local and national quotas. In these cases the break point between different regulations may not simply result in an increase in equipment and manning costs, but may determine where, when and how the fisherman is allowed to fish, or even if he can fish at all. The impact on the earning ability of the vessel can be dramatic, or even catastrophic. In this environment it is not surprising that rule beaters are not simply pushing the limits of conventional design, but dramatic departures that test the expertise and integrity of the naval architect.

The introduction of the VCU as a measure of fishing capacity, and as a way to control the overall fishing effort of the UK fleet is the prevailing design driver of the present time. However the regulatory framework is in a constant state of development, or evolution, with significant changes anticipated in 2002 [13], so the lessons to be learned from the present case are essentially concerned with regulation development, not vessel design. Measuring fishing effort with the current VCU formula has resulted in an unanticipated development of the fishing vessel form. Constrained by the 'deck area' (defined as length by breadth) the designer seeks to maximise the displacement and volume of the vessel. Maximising displacement enables heavier equipment to be installed, and more fuel and fish to be carried, while maximising volume allows an increase in accommodation and areas for working with the gear and catch. As a result the actual catching capability can be considerably greater than that indicated by the measured VCUs. As neither depth nor draught are controlled displacement is maximised by increasing draught and increasing the fullness of the form, especially forward. Volume is maximised by increasing freeboard and making the actual deck area fill as much of the measured area as possible, so wide transoms and exceptionally bluff bows are used. In some cases the entire deck, from transom to stem, is utilised as

the working area, with no forecastle and with the wheelhouse located over the working deck, the nets being hauled forward beneath it. The dimensional constraints are only one half of the VCU formula, with the other half being the engine power. Rule beating in this area results in maximising the diameter of the propeller and placing it in a nozzle, and introducing additional power packs for auxiliary requirements, so reserving all the rated power from the main engine for driving the vessel. De-rating the engine is also practiced, but if this is to be effective the engine must be returned to full power after measurement, which is clearly an illegal case of cheating the rules, and not a legitimate rule beating procedure.

The current type of rule beater is found at its most extreme in the smallest vessels, with a measured length of less than 10 meters. This is because the artificial constraints imposed by the VCU system have been further exaggerated in recent years by the system of allocation of quota. Vessels below this break point have not been allocated an individual quota, but have been free to fish until such time as the allowable catch was reached nationally, at which point the fishery was closed, even to these vessels. This regulatory regime encouraged fishermen to nominally down size from larger vessels in order to enter this relatively unregulated sector of the fleet. The resulting vessels have the capability in terms of crew size, gear handling, endurance, and stowage, of a more traditional vessel of perhaps 15 meters. A schematic of the type is shown in Figure 1, with the extreme geometry associated with these vessels demonstrated by way of a computer model in Figure 2.

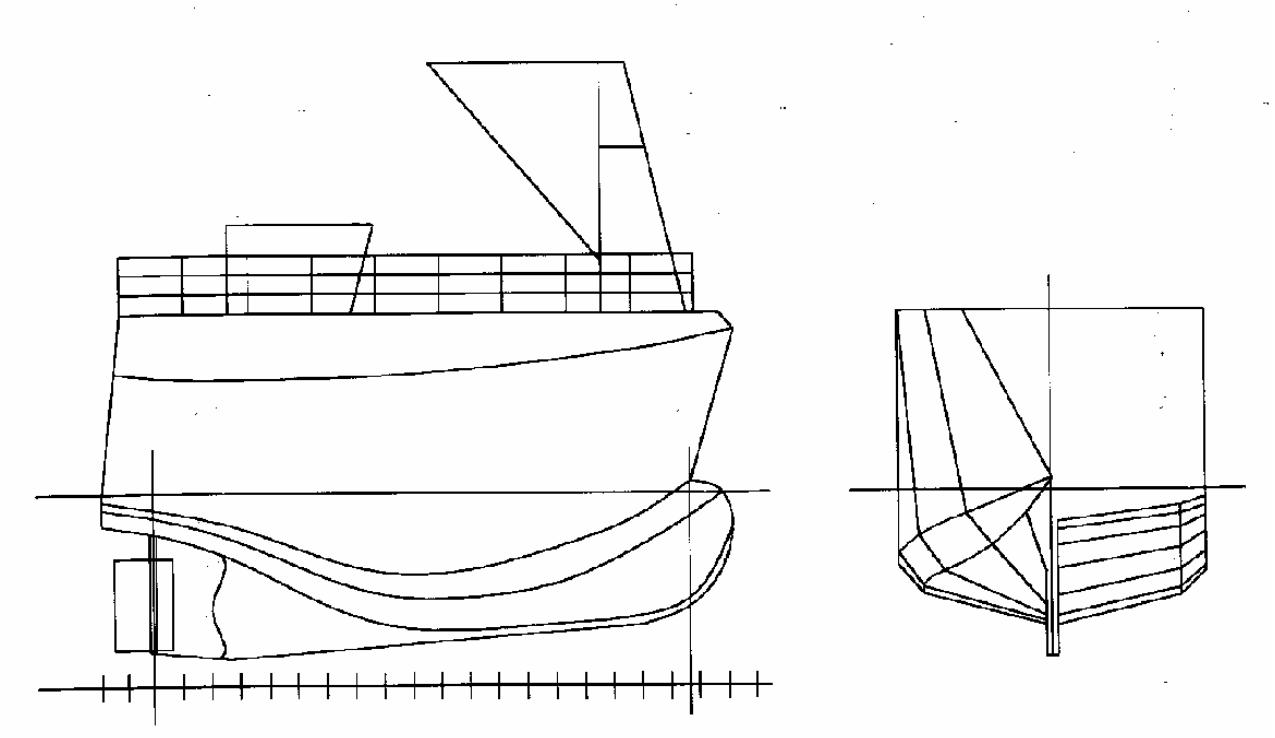

Figure 1: Sketch of under 10 meter Rule Beater

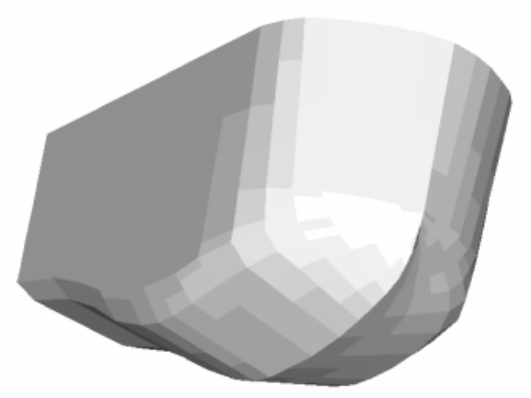

Figure 2: Computer model of under 10 meter Rule Beater

Stability Implications

Fishing vessels intended to have maximum fishing capability for the minimum of measured VCU, 'rule beaters', are designed to have the largest possible displacement and enclosed volume while constraining their planform area, as given by the product of length and breadth. This combination of design goal and constraint inevitably leads to an increase in the depth of the vessel, as once the ends of the vessel have been filled out the only way to increase volume is by enlarging the vessel vertically. This is one of the distinctive characteristics of these designs, their high profile and raised control position.

Increasing the depth inevitably raises the centre of gravity of the vessel, but this is further exaggerated as much of the heavy equipment necessary for fishing operations is located on the main working deck. Raising this deck moves items such as the winches, power block and net storage higher on the vessel. The inevitably high vertical centre of gravity forces the designer to increase the beam of the vessel in order to regain an acceptable value for GM, so giving rise to the second distinctive characteristic of the rule beater designs, their very low length to beam ratio. However the designer may find that simply increasing the beam of the vessel is not an adequate solution to the stability difficulties caused by the high vertical centre of gravity. In the first place there is a limit to how low the length to beam ratio can be allowed to go. In the under 10 metre vessels extreme cases can be found of 2.1, but for larger vessels this would impact too severely on the powering requirement for the vessel. However even if other factors do not restrain the designer from increasing the beam even further stability derived in this way enhances stability at low angles of heel, but reduces it at moderate and high angles. The resulting GZ curve is typical of form stable craft, with the maximum value of GZ at a very low angle. Fishing vessels relying on beam to compensate for their high vertical centre of gravity have difficulty in satisfying the IMO stability criteria, due to the reduction in righting lever as heel angles increase.

The only solution for the designer in this case is to moderate the characteristics of a form stable craft by adding ballast, so bringing back down the centre of gravity until a satisfactory GZ curve can be obtained. This is a most unsatisfactory solution as the designer wishes to reserve all the available displacement for increasing the size of

machinery and other equipment, for carrying fuel, and of course for maximising size of catch that can be stored. Placing permanent ballast in the box keel reduces the deadweight of the vessel, but even so up to 10% of the displacement is utilised for ballast on some of these vessels, this being the only way to obtain satisfactory stability characteristics. This design path is not always successful. Increasing ballast increases the draft of the vessel, which inevitably reduces the height of the metacentre, and may also force the designer to increase the height of the decks yet again, so entering a spiral that moves ever further from an acceptable design solution.

However when convergence is achieved the result is the current extreme form of rule beater design, with a low length to beam ratio, a high above water profile, and a deep draft, that includes a large amount of permanent ballast in the keel. Such designs have one further characteristic that can be commented upon. The masses of the vessel are concentrated at either end of the vessel's extreme depth. Ballast and the main engine (which is itself large for the size of vessel due to poor resistance characteristics and the desire to tow the largest possible nets) are located low down in the vessel, while much other heavy equipment, such as the winches and stored nets, are located high up on the working deck. This polarisation of the location of the main masses on the vessel results in a high mass moment of inertia in roll.

Rule Beaters and Safety

To interpret the statistics that are available for fishing vessel incidents [14] in terms of the impact of regulatory distortion on fishing vessel design is not possible. As the impact of the regulations has been manifest in its most extreme form in the smallest sizes of vessel it seems logical to look to the incident rate for different length groups. The figures for losses in 1999 are given in Table 1, and a graphical presentation of all incidents for the same year in Figure 3. In both cases the data suggests that the under 12 meter fleet, where the rule beaters are most extreme, is the safest sector of the fleet. It should be noted that these figures are presented as a percentage of the registered vessels in the relevant fleet and do not take account of the degree of utilisation of the vessels, the actual hours spent at sea. If a utilisation factor were introduced it would clearly present the smallest class in a less favourable light. It is also likely that minor incidents have been under reported for the smaller vessels where record keeping is less rigorous than the formalised procedures implemented on the large crewed vessels. But even if the figures were adjusted in this way little could be concluded with regard to the impact of the safety record of rule beating vessels as these are not differentiated from the more conventional designs.

Fishing Vessel Losses in 1999			
Length	No. Registered	No. Lost	Percentage lost
Under 12 meters	6163	17	0.28
12 – 24 meters	1002	10	1.00
24 meters and over	295	6	2.03
Total Fleet	7460	33	0.44

Table 1: Fishing Vessel Losses in 1999

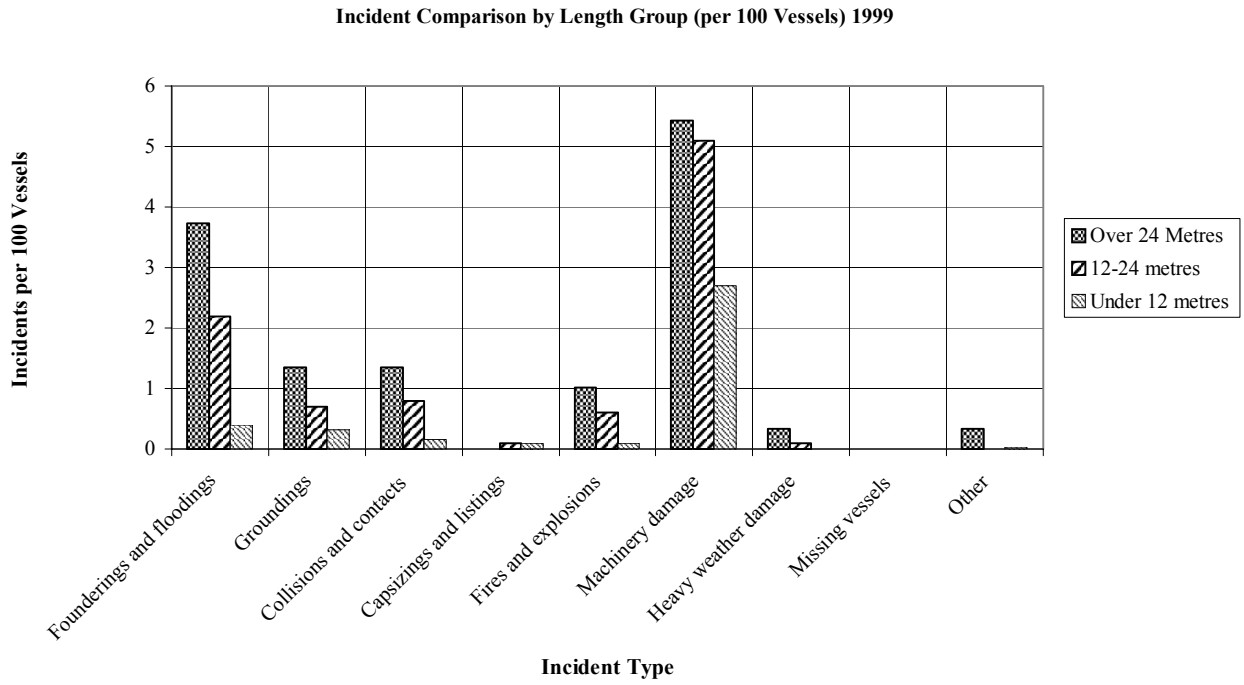

Figure 3. Fishing vessel incidents in 1999

Fishing Vessel Losses Since 1992			
Year	**Total Lost**	**Total on register**	**% Lost**
1992	32	10,953	0.29
1993	38	11,108	0.34
1994	43	10,296	0.42
1995	33	9,337	0.35
1996	26	8,064	0.32
1997	23	7,779	0.30
1998	21	7,605	0.28
1999	33	7,460	0.44

Table 2: Fishing Vessel Losses, 1992-1999

In the fishing industry the imposition of regulatory controls in the form of licenses with catch and capability limits attached, has influenced the fleet in two ways. Firstly, as examined in some detail in this paper, the design of fishing vessels has been driven in unexpected directions. The second effect, which has not been mentioned thus far, is that fishermen have been discouraged from building new vessels. This is because the regulations penalise fleet renewal, whether it be new building to replace older vessels or to aggregate license entitlements (i.e. two smaller vessels are replaced by one larger one). In both cases in order to force a gradual contraction of the total capacity of the fleet a reduction of the VCUs allocated to the license is imposed. Clearly this encourages the fishermen to continue working with older boats for as long as possible as can demonstrated by an analysis of the age of the vessels in the fleet. Over 28% of the fleet is over 25 years old, with the average age of the under 12 meter boats being

28 years, of the 12 to 24 meter boats being 36 years, and of the over 24 meter boats being 40 years [15]. Not only is the fleet old, but it is still aging as the rate of new building is less than half that required to prevent the average age of the fleet increasing further.

The data presented in Table 2 indicates that during the last eight years there is no sign of any improvement in the safety of the fishing fleet. While this could be attributed to many causes it is not unreasonable to suggest that a regulatory regime that discourages the building of new vessels, and encourages the development of extreme characteristics in those vessels that are built, could be one of the main contributors to the safety record.

Conclusion

In this paper the link between the regulations imposed on fishermen and the design of fishing vessels has been examined, and it has been demonstrated that the regulations are driving the evolutionary process in a direction that is unsatisfactory. Without the artificial regulatory constraints vessels could be designed that are fundamentally more appropriate for their purpose. However the fishing industry has to change as it is an undeniable fact that there are too many boats competing to catch too few fish. The industry must recognise that the mission of all fishing vessels has changed, and that they are no longer hunters, but harvesters of a crop. Farmers can reap the corn with a combine harvester, or a tractor, or simply use a scythe, and in different parts of the world all methods can be found. The appropriate technology has to be identified to harvest the resources of the sea in the waters of the UK and Europe. The rules that are regulating the size of the catch, and that are managing the structural changes in the industry, are in a continual state of development due to the complexity of the political, technical and ecological environment in which they operate. If future developments of these rules can be framed in a permissive format, the development of the fleet in future may not conflict with established naval architectural practice [16].

It is surprising that the type of craft described in this paper are economically viable, as the lower fuel efficiency (due to non-optimal hull forms and excessive windage) combined with the potentially reduced opportunity for fishing (due to non-optimal seekeeping characteristics) should be detrimental to the vessels profitability. However the popularity of the under 10 meter rule beaters attests to their commercial success. One reason for this is that these particular boats have been operating in a quota regime that does not include an allocation to each individual boat. A skilful fisherman with a highly efficient vessel can therefore take a disproportionate percentage of the total catch. Expensive but effective fishing operations undertaken over a brief period are more profitable than a more economical less intensive operation if there is effectively a race to grab the allowable catch. Once the fishery is closed both types of vessel are tied up, or turn to alternative sources of income.

It should not be forgotten however that the economic environment that favours all the rule beater designs is entirely artificial, and could be turned on its head by the introduction of slight modifications to either the regulations for capacity measurement, or for quota allocation. With their inefficient use of human and fossil resources an accurate cost benefit analysis of the contribution that these vessels make

to society would demonstrate that short term individual benefit continues to dominate long term societal interests. If the result of this skewed logic is simply that excessive fuel is being used to catch the permitted quantity of fish, or that expensive capital equipment is unused for extended periods of time, perhaps it is an acceptable price to pay for ensuring that the structural changes necessary in the fishing industry occur in a relatively orderly fashion. But if the cost of structural change is also being paid in the form of reduced safety standards, then no one in the industry can afford to be complacent. Clearly further research is needed to compare in detail the safety performance of conventional and rule beating designs.

References

1. Marchaj, C.A., *Seaworthiness – the forgotten factor*, Adlard Coles, London 1986.
2. Hardin, G. 'The tragedy of the commons', *Science*, Vol. 62, December 1968.
3. Gordon, H, 'The economic theory of a common property resource: the fishery', *Journal of Political Economy*, Vol. 62, 1954.
4. Sampson, R. *Sustainability and survivability of the fishing industry*, Final Year Project, The Department of Marine Technology, Newcastle University, 2001.
5. Parkin, J.C. *Policy review of the SFIA*, MAFF, London, 1998.
6. Hatcher, A. and Pascoe, S. *Charging the UK fishing industry*, Centre of Economics and Management of Aquatic Resources, University of Portsmouth, 1998.
7. Holden, M. *The common fisheries policy*, Fishing News Books, Oxford, 1994.
8. O'Connor, R. and McNamara, B. 'Individual transferable quotas and property rights – the New Zealand ITQ system', Colloquium on the Politics of Fishing, edited by Gray, T., Newcastle University, 1996.
9. Gissurarson, H. *The Icelandic solution*, The Institute of Economic Affairs, London, 2000.
10. Scott, A. 'Conceptual origins of rights based fishing', Colloquium on the Politics of Fishing, edited by Gray, T., Newcastle University, 1996.
11. Symes, D. *Property rights, regulatory measures and the strategic response of fishermen*, Fishing News Books, Oxford, 1998.
12. Tucker, C.E. *Study of proposed amendments to the UK fishing licensing system*, Seafish Technical Report No. 344, SFIA, 1988.
13. Symes, D. 'Towards 2002: subsidiarity and the regionalization of the CFP', Colloquium on the Politics of Fishing, edited by Gray, T., Newcastle University, 1996.
14. MAIB, 'Statistics 1992 – 1999', *Annual Report 1999*, HMSO, 2001.
15. Select Committee on Agriculture, *Eighth Report*, House of Commons, London, 1998.
16. Birmingham, R. and Sampson, R. 'Safety and Sustainability in the Fishing Industry: a Design Conflict?' International Conference on Small Craft Safety, The Royal Institute of Naval Architects, London, 22 – 23 May, 2001.

NUMERICAL STUDY OF THE DAMAGE STABILITY OF SHIPS IN INTERMEDIATE STAGES OF FLOODING

Dimitris Spanos, National Technical University of Athens, Ship Design Lab., 9 Heroon Polytechniou Av., 15773 Athens, spanos@deslab.ntua.gr
Apostolos Papanikolaou, National Technical University of Athens, Ship Design Lab., 9 Heroon Polytechniou Av., 15773 Athens, papa@deslab.ntua.gr

SUMMARY

The roll behaviour of a passenger/Ro-Ro vessel in intermediate stages of flooding is investigated by use of a ship motion simulation code and comparison with available experimental data. The systematic numerical investigation on the ship's roll response when water enters suddenly into one compartment and the analysis of the obtained results enables a better understanding of the phenomenon. The response of the ship during transient flooding has been found to be quite non-linear and sensitive to the damage opening.

1. INTRODUCTION

The ship's damage stability in waves has attracted increased research interest in the last decade, in the attempt to answer serious questions arising after recent tragic losses of passenger ships. Assisted by the developments in computer hard- and software, more complicated physical phenomena have been addressed towards better understanding the ship's dynamic stability behaviour in damaged condition. The large amplitude motions of a ship in damaged condition under the action of sea waves and her behaviour in marginal stability conditions has been addressed by various researchers, Vassalos [8], Ishida [2], Papanikolaou [5], [7] de Kat [1], etc.

Actually, the set problem is the investigation of the stability behavior of a damaged ship around a stable equilibrium position. This stable position, if any after damage, is generally different from the stable equilibrium in the intact condition, and is the one reached by the ship under the effect of the floodwater.

Therefore the initial stages of flooding, or the transient flooding, is the stage of change of the ship's equilibrium from that of intact to that of the fully flooded ship in terms of damage hydrostatics. But, the path (transition) between these two conditions is not always possible and also not unique. In case of an impossible path the ship reaches another equilibrium, quite different from that of the fully flooded compartment. Even if the transition is possible, depending on the specific characteristics of the damaged ship, the damage opening and the sea condition, the duration of transient flooding changes and so might change the effects on ship's stability. In both cases the stability of the ship is obviously different from that of the fully flooded ship, considered in hydrostatic calculations and should be therefore evaluated separately.

The present study deals with the behavior of a passenger/Ro-Ro ship in transient flooding. The damaged ship motion and flooding simulation code CAPSIM of NTUA-SDL has been employed to estimate the motion of the vessel when the damage opening is suddenly released and water enters into the compartment. The obtained results are compared with available experimental measurements, published by Ma et al [3]. The study has been carried out in the course of validation studies of the numerical code CAPSIM within the EU funded project NEREUS.

2. SIMULATION BACKGROUND

A brief outline of the employed ship motion simulation code CAPSIM and the underlying theory is provided next. More details can be found in [7], [5], [6].

The flooded ship motion simulation code has been developed at the Ship Design Laboratory SDL, of NTUA. It provides an efficient way to predict the motion of the coupled ship and floodwater system. The model is nonlinear allowing the consideration of large amplitude motions and the stability of the vessel in extreme environmental conditions.

The flooded ship is assumed as a two mass system consisting of the intact ship and the flooded water mass. The ship is considered as a rigid body having six degrees of freedom, while the flooded water is approximated by the lump mass concept, namely a mass being concentrated in its center of mass. Floodwater is assumed moving over predefined surface domain [5], having two degrees of freedom. Considering also the change of mass of water in time, a suitable mathematical model for the motion of the inertia system, with nine degrees of freedom, has been formulated and implemented in the numerical code.

The motion of the inertia system is governed by the momentum conservation of the system masses under the action of external forces. The time rate of change of momentum has been suitably formulated considering the full non-linear character to the motion equations. The external forces are mainly the gravity and the exciting wave forces. The wave forces are treated in the framework of potential theory employing a three-

dimension diffraction code, [4]. Non-linear roll viscous effects are assumed to depend on ship's roll velocity by use of the "equivalent linearisation concept" with the proportionality coefficient semi-empirically estimated. Hydrostatic forces are calculated by integration of pressure in the time domain over the instantaneously wetted ship surface, considering incoming waves and caused ship motions, and allowing the capturing of even complicated geometries by proper surface panelling.

The time rate of change of the floodwater has been approached by use of Bernoulli's equation and modified by a semi empirical, weir flow coefficient to account for the local flow effects at the damage opening. This weir coefficient has been estimated to be equal 0.67 following the accumulated experience by validation of a variety of flooding simulations by experimental data.

3. THE STUDIED SHIP

The presently investigated passenger/Ro-Ro ferry has been tested by Ma et al [3]. The ship was studied in model scale 1/60. Her principal particulars are listed in the Table 1 and her body plan is shown in Figure 2.

	Ship	Model
Lpp	120m	2000mm
B	18.8m	300mm
D	10.0	167mm
T	4.8m	80mm
Displ.	5900tn	27kg
KM	9.39m	156.5mm

Table 1. Main particulars

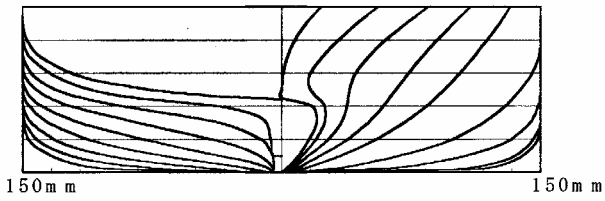

Figure 2. Body plan

There is one compartment in damaged condition extending between stations 4.5 and 6 as shown in Figure 3. Its length is 1/6 of the model length. One rectangular damage opening is located on the compartment's right side having a length according to SOLAS'95 regulations for the study of damage stability by model tests (Res. 14).

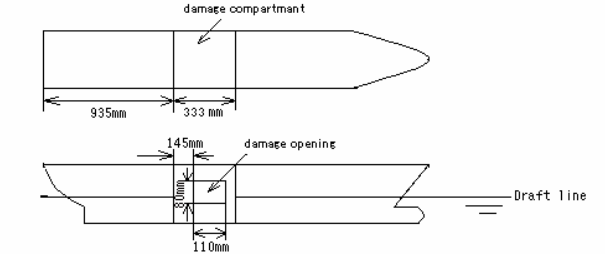

Figure 3. Damage compartment and opening

Two alternative damage compartment arrangements were numerically and experimentally investigated, as shown in Figure 4. Model A and Model B differ only with respect to the existence of a double bottom.

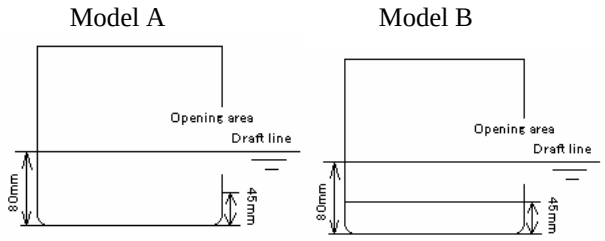

Figure 4. Model arrangements

The lower edge of the damage opening is located 30 mm below the draught line in intact condition for both models, defining the equilibrium position before opening the damage release.

4. SIMULATION RESULTS

The two models A and B described before were investigated in transient flooding using the NTUA-SDL simulation code. Each model is balanced in the intact condition and then suddenly the damage opening is released allowing water to flow into. Under the effect of the floodwater the model performs a roll and a heave decay motion. The model is restrained in the other degrees of freedom following the specifications of the experimental procedure in [3].

Figures 5 and 6 present the response of model A for different values of GM and figures 7 and 8 the results for model B. There are three columns of diagrams. The left one corresponds to the published experimental measurements, the central one to the numerical roll response and the right one to the numerical freeboard. A constant axis scale is used for the calculated results to provide a comparative view of the different GM cases. The same was not possible for the experimental values.

In order to become familiar with these diagrams let us comment one of them, namely the simulated response of Model A with GM=9.6 mm which shows a quite anticipated response. At time equal zero the model balances in intact condition and the damage opening is released. Then water flows into the compartment. The model gradually heels to the opposite side of the opening up to a heeling angle of about 21 degrees. Then the model performs a decay rolling, finally resting around 16 degrees. The corresponding damage freeboard, the distance between the lower edge of the opening and the still water free surface, has an initial value of -30 mm, meaning that water surface exceeds opening edge, at time zero. After resting for about 3 sec then it quickly heels with the opening totally emerging out the water at time 5 sec. The opening does not submerges again, following the decay motion model rests with a lower edge freeboard around 11 mm.

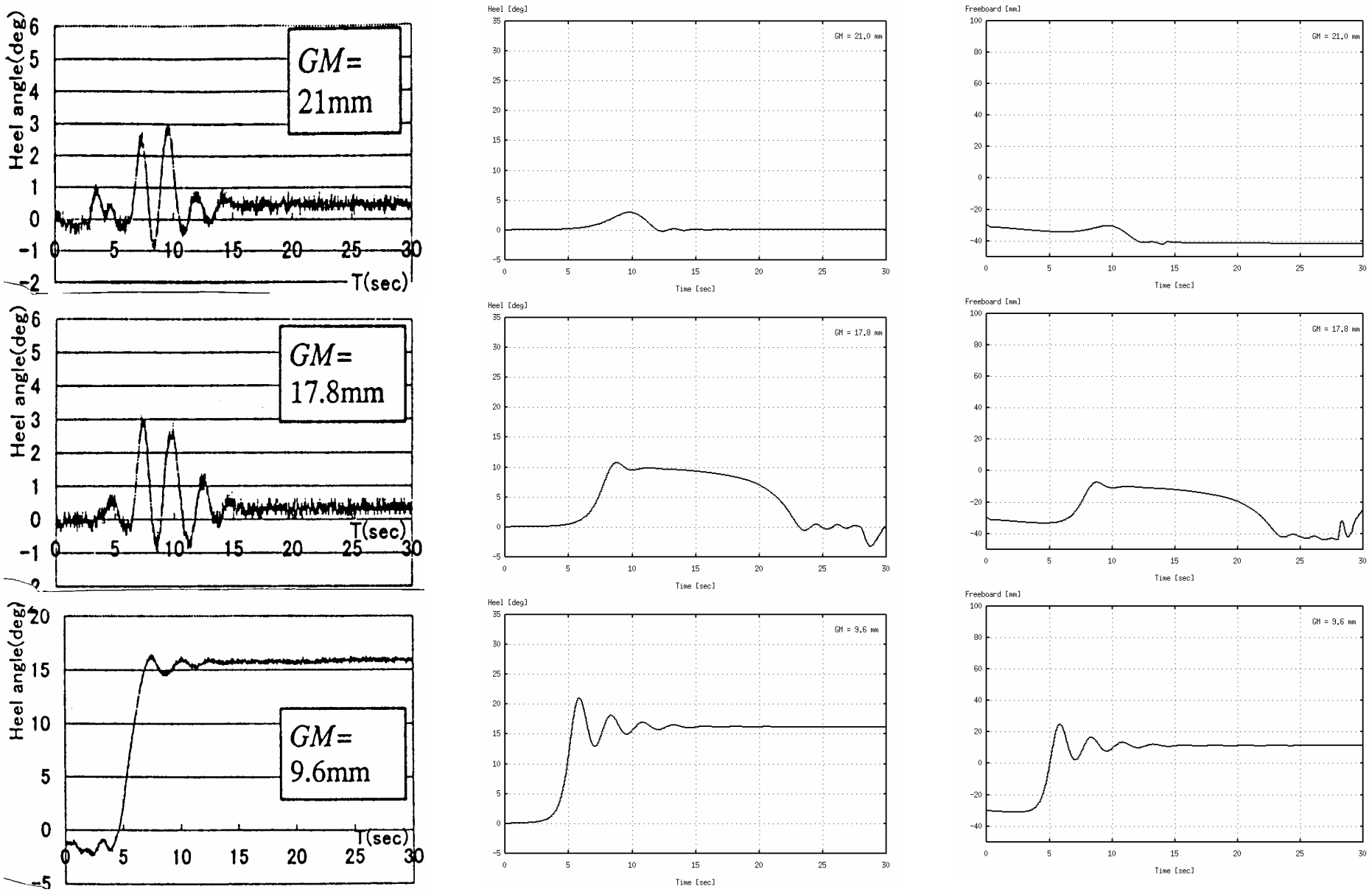

Figure 5. Response of Model A in transient flooding

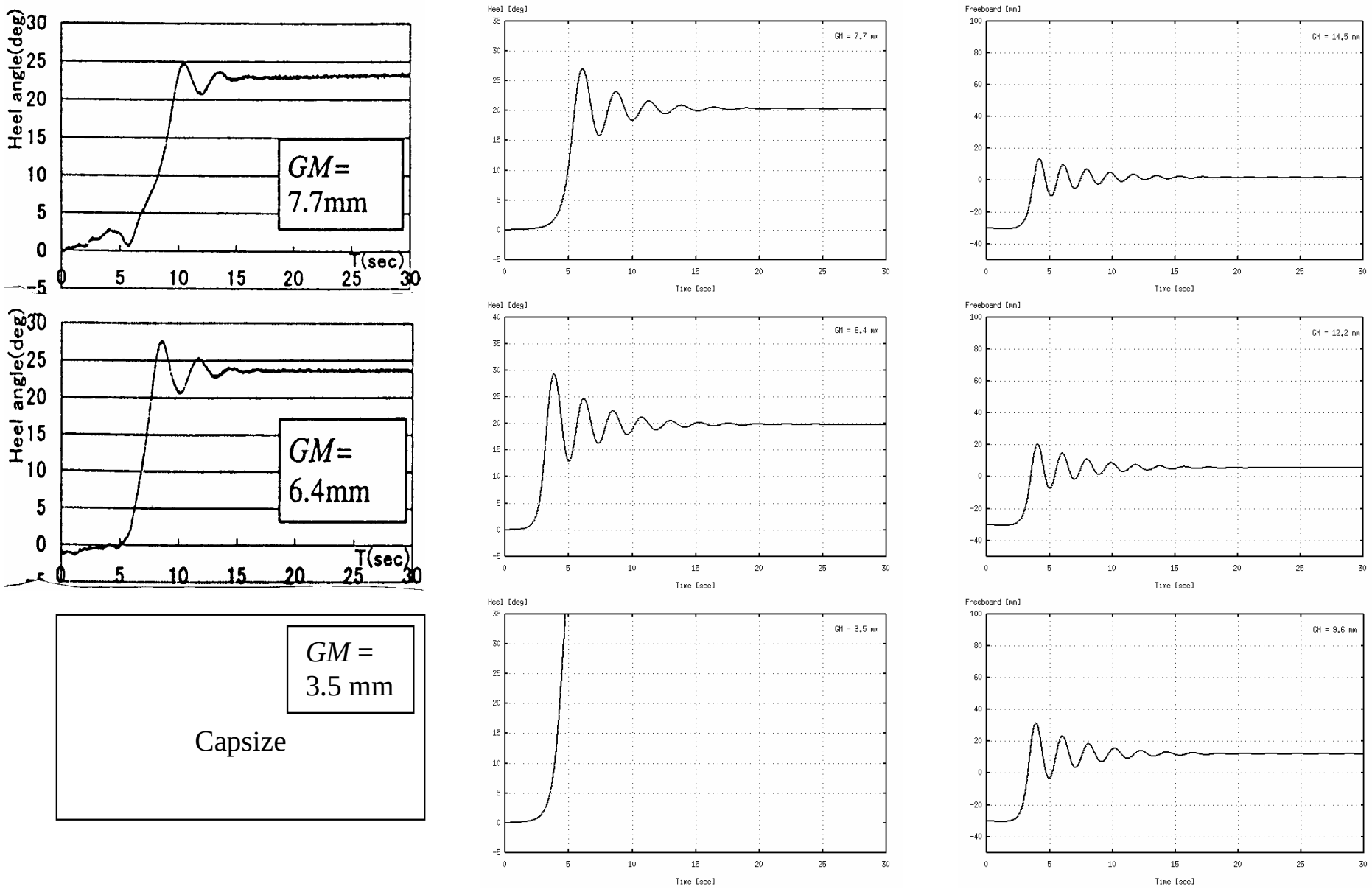

Figure 6. Response of Model A in transient flooding

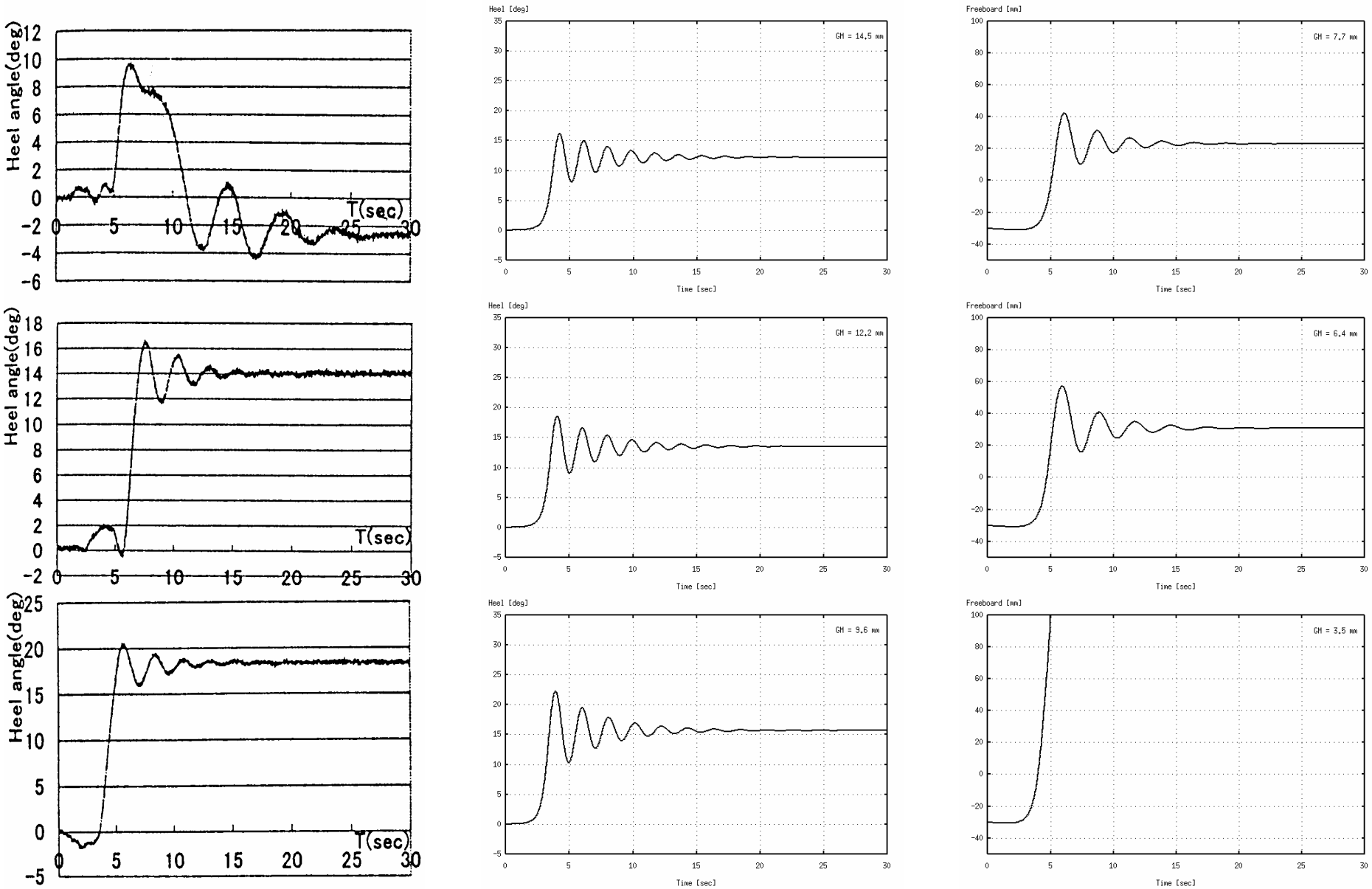

Figure 7. Response of Model B in transient flooding

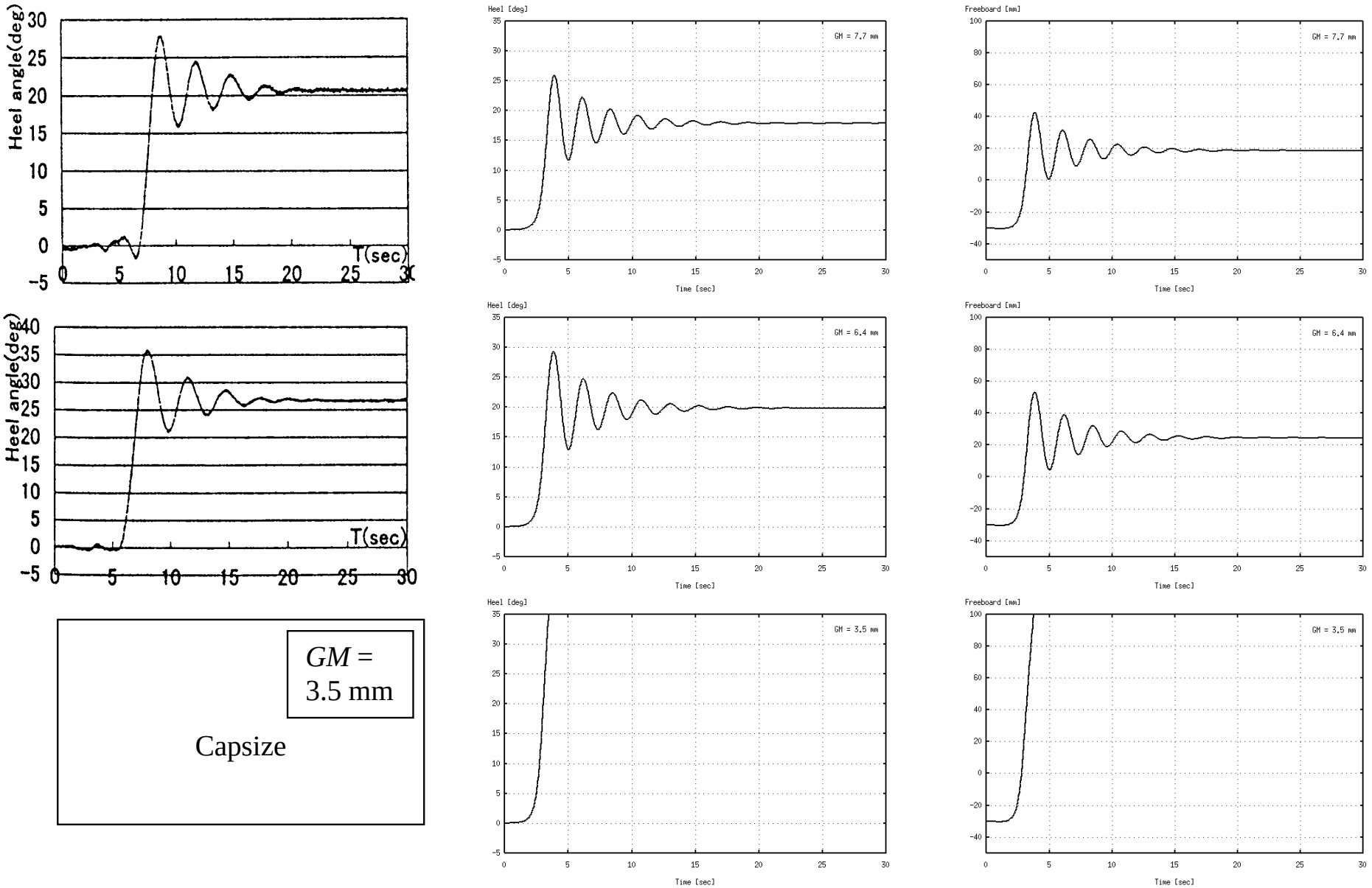

Figure 8. Response of Model B in transient flooding

5. DISCUSSION OF RESULTS

The roll motion results of the vessel in transient flooding, Figures 5 and 6, provide a quite interesting behavior. This presented results concern the behavior of the ship in the initial stages of flooding, in fact of partial flooding. If the damage opening would be extended lower and the water could flood the compartment continuously, then the final position of the damaged model would be unique, namely that resulting by standard stability calculations. The fact that the opening has a certain height, shape and location, is the cause for the partial flooding and the different final positions reached by the model for varying GM values. Therefore the accumulation of water is strongly dependent on the extend, shape and location of the damage opening, and this is the main factor that determines the model behavior.

Regarding the experimental results for the higher values of GM it is observed that the model although it heels some degrees at initial stages of flooding, it finally reduces its heeling angle resting at a quite low heel angle, for model A about half degree opposite and model B about 2.5 degrees against opening. When the GM is reduced the models experience always a finite heeling angle while they capsize for quite small GM value. Numerical calculations show quite similar behavior for the corresponding cases but with partly quantitative differences, which are discussed in the following.

In order to better interpret and understand the behavior of the models A and B the following two diagrams in Figures 9 and 10 respectively, have been prepared.

These diagrams show the equilibrium heel angle of the models, following hydrostatic calculations, as a function of the amount of floodwater into the damage compartment and with parameter KG. For example, in Figure 9, the model A in the presence of 2 kg water inside the compartment obtains an equilibrium stable position at a heeling 15 degrees when the KG=146mm (GM=10.5mm). As a second example, in Figure 10, for the KG=136mm case, the model gradually heels as the floodwater increases, reaching a maximum heel angle about 15 degrees. Then, as the floodwater mass increases for more than about 0.5 kg the ship comes suddenly to the upright position.

These diagrams provide information about the asymptotic behavior of the model, or the heeling of the model if the flooding were quite slow and inertia and hydrodynamic phenomena were absent. During the actual motion, determined by the hydrodynamics of the studied phenomenon, and for a certain amount of floodwater, the model may reach some other heel angle, with its asymptotic equilibrium angle presented in Figures 9 and 10, which can be regarded as the motion attractors when considering the hydrostatic forces as prevailing.

Therefore, taking into account these diagrams, the actual model behavior observed in the experiments can be explained, even for the higher GM values.

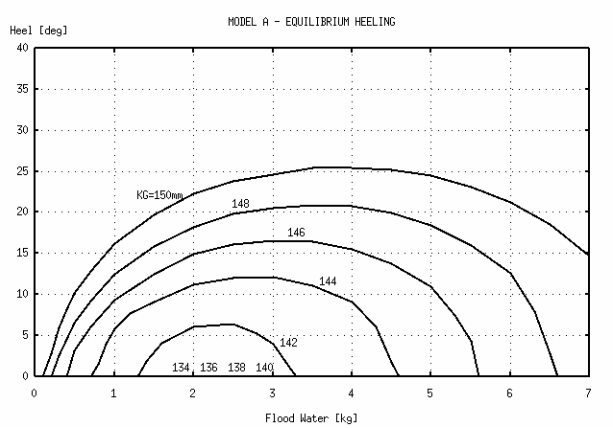

Figure 9. Equilibrium heel angle of Model A

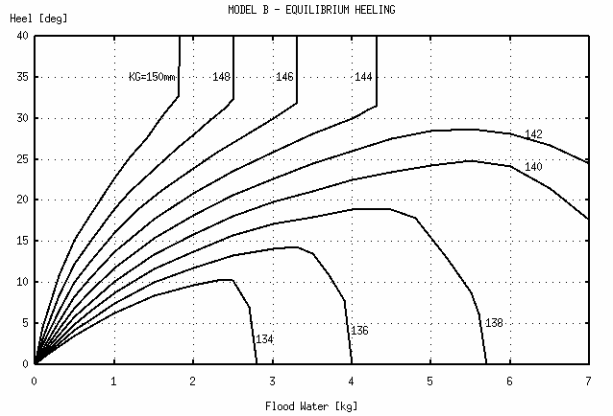

Figure 10. Equilibrium heel angle of Model B

As already stated it becomes obvious that the behavior of the model depends on the amount of floodwater. But at the same time the amount of the floodwater is strongly dependent on the model motion. The submerged portion of the damage opening and the time it remains submerged determine the water inflow, which are directly related to the actual model motion. Considering at the same time the high nonlinear character of the hydrostatics with respect to the floodwater and also other hydrodynamic effects that have not been taken yet into account, the actual motion of the model in transient flooding seems to be quite complicated and sensitive to numerous parameters determining the system. The half kilogram difference of floodwater in case of model B and KG=136mm which leads to 15 degrees difference in heeling could be the result of many of the above not fully explored parameters.

Attention should be paid to the substantial difference between the transient mode of intermediate stages of flooding and the final partial flooding. This distinction is made in order to clarify that intermediate stages of flooding may not finally lead to a fully flooded condition

following damage hydrostatics, but to a partial one. In that case the undesirable conditions of partial flooding are present. Even if the model gets finally fully flooded, depending on the damage opening and sea condition, the model may pass through different partial flooding conditions before it reaches the final stage, then the transient flooding could last for long time.

The shape and location of the damage opening proved to be a quite significant factor for the duration and the final result of transient flooding. Obviously other parameters determining the ship motion, like GM, permeability, as well as exciting wave conditions, like sea state, wave heading, affect the flooding procedure and the actual behavior of the model. They should be studied systematically in future research.

6. CONCLUSIONS

A study on the transient flooding of a passenger/Ro-Ro model using a motion and flooding simulation model has been carried out. Numerical simulation results show satisfactory correlation with the available experimental.

The behavior of the model during the initial stages of flooding proved to be quite non-linear and sensitive to various motion parameters. The shape and location of the damage opening proved to a major factor determining the transient flooding, but also the final position of the flooded model.

Transient flooding over extended time might cause serious stability problems. Pending the thorough validation of numerical simulation codes, intermediate stages of flooding should be studied, at least hydrostatically, very carefully, as they significantly affect the assessment of ship's damage stability in waves.

7. ACKNOWLEDGEMENTS

This work was partially funded by the European Commission project NEREUS (FP5, DG XII, contract number G3RD-CT-1999-00029), dealing with the design of Ro-Ro passenger ships with enhanced survivability in damage condition at sea.

8. REFERENCES

[1]. De Kat J., 'Dynamics of a Ship with Partially Flooded Compartment', Contemporary Ideas on Ship Stability, Elsevier Publishers, Oxford (U.K.) 2000.

[2]. Ishida S., Murashige S., Watanabe I., Ogawa Y., Fujiwara T., 'Damage stability with water on deck of a Ro-Ro passenger ship in waves. Contemporary Ideas on Ship Stability', 2nd Workshop on Stability and Operational Safety of Ships, Osaka, 18-19 November 1996.

[3]. Ma Y., Katayama T., Ikeda Y., 'A Study on Stability of Damaged Ships in Intermediate Stage of Flooding', J. Kansai Soc. N. A., Japan, No. 234, Sep. 2000.

[4]. Papanikolaou A., 'NEWDRIFT V.6: The six DOF three-dimensional diffraction theory program of NTUA-SDL for the calculation of motions and loads of arbitrarily shaped 3D bodies in regular waves', Internal Report, NTUA-SDL, 1989.

[5]. Papanikolaou A., Zaraphonitis G., Spanos D., Boulougouris V., Eliopoulou E., 'Investigation into the capsizing of damaged Ro-Ro passenger Ships in Waves. Proc. 7th Inter. Conf. On Stability of Ships & Ocean Vehicles STAB2000', Australia, Tasmania 2000.

[6]. Spanos D., Papanikolaou A., Boulougouris E., 'On the Rolling and Safety of Fishing Vessels with Water On Deck', VIII Inter. Symp. on Technics and Technology in Fishing Vessels. Ancona, May 2001.

[7]. Spanos D., Papanikolaou A., Zaraphonitis G., 'On a 6-DOF Mathematical Model for the Simulation of Ship Capsize in Waves', Proc. 8th International Conference IMAM'97, Istanbul 1997.

[8]. Vassalos D., Turan O., 'A Realistic Approach to Assessing the Damage Survivability of Passenger Ships', SNAME Transactions. Vol. 102, 367-394, Nov. 1994.

MECHANISMS AND PHYSICS LEADING TO THE CAPSIZE OF DAMAGED SHIPS

J. O. de Kat
R. van 't Veer
MARIN
Wageningen, Netherlands

SUMMARY

This paper focuses on the characteristics of flooding and capsizing of different types of ships. For ro-ro ferries the paper discusses transient flooding in calm water and in waves, including the influence of cross flooding arrangements. Furthermore the progressive flooding and capsizing in waves due to accumulation of water on the car deck are considered and how this may be influenced by the initial conditions at the time of damage occurrence. The paper dwells in some detail on fluid dynamics relevant to flooded compartments that are subjected to oscillatory motions. The capsizing process of a frigate-type ship with a high degree of subdivision is shown to differ from a damaged ro-ro ferry in waves.

1. INTRODUCTION

Over the past decade a significant amount of experience has been gained associated with predicting the capsize behavior of intact and damaged ferries and naval vessels. Experiments and numerical simulations have contributed greatly to an ever-increasing body of knowledge in this field.

The objective of this paper is to provide insights into different physical aspects relevant to the flooding and capsizing of damaged ships in waves. The information presented here is derived from internal research at MARIN, research sponsored by the CRNAV consortium, and from participation in EU projects under the Safer Euroro Thematic Network.

For ro-ro ferries transient flooding is considered in calm water and in waves, including the influence of cross flooding arrangements. Concerning the progressive flooding and capsizing due to deck edge submergence and accumulation of water on the car deck, it is shown that the initial conditions and wave group properties at the time of damage occurrence may have a significant influence on the ship's behavior.

Techniques are discussed for predicting the fluid forces exerted on flooded compartments undergoing oscillatory motions. The paper highlights differences between capsize mechanics of ro-ro ferries and those associated with a frigate-type ship that has a high degree of subdivision.

2. DYNAMICS OF DAMAGED RO-RO FERRY

A significant amount of research involving damaged ro-ro ferries has focused on capsizing associated with the accumulation of water on deck, while drifting in beam seas. Typically model tests are carried out with the vessel starting in the flooded equilibrium condition after damage; this procedure avoids transient effects associated with the initial and intermediate stages of flooding. While subjected to waves, the model will gradually settle in a new equilibrium position, or it will eventually capsize once a critical amount of water has accumulated on the main car deck. An experimental run where the model reaches and remains in a safe equilibrium condition is shown in figure 1.

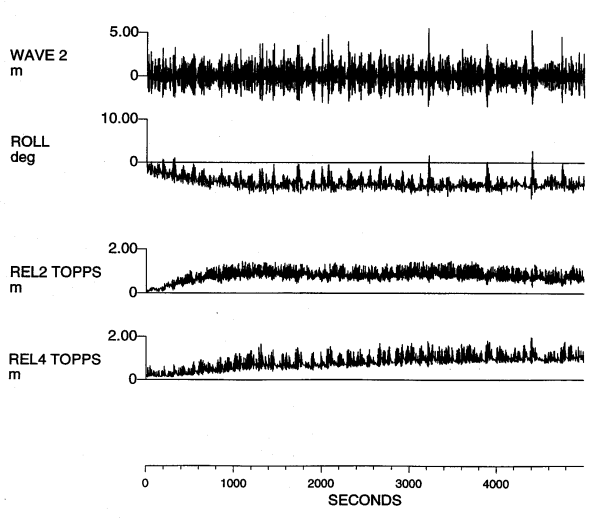

Figure 1 Behaviour of damaged ro-ro vessel while drifting in beam seas (Hs = 4 m)

To investigate the damage behavior of a modern ro-ro ferry with extensive lower hold, Deltamarin designed a vessel for model testing at MARIN. As can be seen in figure 2, the ship has longitudinal bulkheads on the main cargo deck, wing tanks extending from the keel upwards where port and starboard tanks are cross-connected. Part of the research aimed at investigating damage scenarios with the lower hold intact and damaged [1]. Since transient flooding after damage can lead to capsizing (as in the case of the *European Gateway* in the 1980s), this aspect was included in the investigations.

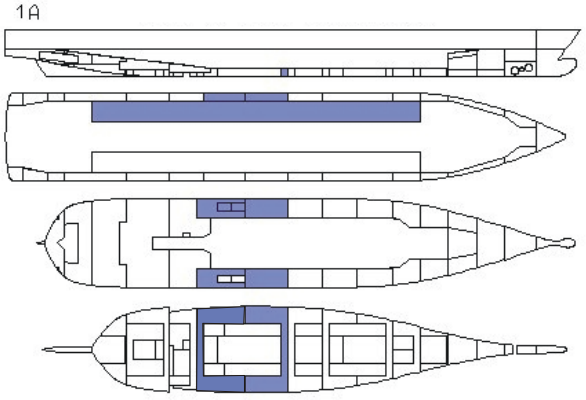

Figure 2 Damage scenario for modern ro-ro ferry

This so-called "ARD" model has been tested in the scenario of figure 2. Figure 3 shows the transient roll response of the ship with an intact GM value of 2.20 m in calm water and in waves following the occurrence of damage. For these tests the vessel started in the intact condition with sealed damage opening (corresponding to standard SOLAS damage). At some point in time, sliding a door created the damage in about 16 seconds prototype. This flooded the model, filled the wing tank on the damage side and flooded the opposite wing tanks through the cross-ducts.

Figure 2 demonstrates that the effects of flooding in calm water and in irregular seas can result in very similar roll response. Furthermore, the roll motions in waves are small compared with the maximum roll angle due to the transient flooding. For this particular configuration the total time of damage creation is of importance -- a long duration damage creation (in the order of one or two minutes) will result in quasi-static flooding without significant transient roll peaks. In this case at the roll peak of about 16 degrees the edge of the car deck was submerged briefly; most of the water captured flowed out of the opening after the maximum roll angle was reached and no critical accumulation of flood water took place.

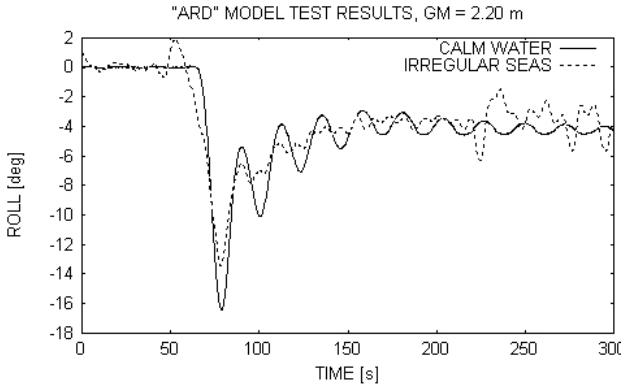

Figure 3 Transient roll response following damage occurrence in calm water and in waves

This transient flooding and motion behavior of the ARD model has been simulated numerically, and good correlation was found. This suggests that the initial water ingress can be modeled assuming a hydraulic flow model. Water ingress experiments with various ship configurations showed that such a flow model describes the physics of flooding and resulting forces adequately [2]. Sloshing effects are not important in this phase of flooding. An example of simulated and experimental roll response is shown in figure 4. The flooding scenario is given in figure 2. Different flooding scenarios and initial GM values gave similar comparisons.

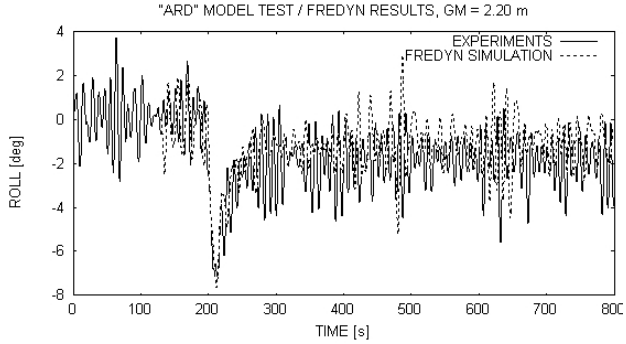

Figure 4 Simulated and experimental roll response following damage occurrence in waves

Cross flooding

The incorporation of cross-flooding arrangements is very effective in reducing final heeling angle in the case of an asymmetric damage scenario. To reduce maximum transient roll peaks during initial flooding of wing tanks, however, such arrangements are largely ineffective. Figure 5 demonstrates this for the ARD model, where the same scenario applies as in figure 2. It shows the measured roll motion and water elevation at the following locations of the damaged compartments underneath the main ro-ro deck (measured close to the cross duct openings): aft port and starboard side

compartments (REL4) and forward port and starboard side compartments (REL6). It takes less than 10 s for the first water quantities to flow through the cross ducts and reach the intact SB compartments, but it takes between 50 and 100 s before cross flooding is completed.

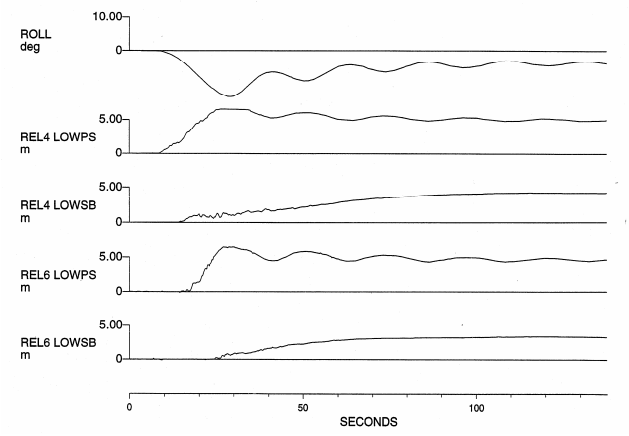

Figure 5 Roll motion and water levels in damaged (PS) tanks and intact (SB) tanks

GM and the heeling moment impulse exerted by the floodwater govern the time it takes for the ship to reach a certain maximum roll peak. The cross-flooding rate determines the time for the ship to reach its static equilibrium. Cross flooding into the intact SB compartments is quasi-static: the oscillatory roll motions do not seem to affect the flooding rate. Complete cross flooding within one roll cycle is not possible for the vessel in this damage scenario.

Influence of initial conditions and wave groups

The behavior of a damaged ro-ro ship in waves depends on the compartment layout below the main deck. This is illustrated by results obtained recently in a model test series conducted at MARIN for the European HARDER project. For this vessel the double bottom area was not connected with a wing tank and no side casings were present. This meant that damage to the side shell would flood the compartment (engine room) and the double bottom below immediately. Part of the double bottom consisted of a cross-duct arrangement between a port and starboard tank.

In the example given in figure 6, the model capsized eventually after the occurrence of damage, but the maximum transient heel angle towards damage (positive) after damage creation is small. There is even a negative roll angle away from the damage. This is due to the large inflow in the engine room, which acts like a "jet" on the side shell of the ship, despite the presence of several large blocks in the E.R. to model the correct permeability and large flow obstructions. The lack of wing tanks results in relatively small transient roll peaks.

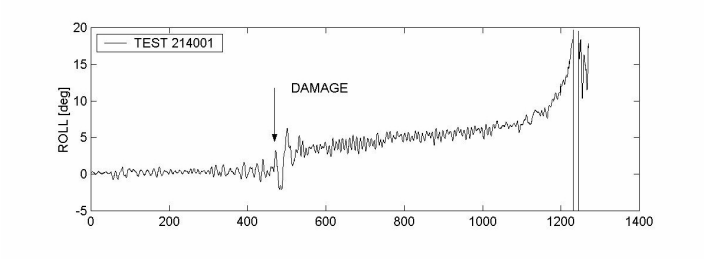

Figure 6 Capsize of ro-ro ferry in waves following occurrence of damage (Hs = 2.5 m, Tp = 9.5 s)

Figure 6 shows also a typical ro-ro vessel capsize. The roll motions in damaged condition are small, and due to the accumulation of water on deck the roll angle increases steadily. The floodwater increases damping (by means of the water mass and increased draught) of the ship and typically the natural roll period increases as well. For a certain time period the roll angle can be more or less steady or slowly increasing until a critical amount of floodwater is reached. The passage of one high wave group may then trigger the final capsize. This capsize point can be clearly seen in the experiments.

Figure 7 shows two capsize events in the same sea state and for the same damage scenario for the HARDER ro-ro ferry discussed above. The difference between the two runs stems from different wave realizations, among others. In the first run the damage opening is created at t = 718 s and the ship remains safe for a long period of time. Large roll angles are found, for example after 1500 seconds in damage condition, but the ship was able to survive those waves and capsizes at a much later stage. In the second run damage occurs at t = 677 s and the ship capsizes within the next 1000 seconds.

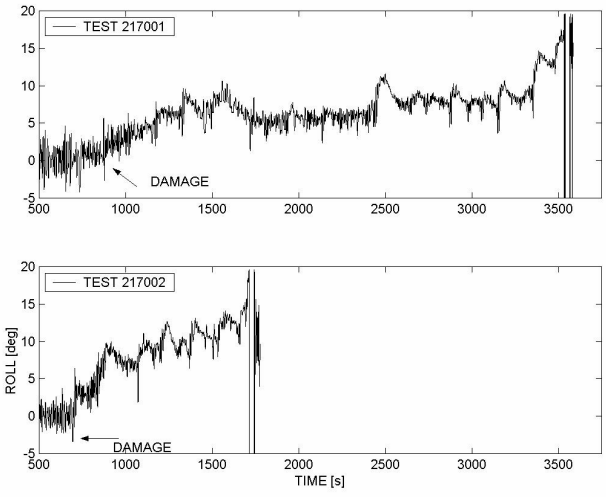

Figure 7 Roll response of ro-ro ferry in capsize conditions (sea state: Hs = 3.5 m, T = 8.0 s)

Analysis of the results in figure 7 suggests that the timing of damage occurrence is important: when damage occurs within a relatively low wave group, no significant flooding takes place at that time, which will delay the possibility of capsize. Alternatively, when damage occurs during the passage of a high wave group, the likelihood of significant water ingress is much higher.

Figure 8 shows for both capsize events the absolute wave elevation measured in-line with the drifting vessel and the relative wave elevation at the deck edge (positive value indicates submergence) determined from the measurements. Figure 9 shows the same information for the first 300 seconds after damage occurrence. For the first run it appears that the damage is created in a group with low waves and the deck edge is hardly submerged during the first 100 seconds. In the second run, however, the damage occurs in somewhat higher waves, immediately followed by the passage of a group with high waves. This changes the flooding process drastically -- in almost every subsequent wave the deck edge submerges, thereby forcing water to accumulate on the car deck, causing an almost monotonically increasing list until the point of capsize is reached.

In this case, the slight trim aft exacerbates the process, as any accumulation of water is here governed by the encounter with critical wave groups and water cannot flow out of the damage opening easily. Thus wave group statistics and damage creation play an important role in the time it takes to capsize.

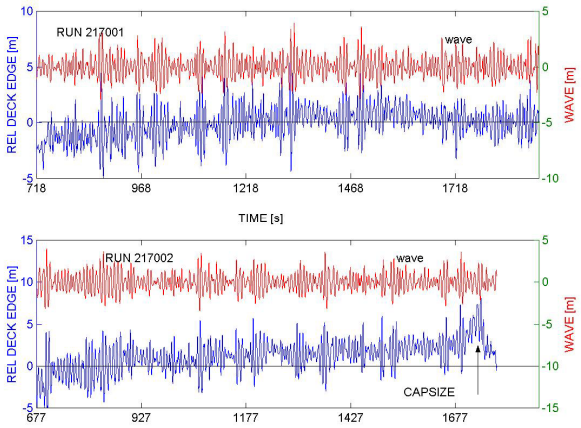

Figure 8 Absolute and relative (at deck edge) wave elevation for capsize events shown in figure 7

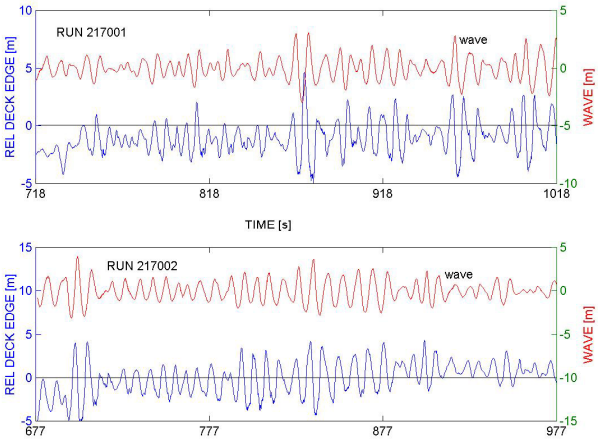

Figure 9 Absolute and relative (at deck edge) wave elevation for capsize events shown in figure 7

3. DYNAMICS OF DAMAGED FRIGATE

Whereas the capsizing process of a ro-ro ferry is governed by the heave response in wave groups and accumulation of water on deck, for a multi-compartment ship like a frigate the process is different. To study the dynamics of floodwater in a frigate-type ship, water ingress and forced oscillation tests have been carried out. Subsequently the capsize behavior in waves and wind has been studied. Results of the water ingress research have been presented in [2]. Additional results are discussed below.

Forced roll oscillations

For validation purposes for the numerical model (FREDYN) a series of forced oscillations were carried out with a schematic ship compartment layout as part of the CRNAV Dynamic Stability Project. A series of 12 small compartments were connected via doors with each other so that water flow was possible between the compartments. The space was filled with water to a certain depth, and then the whole set-up was oscillated in roll. Different frequencies and amplitudes were tested, consisting of sinusoidal motions around a fixed axis. Figure 10 gives an overview of the compartments and the connecting openings.

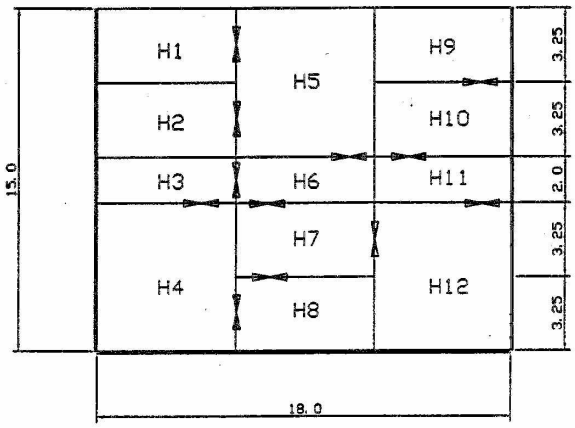

Figure 10 Accommodation space layout with openings for forced roll tests about center line axis through H3, H6 and H11

Figure 11 shows results for the transverse force (FY) and roll moment (MX) acting on the whole section. The sway force is very well predicted, and the roll moment tends to be somewhat overpredicted by FREDYN. This is a trend found in many calculation results. It suggests that the hydraulic model predicts more water flow between the compartments than is the case in the physical tests.

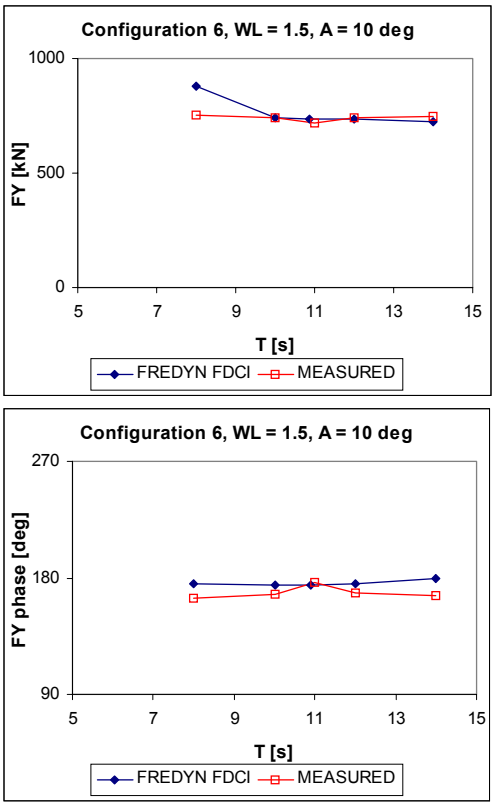

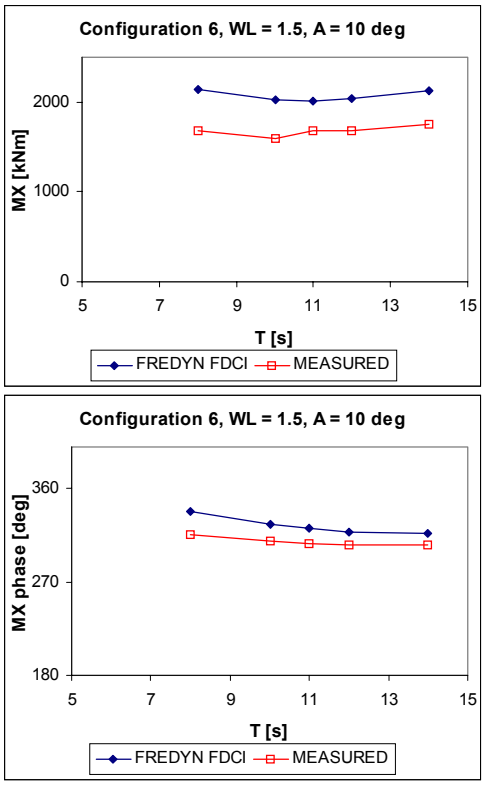

Figure 11 Sway force and roll moment acting on flooded accommodation space as a function of roll period (1.5 m flood level, 10 deg ampl.)

According to the hydraulic model water will immediately flow when there is a difference in water heights between openings; in the physical case there are delaying effects. It might also be due to 3D effects clearly visible in the compartments. The fluid motions were more chaotic than in the simulations in compartment corners and around the door openings. Overall, the comparison is reasonable.

Similar forced oscillation tests were carried out for a configuration where a wing tank on port and starboard side was connected via a cross-duct of diameter 0.3 m (prototype). The wing tanks were large compared to the cross-duct and in the analyses of the tests it appeared that the flow rate between the two compartments was almost nihil. This also indicates that after flooding of a wing tank after damage takes place the interaction between the two tanks diminishes. The water level should be earth-horizontal between the tanks, but with roll amplitudes of 10 degrees the difference in height is not very large. Figure 12 show an example; the correlation with FREDYN is good.

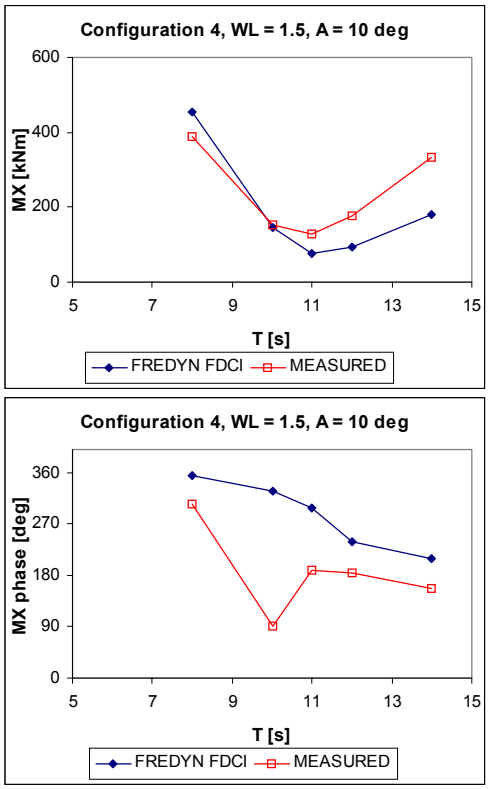

Figure 12 Forced oscillations of compartment with flooded wing tanks and connecting cross duct (measured and simulated roll moment)

For a U-tank compartment consisting of wing tanks and cross duct CFD (2D VoF) computations have been carried out with the program COMFLO. Figure 13 illustrates a vector plot of the fluid velocities for forced roll oscillations; figure 14 shows the associated dynamic pressure variations.

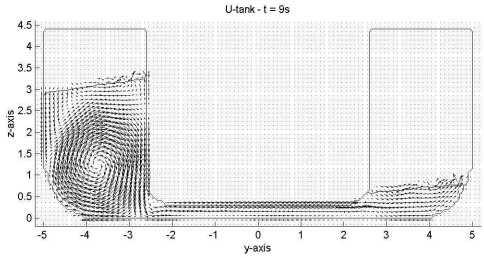

Figure 13 Velocity field in wing tanks and duct during forced roll oscillations

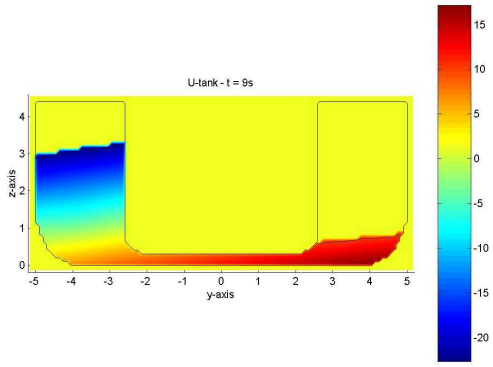

Figure 14 Pressure field in wing tanks and duct during forced roll oscillations

With the same CFD model 3D computations have been performed for a simplified engine room, similar to the one shown in figure 17. Figure 15 shows the predicted and measured roll moment as a function of the roll frequency for a roll amplitude of 10 degrees and 3 m fill level with floodwater. Figure 16 shows a time series of the water elevation at three locations in the compartment. The agreement between measurements and simulations is excellent, even when sloshing is present.

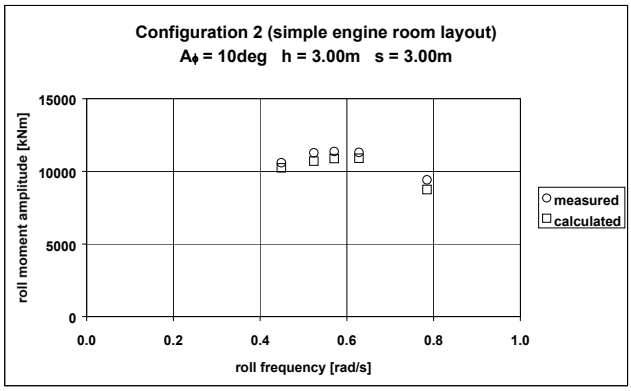

Figure 15 Roll moments acting on flooded engine room

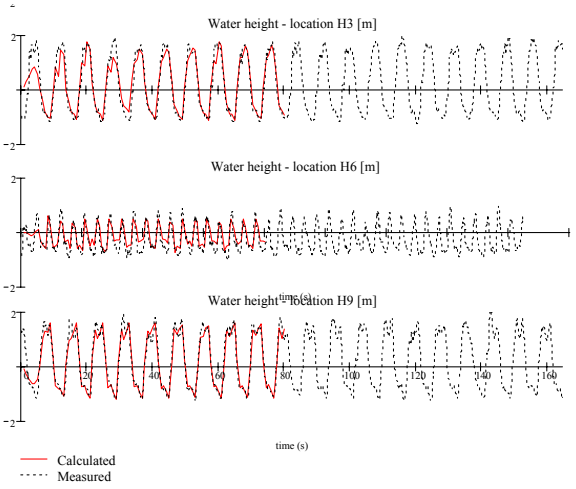

Figure 16 Water levels at three locations in flooded engine room (8 s roll period, 10 deg amplitude)

Capsizing in extreme wave conditions

To illustrate the capsize behavior in an extreme sea state, we consider a generic frigate with a length of around 110 m and displacement of about 3300 tonnes. For this vessel a parametric study has been carried out using numerical simulations, including the influence of compartment layout and damage scenario on capsize boundaries in terms of significant wave height.

It appears that when this vessel capsizes in a seaway under the various conditions considered, it is associated with the passage of a steep, high wave. This applies also to the frigate with a 5 x 4 m damage hole in just the engine room, the layout of which and righting arm (flooded) are shown in figures 17 and 18.

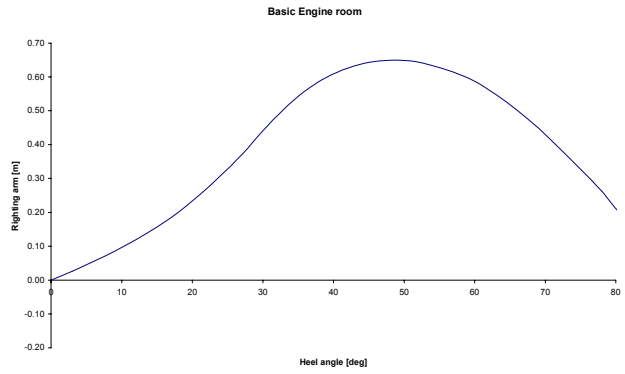

Figure 17 Righting arm curve of frigate with flooded engine room

Figure 19 shows the time series of the last 40 seconds of a typical capsize event; it shows the encountered wave elevation at the CoG (positive is downwards), wave slope at CoG, roll and yaw (90 deg is beam seas). The ship drifts freely at zero forward speed.

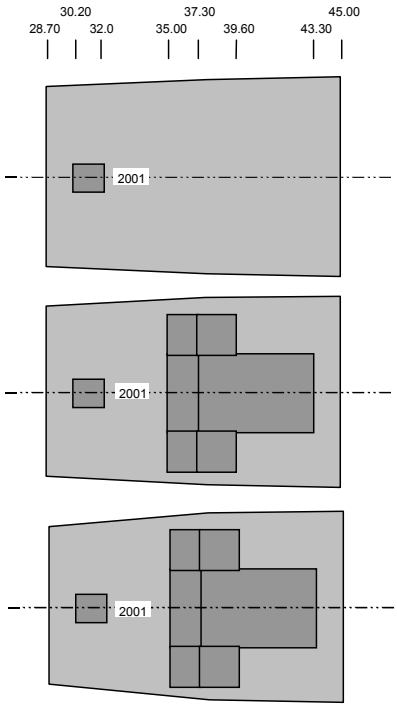

Figure 18 Layout of engine room (plan view)

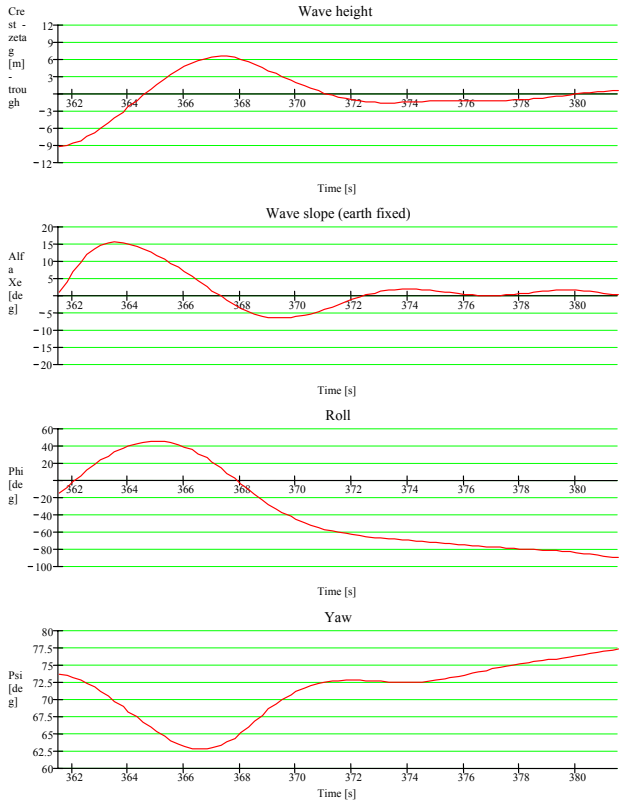

Figure 19 Motions of damaged frigate in extreme sea state (Hs = 11 m, Tp = 12.4 s)

As illustrated in figure 19, a high and steep wave passes the ship from the port side, the maximum slope is around 15 degrees, which causes the ship to undergo an extreme roll to leeward. The ship does not recover from this roll event and capsizes while rolling back; at he time of capsize the wave height is moderate. Figure 20 shows the spatial wave profiles over a length of 400 m as of the capsize inception point (t = 360 s); the zero point coincides with the CoG of the ship. Analysis of these waves suggests that the critical wave height initiating the capsize is around 15 m, and its spatial length is 240 m, i.e. the spatial wave steepness is H/λ = 0.063.

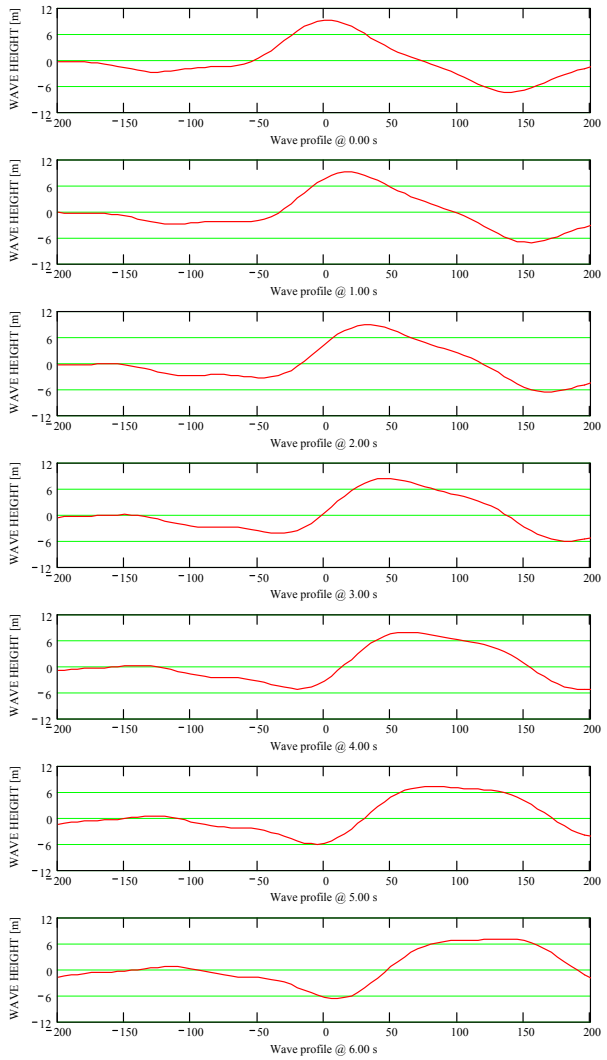

Figure 20 Spatial wave profiles shown every second from inception of capsize

It is possible to predict the occurrence of a wave with given period and height in a sea state when the joint probability density function (pdf) for period and height is known. From such a joint pdf we can derive the pdf of the spatial wavelength and steepness (H/λ), as shown in figure 21. This figure shows that the steepest waves (H/λ = 0.1) occur in the wavelength range of 50 to 200 m. A wave with λ = 240 m is very unlikely to have a steepness exceeding about 0.075. In this case its likelihood of occurrence is closely linked to the probability of capsize, where the duration of the sea state would have to be accounted for.

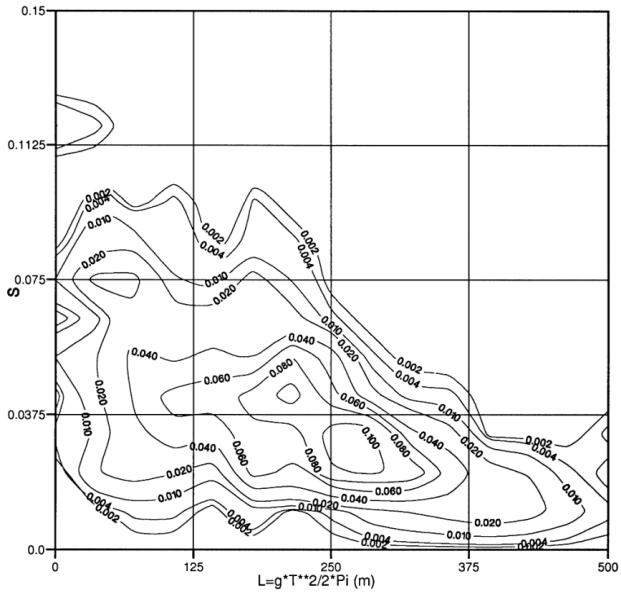

Figure 21 Joint probability density function of wavelength and spatial steepness (Hs = 11 m, Tp = 12.4 s)

5. CONCLUSIONS

The objective of this paper is to provide insights into different physical aspects relevant to the flooding and capsizing of damaged ships in waves.

For ro-ro ferries transient flooding following damage occurrence is discussed in calm water and in waves, including the influence of cross flooding arrangements. It is shown that the transient roll response characteristics are not influenced significantly by the presence of waves. A ship with wing tanks can experience transient roll peaks that are larger than the roll amplitudes in waves once flooded. It is shown that the initial conditions and wave group properties at the time of damage occurrence may have a significant influence on the ship's behavior; damage occurrence in a group of high waves can lead to a capsize within a short time frame.

Techniques are discussed for predicting the fluid forces exerted on flooded compartments undergoing oscillatory motions. The paper highlights differences between capsize mechanics of ro-ro ferries and those associated with a frigate-type ship that has a high degree of subdivision. The capsizing of a damaged frigate can be initiated by the passage of a steep, high wave. Properties of such waves are discussed.

6. ACKNOWLEDGEMENTS

The work presented in this paper on ro-ro ferries has been partly supported by the EU project HARDER (G3RD-CT-1999-00028). The Authors are solely responsible for the contents therein, and it does not represent the opinion of the Community. The Community is not responsible for any use that might be made of data appearing therein.

The work presented in this paper on frigate dynamics has been supported to a large extent by the Cooperative Research Navies (CRNAV) Dynamic Stability Project; participants comprise navies from Australia, Canada, France, Netherlands, United Kingdom and United States, U.S. Coast Guard and MARIN.

7. REFERENCES

[1] J.O. de Kat, M. Kanerva, R. van 't Veer and I. Mikkonen, "Damage Survivability of a New Ro-Ro Ferry", *Proceedings of the 7th International Conference on Stability for Ships and Ocean Vehicles, STAB 2000,* Launceston, Tasmania, Feb. 2000

[2] R. van 't Veer and J.O de Kat, "Experimental and Numerical Investigation on Progressive Flooding and Sloshing in Complex Compartment Geometries", *Proceedings of the 7th International Conference on Stability for Ships and Ocean Vehicles, STAB 2000, Vol. A,* Launceston, Tasmania, Feb. 2000, pp. 305-321

DAMAGE STABILITY MODEL TESTS FOR NAVAL COMBATANTS

William L. Thomas III
Robert J. Bachman
David Taylor Model Basin Seakeeping Department
Naval Surface Warfare Center, Carderock Division
9500 MacArthur Blvd
West Bethesda, Maryland USA 20178-5700
Email *thomaswl@nswccd.navy.mil*
bachmanrj@nswccd.navy.mil

SUMMARY

This paper addresses aspects of damage stability experiments for naval combatants. Since naval combatants are required to engage in combat and remain effective under harsh conditions, it necessary to investigate damage stability beyond the requirements typically defined for RO-RO ferries as specified in SOLAS requirements. This paper discusses test procedures conducted by NSWCCD for naval combatants.

1. INTRODUCTION

Naval combatants and commercial vessels face similar challenges when it comes to damage stability. They are subject to damage and flooding due to running aground, collisions, as well as structural breaches in extreme seas. However, combatants are exposed to the additional hazard of battle damage, which might occur at any point on the ship with hole sizes ranging from 2 cm to insurmountably large. The nature of warfare at sea implies that damage can be inflicted over a wide range of speeds, while maneuvering, in any seaway. Mission requirements can also require the injured warship to maneuver and transit despite damage.

U. S. Naval combatants have been subject to damage stability criteria based on calm water/wind heel relationships that were developed in the 1960's based on experience during World War II [1]. See Figure 1. Compliance with the criteria is based on the calculated equilibrium heel angle of the ship in calm water in terms of the floodable length of the ship. The specific size, shape, and location of the hole are not addressed. Flooding dynamics, as well as the dynamic behavior of the damaged ship in a seaway also are not addressed in the existing criteria.

Recent tragedies involving the flooding of commercial vessels, including the loss of the *Herald of Free Enterprise* in 1987, and the *Estonia* in 1994, have illustrated the need to account for flooding dynamics, and have encouraged the use of model tests to demonstrate compliance with IMO criteria [2]. Given the above considerations, it becomes prudent to address the role of model tests in the evaluation of naval combatants.

2. DAMAGE STABILITY TESTS

The loss of RO-RO ships have drawn attention to the use of model tests as a means to demonstrate suitable levels of survivability for ship designs [3]. This procedure makes the assumption that survival scenarios defined in the model experiment will guarantee an acceptable loss risk for the full-scale ship.

With respect to damage, a naval combatant is subject to a number of variables including:

1. Intact Load Condition
2. Compartmentation (Including status of damage control doors/fittings)
3. Heading
4. Speed
5. Maneuver
6. Damage Location
7. Size, Shape and Depth of Hole created by Damage
8. Wind
9. Seaway

The numerous parameters cited above could define a very large number of configurations that do not make it practical for exclusive use of model experiments to demonstrate acceptable survivability. Future evaluations of naval combatants will require the use

of a combination of model experiments and numerical simulations, to properly model ship dynamics and flooding physics.

2.1 PHILOSOPHY

The extreme nature of warfare encourages innovative ship designs that might extend beyond the range of previous experience. This necessarily leads to advancing the state of the art in simulation tools to accommodate the new designs and the commensurate requirement to validate the amended simulation. The nature of investigating the unknown also implies that unanticipated physical behavior might occur. For these reasons, damage stability experiments should follow a philosophy such that experimental data is collected to:

1. Evaluate model performance of selected scenarios of interest
2. Allow the understanding of flooding physics in the model
3. Properly model ship dynamics
4. Collect sufficient data to validate numerical simulation tools

2.2 MODEL CONFIGURATION

Damage stability experiments at NSWCCD are conducted using a free running radio controlled model. The nominal size of a typical damaged model is 5 meters. This roughly defines the lower limit of length where the necessary equipment can be "stuffed" inside a model. An interesting challenge in model construction is the need to include compartmentation, running gear, instrumentation, and telemetry while limiting the overall size so as to remain within experimental capabilities for making waves. The first challenge is to define the location and extent of compartmentation to be flooded in the model. This can be defined using existing stability rules to define the most critical damage case. In the U. S. Navy, the compartmentation is selected with the worse case flooded condition as defined by DDS-079-1 [1] using the Ship Hull Characteristics Program (SHCP) [4]. The model compartmentation must be watertight to protect the propulsion motors and instrumentation in the non-flooding areas of the model, as well as to prevent undesired free-surface effects due to leakage. Permeabilities are achieved using blocks placed in the compartments representing major machinery. See Figure 2.

Instrumentation consists of data acquisition, command and control, video, and hull breaching mechanism. Six degrees of freedom ship motion responses are measured, to include roll angles up to 90 degrees in each direction of heel. The water levels in the flooded compartments are measured using a matrix of 15 custom-built capacitance probes dispersed throughout the compartments. The probes are housed in perforated aluminum tubes, which isolate each probe from the others in water and provide ventilation. Digital cameras are provided in each compartment to record the behavior of the water in each compartment during and following the flooding process. See the upper left quarter of Figure 3.

The mechanism to provide a hull breach on demand, while otherwise maintaining the integrity of the hull was challenging to design. The NSWCCD design utilizes a polycarbonate panel that slides vertically along tracks that are faired to the hull. The command switch controls a pneumatic valve that actuates a piston, which pulls cables attached to the panel. This configuration provides a fast opening of large holes to investigate transient flooding effects and a quick reset of the mechanism. See Figure 4.

2.3 SCALING

Froude scaling is followed in damaged stability tests due to the influence of gravity on the dynamics. The modeling of ship flooding is also best performed using orifice flow that follows Froude scaling. Since sharp-edged orifice flow theory is used in simulation programs to estimate water ingress, "knife-edges" are cut along the outer edges of the holes representing damage on the model. This provides for the separation of the water boundary and the orifice, minimizing the viscosity effects at the hole, keeping the scaling effects in the Froude realm.

Air entrapment can occur in a flooded compartment introducing scaling effects that can lead to a lower air-water interface level in the model than in the full scale ship when the damaged hole is submerged. This is because the pressure head trying to push water into the compartment is less at the hole depth for the model than it would be for the ship at full scale. This would result in less water in the flooded compartment of the model than for the ship. The air compression scalability issue is avoided by providing adequate ventilation of all flooded spaces during flooding, via the capacitance probe tubes. This is appropriate from the standpoint that upflooding and downflooding is permitted to occur between decks below the damage control deck. Ventilation topside is also considered to be plentiful too.

2.4 EXPERIMENT

It is useful to define the environmental variables in which a ship could become damaged. Wind, current, and waves are the obvious forces roaming the seas. Currents can be strong in some locals, but it is the waves and wind that can have the most critical effect on ship stability. Until recently, damage stability experiments have been performed with captured model arrangements, or non-powered models - in waves and in calm water. Wind and current forces have not yet been integrated with such tests.

At NSWCCD, damage stability tests are performed using radio-controlled models to investigate the effects of transient flooding and flooded equilibrium conditions. Free running radio-controlled models are employed to eliminate cables running between the model and an external platform. This is to minimize any external effect on the capsizing mechanism. Transient flooding is investigated at both zero speed and underway conditions. While at zero speed, transient flooding experiments are performed in benign, flat seas and regular waves. Underway, the transient flooding experiments are performed in calm seas, at several speeds at a constant heading and on opportunity, a maneuvering condition. Each model is also subjected to flooded equilibrium tests in large sea states, as displayed in Table 1.

Model experiments are conducted for several hole sizes corresponding to the specific interests of the investigation. It is useful to investigate hull breaches at the surface, as well as below the waterline.

At least one hole in the test matrix is sized to address the maximum dimensions allowed by the relevant stability criteria. In tests at zero speed, the model is permitted to drift in the seaway, initially at beam seas heading to examine the drifting behavior of the model in the seaway. It is important to note the heading at which the model drifts for validation in simulations because this can impact the accuracy of survivability predictions.

3. CONCLUSIONS

This paper discusses damage stability experiments for naval combatant ships. The requirements for warships extend beyond the scope of typical experiments as defined in SOLAS for RO-RO ships, because combatants are exposed to the hazards of warfare.

As in most investigations, answers provided by model experiments often lead to more questions. As such, it would valuable to conduct further experiments of damage stability. In particular, given that naval combatants may likely be required to continue maneuvering while in a battle condition, it would be advantageous to investigate the effects of maneuvering on the stability of a damaged model. Wind also has a significant effect on stability and is most often accompanying (driving) the large sea states. It, too, would be a beneficial ingredient in future damage stability model tests.

It would also be useful in future experiments to investigate the effects of a hull breach that occurred completely below the water surface and to compare the differences between a rectangular shape hole, which aids in simulation comparisons, and an irregular, perhaps, jagged hole.

4. REFERENCES

[1] Naval Ship Engineering Center, “Design Data Sheet- Stability and Buoyancy of U. S. Naval Surface Ships”, DDS 079-1, Naval Sea Systems Command, Washington DC Aug 1975.

[2] 1995 *SOLAS* Conference, “Appendix to Annex 5, Resolution 14”, *SOLAS 1997 Consolidated Edition.* 1997.

[3] J.O. de Kat, M. Kanerva, R. van 't Veer and I. Mikkonen, "Damage Survivability of a New Ro-Ro Ferry", *Proceedings of the 7th International Conference on Stability for Ships and Ocean Vehicles, STAB 2000,* Launceston, Tasmania, Feb. 2000.

[4] Naval Sea Systems Command, “Ship Hull Characteristics Program-SHCP,” *Users Manual*, CASDAC No. 231072, Dept. of the Navy, Washington DC.

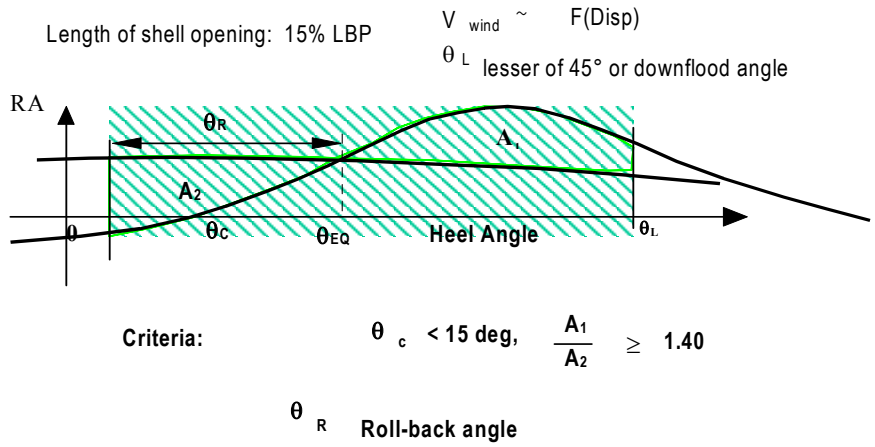

Figure 1 - U. S. Navy Damage Stability Criteria.

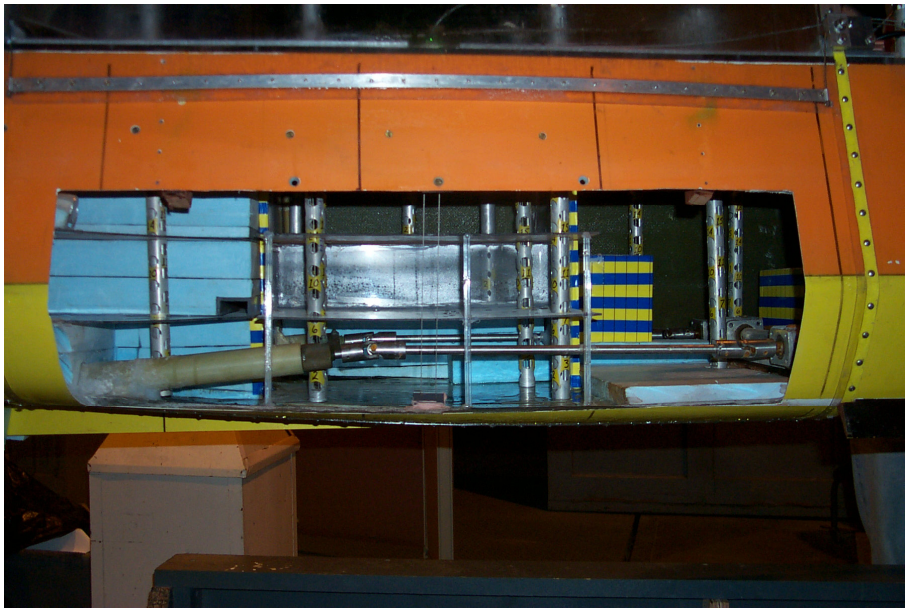

Figure 2 - Starboard view of model showing damaged section. The forward compartment is to the right, the center compartment directly ahead and the aft compartment is to the left. Blue and yellow stripes mark the elevation of compromised lateral bulkheads and blocks.

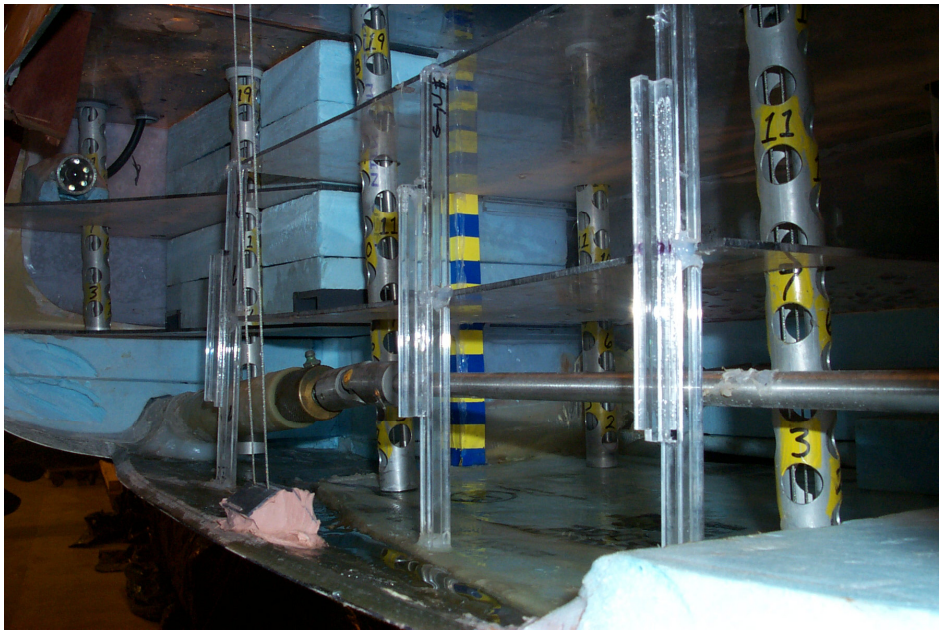

Figure 3 - Looking aft into the center and aft compartments. A camera is located in the upper left corner. The cross-flooding ducts, located in the aft compartment can be seen at the forward and aft ends of the foam block on the second level.

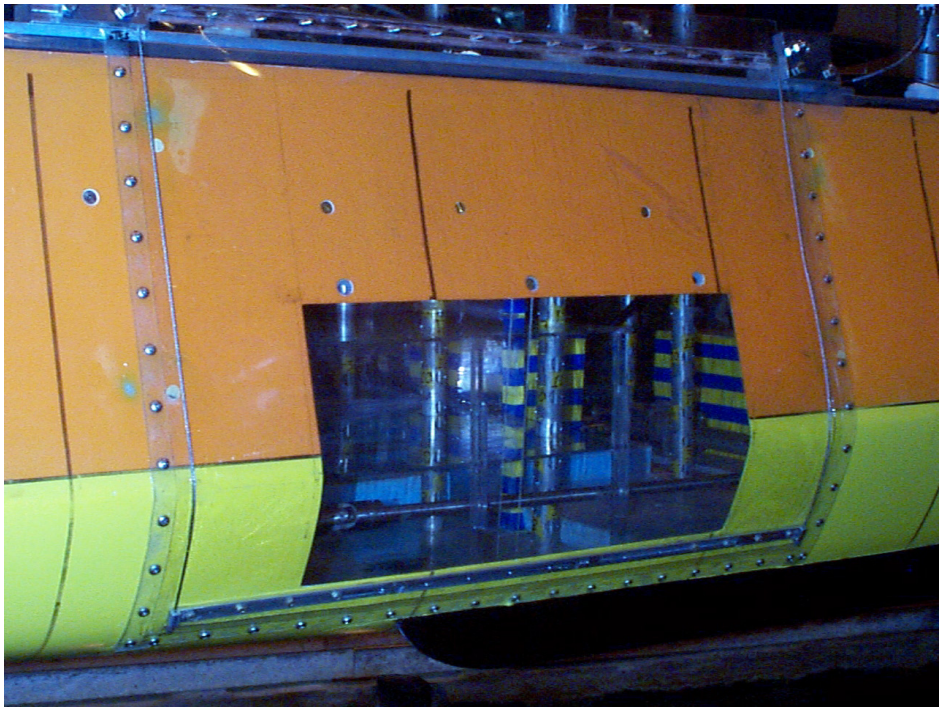

Figure 4 - View of breach mechanism panel

Table 1 – Model Test Matrix

Transient Flooding								
Calm Water			**Regular Waves λ / L = 1.5**					
Speed (Fn)	Hole A	Hole B	H/ λ	Hs (m)	To (sec)	Intact	Flooded Hole A	Flooded Hole B
0.00	X	X	1/50	4.3	11.7	X	X	X
0.10	X	X	1/20	10.6	11.7	X	X	X
0.20	X	X	1/15	14.2	11.7	X	X	X
0.30	X	X	1/10	19.5	11.7	X	X	X
High Speed Turn	X	X	-	-	-	-	-	-

Flooded Equilibrium – Zero Speed							
Sea State	Intact Hull	Flooded					
		Sealed Hole		Open Hole			
				Hole A		Hole B	
		Waveward	Lee	Waveward	Lee	Waveward	Lee
6	X	X	X	X	X	X	X
7	X	X	X	X	X	X	X
Camille	X	X	X	X	X	X	X

EFFECTS OF TRANSIENT MOTION IN INTERMEDIATE STAGES OF FLOODING ON THE FINAL CONDITION OF A DAMAGED PCC

Yoshiho IKEDA and **Tomoko KAMO**, Osaka Prefecture University, Gakuen-cho, Sakai, Osaka, 599-8531 Japan,
ikeda@marine.osakafu-u.ac.jp

SUMMARY

Flooding experiments of a 5000unit pure car carrier are carried out. The experimental results demonstrate that transient motions in intermediate stages of flooding significantly affect the final condition of a damaged and flooded ship. It is revealed that fully flooded condition on the basis of static consideration seldom appears at the final stage

1. INTRODUCTION

Survivability of a ship damaged and flooded by collision is usually evaluated in the ship conditions in the final stage of flooding where water surfaces in the damaged compartment and outside of the ship coincides each other. The damage stability regulations in SOLAS were also deduced on the basis of such a static concept. However, it has been revealed by one of the authors [1][2] that ship conditions in the final stage of flooding do not always coincide to those calculated on the basis of a static assumption. For example, even for flooding into a symmetrical compartment, the final condition is not always in upright. Sometimes such a damaged ship heels in the final stage since the damage opening goes up above water surface and flooding stops in intermediate stages. These facts suggest that the effects of transient motion in intermediate stages of flooding on the final condition should be carefully taken into account for a damaged and flooded ship.

In the present study the effects of transient behaviors of a damaged Pure Car Carrier (PCC) in intermediate stages of flooding on the final conditions are experimentally investigated.

2. EXPERIMENTAL SETUP

A 1/120 scale model of a PCC built by a Japanese shipbuilder is used for the experiments. The principal particulars of the model are shown in Table 1. The general arrangement and the mid-ship section of her are shown in Figs.1 and 2. In the experiments the compartment A is assumed to be a damaged one. The model floats in six-degree of freedom in calm water, the damage opening located on the side of the compartment is released, and ship motions, roll, heave and pitch, are measured until the final stage of flooding. Size and location of lower edge of openings are systematically changed as shown in Fig.3 in order to know the effects of them on transient motions and final results. In the compartment A, four car decks without watertight are modeled. On the decks, many small holes of 0.8mm diameter are made to simulate down-flow through these decks.

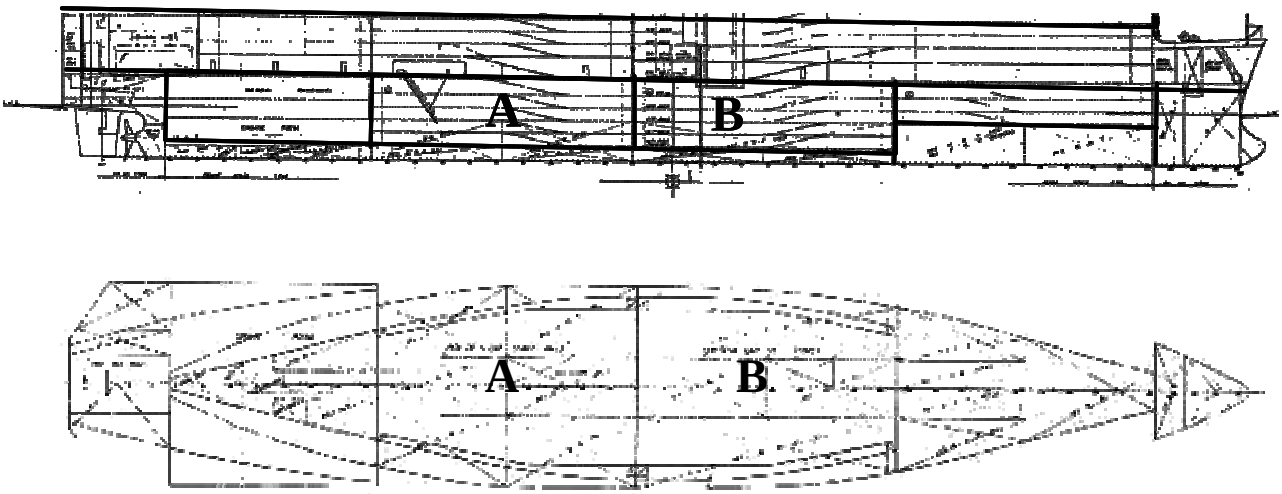

Fig 1. General arrangement of PCC

Table 1 Principal particulars of ship and model

	Ship	Model
Loa	190m	1580mm
Lpp	180m	1500mm
Beam	32.2m	268mm
Depth	13.05m	109mm
Draft	8.925m	74mm
Disp.	29129ton	16.9kg

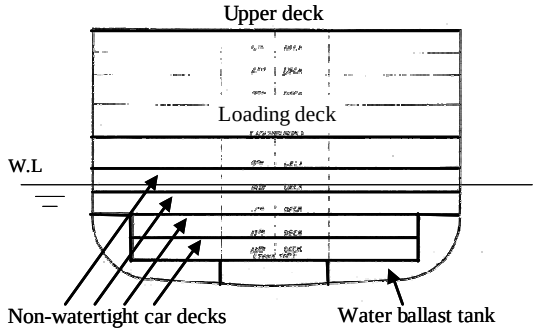

Fig.2 Mid-ship section of PCC

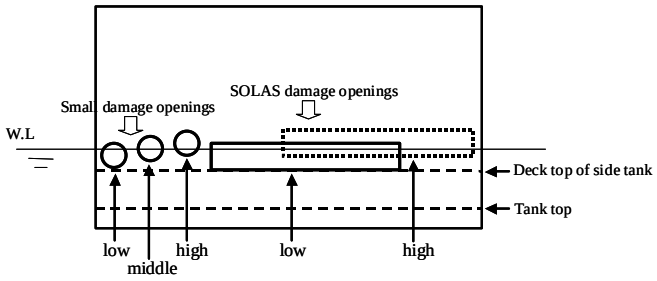

Fig .3 Size and location of damage openings

3. RESULTS AND DISCUSSIONS

The experimental results in the case of a small damage opening are shown in Figs.4 and 5. Flooding in these cases is slow, and the ship motions seem to be almost static. In intermediate stages of flooding, the ship heels to damage side, and gradually recovers to upright position. Flooding continues up to the final condition, where water surface inside and outside coincides each other. This means the damaged compartment is almost fully flooded. It should be noted however that permeability in final stage does not reach 100% but about 70% as shown later in Table 2.

Figs. 6 and 7 show the experimental results in the case of maximum damage length determined in SOLAS. Longitudinal length of the damage opening is 70mm, vertical height of it is 10mm, and the depth the lower edge of the opening from water surface at start of flooding is changed by 2mm and 8mm. As soon as the opening is released, water rushes into the compartment, and the ship heels to the opposite side of the damage opening. Then the opening comes up above water surface, and flooding stops. In the final stage, the ship heels at certain angle, and the amount of flooded water in the damaged compartment is limited. The same conclusion is obtained in the experiments for smaller damage opening of half size of the SOLAS damage opening as shown in Figs. 8 and 9. These experimental results demonstrate that ship motions in intermediate stages of flooding sometimes change the final result.

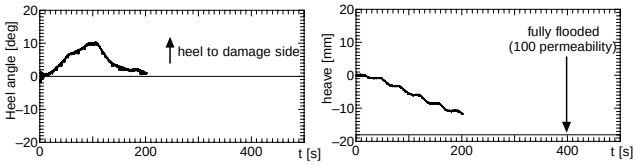

Damage opening ⋯high

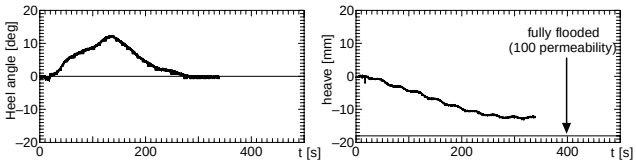

Damage opening ⋯middle

Fig.4 Time histories of ship motions in case of small damage opening with car decks in compartment (GM=23.5mm)

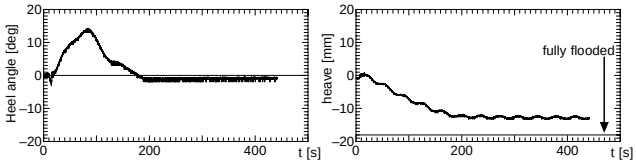

Damage opening ⋯high

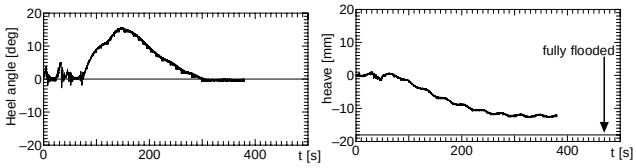

Damage opening ⋯middle

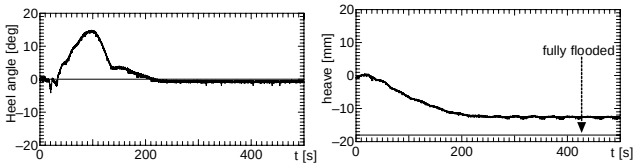

Damage opening ⋯low

Fig.5 Time histories of ship motions in case of small damage opening with car decks in compartment (GM=14.0mm)

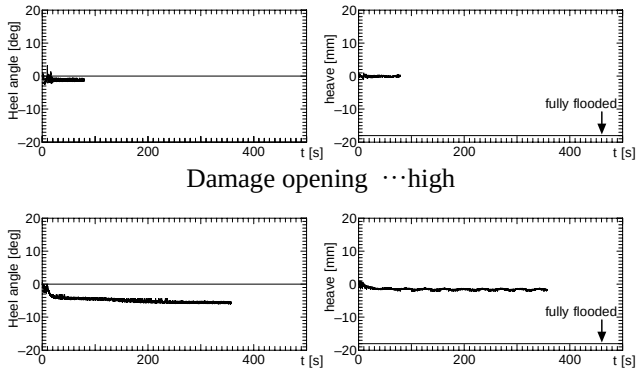

Damage opening ⋯high

Damage opening ⋯low

Fig.6 Time histories of ship motions in case of SOLAS damage opening with car decks in compartment (GM=23.5mm)

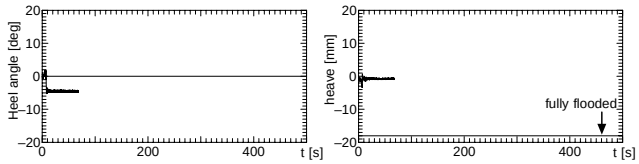

Damage opening ⋯high

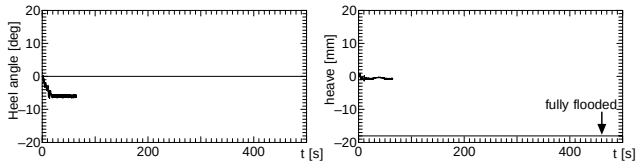

Damage opening ⋯low

Fig.7 Time histories of ship motions in case of SOLAS damage opening with car decks in compartment (GM=14.0mm)

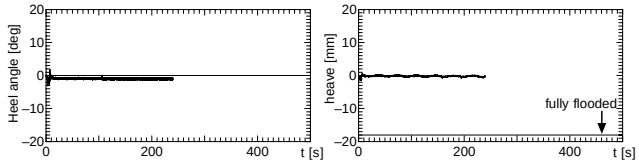

Damage opening ⋯high

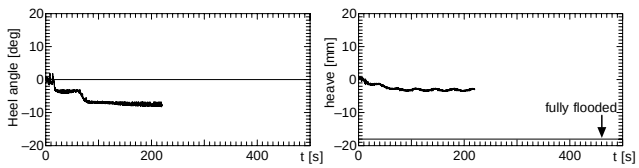

Damage opening ⋯low

Fig.8 Time histories of ship motions in case of half size damage opening of SOLAS's one with car decks in compartment (GM=23.5mm)

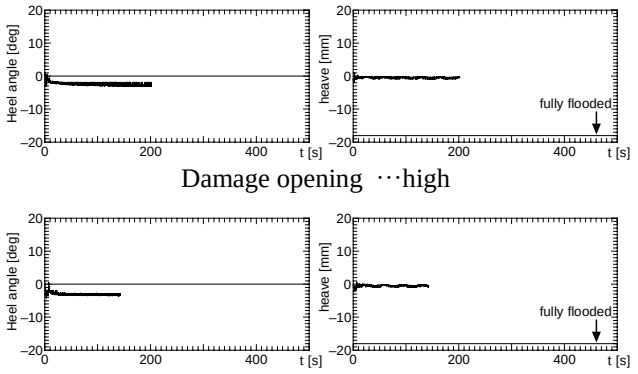

Damage opening ⋯high

Damage opening ⋯low

Fig.9 Time histories of ship motions in case of half size damage opening of SOLAS's one with car decks in compartment (GM=14.0mm)

When the ship has initial heel angle to the opposite side of the damage opening, flooding always stops in intermediate stages of flooding. Fig.10 shows the experimental results for 1.5 degree of initial heel to the side. On the contrary, when the ship has opposite initial heel of the same degree, the opening has been kept underwater, and flooding reaches to almost 50～70% of permeability as shown in Fig.11. These results demonstrate that initial heel angle is also a very important factor to determine the final condition of a damaged ship. It seems to be realistic that a struck ship has a heel angle to the opposite side of damaged opening because the head of the forecastle of a striking ship collides with a struck ship first and this makes the struck ship heel to the opposite side as shown in Fig.12.

All the results are tabulated in Table 2. In the table, final heel angle, permeability of the compartment (=volume of flooded water/volume of compartment), final outside water surface location from the horizontal loading deck are shown. It should be noted the permeability is lower than 100% in all cases. This is because some air is trapped in the compartment. When the ship heels at the final stage, air is usually trapped at ceiling of the compartment. When the ship sinks in nearly upright condition, air is trapped in lower car deck spaces even though the decks are non-watertight. In the experiments, the maximum permeability is only about 70% for a SOLAS damage opening and for a small damage opening. In many cases, the loading deck edge in damaged side is located above water surface. This fact suggests that the upper horizontal compartment can work as buoyancy even when the side plate of the upper compartment is broken by collision in such cases.

In order to know the effects of non-watertight car decks in a damaged compartment, some experiments for the compartment B without any non-watertight car decks are carried out. The experimental results are shown in Table 3. The results are completely different from those mentioned

before. In most of cases, the final conditions are in nearly upright or slightly heeled conditions. This facts suggest that the deck arrangements in a compartment affects ship motions in intermediate stages of flooding and change the final condition of her.

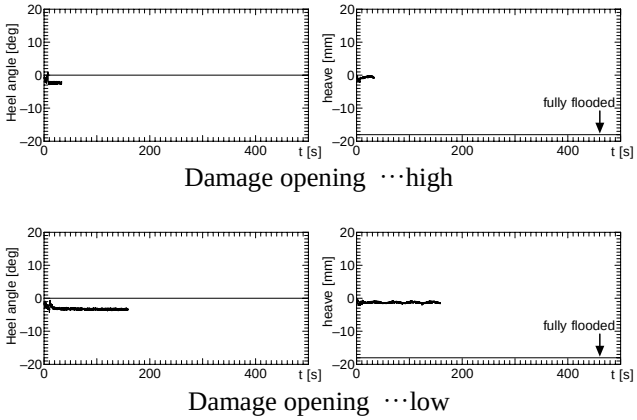

Fig.10 Time histories of ship motions for 1.5 degree of initial heel to the opposite side of damage opening in case of maximum damage opening with car decks in compartment (GM=23.5mm)

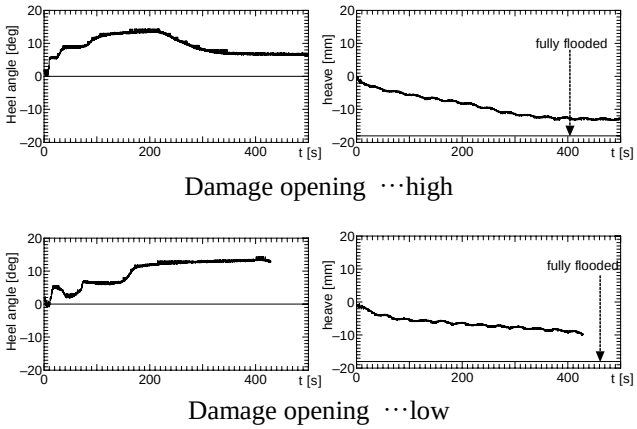

Fig.11 Time histories of ship motions for 1.5 degree of initial heel to the same side of damage opening in case of maximum damage opening with car decks in compartment (GM=23.5mm)

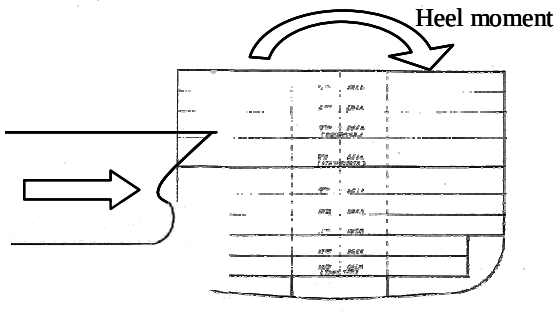

Fig.12 Behavior of a struck ship just after collision

4. CONCLUSIONS

Following conclusions can be deduced from the present experimental study on a damaged PCC.

1) In the case of small damage opening, flooding is almost static, and the final condition is in upright but the permeability is limited to be about 70%. When a ship has small initial heel to the opposite side of a damage opening, flooding stops in intermediate stages, and the final permeability is very small.
2) In the case of SOLAS maximum damage opening and its half size one, flooding stops at intermediate stages of flooding because the damage opening comes up above water surface.
3) Flooding is heavier if there is no non-watertight car decks in a damaged compartment. This fact suggests that such decks in a compartment take an important role to reduce flooding in a damage compartment of a damaged PCC.

The present study was carried out in a joint research project of RR71 in the Shipbuilding Research Association of Japan. The authors would like to express sincere appreciation to the members of RR71 for valuable discussions and to the Association for financial support to the present study. Dr. T. Katayama and Mr. S. Shimoda are appreciated for their help in the experiments.

5. REFERENCES

[1] Ikeda Y., Ma Y., ‘ An Experimental Study on Large Roll Motion in Intermediate Stage of Flooding due to Sudden Ingress Water’, Proc. of 7th International Conference on Stability of Ships and Ocean Vehicles, pp.270-285, Tasmania, 2000

[2] Ma Y., Katayama T., Ikeda Y., ‘A Study on Stability of Damaged Ships in Intermediate Stage of Flooding’, Jour. of Kansai Soc. N. A., Japan, No.234, pp.179-186, 2000 (in Japanese)

Table 2 All results of experiments with car decks in compartment

		opening size	small			half of SOLAS(medium)			SOLAS(large)		
GM	initial heel	opening height	heel	P	FWL	heel	P	FWL	heel	P	FWL
2.82m	-1.5 deg	high	-2.0 deg	6.7%	28.1mm				-2.0 deg	2.8%	28.8mm
		middle	-4.0 deg	8.3%	23.1mm						
		low	-5.0 deg	5.6%	21.2mm				-3.5 deg	8.3%	24.3mm
	0 deg	high	0 deg	69.4%	21.5mm	-1.0 deg	2.8%	31.2mm	-1.0 deg	0.6%	31.6mm
		middle	0 deg	69.4%	21.5mm						
		low				-8.0 deg	16.7%	12.2mm	-5.5 deg	8.3%	19.6mm
	1.5 deg	high							6.5 deg	69.4%	6.2mm
		middle									
		low							13.0 deg	50.0%	-5.9mm
1.68m	-1.5 deg	high	1.0 deg	69.4%	19.2mm						
		middle	-4.0 deg	8.3%	23.1mm						
		low	-5.0 deg	5.6%	21.3mm						
	0 deg	high	1.0 deg	69.4%	19.2mm	-3.0 deg	2.8%	26.5mm	-4.5 deg	5.6%	22.5mm
		middle	0 deg	69.4%	21.5mm						
		low	0 deg	69.4%	21.5mm	-3.0 deg	2.8%	26.mm	-6.0 deg	2.8%	19.4mm
	1.5 deg	high							-3.0 deg	18.8%	25.5mm
		middle									
		low							-5.0 deg	11.1%	20.3mm

・・・Damage opening is below water surface at final stage
・・・Damage opening is above water surface at final stage
P ・・・permeability
FWL・・・final water line from horizontal loading deck
(+; Water line is below the deck)

Table 3 All results of experiments without car decks in compartment

		opening size	small			half of SOLAS(medium)			SOLAS(large)		
GM	initial heel	opening height	heel	P	FWL	heel	P	FWL	heel	P	FWL
2.82m	-1.5 deg	high							-2.0 deg	10.0%	27.8mm
		middle	-4.0 deg	85.0%	7.12mm						
		low	-4.0 deg	85.0%	7.12mm				-4.5 deg	85.0%	6.5mm
	0 deg	high	3.5 deg	85.0%	8.8mm				-1.0 deg	5.0%	29.7mm
		middle	3.5 deg	85.0%	8.8mm						
		low	3.5 deg	85.0%	8.8mm				-2.0 deg	85.0%	12.3mm
	1.5 deg	high									
		middle									
		low									
1.68m	-1.5 deg	high							-4.5 deg	10.0%	21.5mm
		middle	5.5 deg	85.0%	4.1mm						
		low	5.5 deg	85.0%	4.1mm						
	0 deg	high	6.0 deg	80.0%	3.9mm				5.5 deg	85.0%	3.6mm
		middle	6.0 deg	80.0%	3.9mm						
		low	7.0 deg	80.0%	1.5mm				-7.0 deg	50.0%	7.5mm
	1.5 deg	high									
		middle									
		low									

・・・Damage opening is below water surface at final stage
・・・Damage opening is above water surface at final stage
P ・・・permeability
FWL・・・final water line from horizontal loading deck
(+; Water line is below the deck)

CASE STUDY ON STATIC EQUIVALENT METHOD (SEM)

Ilkka Mikkonen, M.Sc., Deltamarin Ltd, Raisio, Finland
ilkka.mikkonen@deltamarin.com

SUMMARY

Static Equivalent Method (SEM) developed by The Ship Stability Research Centre, University of Strathclyde, Glasgow, UK (SSRC) is explored through a calculation case on a modern Ro-Ro Passenger Ferry. Comparison of the results of SEM and IMO Circ.No.1891 (i.e. Stockholm Agreement) is carried out. The merits of the SEM are then considered on the designer's point of view.

INTRODUCTION

A modern Ro-Ro Passenger Ferry designed by Deltamarin Ltd is selected for this study.

Main dimensions of the ship are:
LPP 185.40 m
B 27.50 m
T 6.70 m
H 9.50 m

There are side casings on the trailer deck all the way from stern to bow. No centre casing or flood control doors are fitted on the trailer deck. The ship has an extensive B/5 lower hold. WT compartments of the ship are shown in Figure 1.

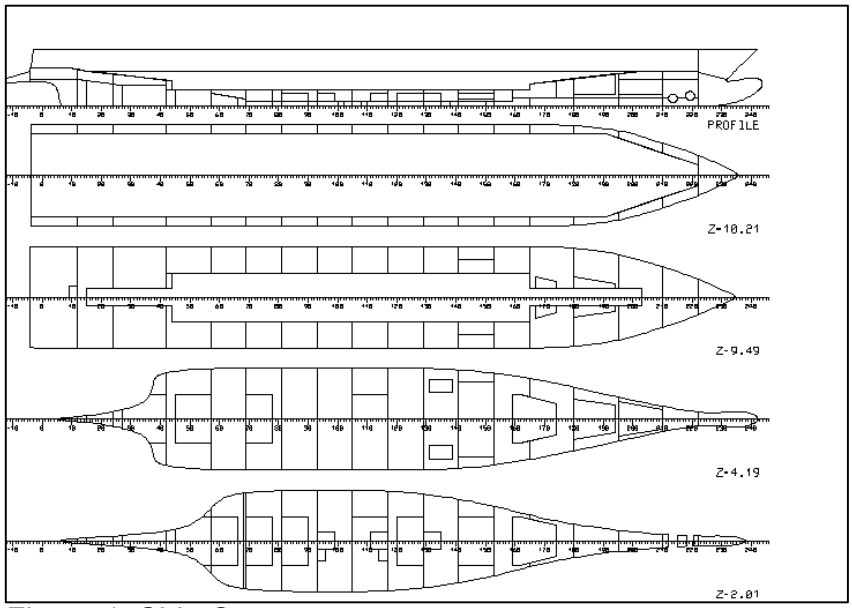

Figure 1: Ship Compartments

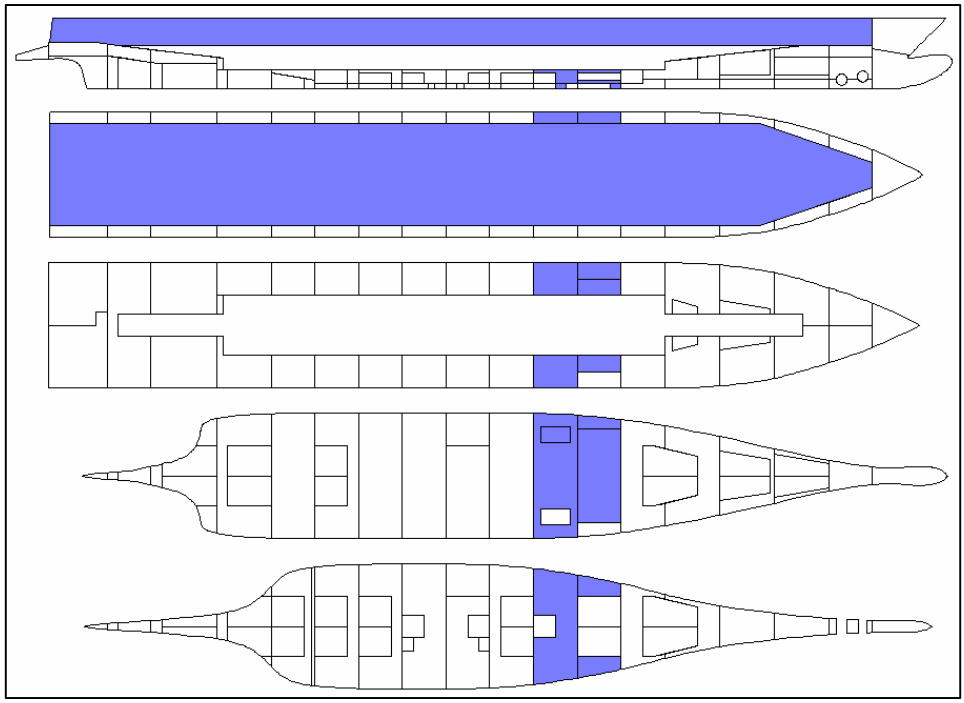

Figure 2: Most severe damage

All two-compartment damage cases according to the SOLAS 90 damage extents have been defined, that is 17 damages in total. Damages of lesser extent have been neglected in this study. The most severe damage is presented in figure 2. GM requirements taking into account the accumulated sea water on the deck according to the IMO Circ.No.1891 with Significant Wave Height of 4.0 m have been calculated. For each of these damages the SEM calculation has then been carried out with the intact condition having exactly the same GM that was found to be the requirement from Circ.No.1891. The resulting Critical Wave Heights from the Original SEM and the Alternative SEM have then been compared with the wave height used in Circ.No.1891 calculation. The merits of the SEM as a “ship designer’s tool” have been considered.

REVIEW OF RESULTS

The Critical Wave Heights have been calculated with the formula given in the original SEM and also with formulae given in the alternative SEM developed to represent 0% and 100% capsize relative frequency. The SEM correlation between the Height of Accumulated Water **h** and the Critical Significant Wave Height $\mathbf{H_s}$ are shown in Table 1.

Original SEM	Alternative SEM	
$h = 0.085 \cdot H_S^{1.3}$	$h_{0\%C} = 0.250 \cdot H_S^{0.83}$	$h_{100\%C} = 0.215 \cdot H_S^{0.81}$

Note: $x\%C$ means $x\%$ ***C***apsize probability

Table 1: Original SEM and Alternative SEM formulae

In Table 2 the most important results are gathered. The columns of the table are:

DAMAGE	Damage identification. Damages are numbered from the aft.
GMREQ	GM requirement calculated according to IMO Circ.No.1891 with Significant Wave Height of 4.0 m.
CRITERIA	The limiting damage stability requirement.
h	The Head of Water **h** calculated according to the SEM.
$H_{s\ original}$	Critical Wave Height calculated according to Original SEM
$H_{s0\%c}$	Wave Height corresponding to h0% Capsize Frequency
$H_{s100\%c}$	Wave Height corresponding to h100% Capsize Frequency
Tot V	Total volume of water on trailer deck
Add V	Volume of accumulated water above sea level

DAMAGE	GMREQ [m]	CRITERIA	h [m]	$H_{s\ original}$ [m]	$H_{s0\%c}$ [m]	$H_{s100\%c}$ [m]	Tot V [m^3]	Add V [m^3]
DDS0+W	1.493	MAXGZP	0.975	6.530	5.151	6.462	307	305
DDS1+W	1.584	MAXGZP	0.865	5.960	4.465	5.581	313	299
DDS2+W	2.324	MAXGZP	0.730	5.231	3.639	4.526	453	344
DDS3+W	2.471	RANGE	0.825	5.745	4.214	5.260	444	362
DDS4+W	2.063	RANGE	0.904	6.161	4.703	5.886	330	318
DDS5+W	1.842	RANGE	0.919	6.240	4.797	6.007	340	331
DDS6+W	1.685	RANGE	0.918	6.239	4.796	6.006	289	288
DDS7+W	1.650	RANGE	0.984	6.579	5.212	6.540	307	300
DDS8+W	2.372	RANGE	0.829	5.766	4.238	5.291	562	453
DDS9+W	2.459	RANGE	0.772	5.461	3.893	4.849	580	434
DDS10+W	2.148	RANGE	0.791	5.563	4.007	4.996	426	351
DDS11+W	2.473	MAXGZP	0.770	5.448	3.879	4.832	596	428
DDS12+W	2.430	MAXGZP	0.782	5.514	3.952	4.925	585	417
DDS13+W	2.386	MAXGZP	0.736	5.261	3.672	4.568	653	434
DDS14+W	2.401	MAXGZP	0.755	5.364	3.786	4.713	644	432
DDS15+W	2.205	MAXGZP	0.796	5.588	4.036	5.032	488	359
DDS16+W	1.662	MAXGZP	0.841	5.829	4.312	5.385	352	305
DDS17+W	1.330	MAXGZP	0.952	6.416	5.011	6.281	335	315

Table 2: Results of SEM calculation

Graphics of the calculation results are provided in Figures 2, 3, 4 and 5.

GM requirements calculated according to Circ.No.1891 vary between 1.330 m and 2.473 m. The highest requirement was caused by the damage into the compartments where the heeling tanks are located. The limiting criteria in the aft and forward part of the ship was the requirement of Maximum GZ taking into account the Passenger Crowding Heeling Moment. At the mid ship area the limiting criteria was the Range of 15 degrees.

The Head of Water **h** causing the angle of equilibrium θ_e that equals the angle θ_{max} derived without accumulated water was rather constant for all damages. Smallest value for **h** was 0.730 m and the maximum 0.975 m. (Note! The initial GM was always changed to correspond the Circ.No.1891 requirement)

The Volume of Water on the Deck calculated according to SEM showed peak values at the same damages that caused the biggest requirements in Circ.1891 calculation which seems quite logical.

At the present case study the SEM calculation showed 0% Capsize Frequency with Significant Wave Height varying between 3.639 m and 5.212 m, the average being 4.320 m, while the corresponding Circ.No.1891 calculation was carried out with H_s of 4.0 m. So the 0% capsize wave height gave in this particular case rather close results to the Circ.No.1891. The Critical Wave Height from Original SEM was clearly higher. The average $H_{s\ original}$ was 5.828 m.

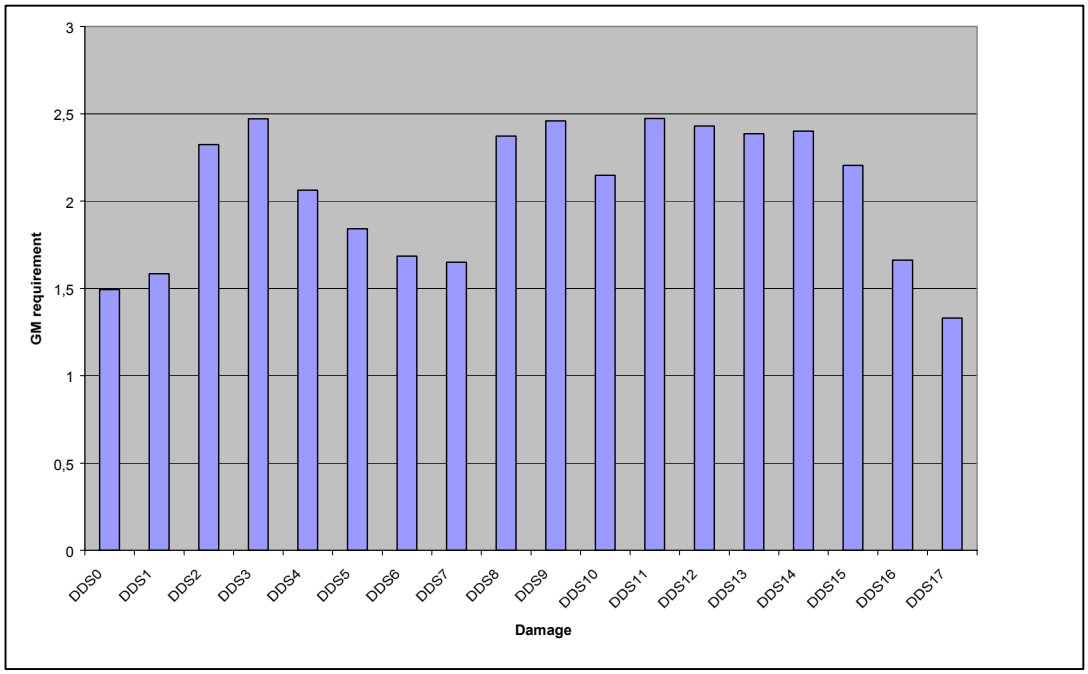

Figure 2: GM requirements acc. IMO Circ.No.1891

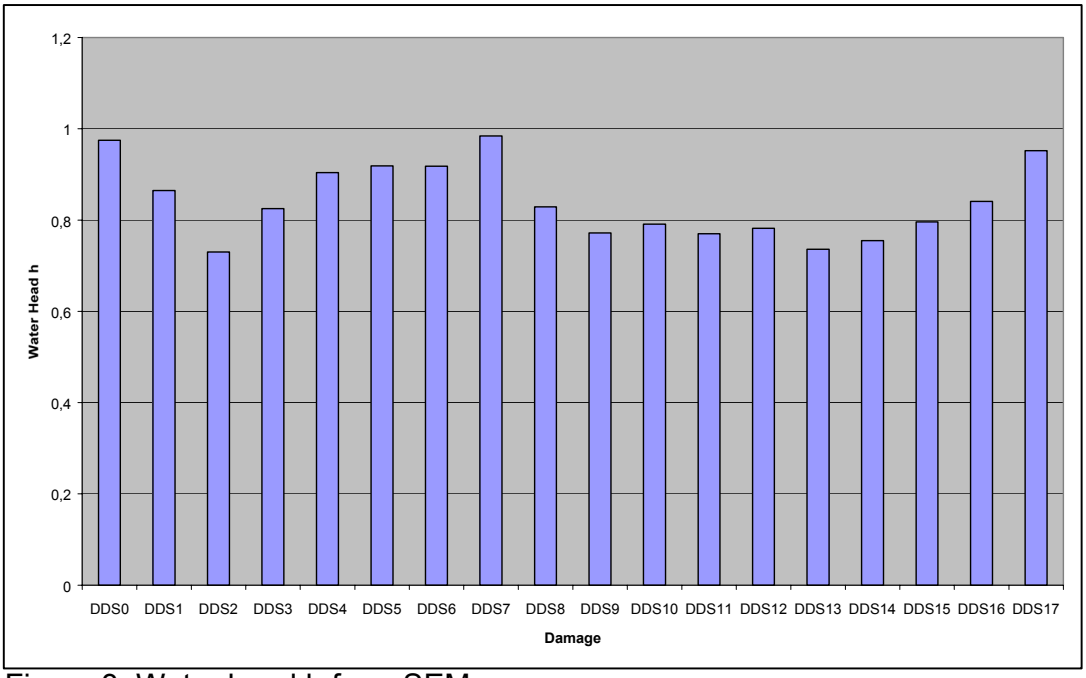

Figure 3: Water head h from SEM

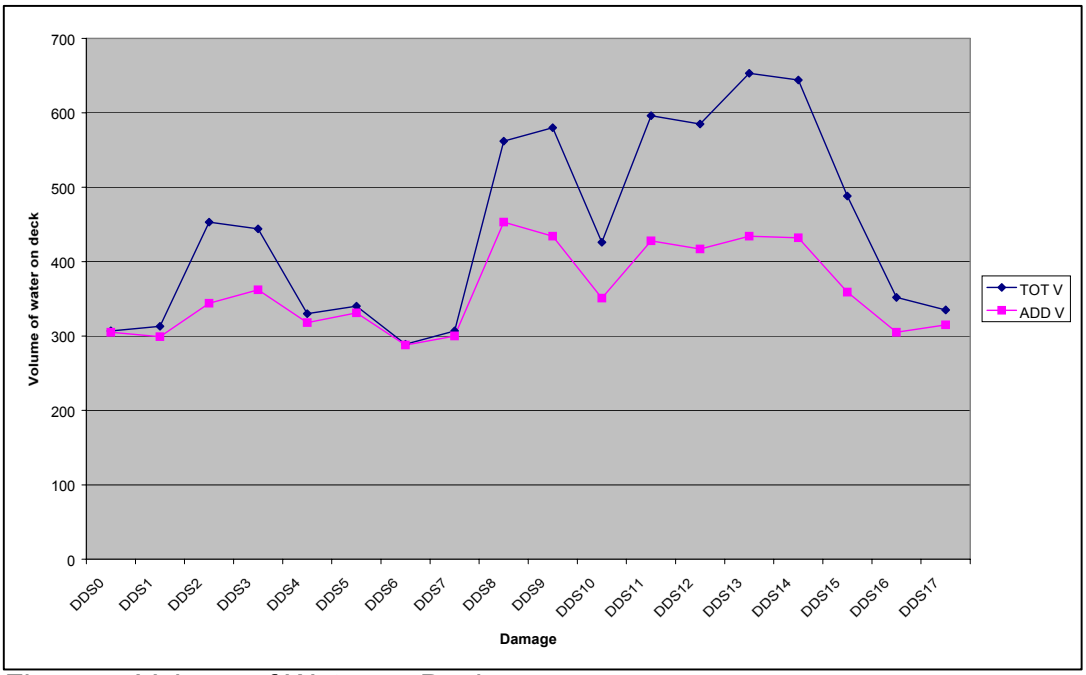

Figure 4: Volume of Water on Deck

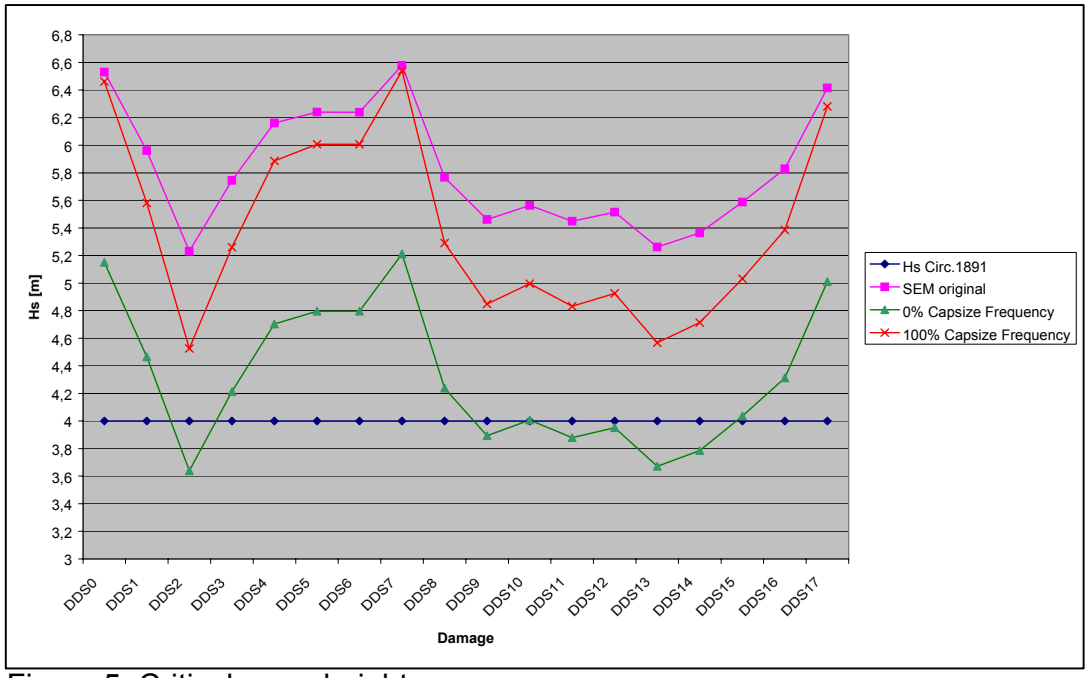

Figure 5: Critical wave heights

CONCLUSIONS

It is a well known fact from earlier experience that the Circ.No.1891 calculation and the alternative model test method can give differing results. The SEM has been tuned to give good correlation with model tests. This good correlation has been found in a lot of calculations, most of those carried out by the SSRC.

The SEM calculation is rather laborious if it is carried out “manually” using graphics of damaged GZ curves. At Deltamarin the first attempts to calculate SEM required several working days per ship. Luckily it is however possible to make most of the work automatic at least in case some modern Naval Architectural Software is used. Today by using Naval Architectural Package NAPA and a small macro program the calculation time for one ship configuration is about 2 – 3 hours.

SEM should be used with great care. Very small adjustments to calculation tolerances and calculation heeling angles seem to cause some tens of centimetres changes to the resulting Critical Wave Height. One reason for this is the normally rather flat form of the damaged GZ curve. The location of the maximum of the GZ curve need to be resolved very accurately.

The best merits of the SEM for a ship designer are that it makes it possible for small and medium sized design offices and small yards to perform analysis on dynamical water on deck performance of the ship without having expensive time domain simulation software and the necessary expertise to use that kind of software. Thus it is possible to

calculate several compartment configurations in order to improve the safety of the final design for the ship.

The SEM can also reduce the amount of the water on deck model experiments needed especially in stability upgrade projects for existing ships with sailing routes on the sea area where The Stockholm Agreement is in force.

REFERENCES

SEM, Static Equivalent Method, Background and Application by
The Ship Stability Research Centre, University of Strathclyde, Glasgow, UK
June 2000

NEREUS, Mid-term report, June 2001

REVIEW OF DESIGN FEATURES AND STABILITY CHARACTERISTICS OF PRE- AND POST SOLAS 90 RO-RO PASSENGER SHIPS

Eleftheria Eliopoulou, Dipl.-Eng., Dr.-Eng. Cand., Ship Design Laboratory, National Technical University of Athens, eli@deslab.ntua.gr

Apostolos Papanikolaou, Professor, Head of Ship Design Laboratory, National Technical University of Athens, papa@deslab.ntua.gr

SUMMARY

This paper presents an analysis of results of systematically collected technical data of Ro-Ro Passenger ships operating mainly in European waters. The data are derived from collaborative work within the EU-projects SAFER-EURORO [1] and ROROPROB [2] as well as from data of an NTUA-SDL in-house technical database. The study enables a variety of conclusions on the past, presently adopted and foreseeable practices in Ro-Ro Passenger Ship Design pertaining to stability and safety characteristics.

1. INTRODUCTION

The Ro-Ro concept is a very popular and efficient mode of transportation especially in Europe, where 50% of the world's Ro-Ro shipping fleet operates.

From the economical point of view, the capability of carrying simultaneously a wide variety of cargoes with minimum infrastructure and shore-based equipment make the particular ship type most competitive. In terms of safety/stability, the vulnerability of large vehicle spaces creates a serious stability and floatability problem in case of flooding due to collision or other incidents leading to car deck flooding (e.g., bow door opening).

The presented work is within the scope of the ROROPROB project, aiming at developing and implementing a new formalized design methodology for optimal subdivision of Ro-Ro Passenger ships based on the probabilistic damage stability approach.

2. TECHNICAL DATABASE

The present RORO Technical Database serves a comprehensive and stand-alone reference of European Ro-Ro Passenger Ferry fleet. It currently includes data of 780 ships of the following types: Passenger/Car Ferries, Passenger/Train/Car Ferries, Vehicle Carriers, Ro-Ro Cargo ships. With respect to the Passenger/Car Ferries, the database is considered to be fully representative of the present status of the entire European Passenger/Car ferry fleet.

2.1 DATABASE STRUCTURE

The database has been developed under MS Access 2000. The registered data refer to available information on the following ship characteristics:

- General characteristics of the vessels (name, former names, owner, flag, area of operation, class, crew, builders, year of build, year of major modifications).
- Main technical characteristics, such as main dimensions, lightship weight, displacement and payload, powering, life saving equipment.
- Special devices such as: propellers, rudders, thrusters, stabilizers, sponsons, stern/bow doors.
- Information on intact stability and loading conditions.
- Basic subdivision below and above main car deck.
- Damage stability information on worst case (equilibrium and values of residual stability)
- Stability standard currently in compliance as well as the next relevant regulation to be in compliance.
- Severe Casualties Records.
- Outline of general arrangement.

2.2 DATABASE ANALYSIS

The following analysis has been carried out with respect to category Ro-Ro Passenger/Car Ferries and attempts to relate technical and global economic ship characteristics to their stability and eventually safety. The sample of analysed data contains 498 ships and is given in *Table 1*.

		Average	Min - Max	Sample
Length Over All	m	126.95	33.02 - 214.9	497
Length Between Perpendiculars	m	116.51	28.01 - 198	486
Breadth Moulded	m	20.19	6.66 - 32	472
Depth to the Main Deck	m	7.03	1.99 - 12.6	269
Draught	m	5.14	1.25 - 8.22	486
Deadweight	t	2716	39 - 15500	476
Lightship	t	6904	317 - 21800	252
Displacement	t	9465	196 - 25300	264
Gross Register Tonnes		12437	198 - 59912	498
Speed	kn	18.98	8 - 31	478
Total Power of Main Engines	HP	16772	456.3 - 90500	496
Year of Built		1980	1952 - 2001	497
Year of Mod/cation of Major Char.		1990	1971 - 2000	80

Table 1: Sample of analysed data

For the study, a major separation into two main categories has been considered, namely: sample of data for ships built

before 1990 and ships built after 1990. This breakdown was essential, firstly because of the change of design philosophy in the last decade and secondly because of the request for compliance with higher stability standards after the introduction of SOLAS 90. Further categorizations have been also considered such as: ships built after 1993 or 1997, in order to have more clearly the effect of the SOLAS 90 and SOLAS 95 requirements. In some cases, the differences are not significant compared to the post-1990 results. In some others, the sample is not considered satisfactory in order to conclude, *Figure 1*. Finally, results based on different stability standard are also provided.

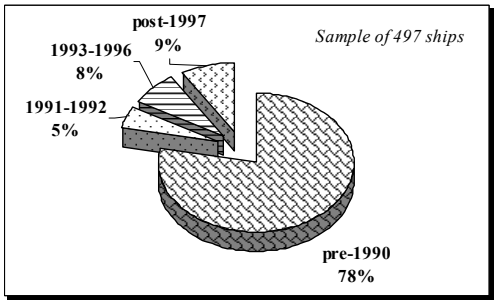

Figure 1: Distribution of sample acc. to Year of Built

3. REVIEW OF RESULTS

3.1 SIZE OF VESSELS

The size of vessels has significantly increased in the last decade along with higher service speeds and powering requirements, creating different generations of Ro-Ro Passenger Ferries and expressing the demand for faster, more comfortable and safer sea transport, *Figure 2* and *Figure 3*.

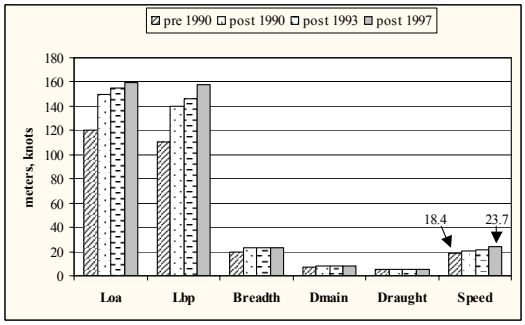

Figure 2: Averages of main dimensions and speed

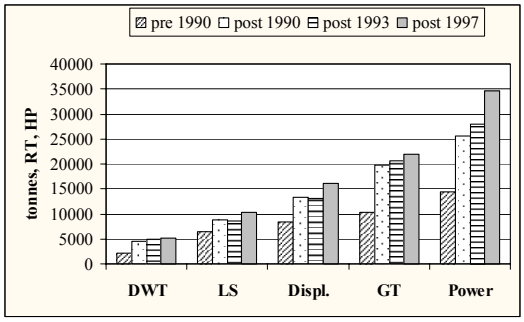

Figure 3: Averages of weights and power of M.E.

3.2 DIMENSIONAL RATIOS & COEFFICIENTS

- L/B ratio: there is no clear trend of the particular ratio. Analysis based on different Lbp categorisation indicates that the ratio decreases for ships built post-1990, especially in the range of Lbp up to 160m. This reflects the relative increase of beam in order the enhanced stability standards to be achieved. On the other hand, length is one major parameter that greatly affects building cost, but also depends on harbour and route limitations.

L/B	Ships of Lbp 100-130m	Ships of Lbp 130-160m	Ships of Lbp >160m
Pre 1990	5.0 - 7.4	4.7 - 7.4	5.8 - 7.4
Post 1990	4.9 - 6.9	5.0 - 6.7	5.3 - 7.4

L/B	Ships Built post 1993	Ships Built post 1997	Ships Built post 1993
	4.9 - 7.4	4.9 - 7.4	
Vs ≥24			5.1 - 7.4

- B/T ratio: Clearly increasing for the new vessels, an indication of increased stability requirements. Draft remains constant or slightly decreasing (shallower ships) for enabling docking of large ferries at existing port infrastructure and accounting for restricted draft routings.

B/T	Ships of Lbp <130m	Ships of Lbp 130-160m	Ships of Lbp >160m
Pre 1990	2.9 - 4.9	2.9 - 4.6	3.3 - 4.7
Post 1990	3.6 - 4.9	3.7 - 4.6	3.2 - 4.7

B/T	Ships Built post 1993	Ships Built post 1997	Ships Built post 1993
	3.2 - 4.9	3.6 - 4.9	
Vs ≥24			3.6 - 4.6

- T/D ratio: The T/D ratio is of particular importance for the damage stability, because of its direct relation to the ship's intact (and damage) freeboard. It is notable that this ratio obviously decreased (indicating increased freeboard), *Figure 4*.

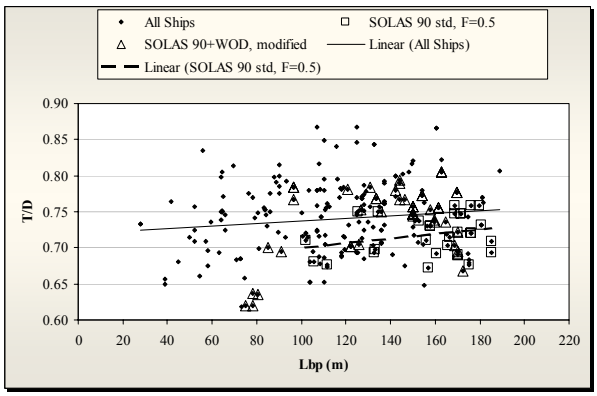

Figure 4: T/D ratio acc. to stability standard

Ships with enhanced stability standard, as built, have a T/D ratio within the range of 0.67-0.76.
Regarding ships that are modified to comply with the enhanced regulations, i.e. SOLAS 90+WOD, high T/D ratios are due to external or/and internal modifications such as sponsons, ducktails, barriers, etc.

- Block Coefficient: typically increased in the average indicating increased hull form efficiency in terms of space and floatability requirements, *Figure 5*.

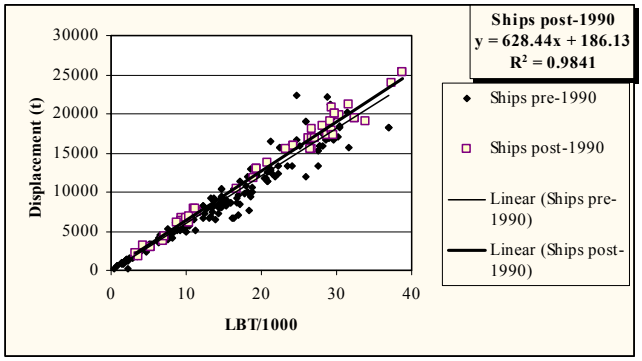

Figure 5: Displacement vs. (LBT/1000)

Regarding pre-1990 results, there is a wide spread of the analysed data, *Figure 6*.

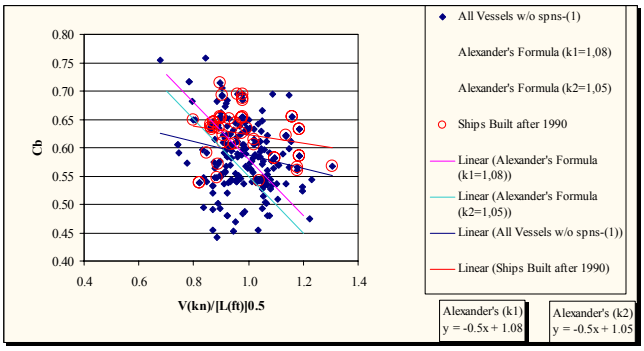

Figure 6: Cb vs. $V/\sqrt{L}$

With respect to minimum values of block coefficients, the significant point is that registered values of 0.45 for some older ships now disappeared.

Cb	Ships Built post 1993	Ships Built post 1997	Ships Built post 1993
	0.54 - 0.72	0.56 - 0.65	
Vs ≥24			0.56 - 0.65

- Powering and related coefficients: The coefficient of the English Admiralty, Cn, reflects the hydrodynamic efficiency of the ship's hull form. It can be noted that vessels built post-1990 have improved hydrodynamic efficiency, *Figure 7,* despite the fact that operational speeds (Froude numbers) and the block coefficients are in the average higher.

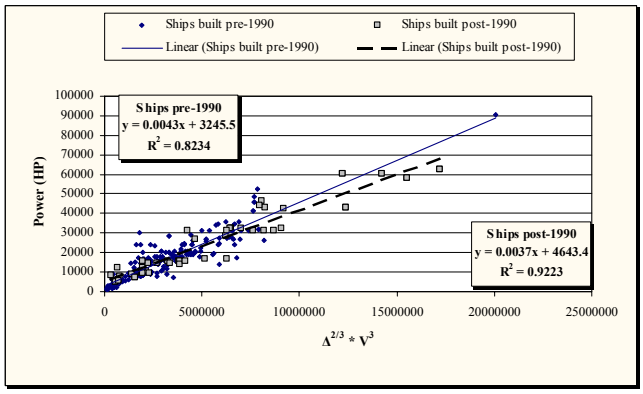

Figure 7: Power vs. [(Displacement$^{2/3}$ * Speed^3)

For ships built post-1993, Cn varies as indicated in the next table.

Cn	Ships Built post 1993	Ships Built post 1997	Ships Built post 1993
	112-312	126-312	
Vs ≥24			202-312

For a given speed, the required horsepower per ton displacement of newer ships is less than for the older ones, *Figure 8.*

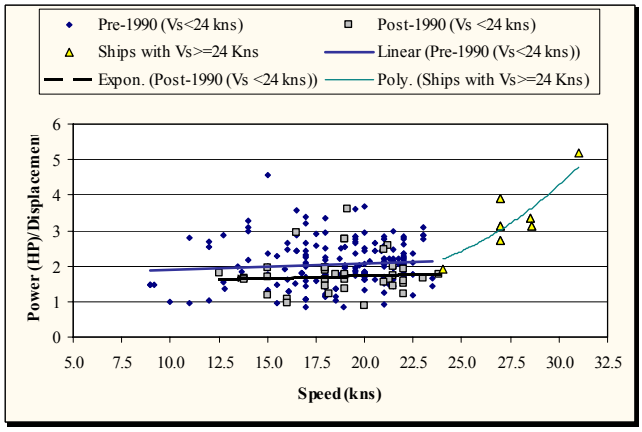

Figure 8: (Power/Displacement) vs. Speed

Figure 9 shows the installed power of Main Engines per passenger with respect to ships carrying more than 1000 passengers.

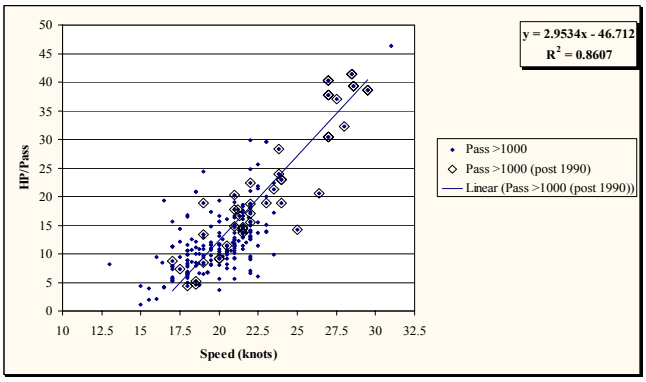

Figure 9: HP/Passengers vs. Speed

3.3 MAIN DIMENSIONS

Regarding the main dimensions, some formulae were deduced that could be useful for the conceptual design stage, *Figures 10 and 11*.

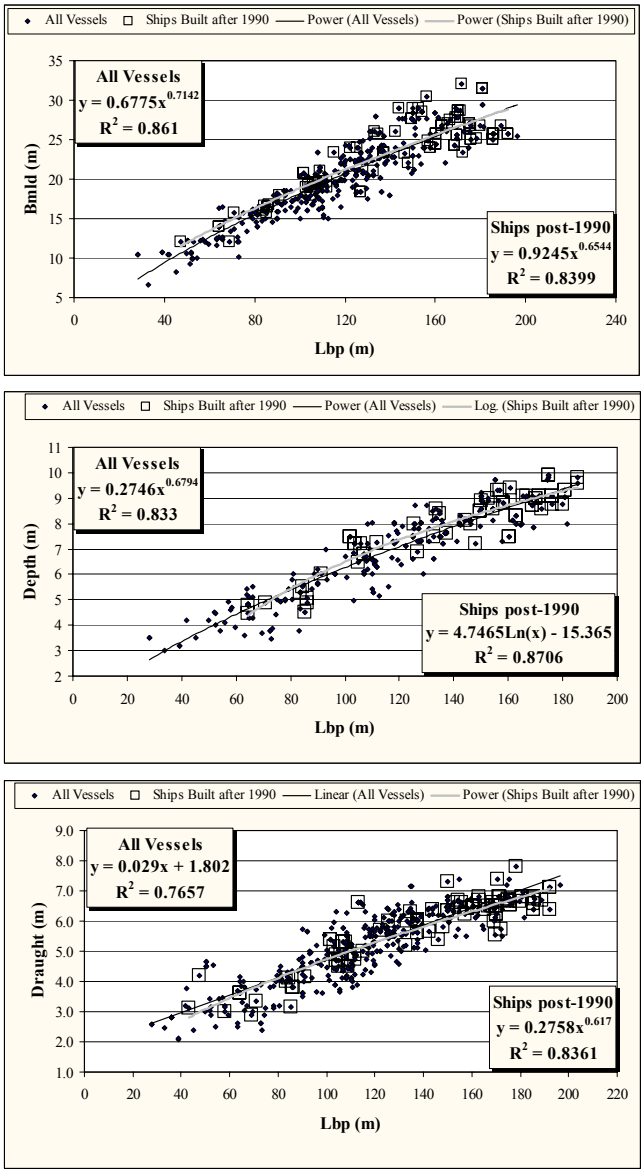

Figure 10: Main Dimensions vs. Lbp

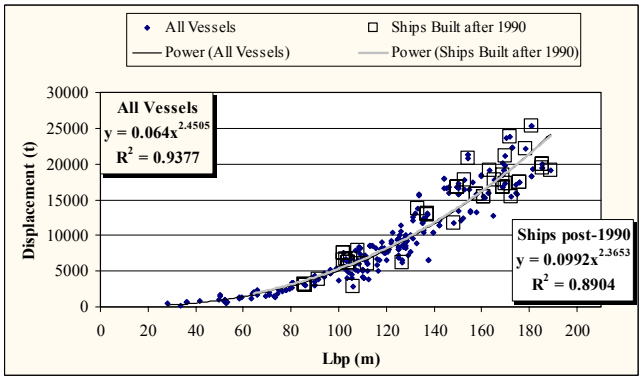

Figure 11: Displacement vs. Lbp

3.4 DISTRIBUTION OF WEIGHTS

Lightship Weight & DWT: For given main dimensions, a vessel built pre-1990 appears to have greater weight of lightship compared to the newer ones. Focusing to the post-1990 ships, lightship is increasing for post-1997 in comparison to ships built in 1990-1996, *Figure 12*.

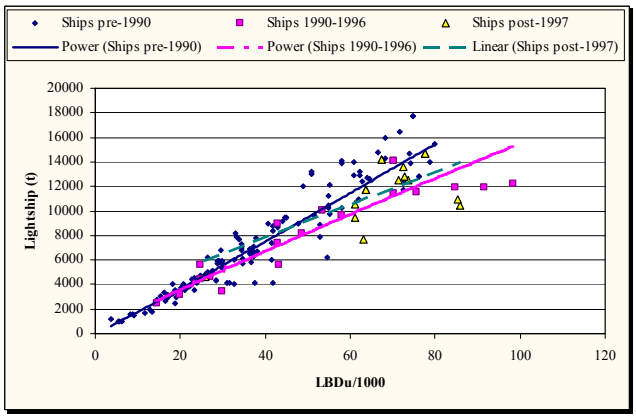

Figure 12: Lightship vs. LBDu/1000

From another point of view, the required compartmentation to meet higher stability standards, leads to an increase of lightship weight due to the additional structural weight, proportional to the number of fitted bulkheads, Papanikolaou et al (2000), *Figure 13*.

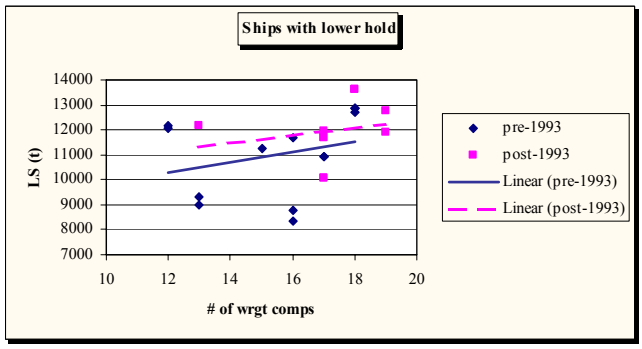

Figure 13: Lightship vs. # of basic transverse watertight compartments

Taking into account the fact that the speed of the vessels continuously increased, DWT/Δ ratios based on speed are presented in *Figure 14*.

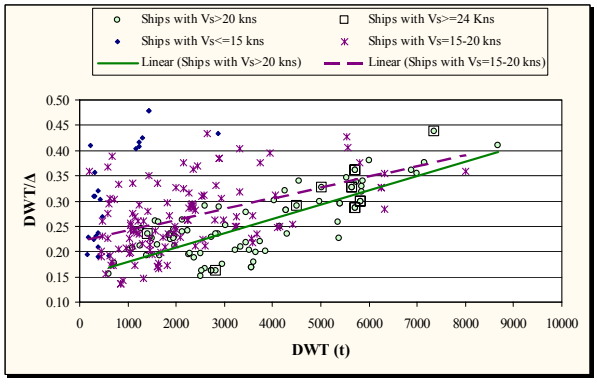

Figure 14: DWT/Displacement vs. DWT

3.5 PAYLOAD

Lanes' length/Lbp ratio: The ratio of the car Lanes' Length/Lbp has significantly increased for the newer ships, indicating the higher efficiency of modern designs. Vessels built before the year 1990 have an average ratio of 7.3, whereas those built after 1990 have a 60% higher ratio of 11.6.

For a given deck waterplane area, ships post-1990 can accommodate a larger number of lane meters than the older ones, *Figure 15*.

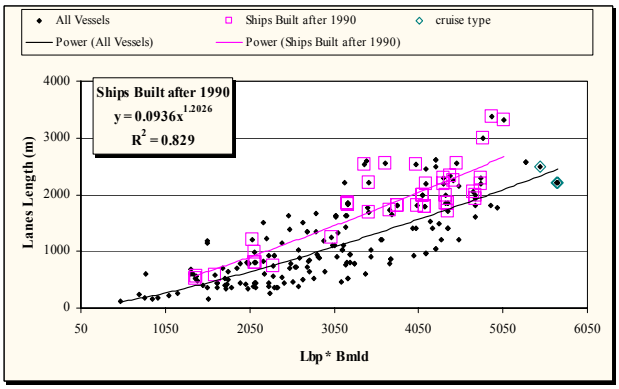

Figure 15: Lanes Length vs. Lbp * Bmld

In domestic voyages, service speeds have been kept at normal levels because it is either impossible by environmental conditions or non-economical to take full advantage of the higher service speeds, *Figure 16.*

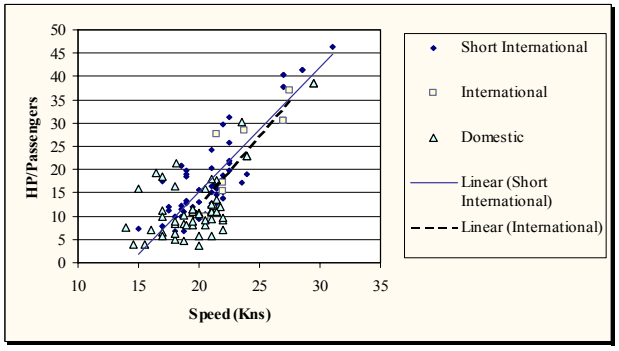

Figure 16: HP/Passengers vs. Speed, per voyage type

3.6 COMPARTMENTATION BELOW MAIN CAR DECK

The introduction of the longitudinal bulkhead concept inside B/5 line has changed the philosophy of design of the internal compartmentation below the main car deck. As a result the considerable floodable volumes have been reduced. The majority of older ships have only transverse bulkheads (TB), as a standard subdivision, to the greater extent of their length, though in newer ships the combination of transverse and longitudinal bulkheads (LB&TB) is a common feature, except for the relatively small ships, *Figure 17*.

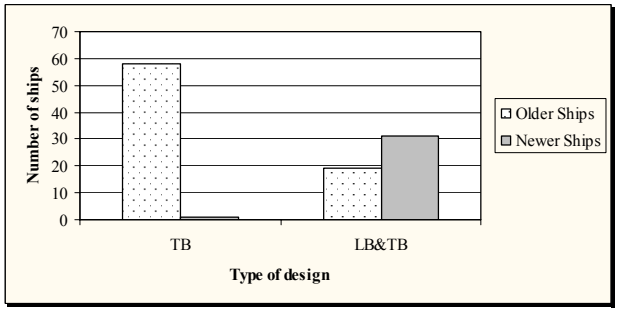

Figure 17: Distribution of type of internal compartmentation below main car deck

The length of primary transverse watertight compartments has been reduced for the newbuildings (and accordingly the number of WT compartments increased) to meet the higher damage stability standards, F*igure 18*.

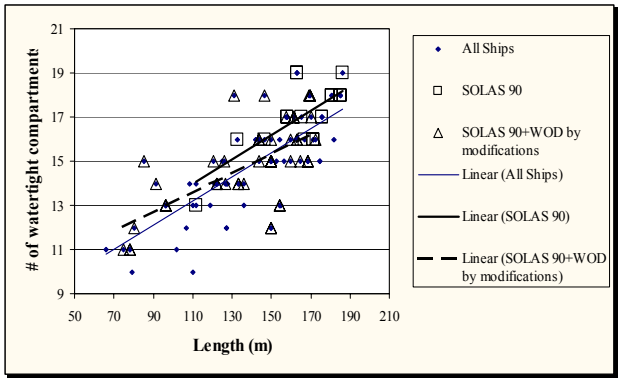

Figure 18: # of watertight compartment vs. Length

In order to utilise the space below the main car deck, as this space cannot be used for accommodation purposes by the latest SOLAS regulations, large lower hold decks inside B/5 line are adopted in new concepts, that in some cases might be exceeding even 50% of ship's length, *Figure 19*.

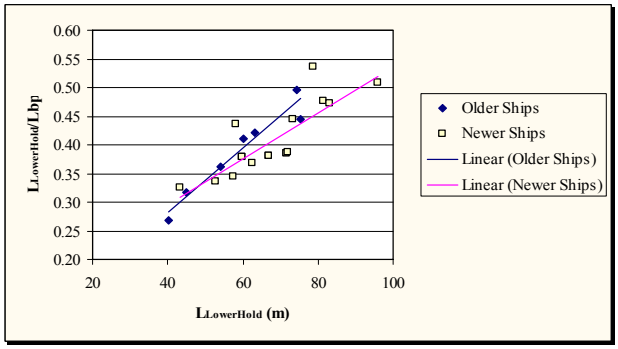

Figure 19: Lower hold Length/Lbp vs. Lower hold Length

Although these large unified spaces are considered intact in typical SOLAS damage conditions, there might be the cause of serious stability problems in cases of actual penetration beyond B/5, if not properly arranged.

The length of engine room appears to become shorter, for given installed power, *Figure 20*. This is attributed to the

consideration of alternative machinery arrangements and the use of more compact machinery units.

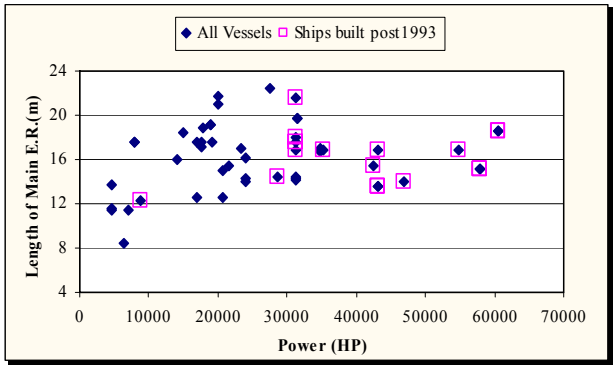

Figure 20: Length of Engine Room vs. installed power

3.7 OUTFITTING

3.7 (a) Stern Ramps

Dimensions of ramps influence their structural design but also ship's operation and efficiency with respect to cargo handling speed.
Normally length varies between 5-12m. Longer ramps of about 20m can also be fitted but are foldable, *Figure 21*.

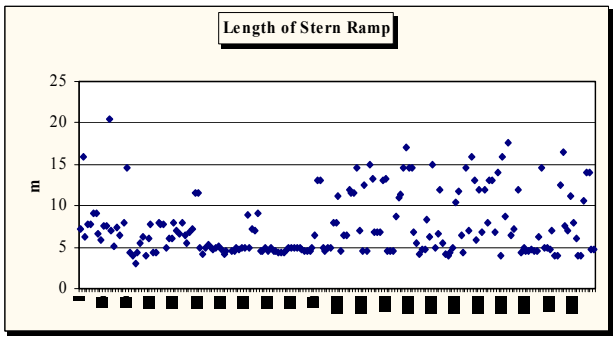

Figure 21: Length of stern ramps

Very wide ramps have been detected at newer ships reaching in some cases 90% of ship's breadth, *Figure 22*.

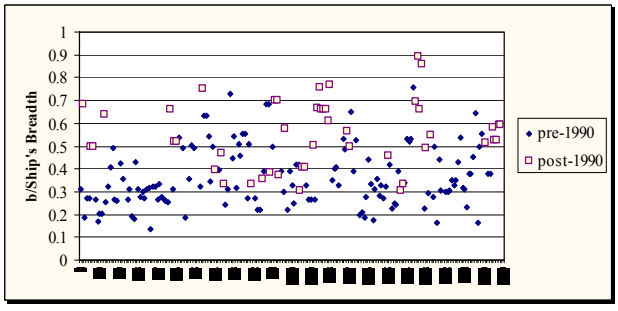

Figure 22: Total breadth of stern ramps/Ship's Breadth ratio

The water ingress through the stern opening might be a problem with poorly maintained stern doors in cases when the seawater level is quite close to the down edge of the ramp. Although newer ships have greater freeboard, it must be noted that in some cases, a roll angle of 9-10 degrees can immerse the down edge of ramps, *Figure 23*.

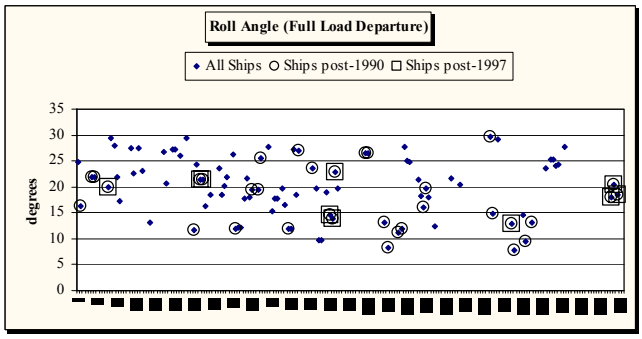

Figure 23: Angle of immersion of down edge

3.7 (b) Thrusters

Bow and even stern thrusters are, nowadays, standard devices for European Ro-Ro Passenger Ferries. Regarding post-1990 ships, the 4% not having fitted thrusters concern small ships of Loa under 70m, *Figure 24*.

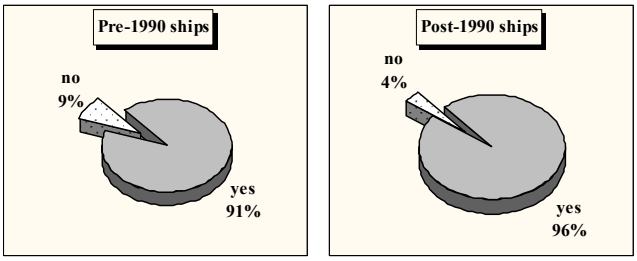

Figure 24: Distribution of existence of thrusters

A significant parameter is also the increased thrusters' power that improves the maneuverability of ships, *Figure 25*.

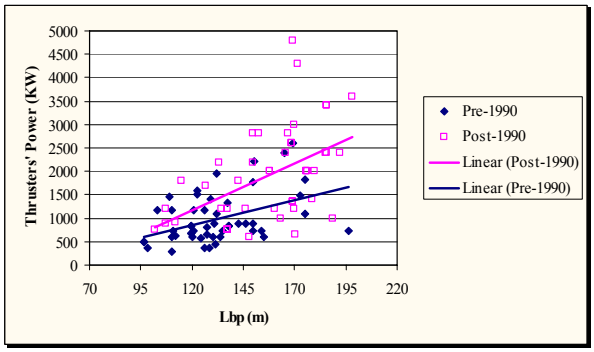

Figure 25: Thrusters' power vs. Lbp

3.8 INTACT STABILITY

Freeboard is an essential parameter affecting the stability and safety of ships both in intact and damage condition. A comparison of the intact freeboards between vessels of different stability standard shows that SOLAS 90 2-compartment standard and A.265 ships dispose comparable and in general larger intact freeboard heights, *Figure 26*.

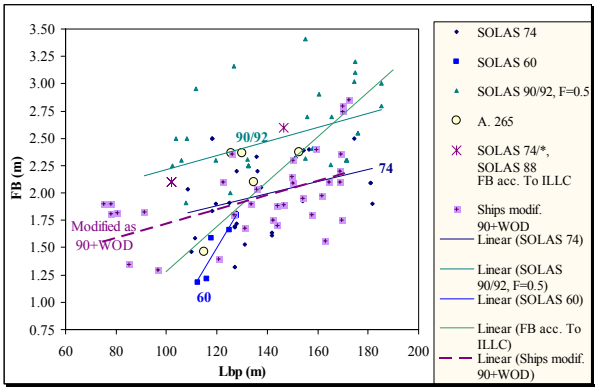

Figure 26: Intact Freeboard vs. Lbp

Note that intact freeboards for the larger new ships are close to and over 2.5 m, what clearly calls for the provision of new docking facilities in some European ports, currently adjusted to freeboards in the range of 1.5 to 2.0m.

Enhanced stability standard clearly requires greater GM values, *Figure 27*. This should generally affect ship's sea kindness, as ships become stiffer in roll and passengers might experience higher transverse accelerations. However, this negative effect of GMt on seakeeping is commonly counteracted by the employment of stabilising fins and of antirolling tanks.

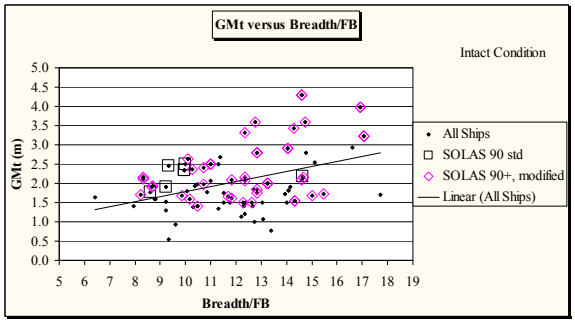

Figure 27: Intact GM vs. Breadth/Intact Freeboard

3.9 DAMAGE STABILITY

Newer vessels have improved damage stability characteristics due to their compliance with enhanced damage stability criteria, *Figure 28*.

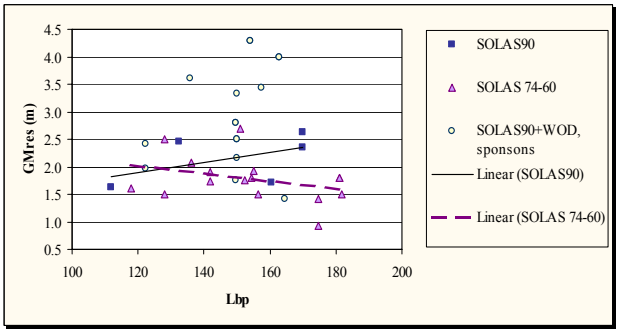

Figure 28: Distribution of residual values of GM

4 CONCLUSIONS

Decisions in the early ship design stage strongly depend on the designer's expertise and knowledge from the past, but also on the knowledge of 'state of the art' technological developments.

Technical ship data to the extent collected herein in a systematic manner are rare, though considered essential in the conceptual-preliminary design stage, that is the stage in which major technical and economic ship characteristics are determined following the owner's requirements and statement of work.

The collected data can be not only exploited in the conceptual design stage, but also for the crosschecking the data of individual designs under consideration. Also, the derived regression formulae might be useful in the set-up of a computer-aided optimisation procedure, as planned in WP3 of the ROROPROB project. Note, however, that in this latter case, special attention should be paid in the careless use of specifically suggested regression formulae, especially in those cases for which the extent of the sample appears small and/or the spread of the collected data large (low R^2 regression values).

5 ACKNOWLEDGES

The work, presented in this paper, was partly supported by the EU-project ROROPROB (C.N. G3RD-CT-2000-00030).

6 REFERENCES

1. SAFER EURORO Ship Design Team, "Technical Database of European Ro-Ro Passenger Ship", NTUA-SDL Report, European Community – DG XII, Brussels, 2000.

2. ROROPROB, "NTUA-REP-T1.3.2&3-D9-D10", European Community – DG XII, Brussels, 2001.

3. Papanikolaou A., Eliopoulou E., Kanerva M., Vassalos D., Konovessis D., "Development of a Technical Database for European Passenger Ship", Proc. IMDC 2000 Conference, Korea, 2000.

SOLAS AND WATERTIGHT DOORS

Furio Degrandi, Fincantieri (TR-ARC)-Trieste, furio.degrandi@fincantieri.it
Giuseppe Mainenti, Fincantieri (TR-ARC)-Trieste, giuseppe.mainenti@fincantieri.it

SUMMARY
The purpose is to induce a more flexibility on the SOLAS interpretation regarding a regulation on the watertight doors.

1. INTRODUCTION

Often, due to the daily contact with the practical problems regarding the shipbuilding, the people in it emploied pay attention to the some specific axpects connected with their activity.
Ship design, as other human activities, have to satisfy the imposed rules to guarantee the safety of the adopted solutions.
The SOLAS is the reference text for the ship designers but sometime it could be an unintentional obstacle to the evolution of the naval technic.

2. DESCRIPTION

An example of the content in the introduction is the Regulation 25-9 of SOLAS (Chapter II, Part B-1) in which the characteristics of the openings in watertight bulkheads and internal decks in cargo ships are listed.
In the point 2 of the regulation is fixed that *" Doors provided to ensure the watertight integrity of internal openings which are used while at sea are to be sliding watertight doors capable ……"*.
In our opinion the literally interpretation of the rule, when it impose the sliding type for a watertight door, limit without a reason the possibility in searching different solutions even if with the same safety grade of the sliding doors.
Moreover it seems to us that the literally interpretation of the above rule contrasts with the content of the Regulation 5 - Equivalence (Chapter I - General provisions, Part A) of the SOLAS in which different solutions are allowed if they assure and demonstrate the same efficacy.
This last rule is very important, in our opinion, because it stimulate the inventiveness and the search of solutions more sticking to the variety of problems, damage consequences in our case, that the ship design have to solve.
Going deeper in the problem, during the activity of the department of Naval Architecture (TR-ARC) of Fincantieri, examining the several flooding condition for same vessels, we observed the possibility to limit more the consequences of the damages, positioning watertight doors in selected locations of the ship.
Unfortunately, the fitting of sliding doors wasn't easy because of the disposable space.
Among the examinated possibilities, an hinged watertight door seemed the best solution.
In the hinged type the absence of the recess for the slidind part of the door was a favourable factor for its fitting.
Nevertheless, because of the possibility of a literally interpretation of the SOLAS that prescribe the sliding type, this solution was doubtful.
Going ever deeper in the problem, the question is: what are the reasons for which SOLAS impose the sliding type?

Examining all the differeces between the sliding and the hinged door only one is the reason for which, in our opinion, the sliding type would be prefer.

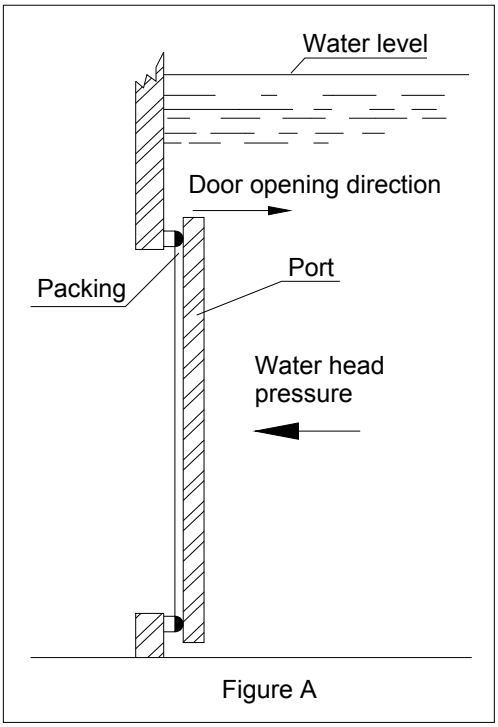

Figure A

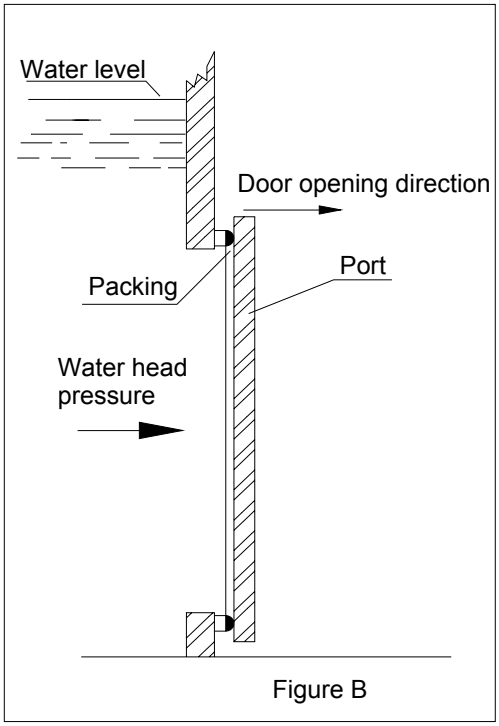

Figure B

Looking at the figure A in which an hinged door is schematized, the water head pressure, acting aganist the port and opposing to the door opening direction, force the packing and helps the closing system to produce the watertightness of the door.

In the figure B, the water head pressure acts according to the opening direction and reduce the closing force acting on the packing.

This means that the hinged type door hasn't, in both side, the same strenght to contrast the water infiltration through the packing.

In the sliding type door, on the contrary, the forcing strenght is the same for both side.

But if we adopt a closing system able to assure the same efficacy to contrast the water infiltration for both side of the port and meeting all the requests as for the sliding door, we think that an hinged door is equivalent to the sliding one.

All this stimulated the Naval Architecture Department of Fincantieri (TR-ARC) in the searching of a simple and reliable solution to the problem.

It was solved and now it's waiting for the practical testing.

3. REFERENCES

' SOLAS ', Consolidated edition 2001, International Maritime Organization. London, 2001

SAFETY EQUIVALENCE – MEANING AND IMPLEMENTATION

Dracos Vassalos and Cantekin Tuzcu
The Ship Stability Research Centre (SSRC), The Universities of Glasgow and Strathclyde, UK, ssrc@na-me.ac.uk

SUMMARY

Deriving motivation from the recent IMO Resolution MSC.99(73) on "Alternative Design and Arrangements" for fire safety and of new proposals at SLF 44 concerning other ship hazards, this paper focuses on the safety equivalence issue, which is at the heart of these exciting new developments. In this respect, it presents an analysis on the level of safety portrayed by current regulatory instruments on assessing damage stability, aiming to demonstrate and quantify the link between deterministic and probabilistic damage stability regulations and performance-based standards. To this end, survivability test results of a representative sample of Ro-Ro passenger vessels, which were model tested according to Stockholm Agreement Resolution 14, are used to provide a reference level against which all other instruments pertinent to damage survivability are tested.

NOMENCLATURE

A	Attained Index of Subdivision
R	Required Index of Subdivision
γ	Peakness parameter
H_s	Significant wave height [m]
s_i	Probability of a ship surviving a specific damage case in a given sea state
p_i	Probability that the compartment(s) under consideration is flooded
s_w	Probability of a ship surviving collision damage with large scale flooding on deck
s_a	Probability of a ship surviving collision damage considering all effects other water accumulation on deck
SEM	Static Equivalent Method
SLF	Sub-committee on Stability and Load Lines and on Fishing Vessels Safety under Marine Safety Committee (MSC) at the International Maritime Organisation (IMO)
T_p	Peak period [sec]
T_0	Zero-crossing period [sec]

1. INTRODUCTION

In the wake of recent shipping casualties involving Ro-Ro ferries, which resulted in severe loss of life, standards for Ro-Ro ship configuration, construction and operation have come under close scrutiny and new legislation has been put into place aimed at improving the safety of these vessels, notably SOLAS '90 as the new global standard for all existing ferries. Furthermore, concerted action to address the water-on-deck problem following the *Estonia* tragedy led to new requirements for damage stability agreed among North West European Nations to account for the risk of accumulation of water on the Ro-Ro deck, known as the *Stockholm Agreement*. Furthermore, in view of the uncertainties in the state of knowledge concerning the ability of a vessel to survive damage in a given sea state, an alternative route has also been allowed which provides a non-prescriptive way of ensuring compliance, through the "*Equivalence*" route, by performing model experiments in accordance with the Model Test Method of SOLAS '95 Resolution 14.

Deriving from systematic research over the past 14 years, numerical simulation models have been developed capable of predicting with good engineering accuracy the capsizal resistance of a damaged ship, of any type and compartmentation, in a realistic environment whilst accounting for progressive flooding. With considerable justification, this approach may be considered as another alternative to complying with Resolution 14, the so-called "*Numerical Equivalence*" route.

The tightening of legislation described above is coupled with serious considerations at IMO for regular application of risk assessment methods, for example, the *Formal Safety Assessment*. In this context, considerable attention has been focusing on the application of probabilistic procedures of damage stability assessment for the evaluation of Ro-Ro vessels and it appears more than likely that developments in the foreseeable future will most certainly adopt a framework of a probabilistic description. The regulatory regime described in the foregoing with respect to assessing the damage survivability of passenger/Ro-Ro vessels has understandably left the shipping industry in a state of confusion and uncertainty concerning the available options, approaches and optimum choice to ensure compliance and to ascertain the level of safety attained with regard to any such choice. Stated specifically, a ship owner today is faced with the following choices concerning damage stability-related standards:

Deterministic Regulations
- SOLAS'90, [1]
- Stockholm Agreement, [2]

Performance-Based Standards
- Numerical Simulations, [3]
- Model Experiments, [4]

Probabilistic Procedures
- Index-A calculations, IMO Resolution A.265(VIII), [5]

- ❖ Index-A calculations, IMO Draft Harmonised Regulations (SLF-42), [6]
- ❖ Index-A calculations, Nordic Project probabilistic framework with water on deck, [7]

Standards in each group are assumed to ensure an "equivalent" level of safety, correspondingly, whilst a summary of the only serious attempt to demonstrate such equivalence among instruments of the first two groups was reported in [8]. The methodology adopted there considers performance-based standards as derived from model experiments and numerical simulations to form a basis against which all other instruments are compared.

When it comes, however, to direct comparisons between deterministic and probabilistically regulations there is an added complication concerning difficulties in finding a common ground. For example, whilst the first deals with prescribed damages, the second deals with the whole range of possible damage scenarios. Notwithstanding this, it is simply amazing that in the 27 years since the introduction of the probabilistic regulations for subdivision and stability of passenger ships as an equivalent to Part B of Chapter II of SOLAS '74, no reported evidence exists of any attempt to establish quantitatively a relationship between probabilistic and deterministic instruments. This paper claims a first in attempting to provide meaningful comparisons for elucidating, for example, what level of the Attained Index A for a given ship would ensure the same level of damage survivability as that deriving from SOLAS considerations.

2. COMPARATIVE ASSESMENT METHODOLOGY

The search in establishing the meaning of the Attained Index and its equivalence to SOLAS standards (in this case SOLAS '90 two-compartment standards) could again be dealt best by considering the results derived in the pursuit of compliance with performance-based standards [8] as the common platform for a rational comparative assessment of the vessel's level of safety derived by what are considered to be equivalent routes. In this respect, the following are noteworthy:

(a) The KG limiting curve derived on the basis of SOLAS '90 two-compartment standards is taken as the basis for KG values to be used in all calculations. In this respect, the worst SOLAS damage is considered as the reference case.
(b) The limiting survival sea state (Hs) is taken from model experiments corrected as necessary (linear interpolation) to account for differences between actual and limiting KG values.

2.1 Test Matrix

A sample of 16 Ro-Ro vessels is considered all complying marginally with SOLAS '90 two-compartment standards. These vessels were selected to form a representative sample of the EU passenger/Ro-Ro fleet considering size, type and compartmentation thus allowing for meaningful comparison and a critical evaluation of emerging trends concerning the level of safety provided by the current damaged survivability assessment methods.

2.2 Wave Environment

The wave environment used in the numerical simulations and physical model tests is representative of the North Sea and is modelled by using JONSWAP spectra as shown in the table below.

Table 1: Sea States (JONSWAP Spectrum with $\gamma = 3.3$)

Significant Wave Height H_s [m]	Peak Period T_P [sec]	Zero-crossing Period T_0 [sec]
1.0	4.00	3.13
2.0	5.66	4.42
2.5	6.33	4.95
3.0	6.93	5.42
4.0	8.00	6.25
5.0	8.95	7.00

$H_s/L_P = 0.04$ ($L_P = 0.25H_s$); $T_P = (2\pi L_P/g)^{1/2}$ ($T_P = 4H_s^{1/2}$); $T_0 = T_P/1.279$

2.3 Deterministic Regulations

SOLAS '90 REGULATIONS

According to SOLAS '90 the following criteria must be met at the final equilibrium condition after damage:

- ❖ A minimum range of 15 degrees beyond the angle of equilibrium, which should not exceed 12 degrees for two-compartment flooding and 7 degrees for one compartment flooding.
- ❖ A minimum area of 0.015m.rad under the residual GZ curve.
- ❖ A minimum residual GM of 0.05m with a maximum GZ of at least 0.10m, increased as necessary to meet certain stipulated heeling moments due to wind heeling, passenger crowding and lifeboat launching.

As indicated in the foregoing, the worst SOLAS damage is chosen by considering minimum stability entities, namely minimum GZmax.

STOCKHOLM AGREEMENT

The Stockholm Agreement requirements demand that a vessel satisfies SOLAS '90 criteria (allowing only for minor relaxation) with, in addition water on deck by considering a constant height, calculated according to Figure 1, depending on the vessel's residual freeboard ad the operational sea state (H_s). In this study the limiting

sea state is calculated by increasing the significant wave height until marginal compliance is achieved.

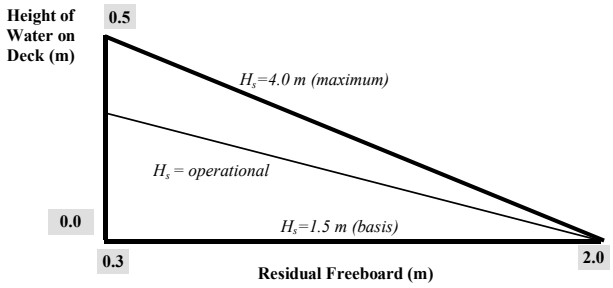

Figure 1: Stockholm Agreement

2.4 Performance-Based Standards

The standards considered under this heading pertain to assessing a given ship in a given damage scenario and operational environment on the basis of her performance (floatability, stability, capsizal resistance, dynamic behaviour) by means of physical or numerical testing. In this respect, considering the uncertainties associated with the problem in question, this route requires invariably the definition of critical damage scenarios to be tested in representative (critical) operational environments as a means of achieving a quantitative representation of a level of safety to be used for comparison purposes. Following this line of thinking, the Model Test Method of SOLAS '95 Resolution 14, [4], was recommended by the IMO Panel of Experts as the "Equivalent" route for compliance with the Stockholm Agreement requirements. Figure 2 below depicts the experimental set-up.

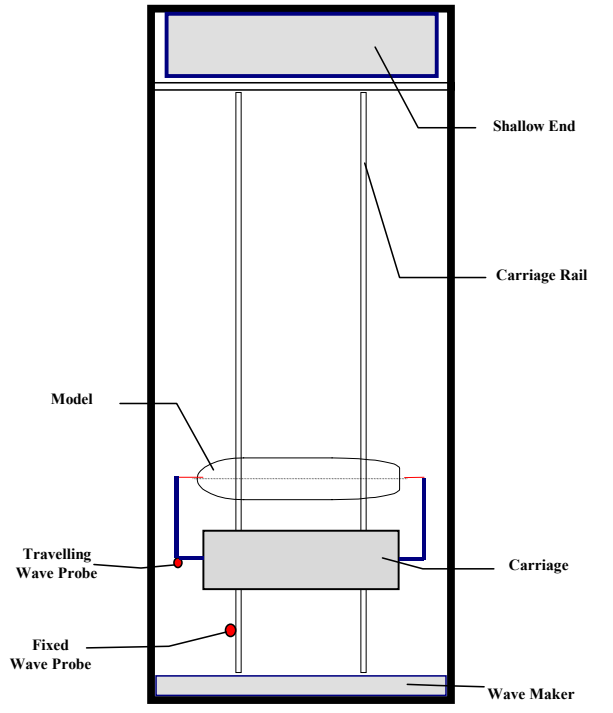

Figure 2: The Model Test method – Experimental Set-up

The Model Test Method comprises testing a ship model in two (typically worst SOLAS and midship) damages and in two sea states of JONSWAP spectral formulation of $4(H_s)^{1/2}$ and $6(H_s)^{1/2}$ peak periods, each test repeated 5 times, thus resulting in 20 tests, survival of which implies compliance with the Stockholm Agreement requirements. The same procedure could be used by either physical or numerical experiments (following exactly the same set-up and procedure) to identify the limiting H_s a vessel could survive and use this as a measure of her safety (damage survivability) or performance-based standard. Following this route, SSRC has completed some 65 physical model test approvals for passenger Ro-Ro vessels operating in northern Europe and some 80 vessels by numerical simulations, thus having available a unique database of performance-related measures of Ro-Ro vessels, including damage survivability boundaries (these are normally given in the form of a band denoting the upper – 100% capsize – and lower – 0% capsize – limits of capsizal resistance) that could be used for comparative assessment as well as in support of derivation of performance-base survival criteria.

2.5 Probabilistic Procedures

The first probabilistic damage stability rules for passenger vessels, deriving from the work of Kurt Wendel on "Subdivision of Ships", [9] were introduced in the late sixties as an alternative to the deterministic requirements of SOLAS '60. Subsequently and at about the same time as the 1974 SOLAS Convention was introduced, the International Maritime Organisation (IMO), published Resolution A.265 (VIII). These regulations used a probabilistic approach to assessing damage location and extent drawing upon statistical data to derive estimates for the likelihood of particular damage cases. The method consists of the calculation of an *Attained Index of Subdivision*, A ($A = \Sigma p_i s_i$, where p_i= probability that this compartment or combination of compartments are being flooded and s_i= probability that the vessel will survive flooding of that (or those) compartments), for the ship which must be greater than or equal to a *Required Subdivision Index*, R, which is a function of ship length, passenger/crew numbers and lifeboat capacity. Index R sets the required safety level, whilst Index A provides a measure of the safety level.

The next major step in the development of stability standards came in 1992 with the introduction of SOLAS part B-1 (Chapter II-1), containing a probabilistic standard for cargo vessels, using the same principles embodied in the aforementioned regulations. The same principle is also the basis for the current IMO regulatory development of "Harmonisation of Damage Stability Provisions in SOLAS based on the Probabilistic Concept of Survival".

An important addition to the probabilistic procedures, particularly for Ro-Ro vessels, was developed during the Nordic Project [7], culminating to a proposal of a

framework for new probabilistic damage stability standards, similar to IMO Resolution A.265 and SOLAS Part B-1.

IMO RESOLUTION A.265 (VIII)

The original method of calculating factor *s* was developed by adopting an experimental approach aiming to establish a simplified relationship between environmental and stability-related parameters for a damaged ship and hence determine capsizal resistance in a given sea. On the basis of limited model tests carried out separately in the United Kingdom, [10] and the USA, [11] such a relationship was established, expressed in the form:

$$(H_s)_{critical} = f(GM_f * F_e / B)$$

where, $(H_s)_{critical}$ $\Rightarrow$ critical significant wave height (characterising a limiting sea state)
GM_f $\Rightarrow$ flooded metacentric height
F_e $\Rightarrow$ effective freeboard
B $\Rightarrow$ beam of the vessel

Deriving from the above, the probability that a ship with a given value of the stability parameter ($GM_f * F_e / B$) will survive damage in a given sea state will be equal to the probability of not exceeding $(H_s)_{critical}$. The formulation given in A.265 (VIII) is:

$$s = k * \sqrt{\frac{Fe * GM_f}{B}}$$

DRAFT HARMONISED REGULATIONS

The approach adopted by the Draft Harmonised Regulations of SLF 42 for calculating factor *s* is to use residual GZ curve parameters similar to cargo ship regulations of SOLAS part B-1 (in Chapter II-1). However, water accumulation on deck is not taken directly into account, which is a major deficiency, particularly for Ro-Ro vessels following large scale flooding.

$$s_i = c \cdot \sqrt[4]{\left(\frac{GZ_{max}}{TGZ_{max}}\right)\left(\frac{Range}{TRange}\right)\left(\frac{Area}{TArea}\right)}$$

C Static heeling coefficient,
GZ_{max} Maximum GZ at final equilibrium,
TGZ_{max} Target value of GZ_{max},
Range Positive stability range,
Trange Target value of positve stability range,
Area Area under positive stability,
Tarea Target value of positive area

NORDIC PROJECT PROBABILISTIC FRAMEWORK

In addition to the effects considered in the above regulations, effects like water on deck and cargo shift have been included. The framework also addresses damage stability modelling, in particular standards for intermediate stages of flooding and cross flooding. The proposed method of calculating the subdivision index follows the basic methodology and principles of the harmonisation work in IMO with two major changes:

- Vertical extent of damage (v-factor) based on results from collision simulations
- Probability of survival (factor *s*), in order to include effect of water on deck, cargo shift and progressive flooding.

The latter, in particular is expressed as a combination of two factors, as explained next:

$s_i = s_a * s_w$, where

s_a = probability to survive pure loss of stability, heeling moments, cargo shift, angle of heel and progressive flooding. As per IMO recommendations $s_a = C \cdot F \cdot K \cdot (GZ_{max} * \cdot range * area)^{1/4}$

s_w = probability to survive water on deck as result of wave action. This can be calculated directly from the wave height distribution, again based upon the critical wave height.

3. SAFETY EQUIVALENCE

Deriving from the foregoing considerations and using the sample of 16 marginal SOLAS '90 two-compartment standard vessels from the SSRC database for which the survival H_s limits have been established experimentally, limiting H_s values were also determined according to Stockholm Agreement and through numerical simulations. In addition the Attained Index of Subdivision has been calculated for all 16 vessels using the three methods of calculation outlined in the foregoing. The results are summarised in Table 2 and Figures 3 and 4 for ease of comparison and discussion purposes.

Table 2: Relative Measures of Safety

Limiting Hs [m]				**Attained Index A**		
Model Test	Operational Limits	Numerical Simulation	Stockholm Agreement	A.265 (VIII)	SLF 42	NORDIC PROJECT
3.23	1.90	3.08	2.00	0.824	0.830	0.776
4.40	4.00	4.38		0.650	0.839	0.832
3.02	2.60	3.14		0.645	0.685	0.658
3.80	3.40	3.42		0.647	0.742	0.627
3.89	3.40	3.52	2.43	0.612	0.857	

3.47	3.40	3.59	4.06	0.512	0.656	
3.07	3.40	3.14	2.17	0.554	0.738	
2.82	2.50			0.763	0.757	0.756
2.91	2.80	2.82	1.60	0.674	0.816	
3.86	3.40	3.83	2.90	0.695	0.868	0.745
3.45	3.00	3.08	2.27	0.737	0.785	0.785
3.49	2.50	3.32	1.60	0.721	0.832	
3.97	3.00	3.30	1.79	0.577	0.837	
4.00	3.40	3.63		0.621	0.795	0.792
4.25	3.00	3.61	1.92	0.613	0.814	
3.03	2.50	2.86	1.77	0.696	0.891	0.852

Based on the derived results, the following points are noteworthy:

- The agreement between the numerical and experimental results, particularly in the range of relevant sea states is very good. This suggests that, numerical tools have reached a stage where survivability boundaries can be successfully predicted and hence performance-based assessment of safety levels be confidently undertaken.
- Ships satisfying SOLAS '90 two-compartment standards (even marginally) appear to survive sea states with H_s over approximately 3m. This result is rather encouraging considering that SOLAS '90 is the global standard for passenger/Ro-Ro ferries.
- The safety level inherent in the Stockholm Agreement calculation method is considerably higher than the level determined through performance-based methods, typically, by 1.25m on average.
- Lack of consideration of water on deck renders A.265 unsuitable for application to passenger/Ro-Ro vessels, as demonstrated by the results (magnitude and trend) presented in Figure 4.
- Both the Draft Harmonised Regulations and Nordic Project framework lead to comparable results, mainly because they both allow directly (Nordic Project) or indirectly (SLF 42) the effect of water on deck. Interestingly, the results show that the level of safety, as represented by Index A, would be higher when water on deck is taken into account explicitly.
- Finally, the 27 year old question could now be answered: for a SOLAS '90 two-compartment standard vessel to survive on the average 3.5m, the average value of Index A (Nordic Project) ought to be 0.75.

4. CONLUDING REMARKS

In the wake of resent marine disasters, number of new instruments for assessing damage survivability have been proposed/adopted, whilst efforts are still ongoing to establish acceptable harmonised damage stability calculations based on probabilistic approaches and on performance-based assessments. It would appear that the latter are here to stay, thus providing added motivation for development in this direction as well as efforts to understand the relative measure of safety provided by each method. This will, in turn promote better understanding of the emerging principle "Equivalent Level of Safety" and facilitate its adoption in the immediate and long term, as a more efficient route to achieving higher safety standards by utilising state-of-the-art knowledge to the full.

5. REFERENCES

[1] IMO Resolution MSC.12 (56) (Annex), "Amendments to the International Convention for the Safety of Life at Sea, 1974: Chapter II-1 – Regulation 8", adopted on 28 October 1988.

[2] IMO Resolution 14, "Regional Agreements on Specific Stability Requirements for Ro-Ro Passenger Ships" – (Annex: Stability Requirements Pertaining to the Agreement), adopted on 29 November 1995.

[3] Vassalos, D, Pawlowski, M and Turan, O, "A Theoretical Investigation on the Capsizal Resistance of Passenger/Ro-Ro Vessels and Proposal of Survival Criteria", Final Report, The Joint North West European Project, University of Strathclyde, Department of Ship and Marine Technology, March 1996.

[4] IMO Resolution 14, "Regional Agreements on Specific Stability Requirements for Ro-Ro Passenger Ships" – (Appendix: Model test method), adopted on 29 November 1995.

[5] IMO Resolution A.265 (VIII), A.266 (VIII), and explanatory notes, 'Regulation on Subdivision and Stability of Passenger Ships (an Equivalent to part B of Chapter II of the 1974 SOLAS Convention)', IMO, London, 1974.

[6] IMO, SDS Working Group,' Development of Revised SOLAS Chapter II-1 Parts A, B and B-1', SLF 42/3,London, 1998.

[7] RUSAAS, S., JOST, A.E.E. AND FRANCOIS, C.: "*Framework for a New Stability Standard*", Final Report, Task 6, The Joint North West European R&D Project, 1996.

[8] Vassalos, D: "Comparative Levels of Safety Achieved by the Stockholm Agreement and SOLAS '95 Regulations", 4th NORDCOMPASS Seminar on 'Ferries and Passenger Ships', Copenhagen, Denmark, February 1998.

[9] Wendel, K, "Subdivision of Ships", Diamond Jubilee International Meeting, New York, June 1968, pp 12-1 to 12-21.

[10] Bird, H. and Browne, R P: "*Damage Stability Model Experiments*", Trans. RINA, Vol. 116, 1974, pp. 69-91; also in: The N. Architect, October 1974, ibid.

[11] Middleton, E H. and Numata, E: "*Tests of a Damaged Stability Model in Waves*", SNAME Spring Meeting, April 1970, Washington DC, paper No. 7.

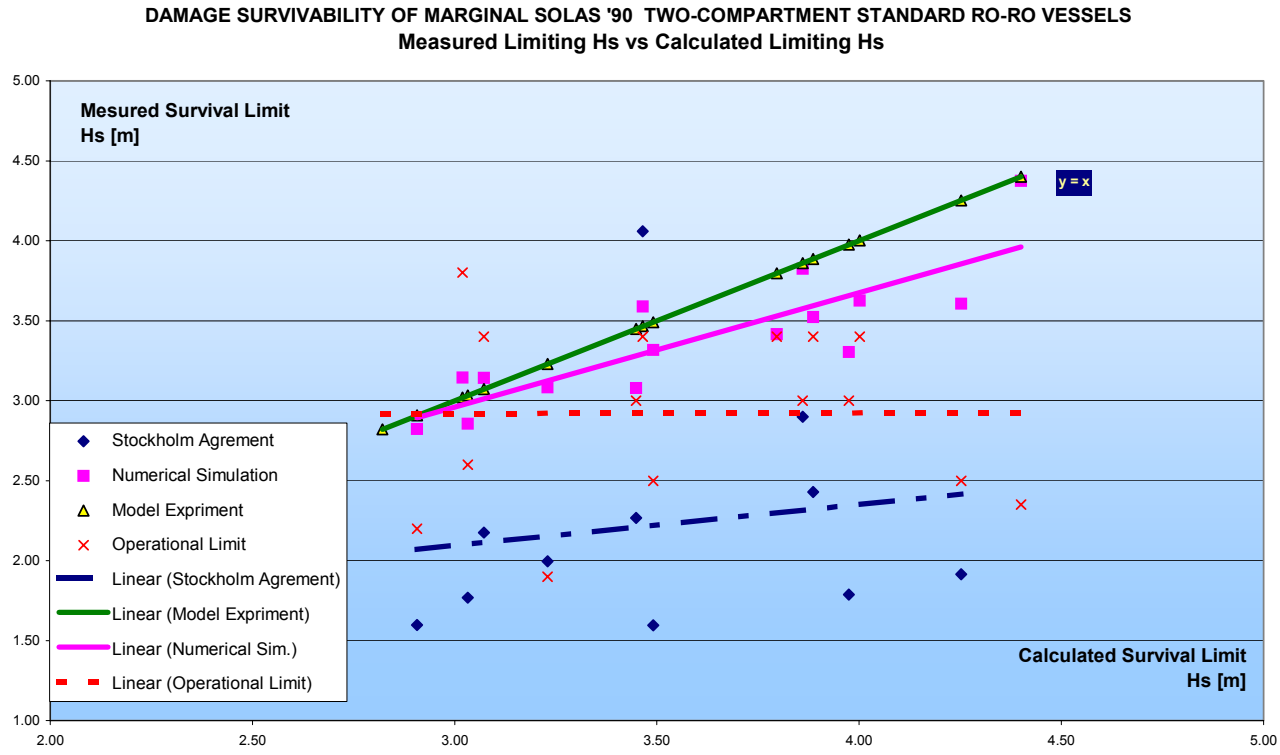

Figure 2: Performance based comparison.

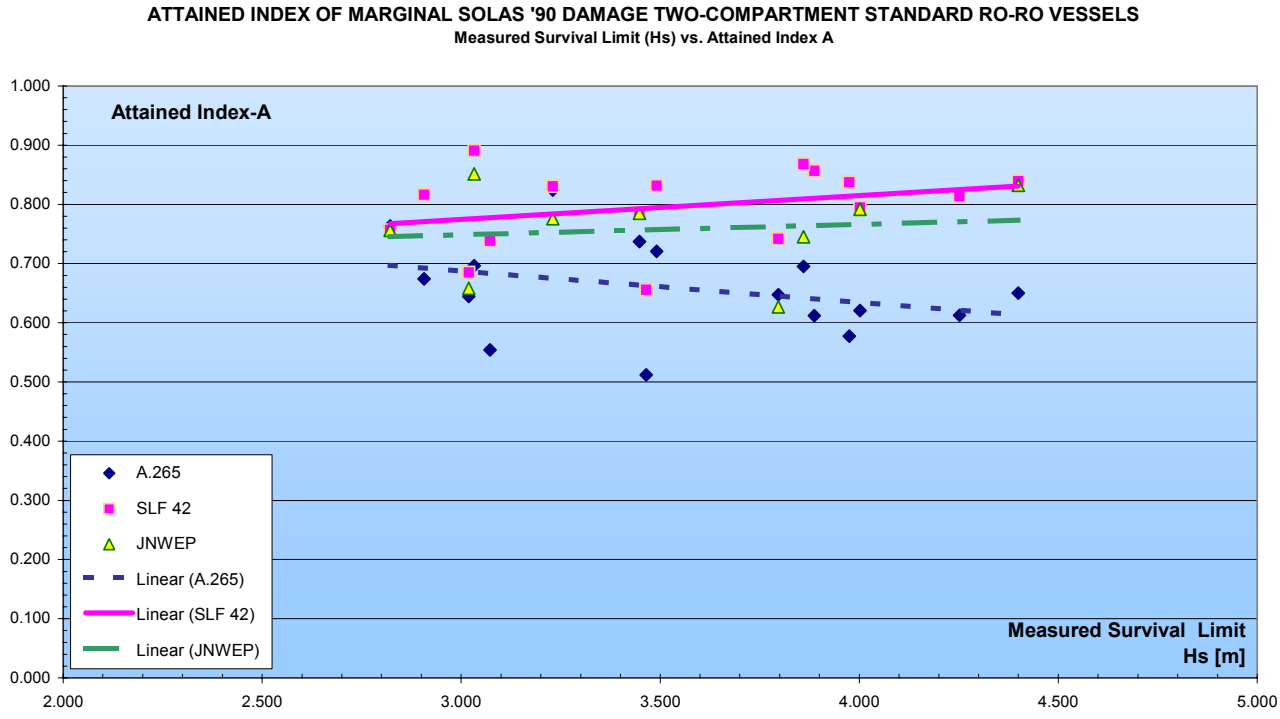

Figure 3: Comparison of Attained Index A for Current Probabilistic Instruments

DAMAGE SURVIVABILITY OF NON-RO/RO SHIPS

Robert Tagg*, **Cantekin Tuzcu*, Maciej Pawlowski**, Dracos Vassalos* and Andrzej Jasionowski***
*The Ship Stability Research Centre (SSRC), The Universities of Glasgow and Strathclyde, UK, ssrc@na-me.ac.uk
**SSRC Visiting Research Fellow, Technical University of Gdansk, Poland, mpawlow@pg.gda.pl

SUMMARY

The Static Equivalent Method (SEM) was developed in the wake of significant research into the capsizing of Ro/Ro vessels following the *Estonia* disaster. This method can predict with reasonable accuracy the survival sea state for specific Ro-Ro damaged conditions. Recent model tests of damaged non-Ro-Ro (or conventional) ships have indicated that the capsize mechanism has many similarities with the mechanism observed in Ro-Ro vessels' capsize, which formed the basis for the development of the SEM. On this basis, using the same idea as in the original research and the same methodology in analysing available experimental and numerical data, a new expression has been developed to account for geometric dissimilarities between Ro-Ro and non-Ro-Ro vessels. The predicted results from the new formulation are compared with the experimental results from recent model tests and the agreement was found to be satisfactory. Based on these preliminary findings, it is believed that this simple method could be applied to all ship types, and efforts to finalise this generalisation are underway at SSRC, as part of the EU project HARDER.

NOMENCLATURE

θ_{max}	Heel angle at which GZ is maximum.
h	Mean elevation of water on deck (the vehicle deck for a Ro-Ro ship or the weather deck for a conventional ship) above the mean sea surface.
H_s	Average significant wave height characterising the critical sea state.
H_{sr}	Reference wave height, where $H_{sr}=(H_s)^b$; a coefficient to be determined by physical and/or numerical experiments.
f	Freeboard to the deck edge at the PNR. For Ro-Ro vessels this is measured at the longitudinal centre of damage. A negative f implies the deck edge is immersed.
F	Residual freeboard in the traditional sense.
PNR	Point of no return, defined as the heel angle for the damaged ship, which when reached whilst progressive flooding is taking place, the ship will normally not recover and will proceed quickly to capsize.
s	The probability of the ship surviving a specific damage condition, in a given sea state.
SEM	Static Equivalent Method

1. INTRODUCTION

The tragic accidents of the *Herald of Free Enterprise* in 1987 and the *Estonia* in 1994 initiated a significant surge of research related to the capsizing of Ro-Ro type ships. This research effort culminated in significant developments that helped the ferry industry to raise safety levels to demanding new heights, in response to strict new regulations, cost-effectively. One of these developments, which is gaining wide acceptance is the Static Equivalent Method (SEM), [1]. The SEM is an empirical capsize model for Ro-Ro ships that can predict with reasonable accuracy the survival sea state for specific damage conditions. The SEM was developed and validated using several model experiments and a large number of numerical simulations.

The EC-funded project HARDER, started March 2000, was set up to systematically investigate the validity, robustness, consistency, and impact of all aspects of the probabilistic damage stability calculations for cargo and passenger ships. One significant aspect of the HARDER project is to devise a generalised formulation of the probability of damage survival for all types of ships and relevant damage scenarios. This plus other related research, includes model testing several aspects of the damage survivability of seven ships, covering a range of ship types and sizes. The model test programme provided additional material for testing the wider applicability of the SEM to other ship types as well as a basis for further refinements of the formulation pertinent to Ro-Ro vessels. This paper examines some of the initial results of the model tests for non-Ro-Ro ships and presents a new formulation that renders SEM applicable to these conventional types of ships.

2. SEM FOR RO-RO SHIPS

The SEM for Ro-Ro ships postulates that the ship capsizes quasi-statically, as a result of accumulation of a critical mass of water on the vehicle deck, the height of which above the mean sea surface uniquely characterises the ability of the ship to survive a given critical sea state. This method was developed following observations of the behaviour of damage ship models in waves. Among the most important observations from the model tests and subsequent investigations [1] are:

1. As the ship reaches the "point of no return" (PNR) it behaves quasi-statically, with subdued roll motion and marginal transverse stability.

2. The PNR generally occurs at an angle very close to θ_{max}.
3. The critical amount of water on the vehicle deck can be predicted from static stability calculations by filling the undamaged vehicle deck with water until the ship lolls at θ_{max}.
4. The unique measure of the ship's survival capability is the height (h) of the water elevated above the sea level at PNR, as shown in Figure 1 (Ro-Ro vessel) and Figure 5 (conventional ship).
5. The model tests and numerical simulations indicated that this elevation of water on deck, h, can be directly correlated to the critical sea state, characterised by H_s.
6. The higher the water elevation (h) at PNR, the higher the sea state needed to elevate the water to this level and capsize the ship.

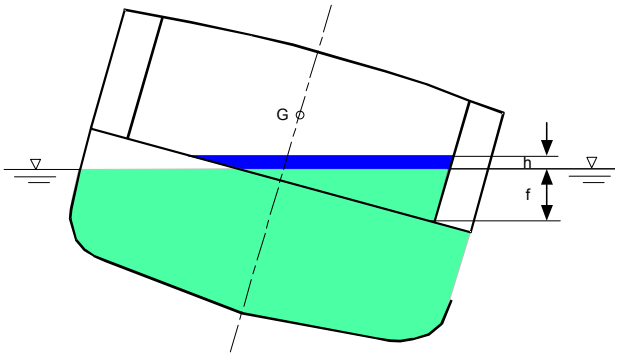

Figure 1: Damaged Ro-Ro vessel with water elevated on the car deck at PNR

3. MODEL TESTS FOR NON-RO-RO SHIPS

The model test programme of HARDER comprises seven ships to be tested in three model basins, as shown next.

1. PRR01 ..... Large Ro/Ro Passenger Ship
2. PRR02 ..... Medium sized Ro/Ro Passenger ship
3. PCLS ..... Large Passenger vessel
4. DCCS ..... Containership
5. DCRR ..... Cargo Ro/Ro vessel
6. DCBC01 ..... Cape Size Bulk Carrier
7. DCBC02 ..... Panamax Bulk Carrier

This paper deals, in particular, with the initial findings from tests of ship 5, the Cargo Ro-Ro, and ship 7, the Panamax Bulk Carrier. The Cargo Ro-Ro involved tests in three configurations, two of which (wing tank damage and combined wing plus lower hold damage) can be considered as non-Ro-Ro configurations since the upper vehicle deck is undamaged. The two non-Ro-Ro configurations are shown in Figure 2 and Figure 3.

The Bulk Carrier tests also involve three configurations, all based on the same midship 2-hold damage scenario, but with three different ship depths to weather deck. The ship with the smallest depth is shown in Figure 4.

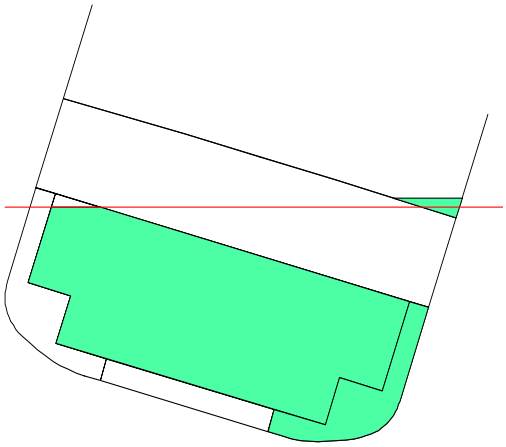

Figure 2: Cargo Ro-Ro with combined wing plus lower hold damage

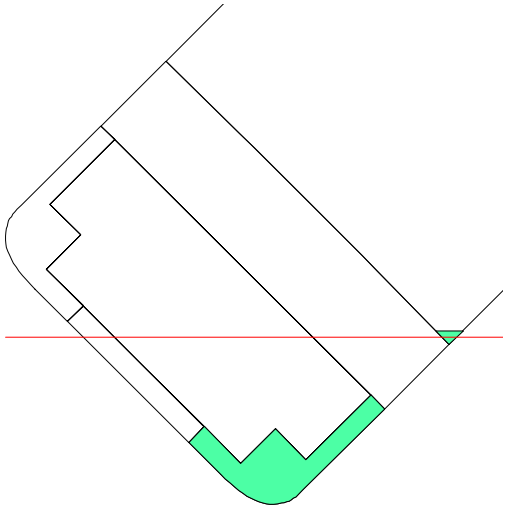

Figure 3: Cargo Ro-Ro with wing tank damage below the car deck

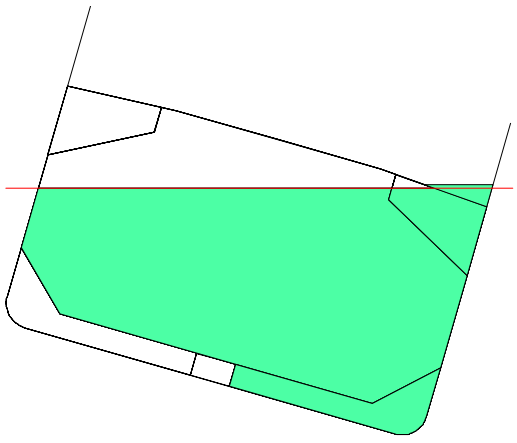

Figure 4: Panamax Bulk Carrier – Configuration 1

These five ship/damage configurations were tested over a range of KGs and sea states to establish the survival boundary. The model tests were performed at Denny

Tank, the University of Strathclyde model testing facility in Dumbarton. The Denny Tank is a conventional towing/wave-making tank measuring 100m x 7m x 2.7m. Unidirectional random waves were modelled using JONSWAP wave energy spectra with the model placed in the tank, free to drift, beam-on to the oncoming waves. Survivability was tested in a number of sea states, each repeated at least five times, so that a clear distinction between capsize and the survival cases could be ascertained and a survival band defined.

From observations of these model tests it became apparent that the ship behaviour near the capsize region is very similar to that seen with Ro-Ro ships. While the mechanics of water ingress and egress to and from an open deck are different than Ro-Ro ships, the mechanics of capsize appeared to be the same. In fact, the quasi-static nature of ship capsize at PNR is even more apparent with conventional ships because of generally smaller metacentric heights and deeper draughts.

4. GENERALISATION OF SEM

The SEM calculation procedure to determine both h can obviously be applied to conventional ships, if the effect of water shipping on the weather deck, unprotected by the ship's sides, is regarded as equivalent to that of water accumulated on the vehicle deck due to large-scale flooding. Essentially the same calculation method can be applied to the ship as if her sides were extended vertically above the open deck, as shown in Figure 5.

This suggestion does not come without a precedence considering that a rise of water on the weather deck has been previously proposed in [2] and subsequently adopted by the US Navy. In the said case the dynamic effects of wave action were represented by a rise 1.2m of water on the weather deck, irrespective of the ship size and freeboard. Subsequent experience has shown that this suggestion is overly conservative for commercial ships considering the typical sea states at the time of a casualty.

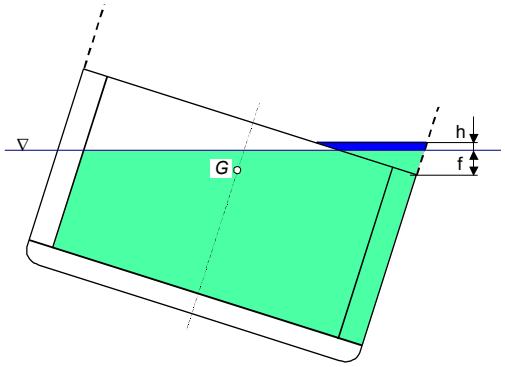

Figure 5: Conventional ship with water elevated on the weather deck at PNR

In view of the foregoing considerations, it would seem appropriate to pursue the same approach with conventional ships as that followed for Ro-Ro vessels by expressing the survival boundary in the non-dimensional form

$$h/H_{sr} = \mathrm{f}(f/H_{sr}),$$

with H_{sr}, h and f to be found with the aid of physical or numerical experiments for damage cases with marginal stability. As a first step, h and f were obtained by static calculations according to the SEM procedure and combined with H_s critical derived from model experiments in an attempt to derive a new formulation pertinent to conventional ships. The results of this effort are shown in Figure 6, the smallest scatter of points in obtained with $H_{sr} = H_s^{0.3}$, in contrast with the value of b of 1.3 derived from Ro-Ro vessel data.

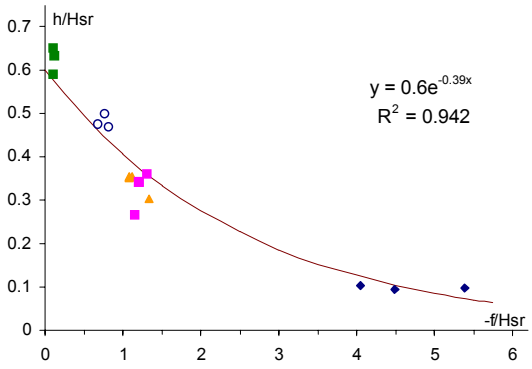

Figure 6: Boundary survivability curve for non-Ro-Ro ships with a modified $b = 0.3$ (total 16 cases)

The reason why the exponent b is different can be attributed to the different modes of water accumulation on deck as well as the geometrical differences between the two ship types (e.g., for conventional ships the non-dimensional freeboard varies in a much wider range than that for Ro-Ro ships). The regression in Figure 6 also shows a strong dependence between the non-dimensional values of h and f, contrary to the case of Ro-Ro vessels where a weak dependence led to the proposal of the formulation $h/H_{sr} = 0.085$, where h/H_{sr} was assumed to be independent of f/H_{sr} or

$$h \approx 0.085(H)^{1.3} \qquad (1)$$

Approximating the exponential in the regression equation of Figure 6 with the first two terms of a series and following some manipulations, the following expression may be derived

$$h \approx 0.6(H)^{0.3} + 0.24f \qquad (2)$$

Considering equations (1) and (2), a generalisation of SEM could be considered in the form

$$h = a(H_s)^b + cf \qquad (3)$$

with ship type dependent coefficients a, b and c.

Awaiting for proper analysis of the available experimental and numerical results, the interim expression (2) was used to compare SEM predictions of survival sea states with those measured from the model test programme of project HARDER and the agreement was found to be satisfactory, as demonstrated in Figures 7-11.

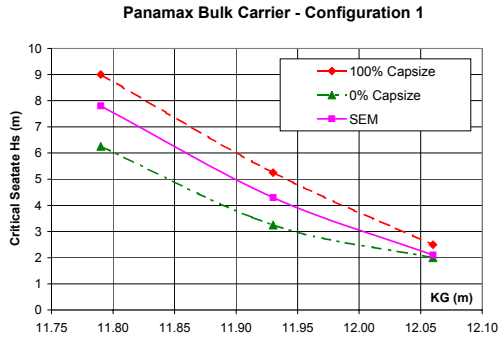

Figure 7: KG vs. Survival Sea State

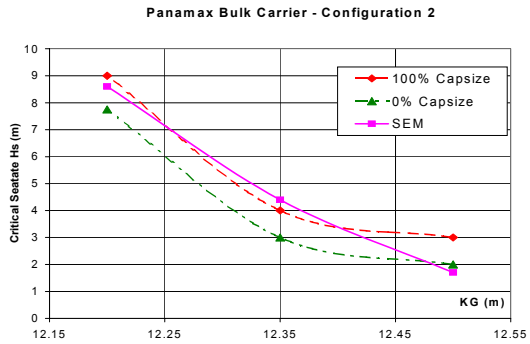

Figure 8: KG vs. Survival Sea State

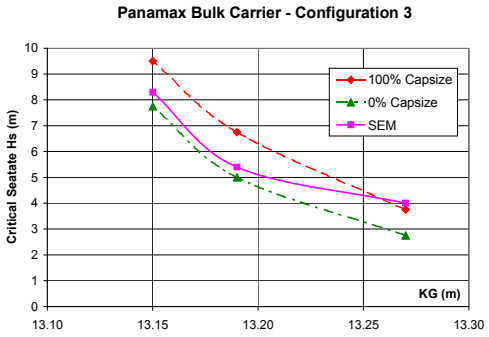

Figure 9: KG vs. Survival Sea State

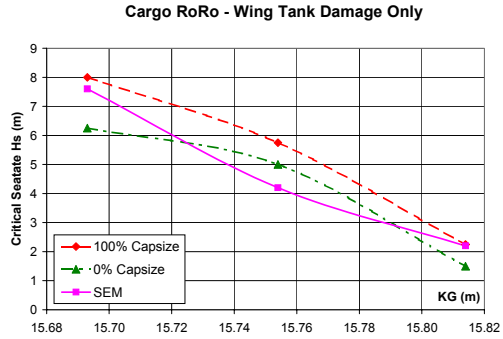

Figure 10: KG vs. Survival Sea State

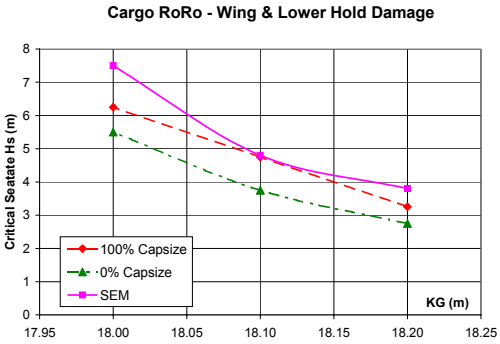

Figure 11: KG vs. Survival Sea State (Large trim by bow)

5. CONCLUSIONS

At this stage of development, the following conclusions are noteworthy:

- A new formulation for predicting the critical survival sea state for conventional (non-Ro-Ro) ship configurations has been presented using the same procedure as proposed for Ro-Ro vessels, simply by by considering the ship sides to extend vertically upwards above the weather deck in the calculation of h and f.
- Based on the above a generalised formulation of SEM has been proposed where any differences between Ro-Ro and conventional ships are represented by different coefficients to be determined by physical and numerical capsize experiemtns.
- Comparisons of the predicted survival sea states between SEM predicted and experimentally measured values show satisfactory agreement.
- Further investigation is required for flooding cases with trim in order to verify the relationships between h, f, and H_{sr} at large trim, as well as where to measure f on a ship with significant trim.

6. ACKNOWLEDGEMENTS

The authors would like to acknowledge the financial support of the European Commission DG Research of the work presented in this paper, which forms part of Project HARDER, Contract No. **G3RD-CT-1999-00028** and to express their gratitude and sincere thanks.

7. REFERENCES

1. Vassalos, D., Pawłowski, M., and Turan, O.,"A Theoretical Investigation on the Capsizal Resistance of Passenger/Ro-Ro Vessels and Proposal of Survival Criteria", Final Report, Task 5, The North West European R&D Project, March 1996.
2. Sarchin, T. H., and Goldberg, L. L.: Stability and buoyancy criteria for U. S. Naval Ships, SNAME *Transactions*, Vol. 59, 1962, pp. 418–458.

PRELIMINARY RESULTS OF EXPERIMENTAL VALIDATION OF PRACTICAL NON-ERGODICITY OF LARGE AMPLITUDE ROLLING MOTION

Vadim Belenky, Independent Contractor to ABS,
ABS Plaza, 16855 Northchase Drive, Houston, TX 77060-6008, USA, email VBelenky@eagle.org
Shiro Suzuki, Yasuyuki Yamakoshi National Research Institute of Fisheries Engineering,
Ebidai, Hasaki-machi, Kashima-gun, Ibaraki, 314-021, Japan, email fblya@nrife.affrc.go.jp

SUMMARY

Practical non-ergodicity (correct math term is cyclic non-stationary quality) means that ergodic hypothesis cannot be used for any practical calculation of nonlinear irregular rolling. In other words, all the probabilistic characteristics have to be averaged over representative ensemble of realization and any result based on one realization is not correct. This was first stated on the base of numerical simulations. It was believed that fold bifurcation is responsible for the effect. It was not clear if contributions from other factors (like water on deck, impacts of breaking waves, influence of others degrees of freedom, etc.) might decrease this effect, so ergodic assumption might be still acceptable for practical purposes.

The model experiment was carried out in the towing tank of National Research Institute of Fisheries Engineering in Japan. There were two series of tests with two models. The first series of tests was done with free drifting model of Japanese purse seiner. Such test yields about 10 minutes realization. Since absence of ergodic qualities can be checked only on significant amount of time, the second series of tests was conducted with restrained model that was not able to drift. The second series produced 30 and 40 minutes realizations of model time that is close to quasi-stationary range of full-scale waves. It was meant that the first series can be used for validation of the second one, in other words, to estimate how significant these restraints are in statistical sense.

The results have shown significant difference in variance estimate on different wave realization that cannot be explained only by statistical errors that may constitute absence of ergodic qualities in practical sense. All the motion recorded were far enough from fold bifurcation region, and at the same time intensive deck flooding with episodic breaking wave hit were observed.

To make sure that GZ non-linearity is not the only reason for ergodicity the second model was tested. It was a rectangular pontoon with almost linear GZ curve.

The paper also rises some methodological issues concerning severe irregular rolling like estimation of "degree of non-ergodicity"

1. INTRODUCTION

Ship response in irregular seas is usually considered as a general stochastic process. This means that we use math abstraction to describe the real world phenomenon. As an abstraction, it is supposed that a stochastic process is infinite in time and has an infinite number of realizations. So, if we fix the time (or, in other words make a time section), we have a usual random number that has an infinite number of values and its own average, variance, distribution and other probabilistic characteristics. These characteristics might be different in different moments of time, however, there are group of stochastic processes, for which the probabilistic characteristic does not depend on time. Every moment brings exactly the same values for the probabilistic characteristics. These processes are considered to be stationary.

Strictly speaking both waves and ship response are not stationary, because waves are changing due to weather and ship response also depends on speed and course, which also are not constant. So, in order to simplify the problem, we consider a period of time when weather, speed and course could be considered as constants; this duration is usually called "period of quasi-stationary". It usually assumed that ship response time does not exceed the period of quasi-stationary.

Averaging the current value of one realization of stationary process, we got so-called time-average estimates for probabilistic characteristics. This way, each realization might have its own mean value, variance, distribution and other estimates. The true estimates for the whole stochastic process are averages of corresponding ones of the realizations.

This means that we can estimate probabilistic characteristics in two ways: using time section or by averaging estimates for each individual realization. Some processes however show identical (in statistical sense) estimates for individual realizations. This makes a problem much simpler – we need just one, long enough realization, to produce estimates. This kind of processes are called "ergodic", and the corresponding quality of such stochastic process – "ergodicity". Usually, sea waves are assumed to be ergodic.

There is a proof that a linear dynamical system, being excited by stationary ergodic process produces also stationary ergodic response. However, nothing like this is provided for nonlinear systems. It creates a question on ergodic qualities of nonlinear rolling and other ship motions that are essential for estimation of capsizing

probability. (So far, we assume nonlinear rolling to be a stationary process at least, which is also questionable from point of view of pure math.)

2. ERGODICITY CHECK BY SIMULATION

Here we give a brief review of the previous results, mainly based by [1-2].

2.1 WAVES

Stochastic elevation of sea wave is usually expressed as

$$\zeta_w(t) = \sum_{i=0}^{N} a_i \sin(\omega_i t + \varphi_{0i}) \qquad (1)$$

Here a_i are amplitudes of components that are defined from spectrum, ω_i is a given set of frequencies and φ_{0i} is a set of random phase numbers distributed uniformly from 0 to 2π. The last figure is responsible for the generation of new realization. Every time the set of phases are calculated and substituted into one, the new realization of the wave process is created. All these realizations, however, would still produce the same spectrum, since amplitudes were not changed.

2.2 RESPONCES

2.2 (a) Linear System

The different realizations of the waves now have to be used for ship rolling simulation. One of the ways to check ergodicity is to calculate an estimate, for example, of the ship roll variance V for consecutive moments of time t_1, t_2, ... t_n: in a form of a function $V(t)$. The procedure has to be repeated for all available realizations, so we have a set of functions $\{V(t)\}_{j=0..k}$

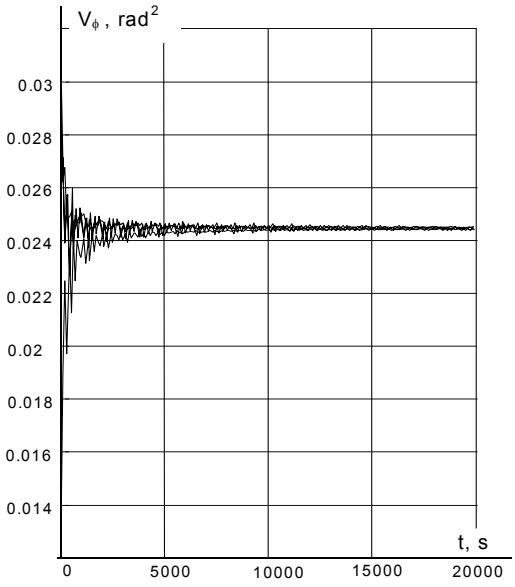

Figure 1. Ergodicity check of linear rolling

If the response is ergodic, all these curves must have one clear limit, as it shown on figure 1, where response of the linear system is shown.
The results on the figure 1 (taken from [1]) was obtained by simulation, so all numerical errors are included, nevertheless there is a clear limit reached in 20,000 seconds –16 hrs. 40 min., that is close to quasi-periodic period.

2.2 (b) Nonlinear System

Now let's check the same rolling-only system, but nonlinear restoring is introduced. The result changes dramatically, see figure 2 (taken from [1])

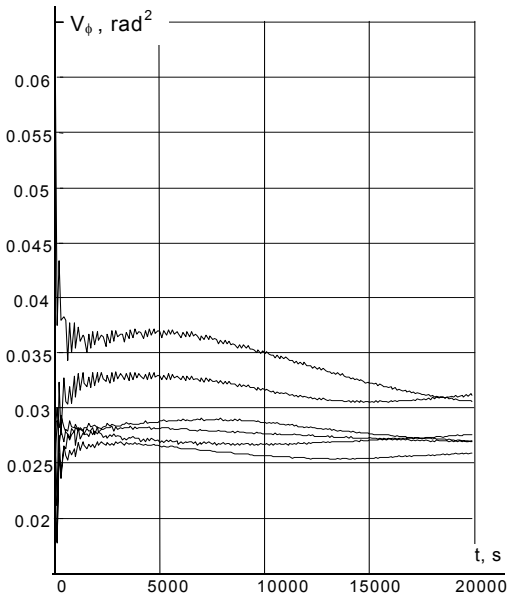

Figure 2 Ergodicity check of rolling with nonlinear restoring

As it is clear from figure 2, the limit is not reached for 16 plus hours, moreover, the shape of the curve might even question the stationary assumption...
A. Degtyarev and A. Boukhanovsky [1] checked this effect, using completely different model of waves and rolling, but finally came to the same conclusion.

3. MODEL TEST SET-UP

The purpose of the model test is to check if the effect of significant absence of ergodicity could be obtained in the conditions of model experiment.

3.1 NRIFE TOWING TANK

The model test was carried out in the towing tank of National Research Institute of Fisheries Engineering in Japan. The tanks dimensions are 137 x 6 x 3 m, equipped with rolling plate type wavemaker, wave absorption beach and self-propelled carriage. The schematic of the wave-maker is shown at figure 3.

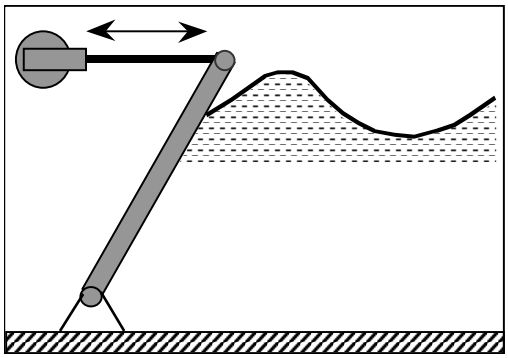

Figure 3: Schematic of the wavemaker

Control system of the wavemaker is capable of reproducing the given electric signal. The control signal elevations was calculated by formula (1) and then transformed to analog form using TEAC DR-F2M Digital Recorder.

3.2 MODELS

Two models were tested: Japanese purse seiner GT-80 (scale 12.6) and box shaped model. The box shaped model had depth larger than breadth, so GZ curve was almost linear. This allowed checking the hypothesis [1] that the absence of ergodicity was caused by rare jumps to higher amplitudes.
The model of GT-80 was tested for two different draughts, in order to check influence of nonlinear damping caused by deck entering water. Bulwark of the model was removed to minimize effect of the green water. Numerical characteristics of the models are given in tables 1 and 2 correspondingly.

Table 1. Characteristics of Purse Seiner GT-80

Characteristics		Full scale	Model
Length O. A., m		36.5	2.900
Length B. P., m		29.0	2.300
Breadth, m		6.80	0.540
Depth, m		2.60	0.206
Draught 1	Draught, m	2.19	0.174
	Displacement, ton	261	0.130
	KG, m	2.38	0.189
	KM, m	3.84	0.304
	GM, m	1.46	0.116
	CB	0.603	0.603
Draught 2	Draught, m	1.74	0.137
	Displacement, ton	180	0.090
	KG, m	2.52	0.200
	KM, m	3.86	0.306
	GM, m	1.33	0.106
	CB	0.528	0.528

The GZ curve for the box –shaped model is shown in figure 4. Both models were equipped with high-precision gyroscope for measuring roll angles. Measurements were recorded by TEAC digital recorder, decoded on a PC and stored in form of ASCII files.

Table 2 Characteristics of box shaped model

Characteristics	Value
Length B. P., m	1.500
Breadth, m	0.300
Depth, m	0.400
Draught	0.246
Displacement, ton	0.111
KG, m	0.087
KM, m	0.305
GM, m	0.0666

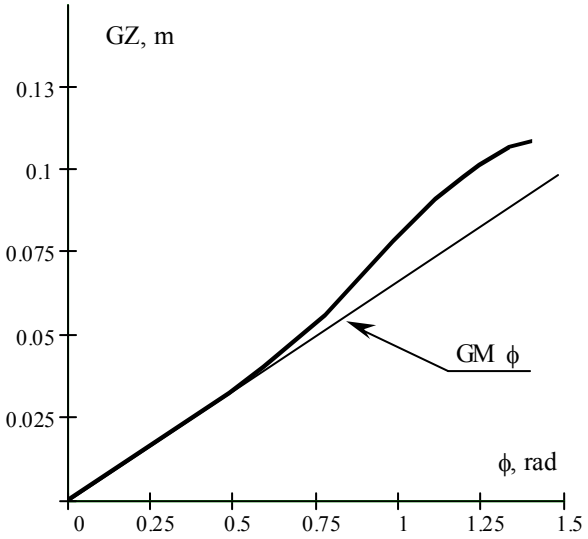

Figure 4: GZ curve of box shaped model

Wave heights were measured in close proximity of the model by string wavemeter. Output signal was amplified and then recorded by TEAC digital recorder, decoded on a PC and stored in a form of ASCII file. The model test layout is shown in figure 5. The model was free to sway, heave and roll, but was restricted in surging, pitching and yawing.

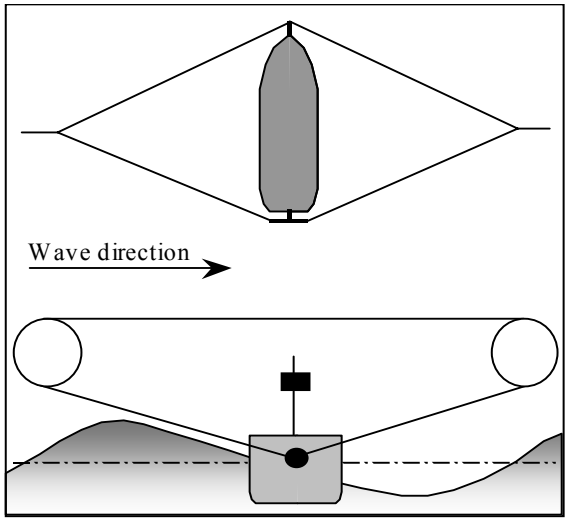

Figure 5: Model test layout

4. TEST PROGRAM

4.1 WAVE GENERATION

Wave spectrum density was calculated using the following formula:

$$s(\omega) = 9.43 \cdot \frac{V_w}{\omega_{wm}} \cdot \left(\frac{\omega_{\max}}{\omega}\right)^6 \cdot \exp\left[-1.5 \cdot \left(\frac{\omega_{\max}}{\omega}\right)^4\right] \quad (2)$$

Here, ω_{max} is cyclic frequency of spectrum's maximum and ω_{wm} is mean cyclic frequency. These two values are assumed to be related as:

$$\omega_{\max} = 0.77\omega_{wm} \quad (3)$$

The entire model test was done for one value of the variance 22.375 cm^2 and frequency of spectrum's maximum 0.7 Hz.

The spectral density of control signal was obtained by multiplying expression (2) by transfer function of the wavemaker that was obtained during special calibration experiment. Then, the controlling signal was calculated by formula (1).

Different realizations were obtained using different set of random initial phases in formula (1). There were total 9 realizations, 30 minutes long each (1 hour 48 min of full-scale time) and 4 realizations, 40 minutes long each (2 hours 22 min full-scale time). The spectral density of one of them (both calculated by formula (2) and actually measured in the tank) is shown on figure 6.

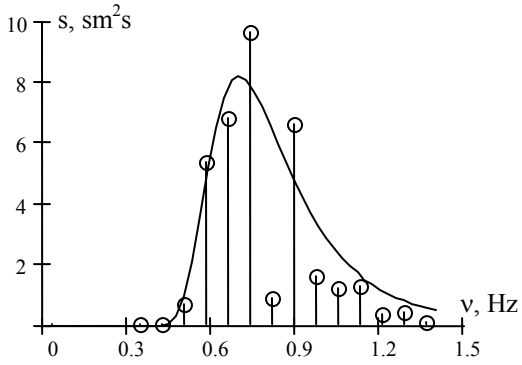

Figure 6. Input and measured wave spectral density

4.2 TEST PROCEDURE

As it was mentioned above there were two models: Japanese purse seiner GT-80 (two loading conditions) and box shaped model (one loading condition), which makes three series of test runs. Each series included three types of tests:

- Free rolling motion;
- Free drift test;
- Stop test.

The model was able to drift freely under action of incident waves during free drift test, however, the length of the tank limited the time of realization that might be recorded. This time (about 10 minutes – model time) is not enough to estimate probabilistic characteristics with accuracy, that would be enough for judgement on ergodicity. So we had to restrain drift of the model, which made it "stop test" and use free drift test results to check an influence of drift restraining. This analysis in not included in this paper.

5. PRELIMINARY ERGODICITY ANLYSIS

5.1 CUMULATIVE VARIANCE

We followed the procedure that was applied for simulation results in [1]. The "cumulative" variances time histories are shown on figure 7 for model GT-80, draught 1, figure 8 for model GT-80 draught 2 and on figure 9 for box shaped model. Four longer curves correspond to 40 minutes realization, nine shorter ones – to 30 minutes realizations.

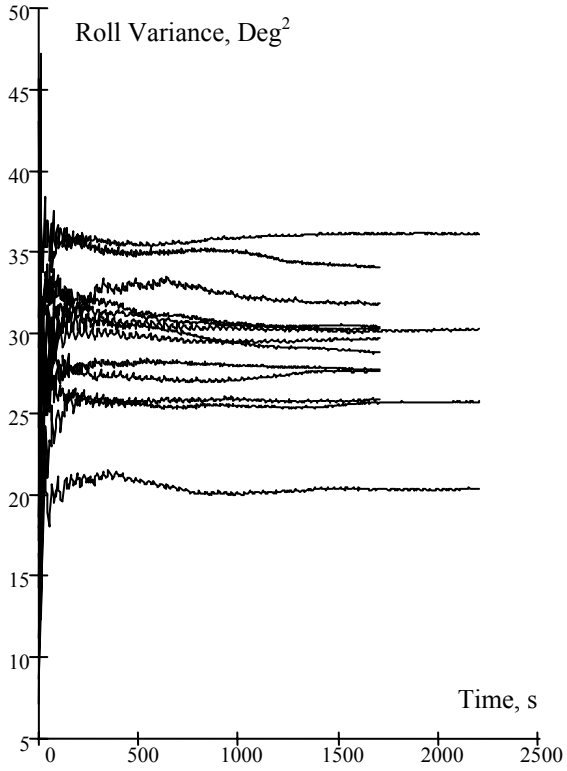

Figure 7. Cumulative variance for GT-80, draught 1

As it is quite clearly seen from figures 7, 8 and 9, all the responses cannot be considered ergodic, at least during testing time. Moreover, majority of the curves tends to almost horizontal asymptotes. This gives a background to a hypothesis, that the process is stationary and does not posses ergodic qualities during quasi-stationary period as well. However it cannot be considered as experimental evidence, yet. The waves in the tank might not be ergodic either, since the wavemaker might be nonlinear dynamic system as well and absence of ergodicity might be a simple reaction on non-ergodic excitation.

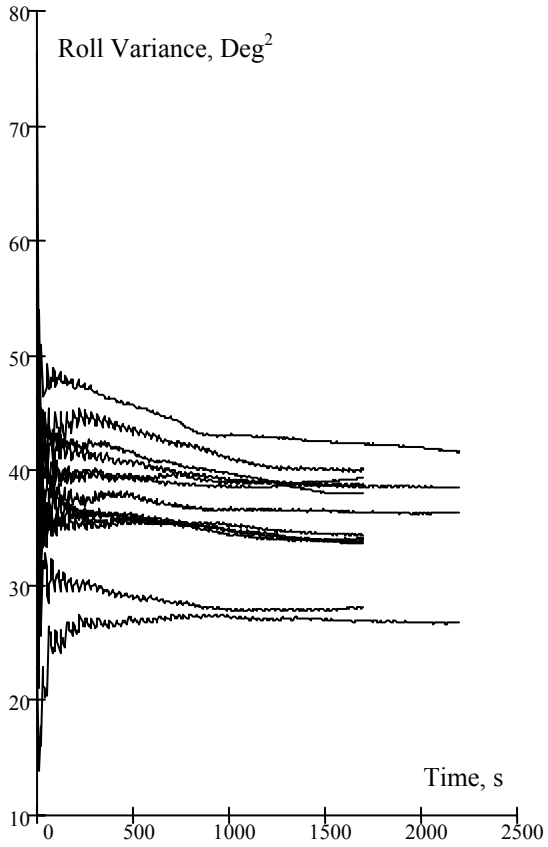

Figure 8. Cumulative variance for GT-80, draught 2

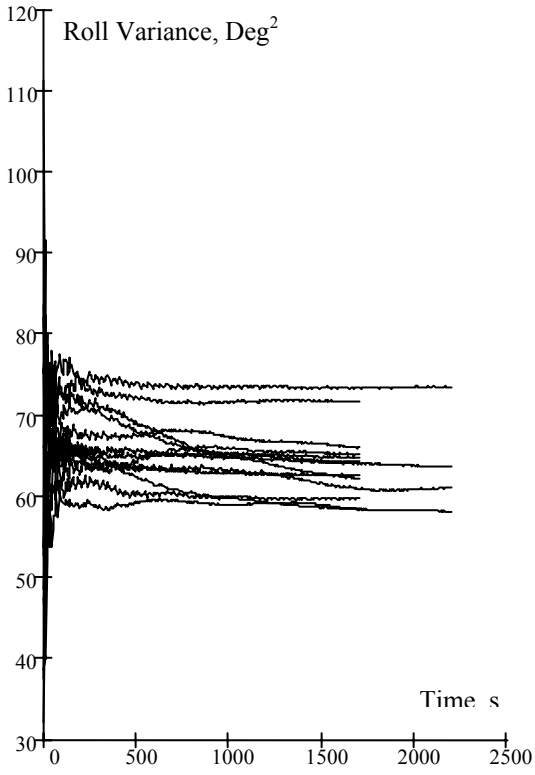

Figure 9. Cumulative variance box shaped model

5.3 ERGODIC QUALITIES OF WAVES

Basically, it is well known, that the waves in the model basin are not a perfect model of the sea waves: physics of wave generation is different. For example, spectrum might be dependent on where the measurements were done exactly in the basin. This error is considered acceptable for vast majority of the model test in irregular waves.

However, absence or presence of ergodicity is critical for this test, if the waves are ergodic, results at figures 7-9 would be enough to reject the hypothesis of ergodicity for tested cases and at least question such a hypothesis in general, when the nonlinear effect is important.

The figure 10 shows the cumulative variances of waves in the towing tank recorded along with the stop test. The wave transducer was located far enough before the model to exclude any influence of wave generated by the model.

As it clearly seen from figure 10, unfortunately, the waves also cannot be considered ergodic.

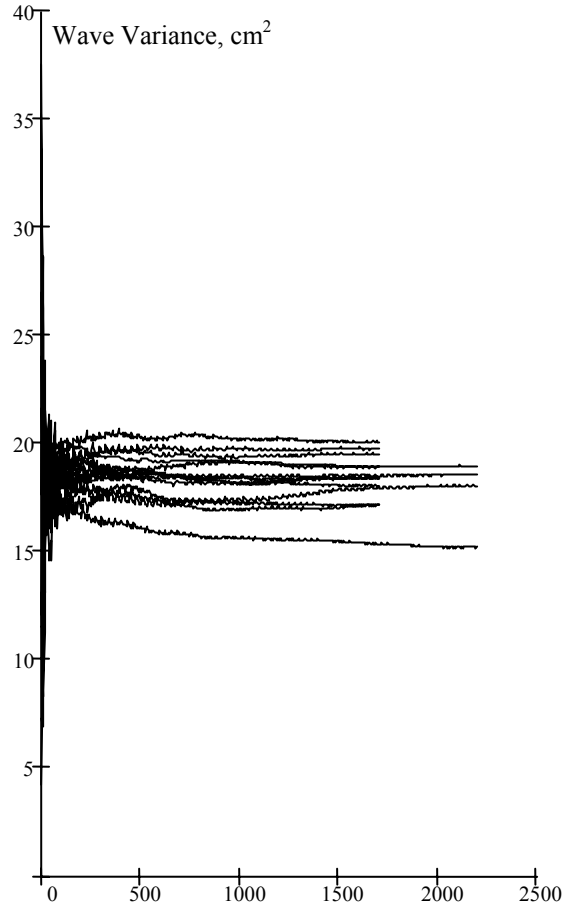

Figure 10. Cumulative variance of waves

So, to conclude anything on applicability of ergodicity hypothesis for nonlinear rolling we have to develop a criterion for ergodicity of the dynamical system exposed

to non-ergodic excitation and somehow separate inherent and input non-ergodicity.

5.4 CRITERIA OF ERGODICITY

Derivation and testing of ergodicity criterion that possesses the above capability deserves separate paper. Here we give it brief consideration without any strict definitions and proofs from math point of view, rather being based on common sense. (Which does not always works but still good enough for preliminary analysis.) Following A. Degtyarev and A. Boukhanovsky [1], we take confidence interval as the main tool for the study.

Any estimate of variance or mean value obtained from finite set of statistics is a random value. Further we will be working with estimate of variance only, however the same method can be applied to any estimate of probabilistic characteristic. The confidence interval is a range that can be calculated for the estimate and contain true value of characteristic with certain given confidence probability β. Here we use β=0.9973.

For the purpose of preliminary analysis, we assume that both distributions of roll process and variance estimate are Gaussian. Then the confidence interval half-width can be calculated as [3]:

$$\Delta V = P_{inv}(\beta, m[V], V[V]) \qquad (4)$$

Here: P_{inv} inverse Gaussian cumulative probability

$m[V]$ – mean value of the variance estimate

$V[V]$ – variance of the variance estimate

Mean value of the variance estimate is the estimate itself if it is calculated with corrected formula:

$$m[V] = \widetilde{V} = \frac{1}{N-1}\sum_{i=0}^{N}\left(\phi_i - m[\phi]\right)^2 \qquad (5)$$

Variance of variance estimate can be calculated via 4th moment of distribution, but since we assume the Gaussian distribution, this figure could be expressed as:

$$V[V] = \frac{2}{N-1}\cdot\widetilde{V}^2 \qquad (6)$$

Finally, the variance estimate with confidence interval can be written as:

$$V = \widetilde{V} \pm \Delta V\,, \qquad (7)$$

and:

$$P\left\{V \in \left[\widetilde{V} - \Delta V, \widetilde{V} + \Delta V\right]\right\} = \beta \qquad (8)$$

Here V is a true value of the variance and $\widetilde{V}$ is its estimate. Again, formulae (4-8) give confidence interval in assumption that the only reason for the difference between estimate and true value is finite volume of statistics. Since we have clear difference between variances estimated by different realizations, we average the estimate over all realizations. Confidence interval also has to be calculated for the estimate averaged over the all available realizations. Also we used the same number of points for each realization to give them equal statistical weight. Results are summarized in the table 3 for rolling and table 4 for waves. Estimates of wave elevation variance were expected to be almost the same for the same realizations, but they are not. This represents influence of model waves, reflection and other factors related to wavemaker work. Repeatability of waves is also important topic, but it is out of scope of preliminary analysis, presented here and will be considered in future papers.

Table 3 Roll Variance Estimates

Variance estimate Deg^2	GT-80 draught 1	GT-80 draught 2	Box shaped model
Realization 1	29.61	38.75	65.07
Realization 2	30.36	37.86	64.14
Realization 3	28.72	33.99	61.99
Realization 4	30.19	39.26	58.17
Realization 5	25.86	27.97	59.59
Realization 6	31.74	40.00	62.35
Realization 7	27.57	33.6	64.64
Realization 8	27.68	34.24	71.5
Realization 9	33.95	33.72	65.85
Realization 10	25.64	36.26	63.91
Realization 11	30.04	38.54	73.25
Realization 12	36.06	42.23	58.29
Realization 13	20.35	26.86	60.71
Average	29.06	35.64	63.81
Variance of Estimate	$7.642\ 10^{-4}$	$1.15\ 10^{-3}$	$3.68\ 10^{-3}$
Confidence Interval	0.154	0.189	0.338

Table 4 Wave Elevation Variance Estimates

Variance estimate cm^2	GT-80 draught 1	GT-80 draught 2	Box shaped model
Realization 1	19.45	20.76	18.24
Realization 2	18.01	19.32	21.36
Realization 3	17.10	17.73	22.35
Realization 4	19.74	19.18	20.81
Realization 5	17.14	16.32	17.58
Realization 6	18.86	18.19	17.47
Realization 7	18.35	17.7	17.19
Realization 8	18.35	17.74	19.97
Realization 9	20.01	19.01	17.91
Realization 10	15.30	15.83	19.45
Realization 11	18.42	18.12	20.92
Realization 12	18.89	19.89	21.28
Realization 13	17.92	17.27	18.59
Average	18.27	18.24	19.47
Variance of Estimate	$3.02\ 10^{-4}$	$3.01\ 10^{-4}$	$3.43\ 10^{-4}$
Confidence Interval	0.0967	0.0965	0.103

It is quite evident from the both tables that were already visually clear from figures 7-10: vast majority of realization estimates does not belong to confidence interval. It is also illustrated on figure 11 and 12 for wave and roll processes correspondingly. Points that present realization variance estimates (with respective confidence interval) are spread far outside of the confidence interval of the estimate averaged over the

whole ensemble. (Only results for GT-80 draught 2 are shown).

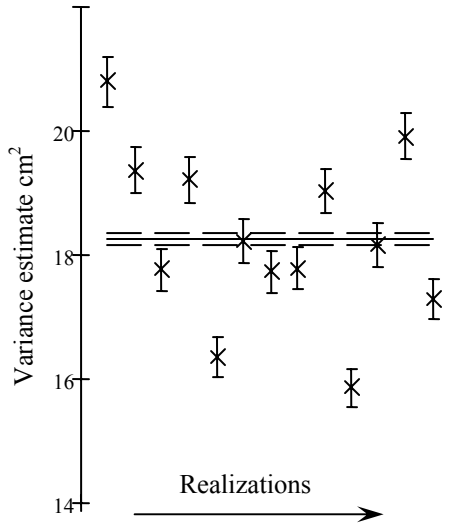

Figure 11 Wave realization estimates vs. wave ensemble estimate (dashed line shows confidence interval for ensemble estimate)

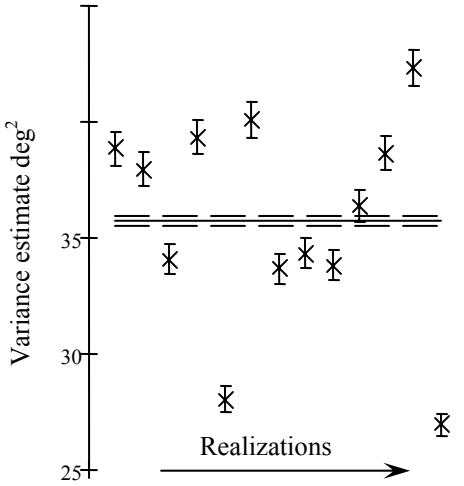

Figure 12 Roll realization estimates vs. roll ensemble estimate (dashed line shows confidence interval for ensemble estimate)

So, the deviation could not be explained just by finite number of statistics. Now let's consider non-ergodicity of the studied processes. For the purpose of preliminary analysis, we treat realization estimates as independent realization of a random number and use "direct" calculation of the variance of variance.

$$V_{NE}[V] = \frac{1}{K-1}\sum_{j=1}^{K}(\widetilde{V}_j - m_{NE}[V])^2 \quad (9)$$

Here m_{NE} is mean value estimate of realization variances calculated with the same assumptions:

$$m_{NE}[V] = \frac{1}{K}\sum_{j=1}^{K}\widetilde{V}_j \quad (10)$$

Again the summation are to be made over realizations, so K is number of recorded ones and equals 13. Now we can use formula (4) for calculation of confidence interval without ergodic assumption:

$$\Delta V_{NE} = P_{inv}(\beta, m_{NE}[V], V_{NE}[V]) \quad (11)$$

Now, criterion on non-ergodicity can be proposed in the following form:

$$E = \frac{\Delta V_{NE}}{\Delta V} \quad (12)$$

If the process is ergodic this criterion will tend to unity, since there no difference how to calculate estimates for ergodic process: by realization or by ensemble. Results of calculation are summarized in the table 5

Table 5 Calculation of ergodic criteria

Value	GT-80 draught 1	GT-80 draught 2	Box shaped model
Ensemble averaged wave variance (from table 4), cm^2	18.27	18.24	19.47
Non-ergodic wave variance of estimate, cm^4	1.58	1.914	3.07
Confidence interval for waves, cm^2	7.00	7.70	9.74
Ergodic criterion for waves	72.40	79.75	94.53
Ensemble averaged roll variance (from table 3), deg^2	29.06	35.64	63.81
Non-ergodic roll variance of estimate, deg^4	15.53	20.63	20.84
Confidence interval for roll, deg^2	21.93	25.27	25.40
Ergodic criterion for roll	142.55	133.97	75.21

Values of the proposed criteria indicate absence of ergodicity, what actually has been seen from figures 7-12. However, the proposed criterion estimates degree of non-ergodicity, in other words, how far an ergodic assumption would be from the reality.

Relative values of the criterion for wave and roll bear an important information. As we can see from the table 5, the criterion values for rolling of GT-80 is about twice as large in comparison of the same for waves. This might be interpreted as the dynamic system "adds" it own non-ergodicity (caused by non-linearity) to already non-ergodic input process.

Such interpretation was confirmed by numerical simulation. As we stated above, the scope of this paper

does not provide an opportunity to give detailed description of the criterion testing. Four cases were simulated: ergodic input with linear system, non-ergodic input with linear system, ergodic input with nonlinear system and non-ergodic input with nonlinear system. It was found that linear system (or inherently ergodic system) does not increase the criterion. Contrary, if the system possesses significant non-linearities, the criterion increases sharply. More details will be available in future publications

Curious enough, that box shaped model actually demonstrates slight decreasing of the criterion. If this effect will be confirmed by more precise analysis, this might be interpreted as an indication that GZ curve is a major nonlinearly affecting on ergodicity of rolling in irregular seas.

6. CONCLUSIONS

The paper describes the model test carried out in towing tank of National Research Institute of Fisheries Engineering of Japan. The purpose of the test was to check applicability of ergodic assumption for severe rolling in beam irregular seas. As of today, preliminary analysis has shown up that:

- Irregular wave produced in the tank is not ergodic stochastic process.
- Roll response of the model tank is not ergodic stochastic process
- There is an indication that non-ergodicity of roll response is also contributed by the non-linearity of the dynamical system
- There is an indication that GZ curve may be the major non-linear factor affecting on ergodic qualities of roll response in beam seas.

7. ACKNOWLEDGEMENTS

This research was funded by Science and Technology Agency of Japan (STA fellowship program Id 269115) and carried out in National Research Institute of Fisheries Engineering. Help of Prof. Naoya Umeda of Osaka University is greatly appreciated.

8. REFERENCES

1. Belenky, V. L., A. B. Degtyarev and A. V. Boukhanovsky. 1998 Probabilistic qualities of nonlinear stochastic rolling. *Ocean Engineering,* Vol. 25:1, 1998, pp. 1-25.
2. Belenky, V.L., Degtyarev, A.B., Boukhanovsky, A.V., probabilistic qualities of severe rolling, *Proc. of Int. Symp. on Ship Safety in a Seaway: Stability, Manoeuvrability, Nonlinear Approach (SEVASTIANOV SYMPOSIUM)*, Kaliningrad, 1995, vol.1
3. Ventsel, E.S. Theory of probability "Nauka" Moscow, 1969, 572 p. (in Russian)

AN EXPERIMENTAL INVESTIGATION INTO THE EFFECTS INITIAL CONDITIONS AND WATER ON DECK HAVE ON A THREE DEGREE OF FREEDOM CAPSIZE MODEL

Michael S. Obar, Young-Woo Lee, and Armin W. Troesch
Department of Naval Architecture and Marine Engineering
University of Michigan, Ann Arbor, Michigan, USA 48109-2145
e-mail: mobar@engin.umich.edu, ywl@engin.umich.edu, troesch@engin.umich.edu

SUMMARY

This paper presents the preliminary results of a three degree-of-freedom (3DOF) vessel capsize experiment and analysis conducted at the University of Michigan Marine Hydrodynamics Lab during the late spring of 2001. A box barge with minimal freeboard was placed in a beam sea and was excited at a super-harmonic three times its roll natural period. The motion of this vessel was captured using a locally developed infrared motion capture system. The video was stored electronically and analyzed using the computer program MATLAB©. The vessel was heeled at varying initial roll angles and released at twelve different locations in the wave train, each corresponding to a quarter of the wave excitation period. This was done to induce various initial conditions at a defined reference point (t_o). The definition of a safe basin of initial conditions and the effects water on deck has on this safe basin will be discussed.

1 INTRODUCTION

The fishing industry has, throughout history, been regarded as an extremely hazardous occupation. Even without the threat of a vessel capsizing, the chances of surviving a long career as a commercial fisherman are not very favourable.

Now, as the quantities of fish and number of species dwindle, and the regulations continue to become more stringent, fishermen must push the capabilities of their vessels to the brink, past which there may be no return. As captains push their vessels with overloading and tempt mother nature with trips into rougher weather, the need to better understand the dynamic nature of a vessels capsize becomes of great importance.

The phenomena of vessel capsize is an extremely complicated dynamic event. Environmental forces, hull design, and vessel loading are just of few of the hundreds of factors that affect the safety and stability of the vessel. In order to better understand this phenomena, the affect of an initial roll angle and velocity pair, coupled with water on deck will be analyzed in this paper.

Roll dynamics are best described by a nonlinear system whose response and eventual state (capsize or non-capsize) is frequently dependent upon initial conditions [1]. Additionally, water on deck produces variable loads that may have large impact on the motions. While there has been significant work investigating water on deck dynamics, e.g. [2]-[11], little attention has been given to the initial state of the vessel subject to these variable loads. Based on the work of Soliman and Thompson [1], an experiment was devised to investigate the affects of varying initial roll angle and roll velocity in a 3DOF system vice a 1DOF system.

2 BARGE PARTICULARS

The model used for the primary experiments was a simple box barge constructed of plywood and coated with West Systems epoxy. See Fig. 1. The model has a Plexiglas "main deck" and an aluminium platform supported by 4 threaded rods. Mounted on the platform are two infrared lights. The length of the model was 66.0cm. The model had a draft of 18.25cm with a freeboard of 1.12cm.

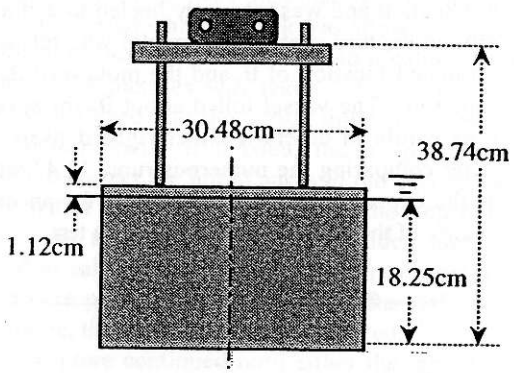

Figure 1: Sketch of barge with dimensions.

The center of gravity was adjusted to give an angle of vanishing stability, experimentally determined, of 11.4°. The deck became awash when the hull heeled approximately 5°, port or starboard. In addition to the angle of vanishing stability, the roll natural period and damping coefficients (linear and quadratic) were determined experimentally.

3 MOTION COLLECTION SYSTEM

It was critical to the analysis of this experiment to develop a system that could capture the motion of the vessel without itself affecting that motion. Two infrared LED lights were mounted on the platform of the model. A COHU 4915 High Performance Monochrome CCD Camera was mounted, in plane with the lights, with the entire test section in view. The manual iris on the camera was then closed until only the IR lights were picked up.

The rest of the test section was blacked out. The camera was connected to an ATI All-in Wonder 128 video card in a Dell PC. The movie was captured at 30 frames per second in an MPEG-1 format and saved on the hard disk for analysis at a later time. The typical movie size was around 30MB.

An intermediary program, Image Explorer Pro, was used to decompose the video into individual frames and save each frame as a JPEG image. Then, using MATLAB, each JPEG was individually loaded and scanned to find the locations of the model and indicator lights. These XY data pairs and the MATLAB workspace were then saved for future analysis. The complete analysis, including data collection, filtering of each frame to identify LED pixel position, and conversion to state six variables and three accelerations, took approximately 20 minutes per test run.

4 PRELIMINARIES

4.1 DETERMINING θ_v, THE ANGLE OF VANISHING STABILITY

A box barge was chosen as the vessel for this experiment due to its hydrostatic simplicity. Once the final weight and platform configuration was settled upon, the location of the center of gravity and θ_v was numerically determined.

The angle of vanishing stability, θ_v, was then determined experimentally. The model was placed in the test section and was manually heeled to a side. Using the motion-capture system, the model was released from the estimated location of θ_v and the motion of the vessel was captured. The vessel lolled about θ_v for several of these runs, while in others it either righted itself or capsized. After comparing the numerous runs, 11.4° was settled on as the experimental θ_v. See Fig. 2 for an example time history of the vanishing stability angle test.

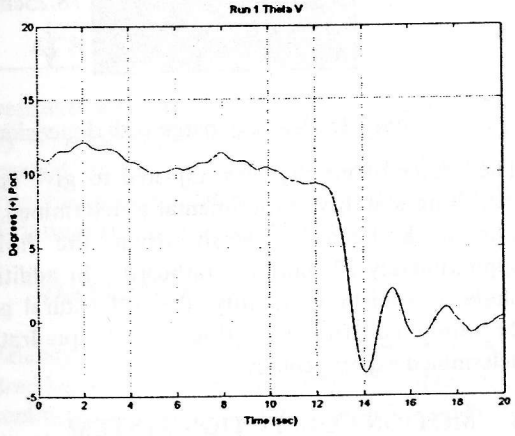

Figure 2: Vanishing Angle Determination Test

4.2 DECREMENT TESTS

Roll decrement tests were conducted in order to determine the roll natural period of the model. The model was heeled to both port and starboard and released. The motion was captured and the logarithmic decrement method was used to determine the natural period. The model was released from three heel angles, both port and starboard. The results of those tests are listed in the Table I below.

TABLE I: Decrement Test Results

Release Angle	Roll fn (Hz)	No. of Cycles
9.92	0.3669	2 analyzed
6.66	0.3605	4 analyzed
4.66	0.3639	8 analyzed
-12.96 *	0.3455 *	4 analyzed *
-10.48	0.3603	5 analyzed
-6.9	0.3645	9 analyzed
	Mean	**Standard Dev**
All 6 Runs	0.3603	0.0077
> 3 Cycles	0.3642	0.0004
> 7 Cycles	0.3589	0.0078

* Release was not clean.

Placing more emphasis on the analysis of runs with release angles less than 7° (these started with little water on deck and provided more cycles to analyze), the natural frequency was estimated to be 0.363 Hz.

4.3 DEFINITION OF t_0 AND RELEASE TIMES

In order to impart various initial conditions, the model was placed at 5 different roll angles and released at 12 different release times for each angle. Knowing the profile of the incident wave train from previous calibration runs (see the Appendix), the initial starting point, t_0,was defined as the first wave crest after the large transient, i.e. the first wave crest in the series of steady state waves. Thus all the transients that lead up to the steady state waves contributed to just the initial conditions defined at t_0. With this t_0 as a reference, it was decided to use an interval of 1/4 of a wave period between each release point and work back 3 wave periods. By releasing the model at set intervals prior to t_0, the model experienced a range of initial values for its six state variables, $(x, \dot{x})_j$ j=1...3, i.e. sway, heave, and roll motions.

4.4 AUTOMATION AND TIMING

In order to synchronize the data collection and motion collection systems, the entire process had to be automated as much as possible. Two computers were used to control the data collection and wavemaker activation. A MAC Quadra 900 running Labview 4.0 recorded the data input from the wave probes and command channels and also controlled the activation and motion of the wavemaker, while a Dell PC recorded the video.

The MAC controlled the signal output channels. The first channel was the command signal to the wavemaker amplifier. The first channel on the data collection card also captured this signal. The second output channel was a 5V low/high signal that controlled the wavemaker activation IR light. This channel was synchronised with the wavemaker command channel and signalled high as soon a command was given to the wavemaker amplifier. The second data collection channel captured this signal.

The third channel gave the control for the model release. A 5V High/Low signal was triggered once the desired release time occurred. Upon triggering, the signal activated a relay, which de-energized the DC magnets and switched on AC current to the magnets. (This helped to break the magnetic field faster.) The channel also powered the Model Release IR light and was monitored by the third data collection channel.

When the model was at the proper setting and the tank settled, the Dell video collection software started. Once a few seconds of the video had been recorded, the data collection card was triggered. It began recording the above-mentioned channels as well as the wave probe. After five seconds of data was recorded, the wavemaker command program was triggered and wave generation began.

In the post-data processing, the data time series and video was synchronized by using the hi/low channels in the data record and the lights in the video record. During the analysis of the scanned videos, the frame (accurate to the nearest 1/30 sec) where the wavemaker and models IR lights trigger, was determined thus synchronizing the video with the wave record.

5 EXPERIMENTAL SETUP AND TEST PROCEDURE

The experiments were conducted in the Gravity Wave Facility at the University of Michigan Marine Hydrodynamics Lab. The Gravity Wave Tank is 35m long, 0.75m wide, and 1.5m deep. It has a computer controlled, plunger style wavemaker. The Gravity Wave Tank also has wind generation capabilities. Although we will not be using this capability, the wind generation equipment limits the depth of the water, e.g. for a maximum wave height of 10cm, the depth of water is limited to 65cm.

For the experiments described here, the model was placed in the tank with its port side towards the wavemaker. The model was fixed in an initial position by electro-magnets suspended from the top of the tank. The release location for every run was 15.44m from the wavemaker. This position was chosen due to the location of the edge of the video frame in relation to the test section. The magnets held the model by brackets mounted on the platform. The electro-magnets were on a pivoting arm, which allowed for the vessel to be set at an initial roll angle. Once the model was released from the magnets, the pivoting arm also allowed the magnets to be swung out of the way of the platform.

The primary wave probe used to capture the wave profile of each run was mounted 8.86m down-tank from the wavemaker. This distance to the wavemaker was limited by the location of the wind generation scoop.

Four reference IR lights were mounted on the exterior of the test section glass in each corner of the video frame. See Fig. 3 for an example frame. The upper right reference light was also used as the video trigger for wavemaker activation and the lower right reference light was used as a trigger for the model release.

The two left hand reference lights were used for determining any camera twist. In order to ensure the camera always remained in the same position a MATLAB plugin allowed camera frames to be taken and imported directly into memory. This allowed for corrections to the camera position prior to every run.

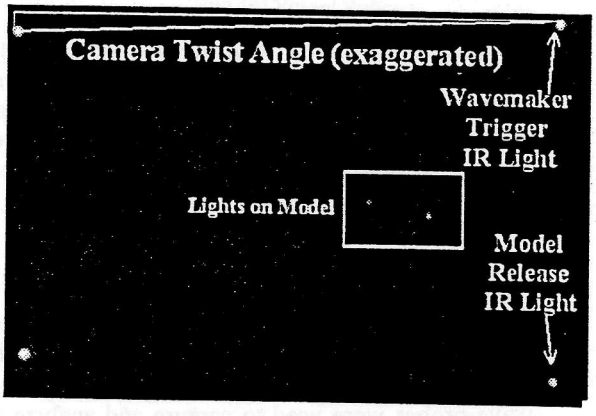

Figure 3: View of test section during run.

The testing began with the camera position verification. Several pictures were taken and compared to a reference picture. The camera was then adjusted slightly until the pictures were aligned with the reference. At the same time, the primary wave probe 40s zero was taken.

Next, the magnetic arms were set to the desired initial roll angle. The model was then placed in position and the magnets energized while the tank was allowed to settle.

After the water surface returned to a calm condition, a second set of pictures was taken. These pictures were instantly analyzed and the actual initial roll angle of the vessel determined. If needed, the magnet arms were adjusted to correct the initial angle to the desired value. A sample matrix is shown in Table A.1 of the Appendix.

Once all adjustments were concluded and the tank returned to calm water, the video capture program and the data capture program were started. After 3-5 seconds of data capture, the wavemaker was energized.

Data capture continued until either the model capsized or it left the test section, drifting out of the camera's view. The data was then saved for future analysis.

6 WAVE DETERMINATION AND ANALYSIS

6.1 WAVE DETERMINATION

The physical dimensions of the Gravity Wave Tank and the wavemaker design limited the available frequency of the waves and wave heights. Being unable to excite the vessel at or near its roll natural frequency of 0.363Hz, it was decided to excite the model at a super-harmonic of 1.089Hz, or 3 times the natural frequency.

The appropriate incident wave height was determined experimentally. Several wave runs were conducted with no artificial initial conditions imparted to the vessel. The vessel was set motionless at the release location and a test wave train was generated. Capsize or no-capsize was recorded and a second wave height was attempted. Once the smallest wave height that consistently capsized the model was identified, the height setting was then reduced.

The goal was to find the largest wave height where the vessel did not consistently capsize. That height, 2.67cm for the particular set of barge particulars and incident wave frequency described here, became the excitation wave height. The intent of this process was to determine an experimental critical wave height [1] where initial conditions imparted upon the vessel would create the likely conditions needed for capsize.

During these early tests, it was noticed that a slight longitudinal variation in the release point of the vessel (i.e. the location of the vessel relative to the wave maker), led to significant changes in the wave height needed to capsize the vessel. The variation could be a little as a few centimetres. The significance of this was noted and will be discussed in the Results/Conclusions sections.

6.2 WAVE ANALYSIS

Once the wave frequency and height was determined, 1.089Hz and 2.67cm, the repeatability of the wave generation capabilities of the tank was verified. Three wave probes were used to capture and analyze the wave profile. The primary wave probe, also used during the data collection phase, was located 8.86m down tank. A second wave probe was placed at the model release location, 15.44m down tank, and a third wave probe was placed at the end of the test section, 16.46m down tank.

6.2 (a) Wave Repeatability

Three runs were conducted with the model removed from the tank and data collection set up for the primary probe (labelled FWD Probe in the plots) and the probe at the release location (labelled Model Probe in the plots). The data collected was analyzed and plotted. Typical results are displayed in Appendix Fig. A1 indicating that wave profiles were repeatable to within 5%.

6.2 (b) Wave Reflection

Due to the finite length of the Gravity Wave Tank, it was important to ensure that the data collection and vessel capsize, occurs prior to the arrival of reflected waves off the far end of the tank. This cut-off time was determined by placing a wave probe at the end of the test section and collecting data for three separate runs.

As seen in Fig. A2, the primary crests and troughs of the steady state wave train can be identified. Once a crest and trough deviated from the mean by 1.5 standard deviations, that zero-crossing was identified as the reflection inception point. In Fig. A2, this point was approximately 62 seconds after wave maker activation. For every data run, the model either capsized or drifted out of the test section well before 60 seconds Thus wave reflection was not an issue with the experiments reported in this work.

6.2 (c) Wave Propagation

The initial transient of the wave front changes as it progresses down the tank. Three calibration runs were conducted, collecting data with the primary probe and a probe located at the release point. As the wave front changes, the excitation the model sees prior to the defined starting phase, t_o, changes as seen in Fig. A3 of the Appendix. This spatial variation of the wave envelope required the capture of the profile of the entire wave surface in the test section.

6.3 TEST SECTION WAVE PROFILE CAPTURE

Due to the fact that the model was allowed to translate down the tank during a run, determining the exact wave elevation at every point in the test section using wave probes was impractical. To capture the spatial behaviour of the wave elevation at every point in the test section, a flourscein solution was dissolved into the tank. The water surface was then illuminated with a laser sheet. Three runs were then conducted without the model in the tank and a video time history was recorded and analyzed. See Fig. 4 for an example video frame. Given the undisturbed wave profile as a function of time and space, it was possible to synchronize time and location of the desired wave crest (or trough) with the barge center of gravity, thus defining the starting reference phase or time, t_o.

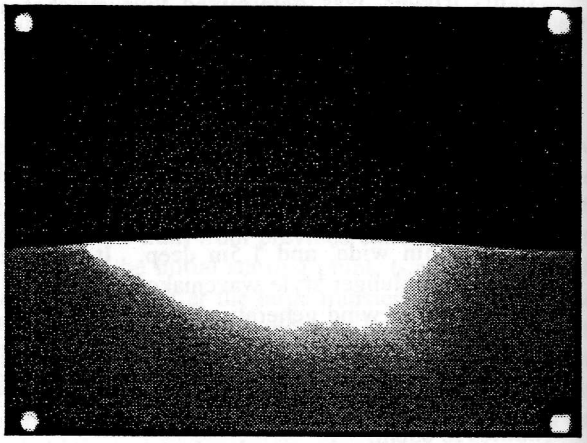

Figure 4: A view of the test section during a run. The cameras iris was opened slightly more than during a regular run.

7 MOTION ANALYSIS

The captured videos were stored in MPEG-1 format. This MPEG was separated into individual frames, e.g. Fig. 5.

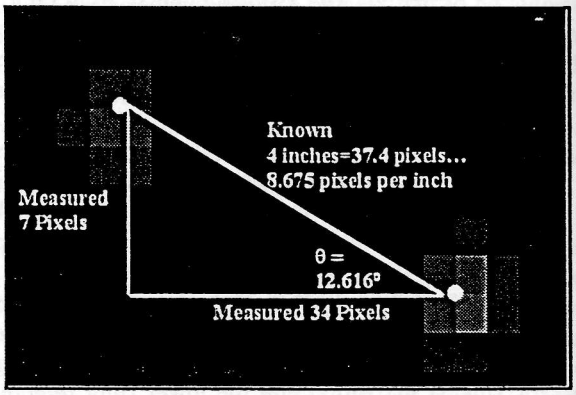

Figure 5: Blow up of the model IR lights and roll angle determination.

For each frame, a MATLAB program determined an ordered set of (x,y) data pairs representing the location of the two IR lights on the model at 1/30 sec intervals.

A third MATLAB program calculated vessel dynamics based upon the IR time series. The reference point for the model was its center of gravity. The roll, heave, and sway motions about the COG are determined using simple geometry.

Figure 6 below displays the captured motion plots. The upper plot shows roll angle vs time. All time-based position plots reference the energizing of the wavemaker at time t = 0. In Fig. 6, the model was released about 21.5 seconds after the wavemaker was energized. The model was held at a release angle of -10 degrees (starboard). The roll angle in Fig. 6 is displayed as the local roll angle. This is the roll angle relative to the wave slope at the location of the center of gravity of the model.

The first circle in the time history denotes the model release time. The second circle at approximately t=27.5sec, is the starting time of the Poincaré samples, t_o. The time interval of the Poincaré samples corresponded to the wave encounter period. The angle of vanishing stability is also marked. Note that there are many instances where the local roll angle exceeds θ_v and does not capsize.

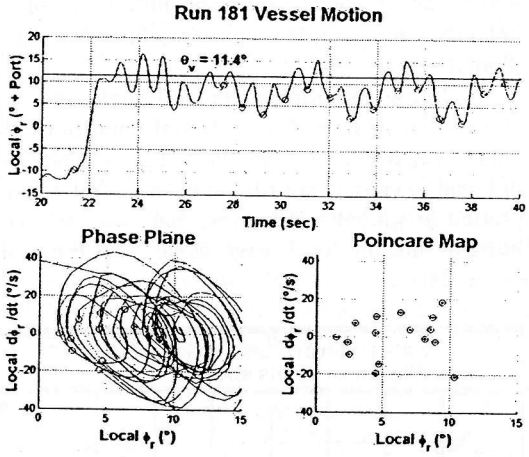

Figure 6: Vessel Non-Capsize Roll Motion (Local Roll Angle)

The motion displayed above is typical of the general trend for every non-capsize run. Runs that were initially released with a starboard roll angle, rolled down tank initially, but eventually settled in to the motion seen above. Runs that were released with a port roll angle rolled up tank immediately and also settled out to the same motion.

Figure 7 contains the same data run, only the analysis is presented with the global roll angle. The global roll angle is referenced to the earth fixed horizontal axis. The Poincaré points are sampled when each wave crest crosses the vessel's center of gravity. Using the local angle, e.g. Fig. 6, the Poincaré points map close to a "roll trough". When plotted on the global plots, e.g. Fig 7, the Poincaré points shift throughout the roll motion crests and troughs. As in Fig. 6, there are periods where the global roll angle exceeds θ_v but does not capsize.

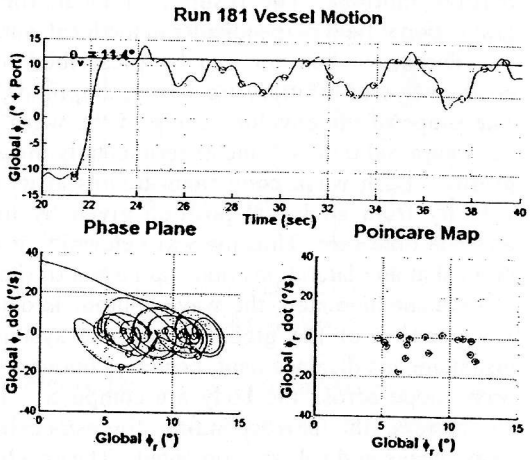

Figure 7: Vessel Non-Capsize Roll Motion (Global Roll Angle)

Figure 8 contains the motion during a capsize run. As with the non-capsize case, the motion of all the capsize situations were similar. While there may have been one or two roll-cycles prior to capsize the vessel tended to capsize and capsize quickly. For the conditions considered in this paper, all the capsize runs capsized into the waves.

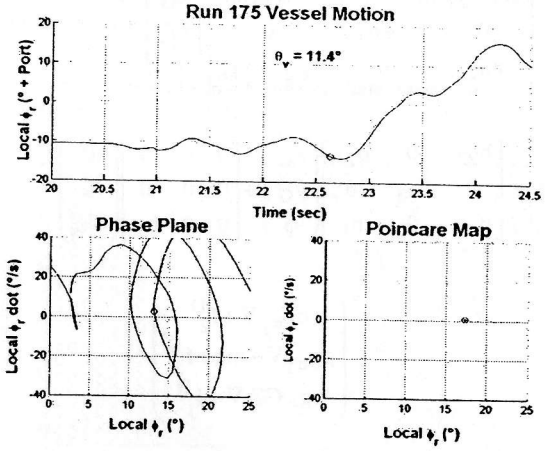

Figure 8: Vessel Capsize Roll Motion (Local Roll Angle)

8 NUMERICAL SIMULATIONS BASED ON A BLENDED HYDRODYNAMIC MODEL

To more fully understand the dynamics shown in Figs. 6-8, calculations were performed using a three degree of freedom "blended" hydrodynamic model. Various blended models have been developed approximating fully nonlinear behaviour with a combination of nonlinear and linear components [12] [13]. In this work, a quasi-nonlinear time domain simulation based on the effective gravitational field and long wave assumption [7] [14] is used. The

approximation will fully account for the effects of deck immersion in the computation of restoring forces and Froude-Krylov forces.

Briefly, the effective gravitational field is a vector combination of the earth's gravitational acceleration and the centrifugal acceleration associated with circular water particle motion. The result is a local, time varying, gravitational field perpendicular to the local water surface.

The wave contour can be prescribed by a single cosine wave of arbitrary frequency, amplitude and phase. The shape of the envelope curve of the wave profile has been adjusted to match the experimentally measured wave profile. Each wave component travels at its own phase velocity from an initial position given by its specified phase at time zero. Thus the wave elevation is completely defined at any lateral position and instant of time. At each subsequent time step, the wave contour is determined at any position of the global coordinate system, and the instantaneous displacement, center of buoyancy and local wave slope across the body are computed. From these parameters, the corresponding forces/accelerations in sway, heave and roll are computed. The accelerations are integrated at each time step to compute the velocities which are then integrated to determine the body position and orientation in sway, heave and roll.

The equations of motion, in a global, stationary axis system, are given in Eq. (1) below. The body position and orientation is given by the coordinates of the center of gravity, (x_G, y_G) and by the roll angle, φ.

$$\begin{bmatrix} m+a_{22} & 0 & a_{24} \\ 0 & m+a_{33} & 0 \\ a_{42} & 0 & I_{c.g.}+a_{44} \end{bmatrix} \begin{pmatrix} \ddot{x}_G \\ \ddot{y}_G \\ \ddot{\varphi} \end{pmatrix}$$

$$+ \begin{bmatrix} b_{22} & 0 & b_{24} \\ 0 & b_{33} & 0 \\ b_{42} & 0 & b_1 \end{bmatrix} \begin{pmatrix} \dot{x}_G \\ \dot{y}_G \\ \dot{\varphi} \end{pmatrix} + \begin{bmatrix} 0 & 0 & 0 \\ 0 & 0 & 0 \\ 0 & 0 & b_2 \end{bmatrix} \begin{pmatrix} 0 \\ 0 \\ \dot{\varphi}|\dot{\varphi}| \end{pmatrix} \qquad (1)$$

$$= \begin{pmatrix} \rho g_{e_2} \nabla + f_2^D \\ \rho g_{e_3} \nabla - mg + f_3^D \\ \rho g_e GZ \nabla + f_j^D \end{pmatrix}$$

The subscripts 2, 3 and 4 denote sway, heave and roll respectively. In the matrix, a_{ij} and b_{ij} are added mass and damping coefficients, f_j^D are diffraction forces and b_1 and b_2 are linear and nonlinear (quadratic) roll damping coefficients. Added mass, damping and wave diffraction forces are assumed constant at each wave frequency and all these coefficients are calculated using the standard linear seakeeping program, SHIPMO[15]. The nonlinear forces are associated with terms that include

g_e- the magnitude of the effective gravity,

g_{e2}, g_{e3} - the sway and heave components of the effective gravity in global axis coordinates,

b_2 - the quadratic roll damping [15],

∇ - the time dependent volume of the hull, including the occurrences of deck immersion or bottom emersion, and

GZ - the time dependent roll righting arm, referenced in the local wave slope/body coordinates.

With this model, the complex dynamic responses of the box barge with a low freeboard floating in regular beam waves can be investigated. Note that the blended model given in Eq. (1) does not include the real-life effects associated with the dynamics of water on deck such as fluid sloshing and water egress.

For the simulations presented in this paper, initial conditions for the other state variables, heave and sway displacements and velocities, were set equal to zero. This is not the case for the experiments and may be a possible explanation for any differences between simulated and experimentally measured capsize boundaries.

9 RESULTS

One hundred and eighty experimental runs were conducted. Three initial-condition sampling points were chosen, t_{o1}, t_{o2}, and t_{o3}, the largest transient crest prior to the regular wave train, the largest transient trough prior to the regular wave train, and the first regular crest in the wave train, respectively. The initial roll angle and roll velocity were sampled at these points and the results are plotted below.

Initial condition pairs, roll angle and roll velocity, are plotted in Figs. 9-12. Initial conditions that did not lead to capsize are left unfilled. Initial condition pairs that did lead to capsize are filled in. These initial conditions are plotted as global roll angles, that is as referenced to the horizon, not the local wave slope. All the plots have the same scale.

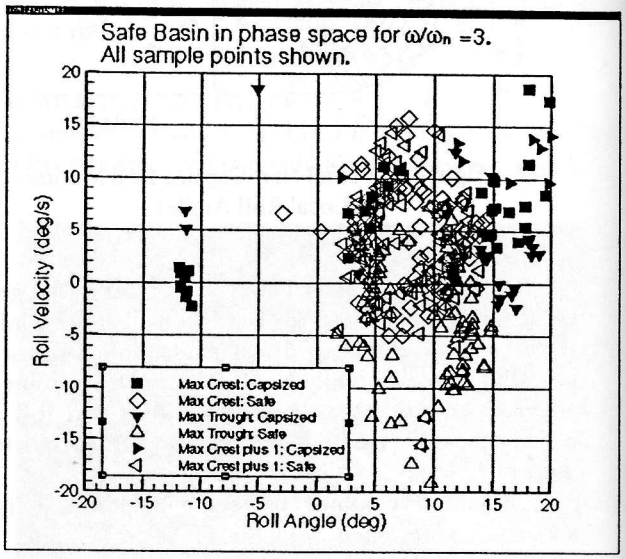

Figure 9: Safe basin with sample points plotted for all phases: Maximum transient crest (t_{o1}), Maximum transient trough (t_{o2}), Maximum transient crest plus one (t_{o3}).

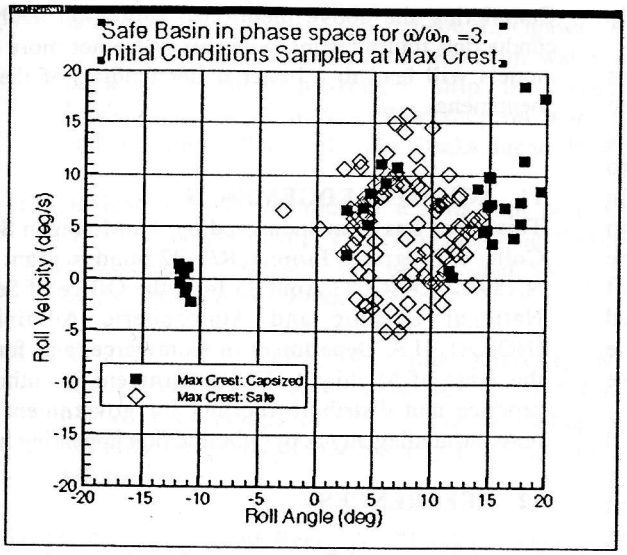

Figure 10: Safe basin from Maximum transient crest sample point (t_{01})

Figure 9 contains all three initial conditions plotted on one graph. This is done to emphasize the general trends in the capsize and non-capsize data. There appear to be differences in the initial condition pairs when chosen from different starting points, however they all map into the same general vicinity. Figures 10, 11, and 12 contain the same data as figure 9, but are categorized based on whether they are referenced to t_{01}, the maximum transient crest, t_{02}, the maximum transient trough, or t_{03}, the maximum transient crest plus one (i.e. the first regular wave crest). Figures 11 and 12 contain a subset of the runs shown in Fig. 10.

Figure 13 is a comparison plot between the numerical simulation runs and the experimental runs, sampled at the maximum transient crest (Fig. 10). The simulations were run with initial conditions spanning $-20 \le \varphi \le 20$ and $-15 \le d\varphi/dt \le 15$.

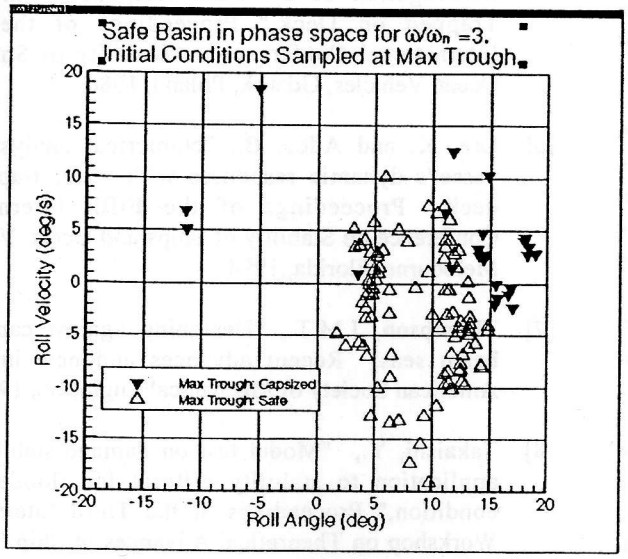

Figure 11: Safe basin from Maximum transient trough sample point (t_{02})

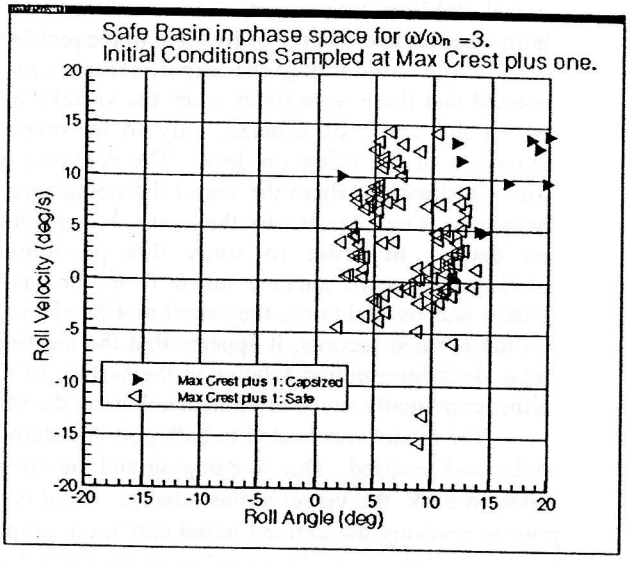

Figure 12: Safe basin from Maximum transient crest plus one (i.e. first regular wave crest) sample point (t_{03})

White areas within the simulation initial condition boundaries of Fig 13 denote safe or non capsize behaviour, as determined by the integration of Eq.(1). There is significant correlation between the experiments and theory even though the simulations did not match initial conditions for heave and sway and additionally, lack a better dynamic model for water on deck. It is clear that more work is needed in this area to improve the predictions. However, it is also gratifying that the concept of nonlinear systems analysis with various basins of attraction (safe or capsize) [1] [7] seems to capture the physics of capsize.

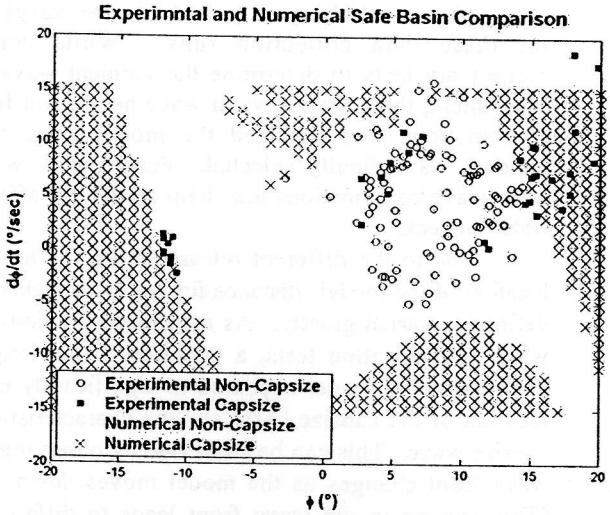

Figure 13: Safe basin plot of numerical and experimental data

10 CONCLUSIONS

The role the initial conditions play in vessel capsize is no doubt an important one. This can be seen where a slight variation in an initial condition can lead to either capsize or non-capsize. In addition, the location where the wave crashes on the deck of the vessel can be significant in

vessel stability assessment. The water on deck clearly introduces another degree of freedom to the problem.

While conducting the experimental runs, it was noticed that there were times when the vessel appeared to be on the verge of capsize, only to be saved by the dynamics of the water on deck. The converse was also true. A situation where the vessel did not appear to be in danger, was exasperated by the next wave crashing down on deck. In order to study this phenomena, the undisturbed wave surface taken from the laser sheet videos was overlaid onto the vessel motion videos. Based on these video records, it appears that the location of the main deck intersection relative to the surface of the wave either continually saved or immediately sank the vessel.

The model was heeled to both port and starboard roll angles and released. Due to damping and the effect of the water on deck, the vessel almost always settled out to port prior to reaching the defined initial condition sample point, t_o. In several cases, the vessel even capsized during the transient wave front. The runs that capsized early were generally those that started heeled to starboard and were released right before the largest transient struck the vessel. During these runs, the model rolled back to port and as the large transient piled water onto the port side of the model, it continued its roll all the way to capsize.

Runs that were released early, tended to settle out to a motion that rolled about 7 to 10 degrees globally to port. Trends in which release times led to which initial conditions, and thus to capsize or not, need to be looked at. Also, quantification of the amount of water on deck and a general location of the "wedge of water's" center of gravity needs to be determined. This should explain the vessels motion settling about a port roll angle between 7 and 10 degrees.

The vessel always capsized into the waves, to port, for these data collection runs. While conducting preliminary tests to determine the incident wave for this experiment, there were several wave height and frequency combinations that capsized the model away from the incident wave finally selected. Future work with these other wave combinations may help clarify the affect of the water on deck.

Due to the different release times, the longitudinal location of the model (distance for the wave maker) at each defined t_o varied greatly. As mentioned previously in the wave determination tests, a variation in the longitudinal position of the model appeared to significantly effect the location of the capsize basin and the characteristics of the capsize wave. This can be addressed by observing how the wave front changes as the model moves down the tank. (This change in the wave front leads to different initial conditions.) However further analysis should be conducted, including running tests starting from the same initial conditions and relative release time but varying the longitudinal release location in the tank.

These experiments and numerical simulations represent a starting point for the development of a practical tool for classifying safe and dangerous dynamic conditions for a specific vessel in a specific loading condition. Completing the above mentioned follow-on analysis and conducting future testing with this and other more complex models will lead to a better understanding of the capsize phenomena.

11 ACKNOWLEDGEMENTS

This paper has been sponsored by the Michigan Sea Grant College Program, Project R/T-32, under grant number NA89AA-D-SG083 Amd #5 from the Office of Sea Grant, National Oceanic and Atmospheric Administration (NOAA), U.S. Department of Commerce, and funds from the State of Michigan. The government is authorized to produce and distribute reprints for government purpose notwithstanding any copyright notation appearing herein.

12 REFERENCES

[1] Soliman and Thompson, 'Transient and steady state analysis of capsize phenomena', Applied Ocean Research, 1991.

[2] Murashige, S. and Aihara, K., "Coexistence of periodic roll motion and chaotic one in a forced flooded ship, International Journal of Bifurcation and Chaos, Vol. 8, No. 3, pp. 619-626, 1998.

[3] Huang, Z.J., Cong, L., Grochowalski, S., and Hsiung, C.C., "Capsize analysis for ships with water shipping on and off the deck," Proceedings of the 22nd Symposium on Naval Hydrodynamics, Washington, DC, 1998.

[4] Huang, Z.J. and Hsiung, C.C., "Nonlinear shallow water flow on deck coupled with ship motion," Proceedings of the 21st Symposium on Naval Hydrodynamics, Trondheim, Norway, 1996a.

[5] Pantazopoulos M. and Adee, B., "An Experimental Investigation of a Vessel Response with Water Trapped on Deck," Proceedings of the Third International Conference on Stability of Ships and Ocean Vehicles, Gdansk, Poland, 1986.

[6] Lee, K. and Adee, B., "Numerical analysis of a vessel's dynamic responses with water trapped on deck," Proceedings of the Fifth International Conference on Stability of Ships and Ocean Vehicles, Melbourne, Florida, 1994.

[7] Thompson, J.M.T., "Designing against capsize in beam seas: Recent advances and new insights," American Society of Mechanical Engineers, 1997.

[8] Takaishi, Y., "Model test on damage stability and application to stability criteria for flooded deck condition," Proceedings of the Third International Workshop on Theoretical Advances in Ship Stability and Practical Impact, Athens, Greece, 1997.

[9] Ishida, S., Murashige, S., Watanabe, I., Ogawa, Y., and Fujiwara, T., "Damage stability with water on deck of a ro-ro passenger ship in waves," Proceedings of the Second Workshop on Stability and Operational Safety of Ships, Osaka, Japan, 1996.

[10] de Kat, J.O., "Dynamics of a ship with partially flooded compartment," Proceedings of the Second Workshop on Stability and Operational Safety of Ships, Osaka, Japan, 1996.

[11] Amagai, K., Ueno, K, and Kimura, N., "Characteristics of roll motion for small fishing boats," Proceedings of the Second Workshop on Stability and Operational Safety of Ships, Osaka, Japan, 1996.

[12] Beck, R. F. and Reed, A., "Modern seakeeping computations for ships", Proceedings 23rd Symposium on Naval Hydrodynamics. 2000.

[13] ISSC, "Extreme hull girder loading", Committee VI.1 report, 14th International Ship and Offshore Structures Congress, Nagasaki, JAPAN, 2000.

[14] Chen, S. L. , Shaw, S. W., Troesch, A. W., "A systematic approach to modeling nonlinear muli-DOF ship motions in regular seas", Journal of Ship Research, Vol. 43, No. 1, 1999.

[15] Beck, R. F. and Troesch, A. W., "Department of Naval Architecture and Marine Engineering student's documentation and users' manual for the computer program SHIPMO.BM", University of Michigan, Ann Arbor, 1990.

A New Method to Predict Vessel/Platform Dynamics in a Realistic Seaway

S. Vishnubhotla, & J. Falzarano
School of Naval Architecture & Marine Engineering,
University of New Orleans, jfalzara@uno.edu

A. Vakakis
Mechanical Engineering Dept.,
University of Illinois

SUMMARY

In this paper, a recently developed approach (Vishnubhotla, Falzarano and Vakakis, 1998 & 2000) is described which makes use of a closed form analytic solution which is exact up to the first order of randomness, and takes into account exactly the unperturbed (no forcing or damping) global dynamics. The result of this is that, very large amplitude nonlinear vessel motion in a random seaway can be analysed with techniques similar to those used to analyse nonlinear vessel motions in a regular (periodic) seaway. The practical result being that dynamic capsizing studies can be undertaken considering the true randomness of the design seaway. The capsize risk associated with operation in a given sea spectra can be evaluated during the design stage or when an operating area change is being considered. Moreover, this technique can also be used to guide physical model tests or computer simulation studies to focus on critical vessel and environmental conditions, which may result in dangerously large roll motions. In order to demonstrate the practical usefulness of this approach, sample application is included. The results are in the form of solutions, which lie in the stable or unstable manifolds and are then projected onto the phase plane. Finally, the eventual goal of utilizing this method or any other similar method is the development of a physics based ship/platform stability criteria, which can reflect the actual vessel characteristics and operating environment.

1. INTRODUCTION

Research studies of non-linear ship and floating offshore platform rolling motion using dynamical systems' approaches have become quite common (Thompson, 1997). However, practical ship design stability criteria still focus on the static restoring moment curve as the sole or dominant indicator of the vessel's resistance to capsizing and only consider the motion in an implicit or very approximate manner. Most non-linear motions studies are limited to single degree of freedom and regular wave (periodic) excitation with few exceptions (see e.g., Hsieh, et al. (1993), Soliman & Thompson, 1990, and Lin & Yim, 1996). It is well known that roll cannot always be exactly decoupled from the other degrees of freedom but more importantly it is well known that sea waves are not regular but in fact are random. It is common in the design of ships and floating offshore platforms to make narrow banded assumptions and predict short-term extremes using the Rayleigh Probability Density Function (PDF) (see e.g., Ochi, 1998). In this study, the highly non-linear near-capsizing behaviour of a small fishing vessel in a random seaway is analysed by using an analytical solution to the differential equation. The availability of such a closed form solution allows safe basin boundary curves for this pseudo-randomly forced system to be generated.

The *Patti-B* was a small fishing vessel, which has the dubious distinction of having capsized twice. This vessel operated off the United States east coast and was unlucky enough to be involved in two capsizings. Initially she capsized in shallow water and her owners salvaged her (NTSB, 1979). The second time the vessel capsized in deeper waters and unfortunately all hands were lost.

2. PHYSICAL SYSTEM MODELING

The focus of this study is highly non-linear rolling motion of small fishing vessel possibly leading to capsizing. For the small fishing vessel, the roll axis is the critical motion axis. Roll is in general coupled to the other degrees of freedom; however, under certain circumstances it is possible to approximately decouple roll from the other degrees of freedom and to consider it in isolation. This allows focus on the critical roll dynamics. The de-coupling is most valid for vessels which are approximately fore aft symmetric which eliminates the yaw coupling. Moreover, by choosing an appropriate roll-center coordinate system, the sway is approximately decoupled from the roll (Webster, 1989). For ships, it has been shown in previous studies that even if the yaw and sway coupling are included the results differ only in a quantitative sense. The yaw and sway act as passive coordinates and do not qualitatively affect the roll (Zhang & Falzarano, 1993).

The other issue is the modelling of the fluid forces acting on the hull. Generally speaking, the fluid forces are subdivided into excitations and reactions (Newman, 1982). The wave exciting force is composed of one part due to incident waves and another due to the diffracted waves. These forces are strongly a function of the wavelength / frequency. The reactive forces are composed of hydrostatic (restoring) and hydrodynamic reactions. The hydrostatics are most strongly non-linear and are calculated using a ship hydrostatics computer program. In order that the zeroth order solutions are

expressed in terms of known analytic functions, the restoring moment curve needs to be fit by a cubic polynomial. It should be noted here that it is not much more difficult to utilize a numerically generated zeroth order solution which is based upon an accurate higher order righting arm curve. The hydrodynamic part of the reactive force is that due to the so-called radiated wave force. The radiated wave force is subdivided into added mass (inertia) and radiated wave damping. These two forces are also strongly a function of frequency. However since the damping is light, and for simplicity, constant values at a fixed frequency are assumed. Generally, an empirically determined non-linear viscous damping term is included. However such empirical viscous damping results are only available for ship hulls. The resulting roll equation of motion is :

$$(I_{44} + A_{44}(\omega_n))\ddot{\phi} + B_{44}(\omega_n)\dot{\phi} + B_{44q}\dot{\phi}|\dot{\phi}| + \Delta GZ(\phi,t) = F(t) \quad (1)$$

The focus of this study is non-linear ship rolling motion in a realistic seaway due to a pseudo-random wave excitation. The effect of seaway intensity is accurately considered. In order to obtain the roll moment excitation spectrum, the sea spectrum is multiplied by the roll moment excitation Response Amplitude Operator (RAO) squared (Equation 2a). The RAO for the small fishing vessel in given in Figure 1a.

The sea spectral model used for the small fishing vessel is the Pierson-Moskowitz (P-M). The P-M sea state equation (Ochi, 1998) is as follows,

$$S^{+}(\omega) = \frac{8.1x10^{-3}}{\omega^{5}} g^{2} e^{-.074(g/U_w/\omega)^4} \quad (2)$$

Where, U_w is the wind speed. The P-M model is used for this case because it corresponds to a fully developed seaway, which is in some sense the most severe. Moreover, the spectrum is a one-parameter spectrum so that solely the effect of seaway intensity can be considered.

Figures 1b and 1c show the *Patti-B*'s excitation spectra and the corresponding time history of the forcing (in non-dimensional form) for a wind speed of U_w = 2.75 meters per second. Figures 2a&b are for larger U_w. The significant wave heights for the sea spectra used for the *Patti-B* range from less than 2.0 foot to almost 7.5 feet. The sea state intensity ranges from about sea state one to four (Bhattachrayya, 1978) which is a reasonable operating condition for the *Patti-B*.

3. THE DYNAMICAL PERTURBATION METHOD

The focus of this investigation is the extension of an approach previously used to study the non-linear dynamics of a small fishing vessel and a very large semi-submersible platform due to pseudo-random wave excitation (Vishnubhotla, Falzarano and Vakakis, 1998 & 2000). The approach is based upon a method originally developed by Vakakis (1993) to calculate in closed form the homoclinic manifolds due to rapidly varying periodic excitation. That approach was generalized to calculate heteroclinic manifolds due to pseudo-random wave excitation. Considering that random excitation is a realistic model for ship and floating offshore platform motions at sea, this method was extended and then applied to consider the case of perturbed heteroclinic manifolds due to an external excitation as approximated by a finite summation of regular (periodic) wave components.

The forcing function would then assume the form shown in equation 3b.

$$S_R^{+}(\omega) = |RAO|^2 \; S^{+}(\omega) \quad (3a)$$

$$F(t) = \sum_{i=1}^{N} F_M(\omega_i)\mathrm{Cos}(\omega_i t + \gamma_i) \quad (3b)$$

where,

$$F_M(\omega_i) = \sqrt{2\, S_R^{+}(\omega_i)\,\Delta\omega} \quad (3c)$$

The solution to equations such as Equation (1) with softening spring characteristics exhibit two greatly different types of motions depending upon the amplitude of the forcing. For small forcing amplitude, the first type of motion is an oscillatory motion, which is generally bounded and well behaved. For large amplitudes of forcing, the motion can be such that a uni-directional rotation occurs. The boundary between these two types of motions is called in the terminology of non-linear vibrations, the separatrix. This curve literally separates the two qualitatively different motions. In the language of non-linear dynamical systems, these curves are called the (upper and lower) saddle connections. The saddles are connected as long as no damping and forcing are considered in the system. Once damping is added to the system, the saddle connection breaks into stable and unstable manifolds. The stable manifolds are most important, because they form the basin boundary between initial conditions, which remain bounded and those that become unbounded. When periodic forcing is added to the system, these manifolds oscillate periodically with time and return to their initial configuration after one period of the forcing. This forcing period is chosen for the Poincaré sampling time of such a periodic system. Unfortunately, no such obvious Poincaré time sampling exists for the pseudo-randomly forced system studied herein.

In this investigation, the random wave forcing is approximated by a summation of periodic components with random relative phase angles. Although this representation approximates the true random excitation as N64, and)T60, for finite N this does not occur. Actually, the "random" signal repeats itself after T_R= 2B/)T. Another relevant time period is the average or zero crossing period T_o . Assuming the spectrum is narrow banded, this might also be a good reference period for a Poincaré map. In lieu of Poincaré maps, we choose to trace out single solution paths, which are

contained in the stable manifolds (see Figure 3). These are then projected onto the phase plane.

The solutions lying in the stable manifolds are calculated using the new approach. This method is a perturbation method, which starts with the un-damped and unforced separatrix. For a simple softening spring (Equation, 4a), this is known in closed form. The critical solutions lying in the stable manifolds are calculated using our approach. This method is a perturbation method that begins with the un-damped and unforced separatrix. For a softening spring, the separtrix is known in closed form. i.e.

$$\ddot{x} + x - k x^3 = 0 \qquad (4a)$$

$$x(\tau) = \frac{1}{\sqrt{k}} \mathrm{Tanh}\left(\frac{\tau - \tau_o}{\sqrt{2}} + 1/2\right) \qquad (4b)$$

$$\dot{x}(\tau) = \frac{1}{\sqrt{2k}} Sech^2\left(\frac{\tau - \tau_0}{\sqrt{2}} + 1/2\right) \qquad (4c)$$

The first order solution is determined by using the method of variation of parameters. The original Equation (1), is scaled into the following form,

$$\ddot{x} + x - kx^3 = \varepsilon(-\gamma\dot{x} - \gamma_q \dot{x} \mid \dot{x} \mid + F(t)) \quad (5)$$

Having scaled the original equation, the solution method basically involves expanding the solution in a perturbation series as,

$$x(t) = x_0(t) + \varepsilon x_1(t)... \qquad (6)$$

The second order equation to be solved is actually a linear equation with time varying coefficients. The coefficients are obtained from the zeroth order solution known from Equations (4a) and (5) squared, i.e.,

$$\ddot{x}_1 + x_1 - 3k x_1 x_0^2 = \hat{F}(x_0, t) \qquad (7)$$

Solution to the zeroth and first order solution terms yields the perturbed manifolds, which are the boundary between the bounded and unbounded motions. This method explicitly determines the critical solution curves, which separate the bounded steady state oscillatory motions from the unbounded motions. These solutions are determined by solving equations (4) and (5) and using them in (6).

The approach taken in this paper although different from our previous analysis is similar enough that all the details need not be completely repeated herein. The basin boundaries correspond to the stable manifolds associated with the positive and negative angles of vanishing stability and are just the damped and forced extensions to the upper and lower separatrices respectively which were previously discussed. These stable manifolds form the basin boundary between bounded (safe, non-capsize) and unbounded (capsizing) solutions. See for example Figure 3a.

Although this method was originally developed by Vakakis (1993) to study intersections of stable and unstable manifolds for equations for which the Melnikov method could not be used, this method is applied herein because it is general enough to yield exact solutions to general equations such as the multiple frequency forcing case being studied herein.

4. RESULTS

The results are for the roll of a small fishing vessel which is probably one of the smallest vessels to venture away far from safety of shore. For the range of seaway considered, the results exhibit qualitatively different types of behaviour; even for these mild seaways considered herein.

An indication of if the basin boundaries will be simple and smooth or fractal and complicated is determined by if the manifolds intersect or not. As a first step in determining whether or not this will occur for the pseudo-randomly forced system is to determine solutions, which lie in both the stable and unstable manifolds. After this is done, the distance between the two solutions can then be determined and this will indicate whether or not a manifold intersection has occurred. When the distance between the two manifolds goes to zero, the manifolds become tangent and this is a critical value of the forcing. Beyond the value of forcing where the manifolds become tangent the manifolds intersect and the safe basin begins to erode. This is exactly what the Melnikov function (Falzarano, et al, 1992) is used for and what is being described herein is simply a more general alternative to the Melnikov approach. The method described herein has several potential benefits over the classical Melnikov approach. These benefits enable the ability to, 1) analyse very general systems for which the Melnikov method is not valid 2) obtain higher order results, and 3) develop a visual projection of the manifolds for single degree of freedom systems.

4.1 Safe Basin Boundary Projected Phase Plane

The results are for physical parameters representing the clam dredge *Patti-B* (Falzarano, et al., 1992) in beam seas and rolling in various intensity Pierson-Moskowitz sea spectra. As stated previously, the sea spectra are approximated by a finite but large number of periodic components. As can be seen, when the wind speed is increased and the seaway intensity increases, the vessel's dynamics change qualitatively. The upper and lower stable manifolds change from smooth curves similar to the unforced system to rather complicated curves indicating the possibility of manifold intersections. The size of the safe operating region of the vessel is somewhat related to when these manifolds intersect and become fractal or complicated. Figures 2a, b & c show moderate to large amplitude sea spectra plotted versus frequency for a range of wind speeds. The wind speed is the single parameter describing the seaway intensity.

Results for time-varying roll motion solutions contained within the upper and lower stable manifolds projected phase planes for these sea spectra are given in Figures 3a-3c. One can see that Figures 3a&b show smooth stable manifolds while Figure 3c shows tangled stable manifolds. When looking at these projected phase plane results, it should be recognized that the solutions depicted represent a time evolution of a single trajectory and are not Poincaré time samplings of the manifold. This explains the wrapping around the fixed point. The random oscillation occurs on the average at the zero crossing period while the solution is slowly evolving towards the fixed point.

4.2 Extended State Space Results

However, once unstable manifolds are also included, the two-dimensional projection of the time-varying solutions, lying in the stable or unstable manifolds, may look deceptive. This is so because true intersections only occur for the same time phase. Therefore a three-dimensional extended state space representation is the only unique representation. In order to illustrate this and in order to determine whether or not intersections have occurred, some typical results for the *Patti-B* are provided. These one-dimensional solution curves are shown in the full three-dimensional extended state space (Fig. 4). These results clearly indicate that the two curves do not intersect for the two given seaway intensities.

A more extensive and systematic investigation is currently underway. In order to more clearly determine if the manifolds intersections have occurred the entire manifold must be generated. Generating the entire manifold would involve varying the initial time t_o and then generating an entire manifold mesh. After this had been done, the distance between the two manifolds, i.e., stable and unstable can then be calculated. This distance going to zero would indicate that manifold intersections were imminent. This would be a critical value of external wave forcing since at a greater value of wave forcing, the safe basin would begin to erode.

5. CONCLUSIONS

The method utilized herein is quite powerful and capable of handling very general systems. The application herein utilized the knowledge of the zeroth order solution, which was known in closed form for this simple system. However, this is not a requirement and actually for more general systems it could be known numerically. Clearly, the safe operating region of the vessel is directly related to when the calculated stable and unstable manifolds intersect and erode the safe basin. It should be re-emphasized here that the results given correspond to single realizations of the given sea spectra. In order to gain a more complete probabilistic understanding of the systems random behaviour, multiple realizations must be considered and analysed. This ensemble of results should then be analysed in terms of averages and standard deviations. However, this has not yet been done in a systematic manner.

The results clearly demonstrate the effect of random excitation on the global dynamics of the vessel about its roll axis. Finally, the eventual goal of utilizing this method or any other similar method is the development of a physics based ship/platform stability criteria, which reflects the actual vessel characteristics and operating environment. Moreover, such a physics based method can be used to gain insight into the importance of relevant capsizing mechanisms in addition to what has been studied herein. Obviously, much more work needs to be done before such a stability criteria is a reality. Some of this work has begun but much more remains to be done.

6. ACKNOWLEDGMENTS

The authors would like to acknowledge the support of the US National Science Foundation, Dynamical Systems and Control Program and program manager Dr. Alison Flatau.

7. REFERENCES

Bhattachrayya, R., *Dynamics of Marine Vehicles*, Wiley, New York, 1978

Falzarano, J., Shaw, S., & Troesch, A., "Application of Global Methods for Analysing Dynamical Systems to Ship Rolling Motion and Capsizing," *International Journal of Bifurcation and Chaos*, Vol. 2, #1, (1992).

Hsieh, H., Shaw, S. & Troesch, A., "A Predictive Method for Vessel Capsize in a Random Seaway," *Nonlinear Dynamics of Marine Vehicles*, ASME (1993)(Ed. J. Falzarano & F. Papoulias).

Lin, H and Yim, S., "Chaotic Roll Motion and Capsizing of Ships Under Periodic Excitation with Random Noise," *Applied Ocean Research*, Vol. 117, 1995.

National Transportation Safety Board (NTSB), "Grounding and Capsizing of the Clam Dredge *Patti-B*," *NTSB Marine Accident Report*, 1979.

Newman, J, *Marine Hydrodynamics*, MIT Press, Cambridge (USA), 1982.

Ochi, M, *Ocean Waves*, Cambridge University Press, Cambridge (UK), 1998.

Soliman, M. & Thompson, JMT, "Stochastic Penetration of Smooth and Fractal Basin Boundaries under Noise Excitation," *Dynamics and Stability of Systems*, Vol. 5, (1990)

Thompson JMT, "Designing Against Capsize in Beams Seas: Recent Advances and New Insight," *Applied Mechanics Reviews*, Vol. 50, No. 5, May 1997.

Vakakis, A., (1993), "Splitting of Separatrices of the Rapidly Forced Duffing Equation," *Nonlinear Vibrations*, ASME Vibrations Conference, September.

Vishnubhotla, S., Falzarano, J. and Vakakis, A., (1998), "A New Method to Predict Vessel/Platform Capsizing in a Random Seaway," *3rd International Conference on Computational Stochastic Mechanics*, Balkema, Holland.

Vishnubhotla, S., Falzarano, J. and Vakakis, A., (1998), "A New Method to Predict Vessel/Platform Capsizing in a Random Seaway," *Philosophical Transactions of the Royal Society*, Special Issue on Nonlinear Dynamics of Ships, May 2000.

Webster, W, "The Transverse motions," Chapter 8 Seakeeping, *Principles of Naval Architecture Volume III*, Society of Naval Architects and Marine Engineers, New York, 1989.

Zhang, F. and Falzarano, J., "Multiple Degree of Freedom Global Transient Ship Rolling Motion: Large Amplitude Forcing," *Stochastic Dynamics & Reliability of Nonlinear Ocean Systems,* ASME (1994).

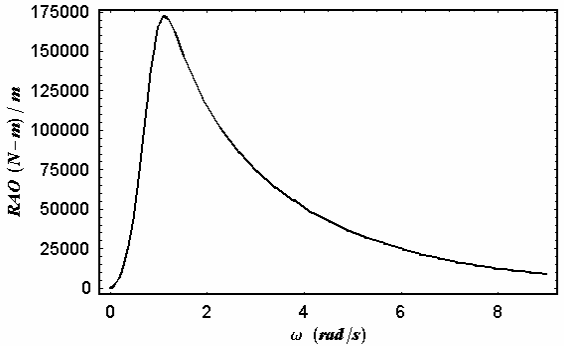

Fig 1a. *Patti*-B Roll Moment Excitation Transfer Function (RAO)

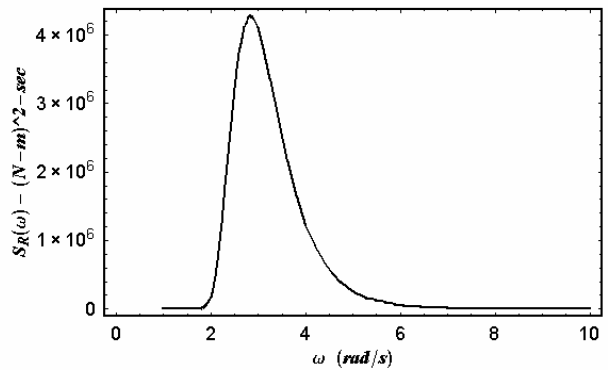

Fig 1b. *Patti*-B Roll Moment Excitation Spectrum, $U_W = 2.75$ ms^{-1}

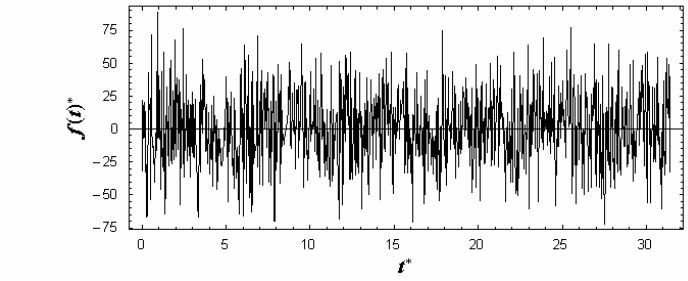

Fig 1c. *Patti*-B Corresponding Roll Moment Excitation Time History (non-dim), $U_W = 2.75$ ms^{-1}

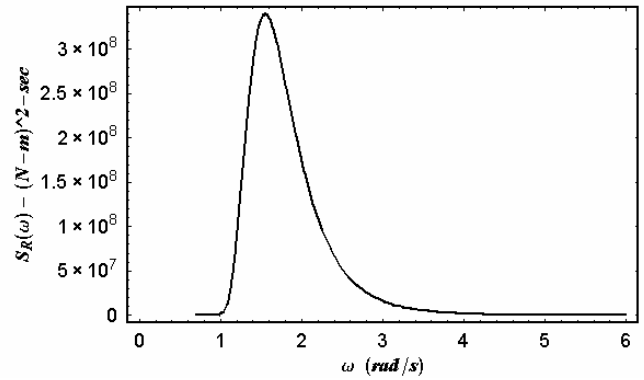

Fig 2a. *Patti*-B Moderate Amplitude Roll Moment Excitation Spectra, $U_W = 5.15$ ms^{-1}

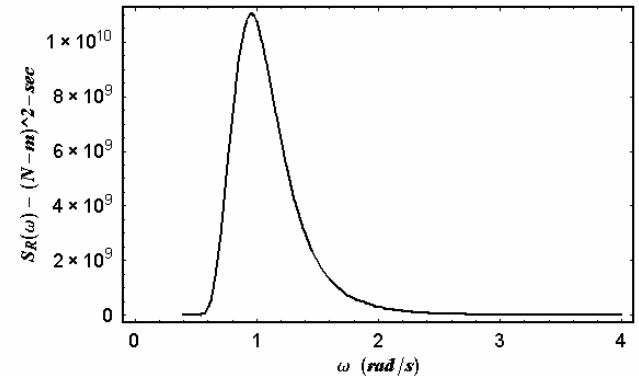

Fig 2b. *Patti*-B Large Amplitude Roll Moment Excitation Spectra, $U_W = 10.0$ ms^{-1}

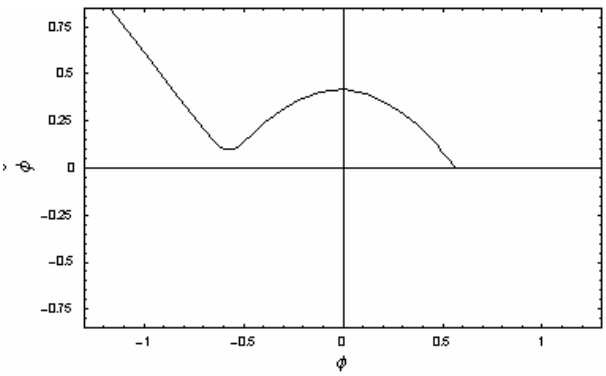

Fig 3a. *Patti*-B Projected Phase Plane for P-M Spectra, $U_W = 2.75$ ms^{-1}

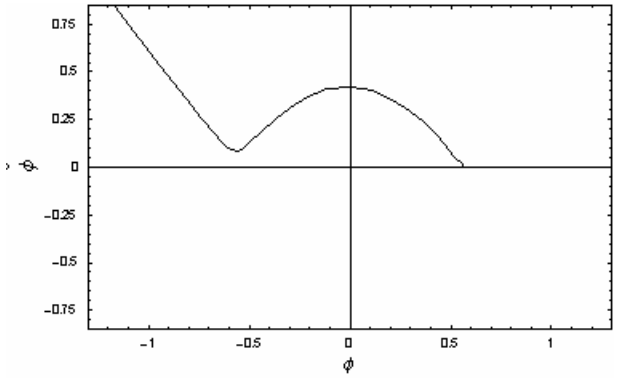

Fig 3b. *Patti*-B Projected Phase Plane for P-M Spectra, $U_W = 5.15$ ms^{-1}

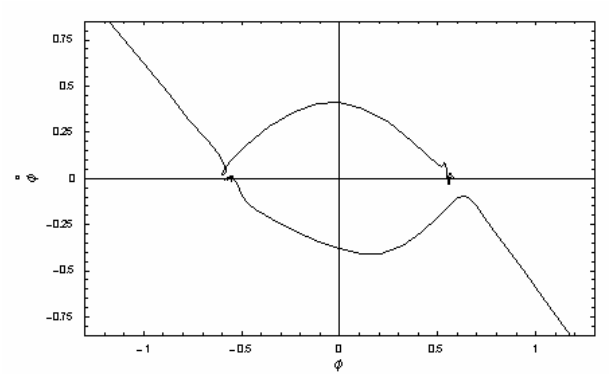

Fig 3c. *Patti-B* Projected Phase Plane for P-M Spectra, $U_W = 10.0$ ms^{-1}

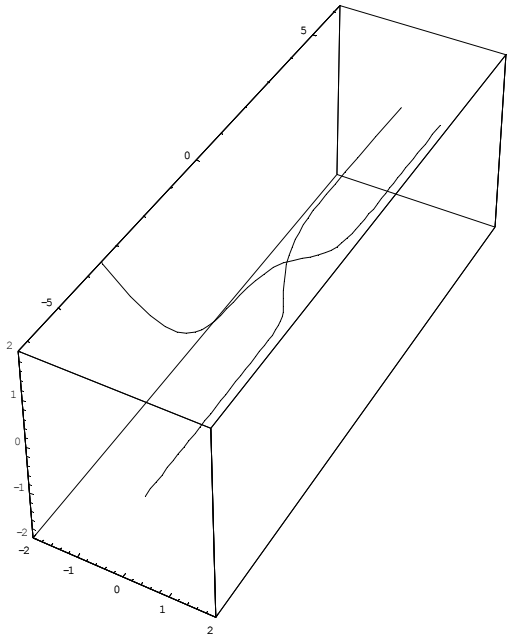

Fig 4a. *Patti-B* Extended Phase Space showing solutions contained in upper stable, $W^{+s}(t)$ and lower unstable manifold $W^{-us}(t)$, $U_W = 2.75$ ms^{-1}

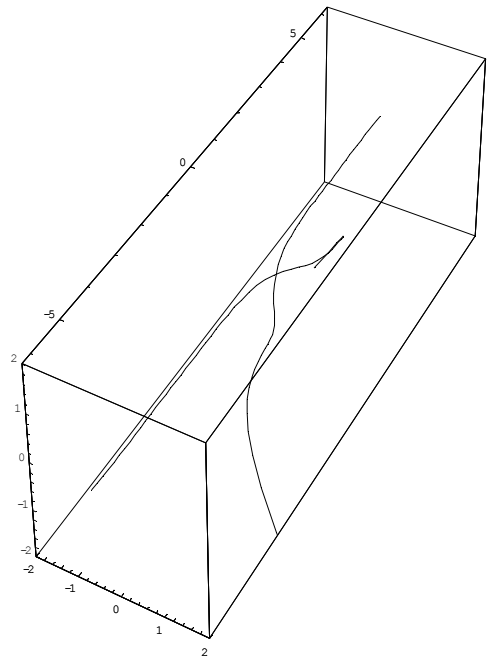

Fig 4b. *Patti-B* Extended Phase Space showing solutions contained in upper unstable, $W^{+us}(t)$ and lower stable manifold $W^{-s}(t)$, $U_W = 2.75$ ms^{-1}

5TH INTERNATIONAL WORKSHOP "STABILITY AND OPERATIONAL SAFETY OF SHIPS"
12-13 SEPTEMBER 2001, TRIESTE, ITALY

CAN MELNIKOV'S METHOD PROVIDE THE RATIONAL ALTERNATIVE TO IMO'S WEATHER CRITERION?

K.J. Spyrou, S. Papagiannopoulos & D. Sakkas

Department of Naval Architecture and Marine Engineering
National Technical University of Athens,
9 Iroon Polytechniou, Zographou, Athens 15773, Greece

Extended abstract

An important recent development in the area of dynamic stability of ships is the introduction of the concept of "engineering integrity" and the use of the so-called Melnikov method for defining the unsafe wave environment in terms of ship capsize[1-4]. This approach seems to provide a rational criterion of dynamic stability that is based on the limiting wave slope that can be sustained consistently during the transient stage of a ship's response to oncoming waves of a certain, deterministic or stochastic, type. The key concept of this approach derives from the observation that the safety margin against capsize of a ship is reduced very sharply soon after some critical level of wave-wind excitation is exceeded due to initiation of area loss in this dynamical system's "safe basin" (= the set of initial conditions which lead to a safe ship motion pattern). This critical excitation level, which depends on the ship's damping and restoring characteristics, can be predicted relatively easily through numerical means (either with repetitive basin plotting until the erosion is shown; or, more accurately, with direct numerical identification of the *heteroclinic tangency*, the global bifurcation phenomenon which initiates the loss of area in the basin). Furthermore, analytical or semi-analytical prediction is also possible on the basis of the method of Melnikov. It is very interesting that this method has been shown to be equivalent with an energy balance applied around the heteroclinic orbit of the corresponding Hamiltonian system.

We are currently investigating whether this approach can generate a design criterion for stability that is superior to the "Weather criterion" of IMO[5]. The latter is known to be relatively simplistic in its account of ship dynamics under the action of waves. Furthermore, we are investigating whether it can be used for design optimisation, and furthermore, whether it can be integrated within a risk-based design methodology. Some of the specific issues that will be discussed during the presentation are the following:

a) The "engineering integrity" concept should be workable for arbitrary restoring curves: The characteristics of the integrity curves for the family of 5th order restoring polynomials, $R(x) = x + ax^3 - (1+a)x^5$, have been investigated. In addition, we have determined the critical excitation that initiates basin erosion, as well as the excitation level at 90% "basin integrity" Fig. 1 [6]. However, some questions still remain here: whether the well-known Melnikov formula for cubic-type restoring is a successful predictor (unlike the Melnikov formula for the biased-case which targets the homoclinic tangency event, whose accuracy has been confirmed); and whether it can be modified in order to account for higher-order restoring polynomials.

b) Application to an existing ship: We have performed a comparison of application of the new criterion versus application of the Weather criterion for an existing RO-RO ferry. A significant advantage of the current method is that it can produce rationally the maximum wave slope for dynamic stability in a beam-sea environment (Fig. 2). Furthermore, the relation between critical wave slope and wind excitation has been set under investigation, given that even a small amount of bias can significantly lower the critical wave slope, combined with the fact that these ships are characterised by large windage areas.

c) Preliminary investigation on the use of the "engineering integrity" concept for design optimisation: We have taken as a basis a simple parameterised family of ship-like hull forms whose offsets are determined with the formula $y = \pm X(x)\, Z(x,z)$. $X(\bar{x}) = \frac{B}{2}\left(1 + a_2\,\bar{x}^2 + a_3\,|\bar{x}|^3 + a_4\,\bar{x}^4\right)$ and

$Z(\bar{x},\bar{z}) = (1+\bar{z})^{n(\bar{x})}$ with the nondimensional longitudinal and vertical positions $\bar{x} = \dfrac{x}{L_{BP}/2}$, $\bar{z} = \dfrac{z}{D}$ and the superscript $n(\bar{x}) = s + t\,|\bar{x}|$ where *s*, *t* are free parameters [7-8]. For a finite set of hulls taken from this family we determine the hull restoring and the damping and then, through dynamic analysis, the critical wave slope for capsize. The effect of bilge-keels on the critical wave-slope is also examined. Eventually, the hull-form with the best stability characteristics is identified.

References

[1] THOMPSON, J.M.T. 1997 Designing against capsize in beam seas: Recent advances and new insights. *Applied Mechanics Reviews*, **50**, 307-325.

[2] FALZARANO, J., TROESCH, A.W. & SHAW, S.W. 1992 Application of global methods for analyzing dynamical systems to ship rolling and capsizing. *International Journal of Bifurcation and Chaos*, **2**, 101-116.

[3] HSIEH, S.R., TROESCH, A.W. & SHAW, S.W. 1994 A nonlinear probabilistic method for predicting vessel capsizing in random beam seas. *Proceedings of the Royal Society*, A**446**, 1-17.

[4] SPYROU, K.J. & THOMPSON, J.M.T. (eds.) 2000: *The Nonlinear Dynamics of Ships*. Theme Issue of the Philosophical Transactions of the Royal Society, A**358**, Mathematical, Physical and Engineering Sciences, Published by The Royal Society of London, ISSN 1364-503X.

[5] IMO (1995) Code on Intact Stability for All Types of Ships Covered by IMO Instruments. Resolution A.749(18), London.

[6] PAPAGIANNOPOULOS, S. *Investigations of ship capsize in beam seas based on nonlinear dynamics theory*, Diploma Thesis, National Technical University of Athens, September 2001.

[7] SAKKAS, D. *Design optimization for maximising dynamic stability in beam seas*, Diploma Thesis, National Technical University of Athens, September 2001.

[8] MIN, K.S. & KANG, S.H. 1998 Systematic study on the hull form design and resistance prediction of displacement-type super-high-speed ships, *Journal of Marine Science and Technology*, **3**, 63-75.

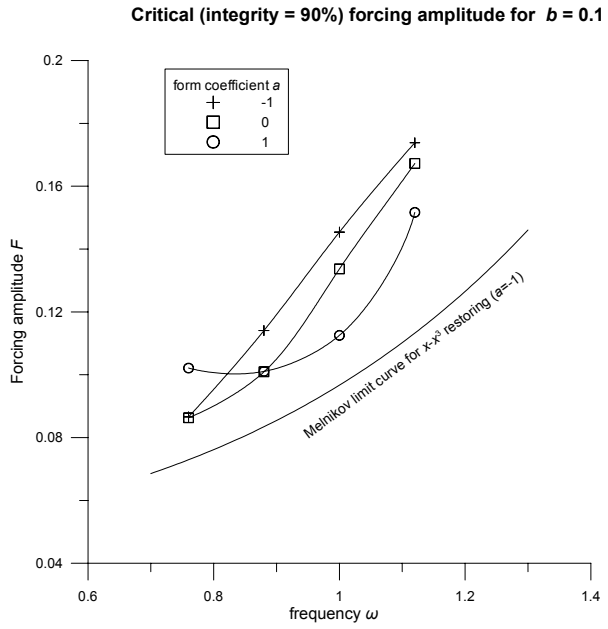

Fig. 1: 90% integrity curves for different types of restoring

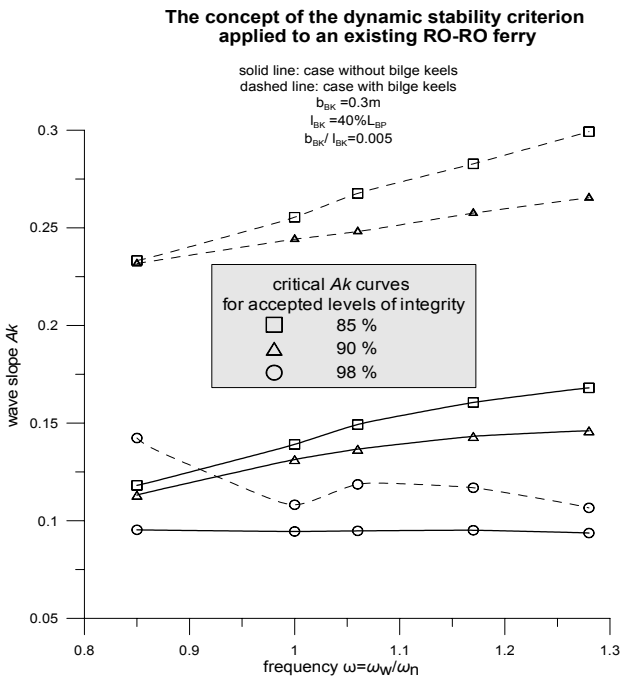

Fig. 2: The new criterion applied to an existing RO-RO.

5TH INTERNATIONAL WORKSHOP "STABILITY AND OPERATIONAL SAFETY OF SHIPS"
12-13 SEPTEMBER 2001, TRIESTE, ITALY

EXACT ANALYTICAL SOLUTIONS FOR ASYMMETRIC SURGING AND SURF-RIDING

K.J. Spyrou

Department of Naval Architecture and Marine Engineering
National Technical University of Athens
9 Iroon Polytechniou, Zographou, Athens 15773, Greece

Extended abstract

It is well-known that the surging behaviour of a ship in following waves of substantial steepness can become strongly nonlinear for a certain range of vessel speeds (normally for Froude numbers higher than 0.3). This nonlinear behaviour is manifested with a gradual change of the ship's response towards an asymmetric pattern of surging even if the considered wave is of a simple sinusoidal form. Typically, the ship spends more time on the crests and less on the troughs, a tendency which becomes more pronounced as the speed is increased further. Furthermore, unusual types of behaviour with a stationary nature and in competition with the periodic pattern arise, featuring a forced motion at a speed equal to the wave celerity and with the ship "locked" between two consecutive wave crests. These phenomena have already been studied on the basis of numerical models for a following as well as for a quartering sea environment and specific explanations of their dynamics have been produced[1]. A typical phase-plane plot of nonlinear surging is shown in Fig.1.

We have recently endeavoured to develop a purely analytical description for the surging behaviour, even for the strongly nonlinear range[2]. This would be very useful for design where closed-form expressions are always preferred. It would benefit also advanced investigations on phenomena such as broaching and loss of transverse stability.

The differential equation of surging motion has a strong nonlinearity in the stiffness term since the wave force is a sinusoidal function of position. There is also a weak nonlinearity in the damping (=difference between resistance and thrust). A general form for the equation of surge on a sinusoidal wave is,

$$\left(m - X_{\dot{u}}\right)\dot{u} + \left[R(u,c) - T(u,c,n)\right] + f\sin(kx) = 0 \qquad (1)$$

The velocity relatively to the wave is $\dot{x} = c - u$. With substitution of suitable polynomial expressions for the thrust and the resistance, eq. (1) becomes,

$$\left(m - X_{\dot{u}}\right)\ddot{x} + \left\{\left[3r_3 c^2 + 2(r_2 - \tau_0)c + r_1\right] - \tau_1 n\right\}\dot{x} + \left[3r_3 c + (r_2 - \tau_0)\right]\dot{x}^2 + r_3\dot{x}^3 + f\sin(kx) =$$
$$= \underbrace{\left(\tau_0 c^2 + \tau_1 c n + \tau_2 n^2\right)}_{T(c;n)} - \underbrace{\left\{r_1 c + r_2 c^2 + r_3 c^3\right\}}_{R(c)} \qquad (2)$$

a) *Surf-riding*:

This calculation is straightforward: If $-1 \le \dfrac{T(c;n) - R(c)}{f} \le 1$ then $-1 \le \sin kx \le 1$. Stationary solutions become possible (surf-riding), located at,

$$x = \frac{2\nu\pi}{k} + \frac{1}{k}\arcsin\left[\frac{T(c;n) - R(c)}{f}\right], \quad x = \frac{(2\nu+1)\pi}{k} - \frac{1}{k}\arcsin\left[\frac{T(c;n) - R(c)}{f}\right] \qquad (3)$$

b) *Asymmetric surging*:

Equation (1) is brought into the following form (4), after substituting the damping terms with an equivalent quadratic on the basis of a least-square fit,

$$(m - X_{\dot{u}})\ddot{x} + \gamma(c;n)\dot{x}|\dot{x}| + f\sin(kx) = T(c;n) - R(c) \tag{4}$$

For an overtaking wave (4) leads to the following expression for the orbits of the phase plane $(x, \dot{x})$,

$$\frac{dx}{dt} = \dot{x} = -\frac{1}{k}\sqrt{c_2 q e^{2pkx} + \frac{2q(\cos kx + 2p\sin kx)}{(1+4p^2)}} - \frac{r}{p} \tag{5}$$

The term $c_2 q e^{2pkx}$ represents the transient part of the solution and it vanishes gradually since $x \to -\infty$ (the ship is trailing behind the waves). Therefore the expression for the steady periodic motion is,

$$\frac{dx}{dt} = \dot{x} = -\frac{1}{k}\sqrt{\frac{2q(\cos kx + 2p\sin kx)}{(1+4p^2)}} - \frac{r}{p} \tag{6}$$

With suitable transformations it can be shown that (6) can be solved explicitly for *t*,

$$t = -\frac{\sqrt{m}}{a}\mathrm{F}\left(\frac{kx - \theta}{2}, m\right) \tag{7}$$

where F is the elliptic integral of the first kind, $\mathrm{F} = \int_0^{\varphi} \frac{1}{\sqrt{1 - m\cos^2 \vartheta}}\, d\vartheta$ with modulus $\sqrt{m}$. In Fig 2 is shown the relation between time and position which shows clearly the distortion from the linear pattern. With inversion of (7) we obtain further the following expression for *x* in terms of *t* (see also Fig. 3),

$$\cos(kx - \vartheta) = 1 - 2\,\mathrm{sn}^2\left(-\frac{a}{\sqrt{m}}t,\ \sqrt{m}\right) \tag{8}$$

When the ship operates away from the strongly nonlinear regime, the *rhs* of (8) tends to obtain the cyclic form $\cos(\omega_e t)$

c) *Condition for heteroclinic connection*

The heteroclinic connection leads to the disappearance of the periodic motion. This phenomenon is linked with broaching and it happens as soon as the unstable stationary solution near the crest falls on the periodic orbit.

Unstable stationary point:
$$\dot{x} = 0$$
$$x = \frac{(2\nu - 1)\pi}{k} - \frac{1}{k}\sin^{-1}\frac{T(c;n) - R(c)}{f} \tag{9}$$

The steady periodic orbit is given by eq. (6). Substitution of (9) into (6) yields the following expression of critical amplitude for the surge wave force,

$$f_{crit} = \frac{R(c;n) - T(n)}{2\gamma}\sqrt{k^2\left(m - X_{\dot{u}}\right)^2 - 4\gamma^2} \tag{10}$$

References

[1] K.J. Spyrou (1996) Dynamic instability in quartering seas: The behaviour of a ship during broaching, *Journal of Ship Research*, SNAME, USA, Vol. 40, No. 1, pp. 46-59.

[2] K.J. Spyrou (2000) On the parametric rolling of ships in a following sea under simultaneous nonlinear periodic surging. *Philosophical Transactions of the Royal Society of London*, A 358, pp. 1813-1834.

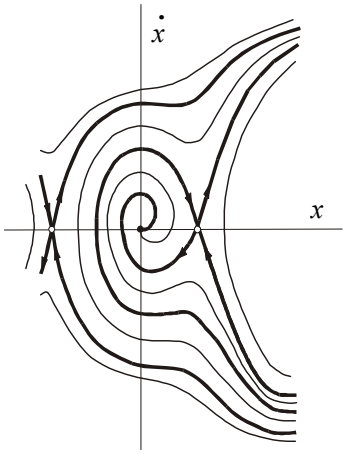

Fig. 1: Typical phase-plane orbits in the range of surf-riding.

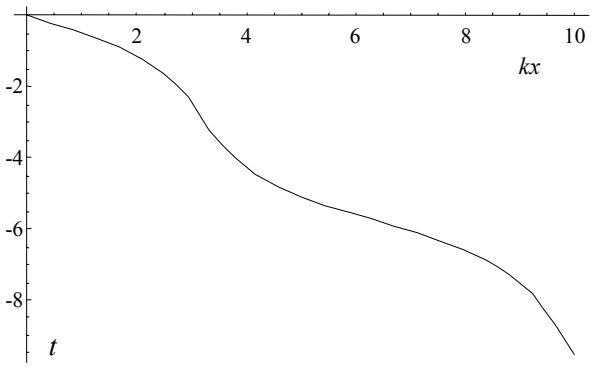

Fig. 2: The relation between time and position is distorted from the linear one in the range of asymmetric surging.

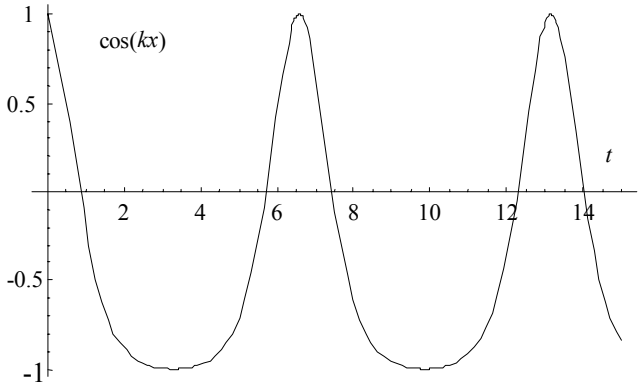

Fig. 3: Surge as described by eq. (8).

WEATHER CRITERION FOR INTACT STABILITY OF LARGE PASSENGER VESSELS

Alberto FRANCESCUTTO (*) & Andrea SERRA (**)

(*) Department of Naval Architecture, University of Trieste, Italy, e-mail: francesc@univ.trieste.it
(**) Cruise Ships Design Department, Fincantieri SpA, Trieste, Italy, e-mail: andrea.serra@fincantieri.it

SUMMARY

The application of intact stability Weather Criterion to the new large passenger ships leads to more stringent requirements than the application of current subdivision and stability rules for damage ships. A critical analysis of Weather Criterion in its hystorical development and in the present version has thus been conducted. In this paper, the calculation method of the rolling amplitude is examined with the aim of identifying weak points needing further studies and to propose some interim modification of existing procedure. It appears that the formulas or graphs used to compute the relevant quantities for the evaluation of ship safety on the base of Weather Criterion appear to overestimate roughly the environmental action. A proposal to correct the evaluation formula for the factor "r" is provided.

NOMENCLATURE

ϕ_0 heeling angle under the action of steady wind
ϕ_1 rolling amplitude
ϕ_2 limiting angle for area computation
lw_1 lever of steady wind
lw_2 lever of wind gust
d , T ship draught
B ship beam
C_B block coefficient
s wave steepness
X_1 factor expressing the roll damping dependence on B/T
X_2 factor expressing the roll damping dependence on C_B
k factor expressing the effect of bilge keels on roll damping
r effective wave slope coefficient
T_ϕ rolling period
OG=KG-d height of centre of gravity on waterline
KG height of centre of gravity on keel
GM initial metacentric height
N coefficient of quadratic roll damping
I' virtual moment of inertia of ship
Δ ship displacement
GZ righting arm
ϕ_{syn} peak roll amplitude

1. INTRODUCTION

In the present version of the Weather Criterion, the ability of the ship to withstand the combined effects of beam wind and rolling should be demonstrated, for each standard condition of loading, with reference to Fig. 1, as follows:

- the ship is subjected to a steady wind pressure acting perpendicular to the ship's centreline which results in a steady wind heeling lever lw_1;
- from the resultant angle of equilibrium ϕ_0, the ship is assumed to roll owing to wave action to an angle of roll ϕ_1 to windward. Attention should be paid to the effect of steady wind so that excessive resultant angles of heel are avoided;
- the ship is then subjected to a gust wind pressure which results in a gust wind heeling lever lw_2;
- under these circumstances, area b should be equal to or greater than area a;
- free surface effects should be accounted for in the standard conditions of loading.

The IMO Recommendation then specifies the methodology that *must* be used to calculate all the relevant quantities.

-

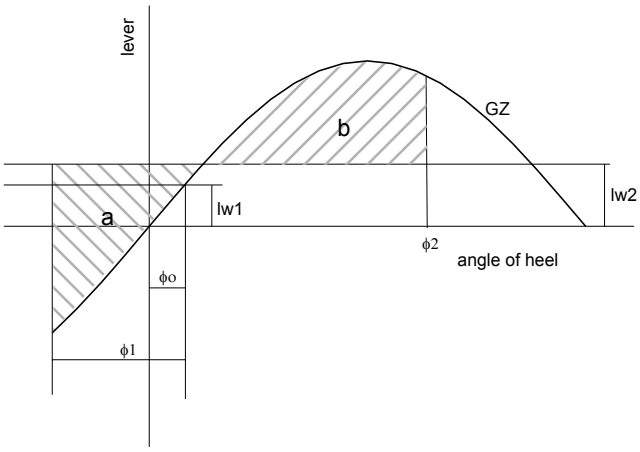

Fig. 1. Illustrating the Weather Criterion

The application of the IMO Weather Criterion (IMO Res. A.562) for intact stability, based on the effects of a severe wind and rolling, to modern large passenger vessels can result in requirements more stringent than those corresponding to the application of general intact stability criteria of intact stability code (IMO Res. A.167 as amended by Res. A.206 and successive) and of current damage stability rules (SOLAS'90). In Fig. 2 the GM limit curves of a large passenger ship are reported as an example. The fact that intact stability requirement in terms of GM (or KG) is more stringent than damage stability rules including both subdivision *and* stability is contradictory. On the other hand, SOLAS'90 is generally considered as a good safety rule, so that the problem is

really that of a better tuning of Weather Criterion to ships of the considered size.

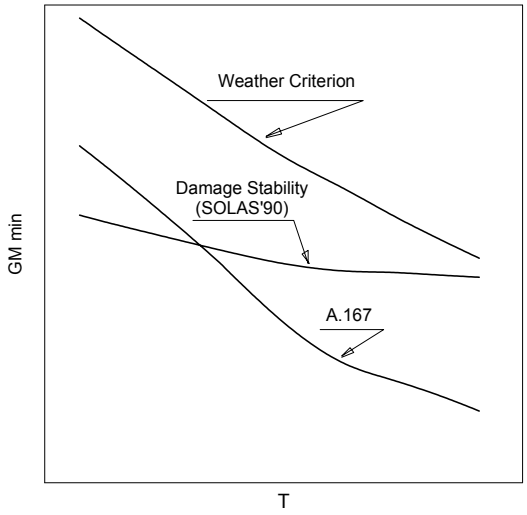

Fig. 2. GM Limit curves for a 77,000 GRT passenger ship with B/T=3.98÷4.27 and OG/T=0.9÷1.15. The even keel condition is indicated.

The matters related to the basic formulation of the weather criterion have thus been reviewed tracing back to the original documents [1]. They are connected with:

- mathematical modelling of roll motion equation. The analysis of large campaigns of experiments by means of powerful parameter identification techniques, applied to the entire roll resonance curve in regular beam waves, indicates that the effective wave slope coefficient can be overestimate especially for ships with OG/T greater than zero. At the same time, the influence of linear damping can be underestimated;
- the evaluation of roll period is based on a regression formula which is not reliable for modern ship forms. In this case, it can lead to an overestimation of the wave steepness.

Some actions to be taken to extend the weather criterion to modern ship forms are envisaged and at the same time it is suggested that appropriate experiments should be conducted for the evaluation of some of the characteristic quantities related to the weather criterion or the satisfaction of the criterion as a whole.

2. ANALYSIS OF WEATHER CRITERION PROCEDURE

The basic physical mechanisms on which the Weather Criterion is based are globally sound and represent pionieristic work done in this field by several researchers, mainly in Japan and Russia. The introduction of Weather Criterion as an additional stability requirement together with the Res. A.167 really improved the safety of navigation. Many issues contained in Weather Criterion however appear to be questionable in themselves and other when extending the range of applicability beyond the original limits. In the following we try to give a global view with some hint for improvement.

2.1 EVALUATION OF ROLL MOTION AMPLITUDE ϕ_1

The roll motion amplitude ϕ_1 in Weather Criterion is calculated through the expression:

$$\phi_1 = 109\, k\, X_1\, X_2 \sqrt{r\, s} \qquad (1)$$

The square root is a consequence of the (questionable) assumption of purely quadratic damping made following Bertin. The k and X_2 factors are not relevant to present discussion and can be found in tabular form whereas the factors r and X_1 are very important and will be discussed in detail.

The factor X1, expressing the effect of B/T ratio on roll damping is reported in Fig. 3.

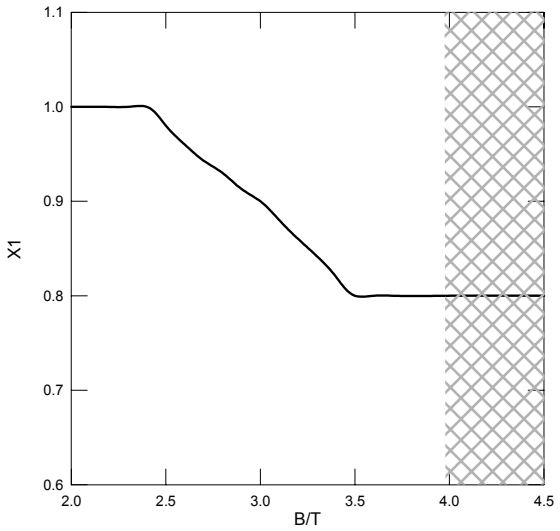

Fig. 3 Effect of B/d on roll damping factor X_1. The shaded area represents the values of B/T typical of modern large passenger ships.

As one can see, the region of interest for large passenger ships (dashed in the figure) is all outside the interval corresponding to the original sample of ships used to evaluate the effect of B/T on damping and the last available value of X_1 is thus used. Due to the high slope of the curve, the assumed extrapolation entails a huge underestimation of damping. Further work in this field is needed, based on roll damping measurements or calculations.

The following choices made-up formula 1:

- 30% reduction of ϕ_{syn} due to the irregular waves;

- $r = 0.73 + 0.6\frac{\overline{OG}}{d}$ (2)

Eq. 2 worths also particular attention, especially for high values of OG/d as it is usual both in very small and very large passenger ships. A research conducted on a sample of very small ships indicated overestimates the wave action by several times. A research conducted on a specimen of conventional ships confirms this overestimate by an average factor 1.5 (Fig. 4). The values originally used to obtain Eq. 2 were in the range -0.4<OG/d<0.6.

It is clear at this point that the influence of the two factors r (from Fig. 4) and X_1 (from Fig. 3) can contribute to a reduction of ϕ_1 for large passenger ships. An additional effect is conncted with the effective wave slope s.

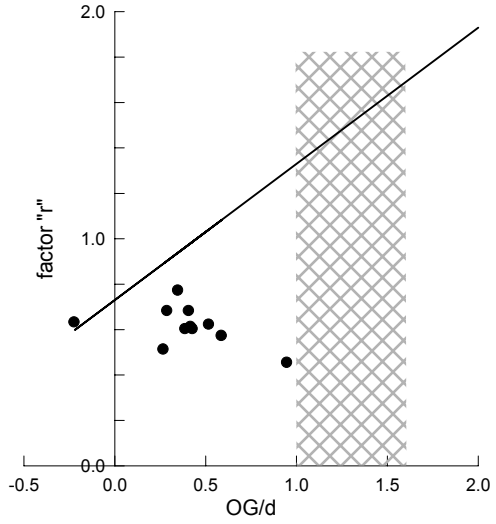

Fig. 4. Effective wave slope coefficient as resulting from Eq. 2 and from experiments. The dashed area represents the interval of values typical of modern large passenger ships. The experimental points are taken from [2,7].

2.2 EVALUATION OF WAVE STEEPNESS

This is based on the theory of Sverdrup-Munk, which was criticised in recent time. On the other hand, the proposers of Japanese original rule assumed a lower limit of 0.038 which is sensibly higher than the tendency limit, as is evident from Fig. 5. For comparison, the wave heights assumed in alternative formulations of height dependence on period (through wavelenght) for "significantly large" waves are presented [8]

In addition the effect of the roll natural period computation is to be considered. The ships we are taking in consideration have indeed quite large rolling periods, over 20 s. The regression formula assumed in Weather Criterion appears not suitable for the evaluation of T_ϕ, since it conducts to an underestimate with the effect of moving the roll peak towards the peak of energy spectra.

3. CONCLUSIONS

From the above presentation we can draw the conclusions that for large passenger ships several formulas or graphs to compute the relevant quantities for the evaluation of ship safety on the base of Weather Criterion appear to overestimate roughly the environmental action

- To coordinate actions aimed to provide new knowledge where this is laking and a tuning of some expressions;

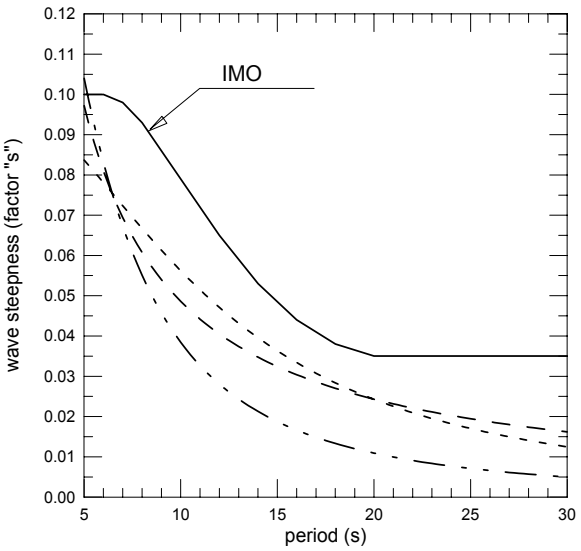

Fig. 5. Wave steepness as a function of roll period T_ϕ assumed in Weather Criterion (solid curve). The modern large passenger ships fall in the assumed flat zone. The dashed curves represent "significantly high waves" assumed in several alternative formulations [8]

- To introduce the possibility to provide direct evidence of fulfillment of the Weather Criterion, or at least to evaluate some relevant quantities connected with, through ad hoc tests or reliable computations;

- To promote a standardisation of testing methodologies provided by some relevant body (for example the ITTC Specialist Committee for Extreme Ship Motions and Capsizing), operating in strict connection/on behalf of IMO;

- As an interim action, to modify the expression (2) given for the computation of the factor r for large passenger ships as follows:

$$\begin{cases} r = 0.73 + 0.6\dfrac{\overline{OG}}{d} \\ \text{but not greater than 1 (one)} \end{cases}$$

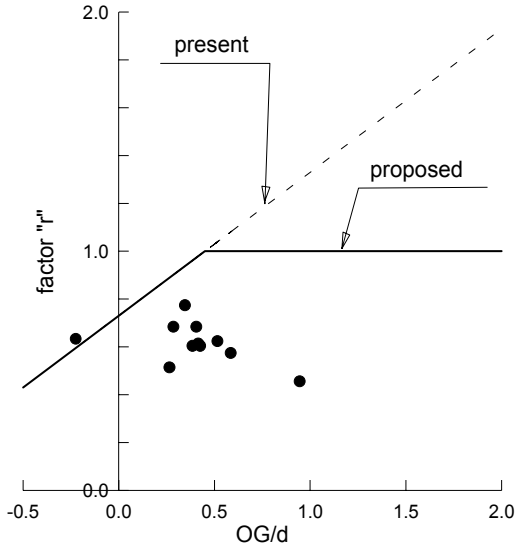

Fig. 6. Proposed dependence of effective wave slope coefficient on center of gravity height on waterline.

4. REFERENCES

1. Francescutto, A., Serra, A., Scarpa, S., "A Critical Analysis of Weather Criterion for Intact Stability of Large Passenger Vessels", Paper n. OFT-1282, Proc. 20th International Conference on Offshore Mechanics and Arctic Engineering - OMAE'2001, Rio de Janeiro, 3-8 June 2001.
2. Contento, G., Francescutto, A., Piciullo, M., "On the Effectiveness of Constant Coefficients Roll Motion Equation", Ocean Engineering, Vol. 23, 1996, pp. 597-618.
3. Contento, G., Francescutto, A., "Intact Ship Stability in Beam Seas: Mathematical Modelling of Large Amplitude Motions", Proc. 3rd Int. Workshop on Theoretical Advances in Ship Stability and Practical Impact, Henronissos Crete, October 1997.
4. Francescutto, A., Contento, G., Biot, M., Schiffrer, L., Caprino, G., "The Effect of the Excitation Modelling in the Parameter Estimation of Nonlinear Rolling", Proc. 8th Int. Offshore and Polar Eng. Conf - ISOPE'98, Montreal, 1998, J. S. Chung Ed., Vol. 3, pp. 490-498.
5. Francescutto, A., Contento, G., "The Modeling of the Excitation of Large Amplitude Rolling in Beam Waves", Proc. 4th Int. Ship Stability Workshop, St.Johns, Newfoundland, September 1998.
6. Francescutto, A., "On the Coupling of Roll Motion with Other Motions in Beam Waves", To appear on Proceedings 14th International Conference on Hydrodynamics in Ship Design - HYDRONAV'2001, Szczecin, 27-29 September 2001.
7. Iskandar, B. H., Umeda, N., "Some Examination of Capsizing Probability Calculation for an Indoneasian RoRo Passenger Ship in Waves", to appear on Journal KSNAJ.
8. Vassalos, D., "A Critical Look into the Development of Ship Stability Criteria Based on Work/Energy Balance", Trans. RINA, Vol. 128, 1986, pp. 217-234.

Some discussions about the probability of capsize Of a Ship in Random beam waves

Xianglu Huang Xinying Zhu
Shanghai Jiao Tong University

Abstract

This paper deal with the problem of probability of a ship capsize in random beam waves. By using the method of nonlinear oscillation together with the theory of stochastic differential equation, some properties of the probability distribution of ship rolling were investigated. Several methods about this problem published recently were commented. Some concluding remarks were presented.

Introduction

The problem of ship capsize on random waves is a complicated problem ,which is hardly to be solved due to the nonlinear property of the problem and the randomness of the motion. Because of the capsize of a ship on waves always link to the large amplitude rolling, so the large amplitude nonlinear rolling has to be investigated. In such case, the motion equation is a **Duffing** equation with soft spring. Ordinarily we adopt a polynomial expression to fit the stability curve of a ship. Due to its asymmetry property, only the odd order terms are kept in the expression. Also considering that the stability will vanish after the rolling angle reached several point, the sign of the terms should fulfil such requirement.

The motion equation can be simply expressed as

$$\ddot{\theta} + \mathbf{2}\xi\omega_{\mathbf{0}}\dot{\theta} + \omega_{\mathbf{0}}^{\mathbf{2}}\theta(\mathbf{1} + \varepsilon\theta^{\mathbf{2}}) = \gamma N(t) \tag{1}$$

in which

θ Ship roll angle

$\mathbf{2}\xi\omega_{\mathbf{0}}$ Linear damping coefficient

$\omega_{\mathbf{0}}$ Natural frequency of roll

ε The coefficient of third order term of stability curve

$N(t) = \dfrac{dW(t)}{dt}$ white noise $W(t)$ Wiener Function

Actually, the wave excitation in(1)should be a time trace with color spectra. But it require large amount of numerical effort to handle such color excitation. Because of we only want to survey qualitatively the effect of randomness on the probability of large amplitude rolling. It should be appropriate to replace the color excitation by the white noise $N(t)$. Converted the original equation into state equations, we obtained the following stochastic differential equations

$$\begin{cases} \dot{x}_1 = x_2 \\ \dot{x}_2 = 2\xi\omega_0 x_2 - \omega_0^2 x_1(1 + \varepsilon x_1^2) + \gamma N(t) \end{cases} \tag{2}$$

in which

$$x_1 = \theta$$

$$x_2 = \dot{\theta}$$

This equation can simply written in the form of vector Ito's stochastic equation

$$d\vec{X} = m(\vec{X},t)dt + \vec{Q}(\vec{X},t)dW(t)$$

in which the drift coefficient is

$$m[\vec{X},t] = \begin{bmatrix} m_1[\vec{X}(t)] \\ m_2[\vec{X}(t)] \end{bmatrix} = \begin{bmatrix} x_2 \\ -2\xi\omega_0 x_2 - \omega_0^2 x_1(1+\varepsilon x_1^2) \end{bmatrix} \tag{3}$$

while the matrix of diffusion coefficients is

$$Q[\vec{X},t] = \begin{bmatrix} Q_1[\vec{X}(t)] \\ Q_2[\vec{X}(t)] \end{bmatrix} = \begin{bmatrix} 0 \\ \gamma \end{bmatrix} \tag{4}$$

Before we start to deal with this stochastic equations, we survey the property of the **Hamilton** system relate to this equation. This system actually is the equation ignore the damping and external excitation. The solution of which is the free oscillation without damping.

$$x_0(t) = \sqrt{\frac{1}{\alpha}}\tanh(\frac{\tau}{\sqrt{2}}) \tag{5}$$

$$y_0^{\pm}(t) = \sqrt{\frac{1}{2\alpha}}\sec h^2(\frac{\tau}{\sqrt{2}}) = \pm(\sqrt{\frac{1}{2\alpha}} - \sqrt{\frac{\alpha}{2}}x_0^2) \tag{6}$$

in which $x_0 = \theta$, $y_0 = \dot{\theta}$, $\alpha = \frac{\varepsilon}{\omega_0^2}$, $\tau = \omega_0 t$, '+' denote the upper half branch of the orbit, while '-' denote the lower part. The different orbit corresponds to the initial rolling angle.

The corresponding phase portrait is shown in following picture.

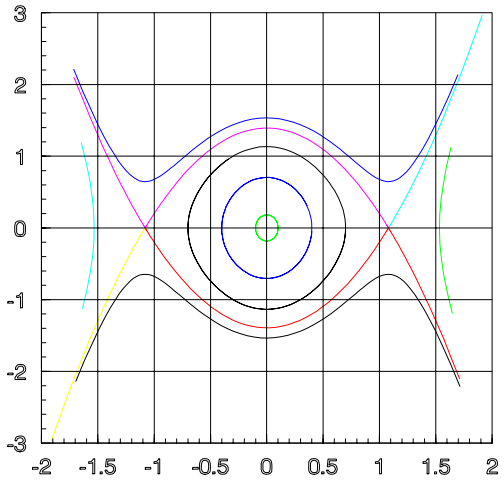

Fig 1. Phase portrait

It is shown on such phase portrait that when the motion reaches the point of the stability vanishing angle， the close orbit will begin to broken. The phase trace will go away to another attractor. So the phase trace which pass through the point corresponds to the stability vanishing angle formed the

boundary between stability and instability flow. **Thompson** has suggested the idea of safe basin in which he linked the initial condition with the happening of the capsize. He has found that if there is some external excitation which result in the happening of capsize, the form of safe basin will have the property of fractal, and the area which enclosed by the boundary of stability will be reduced. It is called the erosion of safe basin. This is a very good idea which can be used to survey the possibility of capsize. But, the difficulty involved is large amount of computation effort . Another method is proposed by **Troesch** et,al . They suggested to used a quantity called phase flux, which is determined by the **Melnikov** function to quantify the area exported outside from the safe basin. Although these two method have made this very complicated problem clear, but they all have the short come as to solve the problem quantitatively. The reason is the method involved in these two method are not statistical. The method of phase flux partly considered the input to have some kind of spectrum. But it is plausible that since capsize is a phenomenen which linked to the large amplitude rolling, how can it be calculated only by the integral of input on the hetro-clinic orbit in a linear manner. For this reason we start to investigate the probability behavior of the rolling motion in time domain, and try to find the relationship between these probability behavior and capsize of a ship.

Determination of PDF of ship rolling on random wave by solving FKP equations

It is obvious that to have the information of ship large amplitude rolling on a random wave train,

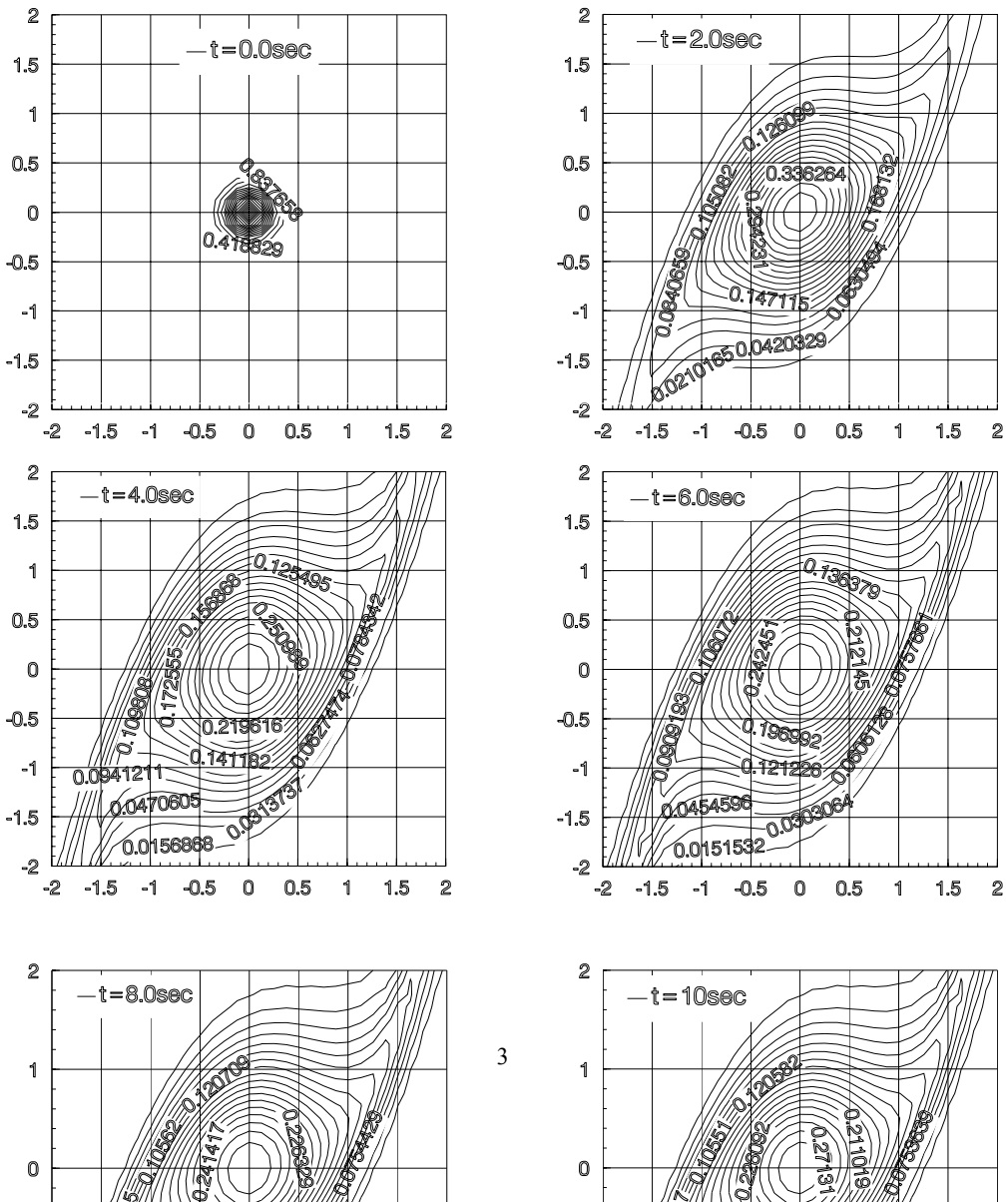

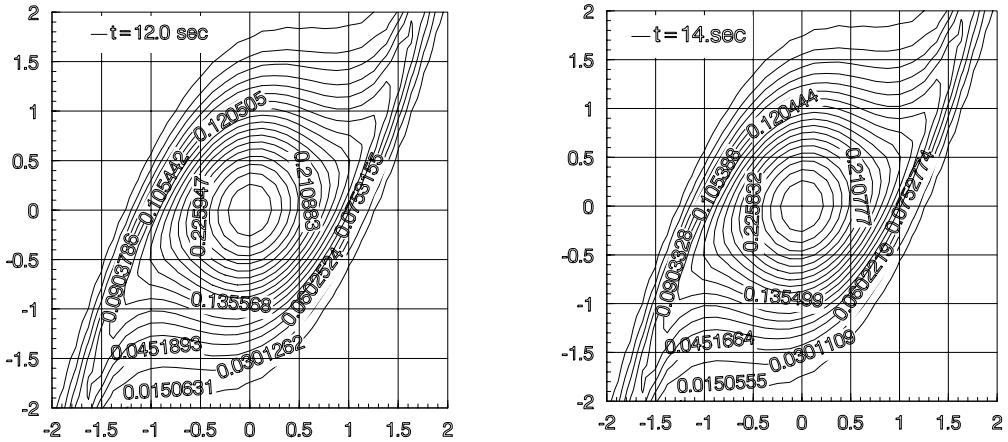

Fig2 The variation of the PDF with time

It should be noted that the PDF is largely depend on the sign of its higher order restoring term. Fig 5 shows the PDF with the same parameter combination as in Fig2 except the sign of third order restoring term is positive.

the appropriate way is to solve the problem in time domain. That is to solve the corresponding Ito's (stochastic differential equations)SDE, which turns to find the solution of corresponding FKP equations under several given initial conditions. For our purpose the SDE has the form of (2). It's FPK equation has the form as

$$\frac{\partial p}{\partial t} = -\frac{\partial m_1 p}{\partial x_1} - \frac{\partial m_2 p}{\partial x_2} + \frac{\partial^2 g_{22} p}{\partial x_2^2} \tag{7}$$

in which

$p(x_1, x_2; t)$ is the probability density distribution function(PDF)

$$G(\vec{X}) = (g_{i,j}(\vec{X})) = \vec{Q}(\vec{X})\vec{Q}(\vec{X})^T = \begin{bmatrix} \mathbf{0} & \mathbf{0} \\ \mathbf{0} & \gamma^2 \end{bmatrix} \tag{8}$$

This two dimensional second order partial equation was solved by a numerical method using Finite Difference Scheme in time domain. The detail of such method can refer to another paper. The calculated result for a combination of parameters as: Ship displacement 480 ton, mass coefficient 1089 ton m^2, damping coefficient 100 ton m and restoring 0.7m with cubic coefficient –0.7. The level of excitation white noise is 0.8 are shown in fig 2

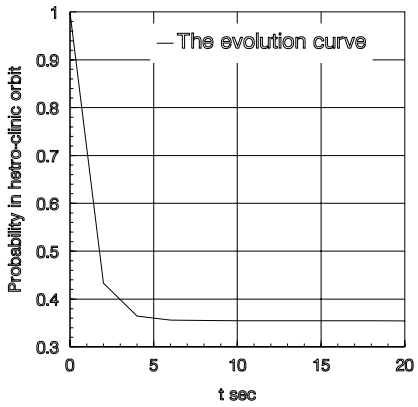

Fig3 The variation of probability inside hetro-clinic orbit with time

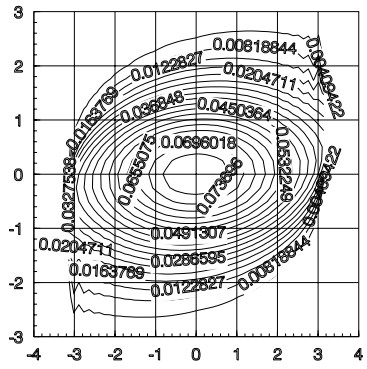

Fig 4 The PDF of a linear system

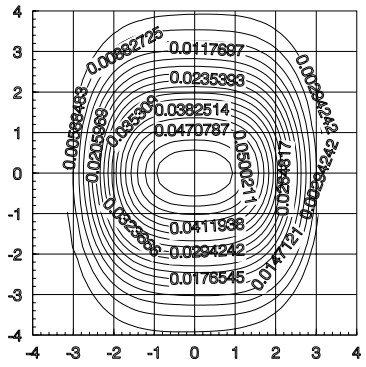

Fig 5 The PDF of a system with positive third order term

From the figs it can be seen that the variation of the PDF of the rolling process in time is diffuse from the center, at which a δ function is located. But is shows that the PDF reaches the stationary

status quickly. Fig 3 is the variation cumulated probability enclosed by the hetro-clinic orbit with the time. It showed that at first the value reduce rapidly and then become slow after 2-3 second. Although the rate of reduction become insignificant after 10 seconds, it still has some small value.

The condition of capsize of a ship on random waves

Although the solution of the FPK equations can be used to show the variation of the PDF with time, it is no use for the determination of the capsize of a ship in a random sea. In order to determine the capsize, we have to at first look further into the process of the happening of the capsize of a ship. The capsize of a ship implies it will goes away from its up righting position to another balance position as 180 degree, in other words turn to up side down. It is known from the first paragraph that for a Hamiltonian system with the soft spring like the ship rolling. The phase portrait has the form of close orbit before it reaches the stability vanishing angle or saddle points. The orbit passing through the point corresponds to the stability vanishing angle is the boundary between the solution of stability flow and instability flow. The instability flow outside the boundary broken into four branches and all goes out to the next attractor. This orbit is called hetroclininc orbit It is clear that in a non-external excitation and no damping oscillation situation, the ship will capsize if it's rolling amplitude large over the stability vanishing angle. But when there is excitation and damping, things will become complicated. In order to make sure if the hetroclinic orbit is stability or instability in forced oscillation case, one can use the **Melnikov** function technique, which is defined as follow:

If there is a system

$$\dot{\boldsymbol{x}} = \boldsymbol{f}_0(\boldsymbol{x}) + \varepsilon \boldsymbol{f}_1(\boldsymbol{x}, t)$$

Then the **Melnikov** function is defined as

$$\boldsymbol{M}(t) = -\int_{-\infty}^{\infty} \{\boldsymbol{f}_0[\boldsymbol{x}_0(\tau)], \boldsymbol{f}_1[\boldsymbol{x}_0(\tau), \tau - t]\} \times \exp[-\int_0^{\tau} \boldsymbol{T}_r \frac{\partial \boldsymbol{f}_0}{\partial \mathrm{x}}(\boldsymbol{x}_0(\boldsymbol{u}))\boldsymbol{du}]\boldsymbol{d}\tau \tag{9}$$

in which

$\boldsymbol{f}_0$ External excitation

$\boldsymbol{x}_0$ The offset of stability/instability flow

$\boldsymbol{T}_r \frac{\partial \boldsymbol{f}_0}{\partial \boldsymbol{x}}$ is the trace of $\frac{\partial \boldsymbol{f}_0}{\partial \boldsymbol{x}}$ matrix

$\{,\}$ Poisson bracket defined as $\{a, b\} = \{a_1 b_2 - a_2 b_1\}$, $a = \{\begin{matrix} a_1 \\ a_2 \end{matrix}\}$, $b = \{\begin{matrix} b_1 \\ b_2 \end{matrix}\}$

Melnikov function measures the distance between the stability and instability flow of the same sandal point. For a system with damping but without external excitation, its **Melnikov** function is a negative constant. Under the action of oscillatory external excitation, the value of **Melnikov** function will oscillate around its mean value ,the amplitude of which is proportional to the external excitation. When the intensity of the external excitation over several threshold, the **Melnikov** function will have zero point. The stability flow will across to the instability flow. The boundary of safe basin will have the fractal character. So the zero value of **Melnikov** function equivalent to the condition of the safe basin erosion.

The **Melnikov** function of a ship without bias can be expressed explicitly as (Jiang 1996)

$$M_{\delta}(t_0, \theta_0) = \widetilde{M}_{\delta}(t_0, \theta_0) - \overline{M}_{\delta} \tag{10}$$

in which

$$\overline{M}_0 = \frac{2\sqrt{2}}{3\alpha}\delta_1 + \frac{8}{15}\left(\frac{1}{\sqrt{\alpha}}\right)^3 \delta_2 \tag{11}$$

$$\widetilde{M}_0(t_0,\theta_0)=\sqrt{\frac{2}{\alpha}}\gamma\pi\Omega\frac{\cos(\Omega t_0+\theta_0+\psi)}{\sinh\left(\frac{\Omega\pi}{\sqrt{2}}\right)} \tag{12}$$

$$\delta_1=\frac{B_{44}\omega_n}{C_1\Delta}\quad \delta_2=\frac{B_{44q}}{I_{44}+A_{44}}\quad \alpha=\frac{-C_3}{C_1}\quad \omega_n=\sqrt{\frac{C_1\Delta}{I_{44}+A_{44}}}\quad \Omega=\frac{\omega}{\omega_n}$$

$$\varepsilon\gamma=HF_{roll}/C_1\Delta$$

$\overline{M}_\delta$ and $\widetilde{M}_\delta(t_0,\theta_0)$ are the average part and time varied part of **Melnikov** function. Then, the condition of the happening of safe basin should be

$$\frac{2\sqrt{2}}{3\alpha}\delta_1+\frac{8}{15}\left(\frac{1}{\sqrt{\alpha}}\right)^3\delta_2=\frac{\sqrt{\frac{2}{\alpha}}\gamma\pi\Omega}{\sinh\left(\frac{\Omega\pi}{\sqrt{2}}\right)} \tag{13}$$

But, in real sea the wave are random. The above expression is not available. In order to survey the effect of random waves on the ship safe basin. We consider that the random waves can be modeled as superposition of a series of regular waves, and at first investigate the effect of a wave train formed by two different sinusoidal waves $\zeta(t)=a_1\cos\omega_1 t+a_2\cos\omega_2 t$ on the safe basin of ship rolling motion.

The zero point of **Melnikov** function of such a wave group is as follows

$$\frac{2\sqrt{2}}{3\alpha}\delta_1+\frac{8}{15}\left(\frac{1}{\sqrt{\alpha}}\right)^3\delta_2=\sqrt{\frac{2}{\alpha}}H\pi\left(\frac{F_{roll1}\Omega_1}{\sinh\left(\frac{\Omega_1\pi}{\sqrt{2}}\right)}+\frac{F_{roll2}\Omega_2}{\sinh\left(\frac{\Omega_2\pi}{\sqrt{2}}\right)}\right) \tag{14}$$

From this expression, it seems the capsize is unlikely to happen in this two regular wave combination case, which implies that the randomness of the wave will reduce the possibility of the capsize.

For a ship rolling on a random waves, the determination of its **Melnikov** function is differ from the determinate cases in two aspects. First, the motion of a ship is random, so the motion will be random too, the variables of motion should attach with a probability and the **Melnikov** function will be a statistical average value. We define that it has the form as

$$\overline{M}_0(t)=\delta_1\int_{-\infty}^{\infty}\int_{y_h^- -\delta y_h^-}^{y_h^- +\delta y_h^-}\int_{x_h^- -\delta x_h^-}^{x_h^- +\delta x_h^-}y_h^2(t)p(x,y,|x',y')dx'dy'dt+\delta_1\int_{-\infty}^{\infty}\int_{y_h^+ -\delta y_h^+}^{y_h^+ +\delta y_h^+}\int_{x_h^+ -\delta x_h^+}^{x_h^+ +\delta x_h^+}y_h^2(t)p(x,y,|x',y')dx'dy'dt$$

$$+\delta_2\int_{-\infty}^{\infty}\int_{y_h^- -\delta y_h^-}^{y_h^- +\delta y_h^-}\int_{x_h^- -\delta x_h^-}^{x_h^- +\delta x_h^-}y_h^2(t)|y_h(t)|p(x,y,|x',y')dx'dy'dt$$

$$+\delta_2\int_{-\infty}^{\infty}\int_{y_h^+ -\delta y_h^+}^{y_h^+ +\delta y_h^+}\int_{x_h^+ -\delta x_h^+}^{x_h^+ +\delta x_h^+}y_h^2(t)|y_h(t)|p(x,y,|x',y')dx'dy'dt \tag{15}$$

$$\widetilde{M}_\delta(t)=\int_{-\infty}^{\infty}\int_{y_h^+ -\delta y_h^+}^{y_h^+ +\delta y_h^+}\int_{x_h^+ -\delta x_h^+}^{x_h^+ +\delta x_h^+}y_h(t)\int_{-\infty}^{\infty}\int_{-\infty}^{\infty}\varsigma(t+t')p(x,y,\varsigma,\dot{\varsigma}|x',y',\varsigma',\dot{\varsigma}')dx'dy'd\varsigma'd\dot{\varsigma}'dt \tag{16}$$

It is known that the **Melnikov** function is the distance between the stability flow and instability flow of the disturbed system. The zero value of **Melnikov** function means the hetroclinic orbit is the stability boundary. The hetroclinic orbit will be stability if

$$\widetilde{M}_{\delta}(t) \le \overline{M}_{0}(t)$$

otherwise it is in-stability. Obviously, this condition determines the erosion of safe basin. These two quantities $\widetilde{M}_{\delta}(t)$ and $\overline{M}_{0}(t)$ are depending on the level of external excitation and are function of time **Troesch** has used the method of **Melnikov** function to calculate the so called phase flux.

By using(13)(14)we have for the ship with the combination of parameters as in section 1.calculate $\widetilde{M}_{\delta}(t)$ 、 $\overline{M}_{0}(t)$ also the cumulated probability enclosed by the hetroclinic orbit was calculated by integrating the PDF inside the hetroclinic orbit. The intensity of the external excitation is from 0.2 to 0.8. The PDF of each case together with the hetroclinic orbit were shown in the following graphics.

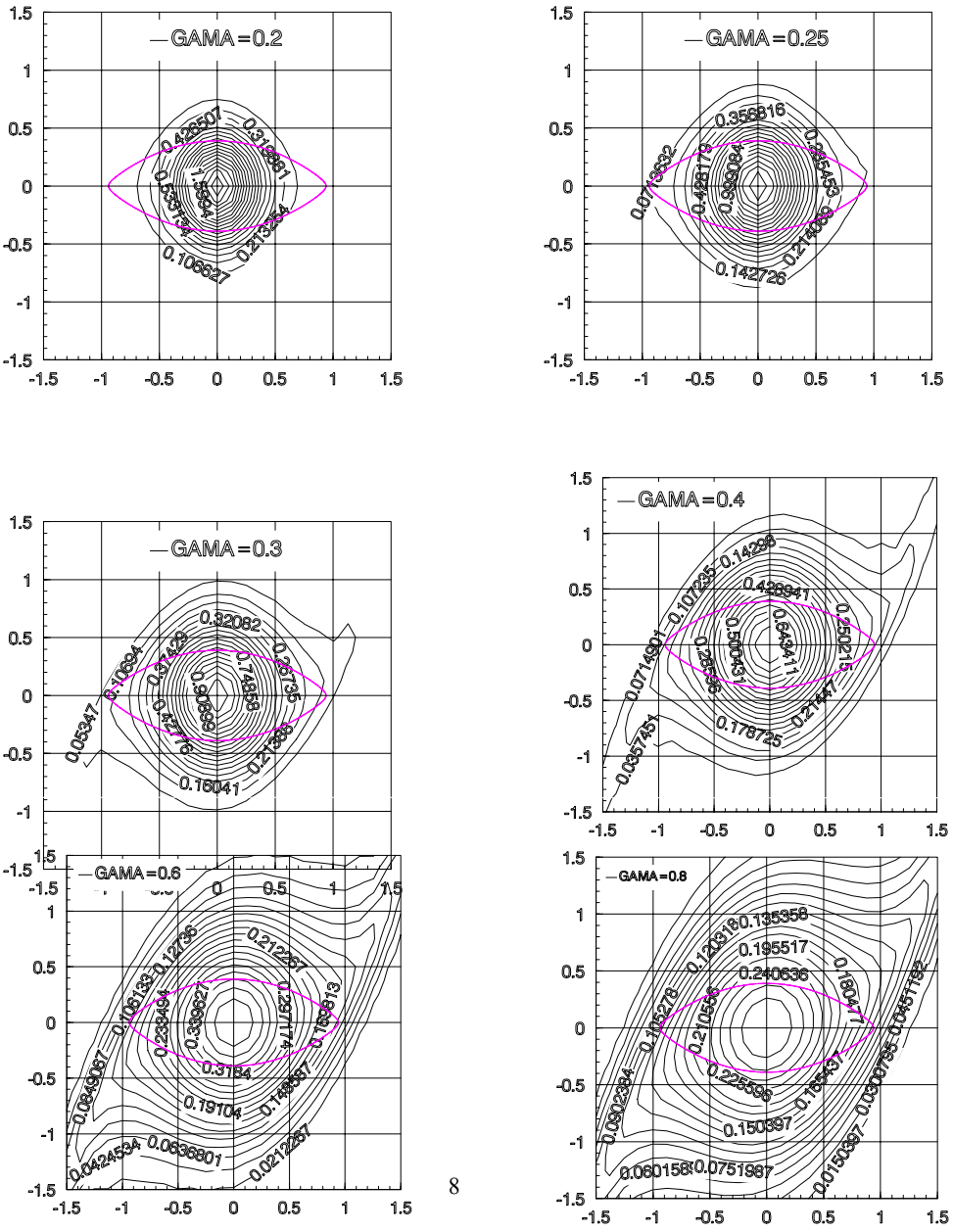

Fig6 The PDF of varies external excitation level

The calculated results of these series of excitation level are included in the following table.

Calculated **Melnikov** function and probability inside the hetroclinic orbit

Level	0.8	0.6	0.4	0.3	0.25	0.2
$\overline{M}_0$	0.3962453	0.4972652	0.6504055	0.7308647	0.7482907	0.6842267
$\widetilde{M}_0$	0.4837243	0.5257167	0.5614390	0.5463681	0.5106571	0.4176435
$\overline{p}$	0.3544042	0.4455447	0.5999293	0.7179332	0.7974694	0.8886672
Status	instability	Instability	stability	stability	stability	Stability

Some discussions

There are some remarks which was illuminated from the above discussions.

At first, we can see that the PDF of the ship rolling has reflected some motion characteristics which may link to the ship capsize. The difference in the appearance between Fig 4.5 and Fig3, show that the form of the stability curves has very strong influence on the probability property of rolling motion especially in large amplitude range. But, it also shows that only PDF itself, can not be used to identify the happening of capsize, and its probability.

The happening of capsize of a ship on a wave train is the transition of ship from its upright position (zero position) to another balance position (180deg), or in other words up side down. In the language of nonlinear mechanics, It means from one attractor goes to another. While such transition is passing through the saddle point, or the stability vanishing angle. This is very important to investigation the role of such stability vanishing angle, since we need in the determination of the happening of ship capsize, the condition at which capsize will happen. Not like in another first passage problem, the condition of capsize is defined by the motion equation itself. In the phase portrait of the corresponding Hamilitonian system, there is a close orbit passing through the saddle point, which is the boundary between the stability flow and instability flow, which is clearly a threshold of capsize in non-external cases. But for a system with external excitation to determine the stability boundary is very complicated. Nevertheless, the hetroclinic orbit is still an important role to be used in the capsize prediction. To judge if this orbit still can be used as a threshold in forced oscillation case , the **Melnikov** function has to be used. The stability of the hetroclinic orbit can be judged from the sign of the **Melnikov** function. It was indicated in the table that the stability character of the orbit is depends on the excitation level. In low excitation intensity, the orbit is stable. Only when γ is over the level 0.6, the boundary become unstable.

Another importance feature is the probability inside the hetroclinic orbit. Calculation shows that the probability will become less and less when the excitation level increase. It means the motion at first remain in the orbit, then will escape from the orbit as the excitation become intense. So, it is clear for the capsize there are two conditions which should be full filled. First the oscillation much reach the orbit then the orbit become unstable. These two conditions all depend on the excitation

level, but in principle there are not the same. We have to consider them separately in determine the condition of capsize.

Reference

1. Jiang, C., Troesch, A.W., & Shaw, S.W. 1996, Highly Nonlinear Rolling Motion of Biased Ships in Random Beam Seas, *Journal of Ship Research*, Vol.40, No.2, pp. 125-135
2. Naess, A. & Johnsen, J.M. 1993, Response Statistics of Nonlinear, Compliant Offshore Structures by the Path Integral Solution Method, *Probabilistic Engineering Mechanics* 8, pp.91-106
3. Rainey, R.C.T. & Thompson, J.M.T 1991, The Transient Capsize Diagram - A New Method of Quantifying Stability in Waves. *Journal of Ship Research*, Vol.35, No.1, pp. 58-62
4. Dong Sheng & Xianglu Huang 2000, The study of lasting time before capsize of a ship under irregular wave excitation Proceedings of 7th International Conference on Stability of Ship and Ocean Vehicles Feb.7-11 2000 Lanceston Tasmania Australia
5. Dong Sheng & Xianglu Huang 1998 Ship's Capsize under Irregular Wave Excitation, 2nd Conference for New Ship & Marine Technology into the 21st Century, Hong Kong,

Analysis of direct and parametric excitation with the Melnikov method and the technique of basin erosion.

Y-M Scolan, ESIM, 13451 Marseille cedex 20, France, scolan@esim.fr

Solutions of nonlinear Mathieu equations are analyzed through two methods: Melnikov method and the technique of basin erosion. A differential equation is formulated for a single degree of freedom. The coupling with another degree of freedom appears parametrically. The way to formulate the equation is similar to the way exposed in Thompson *et al.* (1992). Concerning the rolling motion of ships these circumstances occur when the influence of the wave slope on the restoring can be taken into account.

Here the Melnikov function is calculated and analyzed. Then the space of parameters can be separated into "safe" and "unsafe" areas. The obtained results are compared to optimized numerical direct simulations. The Interpolated Cell Mapping is used (see Tongue and Gu 1988).

As an application the following differential equation is analyzed:

$$\ddot{x} + \beta(\dot{x}) + x(1-x)\Big[1 + G\cos(\omega t + \psi)\Big] = F\sin\omega t \qquad (1)$$

where G and F are the amplitudes of the direct and parametric forcing excitations linked by $F = G\omega^2$. The quantity ω is the ratio of the wave frequency to the natural frequency of the ship (linear) rolling motion. The erosion of the basin of attraction is described in the space of parameters (F,ω). The figure below shows a typical "Dover cliff" limited by a plain line predicted by the Melnikov method. The figure on the right is a zoom for small values of (F,ω).

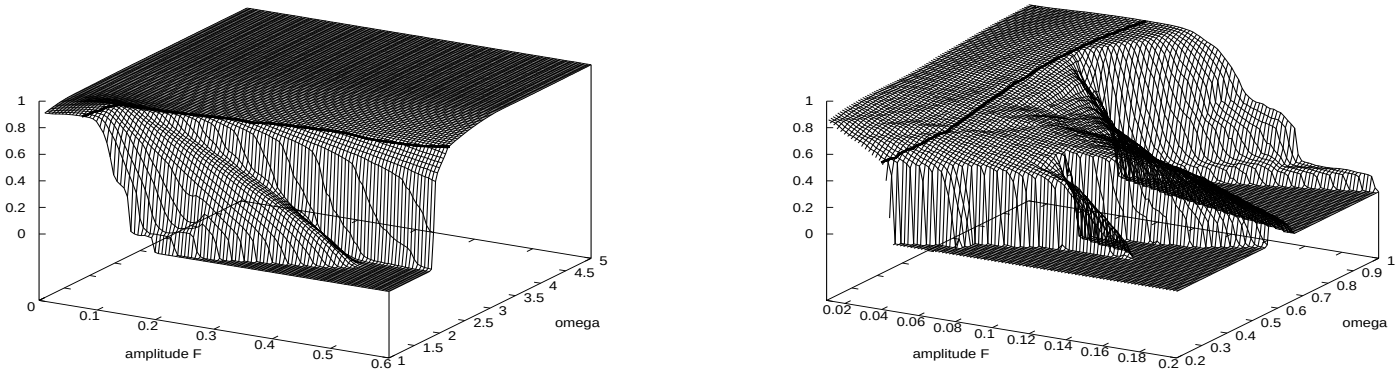

Thompson J.M.T., Rainey R.C.T. & Soliman M.S., 1992, "Mechanics of ship capsize under direct and parametric wave excitation.", Phil. Trans. R. Soc. Lond. A 338, pp 471-490.

Tongue B.H. & Gu K., 1988, "A higher order method of interpolated cell mapping.", J. of Sound and Vibration, 125(1), pp 169–179.

SOME REMARKS ON THE EXCITATION THRESHOLD OF PARAMETRIC ROLLING IN NON-LINEAR MODELLING

Alberto Francescutto[1] & Daniele Dessi[2]

[1]Dept. Naval Architecture, Ocean and Environmental Engineering
University of Trieste, Italy

[2] INSEAN, Italian Ship Model Basin
Roma, Italy

INTRODUCTION I

It is known that the parametric excited rolling in following seas can lead to dramatic roll amplitudes and eventually capsizing.
On the other hand, the parametric rolling in head waves is a less studied phenomenon:
in this case, relative ship velocity is high and consequently the roll damping increases for the effect of forward speed.

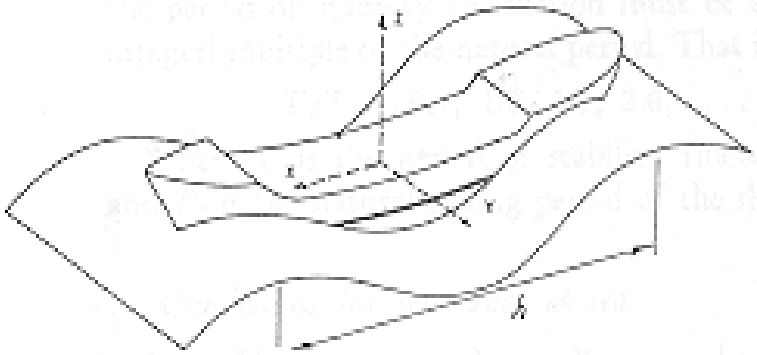

For the onset of parametric rolling:

1. Small deviations from upright position (initial condition on heel angle).

2. **Tuning condition** (with wavelength equal to ship length at waterline) must be $\omega_e / \omega_0 \approx 2$ and may be met **in many operative conditions**.

3. Periodic **fluctuation** of the **transverse stability** sufficiently **high**.

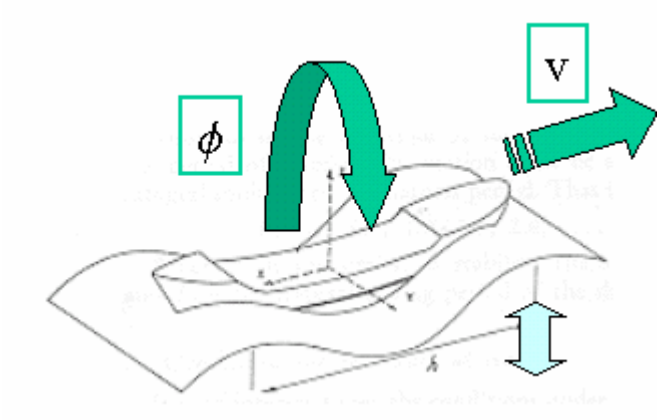

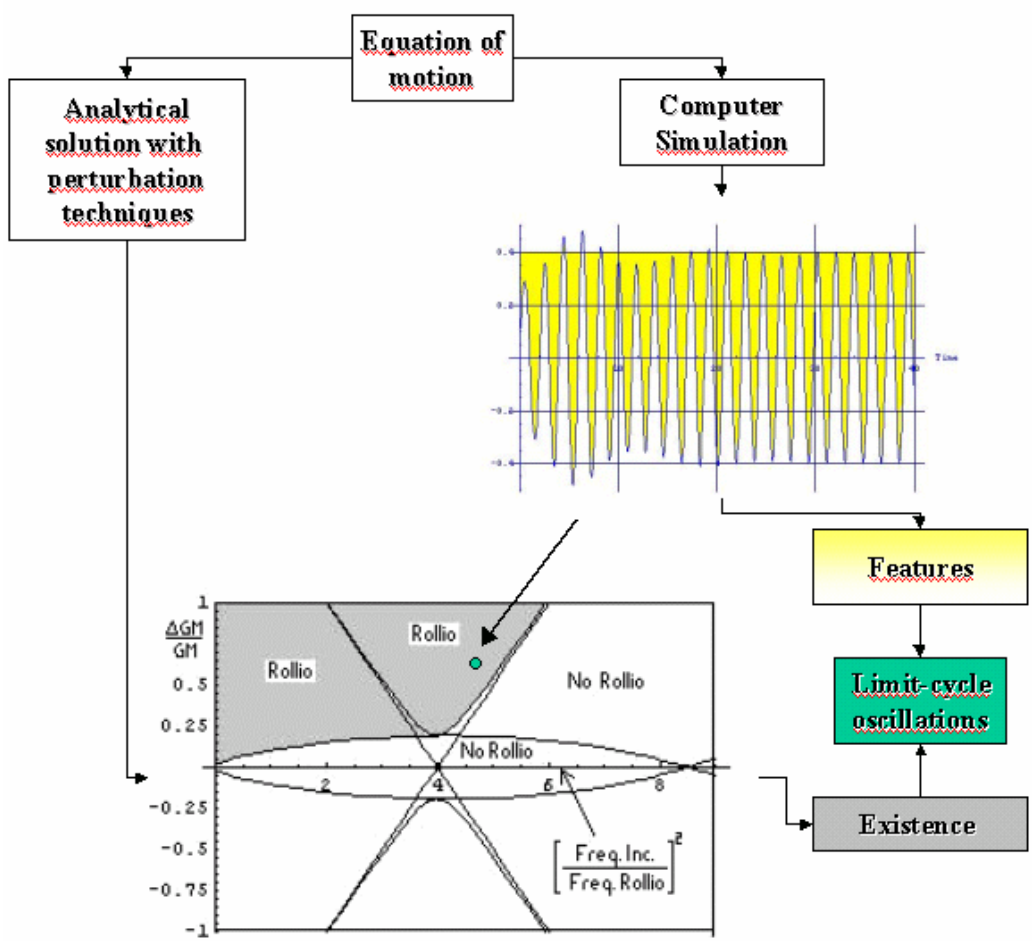

LINEAR APPROACH

Considering a sinusoidal time variation of the transversal metacentric height, the description of ship rolling in a purely longitudinal sea can be obtained by considering the following, linearized mathematical model:

$$\ddot{\phi}+2\mu\dot{\phi}+\omega_0^2\left[1+\frac{\delta\overline{GM}}{\overline{GM}^*}\cos(\omega_e t+\varepsilon)\right]\phi=0$$

By changing the independent variable

$$\omega_e t = 2t'$$

and cancelling the damping by means of a linear transformation $\phi \rightarrow \phi e^{-\mu t}$, we obtain:

$$\ddot{\phi} + 4\frac{\omega_0^2}{\omega_e^2}\left[1 + \frac{\delta\overline{GM}}{\overline{GM}^*}\cos(2t)\right]\phi = 0$$

The Floquet theory (σ characteristic exponent) yields that the solutions of damped Mathieu equation will be:

- diverging if both $-\mu^* \pm \sigma > 0$
- stable if $\mu = \sigma = 0$

$$2 - \frac{\omega_e^2}{2\omega_0^2} < \frac{\delta\overline{GM}}{\overline{GM}^*} < \frac{\omega_e^2}{2\omega_0^2} - 2$$

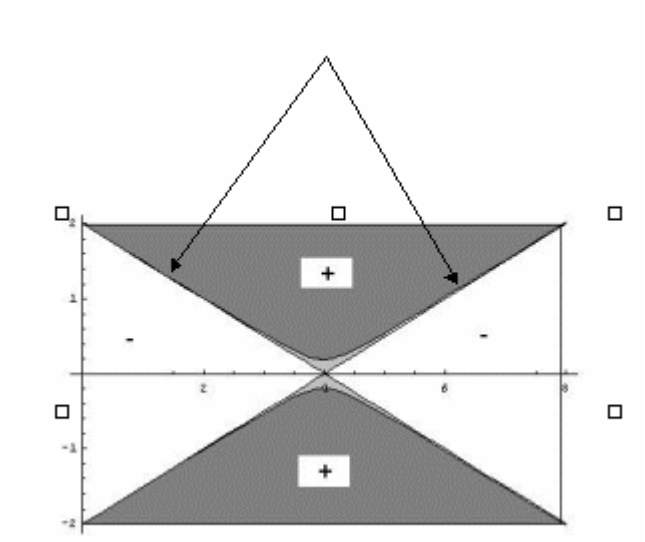

- decaying if both $\mu^* \pm \sigma < 0$.

MODEL TESTING VS. LINEAR APPROACH

Experimental tests on scaled models were performed to determine limit-cycle oscillations (LCO) amplitudes and threshold with respect to ship speed, frequency ratio and metacentric height.

The Figure below is based on data collected from tests in the model basin at DINMA-TRIESTE.

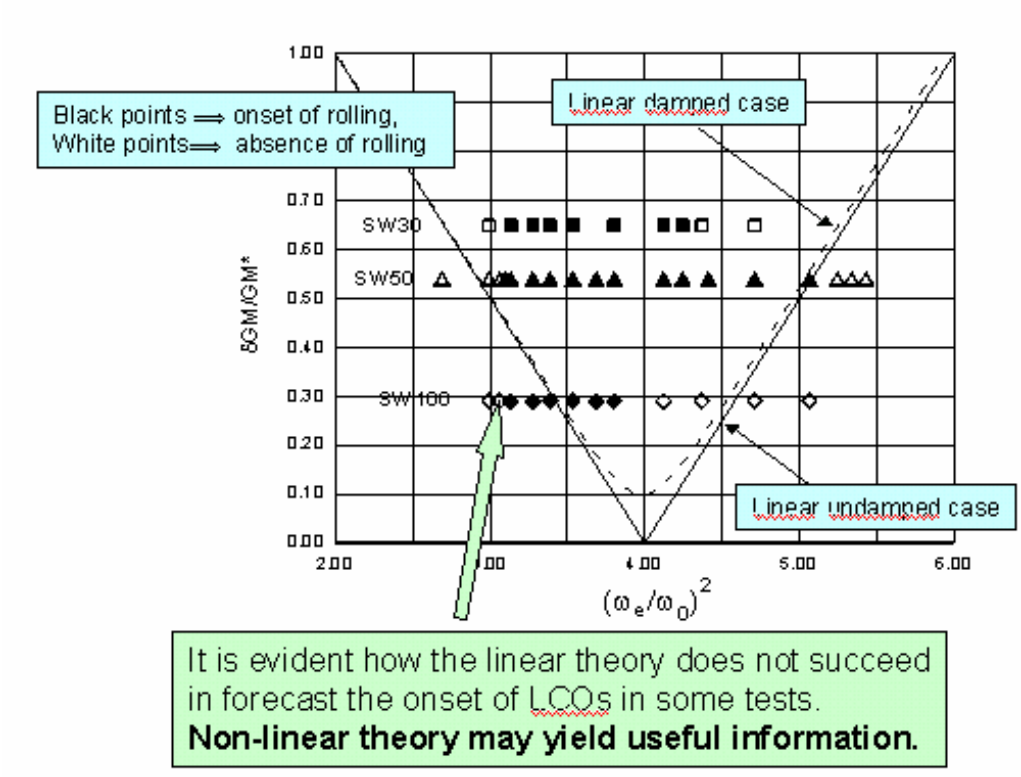

NONLINEAR APPROACH

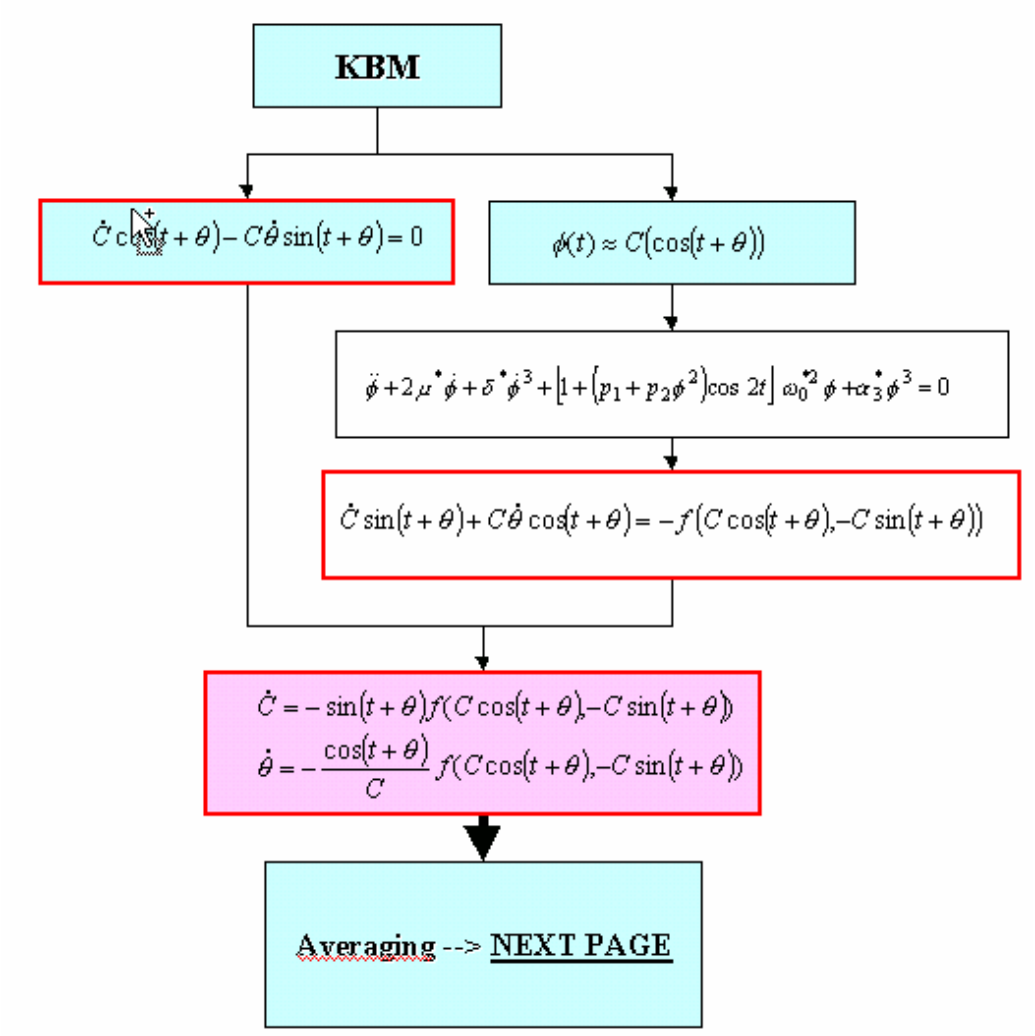

NON-LINEAR APPROACH II

$$\dot{C} = -\sin(t+\theta) f(C\cos(t+\theta), -C\sin(t+\theta))$$

$$\dot{\theta} = -\frac{\cos(t+\theta)}{C} f(C\cos(t+\theta), -C\sin(t+\theta))$$

$$C = \frac{1}{2\pi}\int_0^{2\pi} f(C,\theta)\cos(t)\,dt$$

$$\theta = \frac{1}{2\pi C}\int_0^{2\pi} f(C,\theta)\sin(t)\,dt$$

$$\begin{cases} \sin 2\theta\left[2p_1\omega_0^2 + 2p_2C^2\omega_0^2\right] = 3\delta C^2 + 8\mu \\ \cos 2\theta\left[2p_1\omega_0^2 + p_2C^2\omega_0^2\right] = -2(\omega_0^2 - 1 + \frac{3}{4}\alpha_3 C^2) \end{cases}$$

$$\sin^2 2\theta + \cos^2 2\theta = 1$$

$$C^2 = \frac{8}{3\alpha_3(1+\gamma^2)}\left[-\mu\gamma + (1-\omega_0^2) \mp \frac{1}{2}\sqrt{\frac{\omega_0^4 p_1^2}{4}(1+\gamma^2) - [2\gamma(1-\omega_0^2)+4\mu]^2}\right]$$

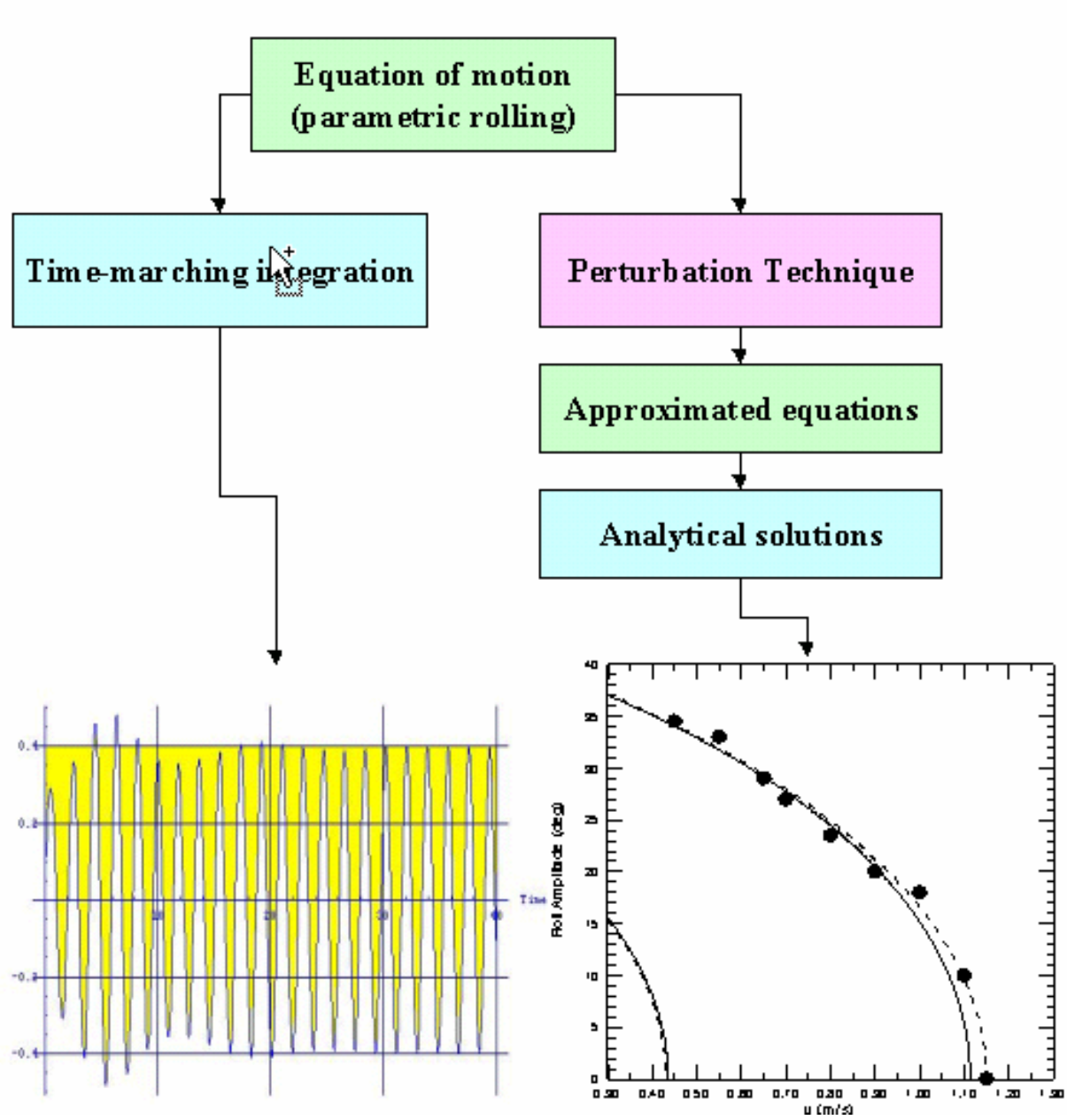
Equation of motion
(parametric rolling)
Time-marching integration
Perturbation Technique
Approximated equations
Analytical solutions
Roll Amplitude (deg)
u (m/s)

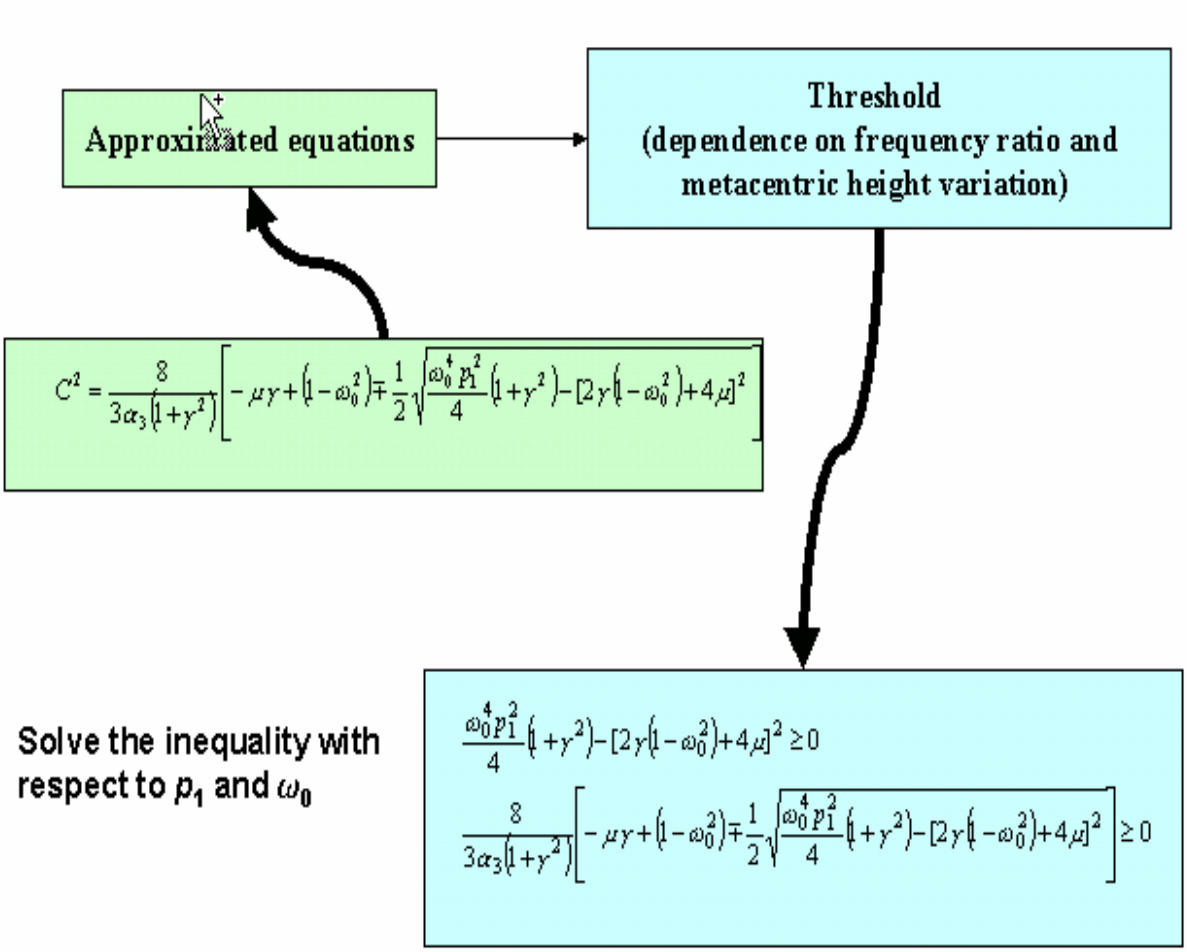

Comparison between theory and experiments

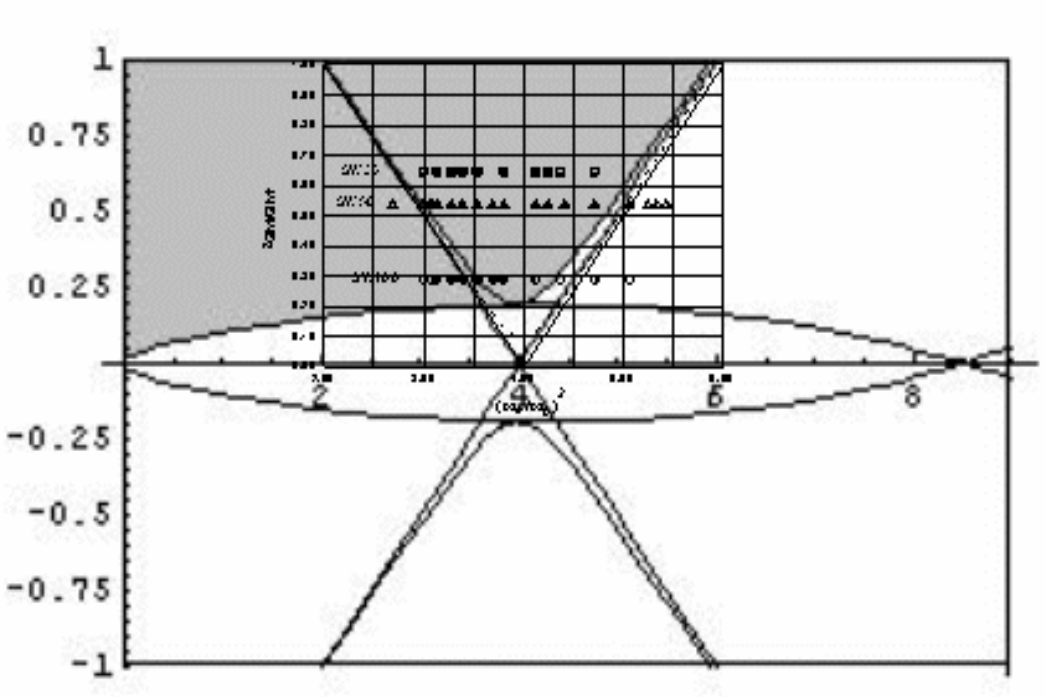

Threshold with Linear and Nonlinear Mathieu Equation

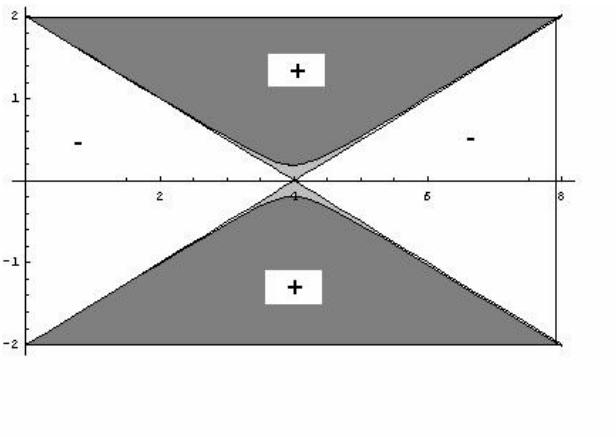

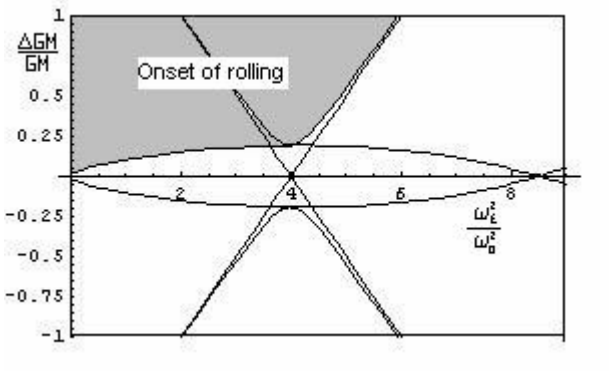

CONCLUDING REMARKS

- The phenomenon of parametric rolling has been investigated from a **mathematical point of view**.

- The **KBM perturbation technique** has been applied to the nonlinear Mathieu equation describing parametric rolling.

- The advantages of analytical solutions via perturbation techniques are:
  - "easy" determination of **amplitudes** of periodic motion
  - possibility to study the **threshold** for the onset of parametric rolling with respect to some coefficients

- It has been shown that **numerical simulation** and **analytical** investigation of simplified equation of motion provide solutions that are in **good agreement** with model testing.

A Numerical Analysis of Violent Free Surface Flow on Flooded Car Deck using Particle Method

Shigeru NAITO, Osaka University, Osaka Japan, naito@naoe.eng.osaka-u.ac.jp
Makoto SUEYOSHI, Osaka University, Osaka Japan, sueyoshi@naoe.eng.osaka-u.ac.jp

SUMMARY

A numerical study concerning violent free surface flow is presented. The sloshing on large car deck, which is extremely non-linear and complicated free surface flow, is numerically analysed using the Particle Method. The long time free surface simulation of large amplitude forced roll oscillation is carried out. Time series of force and moment from fluid on the deck and free surface profiles are presented. In addition, simulated results of very large amplitude free oscillation of floating body with fragmentation of fluid are presented.

1. INTRODUCTION

After the accident of "ESTONIA", a lot of studies concerning damage stability are carried out. In these studies, it has always been pointed out that water invasion to large car deck is extremely dangerous. However it is difficult to analyse this problem by means of ordinary CFD tools. The reason of this is difficulty of complicated free surface dynamics such as fragmentation of fluid. In addition, it is necessary that very shallow water with breaking waves can be treated. Then SOLA-VOF has been used in several past studies for this problem. But long time violent free surface simulation was hardly carried out.
Another difficulty of this problem is the large amplitude floating body motion. Tanizawa[2] carried out BEM non-linear simulation of a floating body in waves. He shows simulations for large amplitude and liquid cargo. However it is difficult to simulate breaking waves and damaged hull's opening using BEM.

MPS (Moving Particle Semi-implicit) method based on macro and deterministic model, which is developed by Koshizuka, is a kind of the particle method. This has following advantages for the present problem.

- Strict conservation of mass
- No numerical diffusion of free surface
- Enough robustness

In order to carry out the long time and violent free surface simulation, these characteristics should not be lacking. The particle method requires enormous computational resources. Nowadays, increase of the computational performance gives availability of the particle method for 2 dimensional problems.

Table 1 : Assessment of Numerical Method.

	BEM	VOF	MPS
conservation of mass	A	B	A
clear surface	A	B	A
computation time	A	B	C
fragmentation of fluid	C	A	A
robustness	B	B	A

A : good B : normal C: no good

Table 1 shows characteristics of three methods for non-linear free surface simulation.
Validation of the computational code is shortly presented in the appendix of this paper.

2. Water on Flooded Large Car Deck

2.1 Numerical Modelling

Numerical simulations are carried out on following assumptions.

- The problem is considered as 2 dimensional one.
- Surface tension and air effects are neglected.

The governing equations for incompressible flow are as follows.

$$\frac{D\mathbf{u}}{Dt} = -\frac{1}{\rho}\nabla P + \nu\nabla^2\mathbf{u} + \mathbf{g} \qquad (1)$$

$$\frac{d\rho}{dt} = 0 \qquad (2)$$

ν Coefficient of viscosity
ρ Density of fluid
$\mathbf{g}$ Gravity acceleration vector
P Pressure
t Time
$\mathbf{u}$ Velocity vector

Equation (1) and (2) are solved using MPS method.
The details of algorithm of MPS method is presented by Koshizuka and Oka[1] (1996).

2.2 Forced Roll Oscillation

RORO ship has a large car deck inside of vessel. Considering sloshing on the car deck, one of important motions is the roll motion.
Figure 1 shows the co-ordinate system and arrangement of simulations. *Fx* is a force acting on both side of tank. *Fy* is a force acting on the deck and ceiling of the tank. *M* is a moment from fluid. The model rectangular tank (0.17x0.07m) is forcedly oscillated in simulations. The first resonance period of the tank, when it is filled with

water at depth h=0.01375(m), is T=0.93 (sec.). Rolling pivot is fixed at 0.02 m above the car deck. Simulations are carried out several patterns.

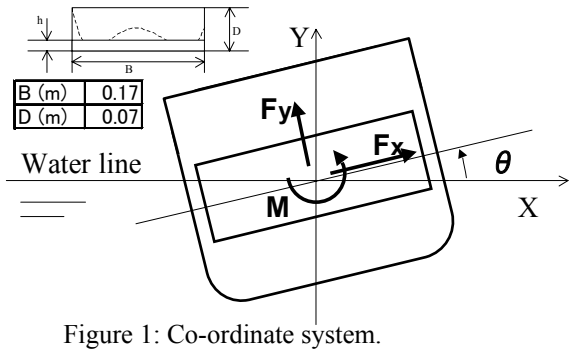

Figure 1: Co-ordinate system.

2.2 (a) Symmetrical Roll Motion

The tank is oscillated without heel angle. Symmetrical sinusoidal motion is given. Figure 2 shows particle configurations for 1.4 seconds. In spite of very large deformation, free surface of water is quite clear.

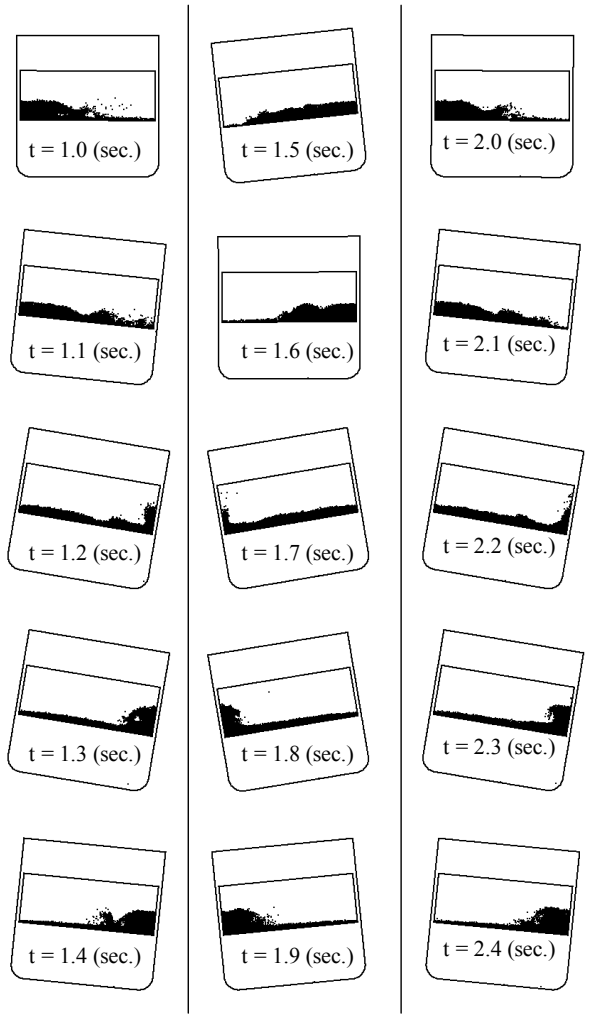

Figure 2: Particle Configurations for symmetric rolling oscillation every 0.1 seconds.

2.2 (b) Increase of Heel Angle as Time-marching

When ship is damaged, the motion of tank is not symmetrical one. Heel angle of the tank increases as time marching. Forced roll angle $\theta(t)$ is given as following equation (2).

$$\theta(t) = at + \theta_0 \sin(\omega\ t + \varepsilon) \qquad (2)$$

Parameters of motion are following, heel angle ratio a =3.0 (degree/sec.), rolling amplitude θ_0 =15.0 (degree) and phase ε =0.0. Figure 3 shows time series of force acting on the tank wall. The transition of sloshing mode as change of heel angle is presented.

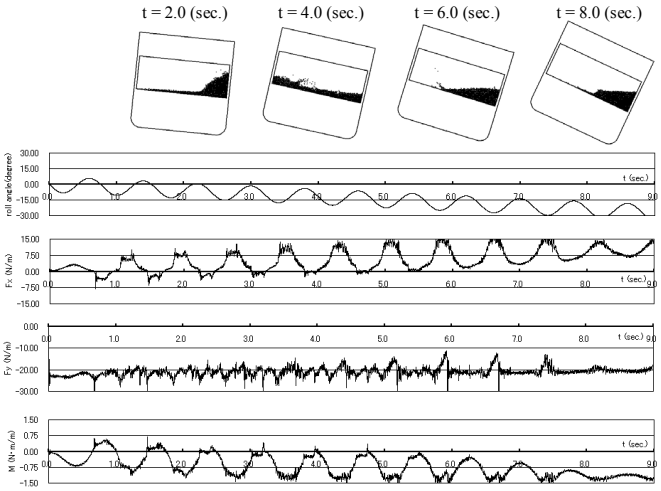

Figure 3: Time series of forces and moment by inner water (roll period 0.8 sec.) and transition of sloshing mode.

2.3 Trailers and Motorcars on the Deck (Example of Estonia)

When RORO ship operates, cargoes, which are mainly trailers and motorcars, usually exist on the car deck. These are fixed on the car deck using some of instruments, chock and harness. Then water on the deck encounters various obstacles. These are pressured by water. Then interaction between floating body and water should be considered on the situation, if binding instruments were broken or sabotaged. Trailers have almost same cross-sections along longitudinal line, and motorcars have usually 3 dimensional forms. However in this study, it is approximate that cargo is fixed and 3 dimensional effects are neglected.

When water invade on the car deck, the ship losses its speed. Fin stabilisers cannot work well on this situation. Then the ship oscillates with large amplitude in waves.

In the simulation, the flooded car deck is forcedly oscillated. Sinusoidal roll motion, whose amplitude is 7.5 degree and the period is 10.0 seconds, is given. The dimension of considered RORO ship's car deck is shown on Table 2. Rolling pivot is fixed at 2.0 m under the car deck. Actual numerical simulations are executed in 1/100 model scale (time scale is 1/10). Initial configuration of obstacles on the car deck is shown Figure 4. Cross

sections of trailers and motorcars are simplified for 2 dimensional simulation. Three cases are simulated. In Case A, the car deck is empty. In case B, 8 numbers of fixed obstacles exist on the deck. In case C, one of obstacles on the deck is freely movable. Figure 5 shows particle configurations for case A, B and C.
Figure 5 shows time series of particle configurations every 0.2 seconds for case A, B and C. When car deck is empty, shallow water runs extremely wild. The turn over splash touches the ceiling of car deck. In case cargoes are fixed, they resist waves and water is well behaved.

Table 2: Dimension of RORO ship's car deck.

Bredth of car deck (m)	24.4
Height of car deck (m)	5.0
Initial level of water (m)	0.5

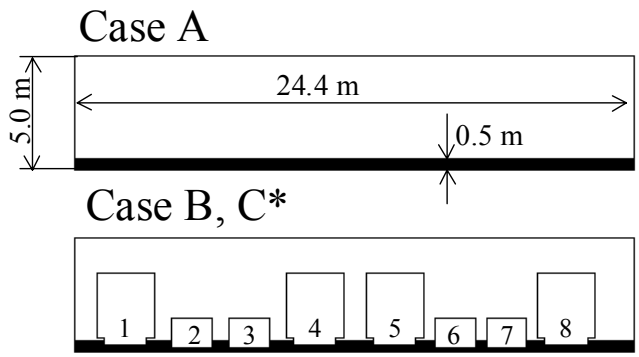

* case C : No. 7 obstacle is movable

Figure 4: Particle configurations for initial time step of simulation of sloshing on RORO ship's car deck.

3. Interaction between Floating Body and Fluid

3 cases of demonstrations using the particle method are shown. Interaction problem between floating bodies and fluid is presented in the previous section too. However in present section, floating bodies, which are in larger water area, are considered. The first example is free rolling of 2D ship which has a flooded tank. Secondly, very large amplitude free oscillation of floating body is shown. Thirdly free oscillation of floating body with openings in waves is shown in a restricted water.

3.1 Free Oscillation of Floating Body with Deck Water

Coupled motion of heave, roll and sway are simulated in time domain. Complicated behaviour of floating body with shallow deck water is presented. Figure 6 shows initial configurations of particles. The initial heel angle of 2 dimensional cross section is 30 degrees and initial velocities of particle, which is arranged as a part of ship, are all zero. 24,611 particles are totally used. Tow cases of simulation are carried out. One is fixed solid cargo on the inner deck. Another is free liquid cargo on it.

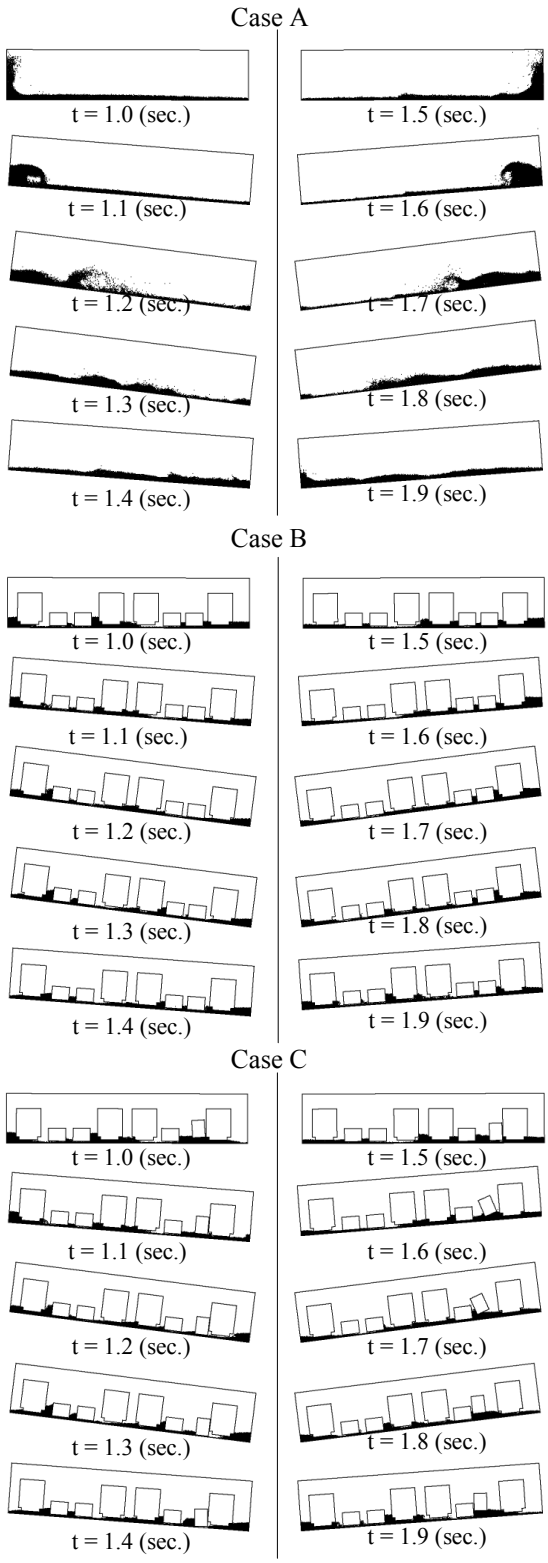

Figure 5: Particle configurations every 0.1 seconds (roll period: T=10.0 (sec.) roll amplitude: θ_0 =10 (degree)).

Figure 7 shows phase plot of simulated roll motion. Black circles on the trajectory are plotted every 1.0 seconds. Figure 8 shows the time series of roll angle. Figure 9 shows particle configurations for the liquid cargo case every 0.1 seconds and every 1.0 seconds. In

the liquid cargo case, as first, the flooded water sloshes on deck. Finally, the flooded ship heels over and stabilises at the point.

3.2 Large Amplitude Free Oscillation of Floating Body

Free falling of floating body with inner free water and water mass is simulated. The floating body makes a touchdown on the free surface and oscillates freely. At the same time the water mass and water of tank unites and large amplitude waves are generated. Figure 10 shows particle configurations every 0.1 seconds.
7,717 particles are used in this simulation.

3.3 Free Oscillation of Floating Body with Opening in Waves

The Floating body has one opening, which is on the right side of hull above water. Inner deck is perfectly dry at initial time step. The right side of tank wall is movable, which play a role of wave generator. The period of generated wave is T=0.8 (sec.) and the amplitude of wave maker is 0.05 m. The left side of tank is fixed wall. Consequently the simulated result involves reflection of waves. 28,908 particles are used.

Figure 11 shows particle configurations for 7.5 seconds every 0.5 seconds. Water invades in floating body every collision with waves. Invading water sloshes on inner deck. Draft of the floating body increases and opening closes with water surface. As a result amount of invading water increases.

4. CONCLUSIONS

This study is aimed to obtain feature of shallow water sloshing using numerical method in time domain. In this study MPS method can be applied to these violent free surface problems successfully.
Various numerical simulations of 2 dimensional violent free surface flow are carried out. As a result, capability of the particle method for shallow water sloshing and large amplitude oscillation of floating body with fragmentation of fluid is presented.
As a next step, 3 dimensional expansion of computational code is required. It is not so difficult, because algorithm of particle method is simple one. A main difficulty for the expansion is limitation of computer performance.
In addition, a development of wave-absorbing zone for particle method should be developed. Especially it is necessary to simulate motion of floating body in the actual sea.

6. REFERENCES

[1] S. Koshizuka and Y. Oka, 'Moving-Particle Semi-Implicit Method for Fragmentation of Incompressible Fluid', Nuclear Science and Engeneering, 123, pp421-434, 1996.

[2] K. Tanizawa, 'Nonlinear Simulation of Floating Body Motions in Waves', ISOPE Proceeding of the 6th, pp414-420, 1996.

[3] A. Francescutto and V. Armenio, M. L. Rocca, 'On the Roll Motion of a Ship with Partially Filled Unbaffled and Baffled Tanks: Numerical and Experimental Investigation', ISOPE Proceeding of the 6th, pp377-386, 1996.

[4] K. AMAGI, N. KIMURA, K. UENO, 'On the Practical Evaluation of Shallow Water Effect in Large Inclinations for Small Fishing Boats', 5th International Conference on Stability of Ships and Ocean Vehicles Proceeding, 1994.

7. APPENDIX

MPS method code used in this paper is validated by comparison with two experiments. One is dam-break flow and another is tank sloshing. Both of them show good agreement between simulations and experiments. Figure 12 shows leading edge of dam-break. Figure 13 shows particle configurations and velocity vectors of tank sloshing. Both of them show pretty good agreements.

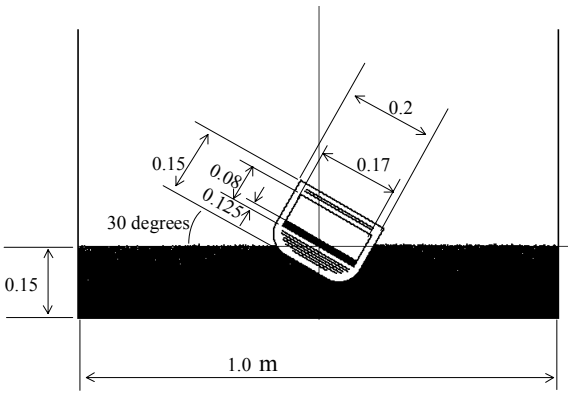

Figure 6: Particle configurations for initial time step.

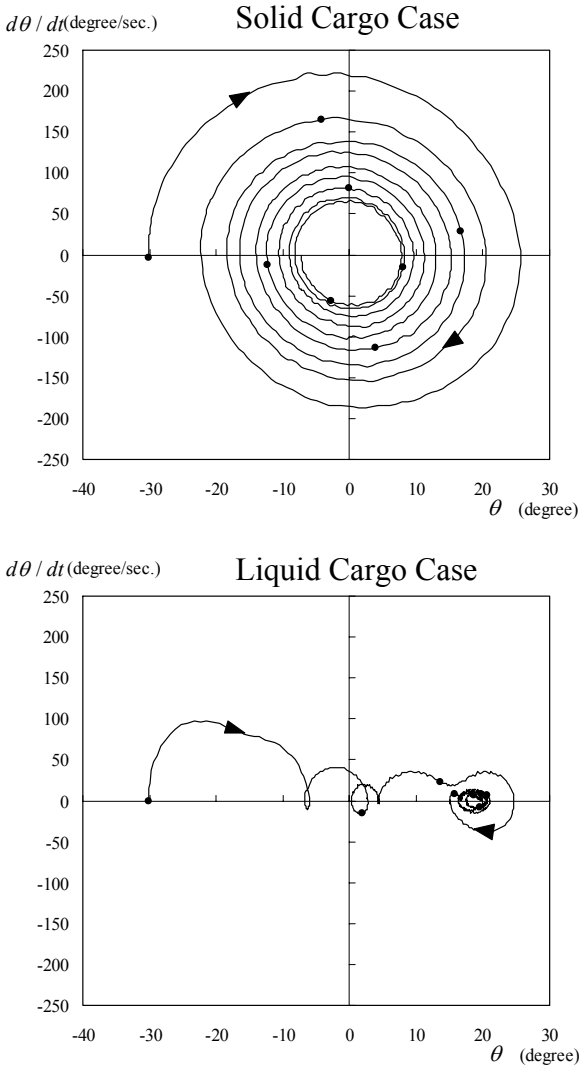

Figure 7: Phase plot of the simulated free roll motion.

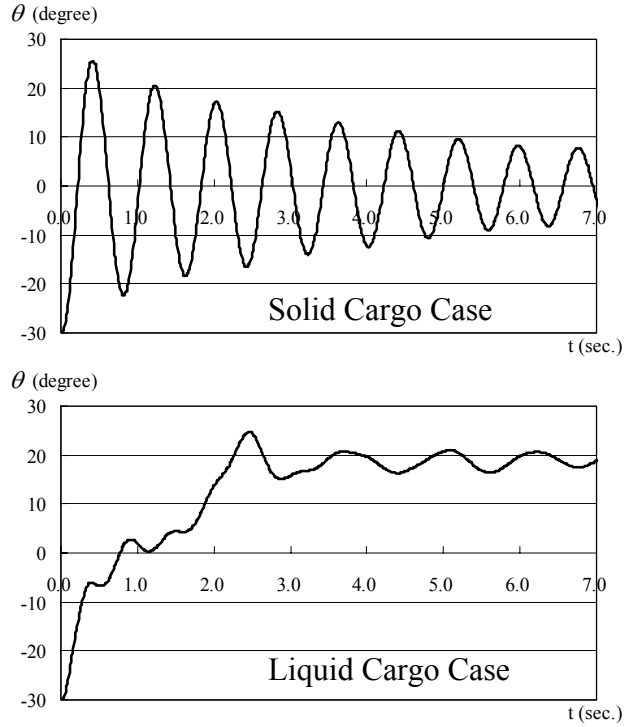

Figure 8: Time series of simulated rolling angle.

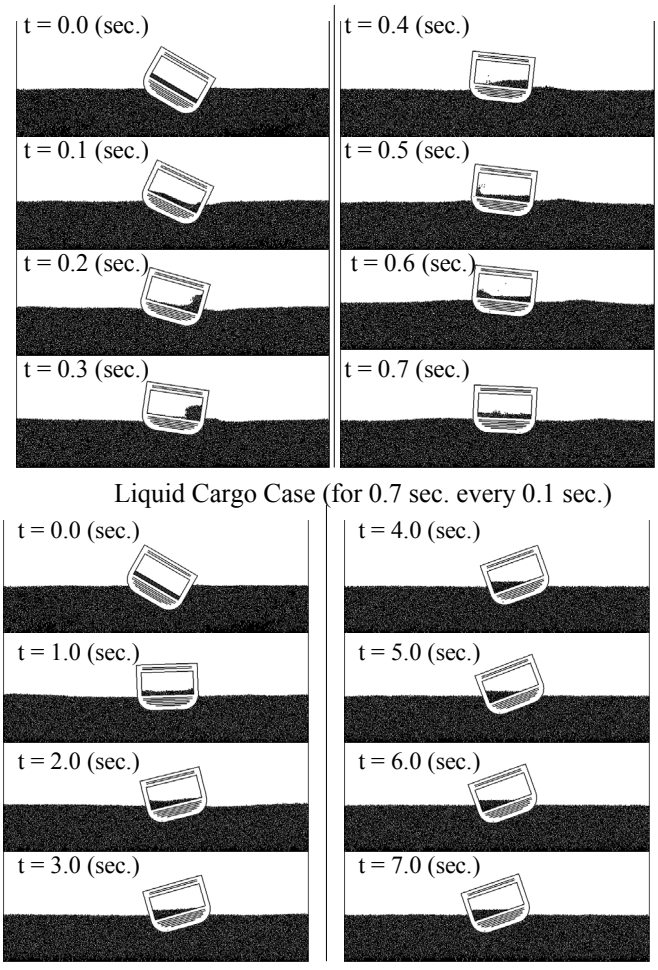

Figure 9: Particle configurations for free rolling of 2D ship with liquid cargo in channel tank.

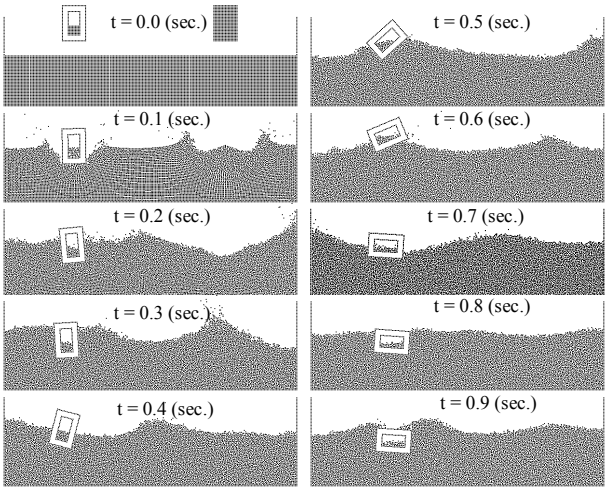

Figure 10: Particle Configurations for Large Amplitude Freedom Oscillation every 0.1 seconds.

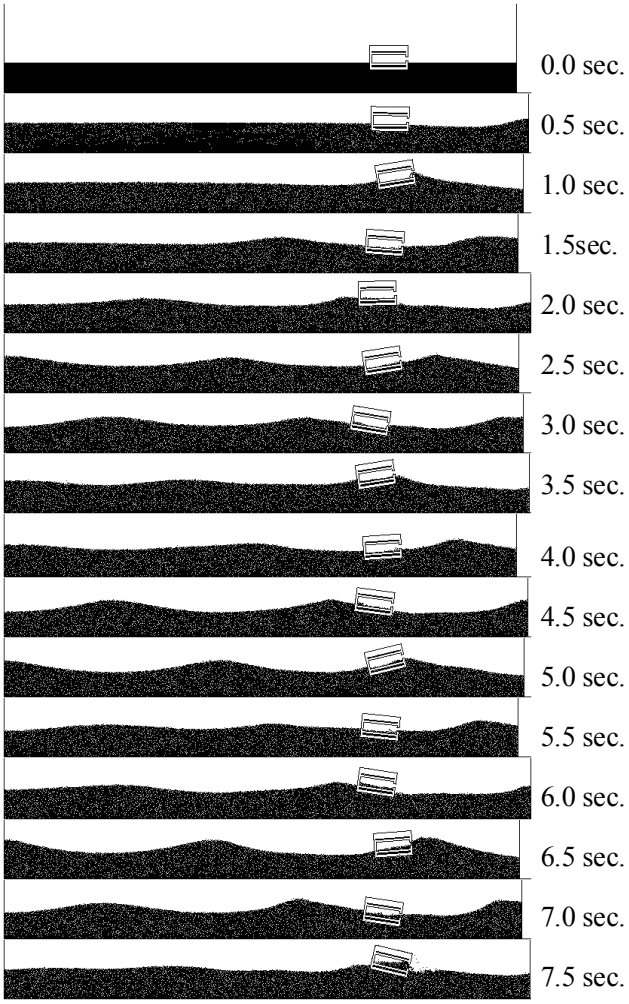

Figure 11: Particle Configurations for Freedom Oscillation of Floating Body with Openings in Waves every 0.5 seconds.

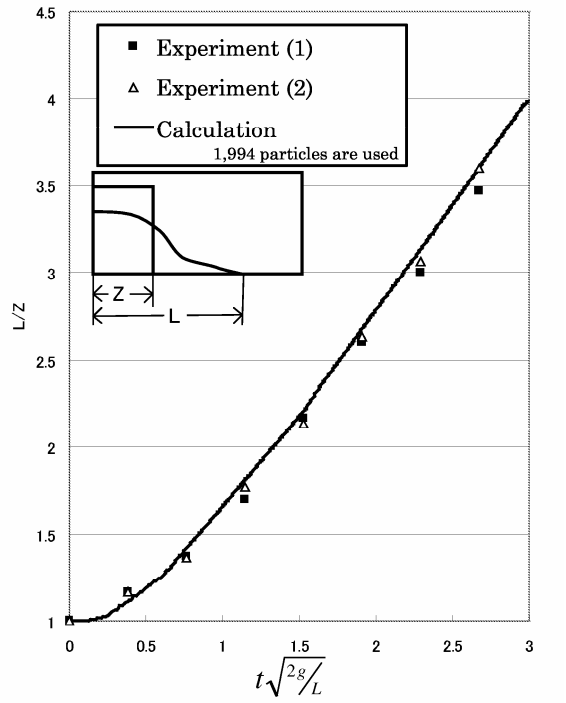

Figure 12: Comparison between experiments and simulations using particle method.

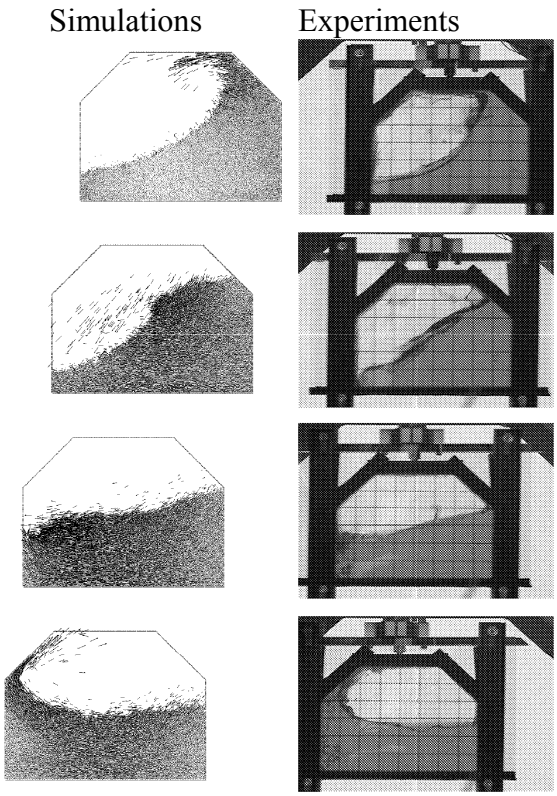

Figure 13: Comparison between experiments and simulations using particle method.

Some topics for discussion on the numerical simulation of large amplitude floating body motions in ship stability problem

Katsuji TANIZAWA

National Maritime Research Institute

Tokyo, JAPAN

1 Introduction

In the last decade, many researchers developed fully nonlinear numerical simulation methods to study large amplitude floating body motions in waves. These numerical simulation methods are generally called Numerical Wave Tank (NWT).

Two dimensional NWTs (2D-NWT) were firstly developed and variety of numerical techniques were examined using them. Now, the research of 2D potential flow NWT is almost finished and many good 2D-NWTs are available to simulate large amplitude floating body motions. We can apply them to study large amplitude responses, parametric resonances, chaotic responses and etc.

Three dimensional NWTs (3D-NWT) were secondly developed and still researchers are working on. One application of 3D-NWT is highly nonlinear wave load acts on vertical columns. Since higher order spectrum methods are not enough to capture steep wave run up on them, fully nonlinear NWTs are required. Three dimensional nonlinear wave interaction is also good application for oceanographers. For naval architects, 3D-NWT can be very attractive tool when floating body is supported. Practical 3D-NWTs are still under investigation.

Now, we are at a good timing to discuss on the application of NWTs to study stability of floating bodies in rough seas. This short article is written to offer some topics we should discuss when we apply NWTs to stability problems.

2 Topics

2.1 Accuracy of NWTs

NWT based on potential theory is known to be very accurate if they are correctly programed. Accuracy check of potential flow NWT is not the topic for discussion any more but for the topic of individual code test. Theoretical backbone of potential flow NWT is very solid. The interaction between floating body motions and ideal fluid motions is also well formulated in the acceleration field. Error due to numerical integration is small enough with correct treatment of singular point. We can say potential flow NWT is as accurate as classical frequency domain method. Tanizawa simulated motions of 2D midship section body in regular waves and compared simulated time histories with measurements [5]. (Fig.1) Kashiwagi simulated hydrodynamic force on 2D bodies by his 2D-NWT and showed the results well agreed with linear theory and experiment up to 3rd order [2]. Kashiwagi also simulated free motions of 2D bodies in regular waves and showed agreement between simulated motions and measured motions were quite good [3]. (Fig.2) Tanizawa proposed benchmark tests of 2D radiation and diffraction problems for ISOPE's NWT workshop and showed simulated results of 2D-NWTs well agreed with each other up to 3rd order, even if NWTs were developed independently by different researchers [7]. Taking the above arguments into account, I think potential flow NWT is accurate and practical tool for the estimation of floating body motions, except roll amplitude in resonant condition. Roll resonant problem is discussed in next section. One unsolved problem I have noticed is estimation of drift force by NWT. Wave drift force is the second order constant force and can be calculated both from wave field and direct pressure integral on wet body surface. Usually, drift force obtained from wave field agrees with experimental value well. However, drift force from

direct pressure integral is not good. I think NWTs may have some problems only for the estimation of 2nd order constant component in hydrodynamic forces by direct pressure integral.

2.2 Viscous effects

For stability problems, viscous effect plays important role. In particular viscous damping is essential when we need accurate estimation of roll amplitude in resonant frequency. In potential flow NWTs, measured roll damping coefficient is used to correct the simulation if necessary. In principle, such a empiricism should be removed and viscous NWT should be applied for such a problem.

Analysis of parametric roll excitation is another problem we should consider viscosity. In this problem, critical wave height of Mathieu instability is the main concern. Tanizawa and Naito applied potential flow NWT to analyze the critical wave height for a bow section shaped 2D body and showed the obtained critical height by NWT is a little lower than experimental result [6]. (Fig.3) This difference is considered to come from viscous effect. Yeung and Liao developed FSRVM (Free surface random vortex method) [8] and successfully introduce viscous effect into potential flow NWT. They applied FSRVM to the analysis of Mathieu instability of a 2D body roll motion with and without bilge keel[9].

2.3 Numerical robustness

As we experience in many cases that free surface is not always stable everywhere but easily breaks locally. However, potential flow NWT assumes stable free surface and very weak against free surface breaking. This weakness limits the application of potential flow NWT. For analysis of damage stability, even if amplitude of wave and body motions are small, motion of shallow internal fluid is usually large and internal free surface is very unstable. To overcome this weak point, we don't need to use time consuming viscous NWT to entire computational domain but use it partially. Grilli combined BEM and VOF to simulate shoaling waves. [1]. Landrini developed gridless code SPlasH and analyzed wave pattern around a Wigley hull by BEM and post-breaking waves by SPlasH. [4] Such approaches are considered to be practical for me. For analysis of damage stability, potential flow NWT can be used to simulate ship and wave motions and viscous NWT can be use to simulate internal fluid motions.

References

[1] Guignard,S., Grilli,S., Marcer,R. and Rey,V. (1999) Computation of shoaling and breaking waves in nearshore areas by the coupling of BEM and VOF method. *9th ISOPE Conf*, vol.3

[2] Kashiwagi,M. (1996), Full-nonlinear simulations of hydrodynamic forces on a heaving two-dimensional body, *J. Soc. Nav. Arch. Japan*, Vol.180

[3] Kashiwagi, M. , Momoda, T. and Inada,M. (1998), Time-domain nonlinear simulation method for wave-induced motions of a floating body, *J. Soc. Nav. Arch. Japan*, Vol.184

[4] Landrini,M., Colagrossi,A. and Tulin,M.P. (2001), Breaking bow and stern waves: Numerical simulations, *16th IWWWFB*

[5] Tanizawa,K., (1997), Nonlinear theory of wave-body interaction based on acceleration potential and its application to numerical simulation (in Japanese), *Ph.D thesis, Osaka Univ.*

[6] Tanizawa, K. and Naito, S. (1997), A study on parametric roll motions by fully nonlinear numerical wave tank, *Proc. of 7th ISOPE Conf.*, Honolulu, Hawaii, vol.3

[7] Tanizawa, K. and Clément, A.H. (2000), Report of the 2nd workshop of ISOPE NWT group, Benchmark test cases of radiation problem, *Proc. of 10th ISOPE Conf.*, Seattle, Vol.3

[8] Yeung R.W. and Liao S.W. (1999), Time-domain solution of freely floating cylinders in a viscous fluid, Proc. 9th ISOPE Conf, vol.3

[9] Liao S.W. and Yeung R.W., (2001), Investigation of the Mathieu instability of roll motion by a time-domain viscous-fluid method,Proc. 16th IWWFB

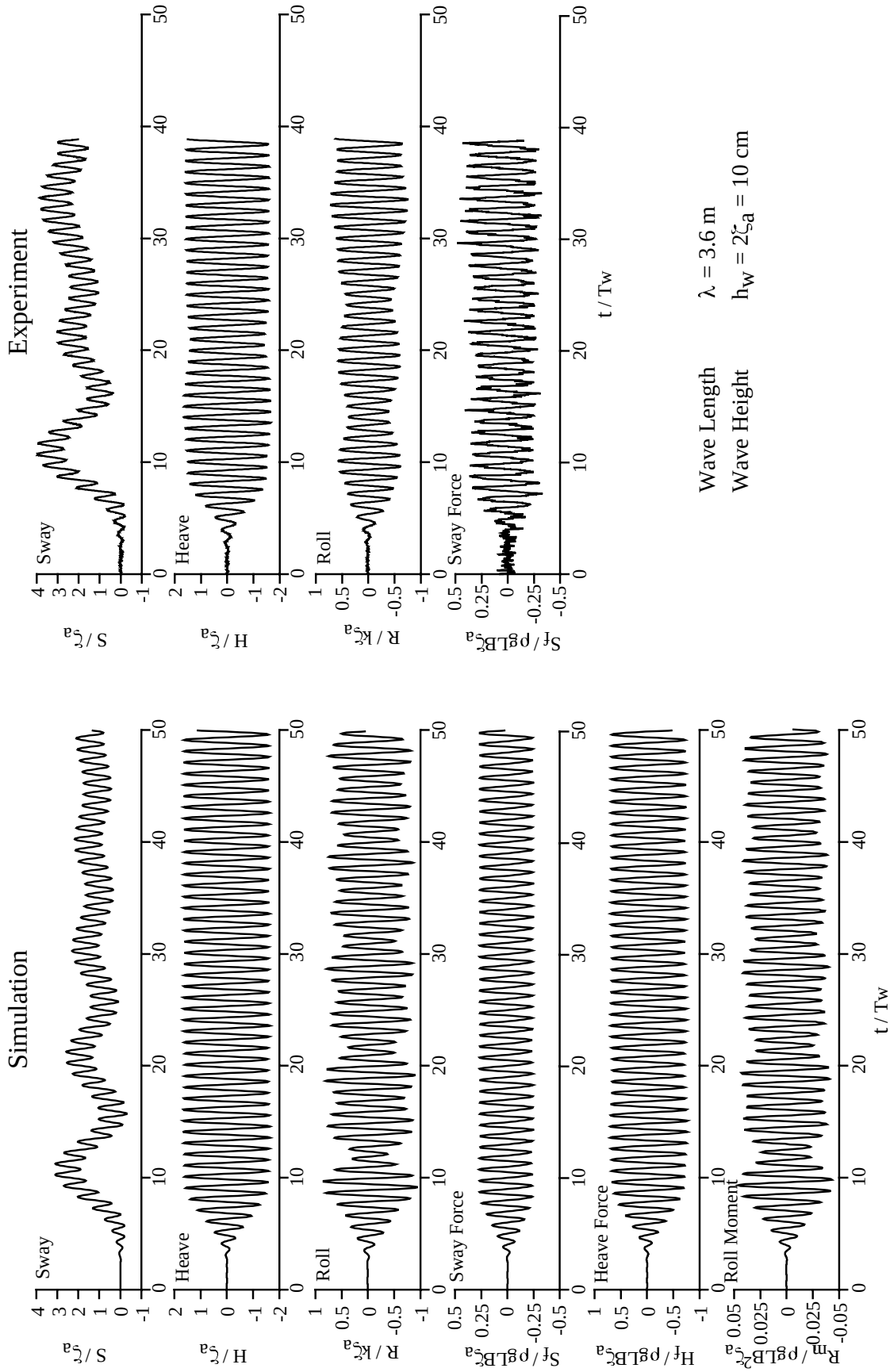

Fig.1 Comparison between simulated and measured body motions in a regular wave by Tanizawa

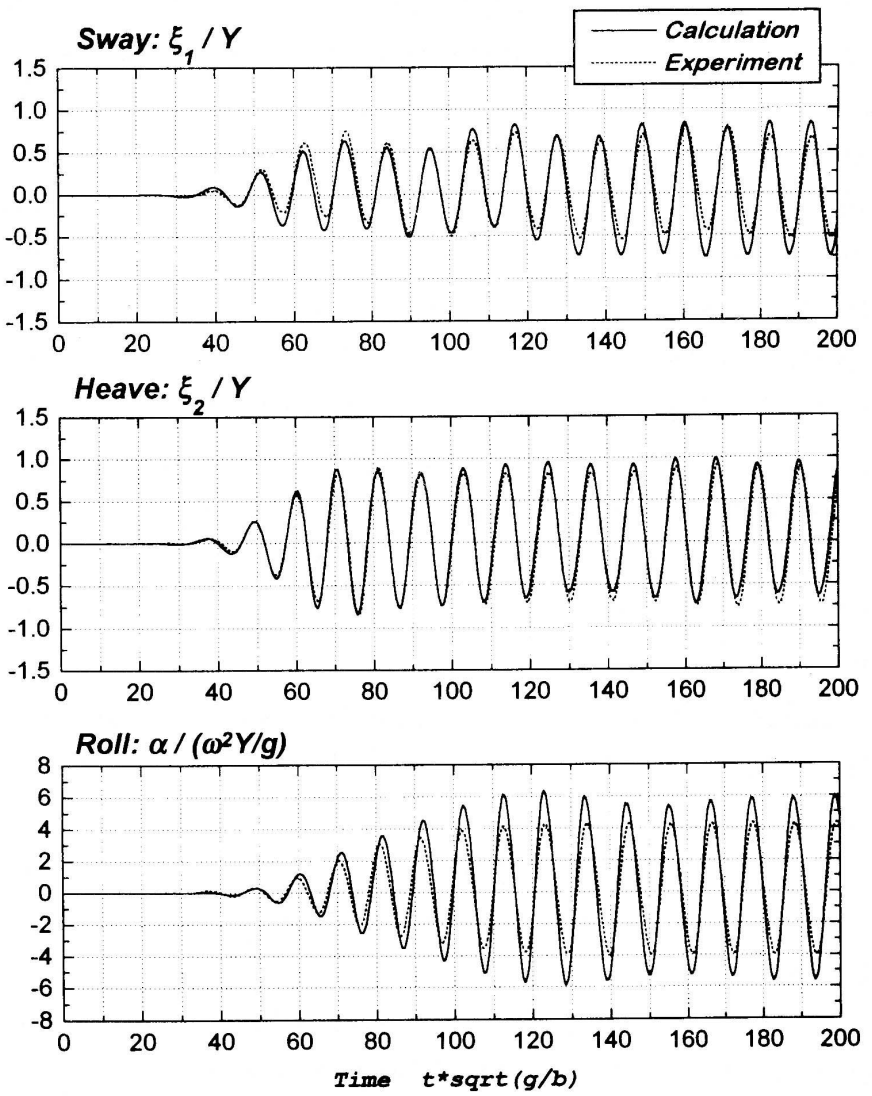

Fig.2 Comparison between simulated and measured body motions in a regular wave by Kashiwagi

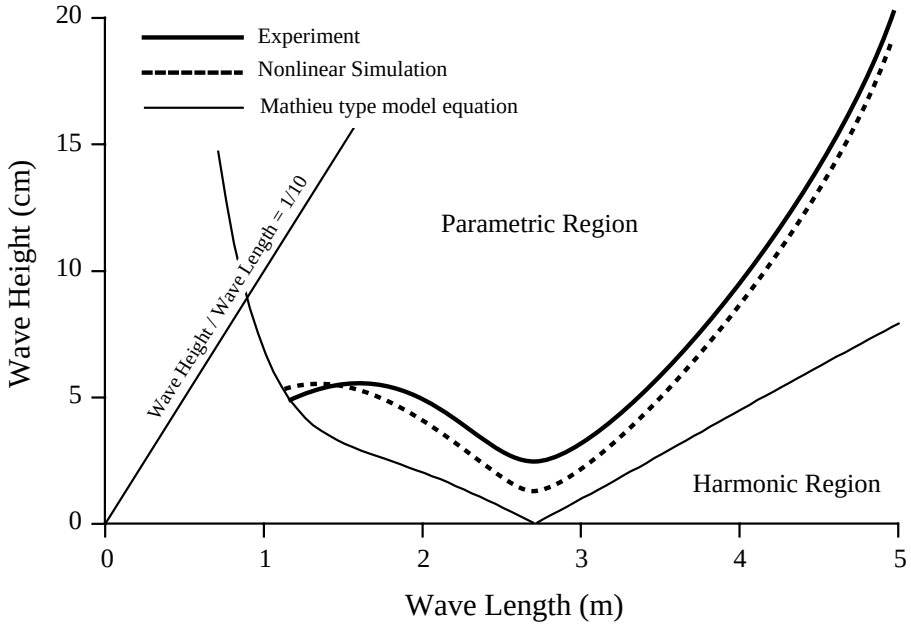

Fig.3 Critical wave height of Mathieu instability, Simulation and measurement.

DIRECT SIMULATION OF FREAK WAVES FOR EXTREME DESIGN CONDITIONS

Antonio CARDO, Riccardo CODIGLIA, Giorgio CONTENTO and **Fabrizio D'ESTE**

DINMA - Department of Naval Architecture, Ocean and Environmental Engineering, University of Trieste
Via Valerio, 10 – 34127 TRIESTE, ITALY
Phone: +39-040-6763424 Fax: +39-040-6763443 e-mail: contento@univ.trieste.it

SUMMARY

This paper describes some recent results obtained at DINMA on the nonlinear behaviour of large unidirectional waves in the presence of frequency focusing. The study is conducted by means of direct numerical simulations in the frame of the inviscid fluid hypothesis. It is shown that given for a given spectrum generated by a wavemaker in a closed basin the nonlinear wave-wave interaction can give a large magnification of the crest elevation if compared to the traditional linear superposition. This is found to be due to the implicit generation of high frequency components. Moreover the phase speeds of the input components exhibit a slight increment and the new frequency component travel with the same speed of the smallest wave of the given spectrum.. Finally the numerical results obtained are compared with laboratory data showing extremely similar characteristics.

INTRODUCTION

"... Loss of a large norwegian ship with the entire crew in the middle of the North Atlantic is not a common event. However at a special occasion two large norwegian bulk ships M/S NORSE VARIANT and M/S ANITA disappeared at the same time at the same location…. Both ships came right into the center of a very extreme weather event with a strong low pressure giving 15 m significant wave heights and mean wave periods close to 10 seconds … with wind velocities near 60 knots. NORSE VARIANT had deck cargo that was damaged and moved by water on deck with the result that a hatch cover was broken and left open. This ship took in large amounts of water and sank before an organised evacuation was finished. Only one member of the crew was rescued on a float. ANITA disappeared completely at sea with the whole crew and no emergency call was ever given.

The Court of Inquiry then concluded that the loss can be explained by an event in which very large wave suddenly broke several hatch covers on deck, and the ship was filled with water and sank before any emergency call was given. …"

On the same stream of the previous indirect witness of the presence of extremely large single waves in rough seas [*Kjeldsen,* 1], *Clauss* [2] suggests that the loss of the semisubmersible OCEAN RANGER could have been due to a single large wave, since weather reports from all the neighbouring platforms in the same geographic area do not mention evident anomalies in the sea state.

On the other hand, evidences given by measurements of the presence of such waves are becoming more and more frequent. Figure 1 (courtesy of Prof. Ove Gudmestad – STATOIL, Norway) shows the wave elevation measured on January 1 1995 at Daupner station. The significant wave height is 11.9 m approximately and the max wave

height detected in the time series is approx. 25.5 m, with a crest height 18.5 m above the still sea level.

It is well known that since the early 50's the predictions of loads on fixed offshore structures and motions of compliant or sailing structures due to surface waves are commonly made by computations on the basis of the statistical/spectral description of the sea elevation.

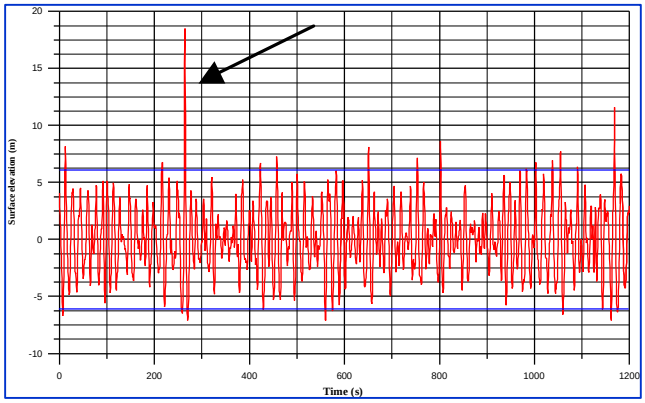

Figure 1. Wave elevation at the Daupner station on January 1 1995 (courtesy of Prof. Ove Gudmestad).

This approach, based on the linear wave model, is now an almost common procedure and it has been recognised that it works reasonably well for the so-called "operational" conditions. The advantages related to the assumption of linearity are enormous and the method is widely accepted.

On the other hand, it is also recognised that the predictions in the so-called "survival" conditions, i.e. extreme wave conditions with very low occurrence probability, cannot recast a linear approach. In particular it may happen that the maximum elevation of the components within the relevant part of the sea spectrum are almost in phase at a specific location leading to the so-called "freak" wave.

From the structural point of view and specifically for the fatigue life, the transit of a freak wave, even not breaking, at the location of a vertical pile (Gravity Based Structures) or an array of floating cylinders (Tension Leg Platforms), can cause the dangerous ringing phenomenon, i.e. the large amplification in few cycles of the response of the structure at its natural frequency. This happens even if the frequency region of the spectrum where most of the energy is concentrated is well below the natural frequency of the structure. Chaplin [3] has related by lab. experiments the occurrence of ringing with the time interval between the zero-downcrossing after the freak wave crest and the next zero-upcrossing. In the same context, Chaplin [3] has shown that focused component waves behave in a fully non-linear manner in a relatively small region around the concentration point. In his experiments the maximum wave elevation is underestimated by linear predictions by 10% approximately, a non negligible amount of energy is (not permanently) shifted to the high frequency range, well above the input spectrum, and at these new frequency components the phase speed shows an almost constant value.

Large single waves are usually strongly asymmetric. Myrhaug and Kjeldsen [4] report that " … in the same time series measured at sea the maximum wave height could deviate with 25%, depending on the choice of analysis, i.e. zero-upcrossing or zero-downcrossing analysis". Such a difference is explained in terms of strong asymmetry of the freak wave profile.

The aim of the research conducted at DINMA on large single waves in a random sea is to investigate the non-linear effects that derive from the interaction of the component waves when focusing occurs, i.e. when or where the phase between them is close to zero. A deeper knowledge of the behaviour of the flow in such extreme conditions can be extremely useful for design purposes also related to safety aspects. Moreover the controlled generation of deterministic wave groups with a given frequency content, aimed at the development of new techniques for seakeeping tests, is one of the subjects of interest in the *23rd ITTC*.

MATHEMATICAL MODEL AND NUMERICAL METHOD IN SYNTHESIS

The details of the mathematical model and of the numerical method employed for the simulations have been widely described in [5-6] so that only a synthesis is given here.

With reference to Figure 2 and according to the assumptions that the fluid is incompressible and inviscid and the flow is irrotational, the velocity potential $\phi(x,y,t)$ yields on *D*. The continuity equation can thus be written as an integral equation

$$\int_{\partial D} \frac{\partial G(\boldsymbol{P},\boldsymbol{Q})}{\partial n}\phi(\boldsymbol{Q})ds - \int_{\partial D} G(\boldsymbol{P},\boldsymbol{Q})\frac{\partial \phi(\boldsymbol{Q})}{\partial n}ds = -\Omega(\boldsymbol{P})\phi(\boldsymbol{P})$$

The free surface profile is assumed single valued $y = \eta(x,t)$ and the fully nonlinear free surface conditions on it become

$$\begin{cases} \dfrac{d\phi}{dt} = -\dfrac{1}{2}(\nabla\phi)^2 - g\eta + \dfrac{\partial\phi}{\partial y}\left(\dfrac{\partial\phi}{\partial y} - \dfrac{\partial\phi}{\partial x}\cdot\dfrac{\partial\eta}{\partial x}\right) - \nu(x)\cdot\phi \\ \dfrac{d\eta}{dt} = \dfrac{\partial\phi}{\partial y} - \dfrac{\partial\phi}{\partial x}\cdot\dfrac{\partial\eta}{\partial x} - \nu(x)\cdot\eta \end{cases}$$

where $\nu(x)$ is the damping factor used at the numerical beach.

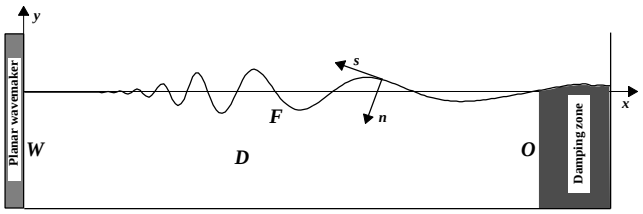

Figure 2. Schematic representation of a numerical 2D wave tank.

As far as the numerical scheme is concerned, Green's equation appropriately modified to include the symmetry condition given by the flat bottom of the tank, is solved by a constant panel method. The time stepping scheme is a 4th order Runge-Kutta method and regridding without smoothing is applied on the whole boundary.

WAVEMAKER MOTION FOR WAVE FOCUSING

Wave-wave interaction at focusing is a strongly nonlinear phenomenon. This mainly regards the dispersion relation, the phase speed and the wave amplitude. Moreover new component waves appear from the interaction of the input frequencies. These nonlinear phenomena have been shown by lab experiments [2, 7-9] and will be highlighted by the results presented here.

The departure from the linear behaviour of the input wave components must be taken into account in the wavemaker control signal since linear wave theory can give inaccurate estimates of the phase speed [3]: a phase shift is systematically observed in the simulations, the largest one occurring at the highest frequencies in the input spectrum.

In this study, linear theory is used for a preliminary estimate of the wavemaker driving signal. The time series at the focusing station is then analysed by means of an FFT and the phase lag detected (it should be zero for perfect focusing!) is used at the wavemaker in a further run. The procedure is repeated until the desired convergence is achieved. In the following this procedure is referred as "phase lag refinement". Furthermore the position of the focusing station in the flume and the start-up time of each frequency component is selected in order to get a useful space and time window at focusing without beach reflections and evanescent modes induced by the wavemaker [10]. Details of this iterative method can be found in [5].

RESULTS

In the following reference is made to the shortest wavelength in the adopted spectrum. The results presented refer to $N_{freq} = 34$ different input frequencies w_i equally spaced in the nondimensional range $\frac{24}{57} \le \omega_i \le 1, \quad i = 1, N_{freq}$, the wave basin is 80 wavelengths long and the relative depth is $d = 0.525$. The focusing station is at $\hat{x} = 12$.

The amplitude spectrum used is such that the steepness of each input wave is always the same and no breaking occurs; it results $\left(\frac{H}{\lambda}\right)_i = \frac{1}{715}$. Figure 3 shows the amplitudes α_{0_i} of the frequency components of the angular motion of a flap wavemaker with rotation axis at the bottom of the tank .

Fig. 4 shows the contour plot of the amplitude spectrum of the wave elevation as a function of the coordinate x along the tank and of the frequency ω. x is varied in the range $7 \le x \le 27$. Fig. 5 shows the intersection of the surface given in Fig. 4 at the focusing station $x = \hat{x} = 12$. It can be seen that the effect of the nonlinear wave-wave interaction on the space variation of the amplitude spectrum results in an almost smooth shift of the energy towards the high frequency range ($\omega > 1$) for $x \le \hat{x}$ whereas an opposite behaviour appears after focusing for $x \ge \hat{x}$. This means that new high frequency components are generated by the focusing process in a relatively small region. This result is strongly supported by experimental ones obtained by Chaplin [3] and shown in Fig. 6. Moreover a non negligible and stable amount of energy can be observed in Fig. 4 for $x > 12$ in the low frequency range, clearly shown even in Fig. 5. It must be observed that the first seiching mode of the basin occurs at a very low nondimensional frequency w=0.0014.

This has been observed also by Tick [11], who developed a perturbative model for random waves. He used a Neumann-type spectrum with a 6 power dependence. His results show that the second order correction to the frequency spectrum exhibits a peak located at approximately twice the frequency of the first order peak and moreover a low frequency contribution appears at frequencies well below the first order spectrum.

Further aspects about the nonlinearities involved can be derived from Fig. 7 where the wave profiles at focusing from the linear and nonlinear simulation, with and without phase lag refinement, are reported. Both wave crests from nonlinear simulations exceed the maximum elevation of the linear wave by a factor 1.3 approx. and the wave profile without phase lag refinement shows an evident vertical asymmetry with a greater slope on the front side with the peak located at a greater distance from the wavemaker.

Finally, the phase speed of the component waves has been computed at the stations $x = 10$, $x = \hat{x} = 12$ (focusing) and $x = 14$ respectively. Fig. 8a-c show the computed nondimensional results (phase speed divided by the linear phase speed of the shortest wave component in the input band) as a function of frequency ω (dots). Solid lines represent the linear phase speeds C, $0.5C$ and $2C$ respectively. From these graphs it can be clearly seen that away from focusing at $x = 10$, $x = 14$ and within the input frequency range the wave celerity behaves in good accordance with linear theory whereas the higher order wave components travel according to the nonlinear effects. At focusing and within input frequency range the celerity is slightly above the linear prediction and the higher order wave components have an almost constant phase speed. This means that the imposed coalescence of in-phase wave components makes the main features of the resulting freak wave dominant in almost the whole spectrum. A similar behaviour has been clearly observed in the experiments by Chaplin [3] shown in Fig. 9. His results derive from time series obtained linking 16 different time series in order to detect intermediate frequencies, if any. His analysis shows that most of the energy content is restricted to the input frequencies and their multiple.

CONCLUSIONS

In this study some effects of the interaction between wave components in a given spectrum have been analysed in the frame of the so-called fully nonlinear numerical wave tank approach. The basic features of the wave interaction for the test case here studied can be summarised in an amplification by a factor 1.3 of the wave height compared to the linear superposition with $\frac{H_{focus}}{H_{1/3}} \approx 3.3$, in a space variation of the spectrum around the focusing station with a non-permanent energy shift in the high frequency range and a more stable energy shift in the low frequency range. Furthermore the strong wave grouping at focusing leads to a slightly higher phase speed within the input range and an almost constant value at higher frequencies. Most of the conclusions here derived are well supported by similar results obtained on an experimental basis.

ACKNOWLEDGEMENTS

This research has been supported by CNR – National Research Council in the frame of the National Strategic Project "Innovative Criteria for Design and Management of Marine and Offshore Systems in the Mediterranean" and by MURST 60%, 2001 "Studio nel dominio del tempo dell'interazione onde-strutture marine in presenza di frontiera libera non-lineare".

REFERENCES

[1] Kjeldsen SP. A sudden disaster – in extreme waves. Proc. Rogue Waves 2000, Brest, France, 2000.

[2] Clauss GF. Task-related wave groups for seakeeping tests or simulation of design storm waves. Applied Ocean Research 1999; 21: 219-234.

[3] Chaplin JR. On Frequency-Focusing Unidirectional Waves. International Journal on Offshore and Polar Engineering 1996; 6(2): 131-137.

[4] Myrhaug D, Kieldsen SP. Steepness and Asymmetry of Extreme Waves and the Highest Waves in Deep Water. Ocean Engineering 1986; 13(6): 549-568.

[5] Contento G., Codiglia R., D'Este F. Nonlinear effects in transient non-breaking waves in a closed basin. Int. Jou. Applied Ocean Research, 2001, 23(1):. 3-13.

[6] Codiglia R, Contento G, D'Este F. Wave-wave nonlinear interaction in the focusing region of large waves. In. NAV'2000 Int. Conference on Ship and Marine Research, Venice, Italy, September 2000, 2: 7.5.1 –7.5.8.

[7] Kriebel D. Simulation of Extreme Waves in a Background Random Sea. In. ISOPE'2000 Int. Conference on Ocean and Polar Engineering, Seattle, USA, May 2000, 3: 31-37.

[8] Stansberg CT. On Spectral Instabilities and Development of Nonlinearities in Propagating Deep-Water Wave Trains. ASCE, Proc. Coastal and Engineering , Venice, Italy, 1993, p. 658-671.

[9] Stansberg CT. On the Nonlinear Behaviour of Ocean Wave Groups. ASCE, Waves'97, 1998, Virginia Beach, USA, 1998, p. 1227-1241.

[10] Dean RG, Dalrymple RN. Water Wave Mechanics for Engineers and Scientists. World Scientific Advanced Series on Ocean Engineering, 1984, Prentice Hall Inc., Englewood Cliffs NJ.

[11] Tick LJ. A non-linear random model of gravity waves. International Journal of Mathematics and Mechanics 1959; 8(5): 643-652.

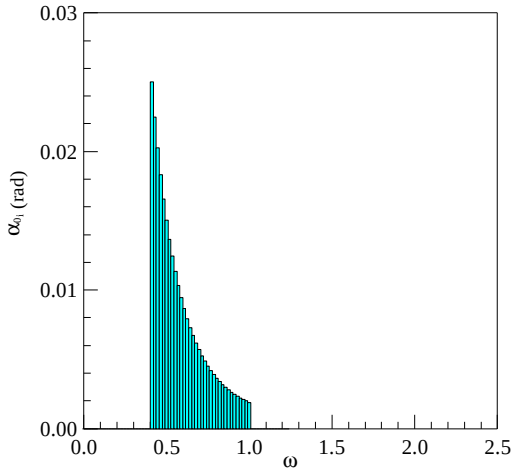

Figure 3 - Amplitudes of the frequency components of the motion of the flap-wavemaker.

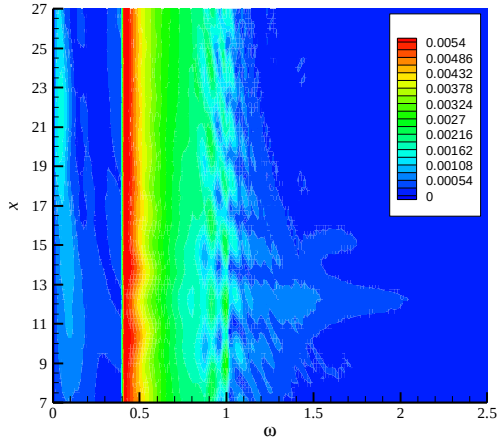

Figure 4 - Contour plot of the amplitude spectrum of the wave elevation as a function of the space coordinate *x* and of the frequency *w*. The focusing station is $\hat{x} = 12$.

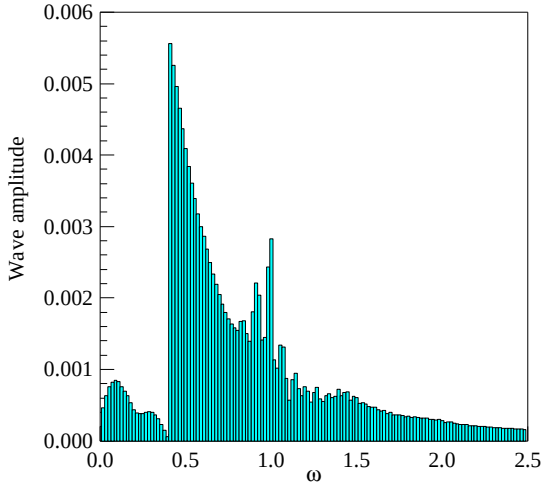

Figure 5 - Amplitude spectrum of the wave elevation at the focusing station $\hat{x} = 12$.

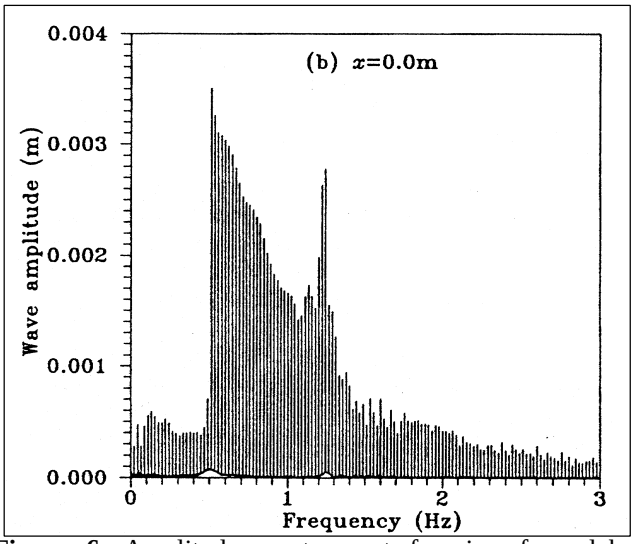

Figure 6. Amplitude spectrum at focusing from lab. experiments [Chaplin, 3].

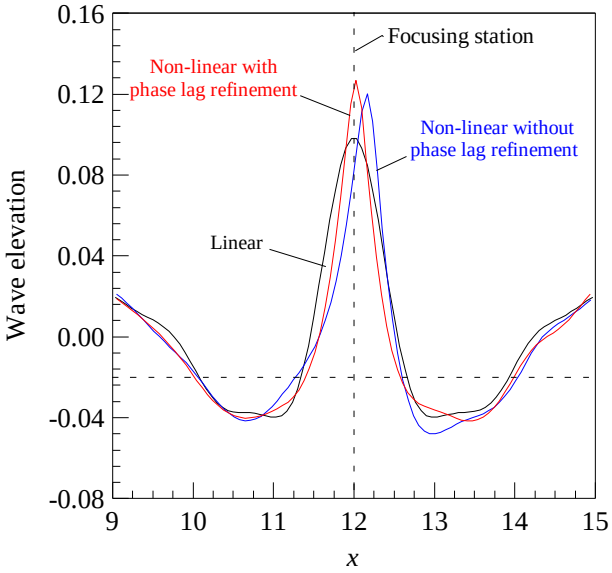

Figure 7. Wave profiles from linear (black) and nonlinear with (red) and without (blu) phase lag refinement.

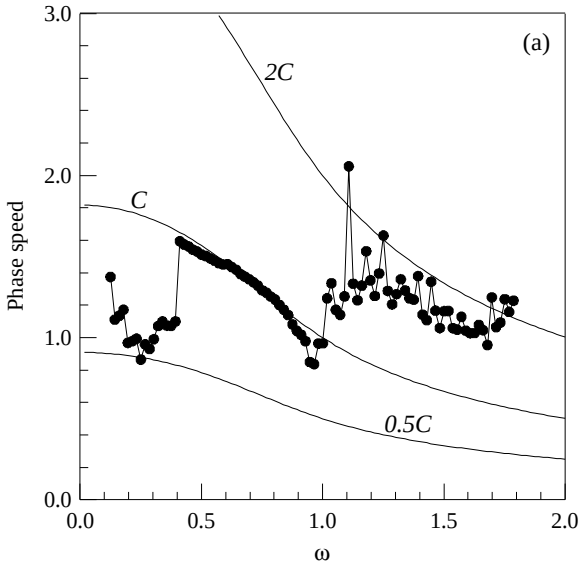

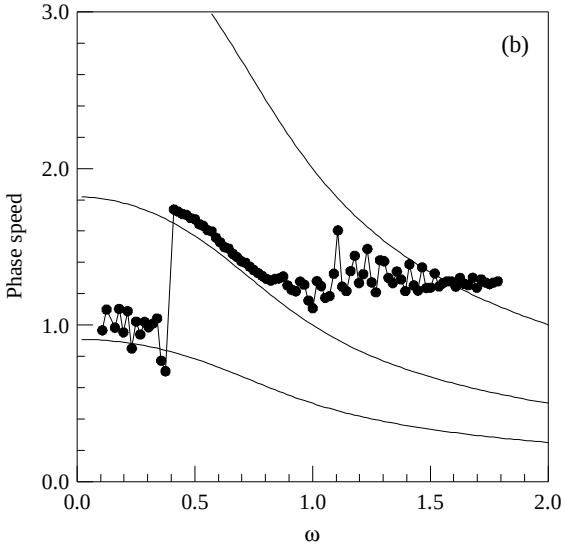

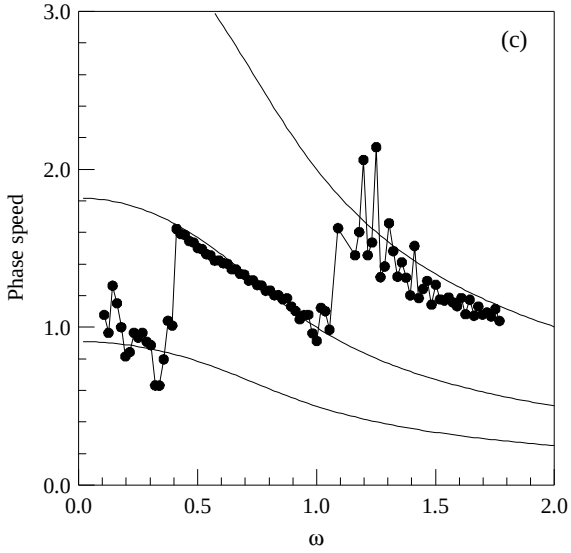

Figure 8a-c. Phase speed as a function of frequency at $x = 10$ (a), $x = \hat{x} = 12$ (b) and $x = 14$ (c). Solid lines represent the linear phase speed C, $0.5C$ and $2C$ respectively

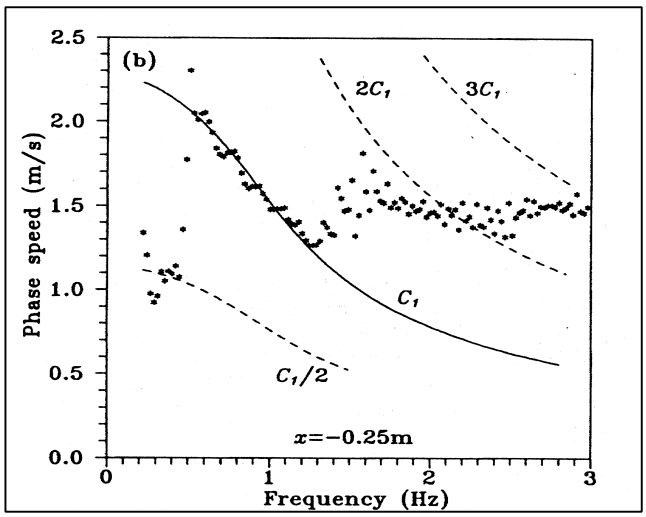

Figure 9. Phase speed at focusing as a function of frequency [Chaplin, 3].

Benchmark Testing of Numerical Prediction on Capsizing of Intact Ships in Following and Quartering Seas

Naoya UMEDA, Department of Naval Architecture and Ocean Engineering, Osaka University,
2-1 Yamadaoka, Suita, Osaka, 565-0871, Japan
umeda@naoe.eng.osaka-u.ac.jp
Martin R RENILSON, Australian Maritime College,
Now at: QinetiQ Haslar, Gosport, Hampshire, PO12 2AG, United Kingdom
MRRenilson@QinetiQ.com

SUMMARY

This paper describes results of the ITTC benchmark testing of intact stability. For these tests, a container ship and a fishing vessel were selected and their hull forms, captive test data and results of capsizing model experiments were provided in advance. Then eight research organisations submitted their own numerical results. By comparing with the experimental results, it was found that some numerical models are able to qualitatively well predict extreme motions, which include capsizing due to parametric resonance and due to broaching. Moreover, the importance of several elements for capsize prediction is noted by mutual comparisons of numerical studies.

1. INTRODUCTION

Responding the reduction of acceptable risk level for safety of lives at sea, performance-based criteria, which may require model experiments to guarantee the safety, are often under discussion at the International Maritime Organisation (IMO) instead of rule-based criteria. For the performance-based criterion, numerical prediction is required before expensive model experiments. However, a standard numerical prediction technique for capsizing has not yet been established. Therefore, in 1999 the International Towing Tank Conference (ITTC)[1] organised a specialist committee for this purpose and planned benchmark testing of numerical predictions with selected data from free running model experiments. For intact stability eight organisations took part in this benchmark testing. This paper summarises the results of these benchmark tests and examines the importance of several elements for numerical prediction of capsizing.

2. FRAMEWORK OF ITTC BENCHMARK TESTING

In the intact benchmark testing programme, two sets of free running model experiments were utilised. The first set was carried out with a 1/60 scaled model of a 15000 gross tonnes container ship (Ship A-1) at the seakeeping and manoeuvring basin of the Ship Research Institute by Hamamoto et al.[2] Here the ship model capsized mainly due to parametric resonance in the lower speed region. The second set was carried out with a 1/15 scaled model of a 135 gross tonnes purse seiner (Ship A-2) at the seakeeping and manoeuvring basin of the National Research Institute of Fisheries Engineering (NRIFE) by Umeda et al.[3] Here the model capsized mainly due to broaching in the higher speed region. The principal particulars and body plans of these ships are shown in Table 1 and Figs 1-2. In the experiment each ship model was steered on a specified course using auto pilot in regular following and quartering waves. They were self-propelled and completely free from any restraints. The angular velocities and angles were measured using an optical gyroscope, and were recorded by an onboard computer. The reference system used in this paper is shown in Fig. 3.

Among the several hundreds of model runs, four runs for each ship were selected for the ITTC benchmark tests as shown in Tables 2-3. Here the nominal Froude number, Fn, and the auto pilot course from the wave direction, χ_c, are control parameters and the wave height, H, and wave length, λ, are the wave parameters. The initial values of ship motions were specified based on measured data except for the sway velocity, which was assumed to be zero because of the limitation of the measurements.

For ships A-1 and A-2, the captive model experiments, e.g. resistance test, self-propulsion test, propeller open test, circular motion tests (CMT), roll decay test and so on, were carried out mainly in NRIFE's seakeeping and manoeuvring basin using an X-Y towing carriage. These data together with hull offset data and the above-mentioned initial values were provided in advance for the participating organisations.

3. RESULTS

The ITTC benchmark test programme for intact stability commenced in March of 2000 and the following organisations submitted their own numerical results by the deadline, March of 2001. For Ship A-1: Flensburger Schiffbau Gesellschaft (attn. Ms. Heike Cramer); Helsinki University of Technology (attn. Prof. J. Matusiak); Maritime Research Institute Netherlands, (attn. Dr. J. O. de Kat); Osaka University (attn. Dr. N. Umeda); Technology University of Malaysia (attn. Dr. A. Maimun); University of Strathclyde (attn. Prof. D. Vassalos) and University of Tokyo (attn. Prof. M. Fujino) participated. For Ship A-2: Memorial University of Newfoundland

(attn. Prof. D. Bass); Osaka University (attn. Dr. N. Umeda) and University of Strathclyde (attn. Prof. D. Vassalos) did. Numerical prediction methods used by the above organisations were summarised in the Appendix and numerical results were shown in Figs. 4-6 with the experimental results. Based on the agreement with the participating organisations, throughout this benchmark programme the results have been presented anonymously. Thus the code used in this paper is not relevant to the above order of organisation names.

Table 1 Principal particulars of the ships.

Items	*Ship A-1*	*Ship A-2*
length : L_{pp}	150.0 m	34.5 m
breadth : B	27.2 m	7.60 m
depth : D	13.5 m	3.07 m
draught at FP : T_f	8.5 m	2.50 m
mean draught : T	8.5 m	2.65 m
draught at AP : T_a	8.5 m	2.80 m
block coefficient : C_b	0.667	0.597
pitch radius of gyration : $\square_{yy}/L_{pp}$	0.244	0.302
longitudinal position of centre of gravity from the midship : x_{CG}	1.01 m aft	1.31 m aft
metacentric height : GM	0.15 m	1.00 m
natural roll period : $T_{\square}$	43.3 s	7.4 s
rudder area : A_R	28.11 m^2	3.49 m^2
propeller diameter : D_P	5.04 m	2.60 m
time constant of steering gear : T_E	1.24 s	0.63 s
proportional gain: K_R	1.2	1.0
differential gain: $K_R T_D$	53.0 s	0.0 s

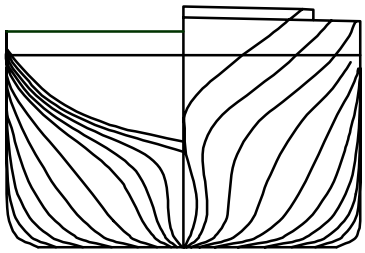

Fig. 1 Body plan of Ship A-1.

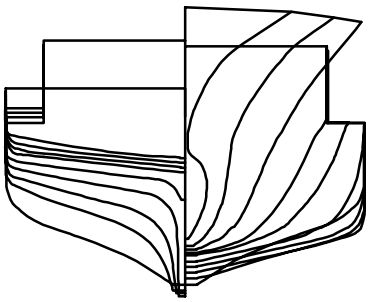

Fig. 2 Body plan of Ship A-2.

The numerical predictions are firstly required to qualitatively agree with the model experiments. Thus, qualitative nature of the results obtained from the experiments and the numerical calculations are overviewed in Tables 4-5. This nature includes capsize, non-capsize, harmonic roll, sub-harmonic roll, surf-riding and broaching. Here as a judging criterion of broaching the authors' proposal[4] is used. That is, broaching is a phenomenon in which both the yaw angle and yaw angular velocity increase despite the maximum opposite rudder angle. The cases where the numerical result does not qualitatively agree with the experimental one are identified with shading.

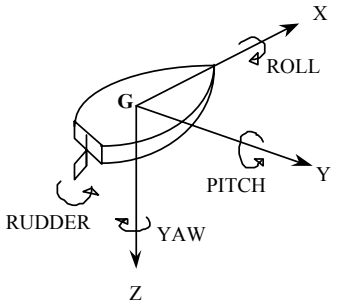

Fig. 3 Reference system.

Table 2 Calculated conditions for Ship A-1.

	H/λ	λ/L_{pp}	Fn	χ_c
(a)	1/25	1.5	0.2	0 degrees
(b)	1/25	1.5	0.2	45 degrees
(c)	1/25	1.5	0.3	30 degrees
(d)	1/25	1.5	0.4	30 degrees

Table 3 Calculated conditions for Ship A-2.

	H/λ	λ/L_{pp}	Fn	χ_c
(a)	1/10	1.637	0.3	-30 degrees
(b)	1/10	1.637	0.43	-10 degrees
(c)	1/8.7	1.127	0.3	-30 degrees
(d)	1/8.7	1.127	0.43	-30 degrees

4. DISCUSSION

For Ship A-1 all the participating organisations used 6 degrees of freedom (DOF) models. However, only Organisation-A submitted results that qualitatively agree with the experiments. Organisation-A calculated radiation and diffraction forces using a strip theory and dealt with manoeuvring forces by the MMG model, utilizing a body coordinate system. It evaluated the Froude-Krylov forces, including roll restoring moment in waves, by integrating incident wave pressure up to the instantaneous water surfaces. With this numerical model, capsizing with sub-harmonic rolling in case (a) and capsizing with harmonic rolling in case (d) were well predicted.

Organisation-G also shows similar agreement but results in capsizing with harmonic rolling in case (a),

which was not observed in the corresponding experiment. The method used here is almost the same as Organisation-A except for radiation and diffraction modelling.

Organisation-E has difficulties in the prediction of the heading angle. In some cases the ship course is changed to bow sea and then a completely different situation occurs. This model is different from the above two organisations in some elements. The radiation forces were calculated using a 3D Green function method with hydrodynamic memory effect. The manoeuvring forces, roll damping moments, resistance and propulsion forces were estimated with databases instead of the captive test data provided.

Table 4 Overview of qualitative results for Ship A-1*.

	exp.	*A.*	*B*	*C*
(a)	cap. (s)	cap. (s)	cap. (h)	no roll
(b)	(s)	(s)	(s)	N/A
(c)	(h)	(h)	N/A	N/A
(d)	cap. (h)	cap. (h)	N/A	N/A

	D.	*E.*	*F*	*G*
(a)	(s)	cap. (s)	cap. (h)	cap. (h)
(b)	cap.(h)	(h)	(h)	(s)
(c)	(h)	cap.	cap.	(h)
(d)	(h)	cap.	cap.	cap. (h)

*Here (h) and (s) mean harmonic and sub-harmonic roll motions, respectively. *cap*. indicates capsizing.

Table 5 Overview of qualitative results for Ship A-2*.

	exp.	*A.*	*B*	*C*
(a)	non-cap	non-cap	non-cap	non-cap
(b)	surf,broach, cap.	surf,broach, cap.	cap.	cap
(c)	non-cap	non-cap	non-cap	non-cap
(d)	cap.	cap.	cap.	cap.

*Here surf and broach mean surf-riding and broaching, respectively.

The method used by Organisation-B is based on a conventional seakeeping approach. That is, the heave, pitch, sway and yaw are assumed to be linear around the averaged course. This organisation reported that this method is not able to calculate the ship runs with a Froude number of 0.3 and over. Organisation-D proposed a method to avoid such the limitation of the seakeeping model by a two-stage approach. Here the motions are assumed to be the sum of linear parts with hydrodynamic memory effect and nonlinear ones. This means that the linear motion was calculated around the instantaneous heading angle instead of the auto pilot course. The agreement between the experiment and this calculation is not so satisfactory. This may be partly because the initial values were different from the specified ones to take the memory effect into account. Organisation-F is a unique example ignoring diffraction forces but the results do not agree well with those from the experiment. In particular, the calculated pitch amplitude is much larger than the measured one.

CFD application to the present problem was attempted by Organisation-C, which had succeeded in several seakeeping predictions. Here the Euer equation was solved by a finite difference method with fully nonlinear free surface and body surface conditions. However, it can provide a solution only for case (a) without lateral motions. If the specified initial values for lateral motions are input, even for case (a) the calculation process failed. In addition, it cannot deal with cases (b), (c) and (d), in which the desired heading angles are not zero. This fact demonstrates that the CFD approach is not yet appropriate for practical use in capsize prediction.

For Ship A-2, only Organisation-A obtained qualitative agreement with the experiment. Here a 4 DOF model was used by assuming that heave and pitch motions trace their static equilibria, which are calculated as the limit of solution sets of a strip theory at zero encounter frequency. The manoeuvring forces were estimated with the MMG model and the wave-induced forces, including hydrodynamic lift due to wave fluid velocity, were calculated with Ohkusu's slender body theory. The wave effects of both the roll restoring moment and the manoeuvring forces were ignored as higher order terms. As a result, this organisation succeeded in predicting capsizing due to broaching associated with surf-riding as well as periodic motions.

Organisation-C used the method that is almost similar to Organisation-A but the nonlinear terms in the manoeuvring models, those of the Froude-Krylov forces and the radiation forces were added. For case (b) it predicted capsizing without surf-riding and with a smaller rudder angle compared to the results from the experiment and those predicted by Organisation-A.

Organisation-B applies a 6 DOF model in which radiation and diffraction were calculated with the 3D Green function for zero forward velocity. Here the change of roll restoring moment due to waves was taken into account but the hydrodynamic lift due to wave fluid velocity was ignored. The hydrodynamic memory effect was included in this calculation, although the initial values were not exactly equal to the specified one. While the predictions of mean yaw angle for cases (a), (c) and (d) are better than those from the other organisations, the predicted rudder angle for case (b) is smaller than the experimental results.

As a whole, these three organisations predicted the results relatively well compared to the experiments for Ship A-2, however, this does not mean that prediction of broaching is easier, because some organisations did not include their own results.

5. SEVERAL ELEMENTS AFFECTING PREDICTION ACCURACY

As mentioned above, the mathematical models for capsizing prediction cover so many elements and there is no guideline which elements should be taken into account.

Mutual comparisons among the organisations do not easily clarify the importance of each particular element because more than two elements are often different from one organisation to another. Therefore, this paper reviews comparative studies of numerical simulations with and without each particular element for Ships A-1 and A-2.

6 DOF vs. 4 DOF or 1 DOF

Although all organisations submitted results with 6 DOF models for Ship A-1, many theoretical studies with 1 DOF models can be found for capsizing due to parametric rolling. Munif [5] estimated the capsizing boundaries for Ship A-1 with a 1 DOF model, a 4 DOF model ignoring heave and pitch motions (4 DOF A model), a 4 DOF model with static equilibria of heave and pitch motions (4 DOF B model) and a 6 DOF model, as shown in Fig. 7. Here the first three models were obtained by simplifying the 6 DOF model. As a result, the following conclusions were made. (1) The 1 DOF model overestimates capsizing danger. (2) The difference between the 4 DOF A model and the 6 DOF model can be significant. (3) The results from the 4 DOF B model almost agree with those from the 6 DOF model and the experiment. The reason for the small difference between the 4 DOF B model and the 6 DOF model is that the natural frequency of heave and pitch motions is far from the encounter frequency in case of ship runs in following and quartering seas.[6]

Memory effect

It is well known that the linear transient motions of a ship with frequency-dependent hydrodynamic forces can be calculated using the convolution integral for hydrodynamic memory effect. However, it is not so clear for capsizing prediction whether the hydrodynamic memory effect should be taken into account or not. This is because an extreme motion leading to capsizing is nonlinear and the hydrodynamic forces acting on a ship running in following and quartering seas do not significantly depend on the encounter frequency.

Hamamoto and Saito[7] carried out a comparative study for a container ship in following seas with and without the memory effect in heave and pitch motions. They concluded that no significant difference exists if the added mass and damping coefficients are calculated for the natural frequency of heave and pitch motions. For the present workshop, Matusiak[8] investigated this problem and concluded that the memory effect can improve the agreement with the experiment for Ship A-1. Here it is noteworthy that exact calculation with memory effect should be carried out from the start of the waves. Thus the present benchmark testing, which does not specify the initial conditions of the fluid motions, is not appropriate for this purpose.

Manoeuvring coefficients

In ship runs in following and quartering waves, prediction of manoeuvring coefficients is important because hydrodynamic lift is dominant. The first question here is whether the effect of nonlinear terms of manoeuvring forces on capsizing prediction is important or not. For Ship A-2, Umeda et al.[9] calculated time series with these nonlinear terms and without them and concluded that the effect of nonlinear terms is negligibly small, as shown in Fig.8. This is because the sway velocity and yaw angular velocity non-dimensionalised with the higher forward velocity are not large even during the process of broaching.

The next problem is the wave effect on the linear manoeuvring coefficients. This problem has been discussed for many years but its effect on capsizing prediction has not yet been fully investigated. Therefore, Hashimoto and Umeda[10] tackled this problem with Ship A-2 for the present workshop. Their main conclusion is that the effect of the waves on the derivatives of manoeuvring forces with respect to the sway velocity can be important.

Nonlinearity in yaw

In a seakeeping theory, ship motions, such as yaw, are often linearised around the inertia system moving with the averaged speed and course of a ship. On the other hand, ship motions are described with a body fixed coordinate system in the field of manoeuvring. Recently Hamamoto [11] introduced a horizontal body coordinate system, which is body fixed but not allowed to roll. At the present workshop, Cramer [12] reported the effect of linearisation of yaw motion with an inertia coordinate system.

Other elements to be examined can be listed as follows:

- wave effect on roll restoring moment
- hydrodynamic lift due to wave fluid velocity[13]
- 3D effect of hydrodynamic forces
- modelling roll damping moment[13]
- roll-yaw coupling[14]
- coupling effect from heave and pitch motions
- trapped water on deck.

Cramer [12] referred to the applicability of numerical models to short-crested irregular waves. Although the capsizing model experiments for Ship A-1 were carried out in both long-crested and short-crested irregular waves [15], the benchmark testing programme deals with only the case in long-crested regular waves. Recently Sera and Umeda [16] executed numerical calculation in short-crested irregular waves with a 1 DOF model, and confirmed the qualitative conclusion, from the experiments, that wave short-crestedness reduces capsizing danger.

6. CONCLUSIONS

As a result of benchmark testing of intact stability, it was found that some numerical models can qualitatively predict capsizing due to parametric resonance and that due to broaching in the limited cases tested. For improving quantitative prediction accuracy further, it is essential that several elements should be examined by comparative studies with and without these elements. For wider validation studies, it is desirable to execute benchmark

tests in capsizing boundary curves as shown in Fig. 7 for Ship A-1.

7. ACKNOWLEDGEMENTS

The authors are grateful to all eight organisations participating this benchmark testing programme and Professor D. Vassalos, the chairman of the ITTC specialist committee on prediction of extreme motions and capsizing. The authors acknowledge effective assistance of Mr. H. Hashimoto, a graduate student of Osaka University. This work was supported by a Grant-in-Aid for Scientific Research of the Ministry of Education, Culture, Sports, Science and Technology of Japan (No. 13555270).

8. REFERENCES

1. The Specialist Committee on Stability (1999) Final Report and Recommendation to the 22nd ITTC, In: Proceeding of the 22nd International Towing Tank Conference, Seoul and Shanghai, 2 : 399-431.
2. Hamamoto, M., T. Enomoto, et al. (1996) Model Experiment of Ship Capsize in Astern Seas -2nd Report-, J Soc Nav Archit Japan, 179 : 77-87.
3. Umeda, N., A. Matsuda et al. (1999) Stability Assessment for Intact Ships in the Light of Model Experiments, J Mar Sci Technol, 4 : 45-57.
4. Umeda, N., A. Matsuda and M. Takagi : (1999) Model Experiment on Anti-Broaching Steering System, J Soc Nav Archit Japan, 185 : 41-48.
5. Munif, A. (2000) Numerical Modeling on Extreme Motions and Capsizing of an Intact Ship in Following and Quartering Seas, Doctor Thesis, Osaka University.
6. Matsuda, A., N. Umeda and S. Suzuki (1997) Vertical Motions of a Ship Running in Following and Quartering Seas, J Kansai Soc Nav Archit, 227 : 47-55, (in Japanese).
7. Hamamoto, M. and K. Saito (1992) Time Domain Analysis of Ship Motions in Following Waves, In : Proceeding of the 11th Australian Fluid Mechanics Conference, Hobart, 1:355-358.
8. Matusiak, J. (2001) Importance of Memory Effect for Capsizing Prediction, In : Proceedings of the 5th International Workshop on Stability and Operational Safety of Ships, Trieste.
9. Umeda, N., A. Munif and H. Hashimoto (2000) Numerical Prediction of Extreme Motions and Capsizing for Intact Ships in Following / Quartering Seas, In : Proceeding of the 4th Osaka Colloquium on Seakeeping Performance of Ships, Osaka, 368-373.
10. Hashimoto, H. and N. Umeda (2001) Importance of Wave Effects on Manoeuvring Coefficients for Capsizing Prediction, In : Proceedings of the 5th International Workshop on Stability and Operational Safety of Ships, Trieste.
11. Hamamoto, M., and Y.S. Kim (1993) A New Coordinate System and the Equations Describing Manoeuvring Motions of a Ship in Waves, J Soc Nav Archit Japan, 173 : 209-220, (in Japanese).
12. Cramer, H. (2001) Effect of Non-Linearity in Yaw Motion on Capsizing Prediction, In: Proceedings of the 5th International Workshop on Stability and Operational Safety of Ships, Trieste.
13. Umeda, N. (2000) Effects of Some Seakeeping/ Manoeuvring Aspects on Broaching in Quartering Seas, In: "Contemporary Ideas on Ship Stability", Elsevier Science Publications (Amsterdam), 423-433.
14. Renilson, M.,R. and T. Manwarring (2000) An Investigation into Roll/Yaw Coupling and Its Effect on Vessel Motions in Following and Quartering Seas, In: Proceedings of the 7th International Conference on Stability of Ships and Ocean Vehicles, Launceston, A:452-459.
15. Umeda, N., M. Hamamoto, Y. Takaishi et al. (1995) Model Experiments of Ship Capsize in Astern Seas. J Soc Nav Archit Japan, 177 : 207-217.
16. Sera, W. and N. Umeda (2001) Effect of Short-Crestedness of Waves on Capsize of a Container Ship in Quartering Seas, J Japan Institute of Navigation, 104: 141-146, (in Japanese).

APPENDIX

Brief descriptions on the prediction methods used by the participating organisations are as follows:

<u>Ship A-1</u>

Organisation -A

- 6 DOF model
- manoeuvring-based time-domain model
- hull radiation : linear strip theory + nonlinear axis transformation
- hull manoeuvring damping : ITTC exp data (linear and nonlinear terms)
- roll restoring: hydrostatics in waves
- roll damping: ITTC exp data + forward speed effect (empirical)
- Froude-Krylov force: nonlinear pressure integral
- diffraction force: linear strip theory + nonlinear axis transformation
- hydrodynamic lift due to wave: none
- hydrodynamic solution method: 2D multi-pole expansion method
- hydrodynamic memory effect: none
- ship resistance: ITTC exp data
- propeller thrust: ITTC exp data
- rudder force: ITTC exp data

Organisation -B

- 6 DOF model
- linear heave, pitch, sway, yaw (frequency domain) + nonlinear surge and roll (time domain)
- hull radiation : linear strip theory
- hull manoeuvring damping : none
- roll restoring: hydrostatics in waves
- roll damping: empirical formula

- Froude-Krylov force: linear strip theory
- diffraction force: linear strip theory
- hydrodynamic solution method: 2D Rankine source method
- hydrodynamic lift due to wave: none
- hydrodynamic memory effect: none
- ship resistance: ITTC exp data
- propeller thrust: none
- rudder force: none

Organisation -C
- 6 DOF model
- CFD time-domain model
- Euler equation (no viscosity)
- fully nonlinear free surface & body surface condition
- finite difference method in time domain
- fluid motion and ship motion are simultaneously solved.
- roll viscous damping: none
- ship resistance & propeller thrust: externally added
- rudder force: none
- H-H type grid (near-field 540,000 grids, far-field 2,600,000 grids)

Organisation-D
- 6 DOF model
- seakeeping-based two-stage model (linear part + nonlinear part)
- linear part (frequency domain): linear strip theory
- hydrodynamic solution method for the strip theory: Frank's close-fit method
- nonlinear part (time domain)

1) cross-coupling terms of body dynamics: included
2) nonlinear part of Froude-Krylov force & roll restoring : pressure integral up to wetted water surface
3) nonlinear parts of radiation & diffraction: none
4) hydrodynamic memory effect: included
5) hull manoeuvring damping : empirical formula
6) roll damping: critical damping ratio
7) ship resistance: ITTC exp data
8) propeller thrust: ITTC exp data
9) rudder force: empirical formula

- quadrilateral panels for hull surface

Organisation-E
- 6 DOF model
- seakeeping-based time-domain model
- hull radiation : linear 3D theory
- hull manoeuvring: semi-empirical formula for hull forces
- roll restoring: hydrostatics in waves (as part of Froude-Krylov forces)
- roll damping: semi-empirical formula (lift damping + quadratic)
- Froude-Krylov force: linear pressure integrated up to free surface
- diffraction force: linear strip theory
- hydrodynamic lift due to wave: cross-flow drag model
- hydrodynamic memory effect: included as part of wave radiation forces
- ship resistance: database for actual ship (measured or calculated)
- propeller thrust: database for actual or standard propellers
- rudder force: semi-empirical formula

Organisation-F
- 6 DOF model
- seakeeping-based time-domain model
- hull linear damping in yaw: ITTC exp data for yaw
- hull linear damping in surge, sway: values for other fishing vessel
- roll restoring: hydrostatics in waves
- roll damping: Ikeda's method
- Froude-Krylov force: nonlinear pressure integral
- diffraction force: none
- hydrodynamic lift due to wave: none
- hydrodynamic solution method: 2D Green function method
- hydrodynamic memory effect: none
- ship resistance: values for other fishing vessel
- propeller thrust: values for other fishing vessel
- rudder force: values for other fishing vessel

Organisation - G
- 6 DOF model
- manoeuvring-based time-domain model
- hull wave-making damping: Tasai's empirical formula
- hull manoeuvring damping : ITTC exp data (linear & nonlinear terms)
- roll restoring: hydrostatics in waves
- roll damping: ITTC exp data + forward speed effect (empirical)
- Froude-Krylov force: nonlinear pressure integral
- diffraction force: Ohkusu's slender body theory
- hydrodynamic lift due to wave: as end term
- hydrodynamic solution method: 2D multi-pole expansion
- hydrodynamic memory effect: none
- ship resistance: ITTC exp data
- propeller thrust: ITTC exp data
- rudder force: ITTC exp data

<u>Ship A-2</u>

Organisation -A
- 4 DOF model with static heave and pitch
- manoeuvring-based time-domain model
- hull added mass : linear slender body theory with double model flow
- hull wave-making damping: none
- hull manoeuvring damping : ITTC exp data (linear terms only)
- roll restoring: hydrostatics in calm water
- roll damping: ITTC exp data + forward speed effect (empirical)
- Froude-Krylov force: linear pressure integral

- diffraction force: Ohkusu's slender body theory
- hydrodynamic lift due to wave: as end term
- hydrodynamic solution method: 2D Green function method
- hydrodynamic memory effect: none
- ship resistance: ITTC exp data
- propeller thrust: ITTC exp data
- rudder force: ITTC exp data

Organisation -B

- 6 DOF model
- seakeeping-based time-domain model
- hull radiation : 3D Green function method (zero forward speed) + forward speed effect
- hull manoeuvring damping : empirical formula
- roll restoring: hydrostatics in waves with incident wave pressure taken into account
- roll damping: empirical formula + forward speed effect (tuning)
- Froude-Krylov force: nonlinear pressure integral
- diffraction force: 3D Green function method (zero forward speed) + forward speed effect
- hydrodynamic lift due to wave: none (no trailing vortex layer)
- hydrodynamic memory effect: included
- ship resistance: empirical formula
- propeller thrust: adjusted to realise the specified speed
- rudder force: empirical formula
- incident wave: second order Stokes wave

Organisation -C

- 4 DOF model with static heave and pitch
- manoeuvring-based time-domain model
- hull wave-making damping: included
- hull manoeuvring damping : ITTC exp data (linear & nonlinear terms)
- roll restoring: hydrostatics in calm water
- roll damping: empirical formula + forward speed effect (empirical)
- Froude-Krylov force: nonlinear pressure integral
- diffraction force: Ohkusu ㅗ s slender body theory
- hydrodynamic lift due to wave: as end term
- hydrodynamic solution method: 2D multi-pole expansion
- hydrodynamic memory effect: none
- ship resistance: ITTC exp data
- propeller thrust: ITTC exp data
- rudder force: ITTC exp data

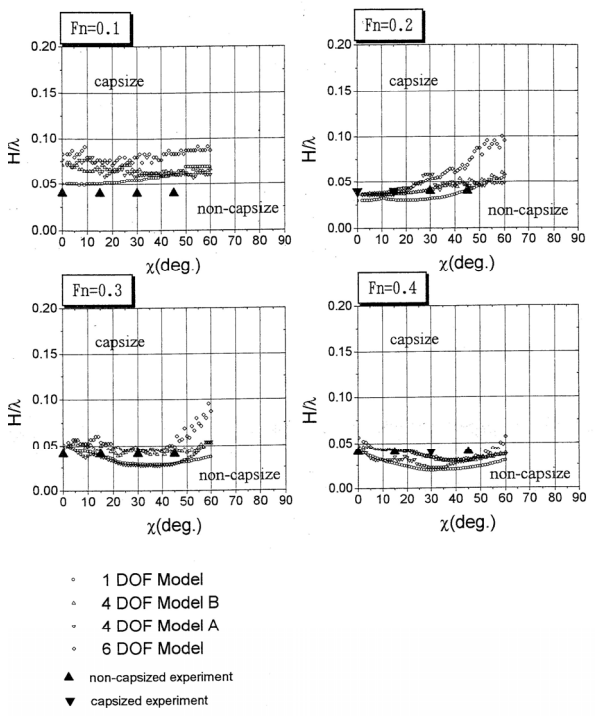

Fig. 7 Capsizing boundaries of Ship A-1 with $\lambda/L=1.5$[5]. Here χ indicates the auto pilot course.

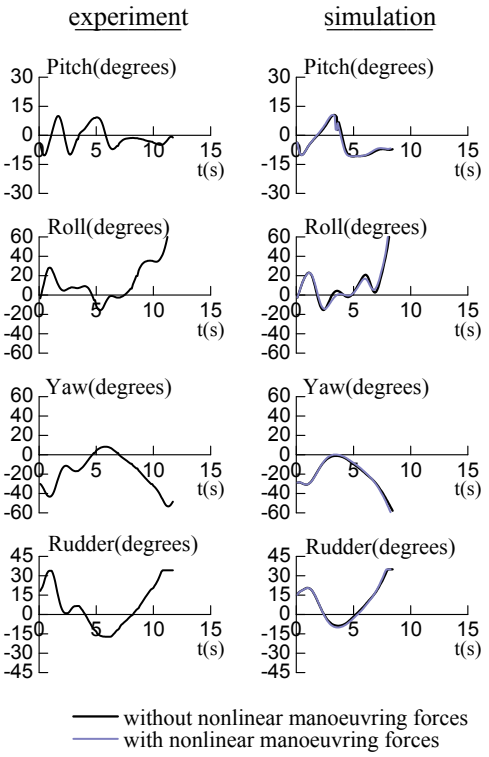

Fig. 8 Effect of nonlinear terms of monoeuvring forces on prediction for Ship A-2 at the case (b).[9]

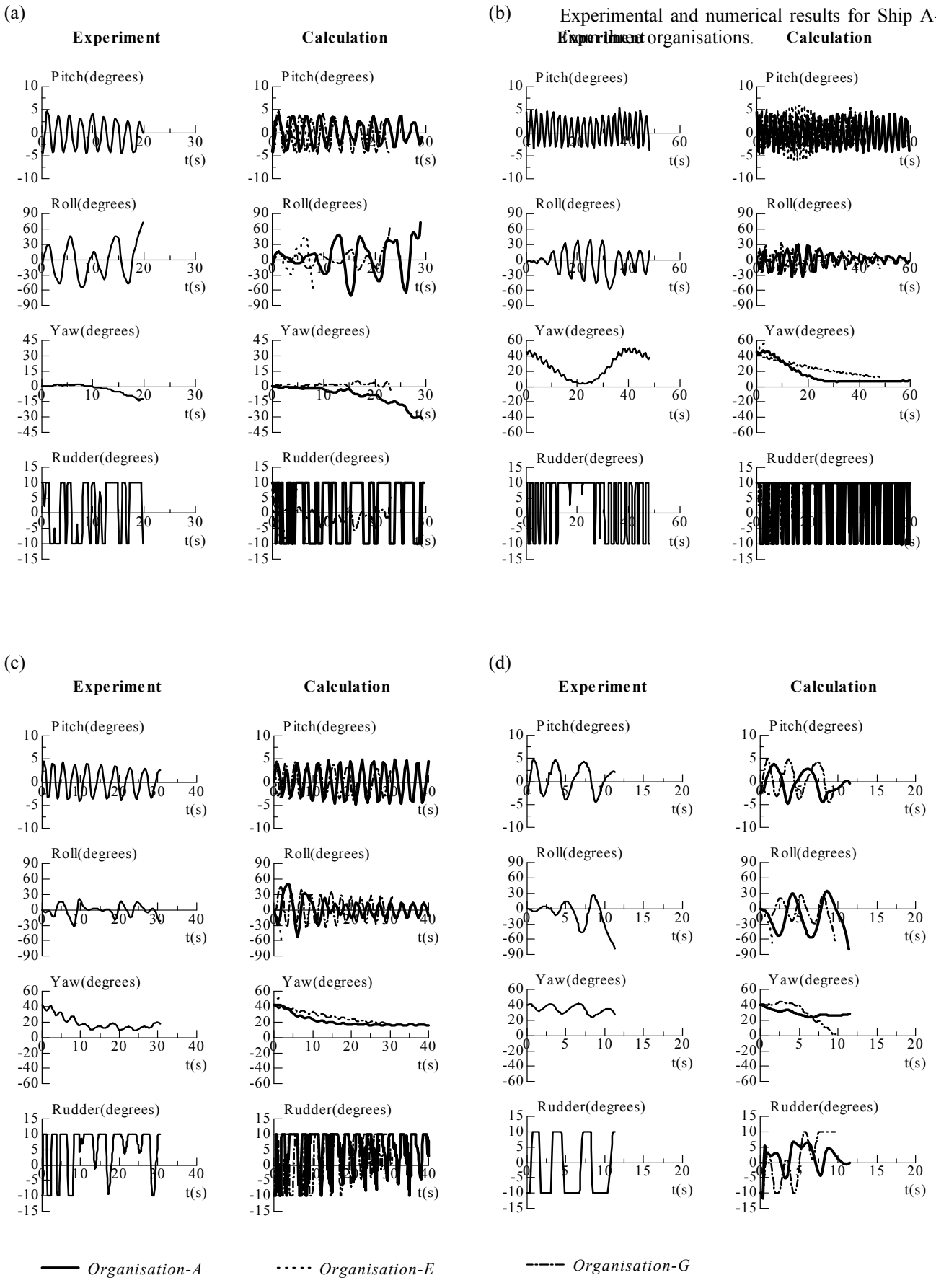

Experimental and numerical results for Ship A-1 from three organisations.

from four organisations.

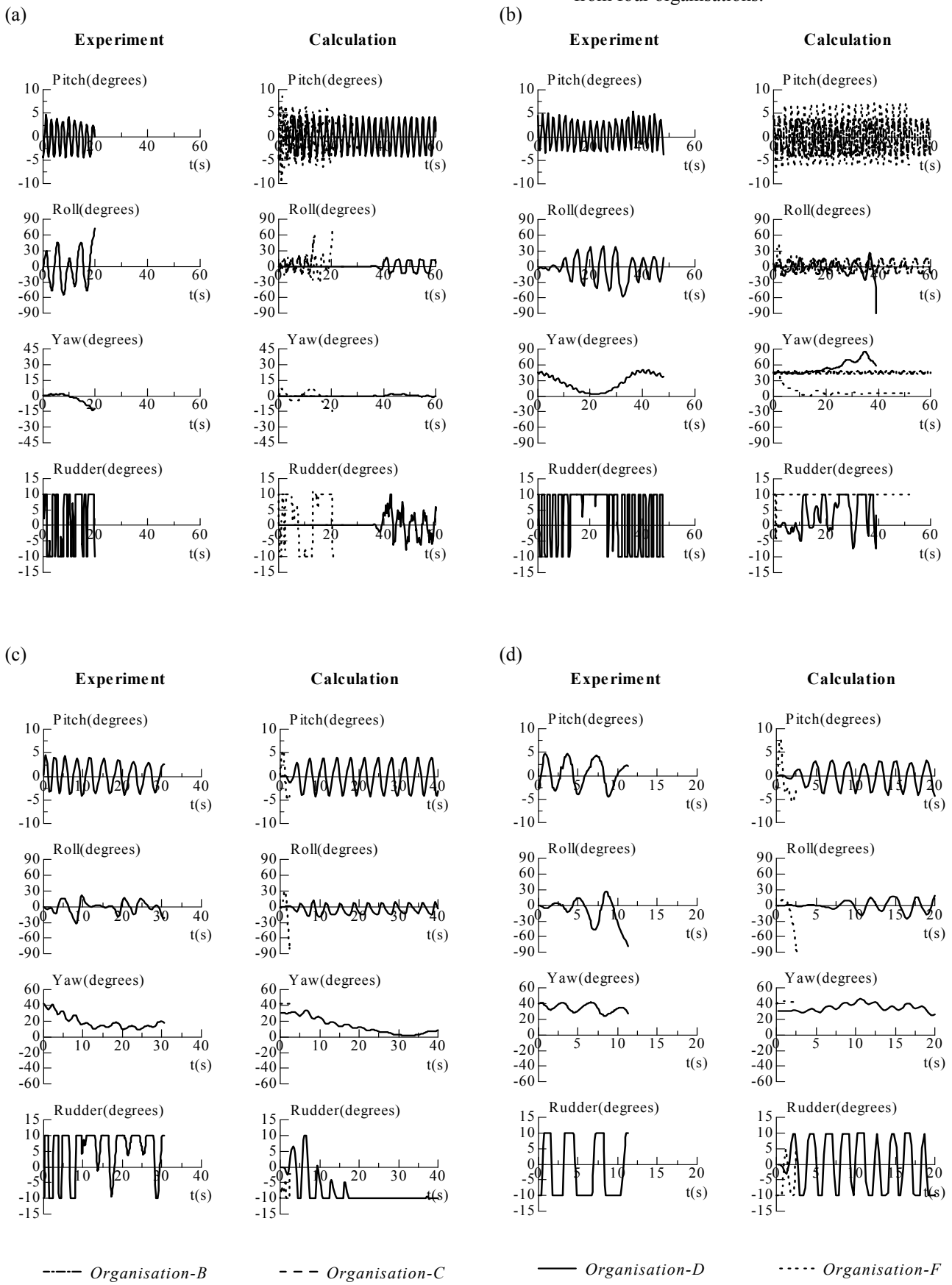

Fig. 5 Experimental and numerical results for Ship A-1

Fig. 6 Experimental and numerical results for Ship A-2.

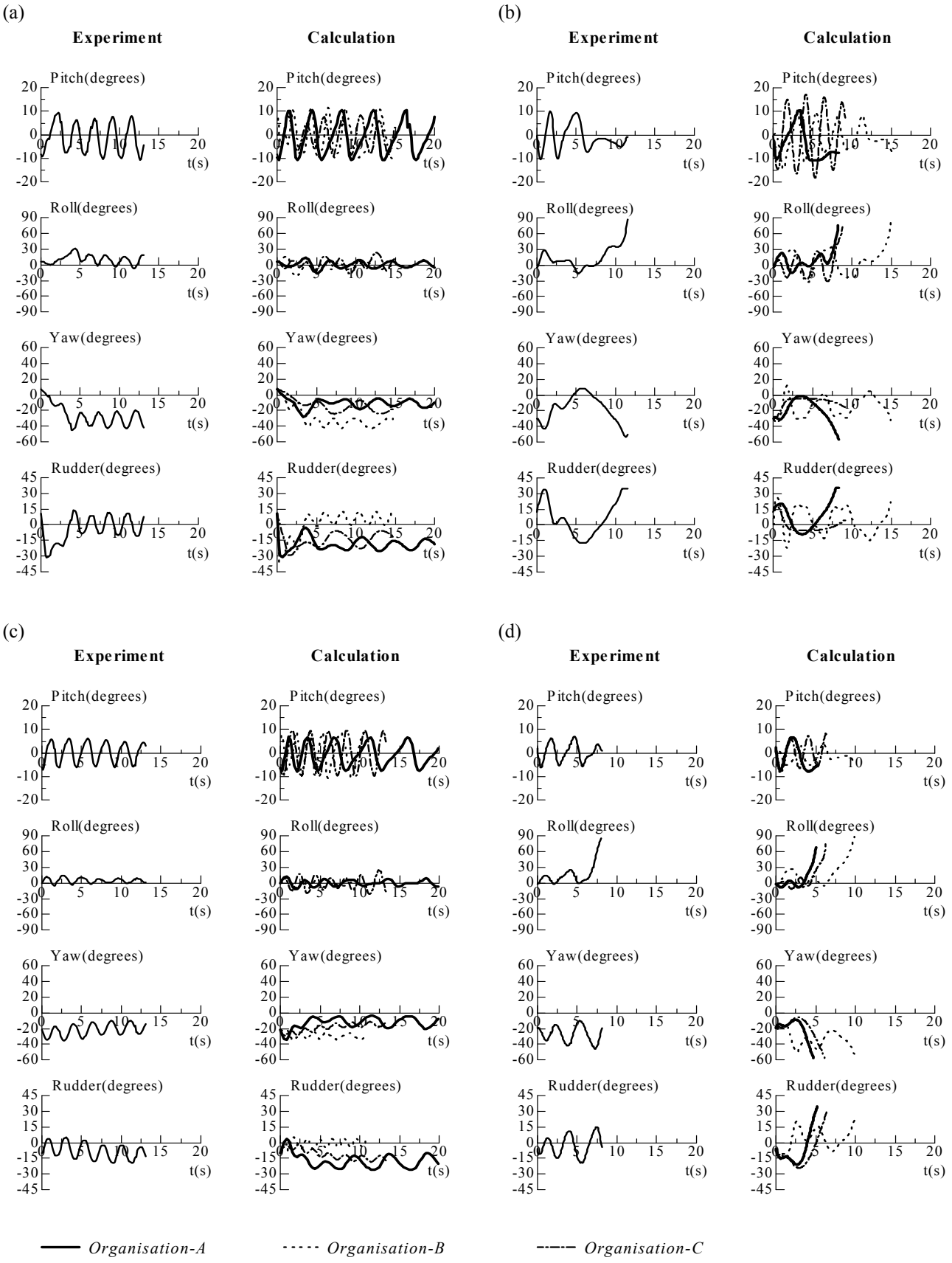

IMPORTANCE OF MEMORY EFFECT FOR CAPSIZING PREDICTION

Jerzy Matusiak, Helsinki University of Technology, Ship Laboratory
Otakaari 4, P. O. Box 4100,FIN-02015 HUT,Finland
Jerzy.Matusiak@HUT.FI

SUMMARY

A two-stage approach [7] to determination of non-linear motions of ship in waves is used in evaluating dynamic stability of ship A-1 of the ITTC benchmark study. Two different models of radiation forces are used. Both are based on the linearity assumption. In the first model radiation forces include the flow memory effect represented by the retardation function. In the second model constant added mass and damping concept is used to represent radiation forces.

1. INTRODUCTION

Linear models of ship dynamics in waves are well established. In most cases they result in a sufficiently accurate prediction of loads and ship motions. Perhaps the biggest benefit of using the linear models is that prediction of exceeding certain level of load or response can be easily derived.

The biggest shortcoming of the linearity assumption is that it precludes prediction of certain classes of ship responses. The linear models cannot predict the loss of ship stability in waves, parametric roll resonance of roll and asymmetry of sagging and hogging. Evaluation of these kind responses requires a proper non-linear modeling of ship dynamics and hydrodynamics. Moreover, the analysis has to be conducted in time domain.

In the two-stage approach [7] to determination of non-linear motions of ship in waves, the fully non-linear model represents the restoring forces and the Froude-Krylov part of wave forces while radiation and diffraction forces are regarded to be sufficiently well represented by the linear approximation. Ship dynamic behavior is represented by a rigid body dynamics having six degrees of freedom. There are no restrictions set on the motion's magnitude. There are two options for evaluating radiation forces. The first one is based on the approach of Cummins [2], which allows to evaluate the radiation forces in time domain without any assumption concerning motion frequency. This approach represents properly the memory effect on the radiation forces. In the second, simplified model, radiation forces are directly related to the added masses and damping coefficients.

Ship behavior in regular waves was evaluated by both approaches of representing the radiation forces. This was done for a container ship model of the Osaka University. The results are compared to the model test results [5].

2 AN OUTLINE OF THE TWO-STAGE APPROACH TO DETERMINATION OF NON-LINEAR MOTIONS OF SHIP IN WAVES

In this chapter only an-outline of the two-stage approach is presented. More detailed description of the approach is presented in [7].

2.1 CO-ORDINATE SYSTEMS USED IN EVALUATING SHIP MOTION

Ship is regarded as a rigid body possessing in general six degrees of freedom. In the following we focus our attention on the general theoretical model of rigid body motion.

Four co-ordinate systems are used for describing general ship motion. These are presented in Figure 1.

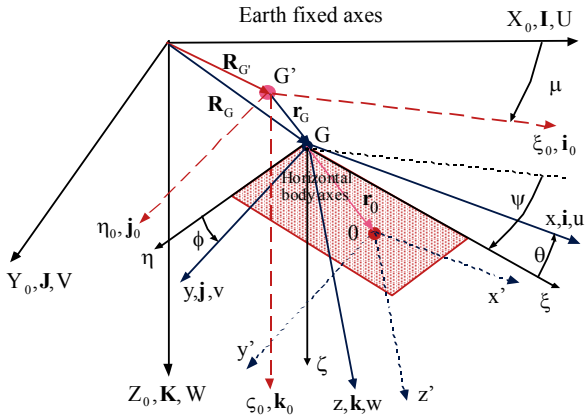

Fig. 1 Co-ordinate systems used in ship dynamics [7].

Inertial co-ordinate system fixed to Earth is denoted by $X_0Y_0Z_0$. X_0-axis points in the wave propagation direction. The X_0-Y_0 plane coincides with the still water level. Ship is on course μ with respect to waves. Course or encounter angle is a time-averaged or initial orientation of ship with respect to the direction of wave propagation. This time-averaged position defines the co-ordinate system $\xi_0\eta_0\zeta_0$. G' is the origin of this co-ordinate system and it is the time-averaged position of the ship's center of gravity. Axis ξ_0 points in the

direction of ship velocity vector $\boldsymbol{V}_S$. The average position of ship is given by the position vector $\boldsymbol{R}_{G'} = X_{G'}\boldsymbol{I} + Y_{G'}$.

The origin of two other Cartesian co-ordinate systems is located at the instantaneous position of ship's origin (point G in Fig.1). Co-ordinate system xyz is fixed to the ship so that the x-axis points towards ship bow. This co-ordinate system is called the body-fixed co-ordinate system. The so-called horizontal body axes co-ordinate system [4] denoted as $\xi\eta\zeta$ moves with ship so that the ξ-η plane stays horizontal that is it is parallel to the plane X_0-Y_0 and ζ-axis stays at ship centreplane. Both the body fixed and horizontal axes co-ordinate systems move with ship with a velocity

Fourth co-ordinate system, denoted by x'y'z', is also body-fixed but with the origin located in other point denoted by 0. In the linear seakeeping theory usually origin 0 lies on the vertical plane that comprises the center of gravity and being the intersection of this plane with the centerplane plane and still waterplane.

Instantaneous position of ship's center of gravity is given by the following displacement components: surge (ξ_0 or x_1), sway (η_0 or x_2) and heave (ζ_0 or x_3). These are the motion components of the center of gravity in the moving with ship velocity $\boldsymbol{V}_s$ inertial co-ordinate system $\xi_0\eta_0\zeta_0$. Translational motion is defined as the motion of ship's origin 0 in the inertial co-ordinate system

$$\boldsymbol{r}_G = \xi_0\boldsymbol{i}_0 + \eta_0\boldsymbol{j}_0 + \varsigma_0\boldsymbol{k}_0 . \tag{1}$$

The velocity of the origin of ship is given as

$$\boldsymbol{U} = \dot{\boldsymbol{r}}_G = \dot{\xi}_0\boldsymbol{i}_0 + \dot{\eta}_0\boldsymbol{j}_0 + \dot{\varsigma}_0\boldsymbol{k}_0 = u\boldsymbol{i} + v\boldsymbol{j} + w\boldsymbol{k} .$$

Angular position of the ship is given by the so-called ship Euler angles denoted in Fig. 1 as ψ, θ and ϕ. These angles bring vehicle from the reference (initial) orientation to the actual orientation of the body-fixed co-ordinate system. The orientation of the body-fixed co-ordinate system varies in time. It is given by the Euler angles. The following matrix relation [1, 3] gives the projection of the velocity expressed in body-fixed co-ordinate system on the Earth-fixed co-ordinates

$$\begin{Bmatrix} \dot{\xi}_0 \\ \dot{\eta}_0 \\ \dot{\zeta}_0 \end{Bmatrix} = \begin{bmatrix} \cos\cos & \cos\sin\sin - \sin\cos & \cos\sin\cos + \sin\sin \\ \sin\cos & \sin\sin\sin + \cos\cos & \sin\sin\cos - \cos\sin \\ -\sin & \cos\sin & \cos\cos \end{bmatrix} \begin{Bmatrix} u \\ v \\ w \end{Bmatrix} \tag{3}$$

Angular velocity $\boldsymbol{\Omega}$ of ship can be expressed in terms of the time derivatives of roll, pitch and yaw as follows

$$\boldsymbol{\Omega} = P\mathbf{i} + Q\mathbf{j} + R\mathbf{k} . \tag{4}$$

The dependence of the derivatives of the Euler angles and angular velocity components expressed in the moving frame is as follows [1]

$$\begin{Bmatrix} \dot{\phi} \\ \dot{\theta} \\ \dot{\psi} \end{Bmatrix} = \begin{bmatrix} 1 & \sin\tan & \cos\tan \\ 0 & \cos & -\sin \\ 0 & \sin/\cos\theta & \cos/\cos\theta \end{bmatrix} \begin{Bmatrix} P \\ Q \\ R \end{Bmatrix} . \tag{5}$$

2.2 GENERAL EQUATIONS OF MOTION

Equations of motion are given by the set of six non-linear ordinary differential equations [3]

$$\begin{aligned} X_g - \mathrm{mg}\sin\theta &= \mathrm{m}(\dot{u} + Qw - Rv) \\ Y_g + \mathrm{mg}\cos\theta\sin\phi &= \mathrm{m}(\dot{v} + Ru - Pw) \\ Z_g + \mathrm{mg}\cos\theta\cos\phi &= \mathrm{m}(\dot{w} + Pv - Qu) \end{aligned} \tag{6}$$

$$\begin{aligned} K_g &= I_x\dot{P} - I_{xy}\dot{Q} - I_{xz}\dot{R} + (I_zR - I_{zx}P - I_{zy}Q)Q \\ &\quad - (I_yQ - I_{yz}R - I_{yx}P)R \\ M_g &= -I_{yx}\dot{P} + I_y\dot{Q} - I_{yz}\dot{R} + (I_xP - I_{xy}Q - I_{xz}R)R \\ &\quad - (I_zR - I_{zx}P - I_{zy}Q)P \\ N_g &= -I_{zx}\dot{P} - I_{zy}\dot{Q} + I_z\dot{R} + (I_yQ - I_{yz}R - I_{yx}P)P \\ &\quad - (I_xP - I_{xy}Q - I_{xz}R)Q. \end{aligned}$$

In equations 6, X_g, Y_g, Z_g, K_g, M_g and N_g depict the components of global reaction force and moment vectors acting on the ship. These are given in the-body fixed co-ordinate system xyz. m and I_{ij} mean ship's mass and the components of the mass moment of inertia. (2)

2.2 LINEAR APPROXIMATION OF THE EQUATIONS OF MOTION

The method starts with a linear approximation of motion estimate in irregular or regular waves. The linear approximation takes care of the diffraction forces and added parameters dependence upon the frequency of motion. Linear approximation of the responses in terms of the velocities

$$\boldsymbol{U}_L = u_L\boldsymbol{i} + v_L\boldsymbol{j} + w_L\boldsymbol{k} \tag{7}$$

$$_L = P_L\mathbf{i} + Q_L\mathbf{j} + R_L\mathbf{k} = \dot{\phi}_L\mathbf{i} + \dot{\theta}_L\mathbf{j} + \dot{\Psi}_L\mathbf{k} \tag{8}$$

is obtained by the standard method such as for instance covered by reference [6]. Note that linear approximation does not distinguish between the inertial and body-fixed co-ordinate system. Motions are given in the co-ordinate system with the origin in the ship's center of gravity. The linearised equations of ship motion can be presented as follows

$$
\begin{aligned}
m\dot{u}_L &= X_L = X_{rad} + X_{diff} + X_{F.K,L} \\
m\dot{v}_L &= Y_L = Y_{rad} + Y_{diff} + Y_{F.K,L} \\
m\dot{w}_L &= Z_L = Z_{restoring,L} + Z_{rad} + Z_{diff} + Z_{F.K,L} \\
I_x\dot{P}_L - I_{xz}\dot{R}_L &= K_L = K_{restoring,L} + K_{rad} + K_{diff} + K_{F.K,L} \\
I_y\dot{Q}_L &= M_L = M_{restoring,L} + M_{rad} + M_{diff} + M_{F.K,L} \\
I_z\dot{R}_L - I_{zx}\dot{P}_L &= N_L = N_{rad} + N_{diff} + N_{F.K,L}.
\end{aligned}
\tag{9}
$$

The indices rad, diff, F.K and restoring stand for radiation, diffraction, the so-called Froude-Krylov and restoring forces and moments. Index L depicts linear approximation to the forces and moments. In the linear approximation wave excitation is assumed to comprise the diffraction and Froude-Krylov forces and moments. The latter are evaluated from the pressures in and undisturbed oncoming wave. In the integration ship hull is assumed to have a constant velocity V_S pointing in the x-direction and integration is conducted up to the still water level.

The terms depicted by the indexes restoring,L are the z-directional force and moments acting on a ship in still water due to infinitely small and slow forced heaving displacement and angular inclination along x- and y-axes. The initial stability model is used to represent them.

2.3 THE NON-LINEAR PART OF THE RESPONSE

At the second stage, non-linear part of ship motions is evaluated in the time domain. This motion takes into account non-linearities of ship hydrostatics and non-linearities of wave loads at large amplitudes of motion. The only motion component that is not decomposed into the linear and non-linear part, is surge. Total surge motion is evaluated using the 1st of equations (6). The effect of added wave resistance, propulsor action and rudder forces are included in this equation. Total ship motion, or other type of response, being a sum of linear approximation and a non-linear part is thus obtained. In other words total responses in terms of velocities are written in the following form

$$
\begin{aligned}
\boldsymbol{U} &= u\boldsymbol{i} + (v_L + v)\boldsymbol{j} + (w_L + w)\boldsymbol{k} \\
\boldsymbol{\Omega} &= (P_L + P)\mathbf{i} + (Q_L + Q)\mathbf{j} + (R_L + R)\mathbf{k},
\end{aligned}
\tag{10}
$$

where variables without subscripts depict non-linear part of the response.

Subtracting the equations (9) of the linear approximation model from equations (6) yields the equations for the non-linear part of response

$$
\begin{aligned}
&m[\dot{u} + (Q_L + Q)(w_L + w) \\
&-(R_L + R)(v_L + v) + g\sin(\theta_L + \theta)] = X \\
&m[\dot{v} + (R_L + R)u - (P_L + P)(w_L + w) \\
&- g\cos(\theta_L + \theta)\sin(\phi_L + \phi)] = Y \\
&m[\dot{w} + (P_L + P)(v_L + v) - (Q_L + Q)u \\
&- g\cos(\theta_L + \theta)\cos(\phi_L + \phi)] = Z
\end{aligned}
\tag{11}
$$

$$
\begin{aligned}
&I_x\dot{P} + [I_z(R_L + R) - I_{zx}(P_L + P) - I_{zy}(Q_L + Q)](Q_L + Q) - I_{xy}\dot{Q} \\
&- I_{xz}\dot{R} - [I_y(Q_L + Q) - I_{yz}(R_L + R) - I_{yx}(P_L + P)](R_L + R) = K \\
&I_y\dot{Q} - I_{yx}\dot{P} + [I_x(P_L + P) - I_{xy}(Q_L + Q) - I_{xz}(R_L + R)](R_L + R) \\
&- I_{yz}\dot{R} - [I_z(R_L + R) - I_{zx}(P_L + P) - I_{zy}(Q_L + Q)](P_L + P) = M \\
&I_z\dot{R} - I_{zx}\dot{P} + [I_y(Q_L + Q) - I_{yz}(R_L + R) - I_{yx}(P_L + P)](P_L + P) \\
&- I_{zy}\dot{Q} - [I_x(P_L + P) - I_{xy}(Q_L + Q) - I_{xz}(R_L + R)](Q_L + Q) = N.
\end{aligned}
$$

Equations (11) govern non-linear part of the rigid body motion in six degrees of freedom. In order to solve them we need to specify the non-linear part of the external (fluid) forces *X,Y,Z* and moments *K,M,N* acting on a body. These are presented in bigger detail in reference [7]. Moreover we use equations (3) and (5) to express body velocities in the inertial co-ordinate system. Numerical integration of these equations together with the division of responses given by equations (10) yields the instantaneous position of ship in the inertial co-ordinate system $X_0Y_0Z_0$. Additional, thirteenth ordinary differential equation of a first order representing the action of auto-pilot is used to control the rudder angle. Integration is conducted using the 4th order Runge-Kutta scheme with an integration step being Δt = 100 ms. Computation is conducted for a full-scale ship. Linear approximation of responses and forces is related to ship's actual position in waves. It takes into account instantaneous heading angle. The zero initial conditions are used for all equations with an exception of surge velocity, which is set initially to a prescribed ship velocity in calm water. In order to dampen the spurious transients, wave amplitude is gradually increased from zero to the prescribed final value $A_{w,final}$ using the expression

$$
\begin{aligned}
A_w(t) &= A_{w,\,final}\left[1 - \left(\cos\frac{\pi t}{2T_f}\right)^2\right] \quad \text{for } t < T_f, \\
A_w(t) &= A_{w,\,final} \text{ for } t \geq T_f,
\end{aligned}
\tag{12}
$$

where t is time and with T_f= 50 seconds in full scale being used.

3 RADIATION FORCES

Radiation forces are approximated by a quasilinear model making use of the added mass and damping concept. These forces can be expressed in the general form as [8]

$$
F_i = -\sum_{j=1}^{6}(a_{ij}\dot{U}_j + b_{ij}U_j) \tag{13}
$$

for i = 1,2,…6 depicting degrees of freedom, or as follows

In equations 14 a_{ij} and b_{ij} depict added masses and damping coefficients referred to the origin located in the center of gravity (G in Fig. 1). These are frequency dependent values. In the present method these

$$
\begin{aligned}
X_{\text{rad}} &= -a_{11}\dot{u} - b_{11}(u - V_S) - a_{15}\dot{Q} - b_{15}Q \\
Y_{\text{rad}} &= -a_{22}\dot{v} - b_{22}v - a_{24}\dot{P} - b_{24}P - a_{26}\dot{R} - b_{26}R \\
Z_{\text{rad}} &= -a_{33}\dot{w} - b_{33}w - a_{35}\dot{Q} - b_{35}Q \\
K_{\text{rad}} &= -a_{44}\dot{P} - b_{44}P - a_{46}\dot{R} - b_{46}R - a_{42}\dot{v} - b_{42}v \\
M_{\text{rad}} &= -a_{55}\dot{Q} - b_{55}Q - a_{53}\dot{w} - b_{53}w - a_{51}\dot{u} - b_{51}(u - V_S) \\
N_{\text{rad}} &= -a_{66}\dot{R} - b_{66}R - a_{64}\dot{P} - b_{64}P - a_{62}\dot{v} - b_{62}v.
\end{aligned} \qquad (14)
$$

coefficients are evaluated by a standard linear seakeeping theory based computer program [6]. Note that radiation forces are oriented in the body-fixed co-ordinate system.

3.1 MEMORY EFFECT INCLUDED USING THE RETARDATION FUNCTION CONCEPT

The radiation forces model represented by the equations 14 is good for a frequency domain linear analysis. Time domain approach requires the so-called convolution integral representation of the radiation forces [2]. In this time approach radiation forces vector $\boldsymbol{X}_{\text{rad}}$ is represented by an expression:

$$
\mathbf{X}_{rad}(t) = -\mathbf{a}_{\infty}\ddot{\mathbf{x}}(t) - \int_{-\infty}^{t} \mathbf{k}(t-\tau)\dot{\mathbf{x}}(\tau)d\tau\,, \qquad (15)
$$

where $\boldsymbol{a}_{\infty}$ is the matrix comprising of the added masses coefficients for an infinite frequency and $\boldsymbol{x}$ is the response vector. Matrix function $\boldsymbol{k}$ is the so-called retardation function which takes into account the memory effect of the radiation forces. This function can be evaluated as follows

$$
\boldsymbol{k}(t) = \frac{2}{\pi}\int_{0}^{\infty} \boldsymbol{b}(\omega)\cos(\omega t)d\omega \qquad (16)
$$

where $\boldsymbol{b}$ is the frequency dependent added damping matrix. The $\boldsymbol{k(t)}$ functions have to be evaluated before the simulation. The Fast Fourier Transform algorithm is used when evaluating discrete values of the retardation functions as follows

$$
K_{k,ij}(k\Delta t) = \frac{N\Delta\omega}{\pi}\,\boldsymbol{FFT}(g_{ij}(x))\,, \qquad (17)
$$

where the original added damping discrete functions are substituted by a 'double-sided function' g(x) as follows:

$$
\begin{aligned}
&g_{ij}(x) = b_{ij}(x) \text{ for } x = \Delta\omega, \Delta\omega N/2 \\
&g_{ij}(N\Delta\omega - x) = b_{ij}(x) \text{ for } x = 0, \Delta\omega(N/2+1).
\end{aligned} \qquad (18)
$$

Note that as a result the retardation function 16 is obtained at N/2 discrete time instants with a time step Δt. FFT analysis is conducted with N = 2048. As a result the retardation functions are represented by 1024 discrete values covering the period of 102.4 seconds. An example of the retardation function for heave is given below.

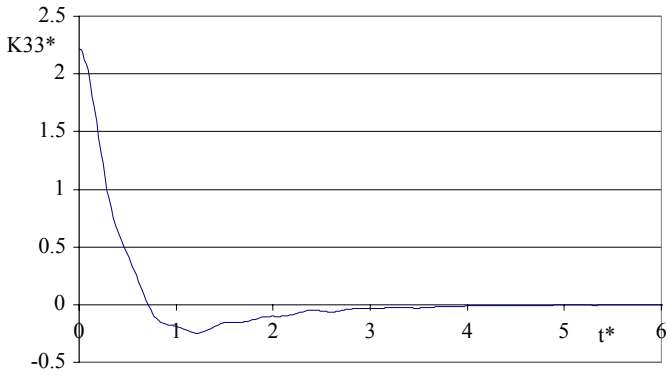

Fig. 2 Non-dimensional heave memory (retardation) function $K_{33}^{*} = K_{33}/\left(m\sqrt{g/L}\right)$ as a function of non-dimensional time $t^{*} = t/\sqrt{g/L}$, where L is waterline length of ship.

3.2 SIMPLIFIED MODEL WITH NO MEMORY EFFECT

The simplified model, which does not take flow memory into account, is based on the assumption that added masses and damping coefficients are constant. For this model two options are used. In case 2a added masses and damping values are evaluated for the prescribed frequency of encounter with an exception of roll coefficients (including cross-coupling of roll with other motion components), which are evaluated for the natural frequency of roll. In case 2b all coefficients are evaluated for the frequency of encounter.

4 RESULTS OF SIMULATION

Model test experiments of the containership conducted at the Osaka University [5] were simulated using three options for the radiation forces modelling. Each simulation run was of a time length 720 seconds full-scale for no-capsizing vessel. If ship capsizes, integration is terminated and time record is shorter. Wave condition is same in all cases. Amplitude of regular wave is A_W = 4.5 [m] and length λ = 225 [m], that is λ=1.5*L. The varied quantities are ship speed and heading. Summary of the simulation is presented in Table below.

Table Summary of the results.

Fn	0.2	0.2	0.3	0.4
Heading [deg]	0	45	30	30
Experiment	capsize	no-capsize	no-capsize	capsize
Case 1	no-capsize	no-capsize	no-capsize	capsize
Case 2a&b	no-capsize	no-capsize	capsize	capsize

Selected time histories of the simulated responses are presented in the following. Simulations do not predict ship capsizing in following regular waves and ship speed *Fn* = 0.2. Although after several wave encounters ship starts to roll heavily (see Fig. 3), this rolling motion is restricted to approximately 12.5 [deg].

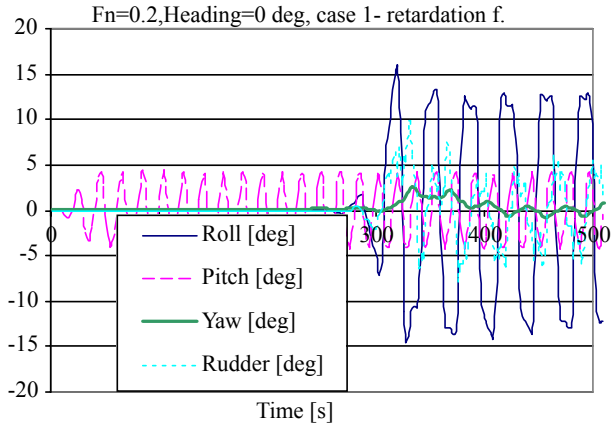

Fig. 3. Angular motions of ship in regular following in the radiation forces.

The case of heading being 30 [deg] and *Fn* = 0.3 is the one where considering memory effect in radiation forces has a positive effect on ship behaviour prediction. As it seen from Figs. 4 and 5, ship survives in this condition both in simulation, in which retardation function is used, and in model tests.

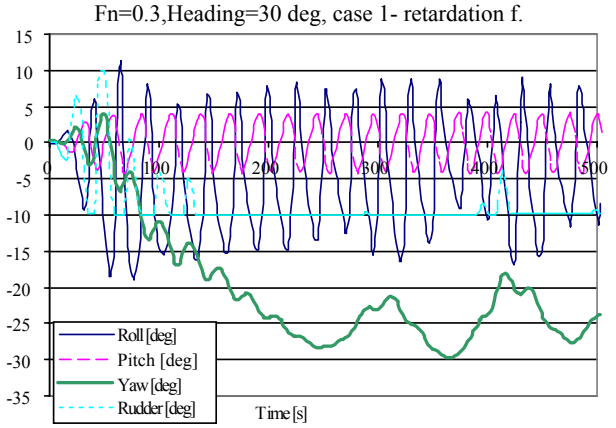

Fig. 4. Angular motions of ship in regular quarteirng waves (heading = 30 [deg]). Ship speed is Fn = 0.3. Memory effect is included in the radiation forces.

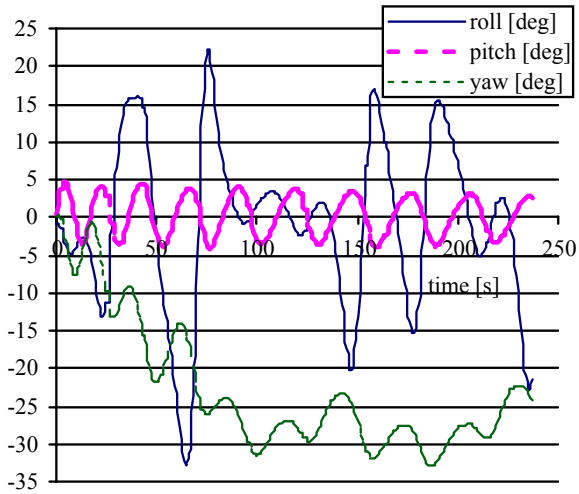

Fig. 5. Angular motions of ship in regular quarteirng waves (heading = 30 [deg]). Ship speed is Fn = 0.3. Model test result scaled to full-scale and yaw defined as a deviation from the initial course. [5].

Both constant added masses and damping models wrongly predict ship capsizing in this condition (see Fig. 6).

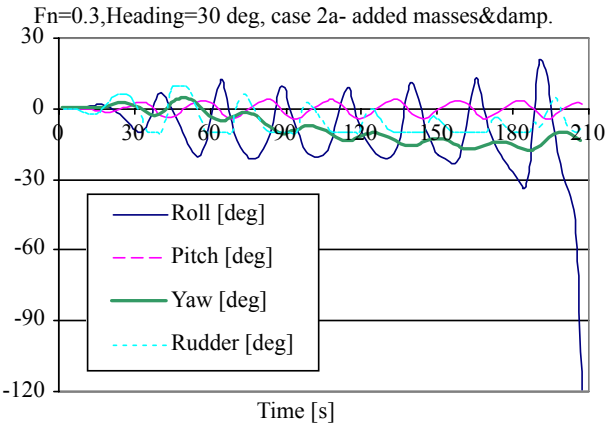

Fig. 6. Angular motions of ship in regular quartering waves. Ship speed is Fn = 0.3 and heading 30 [deg]. Radiation forces are represented by constant added masses and damping coefficients.

The case of highest speed (Fn =0.4) and heading 30 [deg] is shown in Figs. 7, 8 and 9. In model test experiments (Fig. 7) ship capsizes. Same is predicted by simulations (Fig. 8 and 9). In computations it takes longer time for the model to capsize. The reason for this may be in the initial conditions of simulations.

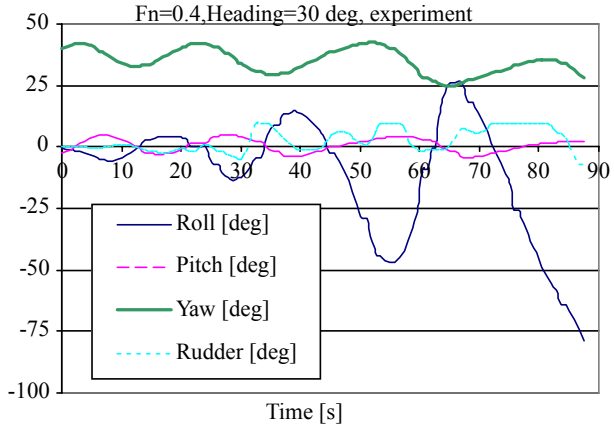

Fig. 7. Model running at Fn = 0.4 capsizes in regular quartering regular waves (heading 30 [deg]). Model test result scaled to full-scale. [5].

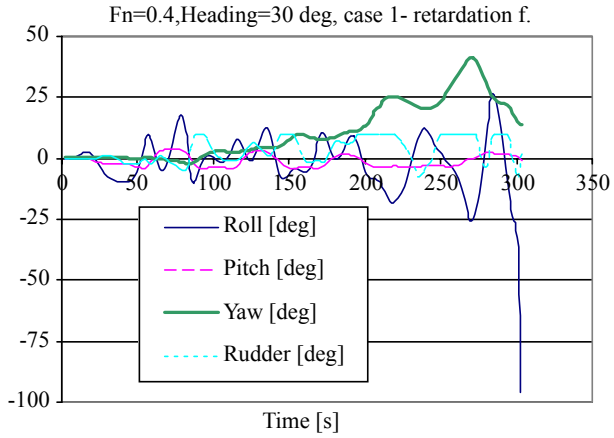

Fig. 8. Containership running at Fn = 0.4 capsizes in regular quartering regular waves (heading 30 [deg]). Simulations include the memory effect.

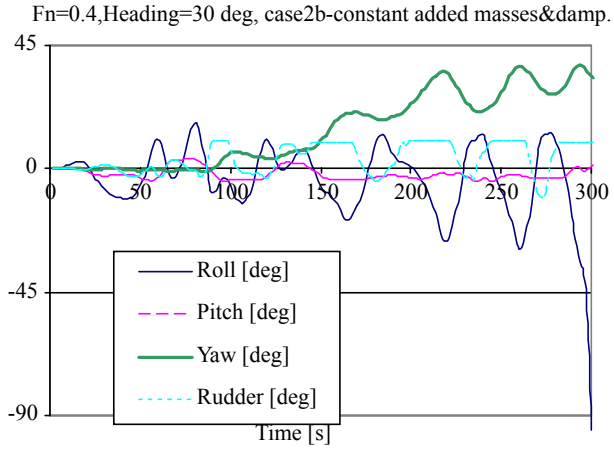

Fig. 9. Containership running at Fn = 0.4 capsizes in regular quartering regular waves (heading 30 [deg]). Simulations conducted using constant added masses and damping approach.

5 CONCLUSIONS

Considering the memory effect when modelling radiation forces yields better results of dynamic behaviour of ship in the context of two-stage approach of prediction non-linear ship motions.

This conclusion is not a surprising one. In time domain analysis, added mass and damping model is in principle applicable for harmonic monochromatic motions only. Dynamic stability of ship is characterized by non-linearities and transient type behavior. Although the retardation function approach implies the linearity assumption, it takes properly into account flow memory effect important in case of transient type behavior.

In the presented method, maneuvering hull forces are represented by the retardation functions and convolution integrals involving them. This potential flow model does not necessarily include all relevant flow features governing yaw and sway motion components. Moreover, this model is based on the linearity assumption. This may be the reason for a poor prediction of ship capsizing in following waves.

6 REFERENCES

1. Clayton B.R.& Bishop R.E.D 1982 Mechanics of marine vehicles, ISBN 0 419 12110-2.
2. Cummins, W.E. The Impulse Response Function and Ship Motions,Schiffstechnik 9 (1962 Nr. 47 S101/109.
3. Fossen, T.,I. 1994 Guidance and control of ocean vehicles, J. Wiley&SonsISBN 0 471 94113 1.
4. Hamamoto, M. and Kim, Y.S., 1993 "A New Coordinate System and the Equations Describing Manoeuvring Motion of a Ship in Waves," J. Soc. Naval Arch., Vol 173,
5. Hamamoto, M and Umeda , N (1998, 2000) Ship A-1 data for a validation of numerical methods. ITTC Committee for Prediction of Extreme Ship Motion and Capsizing.
6. Journee J. M. 1992 Strip Theory Algorithms, report MEMT 24, Delft University of Technology, Ship Hydrodynamics Laboratory.
7. Matusiak, J Two-Stage Approach To Determination Of Non-Linear Motions Of Ship In Waves, 4th Osaka Collouqium on Seakeeping Performance of Ships, Osaka, Japan, 17-21st October, 2000
8. Newman, J.N. 1980. Marine Hydrodynamics. Cambridge, Massachusetts, The MIT Press, 402 s. Washington, D.C 1997

Importance of Wave Effects on Manoeuvring Coefficients for Capsizing Prediction

Hirotada HASHIMOTO and Naoya UMEDA, Department of Naval Architecture and Ocean Engineering,
Osaka University, 2-1 Yamadaoka, Suita, Osaka, 565-0871, Japan
h_hashi@naoe.eng.osaka-u.ac.jp , umeda@naoe.eng.osaka-u.ac.jp

SUMMARY

The wave effects on manoeuvring coefficients, as second order terms of capsizing prediction, were estimated with a slender body theory and compared with the existing results of captive model experiments. Then numerical simulations were carried out with these wave effects and without them and compared with the results of free running model experiments. The comparison demonstrated that the wave effects on derivatives of manoeuvring forces with respect to yaw rate and rudder angle are not so essential for capsizing prediction but those with respect to sway velocity can be essential. Since the wave effects on manoeuvring coefficients do not improve agreements between the numerical prediction and model experiment for capsizing, it is expected to develop a consistent numerical model that takes all second order terms into account.

NOMENCLATURE

a	wave amplitude
a_H	interaction factor between hull and rudder
A_R	rudder area
c	wave celerity
d	mean draft
f_α	rudder lifting slope coefficient
F_n	nominal Froude number
g	gravitational acceleration
GZ	righting arm
H	wave height
I_{xx}	moment of inertia in roll
I_{zz}	moment of inertia in yaw
J	advance coefficient of propeller
J_{xx}	added moment of inertia in roll
J_{zz}	added moment of inertia in yaw
k	wave number
K_p	derivative of roll moment with respect to roll rate
K_r	derivative of roll moment with respect to yaw rate
K_R	rudder gain
K_T	thrust coefficient of propeller
K_v	derivative of roll moment with respect to sway velocity
K_w	wave-induced roll moment
K_δ	derivative of roll moment with respect to rudder angle
K_δ^W	wave effect on derivative of roll moment with respect to rudder angle
K_ϕ	derivative of roll moment with respect to roll angle
l_R	correction factor for flow-straightening effect due to yaw rate
L	ship length between perpendiculars
m	ship mass
m_x	added mass in surge
m_y	added mass in sway
m_y^{2D}	2-dimensional added mass in sway
n	propeller revolution number
N_r	derivative of yaw moment with respect to yaw rate
N_r'	$N_r' = N_r/(\rho L^3 du/2)$
N_r^W	wave effect on derivative of yaw moment with respect to yaw rate
N_v	derivative of yaw moment with respect to sway velocity
N_v'	$N_v' = N_v/(\rho L^2 du/2)$
N_v^W	wave effect on derivative of yaw moment with respect to sway velocity
N_w	wave-induced yaw moment
N_δ	derivative of yaw moment with respect to rudder angle
N_δ^W	wave effect on derivative of yaw moment with respect to rudder angle
N_ϕ	derivative of yaw moment with respect to roll angle
p	roll rate
r	yaw rate
R	ship resistance
t	time
T	propeller thrust
T_D	time constant for differential control
T_E	time constant for steering gear
u	surge velocity
u_w	wave particle velocity in x direction
v	sway velocity
v_w	wave particle velocity in y direction
w_p	effective propeller wake fraction
x_H	longitudinal position of centre of interaction force between hull and rudder
x_R	longitudinal position of rudder
X_w	wave-induced surge force
X_{rud}	rudder-induced surge force
Y	lateral force
ΔY	sectional lateral force
Y_r	derivative of sway force with respect to yaw rate
Y_r'	$Y_r' = Y_r/(\rho L^2 du/2)$
Y_r^W	wave effect on derivative of sway force with respect to yaw rate
Y_v	derivative of sway force with respect to sway velocity
Y_v'	$Y_v' = Y_v/(\rho L du/2)$
Y_v^W	wave effect on derivative of sway force with respect to sway velocity

Y_w wave-induced sway force
Y_δ derivative of sway force with respect to rudder angle
Y_δ^W wave effect on derivative of sway force with respect to rudder angle
Y_ϕ derivative of sway force with respect to roll angle
z_H vertical position of centre of sway force due to lateral motions
χ heading angle from wave direction
χ_c desired heading angle for auto pilot
δ rudder angle
ε_R wake ratio between propeller and hull
ϕ roll angle
Φ velocity potential
γ_R flow-straightening effect coefficient
κ_p interaction factor between propeller and rudder
λ wave length
θ pitch angle
ρ water density
ω wave frequency
ξ_G longitudinal position of centre of gravity from a wave trough
ζ_G vertical distance between centre of gravity and still water plane
ζ_r relative wave elevation for each section
ζ_w wave elevation

1. INTRODUCTION

Since capsizing prediction in following and quartering seas is an important issue for ship safety, benchmark testing for intact stability has been conducted at ITTC[1].

Some mathematical models for capsizing in high-speed region, associated with surf-riding and broaching, have been proposed and compared with free running model experiments. In particular, a mathematical model by Umeda et al.[2-3] qualitatively well predicts such phenomena[4]. In this model, wave steepness, sway velocity and yaw rate are assumed to be small. Thus higher order terms of these small quantities are consistently neglected. As a result, this model considers ship resistance, propeller thrust, lateral righting moment, added inertia force, linear wave exciting forces and linear manoeuvring forces and neglects the second order wave forces, nonlinear manoeuvring forces in calm water and wave effect on the linear manoeuvring forces.

These higher order terms can be candidates of new elements for improving prediction accuracy. Among them mathematical models considering only nonlinear calm-water manoeuvring forces as a higher order term had been proposed by Renilson[5], Spyrou[6], de Kat[7] et al. but importance of these forces on capsizing prediction had not been clarified. Thus the authors[4] examined these effects by conducting comparisons between numerical results with and without the nonlinear calm-water manoeuvring forces and then confirmed these effects on capsizing prediction are rather small.

Hydrodynamic studies on the wave effects on linear manoeuvring forces had started with Hamamoto[8-10]. Then, Son and Nomoto[11] reported that there is a significant difference in stability index of ship lateral motion between a mathematical model with and without these effects. Since their prediction of these hydrodynamic forces is based on the results of PMM tests, we cannot directly apply their results into the present numerical model. Therefore, in this paper, firstly mathematical method for prediction of manoeuvring forces in following and quartering waves by a slender body theory is proposed and comparisons between numerical estimations and existing results of captive model experiments[10-13], such as PMM or CMT, are presented. Secondly we apply this hydrodynamic method into existing model by Umeda et al.[2-3] and compare with the original mathematical model for examining the importance of these effects on capsizing prediction. Because the encounter frequency is low for a ship running in following and quartering seas, we focus on the wave effects on manoeuvring damping forces and neglect the ones on added inertia forces.

2. MATHEMATICAL MODELLING

The numerical model of the surge-sway-yaw-roll motion was developed by Umeda & Renilson[2] and Umeda[3] for capsizing associated with surf-riding in quartering waves. (*Original model*) In cases of ship runs with relatively high forward velocity in following and quartering waves, the encounter frequency becomes very small. Thus, hydrodynamic forces acting on the ship consist mainly of lift components and wave-making components are negligibly small. Therefore, a manoeuvring mathematical model focusing on hydrodynamic lift components can be recommended for broaching.

To take the wave effect of manoeuvring forces into account, the authors modified the above-mentioned model. Two co-ordinate systems used here are shown in Fig.1: (1) a wave fixed with its origin at a wave trough, the ξ axis in the direction of wave travel; and (2) an upright body fixed with its origin at the centre of ship gravity. The state vector, $\mathbf{x}$ and control vector, $\mathbf{b}$, of this system are defined as follows:

$$\mathbf{x} = (x_1, x_2, \cdots, x_8)^T = \{\xi_G / \lambda, u, v, \chi, r, \phi, p, \delta\}^T \quad (1)$$

$$\mathbf{b} = \{n, \chi_c\}^T \quad (2).$$

The modified dynamical system can be represented by the following state equation:

$$\dot{\mathbf{x}} = \mathbf{F}(\mathbf{x};\mathbf{b}) = \{f_1(\mathbf{x};\mathbf{b}), f_2(\mathbf{x};\mathbf{b}), \cdots, f_8(\mathbf{x};\mathbf{b})\}^T \quad (3)$$

where

$$f_1(\mathbf{x};\mathbf{b}) = \{u\cos\chi - v\sin\chi - c\}/\lambda \quad (4)$$

$$f_2(\mathbf{x};\mathbf{b}) = \{T(u;n) - R(u) + \underline{X_{rud}(\xi_G/\lambda, u, \chi, \delta; n)} + X_w(\xi_G/\lambda, \chi)\}/(m + m_x) \quad (5)$$

$$f_3(\mathbf{x};\mathbf{b}) = \{-(m+m_x)ur + Y_v(u;n)v + \underline{Y_v^W(\xi_G/\lambda,u,\chi;n)v} + Y_r(u;n)r + \underline{Y_r^W(\xi_G/\lambda,u,\chi;n)r} + Y_\phi(u)\phi + Y_\delta(u;n)\delta + \underline{Y_\delta^W(\xi_G/\lambda,u,\chi;n)\delta} + Y_w(\xi_G/\lambda,u,\chi;n)\}/(m+m_y) \quad (6)$$

$$f_4(\mathbf{x};\mathbf{b}) = r \quad (7)$$

$$f_5(\mathbf{x};\mathbf{b}) = \{N_v(u;n)v + \underline{N_v^W(\xi_G/\lambda,u,\chi)v} + N_r(u;n)r + \underline{N_r^W(\xi_G/\lambda,u,\chi)r} + N_\phi(u)\phi + N_\delta(u;n)\delta + \underline{N_\delta^W(\xi_G/\lambda,u,\chi;n)\delta} + N_w(\xi_G/\lambda,u,\chi;n)/(I_{ZZ}+J_{ZZ}) \quad (8)$$

$$f_6(\mathbf{x};\mathbf{b}) = p \quad (9)$$

$$f_7(\mathbf{x};\mathbf{b}) = \{m_x z_H ur + K_v(u;n)v + K_r(u;n)r + K_P(u)p + K_\phi(u)\phi + K_\delta(u;n)\delta + \underline{K_\delta^W(\xi_G/\lambda,u,\chi;n)\delta} + K_w(\xi_G/\lambda,u,\chi;n) + mgGZ(\phi)\}/(I_{xx}+J_{xx}) \quad (10)$$

$$f_8(\mathbf{x};\mathbf{b}) = \{-\delta - K_R(\chi-\chi_C) - K_R T_D r\}/T_E \quad (11).$$

Here the underlined parts are newly added to the original model.

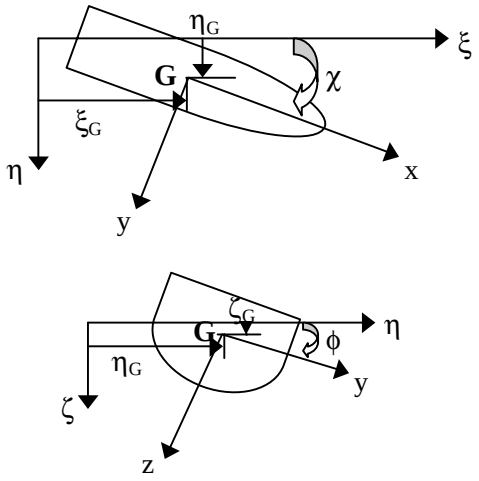

Fig.1. Co-ordinate systems

For the wave effect of linear manoeuvring forces, Hamamoto[8] and then Renilson[9] applied a slender body theory for lateral motions of a simplified hull form without a free surface condition. Later on Fujino et al.[10] utilised a high-speed slender body theory, which considers a free surface condition. In this paper the authors also develop a slender body theory but for an actual hull form, and ignore the free surface condition because the encounter frequency is too small for unsteady wave-making phenomena.

Within the theoretical framework of a slender body theory with a rigid-wall water surface condition[14], the sectional lateral force, $\Delta Y(x)$, can be calculated with the two-dimensional added-mass in sway $m_y^{2D}(x)$ as follows:

$$\Delta Y(x) = -\left(\frac{\partial}{\partial t} - u\frac{\partial}{\partial x}\right)(v+xr)m_y^{2D}(x) \quad (12).$$

Then we consider an incident wave defined with the following elevation, ζ_W , and the velocity potential, Φ.

$$\zeta_W = a\cos(kx\cos\chi - ky\sin\chi + k\xi_G) \quad (13)$$

$$\Phi = -ace^{-k\zeta}\sin k(x\cos\chi - y\sin\chi + \xi_G) \quad (14).$$

In case of a ship in waves, the added-mass can change because of relative wave elevation to the ship, ζ_r , and wave particle velocities, e.g. u_w and v_w, are added to flow velocities. These elements can be modelled as follows:

$$\zeta_r(x,\xi_G,\chi) = \zeta_G(\xi_G,\chi) - x\theta(\xi_G,\chi) - \zeta_W(x,\xi_G,\chi) \quad (15)$$

$$u_w = \frac{\partial\Phi}{\partial x} = -a\omega e^{-k\zeta}\cos\chi\cos k(x\cos\chi - y\sin\chi + \xi_G) \quad (16)$$

$$v_w = \frac{\partial\Phi}{\partial y} = a\omega e^{-k\zeta}\sin\chi\cos k(x\cos\chi - y\sin\chi + \xi_G) \quad (17).$$

Here the heave motion, ζ_G , and pitch motion, θ , can be calculated as the limit of the solution set of a strip theory at zero encounter frequency[15].

Thus, the sectional lateral force in waves can be calculated as

$$\Delta Y = -\{\dot{v} + x\dot{r} - \dot{v}_w\}m_y^{2D}(x,\zeta_r) + (u-u_w)\left(r - \frac{\partial v_w}{\partial x}\right)m_y^{2D}(x,\zeta_r) + (u-u_w)(v+xr-v_w)\frac{\partial}{\partial x}m_y^{2D}(x,\zeta_r) \quad (18).$$

Then, integrating the sectional force along the ship, the total lateral force acting on hull can be obtained as

$$\begin{aligned} Y &= \int_L \Delta Y dx \\ &= -\int_L (\dot{v}+x\dot{r})m_y^{2D}(x,0)dx \\ &\quad - \int_L (\dot{v}+x\dot{r})\zeta_r(x,\xi_G,\chi)\frac{\partial}{\partial z}m_y^{2D}(x,0)dx \\ &\quad + \int_L \dot{v}_w m_y^{2D}(x,0)dx \\ &\quad - \left[uv_w m_y^{2D}(x,0)\right]_L \\ &\quad + u\left[(v+xr)m_y^{2D}(x,0)\right]_L \\ &\quad - 2r\int_L u_w m_y^{2D}(x,0)dx \\ &\quad + u\left[(v+xr)\zeta_r(x,\xi_G,\chi)\frac{\partial}{\partial z}m_y^{2D}(x,0)\right]_L \end{aligned} \quad (19).$$

$$-\left[u_w(v+xr)m_y{}^{2D}(x,0)\right]_L + \int_L \frac{\partial u_w}{\partial x}(v+xr)m_y{}^{2D}(x,0)dx$$

This expression for the hull force and similar formula of the rudder-induced force enables us to provide the wave effect on Y_v and Y_r as follows:

$$\begin{aligned} Y_v{}^W(\xi_G/\lambda,u,\chi) &= u\left[\zeta_r(x,\xi_G)\frac{\partial}{\partial z}m_y{}^{2D}(x,0)\right]_L \\ &\quad -\left[u_w(x,\xi_G,\chi)m_y{}^{2D}(x,0)\right]_L \\ &\quad +\int_L \frac{\partial u_w(x,\xi_G,\chi)}{\partial x}m_y{}^{2D}(x,0)dx \\ &\quad +\frac{3}{2}(1+a_H)\rho A_R f_\alpha \gamma_R u_w(x,\xi_G,\chi) \end{aligned} \tag{20}$$

$$\begin{aligned} Y_r{}^W(\xi_G/\lambda,u,\chi) &= u\left[x\zeta_r(x,\xi_G)\frac{\partial}{\partial z}m_y{}^{2D}(x,0)\right]_L \\ &\quad -\left[u_w(x,\xi_G,\chi)xm_y{}^{2D}(x,0)\right]_L \\ &\quad -2\int_L u_w(x,\xi_G,\chi)m_y{}^{2D}(x,0) \\ &\quad +\int_L \frac{\partial u_w(x,\xi_G,\chi)}{\partial x}xm_y{}^{2D}(x,0)dx \\ &\quad +\frac{3}{2}(1+a_H)\rho A_R f_\alpha \gamma_R l_R u_w(x,\xi_G,\chi) \end{aligned} \tag{21}$$

The first term of each formula indicates the effect of relative wave elevation and the rest does the effect of wave particle velocity.

Similarly, $N_v{}^W$ and $N_r{}^W$ can be obtained as follows:

$$\begin{aligned} N_v{}^W(\xi_G/\lambda,u,\chi) &= u\left[x\zeta_r(x,\xi_G)\frac{\partial}{\partial z}m_y{}^{2D}(x,0)\right]_L \\ &\quad -\int_L u\zeta_r(x,\xi_G)\frac{\partial}{\partial z}m_y{}^{2D}(x,0)dx \\ &\quad -\left[xu_w(x,\xi_G,\chi)m_y{}^{2D}(x,0)\right]_L \\ &\quad +\int_L \frac{\partial u_w(x,\xi_G,\chi)}{\partial x}xm_y{}^{2D}(x,0)dx \\ &\quad +\int_L u_w(x,\xi_G,\chi)m_y{}^{2D}(x,0)dx \\ &\quad +\frac{3}{2}(x_R+a_H x_H)\rho A_R f_\alpha \gamma_R u_w(x,\xi_G,\chi) \end{aligned} \tag{22}$$

$$\begin{aligned} N_r{}^W(\xi_G/\lambda,u,\chi) &= u\left[x^2\zeta_r(x,\xi_G)\frac{\partial}{\partial z}m_y{}^{2D}(x,0)\right]_L \\ &\quad -\int_L ux\zeta_r(x,\xi_G)\frac{\partial}{\partial z}m_y{}^{2D}(x,0)dx \\ &\quad -\left[x^2u_w(x,\xi_G,\chi)m_y{}^{2D}(x,0)\right]_L \\ &\quad +\int_L \frac{\partial u_w(x,\xi_G,\chi)}{\partial x}x^2m_y{}^{2D}(x,0)dx \\ &\quad +\int_L xu_w(x,\xi_G,\chi)m_y{}^{2D}(x,0)dx \\ &\quad +\frac{3}{2}(x_R+a_H x_H)\rho A_R f_\alpha \gamma_R l_R u_w(x,\xi_G,\chi) \end{aligned} \tag{23}$$

We can estimate manoeuvring coefficients in waves by adding these changes into the calm-water value obtained by model experiment.

Furthermore, the wave effects on Y_δ and N_δ can be calculated by

$$\begin{aligned} Y_\delta{}^W(\xi_G/\lambda,u,\chi) &= (1+a_H)\frac{\rho}{2}A_R f_\alpha\left\{2\varepsilon_R(1-w_p)u\right. \\ &\quad \left.\times\sqrt{1+\kappa_p\frac{8K_T}{\pi J^2}}u_w(x,\xi_G,\chi)\right. \end{aligned} \tag{24}$$

$$\begin{aligned} N_\delta{}^W(\xi_G/\lambda,u,\chi) &= (x_R+a_H x_H)\frac{\rho}{2}A_R f_\alpha\left\{2\varepsilon_R(1-w_p)u\right. \\ &\quad \left.\times\sqrt{1+\kappa_p\frac{8K_T}{\pi J^2}}u_w(x,\xi_G,\chi)\right. \end{aligned} \tag{25}.$$

These mean the change of rudder-induced forces is due to the change of wave particle velocity.

3. PREDICTIONS OF HULL MANOEUVRING COEFFICIENTS IN WAVES

Comparisons between numerical results and experimental data in wave effect on the hull manoeuvring coefficients were carried out to confirm the accuracy of a prediction formula, (20)-(23). Firstly for the RR17 trawler, whose body plan is given in Fig.2, comparisons between the numerical results and experimental data are shown in Fig.3. Here the wave steepness is 1/16, the wave length-to-ship length ratio is 1.11. The experimental values were obtained through PMM tests in waves at Osaka University by Nishimura[12]. The calculated values of N_r agree well with the measured ones. The calculations of Y_r and N_v shows only qualitative agreement with the experiments and those of Y_v are acceptable only in amplitude. Secondly, for the SR108 container ship whose body plan is given in Fig.4, comparisons are shown in Fig.5. The experimental values were obtained by Son and Nomoto[11] at Osaka University with the same experimental procedure as the trawler. Here the calculations show reasonably good agreement except for Y_v.

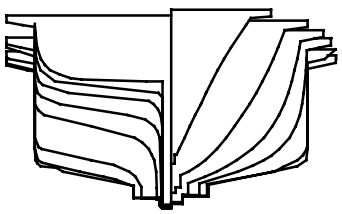

Fig.2 Body plan of the RR17 trawler

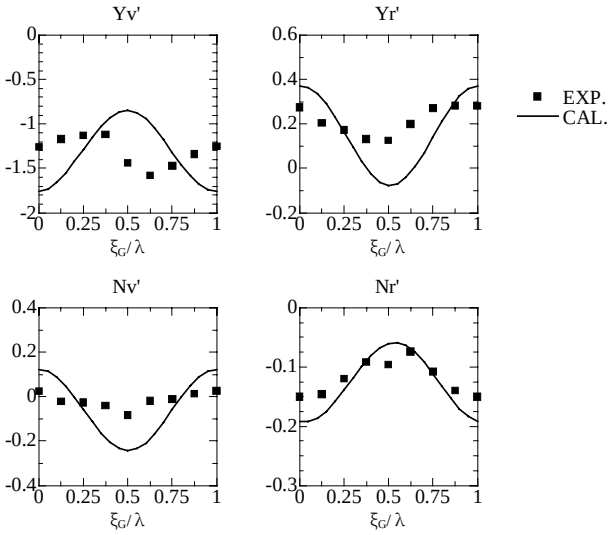

Fig.3 Comparison of manoeuvring coefficients between calculation and experiment[12] for the RR17 trawler with H/λ=1/16, λ/L=1.11, χ=0 degrees and F_n=0.447

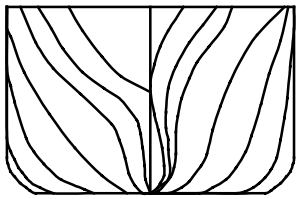

Fig.4 Body plan of the SR108 container ship

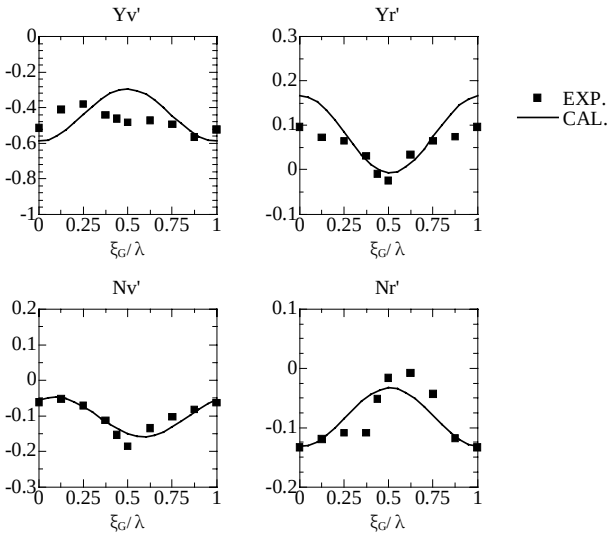

Fig.5 Comparison of manoeuvring coefficients between numerical results and experimental data[11] for container ship with H/λ=1/16, λ/L=1.1, χ=0 degrees and F_n=0.443

For the 135 gross tones purse seiner, known as the ITTC Ship A-2, the captive model experiments were recently carried out with the circular motion technique of a X-Y towing carriage of a seakeeping and manoeuvring basin of National Research Institute of Fisheries Engineering (NRIFE) by Matsuda et al[13]. Body plan of this ship are shown in Fig.6. Here the wave steepness of 1/50, the wave length-to-ship length ratio of 1.5, the non-dimensional yaw rate of 0.2 and the heading angle of 0 and 30 degrees were used. As shown in Figs.7-8, the calculated values of Y_r and N_r provide similar tendency of the measured ones. The measured values here were obtained as the balance by subtracting all other measured forces in Eqs.(6) and (8) from the total measured forces. Thus, these results suggest that the expressions of Eqs.(6) and (8) are reasonable.

As a whole, it is concluded that the prediction formulas of Eqs.(20)-(23) can explain the wave effect on N_r quantitatively, those on Y_r and N_v qualitatively and that on Y_v in amplitude.

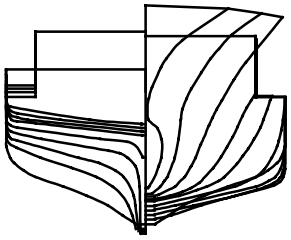

Fig.6 Body plan of the ITTC Ship A-2

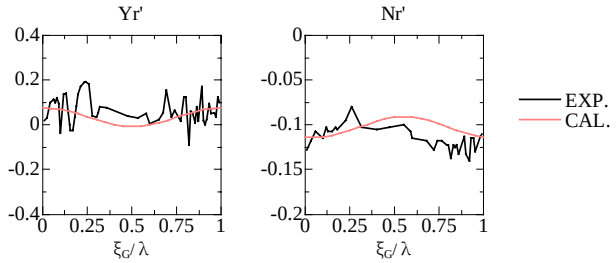

Fig.7 Comparison of Y_r' and N_r' between calculation and experiment[13] for the ITTC Ship A-2 with H/λ=1/50, λ/L=1.5, χ=0 degrees and F_n=0.4

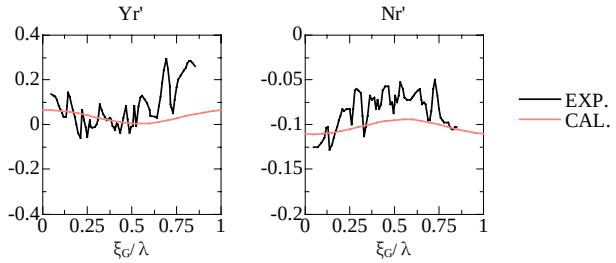

Fig.8 Comparison of Y_r' and N_r' between calculation and experiment[13] for the ITTC Ship A-2 with H/λ=1/50, λ/L=1.5, χ=30 degrees and F_n=0.4

4. PREDICTIONS OF EXTREME SHIP MOTIONS WITH AND WITHOUT WAVE EFFECTS ON MANOEUVRING COEFFICIENTS

Numerical calculations of extreme motions for the ITTC Ship A-2 were carried out by the numerical model with the wave effects on manoeuvring coefficients and that without them and compared also with the free running model experiments at a seakeeping and manoeuvring basin of NRIFE[16]. Here the initial conditions of numerical runs were adjusted to be equal to those in the experiments.

Firstly, the mathematical model only with the wave effects on Y_δ , N_δ and K_δ as higher order terms, (*Modified model I*), was used for numerical calculation. As shown in Fig.9, there is no significant difference between the original and extended models. Therefore, the wave effects on Y_δ , N_δ and K_δ can be regarded as negligibly small.

Secondly, the mathematical model with the wave effects on Y_r, N_r, Y_δ, N_δ and K_δ as higher order terms, (*Modified model II*), was adopted. As can been seen in Fig.10(a), in case of a ship experiencing a stable periodic motion, the new numerical result is almost same as the original numerical result. In Fig.10(b), in case of capsizing due to broaching, it is also rather same as the original calculation. Therefore, we can conclude that the changing of Y_r and N_r in waves is not so important for capsizing prediction in following and quartering seas.

Finally, numerical calculation with mathematical model considering the wave effects on all manoeuvring coefficients, (*Modified model III*), was carried out. In Fig.11(a), in case of periodic motion, absolute value of the average yaw angle is larger than that of the original one and closer to the value of model experiment. This is because some constant yaw moment appears as a result of the product of time-varying manoeuvring coefficient and periodic sway velocity. Some improvements in the pitch and rudder angle are also found. On the other hand, in case of capsizing due to broaching which is shown in Fig.11(b) the yaw angle is rapidly increasing up to positive value and continued to increase despite the opposite steering effort and finally capsized due to this broaching. In this case, capsizing occurred with positive yaw angle while with negative angle in experiment. Because yaw motion here is very different from original numerical model, we examined the components of yaw moment and found manoeuvring force relates to N_v is very large in positive direction and that is very small in original numerical model. This is because the value of manoeuvring forces related to N_v in still water is too small to change ship motion. However, it should be noted that the prediction accuracy for N_v is generally not so satisfactory. Thus, further effort to improve prediction of N_v is necessary. It is also noteworthy that this paper has examined some of higher order terms only and other terms, such as the wave effects of roll moment, have not yet been examined. The final conclusion on the agreements between the experiments and numerical predictions should have been provided only after a consistent second order mathematical model, which include all second order terms, will be established.

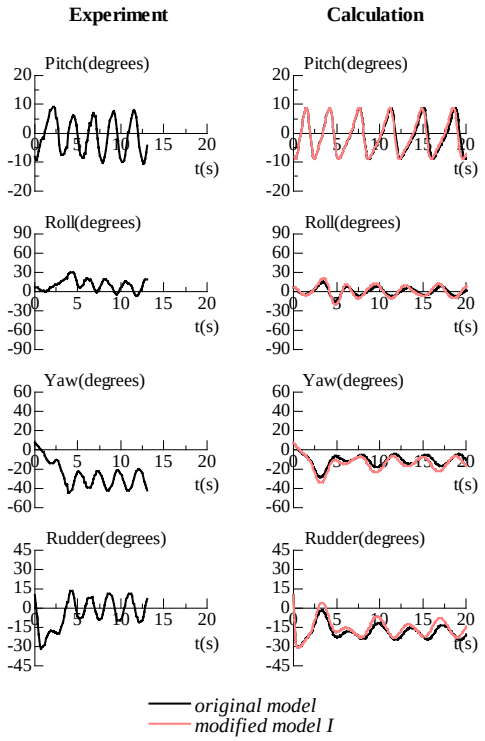

(a) with H/λ=1/10, λ/L=1.637, F_n=0.3 and χ_c=-30 degrees

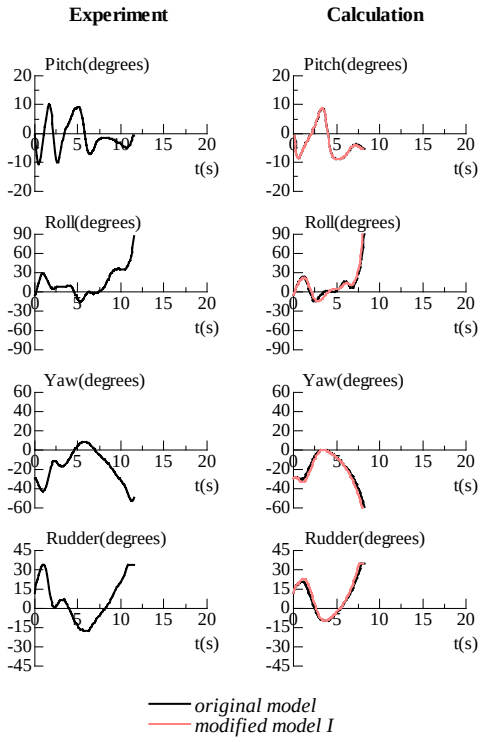

(b) with H/λ=1/10, λ/L=1.637, F_n=0.43 and χ_c=-10 degrees

Fig.9 Comparison between the numerical results with the mathematical model considering the wave effect on Y_δ, N_δ and K_δ, those with original mathematical model and the experimental results

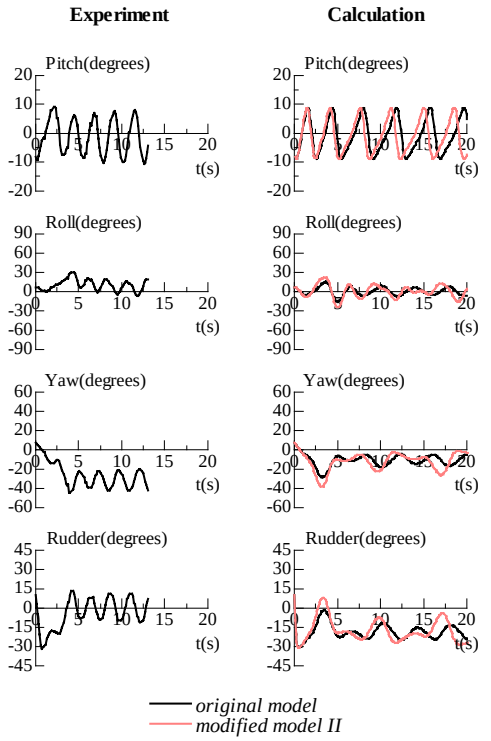

(a) with H/λ=1/10, λ/L=1.637, F_n=0.3 and χ_c=-30 degrees

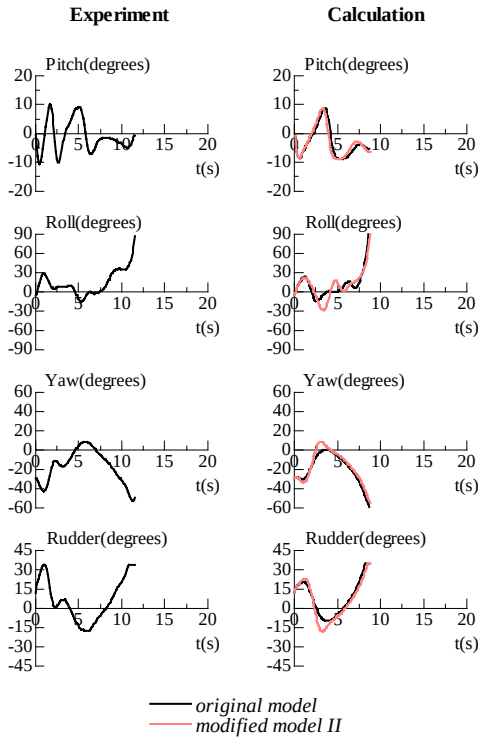

(b) with H/λ=1/10, λ/L=1.637, F_n=0.43 and χ_c=-10 degrees

Fig.10 Comparison between the numerical results with the mathematical model considering changing of Y_r, N_r, Y_δ, N_δ and K_δ, those with original mathematical model and the experimental results

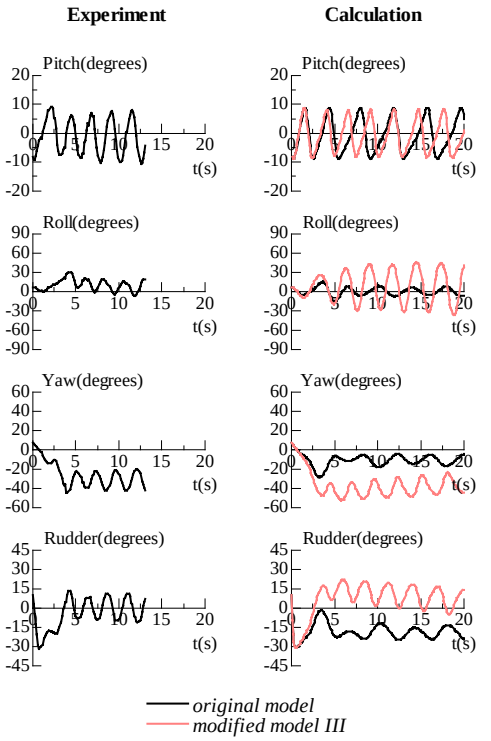

(a) with H/λ=1/10, λ/L=1.637, F_n=0.3 and χ_c=-30 degrees

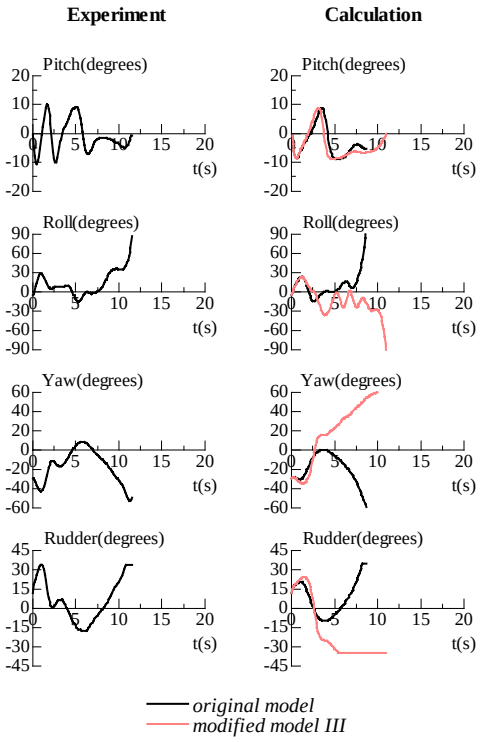

(b) with H/λ=1/10, λ/L=1.637, F_n=0.43 and χ_c=-10 degrees

Fig.11 Comparison between the numerical results with the mathematical model considering the wave effects on all manoeuvring coefficients, those with original mathematical model and the experimental results

5. CONCLUSIONS

The following conclusions can be drawn:

1. The wave effects on the derivatives of manoeuvring forces with respect to yaw rate can be fairly well predicted by a slender body theory, while those respect to sway velocity can be done only in amplitude.
2. The wave effects on the derivatives of manoeuvring forces with respect to yaw rate and rudder angle are not so important for capsizing prediction, while those respect to sway velocity can be significant.
3. The numerical model without the wave effects on the manoeuvring coefficients currently provides better prediction for extreme motions and capsizing than that with them.
4. It is expected to develop a consistent numerical model that takes all second order terms into account.
5. It is also important to improve prediction accuracy for the wave effects on the derivatives of manoeuvring forces with respect to sway velocity.

6. ACKNOWLEDGMENTS

The authors would like to express their sincere gratitude to Mr. A. Matsuda who provided raw data of his experiments and to Dr. M.R. Renilson for his useful discussion. This research was supported by a Grant-in Aid for Scientific Research of the Ministry of Education, Culture, Sports, Science and Technology of Japan (No. 13650967) as well as a grant from the Fundamental Research Developing Association for Ship Building and Offshore.

7. REFERENCES

1. Umeda, N. and M.R. Renilson, (2001), “Interim Report on ITTC Benchmark Testing of Intact Stability”, In: *Proceedings of the 5th International Stability Workshop*, Trieste.
2. Umeda, N. and M.R. Renilson, (1992), “Broaching - A Dynamic Analysis of Yaw Behaviour of a Vessel in a Following Sea”, In: *Manoeuvring and Control of Marine Craft, Computational Mechanics Publications*, 533-543.
3. Umeda, N. (1999), “Nonlinear Dynamics of Ship Capsizing due to Broaching in Following and Quartering Seas”, *J Mar Sci Technol*, 4: 16-26.
4. Umeda, N., A. Munif and H. Hashimoto, (2000), “Numerical Prediction of Extreme Motions and Capsizing for Intact Ships in Following / Quartering Seas”, In: *Proceedings of the 4th Osaka Colloquium on Seakeeping Performance of Ships*, Osaka, pp 368-373.
5. Renilson, M.R. and A. Tuite, (1995), “Broaching Simulation of Small Vessels in Severe Following Seas”, In: *Proceedings of the International Symposium on Ship Safety in a Seaway*, Kaliningrad, 1:15: 1-14.
6. Spyrou, K.J., (1995), “Surf-Riding and Oscillations of a Ship in Quartering Waves”, *J Mar Sci Technol*, 1: 24-36.
7. DeKat, J.O. and W.L. ThomasIII, (1998), ”Extreme Rolling, Broaching and Capsizing - Model Test and Simulations of a Steered Ship in Waves” In: *Proceedings of the 22nd Symposium on Naval Hydrodynamics*, Washington.
8. Hamamoto, M. (1971), “On the Hydrodynamics Derivatives for the Directional Stability of Ships in Following Seas”, *J Soc Nav Arch Japan*, 30: 83-94, (in Japanese)
9. Renilson, M.R. (1982), “An Investigation into the Factors Affecting the Likelihood of Broaching-to in Following Seas”, In: *Proceedings of the 2nd International Conference on Stability of Ships and Ocean Vehicles*, Tokyo, 551-564.
10. Fujino, M., K. Yamasaki and Y. Ishii, (1983), “On the Stability Derivatives of a Ship Travelling in Following Waves”, *J Soc Nav Arch Japan*, 152: 167-179, (in Japanese).
11. Son, K. and K. Nomoto, (1983), “On the Coupled Motion of Steering and Rolling of a Ship in Following Seas, *J Soc Nav Arch Japan*, 152: 180-191, (in Japanese).
12. Nishimura, Y. (1983), “A Study on Broaching-to Phenomenon with Roll Motion Taken into Account”, *Master Thesis, Osaka University*, 1-142, (in Japanese).
13. Matsuda, A. and N. Umeda, (2000), “New Experimental Procedure for Identifying Manoeuvring Coefficients of a Ship Suffering Broaching in Following and Quartering Seas”, In: *Proceedings of the 4th Osaka Colloquium on Seakeeping Performance of Ships*, Osaka, pp 351-356.
14. Lighthill, M.J. (1960), “Note on the Swimming of Slender Fish, *J Fluid Mech*, 9: 305-317.
15. Matsuda, A., N. Umeda and S. Suzuki, (1997), “Vertical Motions of a Ship Running in Following and Quartering Seas, *J Kansai Soc Nav Arch*, 227: 47-55, (in Japanese).
16. Umeda, N., A. Matsuda, M. Hamamoto and S. Suzuki, (1999), “Stability Assessment for Intact Ships in the Light of Model Experiments”, *J Mar Sci Technol*, 4: 45-57.

NUMERICAL MODELLING OF DAMAGE SHIP STABILTIY IN WAVES

Andrzej Jasionowski and Dracos Vassalos
The Ship Stability Research Centre (SSRC), The Universities of Glasgow and Strathclyde, UK, ssrc@na-me.ac.uk

SUMMARY

This paper outlines recent advancements, achieved to date at The Ship Stability Research Centre (SSCR), in modelling of damage ship stability in waves by means of numerical simulations. Some details of the mathematical model are presented with the emphasis put on the water sloshing representation. Fundamental validation studies demonstrate that simplified methods for estimation of fluid motion and resultant loads can successfully be applied for examination of flooded ship behaviour. However, discrepancies in predictions of basic dynamics of a damaged ship with water ingress/egress are identified. Some deficiencies in current understanding of hydrodynamics of a breached hull are highlighted.

NOMENCLATURE

I'_s	Inertia matrix of ship ("s") w.r.t. G_s
I'_w	Inertia matrix of water ("w") w.r.t. G_s
$\vec{v}'_{Gs}, \vec{w}'$	Ship rectilinear and angular velocities
M_w	Mass of floodwater in a single compartment
$\vec{r}'_w$	Position vector of the centre of buoyancy of floodwater "w" in a body-fixed reference system with origin at *Gs*
$\vec{v}'_w$	Velocity vector of the above point
$\vec{M}'_{Gs}$	Resultant of all external moments acting on ship (three-component vector)
$\vec{g}'$	Gravity acceleration vector
$\frac{d}{dt}$	Local time derivative
w_n	Natural frequency of water sloshing
b	Breadth of the tank
h	Fluid level

Superscript denotes that vectors are resolved in ship bound rotating system of reference.

1. INTRODUCTION

The subject of dynamic ship stability in waves with breach in the hull has achieved in recent years much needed attention, not least because of the latest tragic maritime accidents involving significant casualties, but also in view of the growing industrial interest in ships with capacity reaching 10 000 and more passengers onboard, where it is only natural that safety is of prime importance in the whole lifecycle of such vessels.

Assessment of ship performance in terms of her survivability, however, is not straightforward an undertaking, as in addition to complexity of predicting ship behaviour in waves, further intricacies arise in accounting for progressive flooding through the vessels internal layout and ensuing ship-floodwater interactions.

Such dynamic effects of fluid motion on the ship responses, and vice-versa, have been extensively studied in the past from the viewpoint of roll stabilising tanks, oil tankers, water trapped on deck, LNG carriers, and others where the amount of fluid mass in the tank is constant. The problem of a ship undergoing progressive flooding entails further degrees of non-linearity arising from fluid mass variation, which also renders the simulated process non-stationary.

The general difficulties in dealing with the problem accurately derive in great part from the sloshing phenomenon, which mode, influenced by tank geometry, dimensions and position with respect to axis of rotation, the amount of fluid, and amplitude or frequency of motion, [1], displays a character ranging from small-amplitude short waves formation, non-linear standing waves to highly non-linear hydraulic jumps or combinations of the above, [2]. Also the dynamic pressures exerted on the tank surface are of non-linear nature as they comprise both non-impulsive loads related to fluid transfer as well as impulsive localised loading, ref. [2].

Published research on the subject exhibits a variety in levels of sophistication and type of approaches towards solving these problems. Two classes of approaches can be broadly distinguished: techniques employing latest advancements in science of computational fluid dynamics (CFD) and simplified methods based on rigid-body theory.

Recent studies on coupled ship motion and water sloshing, addressing the first of the above appraoches, have been reported by Mikelis et al, [9], Francescutto et al, ref. [10], Bass et al, ref. [11] or de Daalen et al, ref. [12], where the excited due to tank/ship motion internal fluid behaviour is dealt with by solving the Navier-Stokes equation numerically and coupling it with the

simultaneous time-domain solution of more or less complex equations of intact ship motions with then fluid forces taken as external input. Further, de Veer et al, ref. [13], showed some attempts to predict in a similar manner effects of water ingress, with the rate of flooding itself estimated from Bernoulli equation. In addition to water sloshing coupled to 6d.o.f. ship motion prediction model, Woodburn et al, [14], accounts for some fluid interaction between the internal water and the outside sea domain to represent water ingress/egress in somewhat more sophisticated manner.

There does not seem to be much of a doubt that in the fairly foreseeable future these approaches will become a naval architect's routine procedures. As is the general consensus at present, however, these methods require excessive computational as well as expert efforts, preventing their methodological application in studies on dynamic ship stability.

The second class of approach, therefore, has found considerable research interest and recognition of the balance between simplicity and sufficiently meaningful representation of physics. Here, the mass of the liquid is regarded as behaving like a pendulum attached to the ship, with its mass located at the centre of the fluid buoyancy, which in turn is found from intersection of the tank geometry and fluid free surface assumed flat. The fluid free surface is most commonly assumed to always remain parralel to the sea level, e.g. Vassalos et al, [4], [5], de Kat, [3], or more recently assumed to be moving in accordance with some basic physics motion mechnism, e.g. Papanikolaou et al, [7].

The purpose of this paper is to discuss some fundamental validation study on the implications of the above-mentioned simplifications in modelling of the fluid behaviour onboard the flooded ship and building on that demonstrate the degree of agreement achieved in predicting damaged ship dynamics. For this purpose, a very brief overview of the mathematical model for generalised ship motion is given, followed by some details of the floodwater motion mechanism under study. Next, results of numerical simulations of bench-testing of water sloshing derived experimentally by de Bosh and Vugts, ref. [1], are presented together with discussions. Finally, the outcome of predictions of the damage ship dynamic behaviour by means of such an approach is demonstrated, with the concluded nuances pointed out.

2. GENERALISED SHIP MOTION MODEL

Equations for damaged ship behaviour description are derived from fundamental motion principles: the conservation of linear and angular momentum law. The law applied for rigid bodies, whereby this definition is also extended on the internal fluid mass, is resolved in body-fixed system of reference, see Figure 1. Rigorous derivation leads to a set of 6 scalar equations for linear and angular motions. Three such equations for angular motions are presented here in vector form (1).

The right hand side of the equation, $\vec{M}'_{Gs}$, and respective force vector in the set of equations for rectilinear motions, represents all the external forces and moments acting on the vessel expressed in a body-fixed system of reference, $G_s xyz$, located at the ship centre of mass. These forces are predicted with conventional for Naval Architecture methods. The Froude-Krylov and restoring forces and moments are integrated up-to the instantaneous wave elevation, the radiation and diffraction forces and moments are derived from linear potential flow theory and expressed in time domain based on convolution and spectral techniques, respectively. The hull asymmetry due to ship flooding, is taken into account by a "database" approach, whereby the hydrodynamic coefficients are predicted beforehand, and then interpolated during the simulation. The correction for viscous effects on roll and yaw modes of motion is applied based on well-established empirical methods. The second order drift and current effects are also catered for, at present, based on parametric formulations. Naturally the gravity force and moment vectors correspond to ship and flood water weights.

$$
\begin{aligned}
&(I'_s + I'_w)\cdot\frac{d}{dt}\vec{w}' + M_w\cdot\left[\vec{r}'_w\times\left[\frac{d}{dt}\vec{v}'_{Gs}\right]\right] + \\
&+ M_w\cdot\left[(\vec{w}'\times\vec{r}'_w)\times\vec{v}'_w\right] + \\
&+ M_w\cdot\left[\vec{r}'_w\times\left[\frac{d}{dt}\vec{v}'_w + \vec{w}'\times(\vec{v}'_{Gs}+\vec{v}'_w)\right]\right] + \\
&+ \frac{d}{dt}M_w\cdot\left[\vec{r}'_w\times(\vec{v}'_{Gs}+\vec{v}'_w)\right] + \\
&+ \left(\frac{d}{dt}I'_w\right)\cdot\vec{w}' + \vec{w}'\times\left[(I'_s + I'_w)\cdot\vec{w}'\right] = \vec{M}'_{Gs}
\end{aligned}
\qquad (1)
$$

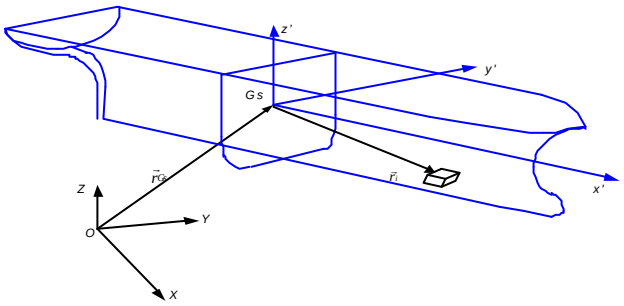

Figure 1 Coordinate system fixed to the centre of gravity of the intact vessel

The whole system, after re-arranging into matrix form as a set of twelve differential equations of the first order, are

solved for position in space of the centre of gravity of the intact ship $\vec{r}_{Gs} = \int \vec{v}_{Gs} \cdot dt$ and three rotations through a 4th order Runge-Kutta-Feldberg integration scheme with variable step size.

3. INTERNAL SLOSHING MODEL

Still undetermined in equation (1), are the relevant vectors for floodwater location, velocity and acceleration, $\vec{r}'_w$, $\vec{v}'_w$ and $\frac{d}{dt}\vec{v}'_w$, respectively. These are the quantities that must be derived from a model representing the sloshing water phenomenon. In case of application of the CFD techniques, these vectors and relevant forces and moments can be derived from pressure integration due to fluid motion. Here, however, simplifications as mentioned in the foregoing, are adopted.

A model, the initial concept of which was presented by Papanikolaou et al in [7], has been developed as a free mass point moving due to the acceleration field and restrained geometrically by predetermined potential surfaces of centre of buoyancy for given amount of floodwater, FMPS (**F**ree **M**ass in **P**otential **S**urface), see Figure 2. This model derived from simple rigid body motion consideration, similar to that leading to equations (1), is presented as a set of equations (2), with graphical explanation in Figure 2:

$$\begin{cases} \frac{d}{dt}\vec{r}'_w = \vec{v}'_w - (\vec{v}'_w \cdot \vec{n}') \cdot \vec{n}' \\ \frac{d}{dt}\vec{v}'_w = \vec{a}'_f - (\vec{a}'_f \cdot \vec{n}') \cdot \vec{n}' \end{cases} \qquad (2)$$

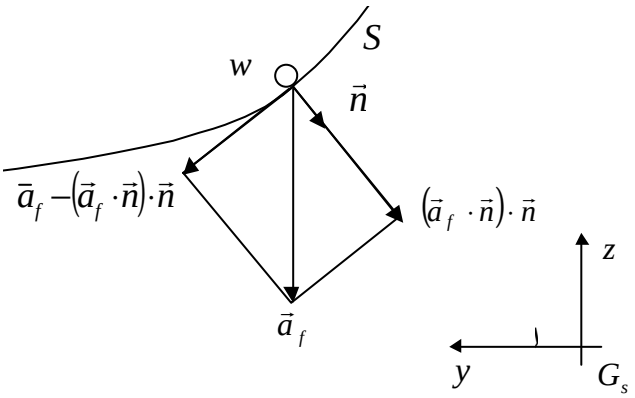

Figure 2 Fluid particle "w" (centre of buoyancy) in acceleration field $\vec{a}_f$ moving on the potential surface S
All the vectors are resolved in $G_s xyz$ system of reference.

The total forcing acceleration vector is:

$$\vec{a}'_f = \vec{g}' - \vec{a}'_s - 2 \cdot \vec{w}' \times \vec{v}'_w - m^* \cdot \vec{v}'_w \qquad (3)$$

Where $\vec{a}_s$, see equation (4), is ship motion-related acceleration vector expressed in body-fixed system of reference.

$$\vec{a}'_S = \frac{d}{dt}\vec{v}'_{Gs} + \frac{d}{dt}\vec{w}' \times \vec{r}'_w + \vec{w}' \times (\vec{v}'_{Gs} + \vec{w}' \times \vec{r}'_w) \qquad (4)$$

$\vec{n}$ is the instantaneous normal vector to the potential surface of floodwater motion, determined from a damage compartment geometry database. Note that the vector is a function of $\vec{r}_w$ and volume of the fluid. Finally, m^* is an artificial coefficient introduced to represent damping of floodwater motion. This coefficient is an *ad hoc* adopted value derived for simple box-shaped compartment from comparisons with experimental data, as discussed later.

With the geometric information about the tank stored in a database, the model is complete. Equation (2) is set up for each flooded compartment within the ship and solved simultaneously with the equations for ship motion.

Having determined fluid motion, the forces and moments due to its displacement can be calculated. For demonstration purposes, the moment vector extracted from equation (1) is used and presented in the form of equation (5), where three components are distinguished to represent inertial moment, gravity moment and non-linear moment, see equations (6), (7) and (8), respectively. Note here that the fluid inertia matrix, I'_w, contains only the inertia of a single mass point located at a position $\vec{r}'_w$ in the ship-fixed system of reference at G_s. Since the mass is constant, the terms containing the time derivative of mass disappear.

$$\vec{M}'_{wat} = \vec{M}'_I + \vec{M}'_g + \vec{M}'_N \qquad (5)$$

Where:

$$\vec{M}'_I = I'_w \cdot \frac{d}{dt}\vec{w}' \qquad (6)$$

$$\vec{M}'_g = M_w \cdot \vec{r}'_w \times \vec{g}' \qquad (7)$$

$$\begin{aligned} \vec{M}'_N &= M_w \cdot [(\vec{w}' \times \vec{r}'_w) \times \vec{v}'_w] + \\ &+ M_w \cdot \left[\vec{r}'_w \times \left[\frac{d}{dt}\vec{v}'_w + \vec{w}' \times (\vec{v}'_w) \right] \right] + \\ &+ \vec{w}' \times [(I'_w) \cdot \vec{w}'] \end{aligned} \qquad (8)$$

4. NUMERICAL STUDIES

Experiments performed by de Bosch and Vugts, [1], have been the basis for studies on fluid sloshing described in this paper. In their experimental research, they performed a series of bench testing on the behaviour of the fluid in the box-shaped tank. The tank, with dimensions of 0.1m in length, 1.0m in breadth and 0.5m in depth, was filled with water, and excited at a range of rotation amplitudes and frequencies. The tank moment amplitude, K_a, as well as the angle ε by which the moment lags behind the rolling was recorded. The moment was expressed as:

$$m_{wat}(t)\big|_x = K_a \cdot \sin(\omega \cdot t - \varepsilon)$$

Since the flow behaviour in such conditions displays very complex nature, as mentioned earlier on, it was perceived of great interest to quantify to what degree the fluid loads can be predicted by simplified methods such as discussed in this paper.

After successful demonstration that a pendulum motion can be accurately simulated by model (2), see Figure 3, a basic prediction of tank natural frequencies was undertaken (note that the dimensions of the tank used for this exercise were 20m in breadth, 20m in length and 20/90m in depth). By comparison with an analytical solution (9), the test revealed that natural frequency could be predicted with reasonable accuracy only for lower filling ratios (fluid height to breadth of the tank), as shown in Figure 4. As the filling increases, the surface over which the centre of volume can travel decreases, and ultimately becomes a single point for full tank. Therefore, the natural period of such tank decreases rapidly if the filling height exceeds approximately half of the tank depth. The same tendency of under-prediction of natural period for higher filling ratios (h/b > 0.3-0.4) is noted also for greater tank depths.

$$\omega_S = \sqrt{\frac{g \cdot \pi}{b} \cdot \tanh\left(\frac{h \cdot \pi}{b}\right)} \qquad (9)$$

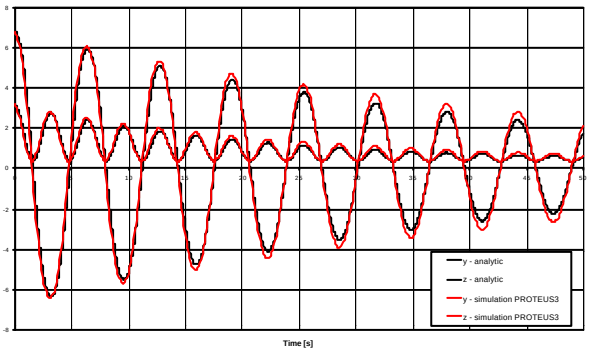

Figure 3 Simulation of the free motion of mass point in sphere-shaped tank, compared with the analytic solution

Further tests with imposed harmonic oscillations were performed to estimate the tank response in terms of forces generated by the fluid. Figure 10 and Figure 11 show amplitudes and phases, respectively, of the total moment (5) around rotation axis x. Notable in these figures is the effect of the damping coefficient μ^*, the value for which thereafter has been adopted as 0.15. For lower values of this coefficient, the predicted moment shows characteristics of an under-damped spring-mass system. With the damping adjusted as mentioned, however, the predicted moment amplitude and phase compare very favourably with the measurements. Although the calculated amplitude curve shows slight difference, as it resembles typical damped spring-mass systems behaviour, it is the accurate estimation of the phase angle, which renders the modelling a very reliable tool for sloshing estimations. Since the filling ratio is relatively low, the natural period is predicted also quite accurately.

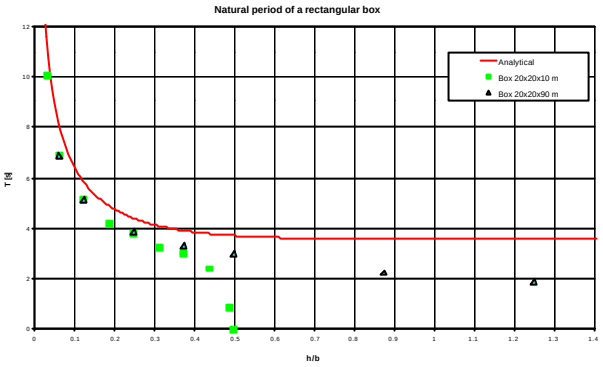

Figure 4 A comparison between the theoretical natural period for a rectangular box and the simulated natural period of fluid motion based on the FMPS model

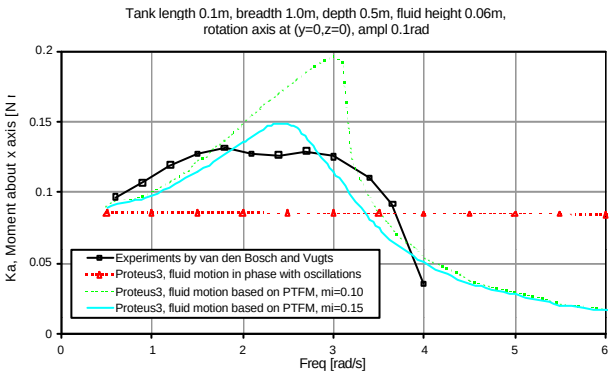

Figure 10 Comparison of fluid moment amplitudes derived by experiments and in-phase and FMPS sloshing models

Additionally, results from a simpler model are shown where the floodwater free surface is assumed to move in phase with the ship rotations. Note that in this case the velocity and acceleration vectors, seen in (8), can be

derived by means of backward differentiation on the instantaneously estimated centre of buoyancy. As can be seen from Figure 10, the moment remains virtually constant irrespective of the frequency of oscillation, with the phase angle shown in Figure 11, by assumption being zero. The moment amplitudes are considerably lower than the values measured experimentally or predicted by model (2) for most of the frequency range, implying that the free surface slopes derived in the latter are consistently exceeding the rotation amplitudes.

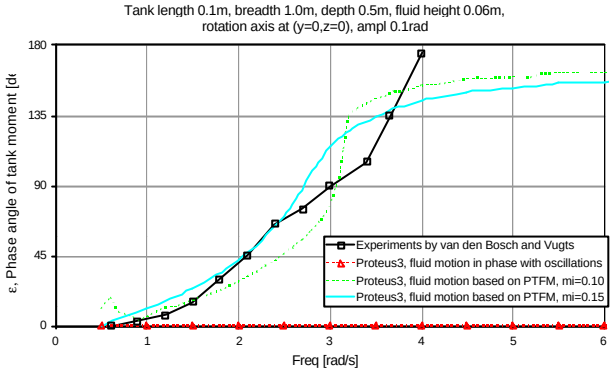

Figure 11 Comparison of fluid moment phase angles derived by experiments and in-phase and FMPS sloshing models

Simulations with different filling ratios confirm consistent predictions of the amplitudes of the tank moments, as is shown in Figure 12.

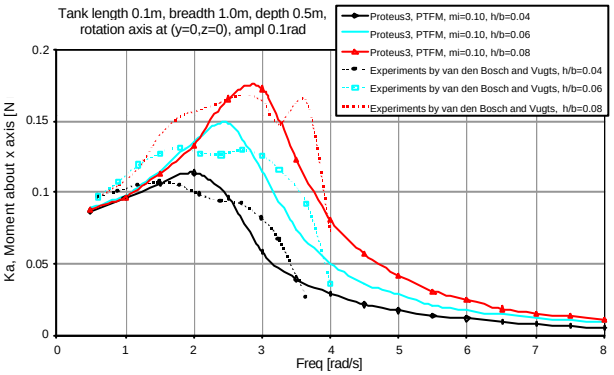

Figure 12 Comparison of fluid moment amplitudes derived by experiments and FMPS sloshing models. Effect of filling ratio.

Finally, partially surprising it was discovered that the most predominant component of the water sloshing moment in this case is due to gravity, as is shown in Figure 13. However, some further testing showed that the non-linear terms are of considerable importance for greater filling ratios (h/b~0.25), which is demonstrated in Figure 14.

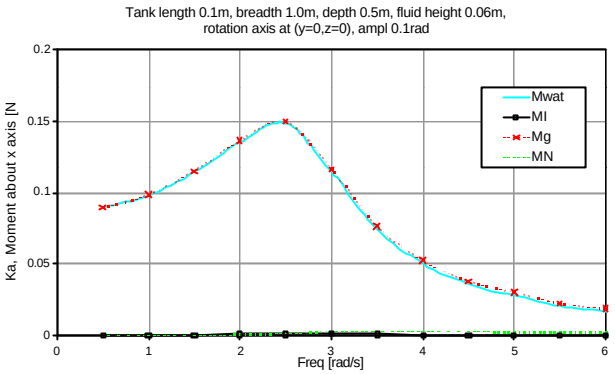

Figure 13 Fluid moment amplitudes derived by FMPS sloshing model. Comparison between different moment components. For low filling ratio, the gravity moment is the predominant component

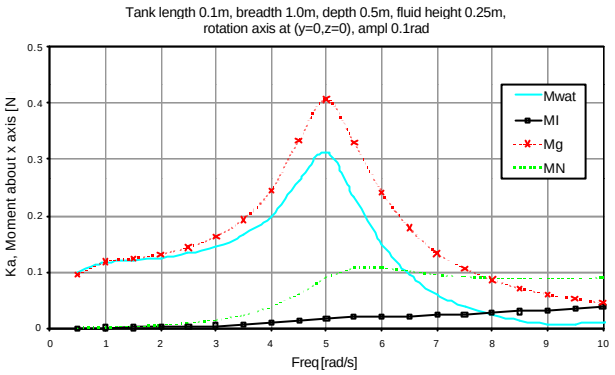

Figure 14 Fluid moment amplitudes derived by FMPS sloshing model. Comparison between different moment components to elucidate importance of non-linear terms for higher fill ratios (h/b~0.25)

The very fundamental case studies discussed above demonstrate that the techniques presented in this paper for predictions of fluid sloshing and its effects, can be confidently applied for examining the dynamic stability of flooded ships. This derives from the fact that the main load components due to fluid transfer can be modelled from basic of dynamic laws, and that the highly non-linear effects present during water sloshing are of minor importance, perhaps relevant for more focused studies on e.g. impulsive loads on localised elements of tank structures.

Length between perpendiculars	170.00	m
Subdivision Length	178.75	m
Breadth	27.80	m
Depth to subdivision deck	9.00	m
Depth to E-Deck	14.85	m
Service Draught	6.25	m
Displacement	17301.7	t
KMT	15.522	m
KG	12.892	m

Deriving from this conclusion, a study into basic dynamic behaviour of a damaged ship has been undertaken. A representative of typical modern passenger

Ro-Ro ship is used in this study, with its general particulars given in the table above and Figure 15. The frequency roll response curve derived numerically as well as by means of physical testing for the intact ship is presented in Figure 15. The agreement achieved is satisfactory. The comparison of the derived responses in damaged condition, however, has proved less favourable. As can be seen in Figure 17, the numerically derived roll response curve does not show any noticeable change in the natural frequency of the damaged ship, which phenomenon is clearly seen in the experimental data. Also the damping present in the damage ship system does not seem to be reproduced sufficiently high.

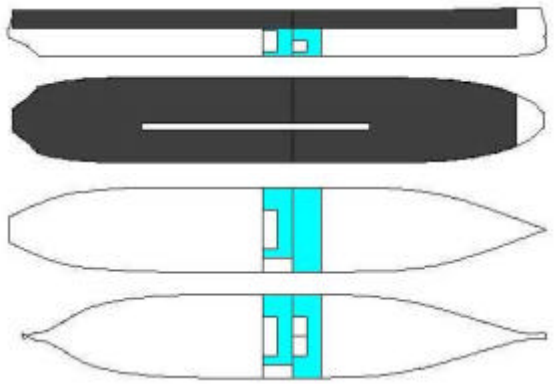

Figure 15 Internal arrangement of damaged compartments on PRR1 vessel.

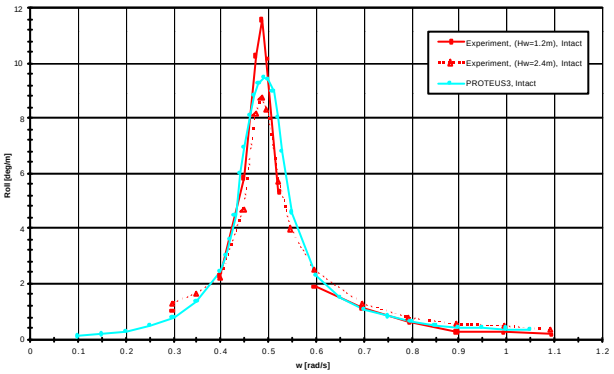

Figure 16 Roll frequency response curve for Ro-Ro vessel PRR1 in intact condition

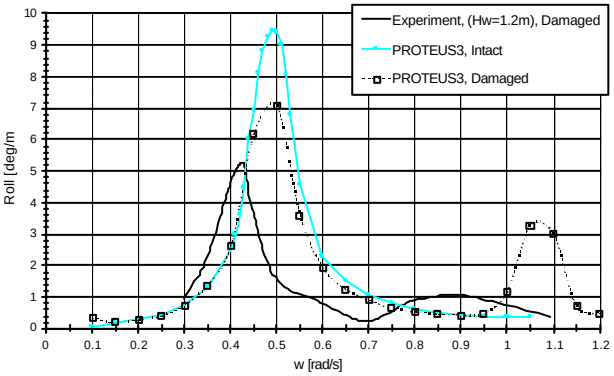

Figure 17 Roll frequency response curve for Ro-Ro vessel PRR1 in damaged condition

Bearing in mind the evidence presented in the foregoing on the ability to represent fluid sloshing in a closed tank with sufficient accuracy, to model intact ship behaviour accurately, and assuming that variation in the ship hydrostatic properties due to damage is negligible for the relevant roll range of up to 10deg, as shown in Figure 18 (GM_I=2.6m, GM_d=2.4m), the following have been suggested as the most likely sources of the discrepancy in modelling of the damaged ship dynamics by the presented method:

a) The natural frequency of the flooded compartment below the car deck and therefore the phase angle between the ship roll and fluid loads are not represented accurately, (approximately 70% of the space, h/b~0.25, is flooded).
b) The constant water ingress/egress (represented herewith by Bernoulli equation) affect the internal fluid behaviour.
c) The constant water ingress/egress affect the ship hydrodynamic properties.

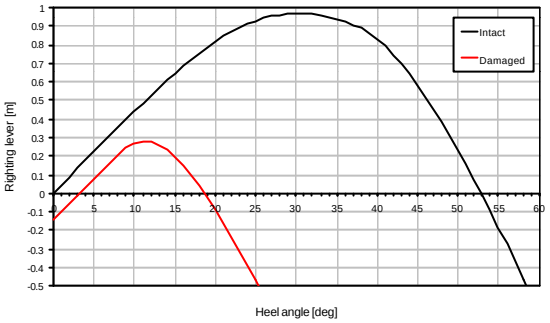

Figure 18 GZ curve for intact and damaged conditions, PRR1 vessel

As a first steps to investigate the above point (c) an *ad-hoc* adjustment has been made, whereby the total roll inertia of the ship has been increased by ~24% (2.2 times the added roll moment of inertia) and the predictions of viscous roll damping with the well known formulae by Himeno, [17], has been increased fivefold. The results of predictions of frequency roll response curves in damaged conditions after such modifications are shown in Figure 19.

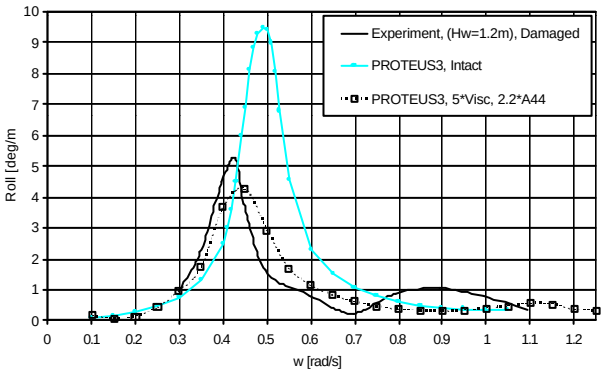

Figure 19 Roll frequency response curve for Ro-Ro vessel PRR1 in damaged condition, adjusted coefficients

The study into the problems highlighted above is ongoing and it is hoped that the sources of discrepancies will soon be identified and possibly resolved.

5. CONCLUSIONS

A mathematical model for the prediction of damaged ship dynamics has been presented. The emphasis has been put on outlining the model for water sloshing. Validation studies undertaken have demonstrated reliability of simplifed modelling of the fluid sloshing phenomenon. Nothwithstanding these advancements, however, some discrepancies in predicting basic dynamics of a damaged ship with water ingress/egress have been identified. Some reasoning behind this has been put forward. However, no firm conclusions can be made at present.

6. ACKNOWLEDGEMENTS

The authors would like to acknowledge the financial support of the European Commission DG Research for the work presented in this paper, which forms part of Project NEREUS, Contract No. G3RD-CT 1999-00029 and to express their gratitude and sincere thanks.

7. REFERENCES

[1] Van den Bosh, J, J, Vugts, J, H, "Roll damping by free surface", Report no. 134, Shipbuilding Laboratory, Delft.

[2] Hamlin, N, A, Lou, Y, K, Maclean, W, M, Seibold, F, Chandras, L, M, "Liquid sloshing in slack ship tanks - theory, observations and experiments", SNAME Transactions, Vol. 94, 1986, pp. 159-195

[3] de Kat, J, "Dynamics of a ship with partially flooded compartment", 2nd StabWshop, Japan, 1996

[4] Vassalos, D., Turan, O., 1994, "A realistic approach to assessing the damage survivability of Passenger ships", TSNAME.

[5] Vassalos, D., Letizia, L., 1995, "Formulation of a non-linear mathematical model for a damaged ship subject to flooding", Sevastianov Symposium, Kalinigrand.

[6] Zaraphonitis, G., Papanikolaou, A., Spanos, D., 1997, "On a 3D Mathematical Model of the Damage Stability of Ships in Waves", STAB'97, Bulgaria.

[7] Papanikolaou, A, Zaraphonitis, G., Spanos, D., Boulougouris, E., Eliopoulou, E., 2000; "Investigation into the capsizing of damaged Ro-Ro passenger ships in waves", STAB'00, Launceston, Tasmania, Australia

[8] Chang, B. C., Blume, P., 1997, "Survivability of Damaged Ro-Ro Passenger Vessels at Sea", 3rd StabWshop, Greece.

[9] Mikelis, N,E, Miller, J, K, Taylor, K, V, "Sloshing in partially filed liquid tanks and its effect on ship motions: numerical simulations and experimental verification", RINA Spring Meetings 1984, Paper No. 7.

[10] Francescutto, A, Contento, G, "An experimental study of the coupling between roll motion and sloshing in a compartment", ISOPE'94, Osaka, 10-15 Apriol, 1994, Paper N. 94-YI1-4

[11] Bass, D., Cumming, D., 2000;"An experimental and numerical investigation of the effects of water trapped on the deck", STAB'00, Launceston, Tasmania, Australia

[12] Daalen E.F.G. van, K.M.T. Kleefsman, J. Gerrits, H.R. Luth, A.E.P. Veldman, 2000, "Anti-roll tank simulations with a volume of fluid (VOF) based Navier-Stokes Solver", 23rd Symposium on Naval Hydrodynamics, paper issued for discussion

[13] R van't Veer, Jan de Kat, 2000 ; "Experimental and numerical investigation on progressive flooding and sloshing in complex compartment geometries", STAB'00, Launceston, Tasmania, Australia

[14] Woodburn, P, Gallagher, P, 2001, "First Principles Design for Damage Resistance Against Capsize, Hydrodynamics of Floodwater Employing CFD", Mid Term Report for NEREUS project, WS Atkins Consultants Ltd

[15] Rakhmanin, N, Zhivitsa, "Predictoin of motion of ships with flooded comparments in a seaway", Proceedings of the STAB'94 Symposium, Melbourne (FL)

[16] Papanikolaou, A, Spanos, D, 2001, *"ITTC Benchmark Study on the Capsizing of a Damaged Ro-Ro Passenger Ship in Waves"*, Final Report, NTUA

[17] Himeno Yoji, "Prediction of ship roll damping – state of the art", Report No 239, University of Michigan, College of Engineering, September 1981

An Introduction to the Session on *"Large amplitude rolling motion and nonlinear ship dynamics"* and a proposal for the establishment of an international group

FOR THE STUDY OF NONLINEAR PHENOMENA IN THE DYNAMIC BEHAVIOUR OF SHIPS AND OF OTHER MARINE STRUCTURES

by

Kostas Spyrou and Alberto Francescutto

In recent years we have witnessed a significant progress in the understanding of complex nonlinear phenomena of dynamic behaviour of ships. Significant new insights concerning mechanisms generating instability in various motions directions have been achieved and new avenues towards the development of rigorous, yet useful, measures for ship design or operation have been opened. Some of these issues will be discussed during the current Workshop. Such a progress would not have been possible without the effective use of a powerful set of concepts, methods and techniques which collectively comprise what has become customary to call a "nonlinear dynamical systems' approach". This approach rests equally on theory and experiment, has a clearly interdisciplinary nature and has found already application in a wide variety of engineering problems. Yet, despite its strong scientific footing, well proven importance and forged connection with application, when considered against a conventional naval architectural background it appears still almost exotic, and privilege of a small group of specialists.

There is a clear need for a coordinated action at international level engaging the several active researchers of the field, which will promote the wider and deeper use of the nonlinear dynamics' ideas and tools in the education and training, the research and the practice of naval architecture and related disciplines. This can be facilitated with the formation of *an international group on nonlinear ship dynamics* which will be working towards objectives such as, but not restricted to, the following:

- Promoting the use of nonlinear dynamics ideas in a wider context within the marine technology research community.
- Reporting about the state-of-the-art and identifying new problems where such ideas can find fruitful application.
- Organising dedicated meetings and acting as a high-level and authoritative scientific forum for the discussion of practical safety measures related with the occurrence of nonlinear phenomena.
- Facilitating joint research initiatives at international level and also the exchange of visits between researchers.
- Liasing with similar groups in other engineering fields as well as with international research or professional maritime organisations.
- Undertaking initiatives for the introduction of the teaching of nonlinear dynamics in the undergraduate and postgraduate curricula of departments of naval architecture or of similar disciplines.
- Promoting the familiarisation of practising naval architects with the basic concepts through publication and the organisation of seminars.

Some of the recent initiatives which this group could build further upon are:

- The workshop on nonlinear ship dynamics which was "run" successfully in the last two STAB Conferences (in Varna & in Launceston),
- the sessions dedicated to Nonlinear Dynamics in the context of the series of international workshops on the Stability and Operational Safety of Ships (in Crete, in Newfoundland and the current one in Trieste) which have attracted in all cases first-class participation,
- the recent publication of a special issue in the Philosophical Transactions of the Royal Society on *the nonlinear dynamics of ships*.

As it is obvious, several detailed issues need to be discussed and resolved that will allow the formation of the group to be successful. Without attempting to pre-judge the debate which is hoped to take place during the preliminary meeting of Nonlinear Dynamics on the 11th of September, some possible matters for discussion could be:

- the specific structure of the group,
- possibilities of representation in international organisations,
- initiatives that could be undertaken in the immediate future.

Organizational Meeting of SNAME Working Group A on Fishing Vessel Stability Criteria
Professor Bruce Johnson, Chair & Professor Pasqualle Cassella Vice Chair, Southern Europe

Agenda

1. **Introduction of attendees**
2. **Review of Charter of SNAME Ad Hoc Panel on Fishing Vessel Operations and Safety** (See Johnson and Womack Paper in 1st day afternoon session) and web site http://www.sname.org/committees/tech_ops/fishing/home.html
3. **Discussion of organizational options for accomplishing the tasks of Working Group A**
    1. Recruit Regional Vice Chairs (or Coordinators) to plan and coordinate F/V information gathering by region including improvements in weather and wave data gathering
    2. Develop a standard format for reporting the results of model tests (and any full scale comparisons) including the essential model geometry characteristics and wave characteristics, such as rather complete statistical characteristics for irregular wave tests and long crested wave characteristics and asymmetries for wave impact capsize tests.
    3. Encourage each region to assemble and report on dynamic stability model tests of the typical F/V types used in that region.
    4. Build a database of dynamic stability tests on fishing vessels and use this database to suggest new risk-based stability criteria.
    5. Work with the ITTC SCEXCAP, to formulate a cooperative fishing vessel research program to develop a complete set of scalable, non-dimensional parameters for designing and building safer vessels. It is expected that the effects of variations in length, beam, draft, freeboard, sheer line, bulwark and deckhouse arrangements and loading conditions can be correlated with a new set of risk-based stability criteria and design parameters for increasing small vessel safety and survivability in a variety of situations. Note that extending hydrostatic analysis software to 180 degrees would greatly enhance the issue of survivability assessment

4. Comments on the use of existing F/V stability standards:

A frequently used interpretation in applying the Torremolinos Protocol stability criteria is that the area under the righting arm curve represents “righting energy”. A possible solution to this misinterpretation is to change the terminology to "unit righting energy" or even “unit static righting energy”. This interpretation is correct since the righting arm is righting energy per unit displacement, m-tons-degrees/ton (ft-tons-degrees/ton). The heeling arm is also the "unit heeling energy" for the same reason. This terminology would imply the correct interpretation that righting energy increases with displacement, all other variables being held constant. If the Workshop agrees with this interpretation, it should be reflected in the ITTC Symbols and Terminology List.

Briefly, scalability in vessel stability characteristics depends on the square-cubed rule, i.e. the heeling forces, which depend on water and wind impact areas, go up with the square of the dimensions but the righting moment depends on the displacement which goes up with the cube of the dimensions.

Correctly interpreting the scalability of the Torremolinos criteria should mean that vessels double in dimensions should survive without capsizing in twice the wave height conditions. However, that is not the interpretation generally given by the existing one-size-fits-all stability guidelines. The wind heel criteria do scale with size, however, since the heeling arm analysis includes being divided by the vessel displacement as is shown in Appendix A.

As an example of what can be done while the F/V community waits for better risk-based stability criteria to be developed, the following status report on a new form of stability letter is offered by John Womack, Vice chair of SNAME Working Group B:

Appendix A
Exploration Into the Preliminary Development of a Weather Dependent Stability Criteria for Small Commercial Fishing Boats

by John Womack, V-Chair of Working Group B

Revised 08/19/01

In a review of weather stability criteria for fishing boats over 24 meters (79 feet) and other commercial vessels, the primary type of criteria in use the Torremolinos Convention criteria or a modified form thereof. Other criteria such as the severe wind & roll criteria, water on deck, lifting weight over the side, or towing large gear are available, but they are currently used to check stability in specialized operating conditions. In all cases, these criteria are designed for a one-size-fits-all generic full storm conditions, often applied against a generic vessel. The one-size-fits-all generic full storm and a generic vessel present several problems for today's small commercial fishing boats.

First, there are many different geographical areas being fished today, each of which has unique sea conditions. For example the size and frequency of the waves encountered in the Gulf of Mexico are significantly different than those on the Mid-Atlantic eastern coastline or the Mid-Atlantic open ocean. Clearly, different stability levels are needed to safely work in the different areas. Additionally, the criteria do not take into account any seasonal differences such as occur on the Mid-Atlantic eastern coastline. These differences in working areas is reflected in current fishing boat designs such as the typical Gulf of Mexico shrimp trawler and the Atlantic Ocean stern trawler, which have evolved over time.

Another problem with these criteria is they are designed for full storm conditions. While correct for fisheries that work long trips more than a day or two steam from a harbor of safe refuge, many fisheries have either short trip times or work close to shore and can reach a safe port in less than a day's steam. For example, the Mid-Atlantic surf clam and ocean quahog trips are 24 to 32 hours dock to dock and range a maximum of 60 to 70 nautical miles from port.

To apply the current generic storm conditions to these vessels is overly conservative. The crews have already figured out that they can safely carry more catch in good weather. Issuing a stability letter with the conservative loading limit set by the current criteria is causing many of the crews to ignore their stability letter. Having available a criteria that provides stability guidance in less than storm conditions will give crews guidance they will trust and follow. Knowing the true risks for each loading condition, the crews will hopefully take the appropriate actions for the expected weather.

The Torremolinos Convention criteria are designed to provide sufficient stability to allow a typical vessel to survive most storms. The basic characteristic of the Torremolinos Convention criteria is minimum area requirements under the righting arm curve to specific angles of heel or the point of uncontrollable down flooding. Additional requirements for initial metacentric height, minimum righting arm values, and the heel angle of the maximum righting arm are also specified. Over time, supplementary requirements have been added to some versions of the Torremolinos Convention criteria such as a minimum range of positive stability or requirements when the maximum righting arm occurs at low angles of heel. A comparison of several versions of the Torremolinos Convention based criteria will be shown at the workshop.

Though the Torremolinos Convention criteria has proven adequate over time, it does have several drawbacks for use in evaluating a fishing boat's stability, particularly in less than storm conditions. The Torremolinos Convention criteria are for a "generic" vessel in a one-size-fits-all storm. The criteria's values do not reflect different geographical or seasonal conditions present in different fishing grounds. The criteria also does not take into account the type of vessel, its hull shape (hard chine or round bilge), the presence or absence of bilge keels or other roll reduction devices, or other unique characteristics, all of which affect a boats response in a seaway. Lastly, the

criteria are not suggested for use on boats less than 79 feet long, nor can the be used to evaluate a boats stability in less than storm weather conditions.

The principal reason for these problems lies in the basic design of the Torremolinos Convention criteria. The criteria use a series of simple static calculations to evaluate a complex dynamic situation; that is the boat's static stability in calm water with generic one-size-fits-all allowances for the dynamic effects of winds and waves. The static calculations of the righting arm only reflect the gross shape of the particular hull, both the part that is submerged and the remaining freeboard. In addition, the selection of specific heel angles such as 30 or 40 degrees for certain parts of the criteria are somewhat arbitrary and do not fit many modern-day fishing boat designs.

The appeal of the Torremolinos Convention criteria is its relatively simple calculation procedure that was practical when slide rules where the computers and planimeters/integrators where the supercomputers. The only change made with the advent of readily available personal computers is allowing the boat to trim to a balanced waterline as opposed to holding a fixed trim at all angles. This change is actually somewhat arbitrary especially for small boats that are more affected by the waves than larger commercial vessels. While the ability to directly dynamically model a small boat's response to a given sea condition is a decade or more away, modifications to the current "static" righting arm curve offer an interim ability to better represent the true dynamics of a particular small boat in a given sea condition.

The "severe wind and roll" criteria offers a more direct approach to evaluate the dynamic energy in wind and waves for a given boat in a given seaway. The basic approach to this criteria type involves two parts; a gust wind heeling arm to model the effects of wind and a roll angle to windward to model the effects of the waves, which are superimposed on the traditional righting arm curve (See PNA or Appendix A of Johnson-Womack Trieste Paper). In this setup area "A" represents the unit kinetic energy (unitized by the boat's displacement) developed by both the natural righting force of the boat and the heeling force from the wind. Area "B" is then the unit potential energy (again unitized by the boat's displacement) available to dissipate the developed kinetic energy.

Versions of this criteria are currently in use such as the USCG's criteria for small fishing boats given in 46CFR 28.575. The USCG's criteria are an adaptation of the IMO developed version. The US Navy also uses a version of the severe wind and roll to evaluate the stability of their vessels from harbor tugs to aircraft carriers in protected to unrestricted ocean service.

By working with these versions as a starting point and exploring new concepts, the intent is to develop a more robust version of the severe wind and roll criteria that can reflect the particular characteristics of the subject boat when working in a given sea condition. The three key components of the severe wind and roll criteria are; the wind heel arm, the roll angle to windward, and the relationship between area "A" and area "B".

The wind heel arm has been well developed over time, though it could stand a review. The IMO/USCG version uses a wind velocity that varies with the height above waterline of the surface in question. For example a pilothouse would be subject to a higher wind velocity than the hull adjacent to the waterline. While theoretically correct in the lab on a level water surface, it is not correct for a small boat bobbing on large waves. The IMO/USCG wind heel arm also does not vary as the vessel heels, which would be expected just as a sailboat would dump wind from its sails as it heels.

The US Navy uses a simple one-wind velocity for all surface areas equation, which is better approach. Their equation also varies the heel arm as the boat heels. The US Navy's wind heel arm equation is;

$$HA = C \times V^2 \times A \times L \times \cos^2(\phi) / W$$ - Where;

C = Dimensionless Coefficient

A = Projected Sail Area, Square Feet or Sq m

V = Nominal Wind Velocity, Knots

L = Lever Arm (Vertical distance from the center of lateral resistance to the centroid of the sail area), Feet or m

ϕ = Heel Angle, Degrees

W = Displacement, Pounds or Newtons

While this may seem as taking a step back, it is also important to remember the more complex a calculation, the greater the chance of a mathematical error could be made. Sometimes simpler is better, especially when the more complex version offers no better accuracy. Additional research into the correct value for the coefficient "C" needs to be done to reflect the unique profiles on the various types of fishing boats in use.

The roll angle to windward is the component of the severe wind and roll criteria that can be used to model a particular boat's response in a given sea. In this area, the IMO/USCG version uses a calculation that takes into account the particular boat's hull shape (hard chine or round bilge), the presence or absence of bilge keels, and the initial stability. While this does reflect some of the subject boats unique characteristics, additional review should be done to investigate the effect of other vessel characteristics such as freeboard, sheer configuration, etc. The IMO/USCG version also assumes a generic one-size-fits-all sea condition. Additional research needs to be done to reflect both different storm conditions for geographical or seasonal variations and the sea conditions in less than storm conditions.

The last component of the severe wind and roll criteria is the relationship between area "A" and area "B". This component is where the adequacy of the boat's stability level can be evaluated. The principal area to be researched is what cutoff point to use for area "B". Typical points used in previous versions are the 2nd intercept point, the point of down flooding, or an arbitrary heel angle such as 40 or 50 degrees. Using, the point of the maximum righting arm should also be investigated as this is unique to the particular boat's stability characteristics.

The relationship between area "A" and area "B" also allows ability to create a risk of capsize analysis to provided additional guidance to the fishing boat crews. Existing criteria coupled with current stability letter formats do not tell a crew how close they are to a limit. The loadings are given as safe/unsafe limits; the crews have no idea how much of a margin is present. There could be a large margin or none at all. By providing the crew with warning that they are approaching a limit will give them the ability to make better operational decisions. For example, if the weather outlook is iffy and they know they will be near a loading limit, they can elect to come in early or load less catch.

To experiment with several simple approaches to developing this new version of the severe wind and roll criteria, trials where run on a typical Mid-Atlantic offshore clamming boat. The trials use educated assumptions to explore some general concepts and trends when using these criteria in less than full storm conditions. Full theoretical and model testing needs to be done to make robust, effective criteria. The trial boat is a former 133-foot offshore supply vessel built in 1966 that around 1984 to 1986 was converted for use in the offshore clam-harvesting fishery. The boat operates on 24 to 32 hour dock to dock trips along the Mid Atlantic and New England coastline, typically ranging from 10 to 60 nautical miles from port. The catch is loaded on deck in steel cages similar to the loading of supplies on a typical offshore supply vessel. Due to the dredging gear, these clamming vessels generally work in winds less than 25 knots in order to keep the dredge in the sea bottom. Because of this wind restriction and the short trip times, this boat is ideally suited to weather dependent safe loading guidelines (See Attached Graphic). Note however, that the selection of the corresponding expected local significant wave heights and the equivalent open ocean significant wave heights need additional work. However, it is felt that the graphical approach using the stop light metaphor is a valid one.

Clearly, significant amounts of research still need to be done to make this workable criterion. In addition to the research mentioned above, many other trial boats from different fisheries and with different characteristics need to be investigated.

F/V # 1 40m OSV Clam Dredger - Safe Loading Table

Fuel Tanks 70% or Lower

All Loaded Cages are on the Main Deck

Dynamic Peculiarities of an Unstable Ship Rolling in Waves

by S. Zhivitsa, Krylov Shipbuilding Research Institute, Russia

Despite classification societies requirement for any ship to have an initial metacentric height being positive, in practice however the accidents when a ship loses her initial stability are quite possible. Among the reasons of that it can be non-correct loading, stock consumption, flooding of the upper compartments, for example, due to extinguish the fire, heavy icing.

Analytical methods accessing ship rolling allow with acceptable accuracy to calculate roll kinematic characteristics always supposing a ship possesses positive initial transversal stability. In situation when a ship looses her initial stability well known methods do not work properly due to strong non-linearity of the ship stability curve in vicinity of static list angle [1], [2].

In principle, as analysis of published works shows [4] - [8], very popular now time-domain simulation technique is able to solve the problem but it will be very time-consuming and tiresome procedure. For avoiding such infinite routine calculations we have tried to investigate behavior of a **s**hip with a **n**egative **i**nitial **s**tability (SNIS) by means of traditional analytical so-called "**v**aried **s**cale method" (VS-method) [3] applied to analysis of non-linear differential equations.

Hereinafter we present the basic results of unstable ship dynamics investigation based on mentioned approach.

As the ship motion mathematical model two "loll type" equations are suggested. The first one is Duffing equation which simulates SNIS rolling in full frequency domain (θ denotes a roll angle)

$$\ddot{\theta} + 2\nu_\theta \dot{\theta} - \alpha \cdot \theta + \beta \cdot \theta^3 = m_0 \cos(\omega t - \rho_0); \qquad (1)$$

the second one is Mathieu equation reflecting the features of a ship rolling at encounter frequency $\omega \approx 2\omega_\theta$ ($\omega_\theta = \omega_\theta(\theta_a)$ - roll natural frequency), where, as known, the ship can undergo the parametric swinging

$$\ddot{\theta} + 2\nu_\theta \dot{\theta} - \alpha(1 + a \cdot \cos \omega t) \cdot \theta + \beta \cdot \theta^3 = 0. \qquad (2)$$

In equation (2) $a = \frac{\Delta\alpha}{\alpha}$ is a relative amplitude of initial stability coefficient α alteration, caused by waves and ship motions. The rest of symbols in both the suggested equations are common ones in ship dynamics.

At representation of restoring moment in the chosen equations we restrict ourselves for simplicity by cubic polynomial because our attention in the work focuses mainly on steady

state rolling regimes with amplitudes far from vanishing angle of a stability curve when the extra terms in GZ curve expansion can not affect strongly the principle dynamic qualities of a ship. As concerns investigation of SNIS behavior in vicinity of the vanish angle this situation has been simulated in details by M. Kan [5], [6].

Applying of cubic polynomial $r(\theta) = -\alpha \cdot \theta + \beta \cdot \theta^3$ allows to obtain the simple relationships which describe main static and dynamic parameters of an initially unstable ship. For instance, static list angle θ_{st} will be determined by simple expression $\theta_{st} = \pm\sqrt{\frac{\alpha}{\beta}}$; a natural small amplitude roll frequency around stable equilibrium angle is calculated by formula $\omega_\theta \approx \sqrt{2\alpha}$; a border between the ship small oscillations around static list angle and large ones around upright angle $\theta_{unst} = 0$ is defined by relationship $\theta_{cr} = \sqrt{2}\cdot\theta_{st}$.

A phase portrait of autonomous SNIS oscillations presented in Fig.1 demonstrates all the regions of the possible steady-state roll regimes.

As to forced oscillations in accordance with VS-method idea a non-linear roll equation

$$\ddot{\theta} + 2\nu_\theta\dot{\theta} + r(\theta) = m_0\cos(\omega t - \rho_0) \tag{3}$$

can be transformed to an equation below

$$Z''(\varepsilon) + \frac{2\nu_\theta}{\dot{\varphi}}Z'(\varepsilon) + Z(\varepsilon) = H(\varepsilon)\,. \tag{4}$$

Equation (4) is linear with $z(\varepsilon) = f[\theta(t)]$, and $\varepsilon = \varphi(t)$, where ε is a new independent variable.

Unknown function $\varphi(t)$ characterizes the variable scale of real time *t* transformation into new one ε. Amplitude function $f[\theta(t)]$ is determined by expression:

$$f(\theta) = \sqrt{2\int r(\theta)d\theta + C}\,; \tag{5}$$

phase function $\eta(t) = \varphi(t) - \varphi(0)$ can be obtained from a solution of more complicate equation

$$t = \int_0^\eta \frac{d\eta}{\dot{\eta}(t)}\,. \tag{6}$$

For restoring moment approximated by the curve $r(\theta) = \pm\alpha \cdot \theta \pm \beta \cdot \theta^3$ right hand side of expression (6) is transformed into the first kind elliptic integral $F(\eta, k)$, and the solution of equation (6) is getting exact but, unfortunately, in an implicit form.

For determination of function $\eta(t)$ in explicit form elliptic integral $F(\eta,k)$ is expanded into trigonometric series. Accuracy of the roll equation solution is determined in dependence on the number of saved terms in the expansion.

Keeping in the expansion two terms the solution of non-linear equation (3) will be structurally the following:

- for small amplitude oscillations around the stable equilibrium positions, such that maximum roll angle $\theta_{max} << \theta_{cr}$, the rolling is characterized by following expression:

$$\theta_{max}^2\sqrt{\frac{\beta}{2}}-\frac{\alpha}{\sqrt{2\beta}}=A_{har}\cos(\omega t-\rho_{har})+A_{sub}\cos[(\omega-\omega_{\theta S})t-\rho_{sub}]+A_{ult}\cos[(\omega+\omega_{\theta S})t-\rho_{ult}]. \quad (7)$$

- for large amplitude oscillations around the unstable equilibrium position (assuming roll amplitude $\theta_0 >> \theta_{cr}$) the roll amplitudes can be determined from equation:

$$\theta\sqrt{\frac{\beta}{2}\theta^2-\alpha}=A_{har}\cos(\omega t-\rho_{har})+A_{sub}\cos[(\omega-2\omega_{\theta L})t-\rho_{sub}]+A_{ult}\cos[(\omega+2\omega_{\theta L})t-\rho_{ult}]. \quad (8)$$

herein:

$$\begin{cases} A_{har}=\dfrac{m_0\omega_{\theta L}}{\sqrt{\left(\omega_{\theta L}{}^2-\omega^2\right)^2+4\nu_\theta{}^2\omega^2}};\rho_{har}=\operatorname{arctg}\dfrac{2\nu_\theta\omega}{\omega_{\theta L}^2-\omega^2};\quad B_L=\dfrac{1}{2}-\dfrac{\pi}{4K(k_L)};\\ A_{sub}=\dfrac{-m_0B_L\omega_{\theta L}}{\sqrt{\left[\omega_{\theta L}^2-\left(\omega-2\omega_{\theta L}\right)^2\right]^2+4\nu_\theta{}^2\left(\omega-2\omega_{\theta L}\right)^2}};\rho_{sub}=\operatorname{arctg}\dfrac{2\nu_\theta\left(\omega-2\omega_{\theta L}\right)}{\omega_{\theta L}^2-\left(\omega-2\omega_{\theta L}\right)^2};\\ A_{ult}=\dfrac{-m_0B_L\omega_{\theta L}}{\sqrt{\left[\omega_{\theta L}^2-\left(\omega+2\omega_{\theta L}\right)^2\right]^2+4\nu_\theta{}^2\left(\omega+2\omega_{\theta L}\right)^2}};\rho_{ult}=\operatorname{arctg}\dfrac{2\nu_\theta\left(\omega+2\omega_{\theta L}\right)}{\omega_{\theta L}^2-\left(\omega+2\omega_{\theta L}\right)^2}; \end{cases}$$

where $\omega_{\theta L}$ - natural roll frequency of large oscillations around the unstable upright equilibrium position that is by means of VS-method defined by formula:

$$\omega_{\theta L}=\frac{\pi\sqrt{\beta\theta_0^2-\alpha}}{2K(k_L)}. \quad (9)$$

The natural roll frequency of small amplitude oscillations around the stable equilibrium positions is defined by another relationship:

$$\omega_{\theta S}=\frac{\pi\sqrt{\alpha-0.5\beta\theta_0^2}}{\sqrt{2}K(k_S)}, \quad (10)$$

where K(k) is a complete elliptic integral of the first kind.

A frequency curve of SNIS rolling in calm water according to formulae (9), (10) is represented in Fig.2.

It is seen from the analysis of expression (8) that for the unstable ship rolling in waves additionally ultra-harmonic oscillations with frequency $(\omega + 2\omega_{\theta L})$ and sub-harmonic ones with frequency $(\omega - 2\omega_{\theta L})$ can exist apart from harmonic oscillations with exciting frequency ω. As the calculating results evidence, amplitudes A_{ult} of higher harmonics in heavy rolling are significantly less than amplitudes of harmonic oscillations, and they can be neglected in practice. As to sub-harmonic regime, amplitudes of such type oscillations can be essential. It is worth noting herein that sub-harmonic oscillations are able to be excited only at exceeding of a certain threshold value of roll damping moment. The latter value is determined using VS-method as well.

Results of calculations driven by expressions (7) and (8) are given in Figs.3, 4.

Examining the SNIS large amplitude roll oscillations close to separatrix (curve 2 in Fig.1), i.e. $\theta_0 > \theta_{cr}$, for specifying of the solution it is necessary to take into consideration at least three terms in the expansion of integral $F(\eta, k)$. As a result, one may find extra overtones with frequencies $(\omega \pm 4\omega_{\theta L})$ near critical amplitude $\theta_{cr} = \sqrt{2}\theta_{st}$ in addition to oscillations with frequencies $(\omega \pm 2\omega_{\theta L})$.Thus the higher number of terms is taken into account in the expansion of the elliptic integral the more complicated forms one can see in the roll oscillations when roll amplitudes are approaching the homoclinic seperatrix. Finally, the ship turns up in the region of stochastic instability characterized by fractal structure in the phase space and by wide spectrum in frequency domain (Figs. 5, 6).

Analyzing Mathieu equation (2) we find approximate relation between amplitude θ_{par} and modulation frequency ω:

$$\theta_{par} = \sqrt{\frac{4}{3\beta}\left[\left(\frac{\omega}{2}\right)^2 + \alpha \pm \frac{1}{2}\sqrt{\alpha^2 a^2 - 4\nu^2\omega^2}\right]}. \qquad (11)$$

The resonance zone of parametric excitation is determined in the case by:

$$\frac{\alpha}{2}(1 - \sqrt{a^2 - 8\nu_\theta{}^2/\alpha}) < \left(\frac{\omega^2}{2}\right)^2 < \frac{\alpha}{2}(1 + \sqrt{a^2 - 8\nu_\theta{}^2/\alpha}). \qquad (12)$$

Obviously, that the inequality (12) will be correct if the condition $a > \frac{4\nu_\theta}{\omega^0_{\theta S}}$. Here $\omega^0_{\theta S} = \sqrt{2\alpha}$ is a frequency of extremely small natural oscillations around stable equilibrium position θ_{st}.

The latter inequality defines the minimum modulation amplitude of SNIS stability diagram

required for parametric resonance excitation at specified roll damping.

According to equation (11) the calculated parametric rolling in head and beam seas of the ship (series 60) with negative initial GM are plotted in Figs.3, 7.

Conclusions

Summarizing all the results obtained we can conclude the following:

The applied mathematical model reflects quantitatively and qualitatively all the principle features of an unstable ship rolling in waves.

It has been shown that the unstable ship rolls differs from the roll of a ship with positive initial metacentric height. With the help of analytical varied scale method of roll equation's analysis the specific oscillation regimes for an unstable ship have been found: depending on frequency and intensity of waves the unstable ship is rolling or with small amplitudes around stable equilibrium positions or with large amplitudes around unstable upright equilibrium position. Crossing the border between the above rolling regimes with small and large amplitudes the ship can be drawn in chaotic roll motion.

It has been determined that in seaway an unstable ship can undergo resonance motions in wide frequency range: in the case of coincidence of an encountering wave frequency and a ship roll natural frequency we have the principle resonance; in the case of an encountering frequency exceeds the natural roll frequency in two times we may have either sub-harmonic resonance of the second kind or parametric resonance; in the case of a wave frequency is three times higher than natural roll one we may observe the sub-harmonic resonance of the third kind.

The analytical expressions are found to determine the maximum roll amplitudes of the ship with negative initial stability for the cases of roll motions in all the above indicated resonance modes. The conditions of their excitation have been obtained as well. The calculations performed in accordance with the above mentioned expessions have been validated by the results of numerical and physical modeling.

References

1. A n a n i e v D. M.- Roll of a Ship with a Negative Initial Stability, Seakeeping qualities and ship design, Proc. of KTIRPIH, Kaliningrad, 1989 (in Rissian).
2. A n a n i e v D. M – Some Problems of Roll Stability, Materialy po obmeny opytom, vyp. 495. Improvement of propulsion, seakeeping and manoeuvrability qualities of ships, Leningrad, Sydostroenie, 1991 (in Russian).

3. B o n d a r N.G. - Non-linear Stationary Oscillations, Kiev, Naukova dumka, 1974 (in Russian).

4. F a l z a r a n o J. M., T r o e s h A. V. - Application of Modern Geometric Methods for Dynamical Systems to the Problem of Vessel Capsizing with Water-on-Deck. 4-th Int. Conference on Stability of Ships and Ocean Vehicles, Naples, 1990.

5. K a n M. - Chaotic Capsizing, Osaka Meeting on Seakeeping Performance, The 20th ITTC Seakeeping Committee, Osaka, 1992.

6. K a n M., T a g u c h i H. - Chaos and Fractals in Nonlinear Roll and Capsize of a Damaged Ship, Proc. of the International Conference on Phisical and Mathematical Modelling of Vessel's Stability in Seaway, Kaliningrad, Russia, 1993.

7. L i a w C. Y., B i s h o p S. R., T h o m p s o n J. M. T. - Heave-Excited Rolling Motion of a Rectangular Vessel in Head Seas. Proc. of the Second International Offshore and Polar Engineering Conference, San Francisco, USA, 1992.

8. L i n H., Y i m S.C.S. - Chaotic Roll motion and Capsize of Ships under Periodic Excitation with Random Noise. Applied Ocean Research, 17, 1995.

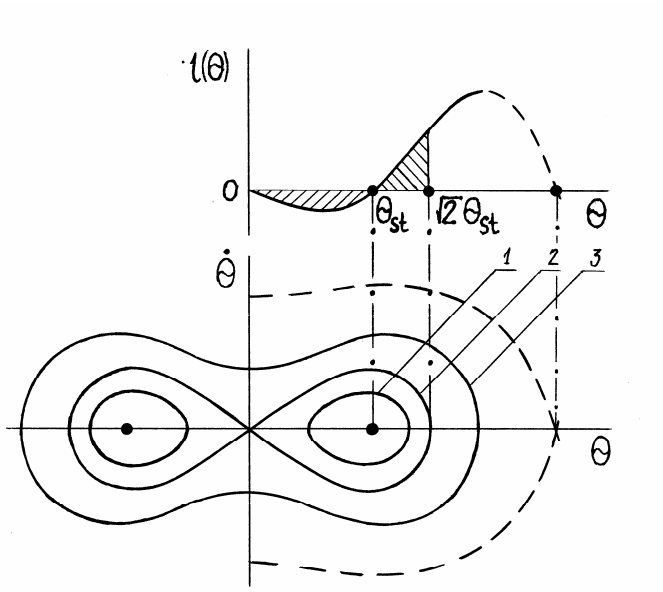

Fig.1 Phase portrait of autonomous roll of the ship with negative initial GM (1 – oscillations around stable equilibrium position; 2 – homoclinic orbit; 3 - oscillations around unstable equilibrium position; - - - - heteroclinic orbit).

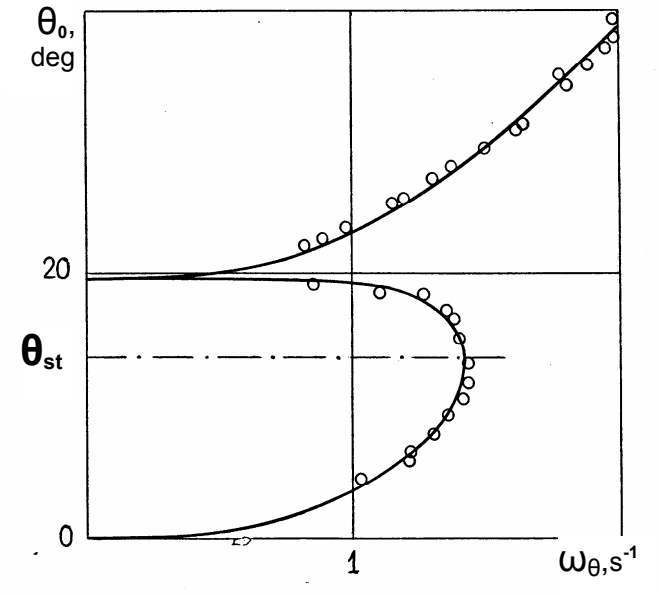

Fig.2 Frequency roll diagram for the unstable ship model of 60th series.

——— Calculations in accordance with (9), (10); ○ - model tests.

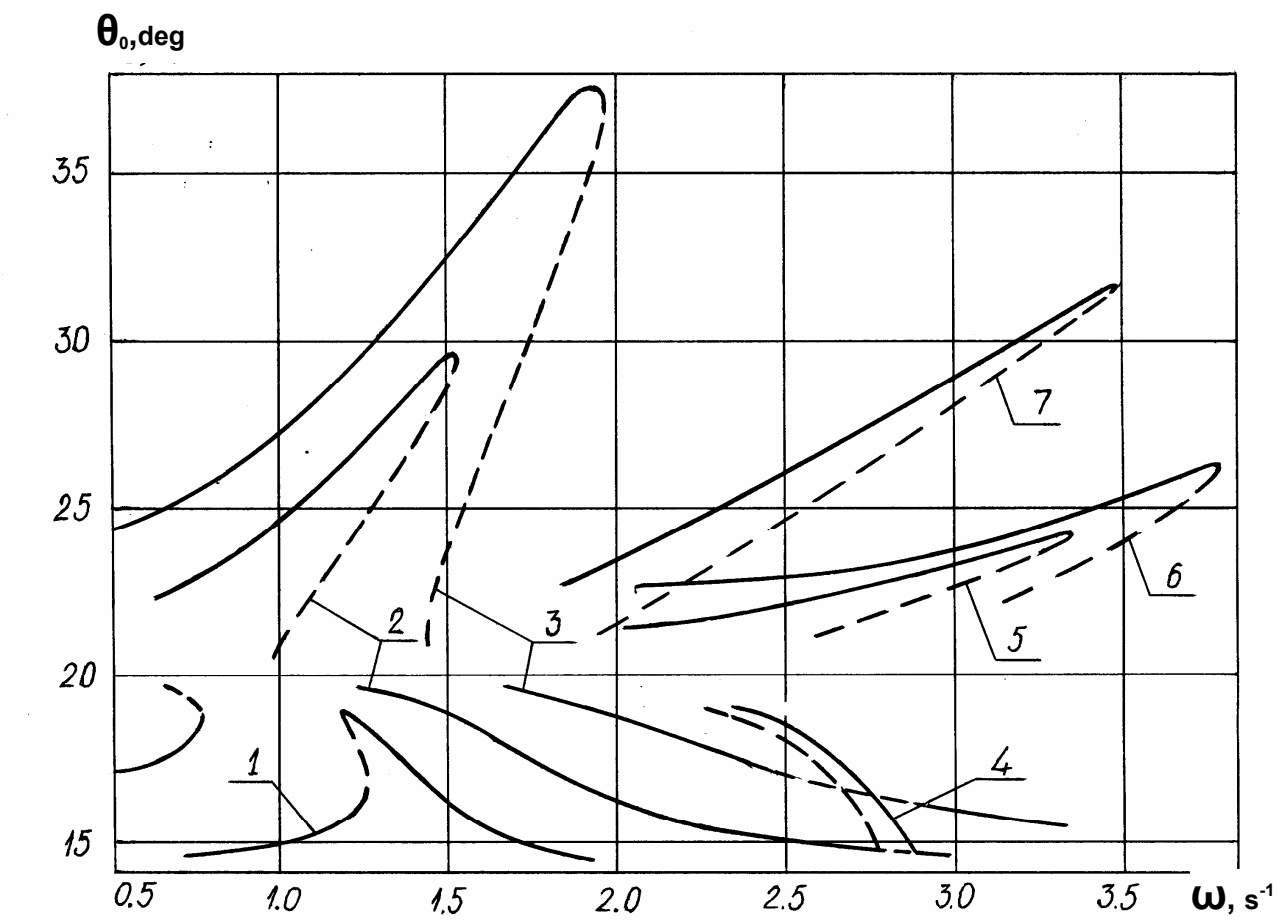

Fig.3 Roll amplitude – frequency diagram for the unstable ship model of 60th series in beam regular waves. Analytic solution.

1 – $m_o = 0.02\ c^{-2}$; 2 - $m_o = 0.1\ c^{-2}$; 3 - $m_o = 0.3\ c^{-2}$: harmonic mode;

4 - $m_o = 0.1\ c^{-2}$: sub-harmonic mode of 2nd kind;

5 - $m_o = 0.1\ c^{-2}$ sub-harmonic mode of 3rd kind;

6 - $m_o = 0.3\ c^{-2}$: sub-harmonic mode of 3rd kind;

7 - $m_o = 0$: parametric oscillations.

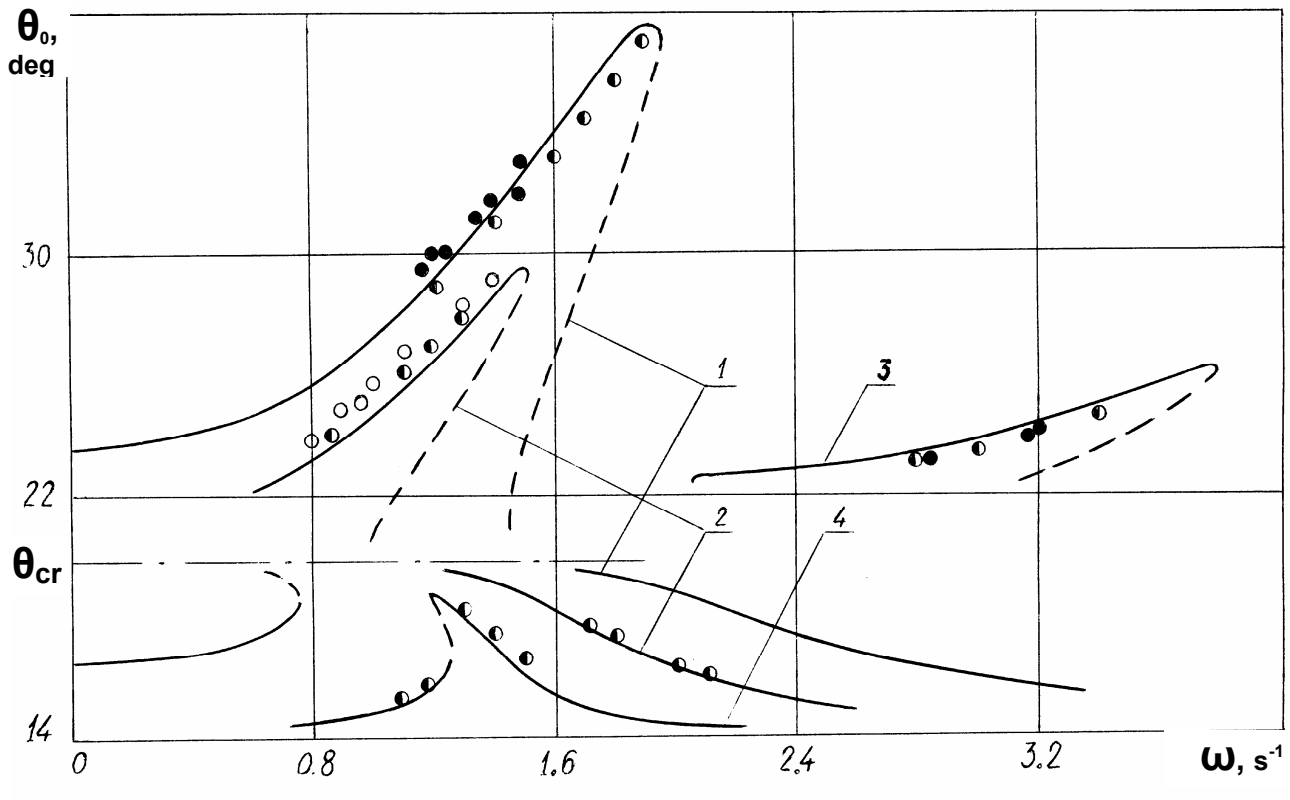

Fig.4 Roll amplitude – frequency diagram for the unstable ship model of 60th series in calm water under harmonic moment excitation.

1 – $m_o = 0.3\ c^{-2}$; 2 - $m_o = 0.1\ c^{-2}$; 4 - $m_o = 0.02\ c^{-2}$: harmonic mode;

3 - $m_o = 0.3\ c^{-2}$: sub-harmonic mode;

$m_o \approx 0.1\ c^{-2}$: model test.

○ - numerical solution of Eq. (1)

● - $m_o \approx 0.3\ c^{-2}$;

○ - $m_o \approx 0.1\ c^{-2}$: model test.

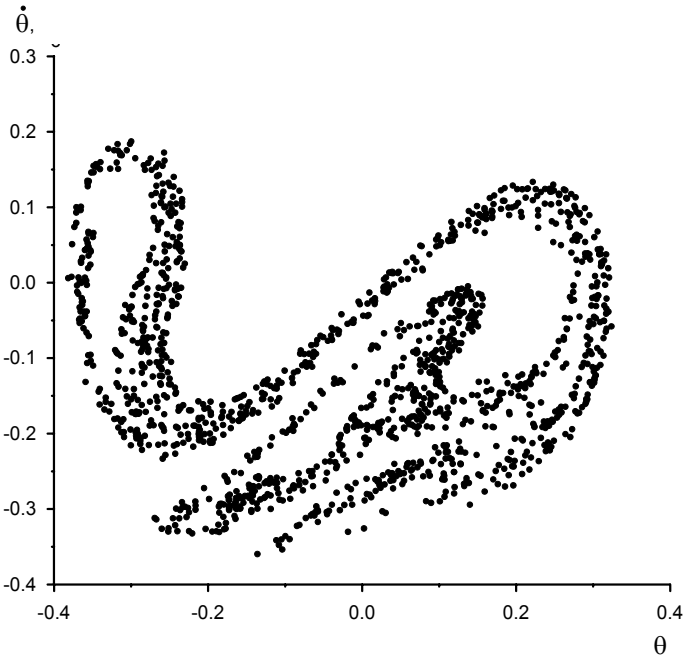

Fig.5 Poincare map corresponding to chaotic motions of SNIS (results of the numerical simulation).

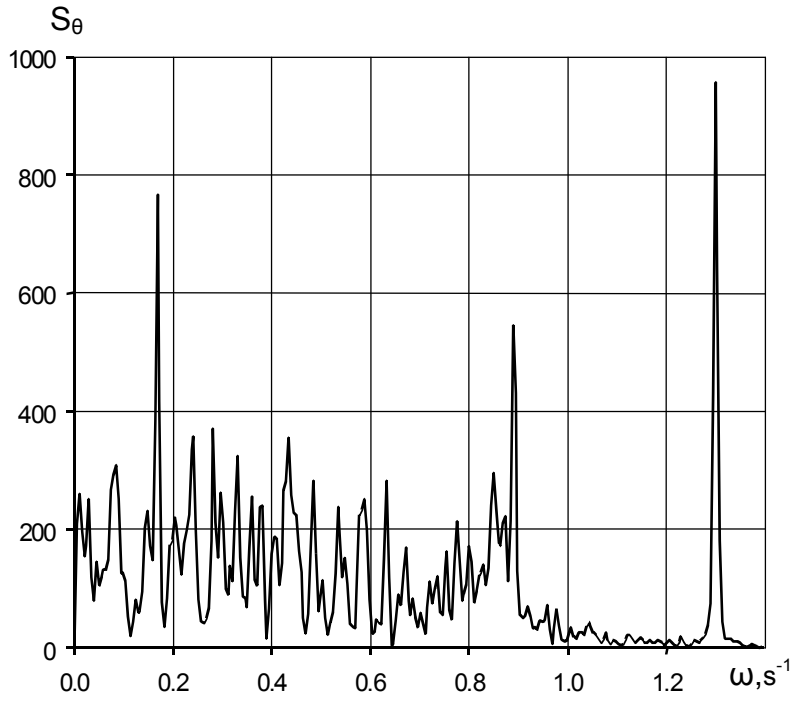

Fig.6 Frequency spectrum of SNIS rolling in chaotic regime (results of the numerical simulation; exciting frequency ω=1.3 rad/s).

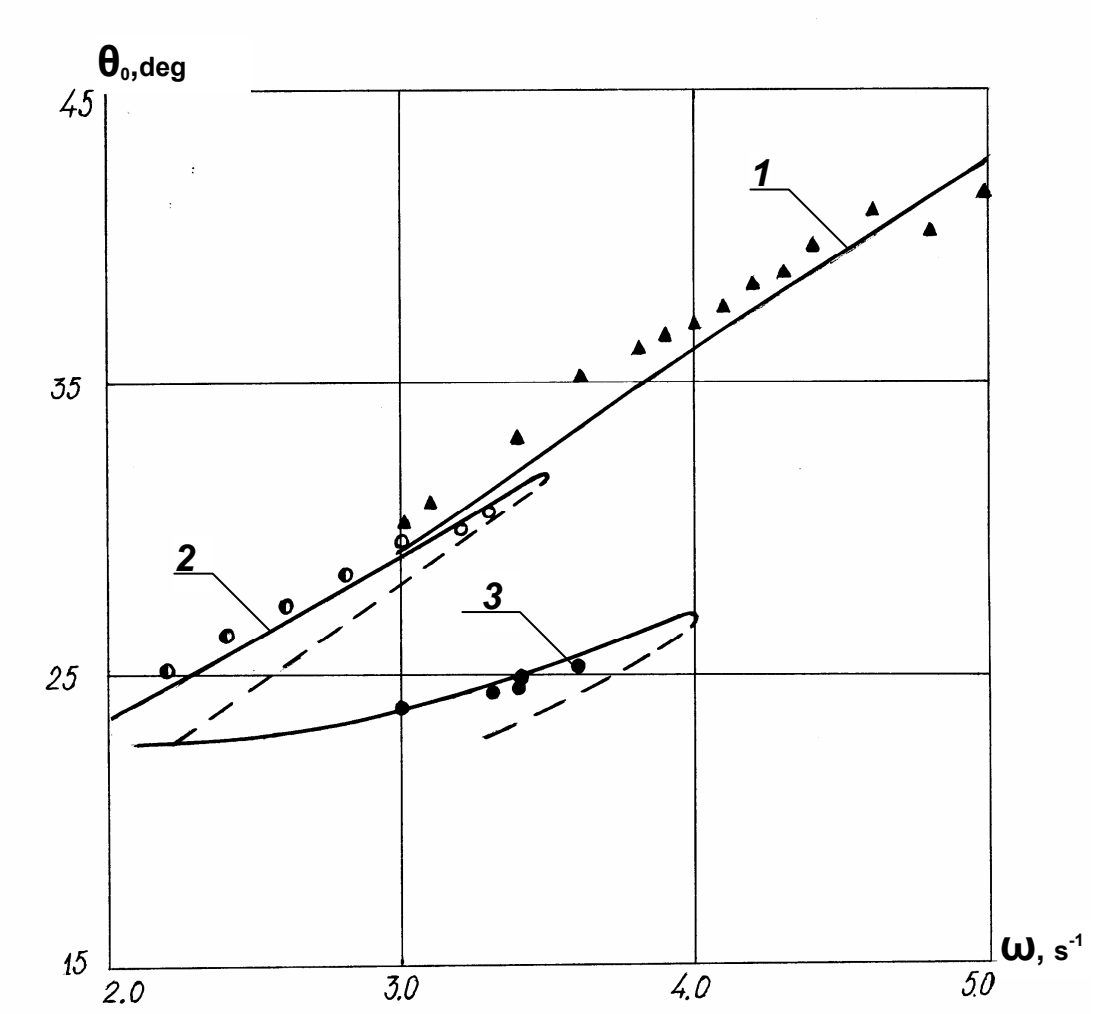

Fig.7 Roll amplitude – frequency diagram for the unstable ship model of 60th series in beam / head regular waves.

1 - parametric oscillations in head sea ;

2 - parametric oscillations in beam sea;

3 - sub-harmonic mode of 3rd kind in beam sea;

○ ,● , ▲ - model tests;

○ - numerical simulation.

On Developing a Rational and User-friendly Approach to Fishing Vessel Stability and Operational Guidance

Bruce Johnson, Working Group A

John Womack, Working Group B

SNAME Panel on F/V Operations and Safety

Tasks of the SNAME F/V Panel

- **Working Group A: Investigate the feasibility of establishing risk-based fishing vessel stability criteria appropriate to the type of vessel and its operating area. (See Dahle 1995)**

- **Working Group B: Evaluate the effectiveness of existing stability letters and develop better ways to communicate to the fishing community the importance of following reasonable stability and survivability guidelines.**

We must cease communicating oversimplified and incorrect fishing vessel stability concepts

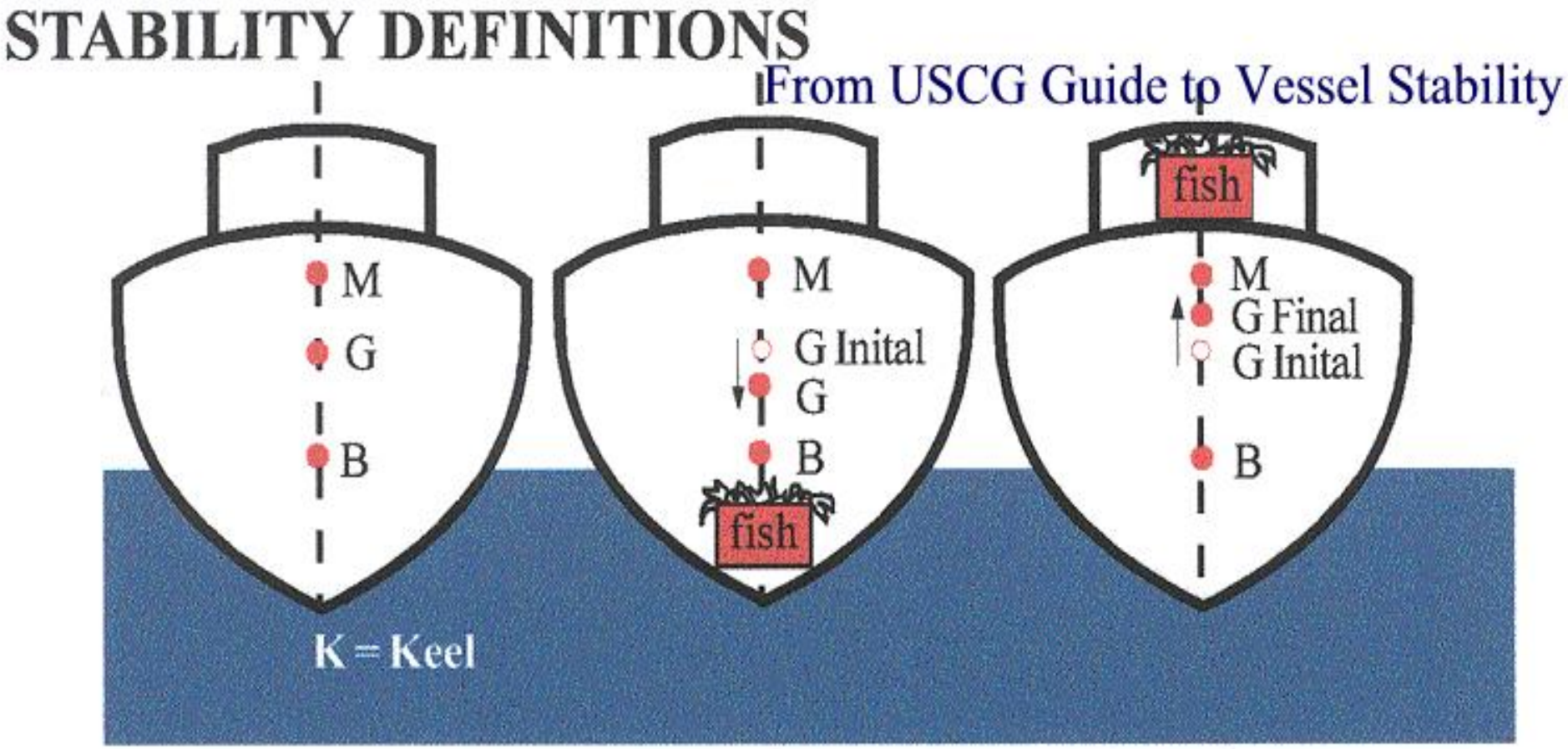

Vessel Upright Stability

FIGURE 1

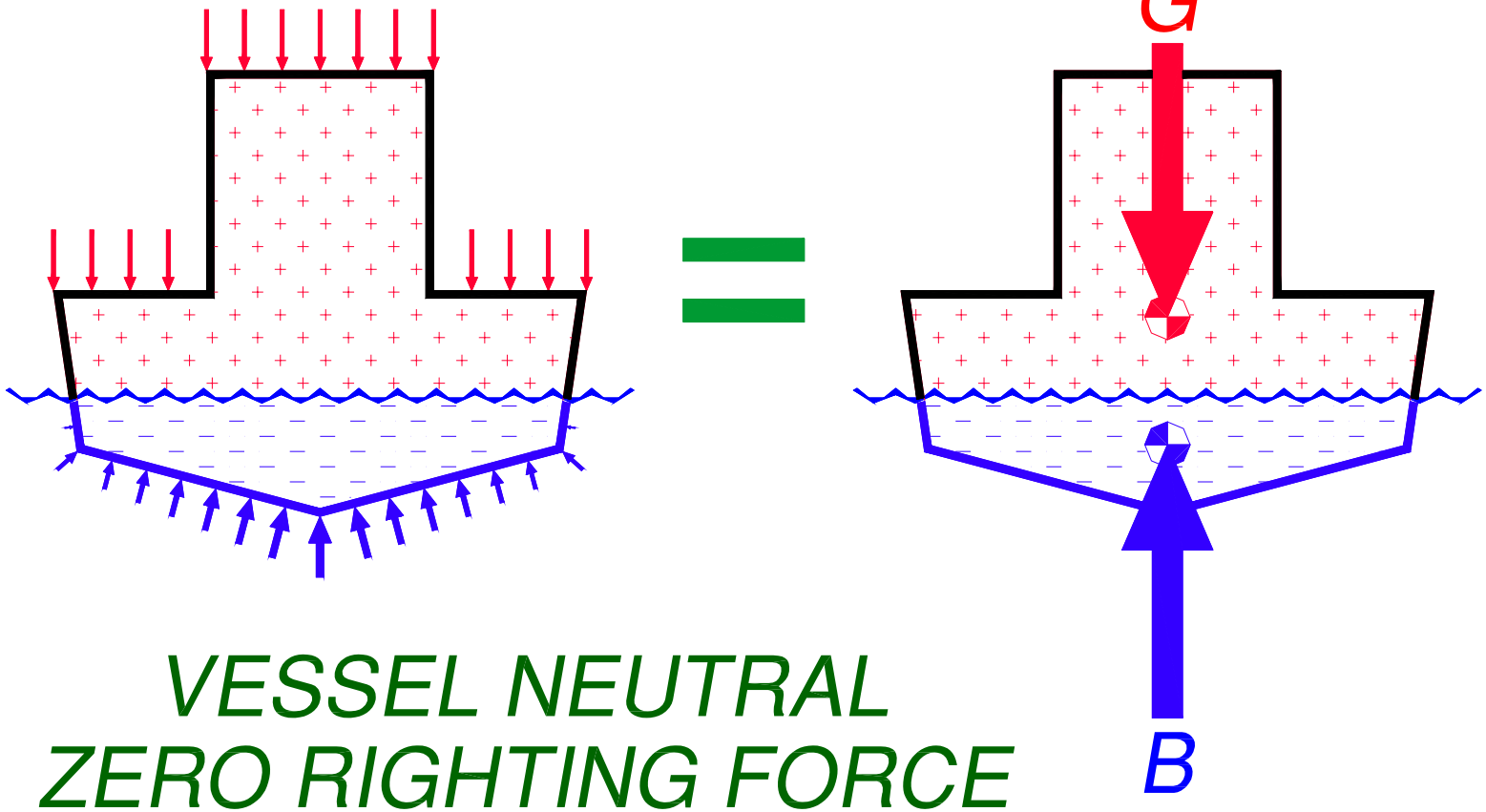

VESSEL NEUTRAL
ZERO RIGHTING FORCE

Inclined Stability

FIGURE 3

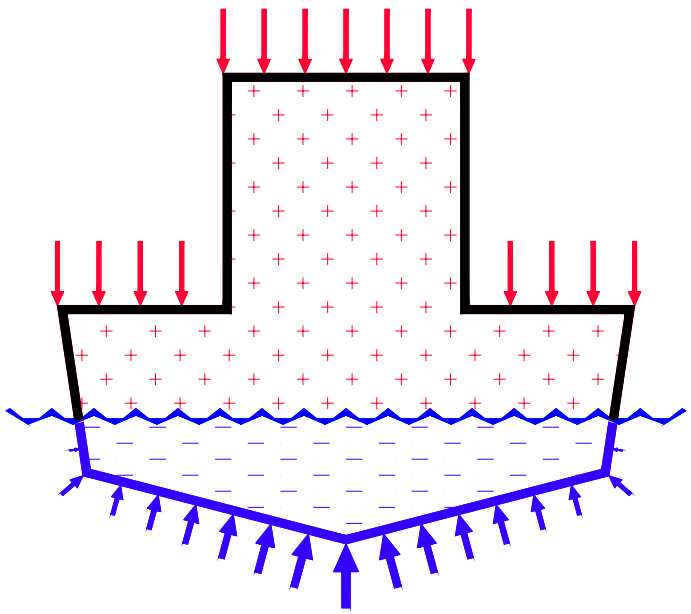

FIGURE 3A

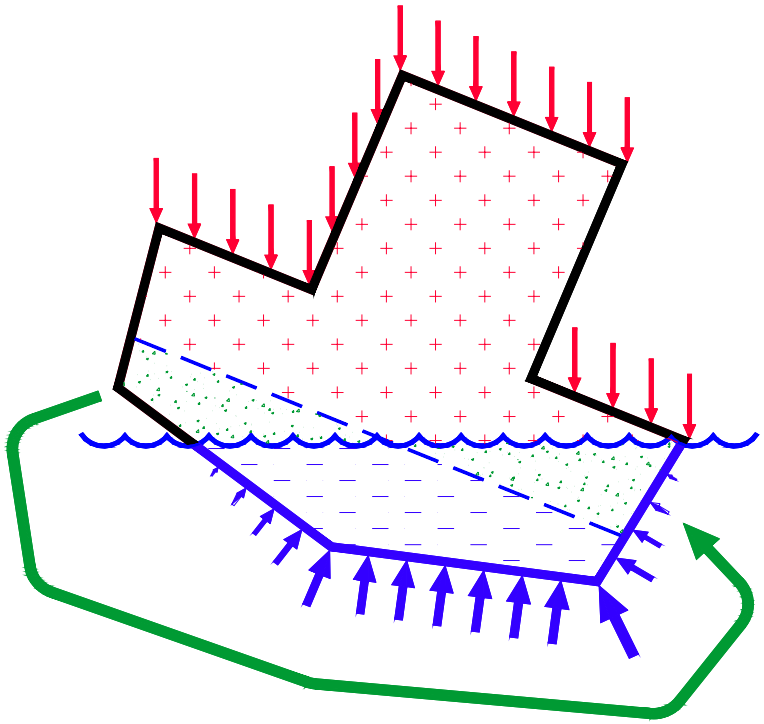

FIGURE 3C

Positive Initial Stability

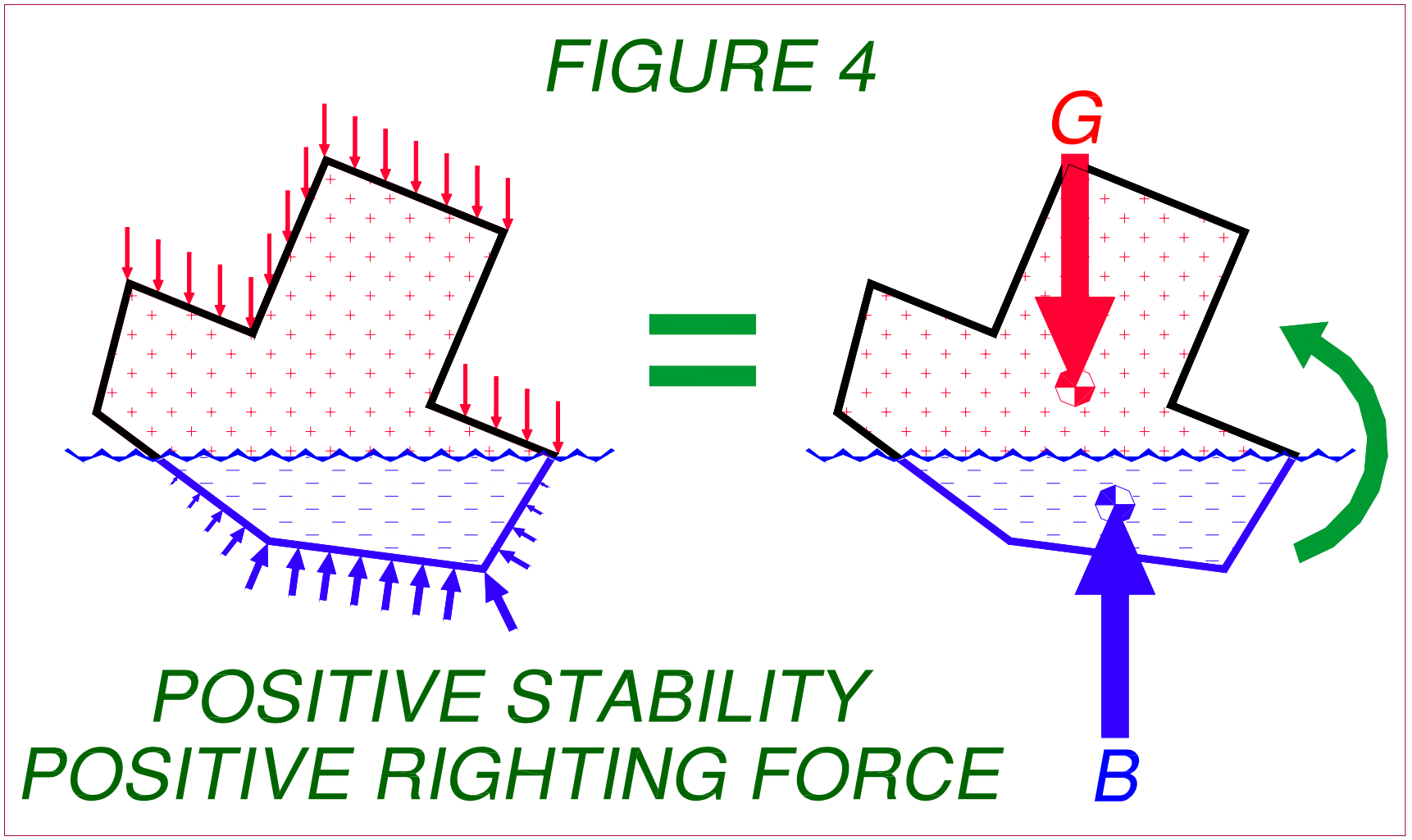

Negative Overall Stability

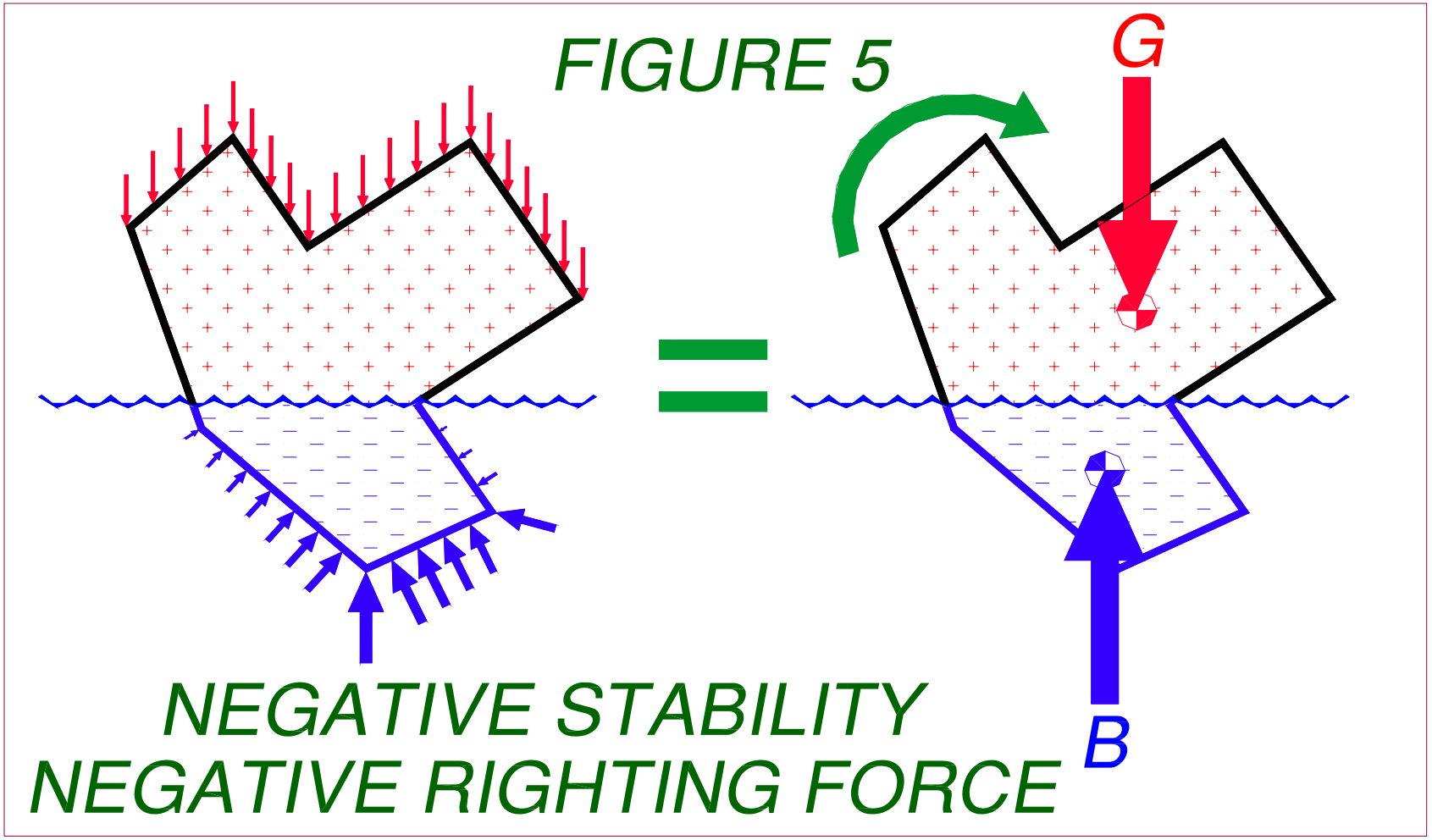

Righting Arm, RA

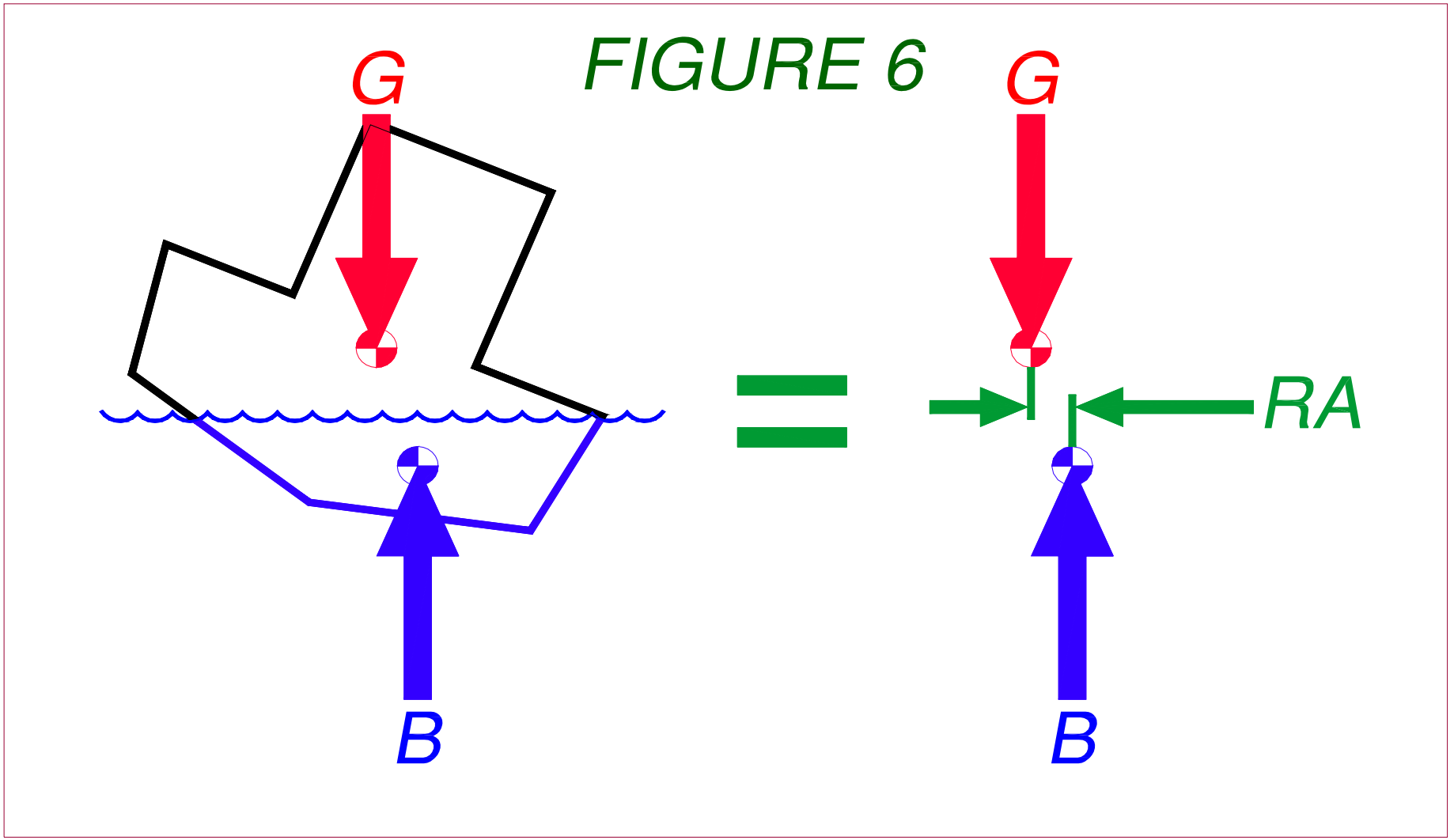

Overall Stability at Various Angles of Heel

FIGURE 7

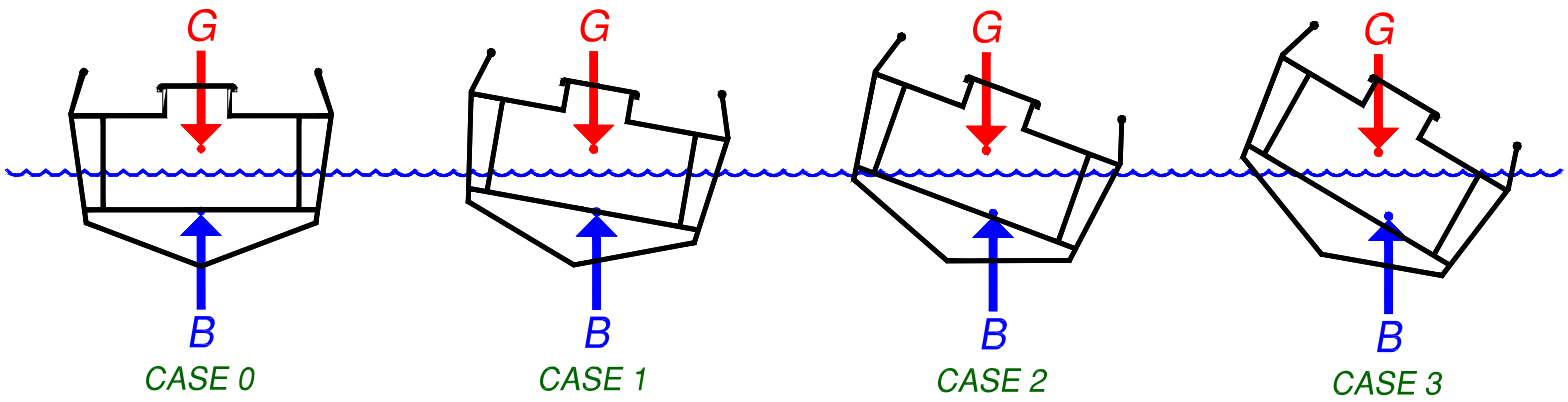

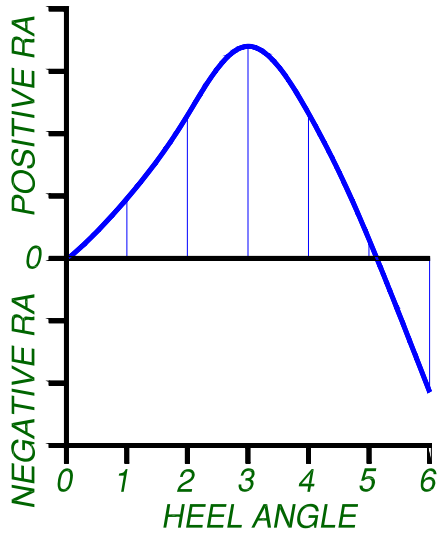

Frequently Used Stability Criteria

FIGURE 8

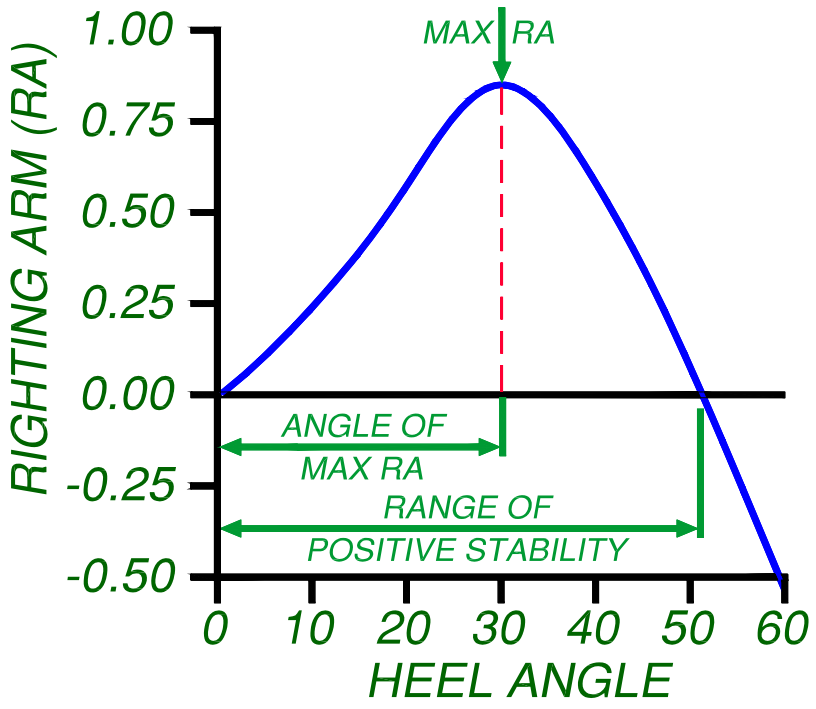

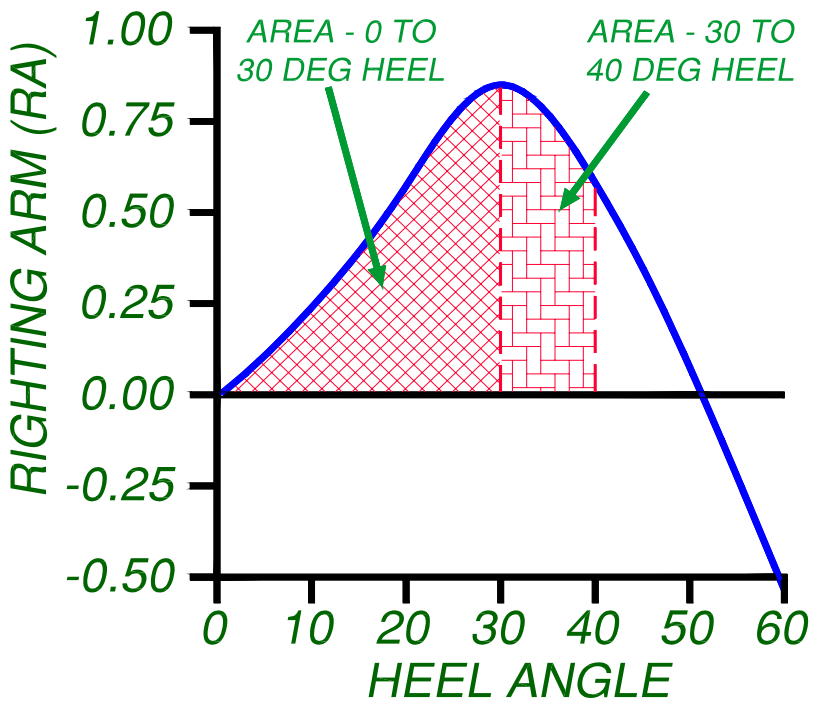

Frequently Used Stability Criteria

- A common interpretation of the Torremolinos Protocol stability criteria is that the area under the righting arm curve represents “righting energy”.
- A possible solution to this misinterpretation is to change the terminology to "unit righting energy" or even “unit static righting energy”. This interpretation is correct since the righting arm is righting energy per unit displacement, m-tons-degrees/ton (ft-tons-degrees/ton).
- (Work and energy are in lb-ft or N-m. See Appendix A, excerpts from PNA 1988, Volume 1, pp 87-93 on Dynamic Stability.)

Scalability

- **Briefly, scalability in vessel stability characteristics depends on the square-cubed rule, i.e. the heeling forces, which depend on water and wind impact areas, go up with the square of the dimensions but the righting moment depends on the displacement which goes up with the cube of the dimensions.**
- **Thus, bigger is almost always better!**
- **Correctly using the Torremolinos criteria should mean that vessels double in dimensions should survive without capsizing in twice the wave height conditions. However, that is not the interpretation generally given by the existing one-size-fits-all stability guidelines.**

Effect of Rise in CG

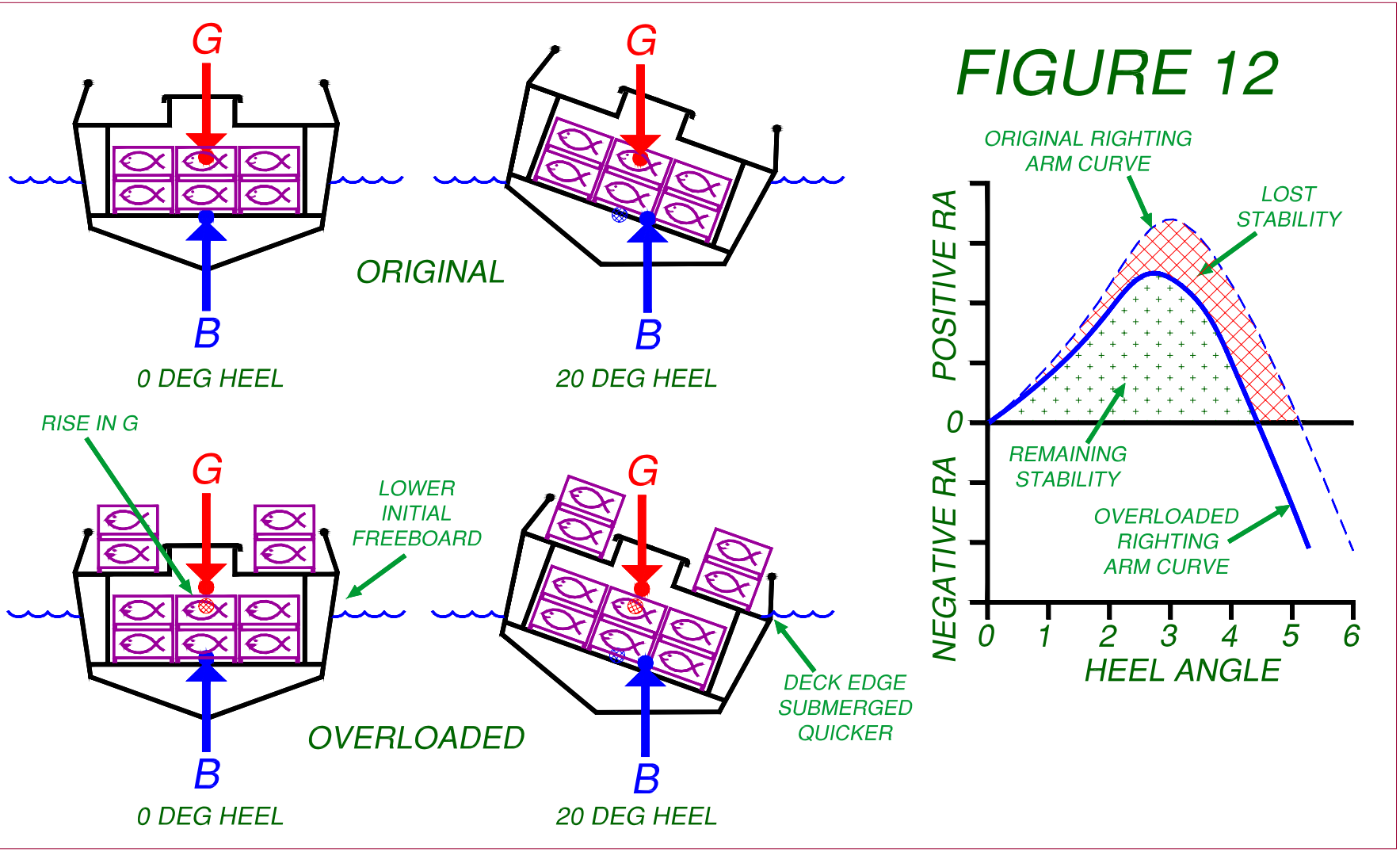

FIGURE 12

Effect of Wind Heeling

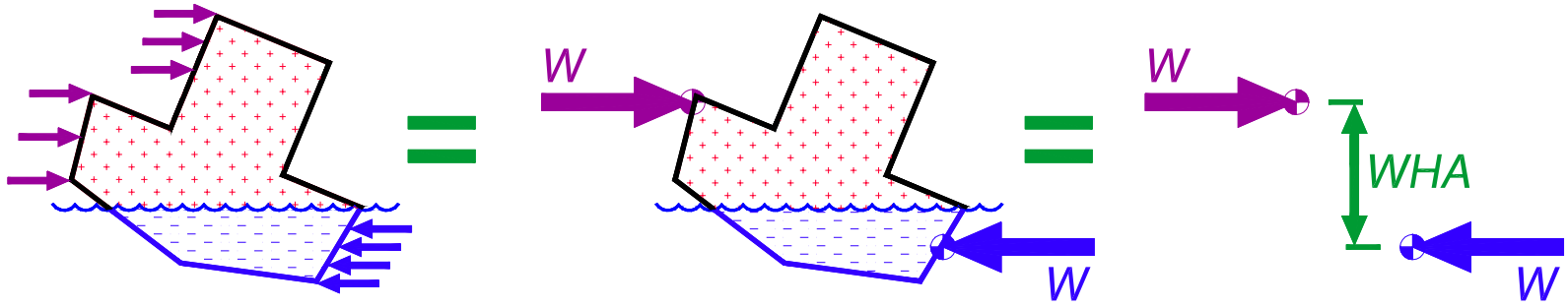

WHA = WIND HEELING ARM

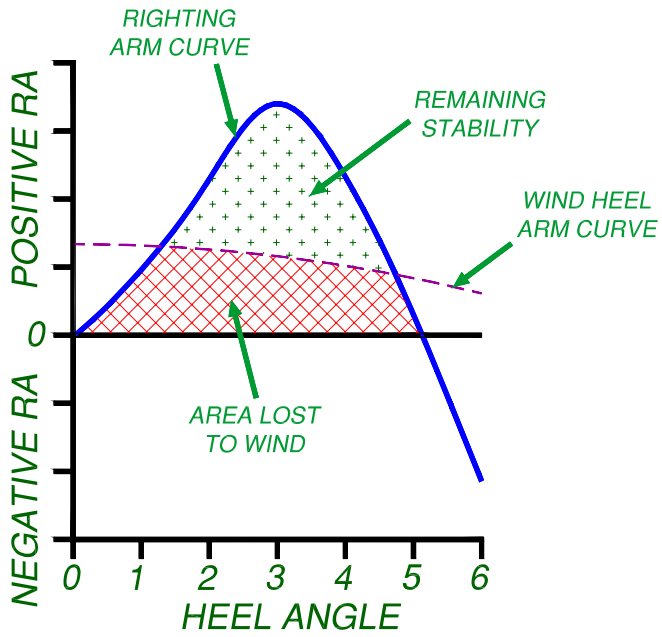

FIGURE 14

Effect of Wind Heeling

- The wind heel criteria do scale with size, as PNA points out, since the both the heeling arm and the righting arm are divided by the vessel displacement.
- This beam sea rolling criteria is used for the following example in the absence of other scalable criteria.
- Working Group A needs to address this problem.

Format Type A - Short Trip Length or Near Shore Operation

- To experiment with several simple approaches to developing this new version of the severe wind and roll criteria, trials were run on a typical Mid-Atlantic offshore clamming boat.
- The trials use educated assumptions to explore some general concepts and trends for using this criteria in less than full storm conditions.
- Full theoretical and model testing needs to be done to make robust, effective criteria.

Format Type A - Short Trip Length or Near Shore Operation

- **The trial boat is a former 133 foot (40m) offshore supply vessel built in 1966 that was converted for use in the offshore clam harvesting fishery.**

- **The boat operates on 24 to 32 hour dock to dock trips along the Mid Atlantic and New England coastline, typically ranging from 10 to 60 nautical miles from port. The catch is loaded on deck in steel cages similar to loading supplies on a typical offshore supply vessel.**

- **Due to the dredging gear, these clamming vessels generally work in winds less than 25 knots in order to keep the dredge in the sea bottom. Because of this wind restriction and the short trip times, this boat is ideally suited to weather dependent loading guidelines.**

Righting Arm Curves, 40 m OSV

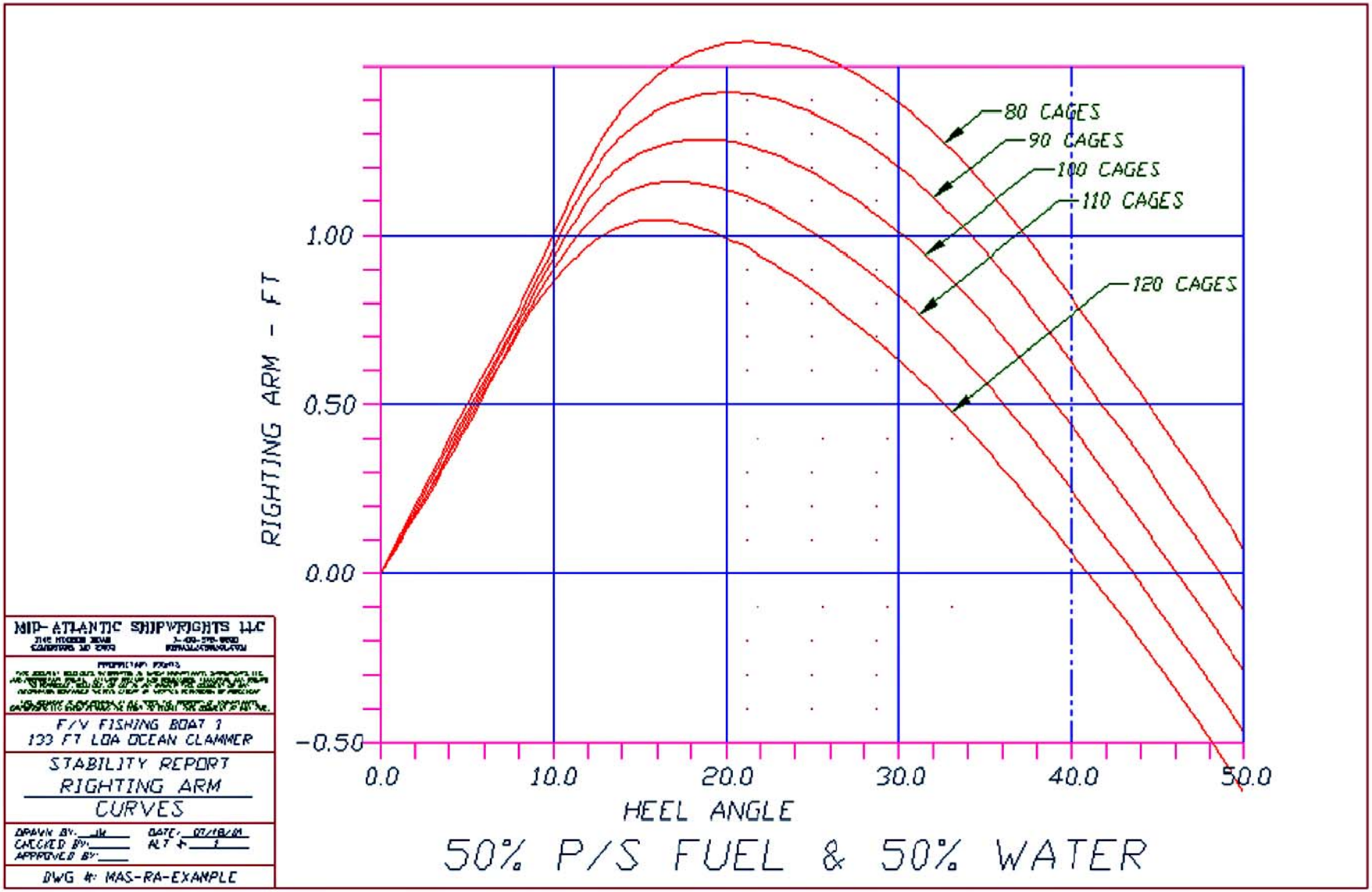

Criteria, 40 m OSV F/V Conversion

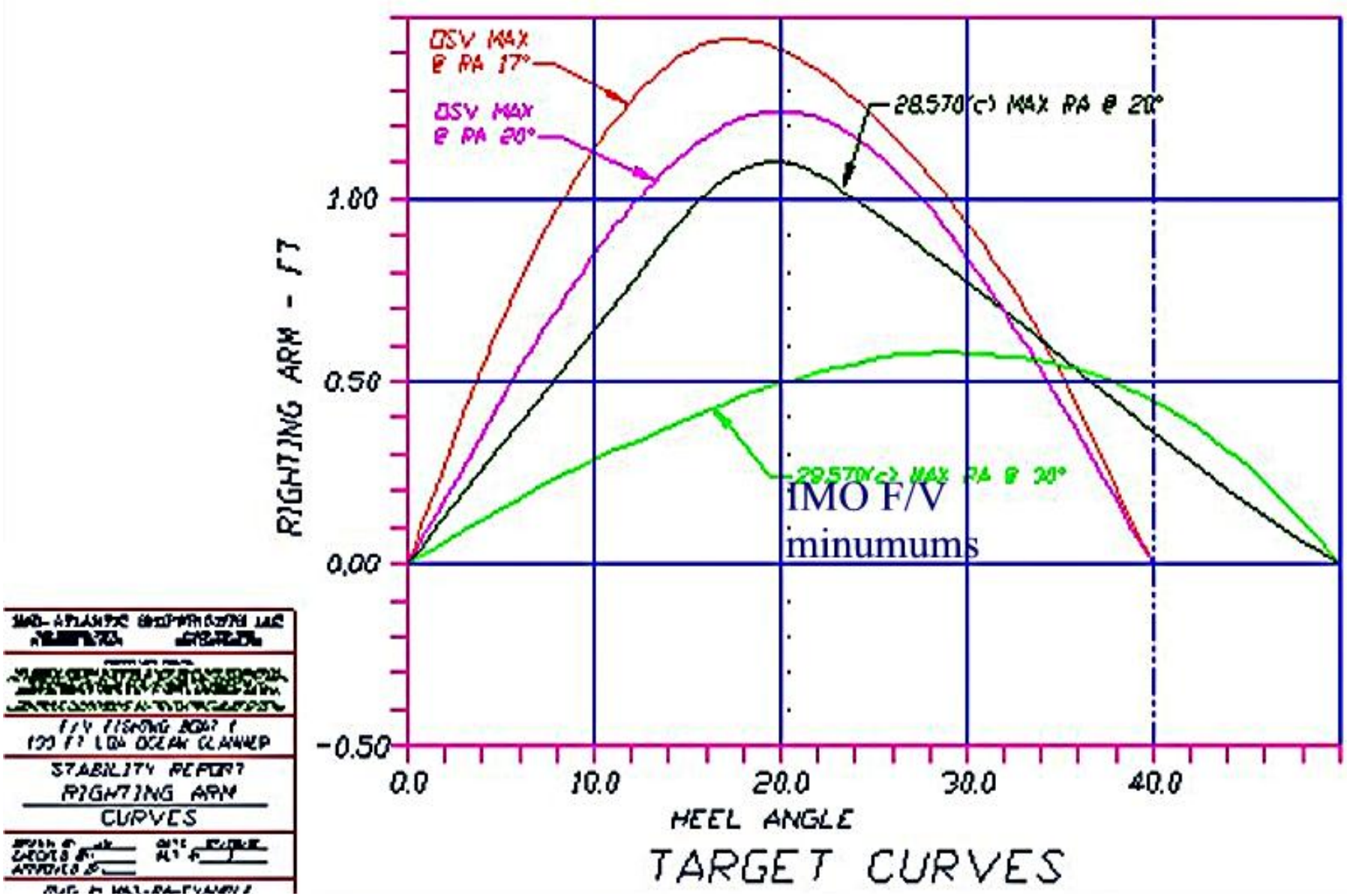

F/V # 1 40m OSV Clam Dredger - Safe Loading Table

Fuel Tanks 70% or Lower

All Loaded Cages are on the Main Deck

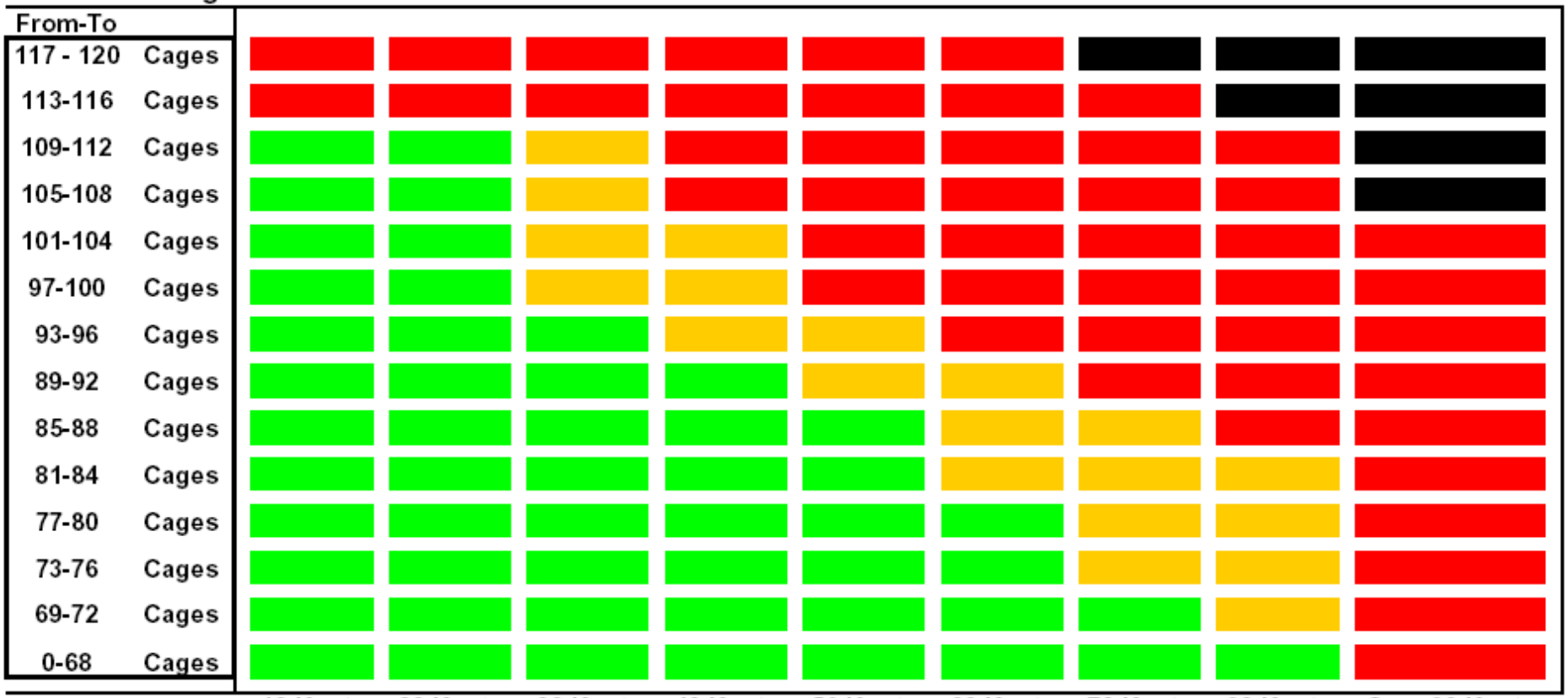

Sustained Wind Speed	10 Knots	20 Knots	30 Knots	40 Knots	50 Knots	60 Knots	70 Knots	80 Knots	Over 80 Knots
Expected Local Hs	0.8 m	1.2 m	2 m	3 m	4 m	6 m	9 m	12 m	> 14 m
Open Ocean Hs	0.8 m	2.5 m	4 m	6 m	8 m	11 m	14 m	16 m	> 16 m

Safe to Operate

Operate with Caution

Unsafe to Operate

Imminent Danger of Capsize

F/V #1 40 m OSV Clam Dredger - Safe Loading Table

Fresh Water Tank any Level

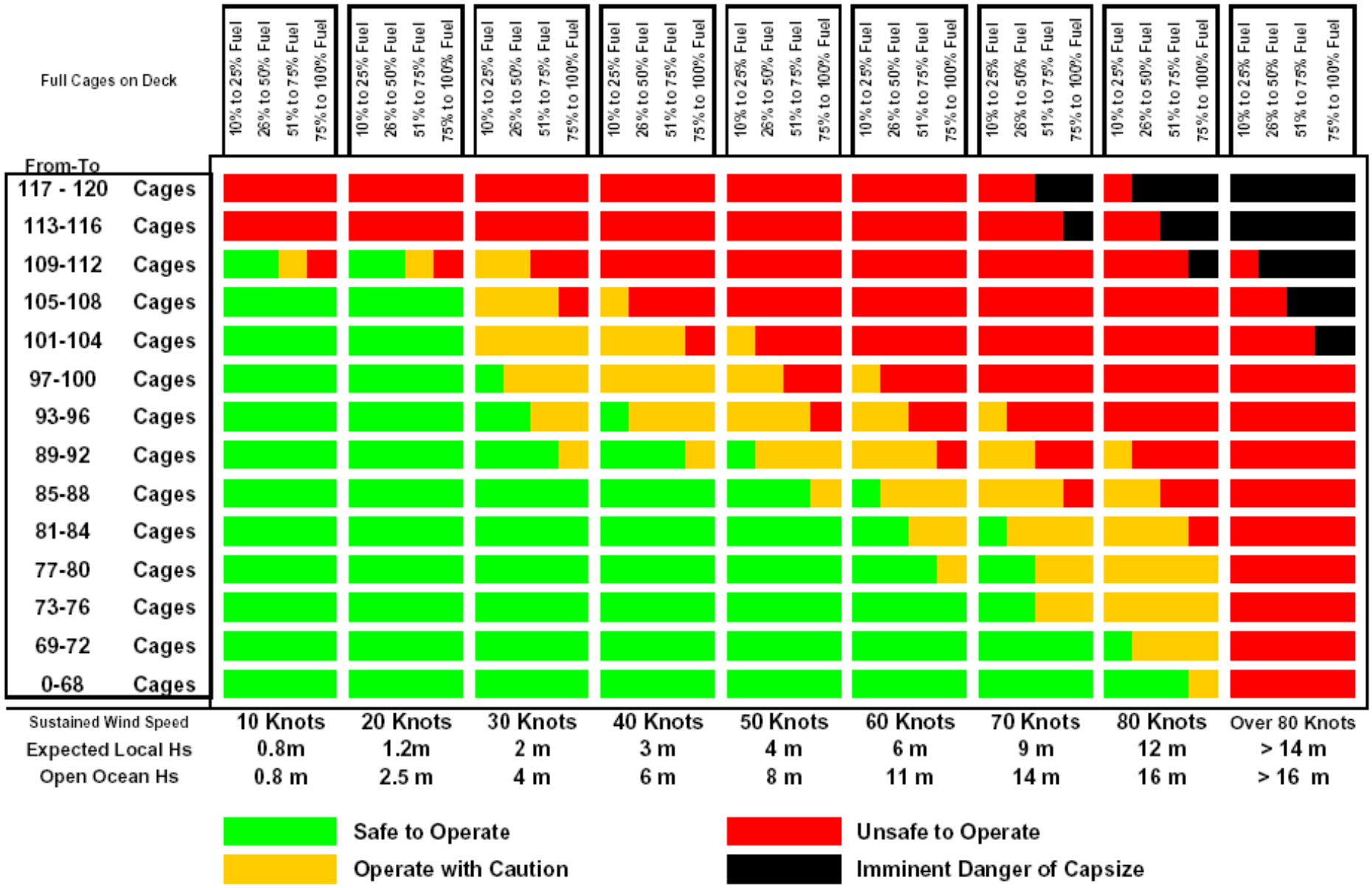

Format Type B - Offshore Operation

- Fishing boats that work on extended trips with no port of safe refuge available within a reasonable steaming range can also take advantage of a risked based loading matrix.
- In this setup, current weather conditions are not factored into the stability review. The fishing boat's stability would be evaluated against an appropriate worst case storm conditions to be expected for its fishing grounds.

F/V #2 40m Stern Trawler - Safe Loading Table B-1 - Unrestricted Ocean Service

Fresh Water Tank any Level

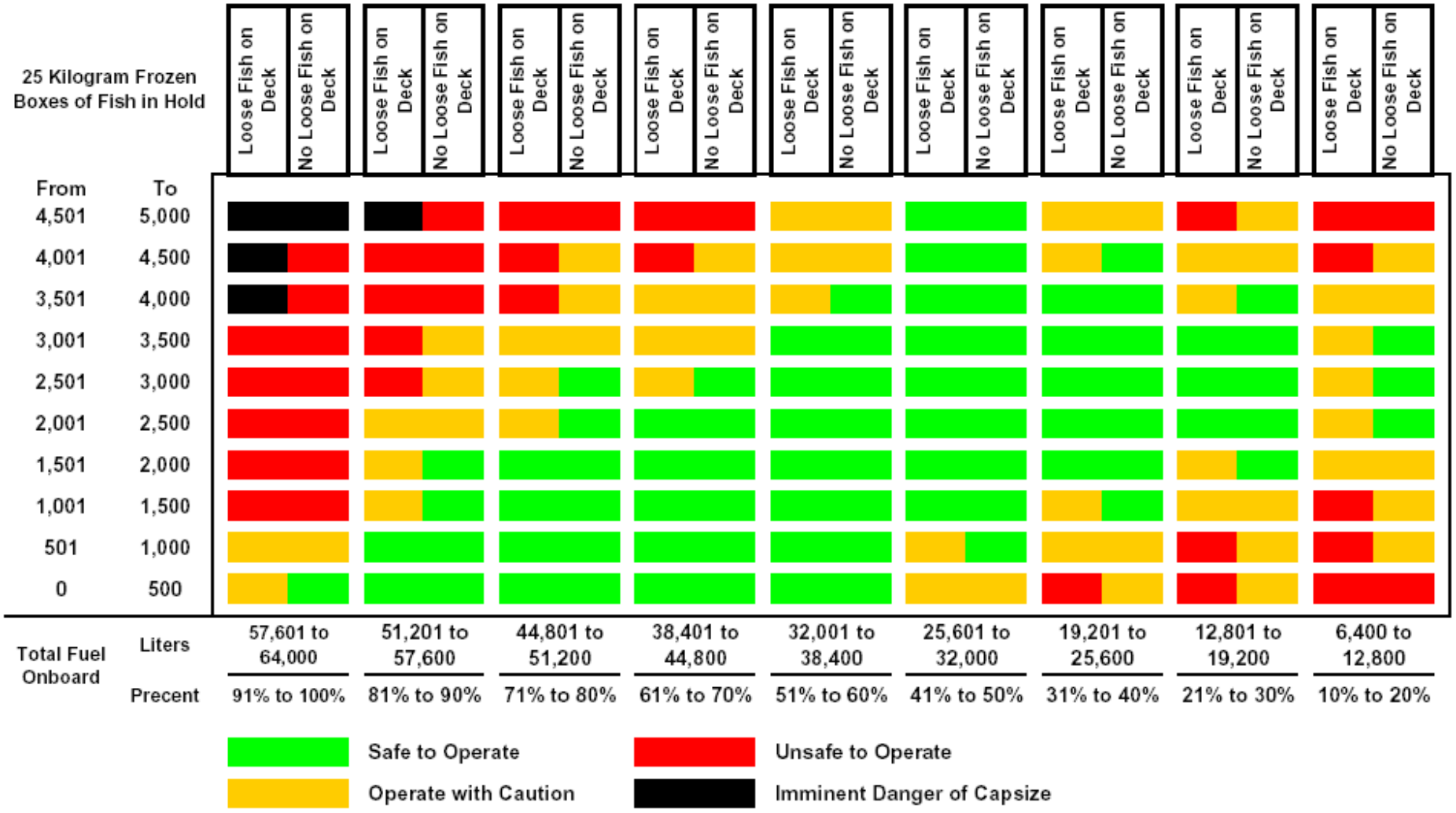

Extracts from An Introduction to Stability

http://www.fao.org/

ftp://ext-ftp.fao.org/pub/Turner/

Jeremy Turner
FAO Rome Italy

ACCIDENTS

DRIFTING

- Bad engine installation
- Bad maintenance of engine
- Lack of trouble-shooting experience
- Lack of fuel

FIRE

- Careless use of open fire
- Bad installation of cooker
- Wrong location of gas bottle

SINKING

- Poor standard of construction
- Bad maintenance

COLLISION

- Lack of navigation and fishing lights
- Lack of radar reflector
- Careless crew

CAPSIZAL

- Poor stability
- Heavy loads on deck
- Water trapped on deck

WORK ACCIDENTS

- Slippery decks
- Unprotected deck equipment and machinery
- Tired crew

How is stability reduced?

- Vessel flooded
- (loss of freeboard plus free surface effect)
- Vessel overloaded
- (reduced freeboard)
- Weights too high
- (reduced freeboard plus CG raised)
- Water on deck
- (free surface effect plus reduced freeboard plus CG raised)
- Half full tanks
- (free surface effect)
- Water in bilges
- (free surface plus reduced freeboard)

THIS BOAT IS IN DANGER OF CAPSIZING

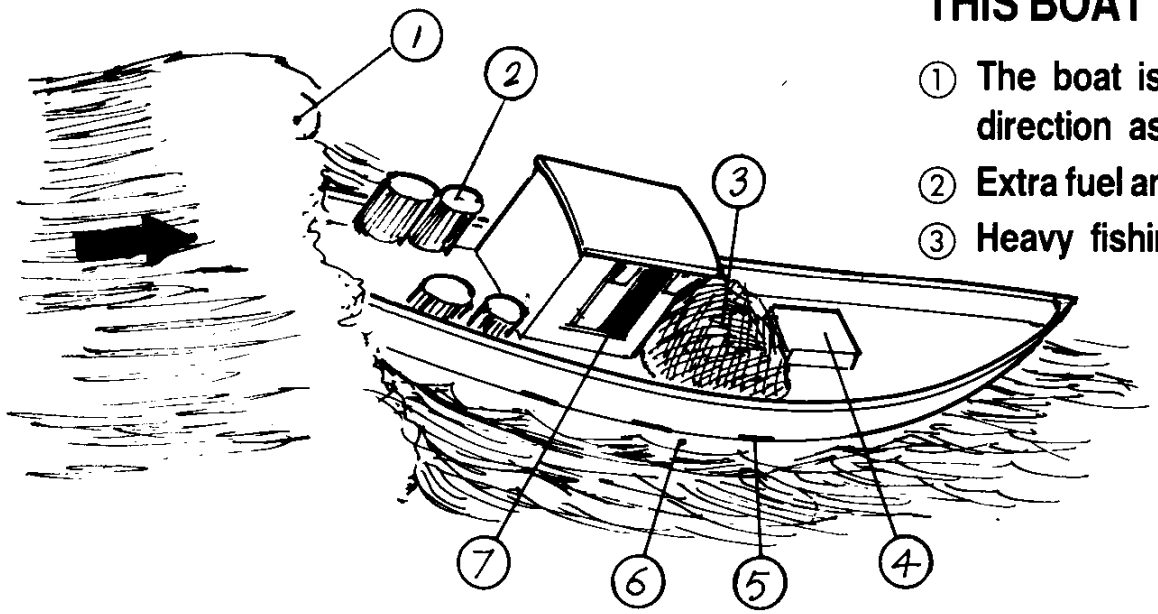

① The boat is going full speed in the same direction as the waves

② Extra fuel and fresh water are in drums on deck.

③ Heavy fishing gear is on deck.

④ Hatch covers are not lashed.

⑤ Freeing ports are small.

⑥ Freeboard is low.

⑦ Deckhouse door is open.

The boat is likely to be thrown broadside to the waves and the fishing gear and drums are likely to slide over the bulwark.

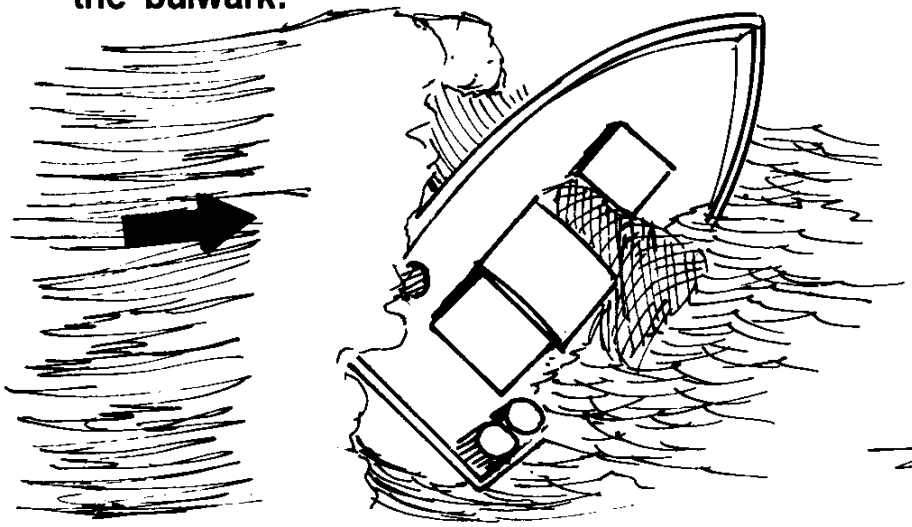

The boat is then likely to capsize with the next large wave.

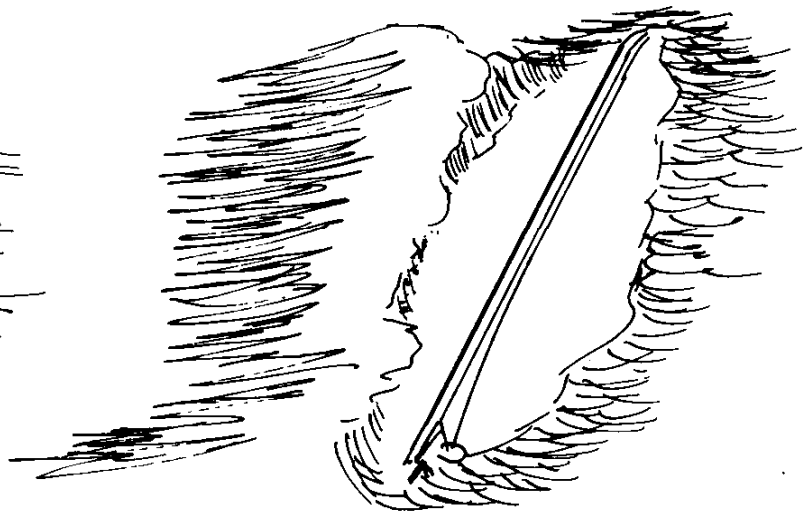

THIS BOAT IS BETTER PREPARED AGAINST CAPSIZING

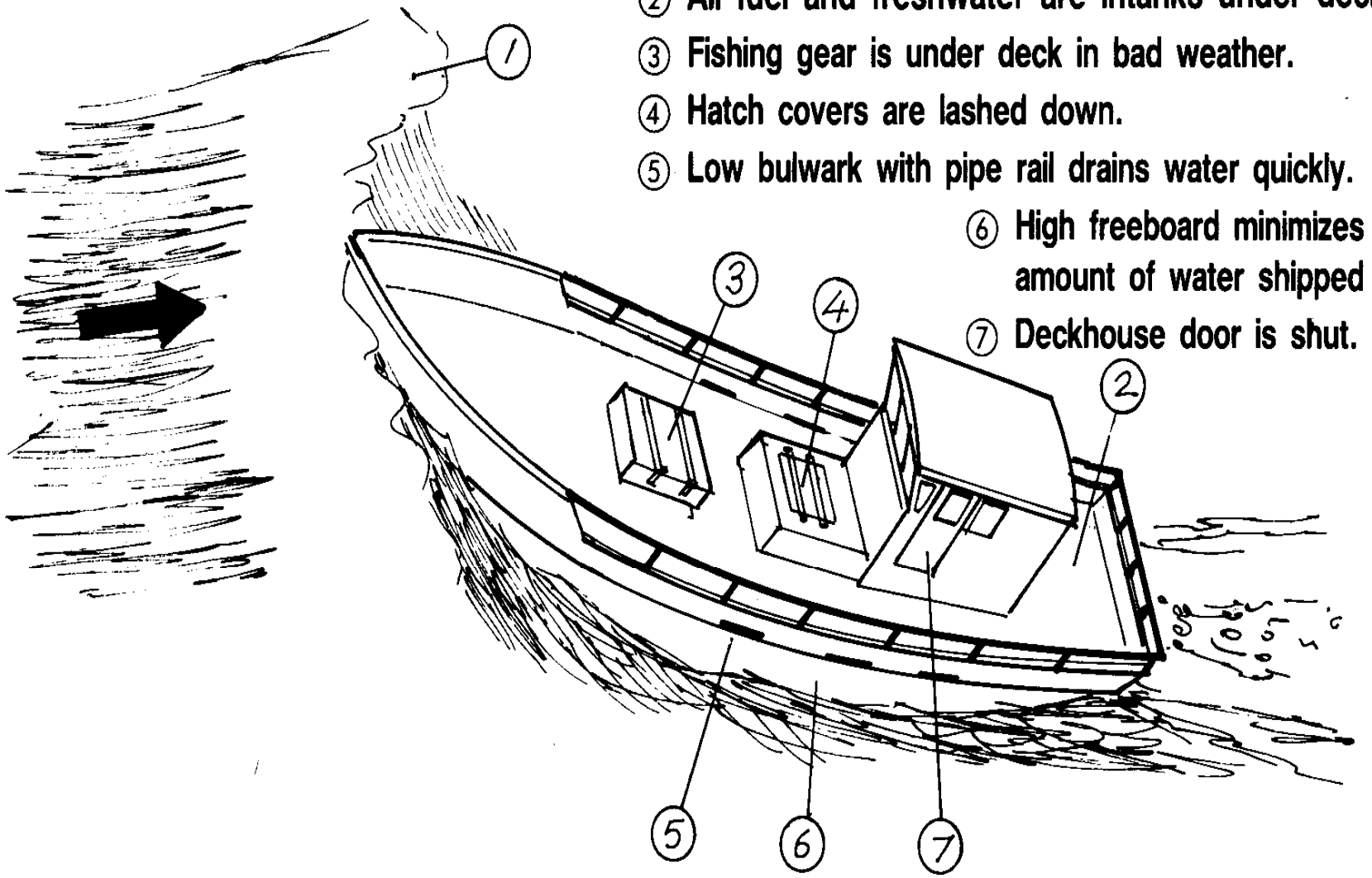

① The boat is going slowly against the waves.
② All fuel and freshwater are intanks under deck.
③ Fishing gear is under deck in bad weather.
④ Hatch covers are lashed down.
⑤ Low bulwark with pipe rail drains water quickly.
⑥ High freeboard minimizes the amount of water shipped in.
⑦ Deckhouse door is shut.

Summary

- Do not overload the vessel
- All fishing gear and other weights should be stowed, prevented from shifting and placed as low as possible
- Freeing ports must be of adequate size and unobstructed
- All doors, windows, hatches etc should be closed in bad weather
- Closing devices must be well maintained
- Fish holds should be longitudinally divided
- Minimize the number of partially full tanks
- Be alert to the dangers of following or quartering seas

Questions and Comments